ISSN 0031 - 9465

PHYTOPATHOLOGIA MEDITERRANEA

Plant health and food safety

Volume 61 • No. 3 • December 2022

60th Anniversary of the foundation of the Mediterranean Phytopathological Union

The international journal of the Mediterranean Phytopathological Union

FIRENZE UNIVERSITY PRESS

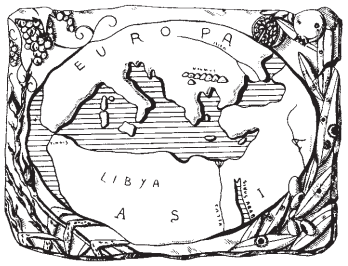

PHYTOPATHOLOGIA MEDITERRANEA

Plant health and food safety

The international journal edited by the Mediterranean Phytopathological Union
founded by A. Ciccarone and G. Goidànich

Phytopathologia Mediterranea is an international journal edited by the Mediterranean Phytopathological Union The journal's mission is the promotion of plant health for Mediterranean crops, climate and regions, safe food production, and the transfer of knowledge on diseases and their sustainable management.
The journal deals with all areas of plant pathology, including epidemiology, disease control, biochemical and physiological aspects, and utilization of molecular technologies. All types of plant pathogens are covered, including fungi, nematodes, protozoa, bacteria, phytoplasmas, viruses, and viroids. Papers on mycotoxins, biological and integrated management of plant diseases, and the use of natural substances in disease and weed control are also strongly encouraged. The journal focuses on pathology of Mediterranean crops grown throughout the world.
The journal includes three issues each year, publishing Reviews, Original research papers, Short notes, New or unusual disease reports, News and opinion, Current topics, Commentaries, and Letters to the Editor.

PHYTOPATHOLOGIA MEDITERRANEA

The international journal of the Mediterranean Phytopathological Union

Volume 61, December, 2022

Firenze University Press

***Phytopathologia Mediterranea*. The international journal of the Mediterranean Phytopathological Union**
Published by
Firenze University Press – University of Florence, Italy
Via Cittadella, 7–50144 Florence–Italy
http://www.fupress.com/pm
Direttore Responsabile: **Giuseppe Surico**, University of Florence, Italy

Phytopathologia Mediterranea
The international journal of the
Mediterranean Phytopathological Union

Firenze University Press
www.fupress.com/pm

Research Papers

Fusarium oxysporum f. sp. *ginseng*, a new *forma specialis* causing *Fusarium* root rot of *Panax ginseng*

Jun WANG[1], Shi FENG[1,2], Baohui LU[1,2], Li NA YANG[1,2], Xue WANG[1,2], Yanjing ZHANG[1,2,*], Jie GAO[1,2,*]

[1] *College of Plant Protection, Jilin Agricultural University, Changchun, 130118, China*
[2] *State-Local Joint Engineering Research Center of Ginseng Breeding and Application, Changchun, 130118, China*
*Corresponding authors. E-mail: yjzhang77@126.com; jiegao115@126.com

Summary. *Panax ginseng* is a valuable medicinal plant which is affected by many diseases during its long cultivation period. Ginseng root rot, caused by *Fusarium oxysporum*, has become severe in China. This soilborne pathogen comprises many *formae speciales* based on host specificity. Ten representative isolates from diseased ginseng rot root showed pathogenicity on ginseng. To identify the *forma specialis* of the *F. oxysporum* strains, host range tests of three representative isolates were carried out on nine plant species. All three isolates caused severe symptoms only on ginseng, but only slight or no visual symptoms on the other eight hosts, indicating that the strains were host-specific to ginseng. Phylogenetic trees were constructed based on sequences of the translation elongation factor 1-α (*EF-1α*) gene, two endopolygalacturonase genes (*Pg1*, *Pg5*) and two exopolygalacturonase genes (*Pgx1* and *Pgx4*). The ten *F. oxysporum* isolates from ginseng clustered into a unique group clearly separated from other *formae speciales* already described. Based on the host range tests and phylogenetic analyses, the isolates of *F. oxysporum* derived from *ginseng* have been identified as a new *forma specialis*, designated *Fusarium oxysporum* f. sp. *ginseng*. This is the first report of *forma specialis* of *F. oxysporum* on ginseng.

Keywords. Soilborne pathogen, host specificity, pathogenicity, *EF-1α*, endopolygalacturonase, exopolygalacturonase.

OPEN ACCESS

Citation: J. Wang, S. Feng, B. Lu, L. Na Yang, X. Wang, Y. Zhang, J. Gao (2022) *Fusarium oxysporum* f. sp. *ginseng*, a new *forma specialis* causing *Fusarium* root rot of *Panax ginseng*. *Phytopathologia Mediterranea* 61(3): 417-429. doi: 10.36253/phyto-13723

Accepted: September 12, 2022

Published: November 25, 2022

Data Availability Statement: All relevant data are within the paper and its Supporting Information files.

Competing Interests: The Author(s) declare(s) no conflict of interest.

Editor: Vladimiro Guarnaccia, DiSAFA, University of Torino, Italy.

ORCID:
JW: 0000-0002-7453-2515
SF: 0000-0002-3851-044X
BL: 0000-0001-8971-973X
LNY: 0000-0002-9304-3207
XW: 0000-0002-4093-4460
YZ: 0000-0003-3663-5633
JG: 0000-0003-2021-819X

INTRODUCTION

Panax ginseng Meyer, a perennial herbaceous plant (*Araliaceae*), is cultivated widely in Northeast China and Korea because of its well-known medicinal value (Yun, 2001; Park *et al.*, 2012). The long cultivation period makes ginseng roots vulnerable to a variety of pathogens (Durairaj *et al.*, 2019). Ginseng root rot caused by *Fusarium* spp. can occur during the whole growth period of ginseng, especially after the third or fourth year (Reeleder *et al.*, 2002; Lee, 2004; Durairaj *et al.*, 2019). In China, incidence of ginseng root rot is usually 10-30%, and as high as 80% in severe cases (Ma *et al.*, 2021).

Fusarium spp. make ginseng roots dark brown, with wet rot, later decaying leaving hollowed-out roots in the soil, and then the inner parts of the roots disintegrate (Lee, 2004). However, the symptoms of infected roots are not obvious in the initial stage. Along with root rot development, the leaves turn yellow in the middle and later stages, and whole plants wilt and die (Lee, 2004; Punja *et al*., 2008). Ginseng root rot is very difficult to control because symptoms on above ground stems and leaves are not obvious in the early stages of the disease.

Fusarium root rot of ginseng was mainly caused by *F. oxysporum* and *F. solani* (Lee, 2004). Pathogenic *F. oxysporum* is a common fungus, causing vascular wilt or root rot symptoms of many plants (Michielse and Rep, 2009; Gordon, 2017). Generally, each strain is pathogenic to one or a few host species. Therefore, *F. oxysporum* pathogenic strains have been grouped into *formae speciales* based on specificity to host species (Gordon and Martyn, 1997; Rana *et al*., 2017). To date, approximately 150 different *formae speciales* of *F. oxysporum* have been described (Armstrong and Armstrong, 1981; Gordon and Martyn, 1997; Edel-Hermann and Lecomte, 2019). Some of these have been further ascribed to races, according to cultivar specificity (Armstrong and Armstrong, 1981; Gordon and Martyn, 1997; Edel-Hermann and Lecomte, 2019).

Identification of *formae speciales* has been based on host range tests using a set of inoculated plant hosts. However, this method is affected by factors in the process of inoculation, including temperature, soil moisture, and light. Molecular identification techniques have advantages compared to the traditional methods, and several useful molecular markers have been developed to identify the *formae speciales* of *F. oxysporum*. These include the translation elongation factor (EF) (Lievens *et al*., 2009), the secreted in xylem (SIX) effector genes (Fraser-Smith *et al*., 2014) and polygalacturonase genes (Hirano and Arie, 2009). Polygalacturonases are important in the process of pathogen infection, especially in the process of hyphae degrading cell walls and infecting plants (Pietro *et al*., 2003). Hirano and Arie (2009) and Ortu *et al*. (2013) demonstrated that polygalacturonase sequences play an important role in the identification of *formae speciales* of *F. oxysporum*. Several new *formae speciales* have been identified by phylogenetic analyses based on endopolygalacturonase and exopolygalacturonase genes. These include *F. oxysporum* f. sp. *crassulae* on *Crassula ovata* (Ortu *et al*., 2013), *F. oxysporum* f. sp. *echeveriae* on *Echeveria agavoides* (Ortu *et al*., 2015a), *F. oxysporum* f. sp. *papaveris* on *Papaver nudicaule* (Ortu *et al*., 2015b), and *F. oxysporum* f. sp. *lavandulae* on hybrid of *Lavandula dentata* and *L. latifolia* (Ortu *et al*., 2018).

With increased ginseng planting area, ginseng root rot has increased in severity, and the control of this disease mainly relies on the use of fungicides. However, control efficiencies were usually low due to the lack of effectiveness of available fungicides and untimeliness of applications. Localization of the pathogen in host vascular systems makes disease management difficult and requires early applications. In addition, the control methods for different species of *Fusarium* and *forma specialis* of *F. oxysporum* are distinct.

There are no reports of identification of the *forma specialis* of *F. oxysporum* causing root rot of ginseng. In this study, host range tests combined with molecular biology technology were used to determine a new *forma specialis* of *F. oxysporum*, *Fusarium oxysporum* f. sp. *ginseng*. This knowledge will provide a foundation for the assessing pathogenic mechanisms of *F. oxysporum*, and control of root rot of ginseng.

MATERIALS AND METHODS

Fungus strains and plants

Fusarium oxysporum isolates were obtained from ginseng root tissues with root rot symptoms, in Jilin Province, China. Other *formae speciales* of *F. oxysporum* were provided by the Agricultural Culture Collection of China (Table 1).

The following nine plant species were evaluated in host range tests: *P. ginseng* 'Damaya', *P. notoginseng* 'Wenshan', *Acanthopanax senticosus* 'Lianguanshan', *Citrullus lanatus* 'Zaojia8424', *Gossypium hirsutum* 'Qianjinwang', *Capsicum annuum* 'Baopi', *Solanum lycopersicum* 'Zhongsu 4', *Pisum sativum* 'Qizhen 76', and *Linum usitatissimum* 'Lanhua'.

Pathogenicity and host range tests

Host planting. Seeds of six plant species (*Citrullus lanatus* 'Zaojia8424', *Gossypium hirsutum* 'Qianjinwang', *Capsicum annuum* 'Baopi', *Solanum lycopersicum* 'Zhongsu 4', *Pisum sativum* 'Qizhen 76', and *Linum usitatissimum* 'Lanhua') were washed and disinfested with 5% sodium hypochlorite for 20 min, and then rinsed three times with sterile water. The seeds were then sown into pots filled with sterilized soil. When the plants grew two pieces of euphylla, the roots of the plants were dug out for inoculation. In the spring, 2-year-old seedlings of *P. ginseng*, *P. notoginseng*, *A. senticosus* were washed and disinfected with 5% sodium hypochlorite for 20 min, and then rinsed three times with sterile water. The roots

Table 1. *Fusarium oxysporum* isolates from *ginseng* and six other *formae speciales* used for pathogenicity and host range tests.

Strains	*Formae speciales*	Hosts	Sources
ACCC30222	*Fusarium oxysporum* f. sp. *vasinfectum*	*Gossypium herbaceum*	Agricultural Culture Collection of China
ACCC31037	*F. oxysporum* f. sp. *pisi*	*Pisum sativum*	Agricultural Culture Collection of China
ACCC36175	*F. oxysporum* f. sp. *niveum*	*Citrullus lanatus*	Agricultural Culture Collection of China
ACCC36465	*F. oxysporum* f. sp. *lycopersici*	*Solanum lycopersicum*	Agricultural Culture Collection of China
ACCC36472	*F. oxysporum* f. sp. *capsicum*	*Capsicum annuum*	Agricultural Culture Collection of China
BNCC85312	*F. oxysporum* f. sp. *linum*	*Linum usitatissimum*	Agricultural Culture Collection of China
0083	*F. oxysporum* f. sp. *ginseng*	*Panax ginseng*	In this study
0414	*F. oxysporum* f. sp. *ginseng*	*P. ginseng*	In this study
DH10-8	*F. oxysporum* f. sp. *ginseng*	*P. ginseng*	In this study
FS03-2	*F. oxysporum* f. sp. *ginseng*	*P. ginseng*	In this study
FS03-5	*F. oxysporum* f. sp. *ginseng*	*P. ginseng*	In this study
FS04-1	*F. oxysporum* f. sp. *ginseng*	*P. ginseng*	In this study
FS13-3	*F. oxysporum* f. sp. *ginseng*	*P. ginseng*	In this study
FS15-1	*F. oxysporum* f. sp. *ginseng*	*P. ginseng*	In this study
TH08	*F. oxysporum* f. sp. *ginseng*	*P. ginseng*	In this study
TH10-2	*F. oxysporum* f. sp. *ginseng*	*P. ginseng*	In this study

were planted in pots filled with sterilized soil. All pots with seeds or roots of plants were cultured in a greenhouse (25 to 28°C, 12 h light/12 h dark cycle). The pots planted with roots were placed under black shading net.

Culture of Fusarium inoculum. The *Fusarium* strain was first activated on PDA medium for 7 d at 25°C. Mycelium plugs at the edges of resulting colonies were taken with a sterile punch, and were placed into 100 mL of potato dextrose broth, which was then incubated for 3 d in an incubation shaker (25°C, 150 r min^{-1}). The resulting conidium suspension was then filtered and adjusted to a final concentration of 1.0×10^6 conidia mL^{-1} to inoculate the plants.

Inoculation methods. For *in vitro* inoculations, the surfaces of 2-year-old healthy ginseng taproots were washed and disinfested with 75% alcohol, and then rinsed with sterile water. The roots were then wounded with a sterilized steel needle to 2 mm depth, and were then each inoculated with 0.5 cm^2 mycelium plugs of one of the ten representative *F. oxysporum* isolates (isolates 0083, 0414, DH10-8, FS03-2, FS03-5, FS04-1, FS13-3, FS15-1, TH08, and TH10-2), which had been derived from ginseng. The inoculated roots were then incubated in a sealed plastic container. Lesion development was observed after 5 to 7 d. Sterile PDA plugs were put on the ginseng taproot as inoculation controls. For *in vivo* inoculation and host range tests, the roots of ginseng and other plant seedlings (*P. notoginseng*, *A. senticosus*, *C. lanatus*, *G. hirsutum*, *C. annuum*, *S. lycopersicum*, *P. sativum*, and *L. usitatissimum*) were each wounded, and then immersed in 1.0×10^6 mL^{-1} conidium suspension of the ten representative isolates (for *in vivo* inoculation) or three representative isolates (0083, 0414, DH10-8, for host range tests), for 30 min (ten replicate plants per strain). The inoculated plants were then transplanted into new pots filled with sterile soil, and these were maintained

in a greenhouse (25° to 28°C, 12 h light/12 h dark cycle). Non-inoculated plants were dipped in sterilized water as experimental controls. All treatments were repeated three times. The whole experiment was repeated for two years.

Assessment methods. Final observations of disease development were carried out 14 to 21 d after inoculation. The roots of plants were dug out of the soil and washed with clean water. A disease index of each plant was evaluated using a 0 to 5 scale, based on that of Song *et al.* (2014) with modification: where 0 = visible lesions; 1 = lesions covering 1-10% of the root surface; 2 = lesions covering 10-20% of the root surface; 3 = lesions covering 20-30% of the root surface; 4 = lesions covering 30-50% of the root surface; and 5 = lesions covering 50-100% of the root surface. Disease severity (DS) for each treatment was calculated using the formula:

$DS = [(0 \times n_0 + 1 \times n_1 + 2 \times n_2 + 3 \times n_3 + 4 \times n_4 + 5 \times n_5)/5 \times N)] \times 100$, where n_{0-5} = the number of plants exhibiting the scores of, respectively, 0, 1, 2, 3, 4 or 5, and N = total number of plants tested (Chiang *et al.*, 2017). Disease severity of nine species of plants was assayed, and the experiments were replicated three times. To confirm the presence of *F. oxysporum*, the tissues of diseased plants were cut into small pieces. These were then surface-disinfected with 70% ethanol for 30 s and then in 1.5% (v/v) NaOCl for 1 min, and were then washed three times with sterile distilled water. The tissue pieces were then placed onto a PDA in Petri dishes and incubated at 25°C for 3 to 4 days. New mycelium and single conidia were transferred onto a new PDA medium to identify the resulting fungi.

Genomic DNA extraction, PCR amplification and sequencing

The genomic DNA of *F. oxysporum* strains isolated from *P. ginseng* was extracted using the Biospin Fungus Genomic DNA Extraction Kit (BioFlux) according to the manufacturer's instructions. The *EF-1 α* gene, two endopolygalacturonase genes (*Pg1* and *Pg5*) and two exopolygalacturonase genes (*Pgx1* and *Pgx4*) were amplified with the primers reported previously (O'Donnell *et al.*, 1998; Hirano and Arie, 2009) (Table 2). The PCR reactions were each carried out in 20 μL volumes, containing 50 ng of gDNA, 1 μL (10 mM) of each primer, 1 unit of Taq DNA polymerase (TaKaRa), 2 μL of Taq DNA polymerase buffer, 1 μL of dNTPs mix with the following program: an initial denaturing step at 94°C for 5 min, 40 cycles each with denaturation at 94°C for 1 min, annealing at 52°C (*Pg1*, *Pg5*, *Pgx1*, and *Pgx4* genes) or 57°C (*EF-1α* gene) for 1 min, extension at 72°C for 1 min (*EF-1α* gene) or 2 min (*Pg1*, *Pg5*, *Pgx1*, and *Pgx4* genes), and final extension at 72°C for 10 min. A negative control (no template DNA) was included in all experiments. PCR profiles were analyzed on 1% agarose gel. After purification with PCR purification kits (Tian-Gen), purified PCR products were sequenced in both directions by Sangon Biotechnology Corporation. The sequences were deposited at GenBank with the accession numbers shown in Table 3.

Phylogenetic analyses

According to the *EF-1α*, *Pg1*, *Pg5*, *Pgx1*, and *Pgx4* genes, specific sequences of different *formae speciales* of *F. oxysporum* were downloaded from GenBank (Table 3). The sequences obtained were used for multiple sequence alignment using the MAFFT program (Katoh and Standley, 2013). Manual corrections were performed in Partition Finder 2 for each alignment in order to delete trimmer regions outside and discard incomplete sequences (Lanfear *et al.*, 2017). Phylogenetic trees were generated for single *EF-1α* gene and multiple *Pg1*, *Pg5*,

Table 2. Primers used in this study for PCR amplification of *EF-1α* and polygalacturonase genes.

Target genes	Primers	Primer sequence (5'-3')	References
EF-1α	Ef1	ATGGGTAAGGAAGACAAGAC	O'Donnell *et al.*, 1998
	Ef2	GGAAGTACCAGTGATCATGTT	
Pg1	endoF	CCAGAGTGCCGATACCGATT	Hirano and Arie, 2009
	endoR2	GCTTAGYGAACAKGGAGTG	
Pg5	PG2F	AGATGCAAGGCCGATGATGT	Hirano and Arie, 2009
	PG2R	TCCATGTACTTCTCCTCACC	
Pgx1	PgxF	TCGTGGGGTAAAGCGTGGT	Hirano and Arie, 2009
	PgxR	TTACTATAGGTCGATCAGCC	
Pgx4	exoF2	TTACTGTCCACGAATGAGAAG	Hirano and Arie, 2009
	exoR	ACCCCAACCCCCCTCATCT	

Table 3. *Fusarium* strains used in the phylogenetic analysis of single *EF-1α* gene and combined polygalacturonase genes.

Formae speciales	Strains	Hosts	Accession numbers on GenBank				
			EF-1α	*Pg1*	*Pg5*	*Pgx1*	*Pgx4*
Fusarium oxysporum f. sp. *ginseng*	0083	*Panax ginseng*	ON316841	MW582553	MW582563	MW505948	MW505957
F. oxysporum f. sp. *ginseng*	0414	*Panax ginseng*	MW532127	MW582554	MW582564	MW505949	MW505958
F. oxysporum f. sp. *ginseng*	DH10-8	*Panax ginseng*	MK962137	MW582555	MW582565	MW505950	MW505959
F. oxysporum f. sp. *ginseng*	FS03-2	*Panax ginseng*	MH698989	MW582556	MW582566	MW505951	MW505960
F. oxysporum f. sp. *ginseng*	FS03-5	*Panax ginseng*	MH698990	MW582557	MW582567	MW505952	MW505961
F. oxysporum f. sp. *ginseng*	FS04-1	*Panax ginseng*	MK962130	MW582558	MW582568	MW505953	MW505962
F. oxysporum f. sp. *ginseng*	FS13-3	*Panax ginseng*	MH748098	MW582562	MW582572	MW505956	MW505966
F. oxysporum f. sp. *ginseng*	FS15-1	*Panax ginseng*	MH748099	MW582559	MW582569	MW532128	MW505963
F. oxysporum f. sp. *ginseng*	TH08	*Panax ginseng*	MH698987	MW582560	MW582570	MW505954	MW505964
F. oxysporum f. sp. *ginseng*	TH10-2	*Panax ginseng*	MH698986	MW582561	MW582571	MW505955	MW505965
F. oxysporum f. sp. *colocasiae*	MAFF744032	*Colocasia esculenta*	–	AB256751	AB256841	AB256883	AB256800
F. oxysporum f. sp. *conglutinans*	MAFF744001	*Brassica oleracea*	–	AB256754	–	AB256886	AB256803
F. oxysporum f. sp. *cucumerinum*	MAFF103054	*Cucumis sativus*	–	AB256755	AB256843	AB256887	AB256804
F. oxysporum f. sp. *cucumerinum*	MAFF744005	*Cucumis sativus*	–	AB256756	AB256844	AB256888	AB256805
F. oxysporum f. sp. *dianthi*	MAFF103072	*Dianthus caryophyllus*	–	AB256757	AB256845	AB256889	AB256806
F. oxysporum f. sp. *fragariae*	MAFF727510	*Fragaria ananassa*	–	AB256759	AB256848	AB256892	AB256809
F. oxysporum f. sp. *lactucae*	MAFF744028	*Lactuca sativa*	–	AB256761	AB256850	AB256894	AB256811
F. oxysporum f. sp. *lagenariae*	MAFF744002	*Lagenaria siceraria*	–	AB256764	AB256853	AB256897	AB256814
F. oxysporum f. sp. *lycopersici*	Saitama ly1	*Solanum lycopersicum*	–	AB256767	AB256856	AB256900	AB256795
F. oxysporum f. sp. *melongenae*	MAFF103051	*Solanum melongena*	–	AB256776	AB256865	AB256909	AB256823
F. oxysporum f. sp. *melonis*	MAFF305122	*Cucumis melo*	–	AB256777	AB256866	AB256910	AB256824
F. oxysporum f. sp. *melonis*	MAFF305544	*Cucumis melo*	–	AB256778	AB256867	AB256911	AB256825
F. oxysporum f. sp. *niveum*	MAFF305543	*Citrullus lanatus*	–	AB256779	AB256868	AB256912	AB256826
F. oxysporum f. sp. *niveum*	NBRC9969	*Citrullus lanatus*	–	AB256780	AB256869	AB256913	AB256827
F. oxysporum f. sp. *phaseoli*	MAFF235727	*Phaseolus vulgaris*	–	AB256781	AB256870	AB256914.	AB256828
F. oxysporum f. sp. *phaseoli*	NBRC9970	*Phaseolus vulgaris*	–	AB256782	AB256871	AB256915	AB256829
F. oxysporum f. sp. *radicis-lycopersici*	KEF-2R1	*Solanum lycopersicum*	–	AB208068	AB208072	AB208080	–
F. oxysporum f. sp. *raphani*	MAFF103058	*Raphanus sativus*	–	AB256787	AB256876	AB256920	AB256833
F. oxysporum f. sp. *raphani*	MAFF305124	*Raphanus sativus*	–	AB256788	–	AB256921	AB256834
F. oxysporum f. sp. *spinaciae*	MAFF103059	*Spinacia oleracea*	–	AB256789	AB256877	AB256922	AB256835
F. oxysporum f. sp. *spinaciae*	MAFF731044	*Spinacia oleracea*	–	AB256790	AB256878	AB256923	AB256836
F. oxysporum f. sp. *tracheiphilum*	MAFF235725	*Vigna unguiculata*	–	AB256791	AB256879	AB256924	AB256837
F. oxysporum f. sp. *tracheiphilum*	MAFF235726	*Vigna unguiculata*	–	AB256792	AB256880	AB256925	AB256838
F. oxysporum f. sp. *tulipae*	MAFF235105	*Tulipa gesneriana*	–	AB256793	AB256881	AB256926	AB256839
F. oxysporum f. sp. *tulipae*	MAFF235109	*Tulipa gesneriana*	–	AB256794	AB256882	AB256927	AB256840
F. oxysporum f. sp. *asparagi*	FOA50	*Asparagus officinalis*	AY337434	–	–	–	–
F. oxysporum f. sp. *melonis*	0348	*Cucumis melo*	DQ016282	–	–	–	–
F. oxysporum f. sp. *lactucae*	BMP1880	*Lactuca sativa*	DQ837670	–	–	–	–
F. oxysporum f. sp. *lactucae*	BMP1375	*Lactuca sativa*	DQ837673	–	–	–	–
F. oxysporum f. sp. *callistephi*	NRRL22536	*Callistephus chinensis*	DQ837679	–	–	–	–
F. oxysporum f. sp. *vasinfectum*	NRRL25231	*Anemone vitifolia*	DQ837680	–	–	–	–
F. oxysporum f. sp. *cepae*	NRRL22538	*Allium cepa*	DQ837681	–	–	–	–
F. oxysporum f. sp. *matthiolae*	NRRL22545	*Matthiola incana*	DQ837682	–	–	–	–
F. oxysporum f. sp. *medicaginis*	NRRL22546	*Medicago sativa*	DQ837690	–	–	–	–
F. oxysporum f. sp. *lycopersici*	FOLR2	*Solanum lycopersicum*	DQ837692	–	–	–	–
F. oxysporum f. sp. *lactucae*	F9501	*Lactuca sativa*	DQ837693	–	–	–	–
F. oxysporum f. sp. *lactucae*	FK09701	*Lactuca sativa*	DQ837694	–	–	–	–

(Continued)

Table 3. (Continued).

Formae speciales	Strains	Hosts	Accession numbers on GenBank				
			EF-1α	*Pg1*	*Pg5*	*Pgx1*	*Pgx4*
F. oxysporum f. sp. *radicis-cucumerinum*	14	*Cucumis sativus*	EF056779	–	–	–	–
F. oxysporum f. sp. *radicis-cucumerinum*	30	*Cucumis sativus*	EF056781	–	–	–	–
F. oxysporum f. sp. *cucumerinum*	ATCC 16416	*Cucumis sativus*	EF056783	–	–	–	–
F. oxysporum f. sp. *lycopersici*	MUCL 14159	*Solanum lycopersicum*	EF056784	–	–	–	–
F. oxysporum f. sp. *conglutinans*	Apr-81	*Brassica oleracea*	EF056786	–	–	–	–
F. oxysporum f. sp. *gladioli*	NRRL 26993	*Gladiolus gandavensis*	EF056787	–	–	–	–
F. oxysporum f. sp. *lilii*	NRRL 28395	*Lilium brownii*	EF056788	–	–	–	–
F. oxysporum f. sp. *melonis*	CBS 423.90	*Cucumis melo*	EF056789	–	–	–	–
F. oxysporum f. sp. *melonis*	CBS 420.90	*Cucumis melo*	EF056790	–	–	–	–
F. oxysporum f. sp. *lilii*	Fol-11	*Lilium brownii*	EU220403	–	–	–	–
F. oxysporum f. sp. *cepae*	NL106-2	*Allium cepa*	EU220404	–	–	–	–
F. oxysporum f. sp. *canariensis*	2675A	*Phoenix canariensis*	FJ895287	–	–	–	–
F. oxysporum f. sp. *canariensis*	4873C	*Phoenix canariensis*	FJ895290	–	–	–	–
F. oxysporum f. sp. *passiflorae*	NRRL 38273	*Passiflora caerulea*	FJ985362	–	–	–	–
F. oxysporum f. sp. *canariensis*	NRRL 38338	*Phoenix canariensis*	FJ985388	–	–	–	–
F. oxysporum f. sp. *cepae*	NRRL 38481	*Allium cepa*	FJ985399	–	–	–	–
F. oxysporum f. sp. *raphani*	NRRL 53154	*Raphanus sativus*	FJ985441	–	–	–	–
F. oxysporum f. sp. *conglutinans*	NRRL 53156	*Brassica oleracea*	FJ985442	–	–	–	–
F. oxysporum f. sp. *conglutinans*	NRRL 53158	*Brassica oleracea*	FJ985443	–	–	–	–
F. oxysporum f. sp. *radicis-lycopersici*	CL-0620	*Solanum lycopersicum*	HM057325	–	–	–	–
F. oxysporum f. sp. *radicis-lycopersici*	CL-06202	*Solanum lycopersicum*	HM057332	–	–	–	–
F. oxysporum f. sp. *lycopersici*	OSU451	*Solanum lycopersicum*	HM057335	–	–	–	–
F. oxysporum f. sp. *canariensis*	PLM-385B	*Phoenix canariensis*	HM591537	–	–	–	–
F. oxysporum f. sp. *canariensis*	PLM-511A	*Phoenix canariensis*	HM591538	–	–	–	–
F. fujikuroi	NRRL 66453	*Vitis vinifera*	KX656207	–	–	–	–

Pgx1, and *Pgx4* genes using the Bayesian Inference (BI) method through the PhyloSuite platform (Ronquist *et al*., 2012; Zhang *et al*., 2020).

RESULTS

Pathogenicity assays

The samples of diseased ginseng roots were collected, and a total of 272 isolates of *F. oxysporum* were obtained in pure cultures. In the *in vitro* experiment, after 5–7 d, all of the ginseng roots inoculated with the ten representative isolates showed water-soaked root rot lesions (Figure 1, A and B), whereas no lesions were observed in the control roots (Figure 1, C and D). For the *in vivo* inoculations of whole plants in the greenhouse, typical root rot symptoms were observed 14 d after inoculation with the ten representative isolates. The symptoms included yellowing of leaves and brown necrotic lesions on the root surfaces. As the symptoms developed, all of the infected ginseng plants were dead at 21 d post-inoculation, with dark brown and soft root rot (Figure 1, E and F). No symptoms were observed on the control ginseng plants (Figure 1, G and H). The same pathogens were re-isolated from the diseased ginseng roots, fulfilling the Koch's postulates.

Greenhouse host range tests

In the host range tests, three representative *F. oxysporum* strains derived from ginseng roots were inoculated onto nine species of plants. The three ginseng isolates (0083, DH10-8, and 0414) caused severe rot symptoms on ginseng roots, with disease mean severities ranging from 86.67 to 96.67. However, the isolates 0083, 0414, and DH10-8 only slightly infected *A. senticosus*, *P. notoginseng*, *P. sativum*, *C. lanatus*, and *S. lycopersicum*, with disease severities less than 7.00 (Figures 2 and 3). Six *formae speciales* of *F. oxysporum* from other hosts (Table 1) did not infect, or only slightly infected ginseng,

Figure 1. Pathogenicity of *Fusarium oxysporum* derived from ginseng on 2-year-old ginseng taproots (A, B) and whole plants (E, F). Healthy controls inoculated with PDA plugs (C, D) and sterilized water (G, H) are also shown.

with disease severities less than 11.00. These isolates also caused obvious symptoms on corresponding host plants with disease severities greater than 73.00. For example, *F. oxysporum* f. sp. *pisi* (ACCC31037) was only highly pathogenic to *P. sativum* (disease severity = 92.67), while *F. oxysporum* f. sp. *capsicum* (ACCC36472) was only highly pathogenic to *C. annuum* (disease severity = 96.00) (Figures 2 and 3). These results indicated that the *F. oxysporum* isolates from ginseng root were host-specific to ginseng.

Phylogenetic analyses

The amplification products of the *EF-1α*, *Pg1*, *Pg5*, *Pgx1*, and *Pgx4* genes were, respectively, approx. 750, 1560, 1800, 1800 and 1400 base pairs (bp) long. The nucleotide sequences were submitted and deposited in GenBank, and the GenBank accession numbers are shown in Table 3. Phylogenetic analyses were carried out using the single gene *EF-1α* sequences, and a combined *Pg1*, *Pg5*, *Pgx1* and *Pgx4* gene sequences, from the ten isolates from ginseng and those of other *formae speciales* of *F. oxysporum* from the GenBank database (Table 3). In the phylogenetic trees constructed with the single gene *EF-1α* sequences, the ten isolates from ginseng formed a single and distinct clade, separate from the other *formae speciales* of *F. oxysporum* (Figure 4). Similarly, the phylogenetic tree constructed using the combined sequences of the genes *Pg1*, *Pg5*, *Pgx1*, and *Pgx4* also clearly clustered the ginseng isolates in an independent clade distinguished from the other *formae speciales* of *F. oxysporum* isolates (Figure 5). These results showed that the ten isolates obtained from *P. ginseng* were clustered together to form a unique clade which was clearly separated from other *formae speciales* of *F. oxysporum*.

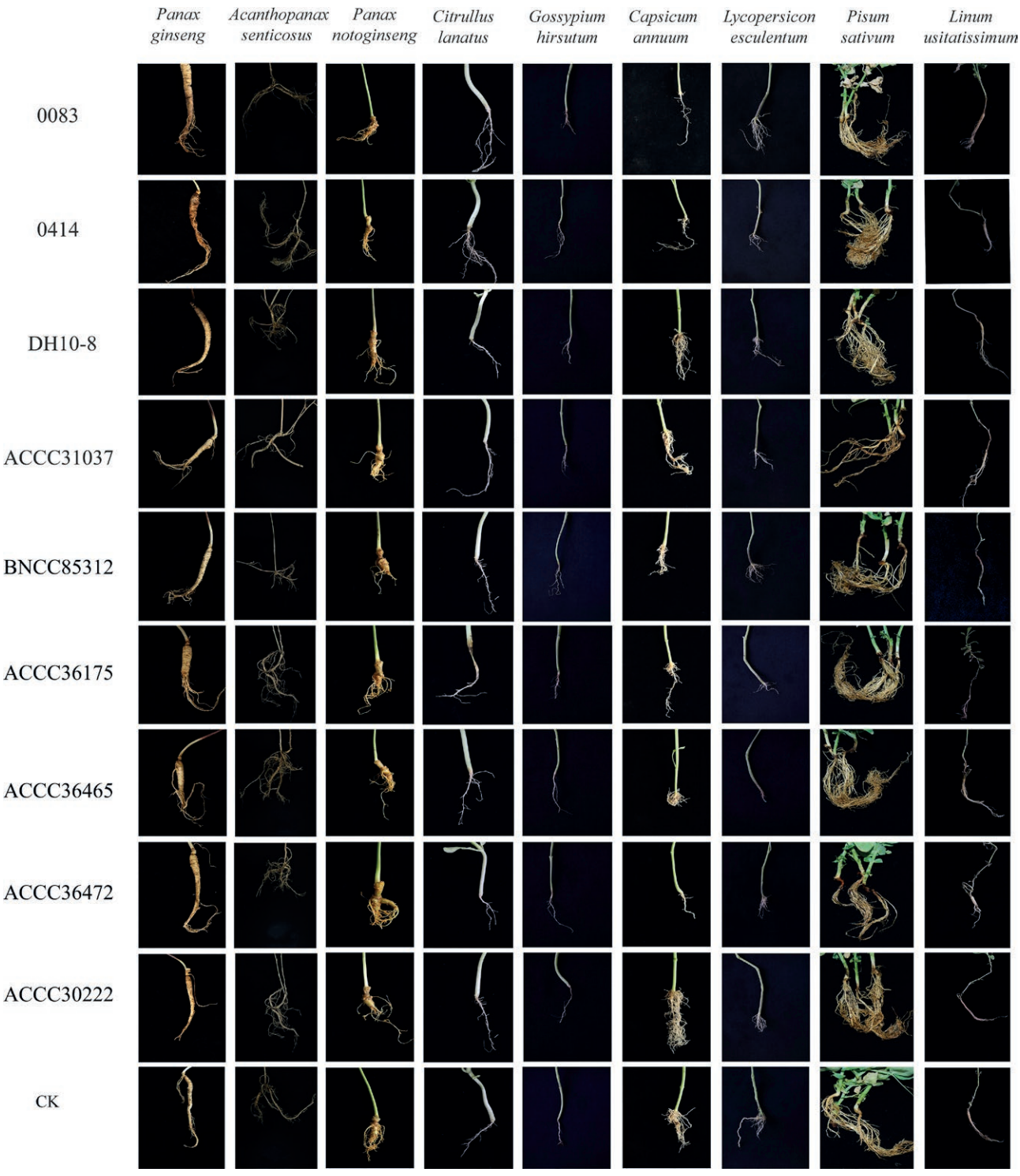

Figure 2. Symptoms on nine species of plants inoculated with *Fusarium oxysporum* derived from ginseng and six other *F. oxysporum formae speciales*.

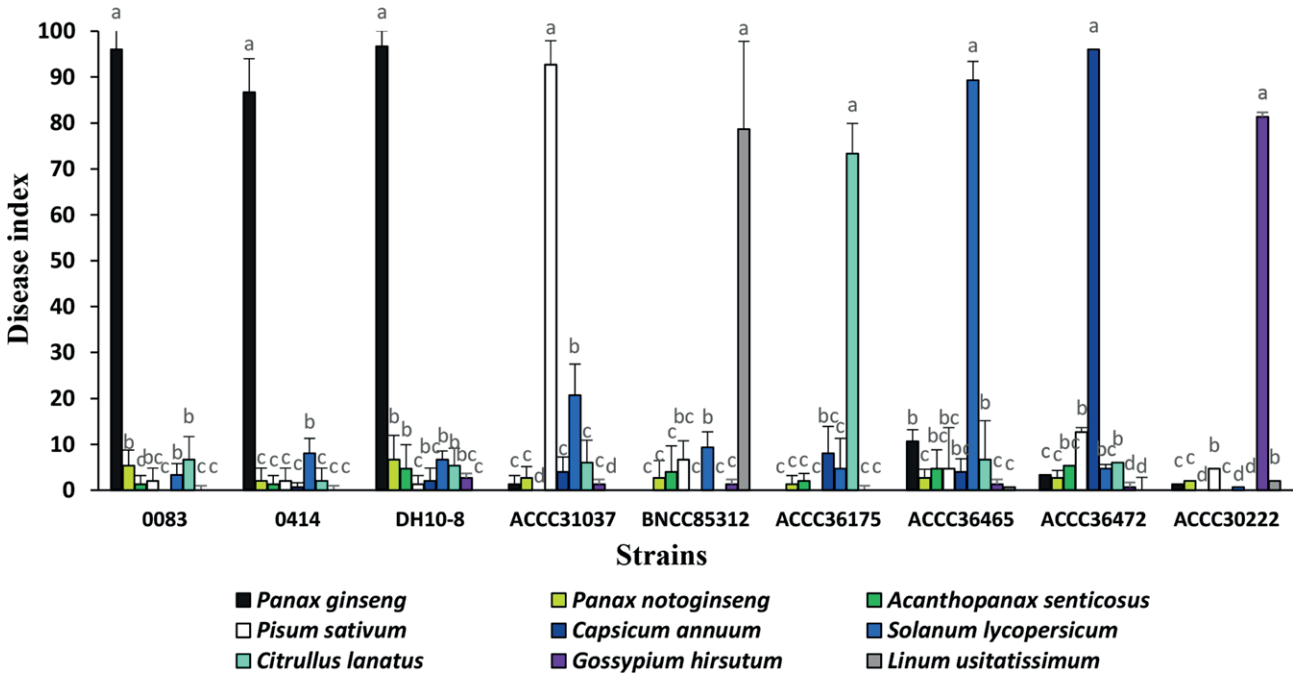

Figure 3. Mean disease severity indices of plant root rot caused by *Fusarium oxysporum* derived from ginseng, and six other *F. oxysporum formae speciales*. Means accompanied by different lowercase letters among treatments within a given strain are different ($P < 0.05$).

DISCUSSION

Fusarium oxysporum, is a major pathogen causing plant vascular wilts and root rots, but strains of this fungus often infect only one or a few plant species, indicating that they are usually host-specific. Therefore, based on host specificity, pathogenic strains of *F. oxysporum* have been grouped into *formae speciales* (Gordon and Martyn, 1997). In the present study, host range tests were used to identify a new *forma specialis* of *F. oxysporum* isolated from ginseng. Phylogenetic analysis based on the *EF-1α* gene and four polygalacturonase genes (*Pg1*, *Pg5*, *Pgx1*, and *Pgx4*) confirmed the results of host range tests, suggesting the presence of a new *forma specialis* of *F. oxysporum*. A novel *forma specialis*, *F. oxysporum* f. sp. *ginseng*, is therefore proposed, which causes root rot of ginseng.

Traditional identification of *formae speciales* mainly through pathogenicity tests on particular hosts or groups of hosts. In the present study, *P. ginseng*, *P. notoginseng*, *A. senticosus*, *C. lanatus*, *G. hirsutum*, *C. annuum*, *S. lycopersicum*, *P. sativum*, and *L. usitatissimum* were selected for host range tests. The results showed that *F. oxysporum* isolated from ginseng could only cause severe root rot of ginseng, and did not infect other hosts or infected some only slightly. In addition, low levels of root rot symptoms were observed in some plants inoculated with *formae speciales* of *F. oxysporum* nonpathogenic to them. It is likely that the artificial inoculation method in a greenhouse enhances host infection, and infections could be less under field conditions. In addition, the results of the host range tests could also be influenced by environmental conditions and the species (and/or cultivar) of host plants.

Because of abundance of plant species, host range tests are time-consuming and laborious (Correll, 1991). With the development of molecular biology and sequencing technologies, some DNA markers and transposon insertions based on genomic DNA sequences have been developed as alternative methods for identification of the *formae speciales* of *F. oxysporum*. Phylogenetic analysis based on the mitochondrial small subunit (*mtSSU*) ribosomal RNA gene, the rDNA intergenic spacer (IGS) region, and the *EF-1α* gene have helped to reveal the genetic and evolutionary relationships within and among *formae speciales* of *F. oxysporum* (Lievens *et al.*, 2008). Furthermore, some pathogenicity-related genes, such as secreted in xylem (*SIX*) effector (Lievens *et al.*, 2009) and polygalacturonase genes (Hirano and Arie, 2009) have become important tools used for high resolution discrimination of different *formae speciales* of *F. oxysporum*. Several new *formae speciales* have recently been identified by phylogenetic analyses based on *EF-1α* and polygalacturonase genes (Ortu *et al.*, 2013; Ortu *et*

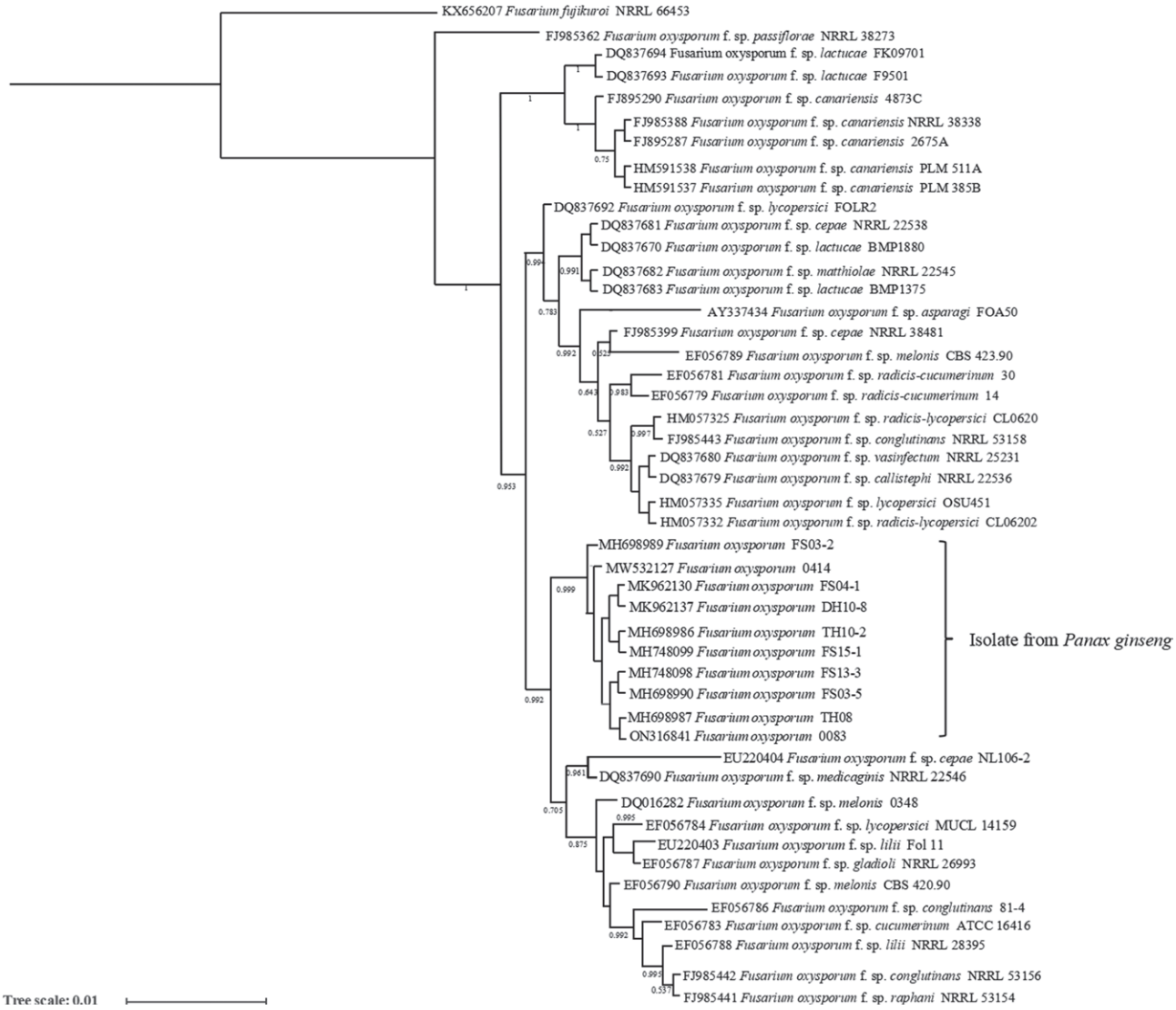

Figure 4. Phylogenetic tree based on *EF-1α* gene sequences of different *formae speciales* of *Fusarium oxysporum*, using Bayesian inference (BI) methods in the PhyloSuite platform. *Fusarium fujikuroi* was used as an outgroup. Numbers under branches indicate a posterior probability > 0.5.

al., 2015a; Ortu *et al*., 2015b; Ortu *et al*., 2018). Phylogenetic analysis based on these genes has demonstrated the usefulness of these regions for the identification of *F. oxysporum forma speciales*.

Compared with traditional pathogenicity testing, molecular identification of *forma specialis* of *F. oxysporum* based on the genomic DNA has many advantages. It is highly specific and sensitive, and is rapid and easy to operate in a laboratory. However, molecular identification of *forma specialis* combined with traditional identification methods such as morphology and pathogenicity tests, increases precision of results. Therefore, identification of *formae speciales* is commonly based on pathogenicity assays and is supported by molecular identification tools. For soilborne pathogens such as *F. oxysporum*, it is important to develop diagnosis tools to discriminate between species and *formae speciales*, because these will detect the risk of the infection, and provide information to guide corresponding disease management treatments.

ACKNOWLEDGEMENT

This research was supported by the Scientific and Technological Developing Project of Jilin Province (20210204047YY).

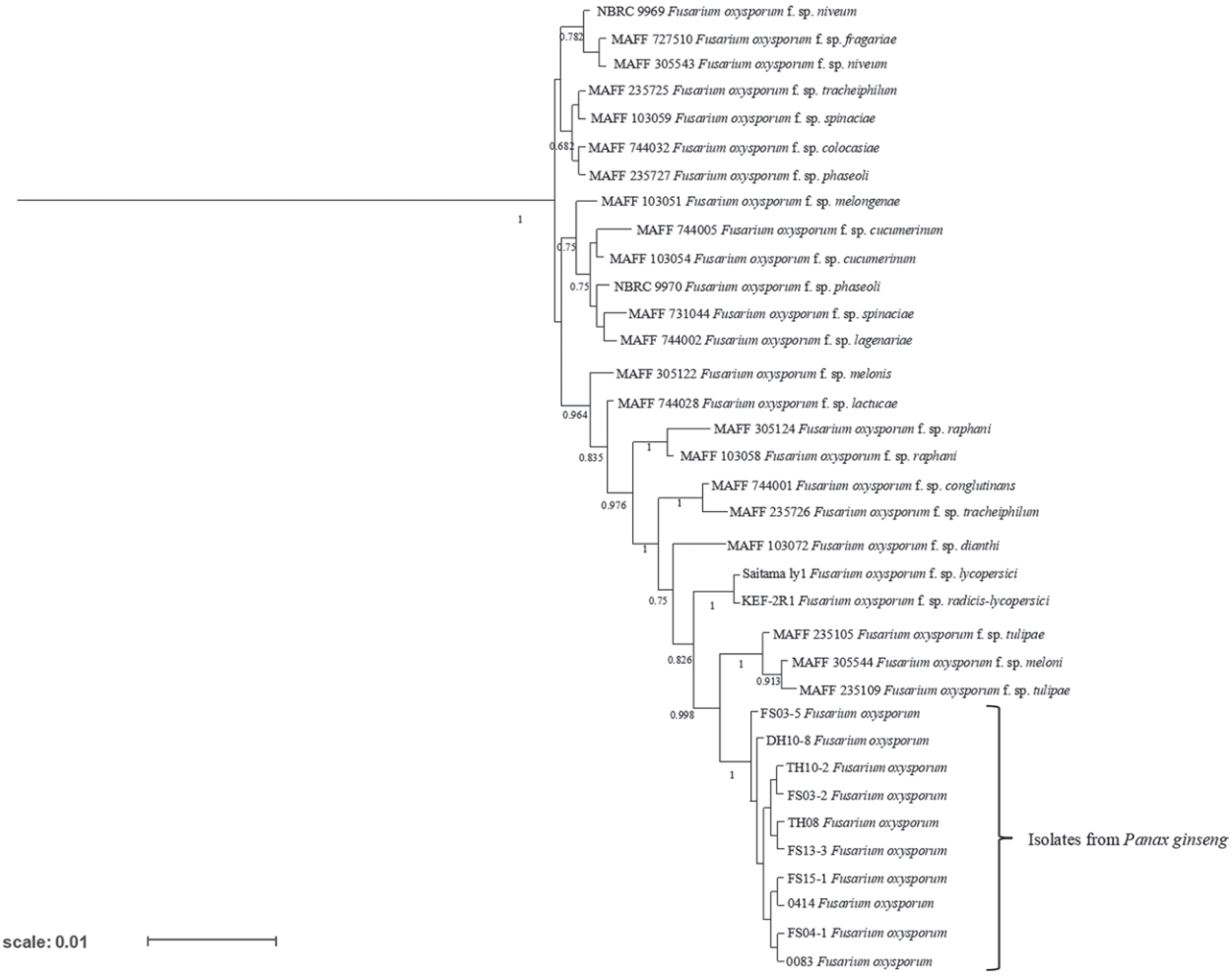

Figure 5. Phylogenetic tree based on combined *Pg1*, *Pg5*, *Pgx1* and *Pgx4* gene sequences of different *formae speciales* of *Fusarium oxysporum*, using Bayesian inference (BI) methods in the PhyloSuite platform. Numbers under branches indicate a posterior probability > 0.5.

LITERATURE CITED

Armstrong G.M., Armstrong J.K., 1981. *Formae speciales* and races of *Fusarium oxysporum* causing wilt diseases. In *Fusarium: Diseases, Biology, and Taxonomy* (Nelson, P. E., Toussoun, T. A., and Cook, R. J., ed.). The Pennsylvania State University Press, University Park, United States of America, 391–399.

Chiang K.S., Liu H.I., Bock C.H., 2017. A discussion on disease severity index values. Part I: warning on inherent errors and suggestions to maximise accuracy. *Annals of Applied Biology* 171: 139–154. https://doi.org/10.1111/aab.12362

Correll J.C., 1991. The relationship between *formae speciales,* races, and vegetative compatibility groups in *Fusarium oxysporum*. *Phytopathology* 81: 1061–1064.

Durairaj K., Velmurugan P., Vedhanayakisri K.A., Chang W.S., Senthilkumar P., Choi K.M., . . . Oh B.T., 2019. Reprint of "Molecular and phenotypic characterization of pathogenic fungal strains isolated from ginseng root rot". *Physiological and Molecular Plant Pathology* 105: 28–33. https://doi.org/10.1016/j.pmpp.2018.11.005

Edel-Hermann V., Lecomte C., 2019. Current status of *Fusarium oxysporum formae speciales* and races. *Phytopathology* 109: 512–530. https://doi.org/10.1094/PHYTO-08-18-0320-RVW

Fraser-Smith S., Czislowski E., Meldrum R.A., Zander M., O'Neill W., … Aitken E.A.B., 2014. Sequence variation in the putative effector gene SIX8 facilitates molecular differentiation of *Fusarium oxysporum* f. sp. *cubense*. *Plant Pathology* 63: 1044–1052. https://doi.org/10.1111/ppa.12184

Gordon T.R., 2017. *Fusarium oxysporum* and the *Fusar-*

ium wilt syndrome. *Annual Review of Phytopathology* 55: 23–39. https://doi.org/10.1146/annurev-phyto-080615-095919

Gordon T.R., Martyn R.D., 1997. The evolutionary biology of *Fusarium oxysporum*. *Annual Review of Phytopathology* 35: 111–128. https://doi.org/10.1146/annurev.phyto.35.1.111

Hirano Y., Arie T., 2009. Variation and phylogeny of *Fusarium oxysporum* isolates based on nucleotide sequences of polygalacturonase genes. *Microbes & Environments* 24: 113–120. https://doi.org/10.1264/jsme2.me08554

Katoh K., Standley D.M., 2013. MAFFT multiple sequence alignment software version 7: Improvements in performance and usability. *Molecular Biology and Evolution* 30: 772–780. https://doi.org/10.1093/molbev/mst010

Lanfear R., Frandsen P.B., Wright A.M., Senfeld T., Calcott B., 2017. PartitionFinder 2: New methods for selecting partitioned models of evolution for molecular and morphological phylogenetic analyses. *Molecular Biology and Evolution* 34: 772–773. https://doi.org/10.1093/molbev/msw260

Lee S.G., 2004. Fusarium species associated with ginseng (*Panax ginseng*) and their role in the root-rot of ginseng plant. *Research in Plant Disease* 10: 248–259. https://doi.org/10.5423/RPD.2004.10.4.248

Lievens B., Rep M., Thomma B.P., 2008. Recent developments in the molecular discrimination of *formae speciales* of *Fusarium oxysporum*. *Pest Management Science* 64: 781–788. https://doi.org/10.1002/ps.1564

Lievens B., van Baarlen P., Verreth C., van Kerckhove S., Rep M., Thomma B.J., 2009. Evolutionary relationships between *Fusarium oxysporum* f. sp. *lycopersici* and *F. oxysporum* f. sp. *radicis-lycopersici* isolates inferred from mating type, elongation factor-1α and exopolygalacturonase sequences. *Mycological Research* 113: 1181–1191. https://doi.org/10.1016/j.mycres.2009.07.019

Ma Y., Xu H., Song M., Feng Z., Shao Z., … Gao J., 2021. Relationship analysis between ginseng root rot diseases and main chemical properties, enzyme activities of rhizosphere soil. *Journal of Jilin Agricultural University*. https://doi.org/10.13327/j.jjlau.2021.1246

Michielse C.B., Rep M., 2009. Pathogen profile update: *Fusarium oxysporum*. *Molecular Plant Pathology* 10: 311–324. https://doi.org/10.1111/j.1364-3703.2009.00538.x

O'Donnell K., Kistler H.C., Cigelnik E., Ploetz R.C., 1998. Multiple evolutionary origins of the fungus causing Panama disease of banana: Concordant evidence from nuclear and mitochondrial gene genealogies. *Proceedings of the National Academy of Sciences* 95: 2044–2049. https://doi.org/10.1073/pnas.95.5.2044

Ortu G., Bertetti D., Gullino M.L., Garibaldi A., 2013. A new *forma specialis* of *Fusarium oxysporum* on *Crassula ovata*. *Journal of Plant Pathology* 95: 33–39.

Ortu G., Bertetti D., Gullino M.L., Garibaldi A., 2015a. *Fusarium oxysporum* f. sp *echeveriae*, a novel *forma specialis* causing crown and stem rot of *Echeveria agavoides*. *Phytopathologia Mediterranea* 54: 64–75. https://doi.org/10.14601/Phytopathol_Mediterr-13533

Ortu G., Bertetti D., Patrizia M., Gullino M.L., Garibaldi A., 2015b. *Fusarium oxysporum* f. sp. *papaveris*: a new *forma specialis* isolated from iceland poppy (*Papaver nudicaule*). *Phytopathologia Mediterranea* 54: 76–85.

Ortu G., Bertetti D., Gullino M.L., Garibaldi A., 2018. *Fusarium oxysporum* f. sp. *lavandulae*, a novel *forma specialis* causing wilt on *Lavandula* × *allardii*. *Journal of Plant Pathology* 100: 391–397. https://doi.org/10.1007/s42161-018-0084-0

Park H.J., Kim D.H., Park S.J., Kim J.M., Ryu J.H., 2012. Ginseng in traditional herbal prescriptions. *Journal of Ginseng Research* 36: 225–241. https://doi.org/10.5142/jgr.2012.36.3.225

Pietro A.D., Madrid M.P., Caracuel Z., Delgado-Jarana J., Roncero M.I.G., 2003. *Fusarium oxysporum*: exploring the molecular arsenal of a vascular wilt fungus. *Molecular Plant Pathology* 4: 315–325. https://doi.org/10.1046/j.1364-3703.2003.00180.x

Punja Z.K., Wan A., Goswami R.S., 2008. Root rot and distortion of ginseng seedling roots caused by *Fusarium oxysporum*. *Canadian Journal of Plant Pathology* 30: 565-574. https://doi.org/10.1080/07060660809507556

Reeleder R.D., Roy R., Capell B., 2002. Seed and root rots of ginseng (*Panax quinquefolius* L.) caused by *Cylindrocarpon destructans* and *Fusarium* spp. *Journal of Ginseng Research* 26: 151–158. https://doi.org/10.5142/JGR.2002.26.3.151

Ronquist F., Teslenko M., van der Mark P., Ayres D.L., Darling A., … Huelsenbeck J.P., 2012. MrBayes 3.2: efficient Bayesian phylogenetic inference and model choice across a large model space. *Systematic Biology* 61: 539–542. https://doi.org/10.1093/sysbio/sys029

Rana, A., Sahgal, M., Johri, B.N., 2017. *Fusarium oxysporum*: Genomics, diversity and plant–host interaction. In: *Developments in Fungal Biology and Applied Mycology* (Satyanarayana, T., Deshmukh, S., Johri, B., ed.). Springer, Singapore, 159–199. https://doi.org/10.1007/978-981-10-4768-8_10

Song M., Yun H.Y., Kim Y.H., 2014. Antagonistic *Bacillus* species as a biological control of ginseng root rot caused by *Fusarium* cf. *incarnatum*. *Journal of Gin-*

seng Research 38: 136–145. https://doi.org/10.1016/j.jgr.2013.11.016

Yun T.K., 2001. Brief introduction of *Panax ginseng* C.A. Meyer. *Journal of Korean Medical Science* 16: S3–S5.

Zhang D., Gao F., Jakovlić I., Zou H., Zhang J., Li W.X., Wang G.T., 2020. PhyloSuite: An integrated and scalable desktop platform for streamlined molecular sequence data management and evolutionary phylogenetics studies. *Molecular Ecology Resources* 20: 348–355. https://doi.org/10.1111/1755-0998.13096

Phytopathologia Mediterranea
The international journal of the
Mediterranean Phytopathological Union

Firenze University Press
www.fupress.com/pm

Short Notes

Curvularia americana and *Curvularia tropicalis* cause leaf and crown necrosis on Bermuda grass in Italy

Giovanna GILARDI[1], Massimo MOCIONI[2], Maria Lodovica GULLINO[1], Vladimiro GUARNACCIA[1,3,*]

[1] *Centre for Innovation in the Agro-Environmental Sector, AGROINNOVA, University of Torino, Largo Braccini 2, 10095 Grugliasco (TO), Italy*
[2] *ANT–NET srl, Via Livorno 60, Torino, Italy*
[3] *Department of Agricultural, Forest and Food Sciences (DISAFA), University of Torino, Largo Braccini 2, 10095 Grugliasco (TO), Italy*
[*]Corresponding author. E-mail: vladimiro.guarnaccia@unito.it

Summary. *Curvularia americana* and *C. tropicalis* are described as causes of leaf and crown necroses on Bermuda grass (*Cynodon dactylon* x *Cynodon transvaalensis)* in Veneto, Northern Italy. These pathogens were characterized using morphological characters, and a multilocus molecular phylogenetic analysis based on the nuclear ribosomal internal transcribed spacer (ITS) region, the partial glyceraldehyde-3-phosphate dehydrogenase (*gapdh*) and translation elongation factor-1α (*tef1-α*) genes. Pathogenicity tests and the fulfilment of Koch's postulates confirmed *C. americana* and *C. tropicalis* as foliar pathogens of Bermuda grass. This is the first report of *C. americana* and *C. tropicalis* as pathogens of Bermuda grass, and the first record these two fungi in Europe.

Keywords. *Cynodon*, turf disease, multi-locus typing, golf courses.

OPEN ACCESS

Citation: G. Gilardi, M. Mocioni, M.L. Gullino, V. Guarnaccia (2022) *Curvularia americana* and *Curvularia tropicalis* cause leaf and crown necrosis on Bermuda grass in Italy. *Phytopathologia Mediterranea* 61(3): 431-437. doi: 10.36253/phyto-13825

Accepted: October 3, 2022

Published: November 25, 2022

Data Availability Statement: All relevant data are within the paper and its Supporting Information files.

Competing Interests: The Author(s) declare(s) no conflict of interest.

Editor: Alan J.L. Phillips, University of Lisbon, Portugal.

ORCID:
GG: 0000-0002-6420-7444
MLG: 0000-0002-7706-1915
VG: 0000-0003-3188-7743

INTRODUCTION

Bermuda grass is a popular turfgrass in temperate, tropical and subtropical regions. Genus crosses and triploid interspecific hybrid Bermuda grass cultivars were developed for various characteristics, including high turf quality, tolerance to low mowing heights, and resistance to pests (Brecht *et al.*, 2007). Hybrid Bermuda cv. Miniverde grass is the product of the interspecific cross between *Cynodon dactylon* and *Cynodon transvaalensis*. In Italy in the last 20 years, use of Bermuda grass is increasing for high maintenance turfgrasses (such as on golf courses and football fields). More than 50 golf courses in Italy have converted the original fairways and tee areas to Bermuda grass, to reduce water consumption and other maintenance inputs. Hybrid Bermuda grass, and other warm season grasses (*Zoysia* spp. and *Paspalum* spp.), are being used under Italian conditions to obtain a high-quality turf,

and to reduce pesticide use in public areas, as requested by the National Action Plan since 2014. Bermuda grass is currently being used to replace bentgrass on golf greens (Magni *et al*., 2018), being less sensitive to water stresses and diseases than other turf species (Turgeon and Kaminski, 2019).

In August 2020, symptoms of a previously unknown disease were observed on *Cynodon dactylon* × *Cynodon transvaalensis* ' Miniverde' in a golf green in the Padova province, Veneto (Northern Italy). The golf course area (approx. 0.5 ha) was covered with Bermuda grass in 2018. The symptoms consisted of leaf spots which were reducing the playability and the smoothness of the green surfaces.

The aims of the present study were: i) to isolate the causal agents associated with the affected host tissues; ii) to test the pathogenicity of isolates by fulfilling Koch's postulates; and iii) to characterize the isolated fungi using morphological, molecular and phylogenetic tools.

MATERIAL AND METHODS

Symptoms and isolation of fungi

The first symptoms appeared in May 2020 (3 years after the turfgrass was established), as necrotic areas (diam. 2–10 cm) of affected plants. At the end of the growing season smaller spots were completely recovered, but in October 2020 the affected areas of the turf developed involving up to 10–15% of the area (Figure 1a). Diseased plants showed necrotic leaves and crowns with small, dark, sunken spots (Figure 1b). The infected tissues from leaves and crowns (Figure 2) were surface sterilized by immersion in 1% sodium hypochlorite for 1 min, followed by rinsing twice in distilled water, and then drying on sterile absorbent paper. Small fragments (1–2 mm) were cut from the edges of healthy and necrotic tissues and plated on potato dextrose agar (PDA, Oxoid) amended with 25 μg mL^{-1} of streptomycin sulphate (PDA-S, Sigma-Aldrich). The plates were incubated at 25±1°C under a 12 h photoperiod. Hyphae from the margin of each isolate were placed on PDA-S, then, 5 d later, single conidia were transferred into PDA plates to establish pure cultures. Representative isolates with different macroscopic morphological characteristics were selected (5A, 5B, 15A, 15B and 15C) for further molecular characterization. Stock cultures of these isolates are maintained at 4°C and at -20°C in the AGROINNOVA (University of Torino) culture collection, Torino, Italy.

Pathogenicity tests

Isolates 5A, 5B, 15A, 15B and 15C were inoculated on 50-d-old healthy plants of *Cynodon dactylon* x *Cynodon transvaalensis* cultivated in plastic trays (30 × 50 cm, 12 L volume), containing steam disinfected peat plant growth medium. The isolates were grown on PDA amended with streptomycin sulphate (25 mg L^{-1}) and kept at 25°C with a 12 h photoperiod for 7 d. The turfgrass sods were each sprayed with a conidium suspension (final concentration of 10^6 conidia mL^{-1}) for each isolate (n. 2 trays per isolate). Non inoculated grass was sprayed with sterile water as experimental controls. Inoculated and non inoculated grass were then kept in a growth chamber at 25°C with a 12 h photoperiod. Fifteen days after inoculation, the symptom severity (SS) associated with each inoculated isolate was evaluated. Small portions (0.3 cm) of symptomatic leaf and crown tissues were placed onto PDA and maintained under the incubation conditions described above. Fungal colonies morphologically similar to those inoculated were con-

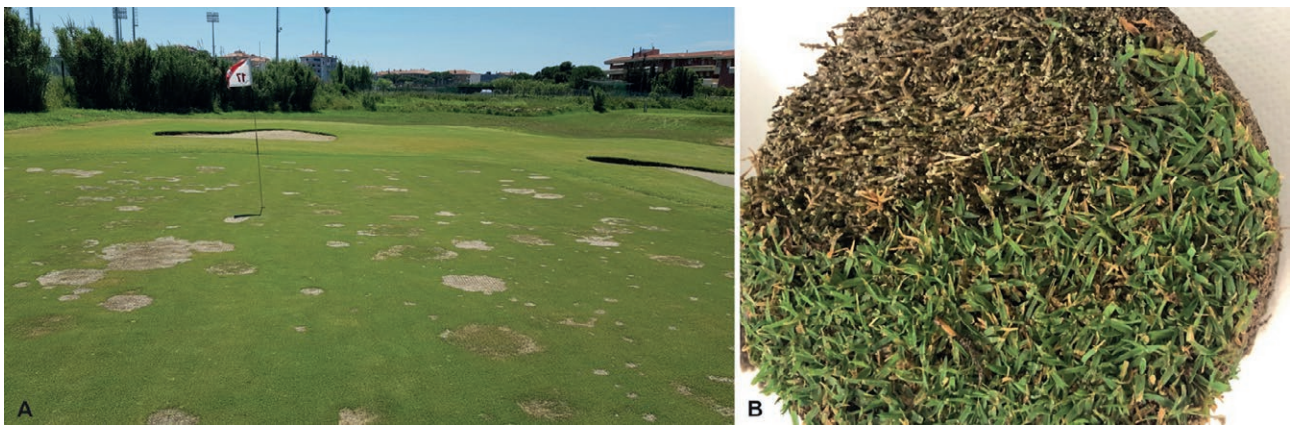

Figure 1. Necrotic areas caused by *Curvularia americana* and *C. tropicalis* observed on a golf course green (A), and affected leaves (B).

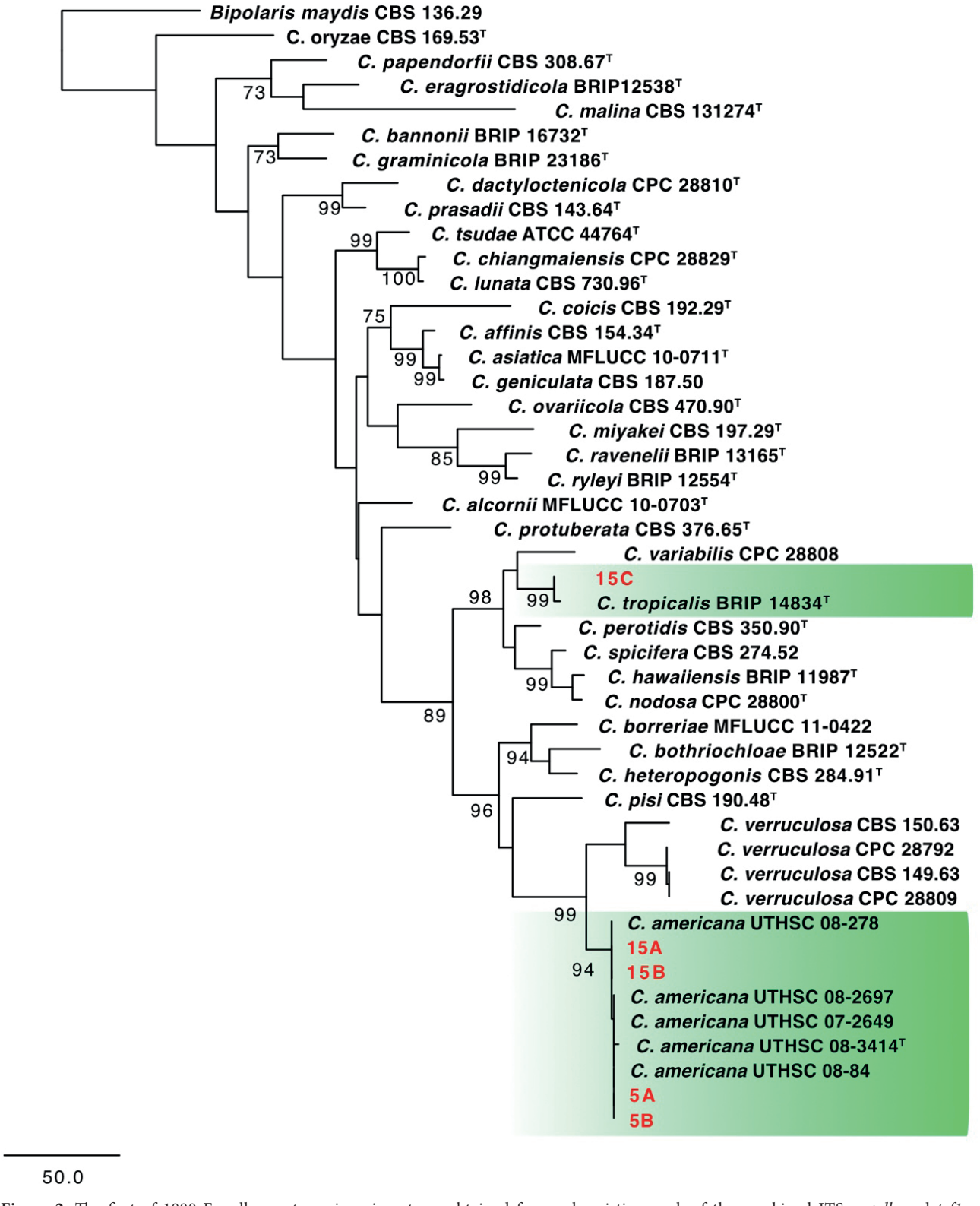

Figure 2. The first of 1000 Equally most parsimonious trees obtained from a heuristic search of the combined ITS, *gapdh* and *tef1-α* sequence alignments of *Curvularia* spp. Bootstrap support values are shown at the nodes. The strains isolated in the present study are shown in red font, and the scale bar represents number of changes. The tree was rooted to *Bipolaris maydis* (CBS 136.29). [T] indicates ex-type cultures.

sistently reisolated, and were identified based on their colony characteristics and on nuclear ribosomal internal transcribed spacer (ITS) sequencing.

Phenotypic characterization

Agar plugs (5 mm diam.) of representative isolates of each morphology group 5B and 15C were taken from the edge of 10-d-old cultures and transferred to the center of 9 cm diam. Petri dishes containing PDA. These plates were then incubated at 25±1°C under a 12 h photoperiod for 7 d. Colony characters, colour and diameter were observed/measured after 7 d. Cultures were examined over time for development of ascomata, conidiomata and setae. The morphological characteristics were assessed examined by mounting fungal structures in water and examining at 40× magnification (Nikon Eclipse 55i microscope), and 40 measurements were determined for two isolates (5B and 15C).

DNA extraction, polymerase chain reaction (PCR) amplification, and sequencing

Total DNA was extracted from 0.1 g of mycelium of each isolate grown on PDA, using the E.Z.N.A.® Fungal DNA Mini Kit (Omega Bio-Tek), following the manufacturer's instructions. Species identifications were achieved through DNA amplification and sequencing of a combined dataset of genes: the ITS regions, and the partial glyceraldehyde-3-phosphate dehydrogenase (*gapdh*) and translation elongation factor-1α (*tef1-α*) genes. ITS region of each isolate was amplified using the universal primers ITS1 and ITS4 (White *et al*., 1990). The primer GDF1 and GDR1 were amplified to amplify part of the *gapdh* gene (Guerber *et al*., 2003). The primers EF1-983 and EF1-2218R (Manamgoda *et al*., 2012) were used to amplify part of the *tef1-α* gene. The PCR amplification mixtures and cycling conditions adopted for the three loci were followed as described for the respective cited references (above). An amount of 5 µL of PCR product for each PCR reaction was examined by electrophoresis at 100V on 1% agarose (VWR Life Science AMRESCO® bio chemicals) gels stained with GelRed™. PCR products were sequenced in both directions by Eurofins Genomics Service. The DNA sequences generated were analyzed and consensus sequences were computed using the Genious v. 11.1.5 (Geneious Prime).

Phylogenetic analyses

New sequences obtained in this study were blasted against the NCBI's GenBank nucleotide database to determine the closest relatives for develop a taxonomic framework of the studied isolates. Alignments of different gene regions, including sequences obtained from this study and sequences downloaded from GenBank, were initially performed with the MAFFT v. 7 online server (http://mafft.cbrc.jp/alignment/server/index.html) (Katoh and Standley, 2013), and then manually adjusted in MEGA v. 7 (Kumar *et al*., 2016). The program Geneious v. 11.1.5 (Geneious Prime) was used to assemble the generated sequences of DNA and consensus sequences were computed. Alignments of different loci were manually adjusted in MEGA v. 7 (Kumar *et al*., 2016). *Bipolaris maydis* (CBS 136.29) was used as the outgroup. The phylogeny was based on Maximum Parsimony (MP) analysis which was performed through Phylogenetic Analysis Using Parsimony (PAUP) v.4.0b10 (Swofford, 2003). Phylogenetic relationships were estimated through heuristic searches with 100 random addition sequences. Tree bisection reconnection was used, with the 'best trees' as the branch swapping option, with alignment gaps treated as fifth base and all characters weighted equally. Parsimony and the bootstrap analyses (Hillis and Bull, 1993) were based on 1000 replications and on tree length (TL), consistency index (CI), retention index (RI) and rescaled consistence index (RC). The sequences obtained in the present study (Table 1) were deposited in GenBank.

RESULTS

Fungal isolations

Brown to black fungal colonies consistently developed from inoculated leaves (30% frequency) and crowns (46% frequency), after incubation of 48 to 72 h on PDA.

Pathogenicity tests

Symptoms described above for leaves and crowns developed on all inoculated plants 15-20 d after inoculation, causing 30 to 40% areas of necroses. The non inoculated plants remained healthy. *Curvularia americana* and *C. tropicalis* were isolated from the symptomatic tissues and their identities were confirmed sequencing the *tef1-α* gene as the most informative, fulfilling the Koch's postulates.

Phenotypic characterization

Black to brown colonies were observed for isolate 5B and 15C. Colonies grown on PDA reached 64 mm diam.

Table 1. Collection details and GenBank accession numbers of isolates included in this study.

Species	Isolate No.[1]	Host	Location	GenBank No.[2]		
				ITS	*gapdh*	*tef1-α*
Bipolaris maydis	CBS 136.29^T	*Zea mays*	USA	AF071325	KM034846	KM093794
C. affinis	CBS 154.34^T	Unknown	Indonesia	KJ909780	KM230401	KM196566
C. alcornii	MFLUCC 10-0703	*Zea mays*	Thailand	JX256420	JX276433	JX266589
C. americana	5A	*Cynodon dactylon* x *C. transvaalensis*	Italy	*OP081046*	*OP114771*	*OP103749*
	5B	*Cynodon dactylon* x *C. transvaalensis*	Italy	*OP081047*	*OP114772*	*OP103750*
	15A	*Cynodon dactylon* x *C. transvaalensis*	Italy	*OP081048*	*OP114773*	*OP103751*
	15B	*Cynodon dactylon* x *C. transvaalensis*	Italy	*OP081049*	*OP114774*	*OP103752*
	UTHSC 08-3414^T	Human leg	USA	HE861833	HF565488	_
	UTHSC 07-2649	Human toe tissue	USA	HE861834	HF565486	_
	UTHSC 08-84	Human nasal sinus	USA	HG779015	HG779115	_
	UTHSC 08-278	Human peritoneal dialysis fluid	USA	HE861832	HF565487	_
	UTHSC 08-2697	Human leg	USA	HG779016	HG779117	_
C. asiatica	MFLUCC 10-0711^T	*Panicum* sp.	Thailand	JX256424	JX276436	JX266593
C. bannonii	BRIP 16732^T	*Jacquemontia tamnifolia*	USA	KJ415542	KJ415404	KJ415450
C. borreriae	MFLUCC 11-0422	Unknown *Poaceae*	Thailand	KP400638	KP419987	KM196571
C. bothriochloae	BRIP 12522^T	*Bothriochloa bladhii*	Australia	KJ415543	KJ415403	KJ415449
C. chiangmaiensis	CPC 28829^T	*Zea mays*	Thailand	MF490814	MF490836	MF490857
C. coicis	CBS 192.29^T	*Coix lacryma-jobi*	Japan	AF081447	AF081410	JN601006
C. dactyloctenicola	CPC 28810^T	*Dactyloctenium aegyptium*	Thailand	KJ415545	KJ415401	KJ415447
C. eragrostidicola	BRIP 12538^T	*Eragrostis pilosa*	Australia	MH414899	MH433643	MH433661
C. geniculata	CBS 187.50	Unknown seed	Indonesia	KJ909781	KM083609	KM230410
C. graminicola	BRIP 23186^T	*Aristida ingrata*	Australia	JN192376	JN600964	JN601008
C. hawaiiensis	BRIP 11987^T		USA	KJ415547	KJ415399	KJ415445
C. heteropogonis	CBS 284.91^T	*Heteropogon contortus*	Australia	KJ415549	JN600969	JN601013
C. lunata	CBS 730.96^T	*Homo sapiens*	USA	JX256429	JX276441	JX266596
C. malina	CBS 131274^T	*Zoysia matrella*	USA	JF812154	KP153179	KR493095
C. miyakei	CBS 197.29^T	*Eragrostis pilosa*	Japan	KJ909770	KM083611	KM196568
C. nodosa	CPC 28800^T	*Digitaria ciliaris*	Thailand	MF490816	MF490838	MF490859
C. oryzae	CBS 169.53^T	*Oryza sativa*	Vietnam	KP400650	KP645344	KM196590
C. ovariicola	CBS 470.90^T	*Eragrostis interrupta*	Australia	JN192384	JN600976	JN601020
C. papendorfii	CBS 308.67^T	*Acacia karroo*	South Africa	KJ909774	KM083617	KM196594
C. perotidis	CBS 350.90^T	*Perotis rara*	Australia	JN192385	KJ415394	JN601021
C. pisi	CBS 190.48^T	*Pisum sativum*	Canada	KY905678	KY905690	KY905697
C. prasadii	CBS 143.64^T	*Jasminum sambac*	India	KJ922373	KM061785	KM230408
C. protuberata	CBS 376.65	*Deschampsia flexuosa*	UK	KJ922376	KM083605	KM196576
C. ravenelii	BRIP 13165^T	*Sporobolus fertilis*	Australia	JN192386	JN600978	JN601024
C. ryleyi	BRIP 12554	*Sporobolus creber*	Australia	KJ415556	KJ415390	KJ415437
C. spicifera	CBS 274.52	soil	Spain	JN192387	JN600979	JN601023
C. tropicalis	15C	*Cynodon dactylon* x *C. transvaalensis*	Italy	*OP081050*	*OP114775*	*OP103753*
	BRIP 14834	*Coffea arabica*	India	KJ415559	KJ415387	KJ415434
C. tsudae	ATCC 44764^T	*Chloris gayana*	Japan	KC424596	KC747745	KC503940
C. variabilis	CPC 28808	*Eleusine indica*	Thailand	MF490819	MF490841	MF490862
C. verruculosa	CBS 149.63	*Elaeis guineensis*	Nigeria	HF934909	HG779110	_
	CBS 150.63	*Punica granatum*	India	KP400652	KP645346	KP735695
	CPC 28792	*Cynodon dactylon*	Thailand	MF490825	MF490847	MF490868
	CPC 28809	*Eleusine indica*	Thailand	MF490824	MF490846	MF490867

[1] ATCC: American Type Culture Collection, Virginia, USA; BRIP: Biosecurity Queensland Plant Pathology Herbarium, Brisbane, Queensland, Australia; CBS: Westerdijk Fungal Biodiversity Institute, Utrecht, the Netherlands; CPC: Culture collection of P.W. Crous, housed at the Westerdijk Institute, Utrecht, the Netherlands; MFLUCC: Mae Fah Luang University Culture Collection, Chiang Rai, Thailand. ^{T} indicates ex-type cultures.

[2] ITS: internal transcribed spacers 1 and 2 together with 5.8S nrDNA; *gapdh:* partial glyceraldehyde-3-phosphate dehydrogenase gene; *tef1-α*: translation elongation factor 1-α gene. Sequences generated in this study indicated in italics.

for isolate 5B and 68 mm diam. for 15C after 7 d at 25°C. Conidia each had three horizontal septa, and were curved at the third cell from the base. This cell was longer and darker than the others. Cells at each end were subhyaline and intermediate cells were medium brown. Conidia of isolate 5B measured 16.9 to 25.6 µm (mean = 21.4 µm) × 6.6 to 11.3 µm (mean = 8.5 µm), resembling the conidia of *C. americana* (Madrid *et al*., 2014). Conidia produced by the isolate 15C measured 20.3 to 30.1 µm (mean = 24.9 µm) × 7.9 to 10.6 µm (mean = 8.9 µm), resembling the morphological characteristics of conidia of *C. tropicalis* (Tan *et al*., 2014).

Phylogenetic analyses

The combined locus phylogeny consisted of 46 sequences. A total of 1670 characters (ITS: 1–493, *tef1-α*: 500–1355, *gapdh*: 1362–1670) were included in the phylogenetic analysis. A maximum of 1000 equally most parsimonious trees were saved (Tree length = 1291, CI = 0.510, RI = 0.750, RC = 0.382). Bootstrap support values from the parsimony analysis are plotted on the MP tree presented in Figure 2. In the combined analysis, four of the isolates (5A, 5B, 15A and 15B) obtained from symptomatic *Cynodon* plants clustered with the reference strains of *Curvularia americana*, while one isolate (15C) was grouped with *C. tropicalis* in two separate highly supported clades embedded in *Curvularia*.

DISCUSSION

Curvularia has extensive international distribution, and includes pathogens or saprobes of a wide range of plant hosts (Marin-Felix *et al*., 2020) of the family *Poaceae*. These fungi are important pathogens of grass and staple food crops, including rice, maize, wheat and sorghum (Marin-Felix *et al*., 2017a). *Curvularia* includes than 40 species that are distinguished by differences in the conidium morphology and numbers of septa, and in colony morphology (Zhang *et al*., 2004; Chung and Tsukiboshi, 2005). *Curvularia* includes saprophytes, endophytes and pathogens (Sanchez-Marquez *et al*., 2008), which form a complex with *Cochliobolus* and *Bipolaris* affecting mostly grasses (*Poaceae*) with wide international distributions. The taxonomy of this complex is confusing as frequent nomenclatural changes and refinements have occurred. There is no clear morphological boundary between the asexual genera *Bipolaris* and *Curvularia* (Manamgoda *et al*., 2012), so accurate identifications are based on multilocus sequencing analyses (Manamgoda *et al*., 2012; Tan *et al*., 2014, 2018; Marin-Felix *et al*., 2017a, 2017b), and these are fundamental for achieving specific disease management strategies. For this reason, the species identification in the present study was based on a robust phylogenetic analysis developed through three genomic loci, with high informative level provided to distinguish species within *Curvularia*.

In 2003, the presence of pathogenic *Curvularia* spp. was reported in Wuhan, China, on hybrid Bermuda grass, in a sport turfgrass of *C. dactylon* × *C. transvaalensis* hybrid (Huang *et al*., 2005). A foliar disease of hybrid Bermuda grass, caused by *Curvularia malina*, was observed on several golf courses in China after April 2011 (Zhang *et al*., 2017). A novel species of *Curvularia* was also identified in 2017 as a foliar pathogen of *Cynodon dactylon* in the south of the United States of America (Peterson *et al*., 2017). *Curvularia americana* was reported on *Oryza sativa* in Iran (Heidarian *et al*., 2020) and on *Vitis* sp. in China (Jayawardena *et al*., 2018), and *C. tropicalis* was found associated with leaves of *Coffea arabica* in India (Tan *et al*., 2014).

The present study is the first to report *C. americana* and *C. tropicalis* causing leaf and crown necroses on Bermuda grass in Italy. This study is also the first to record these two species in Europe. Pathogenicity of these fungi was confirmed on Bermuda grass, and symptoms of leaf yellowing and necrosis, and of crown rot were obtained after inoculations under controlled conditions. Despite the use of warm season grasses which are usually less susceptible to the major turf diseases, golf courses and football field environments could induce conditions suitable for disease development, through pathogen sporulation and spread. High temperatures and humidity are likely to be involved with turfgrass diseases caused by *Curvularia* spp. Because of these environments and the susceptibility of turfgrasses to several pathogens, accurate diagnoses of these pathogens are essential for effective disease management. This study highlights the need for accurate diagnostic tools for the identification of pathogens affecting Bermuda grass.

ACKNOWLEDGEMENTS

This study was funded by the Ministry of Education, Universities and Research (MIUR), Local research (ex 60%). The authors thank Prof. M. Mezzalama (AGROINNOVA - University of Torino) and Ms. Erica Napoletano for technical support, and the "Golf Club della Montecchia" for availability and support with specimen collection.

LITERATURE CITED

Brecht M.O., Stiles C.M., Datnoff L. E., 2007. Evaluation of pathogenicity of *Bipolaris* and *Curvularia* spp. on dwarf and ultradwarf bermudagrasses in Florida. Online. *Plant Health Progress* 8: 30.

Chung W.H., Tsukiboshi T., 2005. A new species of *Curvularia* from Japan. *Mycotaxon* 91: 49–54.

Guerber J.C., Liu B., Correll J.C., Johnston P.R., 2003. Characterization of diversity in *Colletotrichum acutatum sensu lato* by sequence analysis of two gene introns, mtDNA and intron RFLPs, and mating compatibility. *Mycologia* 95: 872–895.

Heidarian Z., Arzanlou M., Ahmadpour A., 2020. Molecular phylogeny and morphology differentiate several new records and novel hosts for *Curvularia* species in Iran. *Nova Hedwigia* 111: 151–171.

Hillis D.M., Bull J.J., 1993. An empirical test of bootstrapping as a method for assessing confidence in phylogenetic analysis. *Systematic Biology* 42: 182–192.

Huang J., Zheng L., Hsiang T., 2005. First report of leaf spot caused by *Curvularia verruculosa* on *Cynodon* sp. in Hubei, China. *Plant Pathology* 54: 253.

Jayawardena R. S., Purahong W., Zhang W., Wubet T., Li X. H., … Yan J., 2018. Biodiversity of fungi on *Vitis vinifera* L. revealed by traditional and high-resolution culture-independent approaches. *Fungal Diversity* 90: 1–84.

Katoh K., Standley D.M., 2013. MAFFT Multiple sequence alignment software version 7: improvements in performance and usability. *Molecular Biology and Evolution* 30: 772–780.

Kumar S., Stecher G., Tamura K., 2016. MEGA7: Molecular Evolutionary Genetics Analysis version 7.0 for bigger datasets. *Molecular Biology and Evolution* 33: 1870–1874.

Madrid H., Da Cunha K.C., Gené J., Dijksterhuis J., Cano J., Sutton D. A., … Crous P., 2014. Novel *Curvularia* species from clinical specimens. *Persoonia-Molecular Phylogeny and Evolution of Fungi* 33: 48–60.

Magni S., Gaetani M., Caterugli L., Minelli A., Volterrani M., … Grossi N., 2018. Evaluation of warm season turfgrasses for putting green in two locations in Italy. In: Proceedings 6th European Turfgrass Society Conference, 42–44.

Manamgoda D.S., Cai L., McKenzie E.H.C., Crous P.W., Madrid H., … Hyde K.D., 2012. A phylogenetic and taxonomic re-evaluation of the *Bipolaris - Cochliobolus - Curvularia* Complex. *Fungal Diversity* 56: 131–144.

Marin-Felix Y., Groenewald J.Z., Cai L. … Crous P.W. 2017a. Genera of phytopathogenic fungi: GOPHY 1. *Studies in Mycology* 86: 99–216.

Marin-Felix Y., Senwanna C., Cheewangkoon R. … Crous P.W. 2017b. New species and records of *Bipolaris* and *Curvularia* from Thailand. *Mycosphere* 8: 1556–1574.

Marin-Felix Y., Hernández-Restrepo M., Crous P.W., 2020. Multi-locus phylogeny of the genus *Curvularia* and description of ten new species. *Mycological Progress* 19: 559–588.

Peterson T.M., Young-Ki Jo, Phillip L.V., Hoffmann F.G., 2017. *Curvularia malina* sp. nov. incites a new disease of warm-season turfgrasses in the southeastern United States. *Mycologia* 108: 915–924.

Sanchez-Marquez S., Bills G.F., Zabalgogeazcoa I., 2008. Diversity and structure of the fungal endophytic assemblages from two sympatric coastal grasses. *Fungal Diversity* 33: 87–100.

Swofford D.L., 2003. PAUP*. Phylogenetic analysis using parsimony (*and other methods) v. 4.0b10. Sunderland; MS, USA: Sinauer Associates.

Tan Y.P., Madrid H., Crous P.W., Shivas R.G., 2014. *Johnalcornia* gen. et. comb. nov., and nine new combinations in *Curvularia* based on molecular phylogenetic analysis. *Australasian Plant Pathology* 43: 589–603.

Tan Y.P., Crous P.W., Shivas R.G., 2018. Cryptic species of *Curvularia* in the culture collection of the Queensland Plant Pathology Herbarium. *Mycokeys* 35: 1–25.

Turgeon A.J., Kaminski J.E., 2019. Turfgrass management, Turfpath, LLC, State College, Pennsylvania, USA, 392 pp.

White T.J., Bruns T., Lee S., Taylor J.W., 1990. Amplification and direct sequencing of fungal ribosomal RNA genes for phylogenetics. In: *PCR Protocols: a Guide to Methods and Applications*. (Innis M.A., Gelfand D.H., Sninsky J.J., White T.J., ed.). Academic Press, San Diego, California, 315–322.

Zhang M., Zhang T.Y., Wu W.P., 2004. A new name and a new variety in *Curvularia*. *Mycosystema*, 23:177–178.

Zhang W., Liu J., Huo P., Huang Z. 2017. *Curvularia malina* causes a foliar disease on hybrid. *European Journal of Plant Pathology* 151: 557–562.

Phytopathologia Mediterranea
The international journal of the
Mediterranean Phytopathological Union

Firenze University Press
www.fupress.com/pm

Research Papers

Optimisation of sampling and testing for asymptomatic olive trees infected by *Xylella fastidiosa* in Apulia region, Italy

Anna Maria D'ONGHIA*, Franco SANTORO, Serena Anna MINUTILLO, Dajana FRASHERI, Marilita GALLO, Stefania GUALANO, Giuseppe CAVALLO, Franco VALENTINI

Centre International de Hautes Etudes Agronomiques Méditerranéennes Bari (CIHEAM Bari), Via Ceglie, 9 - 70010 Valenzano (BA), Italy
*Corresponding author. E-mail: donghia@iamb.it

Summary. Early detection of *Xylella fastidiosa* outbreaks in Apulian olive groves is crucial, especially in buffer zones and pathogen-free areas where olive trees are asymptomatic. Three studies were conducted. Two were on the spatial and temporal progression of *X. fastidiosa* infections in tree canopies of asymptomatic or mildly symptomatic olive trees of tolerant ('Leccino') and susceptible ('Cellina di Nardò' and 'Ogliarola salentina') cultivars. Despite different trends in pathogen infection rates and concentrations between 'Leccino' and susceptible olive cultivars over the study period, results showed that sampling was most effective in the mid-upper part of tree canopies throughout the year, excluding the warmest and coldest periods. Stem xylem tissues were the most appropriate for detecting the pathogen compared to lower parts of mature leaves with petioles, using serological and molecular assays. Based on these results, a third study was conducted to compare molecular and serological tests (qPCR, real-time LAMP, DAS-ELISA, DTBIA) for detection of *X. fastidiosa* in the mid-upper part of asymptomatic branches of infected 'Leccino' trees that were sampled in an appropriate collection time, using stem xylem tissue as the most appropriate matrix for testing. The molecular methods showed the greatest sensitivity, with no undetermined results, while among the serological assays, DTBIA was more sensitive than DAS-ELISA. An improved protocol for monitoring asymptomatic olive trees is recommended.

Keywords. Plant matrices, diagnosis, qPCR, real-time LAMP, DAS-ELISA, DTBIA.

OPEN ACCESS

Citation: A.M. D'Onghia, F. Santoro, S.A. Minutillo, D. Frasheri, M. Gallo, S. Gualano, G. Cavallo, F. Valentini (2022) Optimisation of sampling and testing for asymptomatic olive trees infected by *Xylella fastidiosa* in Apulia region, Italy. *Phytopathologia Mediterranea* 61(3): 439-449. doi: 10.36253/phyto-13732

Accepted: October 17, 2022

Published: November 25, 2022

Data Availability Statement: All relevant data are within the paper and its Supporting Information files.

Competing Interests: The Author(s) declare(s) no conflict of interest.

Editor: Joel L. Vanneste, Plant and Food Research, Sandringham, New Zealand.

ORCID:
AMD'O: 0000-0002-1817-4637
FS: 0000-0003-0793-866X
SAM: 0000-0002-6403-0685
DF: 0000-0001-6423-2394
MG: 0000-0003-4981-485X
SG: 0000-0002-2221-6529
GC: 0000-0001-9192-9955
FV: 0000-0001-5724-8291

INTRODUCTION

Xylella fastidiosa (Wells *et al.*, 1987), a xylem-limited Gram negative bacterium, causes a number of serious plant diseases, including Pierce's disease of grapevine and citrus variegated chlorosis (CVC), and this pathogen can infect more than 655 plant species among crops, ornamentals, wild vegetation and forestry (EFSA *et al.*, 2022). The bacterium is classified into six genetically different subspecies: *fastidiosa*, *multiplex*, *pauca*, *sandyi*, *tashke*,

and *morus,* each with its own host range (Schaad *et al*., 2004; Randall *et al*., 2009; Janse and Obradovic, 2010; Nunney *et al*., 2014).

Xylella fastidiosa was first recorded in Europe and Mediterranean region in olive trees in the Apulia region of Southern Italy (Saponari *et al*., 2013). A novel strain of *X. fastidiosa* subsp. *pauca*, De Donno strain ST53 (Elbeaino *et al*., 2014; Loconsole *et al*., 2016) causes the dramatic 'Olive Quick Decline Syndrome (OQDS)'. This strain, which primarily infects olive trees (*Olea europaea* L.), is transmitted by three spittlebugs, among which *Philaenus spumarius* is the most efficient (Ben Moussa *et al*., 2016; Cavalieri *et al*., 2019). *Xylella fastidiosa* causes withering, desiccation, leaf scorch and some dieback in olive trees, symptoms that can extend over entire canopies and lead to death of susceptible cultivars, within a few years from the onset of the symptoms (Martelli *et al*., 2016). With no pathogen control methods being available, strategies for managing *X. fastidiosa* infections currently rely on vector control and the use of *X. fastidiosa*-resistant cultivars (Morelli *et al*., 2021). Apulian native olive cultivars, such as 'Cellina di Nardò' and 'Ogliarola salentina', are highly susceptible and succumb to the disease, while 'Leccino' and 'Favolosa FS-17' show some resistance to the infections (Boscia *et al*., 2017).

Apulia is the most important olive oil producing region in Italy (ISTAT, 2021) and is almost totally covered with olive trees, so spread of the bacterium by vectors has been rapid and destructive. The pathogen is a serious threat to the olive industry and to the landscape of this region, and the heritage value of centuries-old olive trees is also important (Strona *et al*., 2017; Schneider *et al*., 2020).

Early detection of *X. fastidiosa* in olive trees through monitoring programmes is important for assessing new outbreaks, especially when there are no or very mild symptoms, particularly in early stages of infections and because some trees are resistant/tolerant to the pathogen. Following the EPPO diagnostic protocol PM 7/24 (4) *Xylella fastidiosa* (2019) for survey of the bacterium in olive trees, samples should be collected close to the symptomatic portions of branches or should be representative of whole tree canopies for asymptomatic trees. Sampling of olive could also be carried out throughout year, regardless of temperature and physiological phases, because symptoms associated with *X. fastidiosa* infections are persistent, although more strongly expressed in summer.

Several official diagnostic assays are available for the detection of *X. fastidiosa* in olive trees (Harper *et al*., 2010; Djelouah *et al*., 2014; Loconsole *et al*., 2014; Yaseen *et al*., 2015), using leaf petioles and midribs from mature leaves, which are the most suitable source for diagnosis due to the high number of xylem vessels they contain (Hopkins, 1981). Serological tests are usually performed in large-scale monitoring of *X. fastidiosa* in infected and containment areas, where the concentration of the bacterium is expected to be high. Instead, molecular tests are recommended for *X. fastidiosa*-free areas and buffer zones. However, apart from diagnostic sensitivity and specificity, these tests differ in terms of required processing time, necessary technical skills, and specialised instrumentation, which impact the efficiency of *X. fastidiosa* monitoring programmes, especially from an economic viewpoint.

Concentration of the bacterium and its distribution in olive trees are not uniform and depend on pathogen strains, olive cultivars and environmental factors (primarily air temperature and soil water content). As well, EPPO sampling procedures for official monitoring of *X. fastidiosa* in pathogen-free areas are not fully supported by specific research results. For these reasons, the present study aimed to maximize probability of detecting *X. fastidiosa* ST53 in canopies of asymptomatic or mildly symptomatic olive cultivars in the Apulian *X. fastidiosa*-demarcated area. It was therefore necessary to develop effective sampling and testing procedures for detecting the pathogen in olive trees on a large scale.

To this aim, two studies were carried out on the temporal, spatial and quantitative evolution of the *X. fastidiosa* population at olive canopy level of the tolerant 'Leccino' cultivar in comparison with susceptible olive cultivars, using different matrices and diagnostic methods. Results achieved led to a third study for the detection of *X. fastidiosa* in infected 'Leccino' olive trees that were asymptomatic or showed mild infection symptoms through the comparative evaluation of four diagnostic assays, including: Double antibody sandwich - enzyme-linked immunosorbent assay (DAS-ELISA), Direct tissue blot immunoassay (DTBIA), real time Loop-mediated isothermal amplification (real time LAMP), and quantitative polymerase chain reaction (qPCR). For field data acquisition, the XylApp software (Santoro *et al*., 2017) was used, and samples were analysed in the official plant quarantine laboratory of CIHEAM Bari (Italy).

MATERIALS AND METHODS

Spatial, temporal and quantitative evolution of the infections

A preliminary study was conducted in 2017 on 80 'Leccino' (*X. fastidiosa*-tolerant) and 46 'Cellina di

Nardò' (susceptible) olive cultivars in a 50-year-old olive grove in the *X. fastidiosa* infected zone (Lecce province, Apulia). In March, the status of infection in the grove was assessed by testing all the olive trees using DAS-ELISA. For each tree, four semi-hardwood twigs with mature leaves (15–20 cm in size) were collected from the mid-upper and on four sides of the tree canopy (EPPO, 2019). A total of five *X. fastidiosa*-positive trees for each cultivar were selected, based on absence or low levels of symptoms (Boscia *et al.*, 2017). Asymptomatic branches were chosen for sampling. This study aimed to evaluate three levels of canopy and twig portions for preliminary screening, before performing a more in-depth sampling in the second study. The canopy of these trees was divided into three height levels: low (L_1), medium (L_2), high (L_3). Four twigs were randomly collected at each level and each twig was divided into three portions: basal, middle, apical. A total of 240 twigs per cultivar were collected in May and July and twig sections were tested for *X. fastidiosa* using DTBIA, following the protocol of Djelouah *et al.* (2014). DTBIA-negative samples were retested using real-time LAMP following the protocol of Yaseen *et al.* (2015).

Preliminary results from the first study led to a more extensive investigation in the period from December 2017 (T_0) to March 2019 (T_4), focusing on two canopy levels using semi-hardwood twigs. Due to the high *X. fastidiosa* infection pressure in the grove used in the first study, the second study was carried out in two olive groves (approx. 50 years old) located in the Northern part of the *X. fastidiosa* infected zone bordering the containment area. In this area, one olive grove was found with the tolerant 'Leccino' (189 trees), the target cultivar, but not with the susceptible 'Cellina di Nardò', which was replaced with the susceptible 'Ogliarola salentina' (109 trees). The total infection rates in these two groves were first assessed by DAS-ELISA at T_0 in December 2017 (EPPO, 2019). Based on these results and absence of symptoms or presence of mild symptoms, ten infected trees per cultivar were chosen, and asymptomatic branches were periodically tested at two canopy levels (low and high) at four collection times: June 13, 2018 (T_1), September 6, 2018 (T_2), December 18, 2018 (T_3), March 6, 2019 (T_4).

A total of eight semi-hardwood twigs with mature leaves per tree (four from each canopy level) were tested for *X. fastidiosa* at each collection time, using DAS-ELISA, DTBIA and qPCR (Harper *et al.*, 2010), and xylem tissues either from twigs or from mature leaves (lower portion of the leaf with petiole). Each twig with mature leaves was considered as a sample. Throughout the whole sampling period, a total of 640 samples from both cultivars were analysed by serological assays (80 samples per cultivar at each collection time) and half of the samples were randomly selected for qPCR tests. As shown in Figure 1, the same portion of each host matrix was first analysed by DTBIA (two prints per sample) and afterwards by DAS-ELISA (0.5 g per sample) and qPCR (0.3 g per sample).

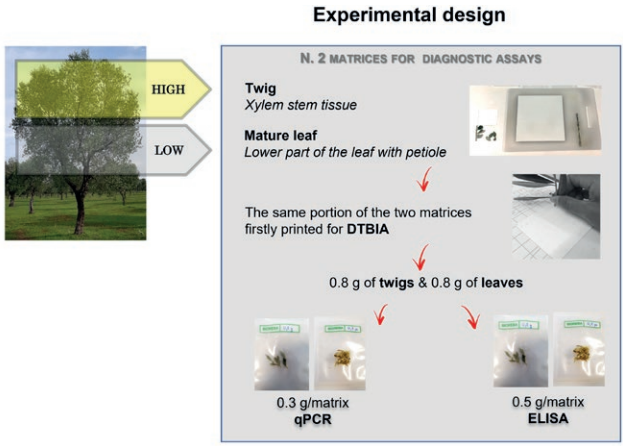

Figure 1. The experimental design used for sampling olive trees. This shows the two canopy levels that were sampled (four semi-hardwood twigs with mature leaves were collected from each level), and the analyses for detection of *Xylella fastidiosa* using two matrices: the stem xylem tissue and the lower part of the mature leaves with their petioles. Each host matrix was first printed on nitrocellulose membrane for DTBIA and was then used for qPCR and DAS-ELISA.

Diagnostic assays

DAS-ELISA was applied using a commercial kit (Agritest S.r.l.) following the manufacturer's instructions. The reaction was determined to be positive if, at regular intervals within 120 min, the absorbance value (at 405 nm) with a microplate reader was three times greater than the mean absorbance of negative control samples. Samples were considered undetermined when the absorbance value was at least two times greater than the mean absorbance of negative control samples. For "undetermined" samples, testing was repeated using the same matrix sample.

DTBIA was carried out using the protocol of Djelouah *et al.* (2014). Twig sections (2–5 mm diam.) and mature leaf petioles were printed on nitrocellulose membranes. Each type of sample was printed twice. Blotted membranes were immersed in 1% bovine serum albumin at room temperature, and then with antigen-specific alkaline phosphatase-labelled antibodies to *X. fastidiosa* (Agritest S.r.l.) at a dilution of 1:500. They were then

dipped in a substrate solution containing one tablet of Sigma Fast TM BCIP-NBT at room temperature until purple-violet colour appeared in the positive controls. The reaction was stopped by washing with tap water. The sample was considered positive when a clear purple violet colour reaction, in one or more prints, was visible with a 10× magnification stereoscope. For a mild positive reaction, results were considered undetermined, and the test was repeated with the same matrix sample.

qPCR was applied after using the CTAB-based protocol for total DNA extraction from 0.3 g of xylem tissue per host matrix. For absolute pathogen quantification, inactivated bacterial cells of *X. fastidiosa* subsp. *pauca* ST53 (supplied by CNR Bari, Italy) were used for generating the standard calibration curves. Inactivated bacterial suspension with an initial OD_{600} of 0.5, corresponding to ca. 10^8 CFU mL^{-1}, was spiked into crude extract of healthy olive xylem tissues to obtain serial ten-fold dilutions ranging from 10^7 to 10^5 CFU mL^{-1}. Bacterium quantifications from samples were inferred by the standard calibration curve, using Cqs from qPCR. Reactions were performed on 50 ng μL^{-1} total DNA. In all analyses, appropriate negative controls containing no template DNA were used. Amplifications and data analyses were carried out using CFX96™ Real-Time PCR Detection Systems (BIO-RAD). Samples were considered positive for Cq values not exceeding 32 and undetermined for 33 to 34 Cq. In cases of no amplification curves or Cq values exceeding 35, samples were considered negative (molecular detection of *X. fastidiosa* by real-time tests https:// upload.eppo.int/download/298ocd8b7f525).

Real-time LAMP was carried out using a commercial kit (Enbiotech S.r.l.), following the manufacturer's instructions, and based on primers developed by Harper *et al.* (2010; erratum 2013) and modified by Yaseen *et al.* (2015). An aliquot (5 µL) of crude sap, prepared for DAS-ELISA using xylem tissues from each matrix (mature leaf with petioles and twig samples), was processed in two steps (DNA extraction and real-time LAMP). Amplifications and data analyses were carried out using CFX96™ Real-Time PCR Detection Systems (BIO-RAD). Samples were considered positive in presence of amplification curves within 30 min from the beginning of each reaction.

Comparative evaluation of serological and molecular tests

Based on results obtained in the two previous studies, a comparative evaluation of serological (DAS-ELISA, DTBIA) and molecular (qPCR, real-time LAMP) tests for the detection of *X. fastidiosa* was carried out on 75 asymptomatic/mildly symptomatic infected trees of the tolerant 'Leccino' cultivar. Four semi-hardwood twigs from four sides at the high canopy level of each tree were collected and tested in October 2019. A portion from each twig was printed twice on nitrocellulose membranes for the DTBIA tests. Xylem tissue from the same twig portion (approx. 1 g) was divided into two equal parts: one was homogenized to obtain plant sap for DAS-ELISA and real time LAMP tests, and the other part was used for qPCR. Positive controls from Agritest S.r.l. and Enbiotech S.r.l. commercial kits were used for serological assays and real-time LAMP, respectively, whereas inactivated bacterial cells of *X. fastidiosa* subsp. *pauca* ST53 (supplied by CNR Bari, Italy) were used for qPCR. Negative controls were obtained from healthy olive plants maintained in the insect-proof greenhouse of CIHEAM Bari (Italy). Serological and molecular tests for the detection of *X. fastidiosa* were performed following the EPPO diagnostic protocol PM 7/24 (4) *Xylella fastidiosa* (EPPO, 2019).

Statistical analyses

Descriptive and parametric statistical analyses were carried out for the two studies on xylem tissues from twigs and mature leaves (lower part with petioles) of *X. fastidiosa*-infected olive trees. Incidence of infection, with respect to the type of olive cultivars (susceptible 'Cellina di Nardò' and 'Ogliarola Salentina' and tolerant 'Leccino'), was estimated using the relative frequency of selected trees *versus* the total number of trees tested by serological and molecular methods. Pathogen concentrations were expressed as a base-10 logarithmic scale (Log CFU mL^{-1}).

To investigate differences and infection evolution rates, and pathogen concentrations with respect to different conditions, six categorical variables were defined: varietal susceptibility ('Cellina di Nardò' *vs* 'Ogliarola salentina', 'Leccino'), canopy level (low, medium, high), twig portion (basal, medium, apical), plant matrix (xylem tissue from the lower part of mature leaves with petioles and from twigs), sampling time (T_1, T_2, T_3, T_4), and diagnostic method (DTBIA, DAS-ELISA, qPCR). Parametric univariate tests ("one way" and "factorial" ANOVAs) were applied to test for separability and interactions between levels of defined categorical variables. The applicability condition of the univariate models was verified by normality tests on the data (Shapiro-Wilks), admitting a slight deviation from the ideal condition, and Levene's test to verify the homogeneity of variances. The comparison between serological (DAS-ELISA, DTBIA) and molecular (qPCR, real-time LAMP) tests, with respect to the condition of infected plants of

the tolerant 'Leccino' with no or mild symptoms, was assessed through evaluation of the relative percentages of positive, false negative and undetermined samples detected by the diagnostic techniques. Microsoft Excel® was used for preparation of some datasets. All statistical analyses with derived graphs were carried out using Statistica 7 software (StatSoft Inc.).

RESULTS

Spatial, temporal and quantitative evolution of the infection

Results from the preliminary study in 2017 showed that the average infection rates from the three canopy levels of the five olive trees per cultivar (240 twigs per cultivar) were the least in the tolerant 'Leccino' (23.1%) compared to that of the susceptible 'Cellina di Nardò' (89.3%). In the susceptible cultivar, most of the tested twigs were *X. fastidiosa*-infected, whereas in 'Leccino' the number of infected twigs was much less. In addition, no DTBIA-negative sample was assessed as positive by real-time LAMP.

For host canopy levels, a statistically significant difference in infection rate was detected only in the low canopy level (L_1) compared to L_2 and L_3 of 'Leccino' (one way ANOVA), whereas no significant difference in infection rate among the three canopy levels was shown for the susceptible cultivar (Figure 2, A and B).

Effects of the distribution of infection along three longitudinal portions of olive tree twigs (apical, middle, basal) were analysed by a factorial ANOVA analysis, with respect to the two different cultivars (Figure 3). The results showed no significant differences in the infection rate between the three portions of the two cultivars, although the greatest values were found in the apical twigs of 'Leccino'.

The second study (December 2017 to March 2019) on ten asymptomatic/mildly symptomatic trees/cultivar analysed effects of two canopy sampling levels using different diagnostic methods and two host matrices (factorial ANOVA). The total number of positive samples over the full sampling period was greater for the upper part of tree canopies of the susceptible cultivar 'Ogliarola salentina', regardless of the plant matrix or diagnostic test used (Figure 4, A and B). The same result, but less evident, was obtained for the 'Leccino' cultivar. The statistical model revealed a greater percentage of positives in the xylem tissues of twigs (approx. 5 - 10%) compared to leaf tissues, regardless of the diagnostic test used, variety susceptibility, and host canopy level (Figure 4 B). These results were more marked from qPCR, which had greater diagnostic sensitivity than the serological tests.

In the susceptible 'Ogliarola salentina', infection rates for twig samples detected with qPCR ranged from 45% in the low canopies to 75% in the high canopies. This effect was much less marked in tolerant 'Leccino' trees where low canopy samples gave 40% infection and high canopy samples gave 48% infection. DTBIA and DAS-ELISA gave similar results for both cultivars using twig tissues (Figure 4 B). However, DTBIA was more sensitive for detecting infections in leaf tissues in 'Ogliarola salentina' (Figure 4 A).

For the evolution of infection incidence (positive samples for each host canopy level), statistically signifi-

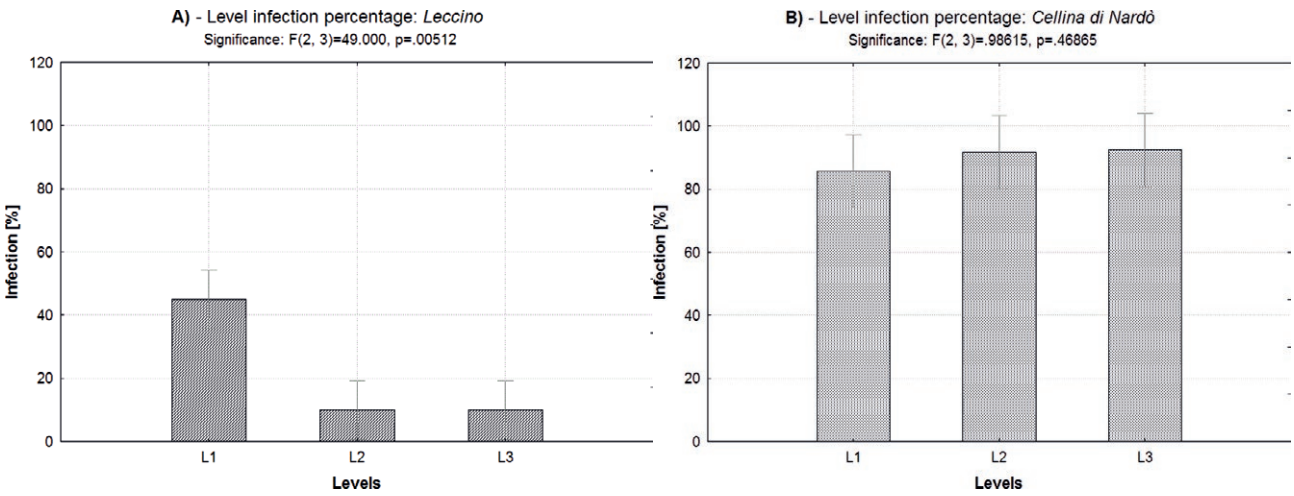

Figure 2. Mean infection rates in 'Leccino' (A) and 'Cellina di Nardò' (B) olive cultivars, as indicated from testing 240 twig samples per cultivar at the three canopy levels: low (L_1), medium (L_2), high (L_3).

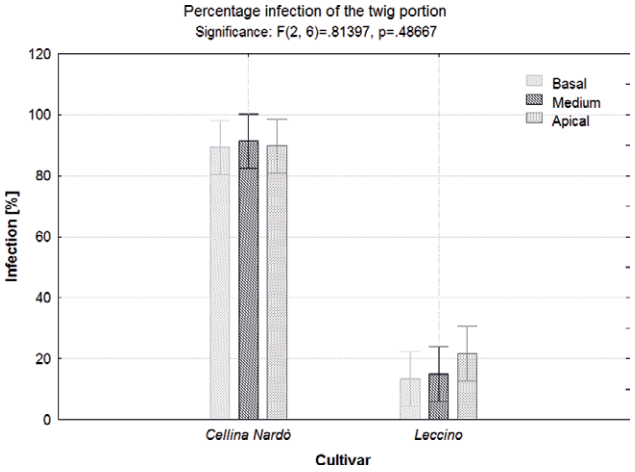

Figure 3. Mean infection rates for different olive twig portions (basal, middle, apical) for the *Xylella fastidiosa* tolerant 'Leccino' and the susceptible 'Cellina di Nardò' cultivars.

cant differences were recorded within the sampling period (F = 84.16, *P* = 0.00000) and according to the cultivar factor (F = 15.13, *P* = 0.0000); no differences for host canopy level, plant matrix, and diagnostic method were detected (Figures 5 and 6). 'Ogliarola salentina' showed a progressive increase over time in infection rates at both host canopy levels for both types of plant matrices (Figures 5B and 6B). This trend was more evident for twigs from the high canopy level, reaching values close to 100% infection at the last collection month. In contrast, percentage of infection for 'Leccino' fluctuated regardless of host canopy level or matrix type, with ranging from approx. 30 to 50% for qPCR-positive samples (Figures 5A and 6A). In this cultivar, the infection rates increased from September to December and then decreased from December to March. In contrast, decreased infection was observed in the period June to September. In general, a slight increase in incidence of infection was detected in the high host canopy level, using twig tissue samples.

For the different diagnostic methods, in general qPCR gave the greatest numbers of positive results regardless of olive variety, host canopy level and type of plant matrix (Figures 5 and 6). However, the greatest diagnostic sensitivity of qPCR was more evident in 'Leccino' when twigs were used for testing (Figure 6A). The two serological methods gave similar results with twigs from both olive varieties (Figure 6). In contrast differences were recorded when leaves were used (Figure 5). In this case, DTBIA was more sensitive than DAS-ELISA, showing the greatest diagnostic sensitivity in the high canopy level of 'Ogliarola salentina' (Figure 5B).

For evolution of overall mean *X. fastidiosa* concentration (Log[CFU mL^{-1}]) in both cultivars, at each collection time during the sampling period (T_1, T_2, T_3, T_4), the statistical analyses confirmed significant differences between the four assessed concentrations (F = 24.2, *P* = 0.00002, with Shapiro-Wilk: W = 0.98, *P* < 0.001, and Levene test: F = 2.94, *P* < 0.001), highlighting September 2018 as the month with the lowest mean value (4.426 Log[CFU mL^{-1}] or approx. 26,000 CFU mL^{-1}), and March 2019 with the greatest mean value (5.166 Log[CFU mL^{-1}] or approx. 140,000 CFU mL^{-1}) (Figure 7).

The overall average concentration of *X. fastidiosa* detected in 'Leccino' (approx. 50,000 CFU mL^{-1}) was less than that measured in the susceptible 'Ogliarola salentina' (approx. 100,000 CFU mL^{-1}) (F = 18.915, *P* =

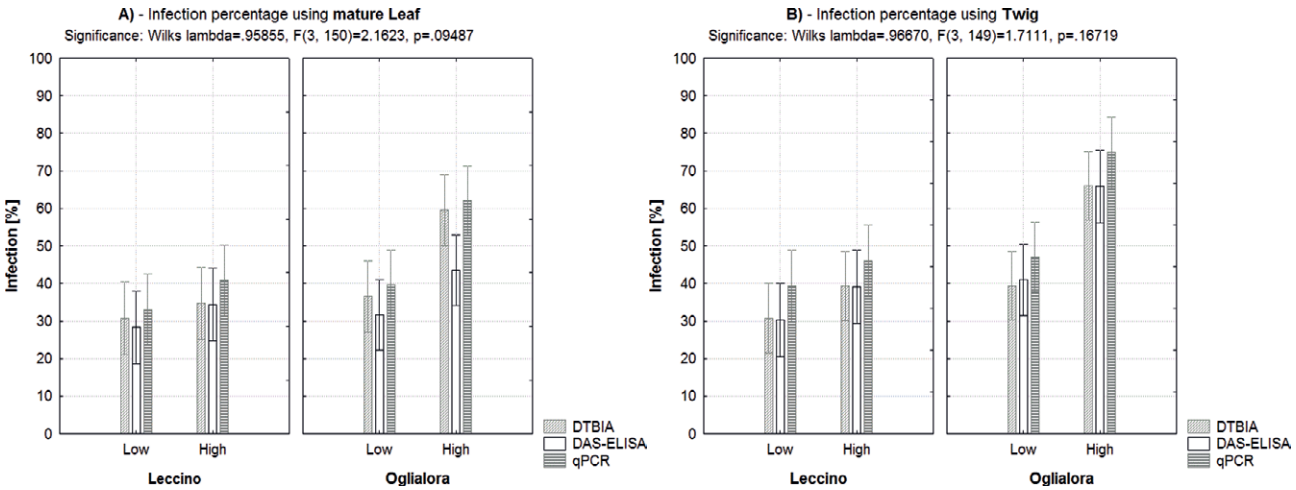

Figure 4. Mean *Xylella fastidiosa* infection rates in two olive cultivars ('Ogliarola salentina' and 'Leccino') assessed using xylem tissue from leaves (A) and twigs (B), from two host canopy levels (high, low) and using three diagnostic methods (DAS-ELISA, DTBIA, qPCR).

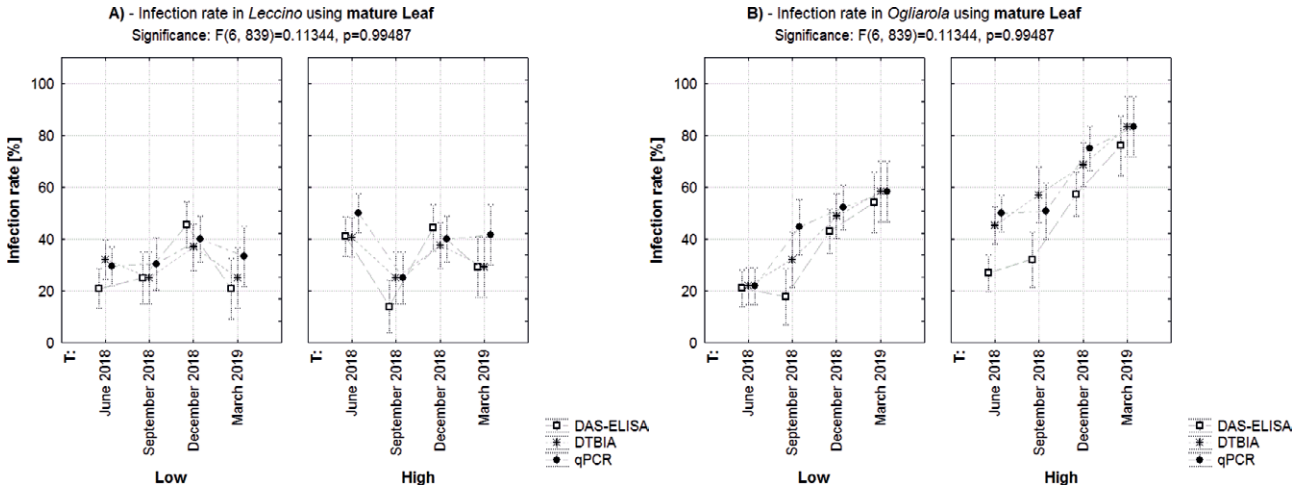

Figure 5. Mean *Xylella fastidiosa* infection rates in 'Leccino' (A) and 'Ogliarola salentina' (B) olive trees assessed using the host leaves, and three diagnostic assays at four different sampling times (T).

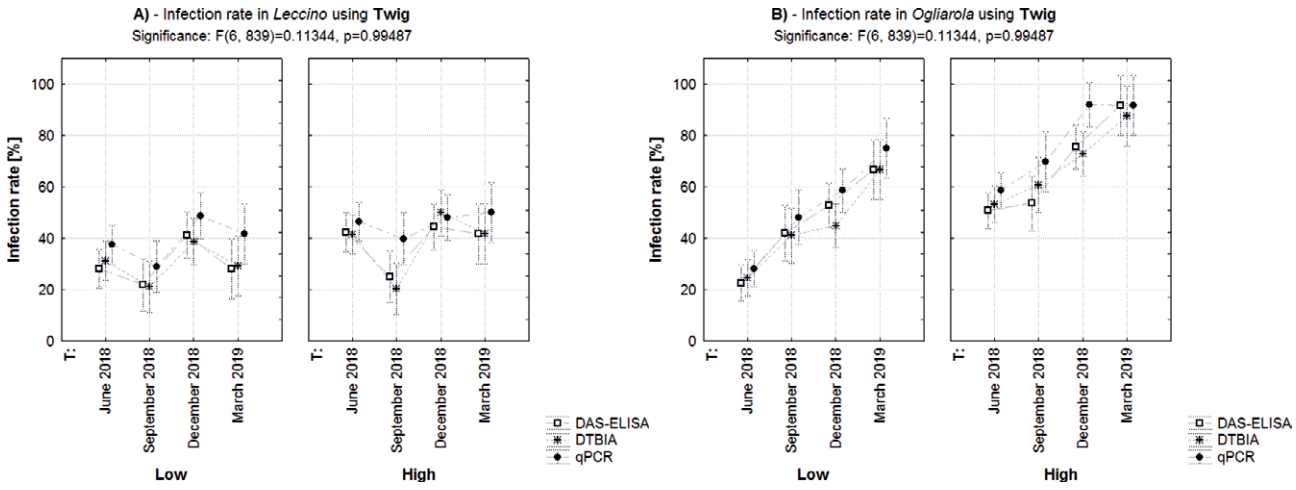

Figure 6. Mean infection rates in olive trees of 'Leccino' (A) and 'Ogliarola salentina' (B) assessed using the host twigs and three different diagnostic assays at four different sampling times (T).

0.00002), and the overall mean amount of bacterial cells extracted from mature leaves (approx. 53,000 CFU mL^{-1}) was less than that extracted from twigs (approx. 100,000 CFU mL^{-1}) ($F = 15.1$, $P = 0.00011$).

Figure 8 shows the time course of *X. fastidiosa* concentrations expressed in logarithmic units for the two olive cultivars in the two assessed host tissue types.

Only in 'Leccino', the evolution of *X. fastidiosa* concentration in the June-December period was similar to that of the infection rate in leaf tissues, i.e., this decreased from June to September, followed by an increase until December. In contrast, a different trend in this cultivar was observed for twigs, which showed decreases in bacterial population size from June to December, followed by increases from December to March. Unlike the infection rate, the pathogen concentration trend was different in 'Ogliarola salentina', which showed a decrease in the summer period using both matrices, followed by increases in the remaining months. In both olive varieties, however, there was a steady increase in pathogen concentrations from December to March, regardless of the tissues assayed. In general, twigs yielded greater pathogen concentrations than leaves (Figure 8).

Comparative evaluation of serological and molecular tests

The comparisons of the different diagnostic tests for the detection of *X. fastidiosa* on asymptomatic branch-

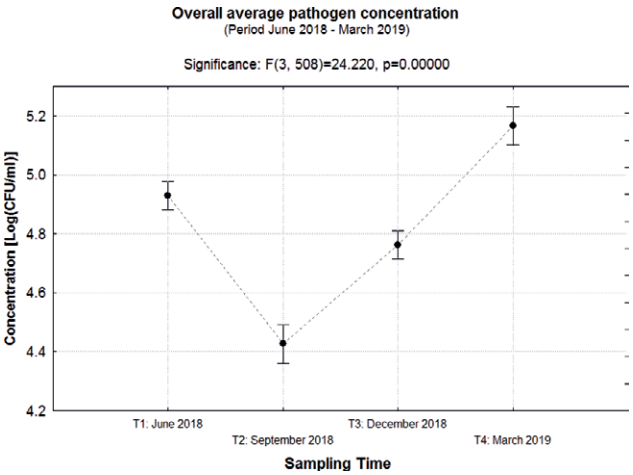

Figure 7. General trend of mean *Xylella fastidiosa* concentrations in two olive cultivars at four sampling times (T1 to T4) during 2018/19.

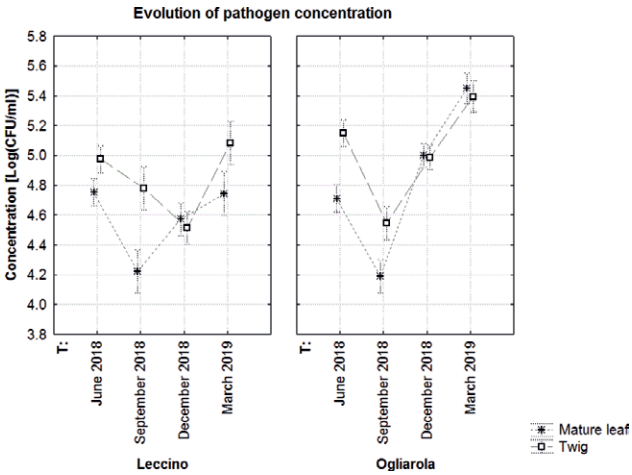

Figure 8. Mean *Xylella fastidiosa* concentration in different tissues (lower parts of mature leaves with petioles and twigs) of two olive cultivars at different sampling times (T).

es of 'Leccino' trees was based on the most effective sampling procedure and most suitable collection time obtained in the previous studies. The proportions of positives, false-negatives and undetermined samples detected with the four diagnostic tests showed that qPCR was the most sensitive, followed by real-time LAMP, DTBIA and DAS-ELISA. DTBIA detected 90.7% of the infected trees, with 5.3% of false-negatives and 4.0% of undetermined samples. ELISA was less sensitive for infected trees (86.7%), with a greater proportion of false-negatives (12%) and fewer undetermined samples (1.3%). For the molecular tests, qPCR (98.7%; 1.3% false-negatives) performed slightly better than real time LAMP (97.3%; 2.7% false-negatives) and without undetermined results. The only false-negative sample detected using qPCR was positive by real-time LAMP and DTBIA. Both serological techniques gave greater proportions of false-negatives and undetermined results when compared with the molecular tests, which showed few false-negatives. All undetermined samples in the serological tests gave positive results in the second round of testing, thus increasing the performance of DTBIA by approx. 3% compared to ELISA.

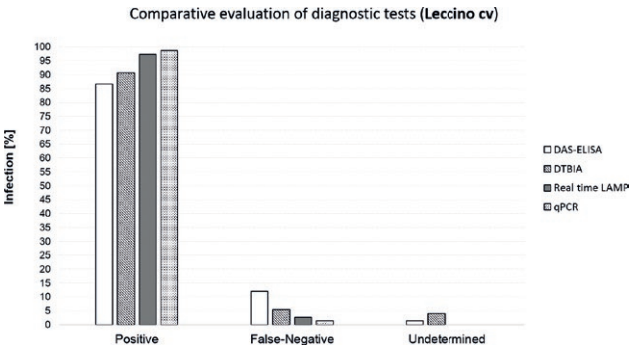

Figure 9. Infection levels indicated in different *Xylella fastidiosa* diagnostic tests (DTBIA, DAS-ELISA, qPCR, real-time LAMP), expressed as percentages of positive, false-negative and undetermined samples.

DISCUSSION

This research has provided relevant technical results for optimizing sampling and analyses of olive trees for *X. fastidiosa* in buffer zones and pathogen-free areas. In these areas, trees infected by this pathogen could be asymptomatic or mildly symptomatic, depending on cultivar susceptibility or low bacterial content in new infections. Therefore, studies on the spatial and quantitative distribution of the bacterium in the olive canopies, and the seasonal dynamics of the pathogen in naturally infected olive trees have focused on the tolerant 'Leccino' cultivar compared with susceptible olive cultivars.

The difference in the host canopy distribution of the pathogen between tolerant and susceptible olive cultivars was evident in most of the situations analysed. Comparing results of the first two studies, it appears that in addition to the increase in the number of samples (from five to ten trees per cultivar) and collection times (from two to four), and the robust statistical analysis conducted in the second study, the different infection pressure at the two study sites may also have influenced the results obtained for both cultivars. However, sampling of the high host canopy level in the second study yielded the

best results for both cultivars. These trends were much less evident in 'Leccino'. For this cultivar, the resistance mechanism likely reduces the pathogen multiplication rate and spread in host plants (Giampetruzzi *et al*., 2016).

For host xylem tissue samples, a difference was also noted between the two cultivars, i.e., xylem tissue from twigs gave better results than for leaf samples in the susceptible 'Ogliarola salentina'. This trend was less evident in 'Leccino'. In contrast, use of xylem tissue from twigs was the most effective for the quantitative detection of the pathogen in both varieties, to a greater extent in the case of 'Leccino'.

These results confirm the differences between the two varieties, both for symptom expression and for spatial, temporal, and quantitative distribution of *X. fastidiosa* infections.

A fluctuating trend in infection rates was observed in 'Leccino', where the infection apparently remained within a range, regardless of canopy level, tissue type, and diagnostic method. Pathogen detection decreased from June to September and increased from September to December, followed by a slight decrease in the winter period. In contrast, 'Ogliarola salentina' had a continuous increase in infection rate, reaching almost 100% in different canopy parts at the end of the sampling period.

The quantitative evolution of *X. fastidiosa* concentrations also differed between the two cultivars, for twig tissues in the June-December period. There was a decrease in bacterial concentrations in 'Leccino', with Ct values greater in twigs than in leaves. The increase in pathogen concentration in the winter months occurred irrespective of cultivars, tissue types or canopy levels. Effects of air and xylem temperatures estimated by regression models have indicated buffer effects of trunk tissues, especially for maximum temperatures occurring during summer (Román-Écija *et al*., 2022). These effects could explain the different results obtained with xylem tissues from twigs compared to those from leaves.

De Pascali *et al*. (2019) indicated that *X. fastidiosa* resistance in 'Leccino' could be linked to low resistance to water stress which enhances the defence mechanisms, as compared to 'Ogliarola salentina'. In addition, effects of temperature on *in vitro* cell cultures of the pathogen and on xylem vessel temperature dynamics in olive grove showed that extreme low or high temperatures differentially influence growth and survival of *X. fastidiosa* strains (Román-Écija *et al*. (2022). Temperatures between 4 and 10°C did not affect cell survival, while incubation at 36 and 40°C for 7 d killed the bacterial cells. However, the widest optimum growth temperature range was estimated for *X. fastidiosa* subsp. *fastidiosa* (19 to 33°C) and for subsp. *multiplex* (20 to 31°C), while *X. fastidiosa* subsp. *pauca* strains had lower optimal ranges (19 to 27°C).

The olive groves studied here, like most of those in southern Apulia, were not irrigated, and the trees in this region are usually under water stress during the summer months. This could explain the decrease of *X. fastidiosa* infection rates and pathogen populations in 'Leccino' from June to September. Also during the study period between 2018 and 2019, the temperature trends in the vicinity of the two olive groves (measured approx. 10 km away) showed that the summer was hot, with average temperatures often exceeding 36°C for whole weeks (July and August were the warmest months), followed by a mild autumn with an average minimum temperature rarely below 10°C (November was the coldest month), and a mild winter with average minimum temperature of 5 to 6°C (January, February and March were the coldest months). Low daily temperature values (1.5–3.5°C) occurred occasionally between January and February, and never exceeded more than 1 d duration (data provided by the weather station of the Regional Agency for Environmental Prevention and Protection, ARPA: http://www.webgis.arpa.puglia.it/meteo/index.php). As *X. fastidiosa* subsp. *pauca* strains have low optimal temperature ranges (19 to 27°C), the pathogen decline in both cultivars in late summer (September) was probably influenced by the persistent high temperatures during midsummer. Mild autumn and winter temperatures did not seem to inhibit the bacterium.

Results of diagnostic tests used during the second study were confirmed in the comparative study that was conducted only on asymptomatic/mildly symptomatic infected 'Leccino' trees in a suitable sampling month (October), by testing xylem stem tissues from asymptomatic branches in the mid-upper parts of the tree canopies.

Choice of the most suitable tests for *X. fastidiosa* monitoring programmes depends on several factors, but most importantly, their sensitivity. Although qPCR was the most sensitive test, in large-scale monitoring programmes, samples are usually processed with serological tests, that are less expensive and do not require sophisticated equipment. Real-time LAMP (97.3% detection) was slightly less sensitive than qPCR (98.7%), but has several advantages, as it is user-friendly and less time-consuming. It can be performed either with a real-time instrument for processing many samples, or with hand-held devices for fewer samples, allowing pathogen detection on site (Yaseen *et al*., 2015). Among serological tests, DTBIA also offers several advantages, but it requires well-trained personnel to read mild positive reactions with microscope. This is a limitation to the

use of DTBIA in most diagnostic laboratories, which often prefer to use DAS-ELISA for large-scale monitoring of *X. fastidiosa* (Djelouah *et al*., 2014). Considering the high sensitivity of both molecular assays compared to serological tests, qPCR and real-time LAMP are the preferred tests to detect low pathogen concentration in asymptomatic olive trees.

Results obtained on the 'Leccino' cultivar provide technical indications for optimizing sampling and testing procedures to increase probability of detecting new *X. fastidiosa* infections in asymptomatic olive trees, especially when buffer zones and pathogen-free areas are monitored. As recommended by EPPO and substantiated by this work, the mid-upper parts of olive canopies are the most efficient for sampling asymptomatic trees. Different from the EPPO procedure is the sampling period and the olive xylem tissues to be used in diagnostic assays. For sampling period, this should consider the environmental temperature range rather than the seasonal period, as recommended by EPPO (late spring to autumn). Thus, sampling can be conducted year-round, avoiding the warmest periods (temperatures above 36°C for weeks), and the coldest periods (temperatures below 10°C for weeks). In addition, xylem tissues of semi-hardwood twigs should be preferred over the basal parts of mature leaves with petioles for detection of the pathogen using serological and molecular assays. For the diagnostic tests recommended by EPPO, DTBIA should be the preferred test for monitoring in *X. fastidiosa*-infected and containment areas, while qPCR or real-time LAMP are appropriate for buffer zones and pathogen-free areas. However, the advantages of real-time LAMP over qPCR make this test more suitable for large-scale *X. fastidiosa* monitoring programmes.

ACKNOWLEDGMENTS

This research received funding from the European Union's Horizon 2020 research and innovation programme, under grant agreement N. 727987 '*Xylella fastidiosa* Active Containment Through a Multidisciplinary Oriented Research Strategy' XF-ACTORS. The authors thank Mariam El-Hajj and Gianfranco Cataldi (CIHEAM Bari) for technical assistance in sample collection, and Elvira Lapedota (CIHEAM Bari) for language editing of this paper. Author contributions: A.M.D., F.S. and F.V. originally conceived the research design and choice of the study sites. M.G., F.V. and G.C. carried out field data acquisition and sampling. S.A.M., D.F., M.G. and F.V. performed diagnostic assays. S.G., F.S. and A.M.D. contributed to data analyses and interpretation; and A.M.D. wrote the original draft of the manuscript. All authors contributed to the manuscript revision and read and approved the submitted version. The authors declare that there are no conflicts of interest.

LITERATURE CITED

Ben Moussa I.E., Mazzoni V., Valentini F., Yaseen T., Lorusso D., D'Onghia A.M., 2016. Seasonal fluctuations of sap-feeding insect species infected by *Xylella fastidiosa* in Apulian olive groves of southern Italy. *Journal of Economic Entomology* 109: 1512–1518. https://doi.org/10.1093/jee/tow123

Boscia D., Altamura G., Ciniero A., Di Carolo M., Dongiovanni C., … Martelli G.P., 2017. Resistenza a *Xylella fastidiosa* in diverse cultivar di olivo. *L'Informatore Agrario* 11: 59–63.

Cavalieri V., Altamura G., Fumarola G., di Carolo M., Saponari M., … Dongiovanni C., 2019. Transmission of *Xylella fastidiosa* subspecies *pauca* sequence type 53 by different insect species. *Insects* 10: 324. https://doi.org/10.3390/insects10100324

De Pascali M., Vergine M., Sabella E., Aprile A., Nutricati E., Nicolì, F., … Luvisi A., 2019. Molecular effects of *Xylella fastidiosa* and drought combined stress in olive trees. *Plants* 8, 437. https://doi.org/10.3390/plants8110437

Djelouah K., Frasheri D., Valentini F., D'Onghia A.M., Digiaro M., 2014. Direct tissue blot immunoassay for detection of *Xylella fastidiosa* in olive trees. *Phytopathologia Mediterranea* 53: 559–564.http://dx.doi.org/10.14601/Phytopathol_Mediterr-14603

Elbeaino T., Valentini F., Abou Kubaa R., Moubarak P., Yaseen T., Digiaro M., 2014. Multilocus sequence typing of *Xylella fastidiosa* isolated from olive affected by "olive quick decline syndrome" in Italy. *Phytopathologia Mediterranea* 53: 533–542.

European Food Safety Authority (EFSA), Delbianco A., Gibin D., Pasinato L., Morelli M., 2022. Update of the *Xylella* spp. host plant database–systematic literature search up to 30 June 2021. *EFSA Journal* 20, e07039. https://doi.org/10.2903/j.efsa.2022.7039

EPPO, 2019. PM 7/24 (4): *Xylella fastidiosa*. *OEPP/EPPO Bulletin* 49: 175–227.

Giampetruzzi A., Morelli M., Saponari M., Loconsole G., Chiumenti M., … Saldarelli P., 2016. Transcriptome profiling of two olive cultivars in response to infection by the CoDiRO strain of *Xylella fastidiosa* subsp. *pauca*. *BMC Genomics* 17: 475. https://doi.org/10.1186/s12864-016-2833-9

Harper S.J., Ward L.I., Clover G.R.G., 2010. Development of LAMP and real-time PCR methods for the rapid detection of *Xylella fastidiosa* for quarantine and field applications. *Phytopathology* 100: 1282–1288 (erratum 2013). https://doi.org/10.1094/PHYTO-06-10-0168

Hopkins D.L., 1981. Seasonal concentration of the Pierce's disease bacterium in grapevine stems, petioles, and leaf veins. *Phytopathology* 71: 415–418.

ISTAT 2021: http://dati.istat.it/index.aspx?lang=en&SubSessionId=0ad38105-3f4e-4157-a8c8-72a502f72067Territory=Puglia

Janse J.D., Obradovic A., 2010. *Xylella fastidiosa*: its biology, diagnosis, control and risks. *Journal of Plant Pathology* 92: S35–S48.https://www.jstor.org/stable/41998754

Loconsole G., Potere O., Boscia D., Altamura G., Djelouah K., ... Saponari M., 2014. Detection of *Xylella fastidiosa* in olive trees by molecular and serological methods. *Journal of Plant Pathology* 96: 7–14. http://dx.doi.org/10.4454/JPP.V96I1.041

Loconsole G., Saponari M., Boscia D., D'Attoma G., Morelli M., … Almeida R.P.P. 2016. Intercepted isolates of *Xylella fastidiosa* in Europe reveal novel genetic diversity. *European Journal of Plant Pathology,* 146: 85–94. https://doi.org/10.1007/s10658-016-0894-x

Martelli G.P., Boscia D., Porcelli F., Saponari M., 2016. The olive quick decline syndrome in south-east Italy: a threatening phytosanitary emergency. *European Journal of Plant Pathology* 144: 235–243. https://doi.org/10.1007/s10658-015-0784-7

Morelli M., García-Madero J.M., Jos Á., Saldarelli P., Dongiovanni C., … Compant S., 2021. *Xylella fastidiosa* in Olive: A Review of Control Attempts and Current Management. *Microorganisms* 9:1771. https://doi.org/10.3390/microorganisms9081771

Nunney L., Ortiz B., Russell S.A., Ruiz Sánchez R., Stouthamer R., 2014. The Complex Biogeography of the Plant Pathogen *Xylella fastidiosa*: Genetic Evidence of Introductions and Subspecific Introgression in Central America. *PLOS ONE* 9: e112463. https://doi.org/10.1371/journal.pone.0112463

Randall J.J., Goldberg N.P., Kemp J.D., Radionenko M., French J.M., … Hanson S.F., 2009. Genetic analysis of a novel *Xylella fastidiosa* subspecies found in the southwestern United States. *Applied and Environmental Microbiology* 75: 5631–5638. https://doi.org/10.1128/AEM.00609-09

Román-Écija M., Landa B.B., Testi L., Navas-Cortés J.A., 2022. Modelling temperature response of *Xylella fastidiosa* strains, and xylem vessel temperature in woody plants. In Abstracts of invited, oral and poster papers of the 16th Congress of the Mediterranean Phytopathological Union, April 4–8, 2022, Limassol, Cyprus (Laura Mugnai ed.), *Phytopathologia Mediterranea* 61: 194.

Santoro F., Gualano S., Favia G., D'Onghia A.M., 2017. IT platform based on smart device and web-application for the survey of *Xylella fastidiosa*. In: *Xylella fastidiosa & the Olive Quick Decline Syndrome (OQDS): a Serious Worldwide Challenge for the Safeguard of Olive Trees* (A.M. D'Onghia, S. Brunel, F. Valentini, ed.), CIHEAM publications, Options Mèditerranéennes, A/121: 47–48.

Saponari M., Boscia D., Nigro F., Martelli G.P., 2013. Identification of DNA sequences related to *Xylella fastidiosa* in oleander, almond and olive trees exhibiting leaf scorch symptoms in Apulia (Southern Italy). *Journal of Plant Pathology* 95: 668.

Schaad N. W., Postnikova E., Lacy G., Chang C. J., 2004. *Xylella fastidiosa* subspecies: *X. fastidiosa* subsp. *piercei*, subsp. nov., *X. fastidiosa* subsp. *multiplex* subsp. nov., and *X. fastidiosa* subsp. *pauca* subsp. nov. *Systematic and Applied Microbiology* 27: 290–300. https://doi.org/10.1078/0723-2020-00263

Schneider K., Van der Werf W., Cendoya M., Mourits M., Navas-Cortés J.A., … Oude Lansink A., 2020. Impact of *Xylella fastidiosa* subspecies *pauca* in European olives. In *Proceedings of the National Academy of Sciences* 117: 9250–9259. https://doi.org/10.1073/pnas.191220611

Strona G., Carstens C.J., Beck P.S.A., 2017. Network analysis reveals why *Xylella fastidiosa* will persist in Europe. *Scientific Reports* 7: 71. https://doi.org/10.1038/s41598-017-00077-z

Wells J. M., Raju B.C., Hung H.-Y., Weisburg W.G., Mandelco-Paul L., Brenner D. J., 1987. *Xylella fastidiosa* gen. nov., sp. nov: Gram-Negative, xylem-limited, fastidious plant bacteria related to *Xanthomonas* spp. *International Journal of Systematic and Evolutionary Microbiology* 37: 136–143. https://doi.org/10.1099/00207713-37-2-136

Yaseen T., Drago S., Valentini F., Elbeaino T., Stampone G., … D'Onghia A.M., 2015. On-site detection of *Xylella fastidiosa* in host plants and in "spy insects" using the real-time loop-mediated isothermal amplification method. *Phytopathologia Mediterranea* 54: 488–496. https://doi.org/10.14601/Phytopathol_Mediterr-15250

Phytopathologia Mediterranea
The international journal of the
Mediterranean Phytopathological Union

Firenze University Press
www.fupress.com/pm

Research Papers

Trunk anatomy of asymptomatic and symptomatic grapevines provides insights into degradation patterns of wood tissues caused by Esca-associated pathogens

Hanns-Heinz KASSEMEYER[1,5,*], Fabian KLUGE[1], Evi BIELER[4], Markus ULRICH[6], Jörg GRÜNER[2,3], Sigfried FINK[2], Markus DÜRRENBERGER[4], René FUCHS[1]

[1] *State Institute for Viticulture and Enology Freiburg, Plant Pathologie & Diagnostics, 79100 Freiburg im Breisgau, Germany*
[2] *Albert-Ludwigs-Universität Freiburg, Faculty of Environment and Natural Resources, Forest Botany, Albert-Ludwigs-Universität Freiburg, 79085 Freiburg im Breisgau, Germany*
[3] *FVA - The Forest Research Institute Baden-Wuerttemberg, Forest Protection, 79100 Freiburg im Breisgau, Germany*
[4] *University Basel, Swiss Nano Science Institute, Nano Imaging Lab, 4056 Basel, Switzerland*
[5] *Albert-Ludwigs-Universität Freiburg, Faculty of Biology, Plant Biomechanics Group and Botanic Garden, 79104 Freiburg im Breisgau, Germany*
[6] *Center for Agricultural Technology Augustenberg (LTZ), Plant health & Pesticide reduction, 76227 Karlsruhe, Germany*
*Corresponding author. E-mail: hanns-heinz.kassemeyer@wbi.bwl.de

Summary. Wood colonizing fungi are specialists that exploit the lignocellulose of cell wall components in host wood cylinders as a carbon sources. Some of these specialized fungi, including *Fomitiporia mediterranea* (Fmed) and *Phaeomoniella chlamydospora* (Pch), cause the disease Esca of grapevine. This disease complex includes grapevine leaf stripe disease (GLSD) of canopies and white rot and black wood streaking in trunks. The present study gained insights into the activity of Esca pathogens in host xylem of the trunk tissues at an anatomical level. Lesions with white rot and brown wood streaking were microscopically analyzed, and the structures of affected tissues were compared with intact xylem. In trunks with white rot, demarcation zones separated intact tissues from the lesions. Immediately adjacent to the demarcation zones, cell wall decomposition initiated in the xylem. At this initial stage, cavities appeared in the secondary cell walls of libriform fibres, which expanded and closely resembled the degradation pattern of soft rot. In the advanced stage, the fibre cell walls were completely decomposed, and the vessels were attacked with a degradation pattern similar to white rot. Only remnants of the xylem elements remained, forming amorphous matrices. These decomposition patterns occurred in field samples and in wood cores artificially infected with Fmed. The obvious compartmentalization of the tissue affected by Fmed indicated a defense reaction in the xylem, according to the CODIT model. In contrast, brown wood streaking affected only small groups of vessels, adjacent libriform fibres and parenchyma. Dark inclusions in cells and tyloses in vessels indicate a defense reaction against the pathogens

OPEN ACCESS

Citation: H.-H. Kassemeyer, F. Kluge, E. Bieler, M. Ulrich, J. Grüner, S. Fink, M. Dürrenberger, R. Fuchs (2022) Trunk anatomy of asymptomatic and symptomatic grapevines provides insights into degradation patterns of wood tissues caused by Esca-associated pathogens. *Phytopathologia Mediterranea* 61(3): 451-471. doi: 10.36253/phyto-13154

Accepted: October 20, 2022

Published: November 25, 2022

Data Availability Statement: All relevant data are within the paper and its Supporting Information files.

Competing Interests: The Author(s) declare(s) no conflict of interest.

Editor: Luisa Ghelardini, University of Florence, Italy.

ORCID:
H-HK: 0000-0001-8675-787X
JG: 0000-0003-1673-5071
RF: 0000-0001-5056-5323

causing brown wood streaking. Artificial inoculation of sterile wood cores with Pch confirmed the contribution of this pathogen to brown wood streaking. This research provides insights into the structural and functional anatomy of intact and infected tissues of grapevines, which clarify the etiology of Esca, and provide new knowledge for developing new approaches to control of this disease complex.

Keywords. White rot, xylem, cell wall degradation, CODIT-model, *Fomitiporia mediterranea, Phaeomoniella chlamydospora*.

INTRODUCTION

Grapevines (*Vitis vinifera*) are woody liana plants, with anatomical structure of the secondary xylem adapted to the climbing vine growth habit. The secondary xylem of woody plants is a niche for specialist fungi that can exploit cell wall lignocellulose as carbon sources as well as ions dissolved in the hydrosystem (Yadeta and Thomma 2013). Secondary xylem of grapevine provides substrates for several wood-colonizing fungi causing grapevine trunk diseases (GTDs), including Esca. Esca has been known for many years (Viala 1926; Mugnai et al., 1999), but in the last three decades, the increasing incidence of this disease has gained economic importance as it causes premature vine decline. (Gramaje *et al*., 2018; Guerin-Dubrana *et al.,* 2019).

Grapevine leaf stripe disease (GLSD) is the most obvious and distinct manifestation of Esca, but GLSD was designated by Surico (2009) as a particular disease complex. There is a consensus that Esca, including GLSD, is caused by colonization of host secondary xylem by wood-destroying fungi. In xylem of affected trunks zones develop with characteristic symptoms of white rot and brown streaking (Viala, 1926; Mugnai *et al,* 1999; Chiarappa, 2000; Surico *et al*., 2000; Surico 2009; Bertsch *et al*., 2013; Bruez *et al*., 2016; 2020; Gramaje *et al*., 2018; Mondello *et al*., 2018; Fischer and Peighami Ashnaei, 2019; Hrycan *et al*., 2020; Vaz *et al*., 2020; Pacetti *et al.,* 2021).

White rot in grapevine trunks is caused by species of *Basidiomycota*, including *Fomitiporia mediterranea* (Larignon and Dubos 1997; Mugnai *et al*., 1999; Cortesi *et al*., 2000; Fischer, 2001; Fischer and Kassemeyer, 2003; Larsson *et al*., 2006; Hofstetter *et al*., 2012; Bertsch *et al*., 2013; Bruez *et al*., 2016; 2020; Baranek *et al*., 2018, Elena *et al*., 2018; Del Frari *et al*., 2019; 2021; Brown *et al*., 2020; Moretti *et al*., 2021; Ye *et al*., 2021; Pacetti *et al*., 2022). Other species of the *Hymenochaetales* are also involved, including *Tropicoporus* sp., *Inonotus* sp., *Fomitoporella* sp. and *Phellinus* sp. (Cloete *et al*., 2015; Brown *et al*., 2020). Two types of white rot of woody plants have been described: (i) selective delignification, where first lignin and then hemicellulose and cellulose are preferentially degraded; and (ii) simultaneous degradation of all cell wall components (Blanchette, 1984; Schwarze, 2007). The causal agents of brown wood streaking include *Ascomycota* species from *Phaeomoniellales* (e.g. *Phaeomoniella chlamydospora* and *Phaeoacremonium minimum* (teleomorph *Togninia minima*)), and *Botryosphaeriales* (e.g. *Diplodia seriata* and *Neofusicoccum parvum*) (Larignon and Dubos 1997; Crous and Gams 2000; Crous *et al*., 2006; Úrbez-Torres *et al*., 2008; 2011; Mutawila *et al*., 2011; Lecomte *et al*., 2012; Fischer *et al*., 2016; Massonnet *et al*., 2017; 2018a; b; Reis *et al*., 2019; Claverie *et al*., 2020).

Restricted areas of brown wood streaking are most likely the result of host defense reactions such as deposition of phenolic compounds in the affected cells (Troccoli *et al*., 2001; Del Rio *et al*., 2004; Bruno and Sparapano, 2006b, 2007; Agrelli *et al*., 2009; Amalfitano *et al*. 2011; Mutawila *et al*., 2011; Lambert *et al*., 2012, 2013; 2012; Calzarano *et al*., 2016; Gómez *et al*., 2016; Pierron *et al*., 2016; Rusjan *et al*., 2017; Spagnolo *et al*., 2017; Stempien *et al*., 2017; Khattab *et al*., 2020; Labois *et al*., 2020, 2021). The numerous studies on the pathogen spectrum of Esca (including GLSD) and on the host plant responses have provided valuable insights into the etiology of the disease. However, detailed knowledge is not available on the degradation patterns caused by these pathogens in xylem of affected grapevines.

The present study aimed to gain insights into the decomposition patterns in grapevine secondary xylem, caused by two Esca pathogens. The architecture of secondary xylem plays a crucial role in the colonization dynamics by the pathogens. For this reason, visualization of the structural and functional anatomy of this host tissue was required. Based on anatomical knowledge, a detailed characterization became possible of the degradation patterns in the secondary xylem of infected trunks. Wood samples from trunks of symptomatic and asymptomatic grapevines, and from wood cores artificially inoculated with *Fomitiporia mediterranea* (Fmed) and *Phaeomoniella chlamydospora* (Pch), were examined using microscopy. Pathogen pathways in trunk tissues and the decomposition processes caused by the fungi were characterized.

MATERIAL AND METHODS

Sampling and macroscopic documentation

In 2019, 2020 and 2021, trunks of *Vitis vinifera* L. "Mueller-Thurgau" and "Pinot noire" vines expressing GLSD symptoms were collected from experimental plots at the State Institute for Viticulture in Freiburg (Germany). Samples of asymptomatic grapevines from the same experimental plots were used for comparisons. The grapevines were planted in 1999 ("Mueller-Thurgau") and 1983 ("Pinot noire"), and were in adjacent plots on loess-clay soil facing southwest, located south of Freiburg (Germany) (47°45'20''N; 7°50'04''E; 280 m altitude). Incidence of Esca was 46.2% for the "Mueller-Thurgau" vines and 27.0% for"Pinot noir". In addition, samples from 2003 were collected from the same field, and further samples were collected between 2014 and 2018 from GLSD-symptomatic and asymptomatic grapevines from different regions of southwestern Germany. Longitudinal and cross-sections were made from the trunks with a band saw and the conditions of the sections were documented. For the microscope analyses, samples each measuring 10 × 8 × 4 mm were excised from wood segments with lesions and intact secondary xylem. Furthermore, approx. 1 cm thick transverse or longitudinal sections of trunks were rubbed with sandpaper of increasing grit size (80 to 480) to produce surfaces for stereo microscope observation.

Artificial inoculation of wood cores

From GLSD-asymptomatic grapevines grown in the vineyard described above, cores of 5 mm diameter were taken from the central areas of sampled trunks using a drill bit (5 mm diam.). Trunk sampling was radial, that all zones of each wood cylinder were included in the drill core. The wood cores were then autoclaved (121°C, 20 min.) to avoid contamination by pathogenic and endophytic fungi. The samples were then placed into Petri dishes (90 mm diam.) containing malt extract agar (30 g malt extract, 5 g yeast extract, 20 g agar, 1 L deionized water), and were inoculated with mycelium pieces from *Fomitiporia mediterranea* M. Fischer, (accession No. 45/23 from *V. vinifera* cv. Mueller-Thurgau Blankenhornsberg) or *Phaeomoniella chlamydospora* Gams W., Crous P., Wingfield M.J & Mugnai L., (accession No. CBS 229.95), and were incubated at 24°C. Samples were taken from the inoculated wood cores 2 to 4 months after inoculation for the preparation of semi-thin wood sections.

Light microscopy

The wood specimens were fixed in 2% glutardialdehyde in phosphate buffer (pH 7.4) in a vacuum for 24 h and then rinsed three times in deionized water. The samples were then dehydrated in an increasing concentration of isopropanol, and then embedded in methacrylate resin. Semi-thin sections (3 µm and 1 µm) were made with a rotation microtomes (LEICA Reichert & Jung Supercut 2065 and 2044). The sections were rinsed overnight in isopropanol to remove the resin, and were then fixed on glass slides and stained in a programmable slide stainer (ZEISS HMS TM Series) with 2 % safranine and 1% acriflavine (12 h), 1% acid-yellow (30 min) and 1% methylene-blue (5 min). For fluorescence microscopy (FM), the slides were stained with 5 µM acridine orange. After staining, the specimens were embedded in Eukitt (O. Kindler). The microscopic analyses were carried out with a light (brightfield) and fluorescence microscope (ZEISS Axio Imager Z1, Carl Zeiss AG), equipped with the optical sectioning system (ZEISS Apotome 2) for structural illumination and a digital imaging system (ZEISS Axiocam MR35, ZEN 2,9 pro imaging processing software, Carl Zeiss AG). The specimens stained with acridine orange were analysed by epifluorescence using the FITC filter combination 38 HE (excitation 460-488 nm, emission 500-557 nm). The overview images of the wood longitudinal and cross sections were acquired using a ZEISS Stereo LumarV12 with motorized x-, y-, z-axis positioning control, and ZEISS Axiocam 305 and ZEN 3.2 pro image processing software (Carl Zeiss AG).

Scanning electron microscopy

Host xylem structure was visualized using a scanning electron microscope (SEM). The surfaces of specimens excised as described above were ground and polished using the Leica EM TXP Target Surfacing System (Leica Microsystems) before being examined in the SEM. After sputtering the specimens with 20 nm of gold, the wood structure was analyzed using a High Resolution Field-Emission (Cold Emission) Scanning Microscope FEI Nova Nano SEM 230 (FEI Company). To preserve the structure of the fungi colonizing the wood tissues, fresh samples were additionally analyzed with a Cryo-SEM (Philips XL30 ESEM, Koninklijke Philips N.V.) equipped with a cryo preparation unit (Gatan Alto 2500, Gatan Inc.). Small slices (approx. 4 mm thick) were excised from trunk segments with a scalpel, and were mounted on specimen holders with low-temperature mounting medium. Cryofixation was carried out using

nitrogen slush (< -185°C) in the cryo-preparation unit. The frozen samples were then sputtered with 20 nm gold in a high vacuum cryo-preparation chamber, and examined with a SE detector operating with an acceleration voltage of 5–10 kV at high vacuum and -150°C. The SEM and Cryo-SEM images were acquired and documented with DISS5 Software from REM-X GmbH Bruchsal.

RESULTS

Anatomy of intact host secondary xylem

In the cross-sections of both varieties, wide-lumened vessels occurred more frequently in the early wood than in the late wood, followed by a number of narrow-lumened vessels (Figure 1, Figure 2 A and B). The lateral walls of the vessels and tracheids were scalariform with bordered pits (Figure 3 A and B; Figure 4 A). In the centre of the pits, the middle lamella and primary cell wall formed a membrane (Figure 3 A). A paratracheal sheath of parenchymatic cells was associated with each vessel, which extended parallel in axial direction (Figure 2 A; Figure 4 A). Semi-bordered pits connected the vessels with the associated cells (vessel associated cells - VACs) of the paratracheal sheaths (Figure 4 A). Longitudinal and tangential sections showed that each vessel formed an axial continuum without transverse walls over a long distance due to the remission of the transverse walls (Figure 4 B). In contrast, the tracheids had compartments whose lateral walls tapered at the apex and formed an end plate (Figure 4 B). A row of thick-walled,

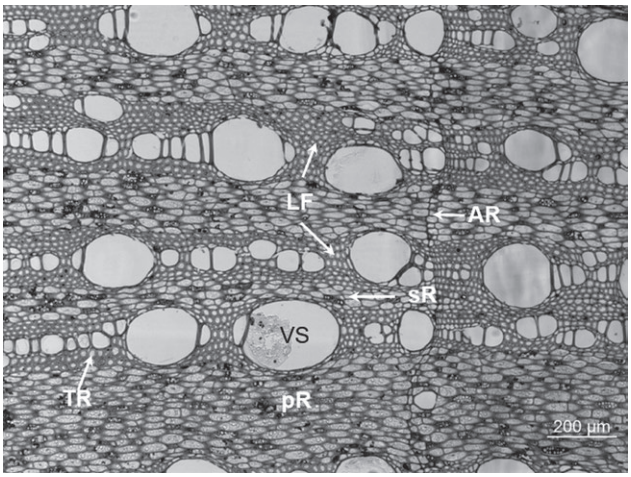

Figure 1. Cross section from intact xylem of *Vitis vinifera* "Mueller-Thurgau". Xylem with vessels (VS), tracheids (TR), libriform fibres (LF) primary wood rays (pR), secondary wood ray (sR), and annual ring (AR) are indicated. Bright field micrograph, 5× magnification.

libriform fibres surrounded the vessels and tracheids, forming a compact bond without intercellular spaces (Figure 5). Radial and tangential sections displayed tapered longitudinal tips of the libriform fibres, similar to the tracheids (Figure 4 B). Fluorescence microscopy revealed the highly fluorescent middle lamella and the different layers of libriform fibre cell wall (cw) in the samples stained with acridine orange. A thick laminated structure (S_2 layer) was visible between a thin outer (primary cell wall and S_1 layer of secondary cell wall) and inner S_3 layer (Figure 5). Pits, each containing a septum

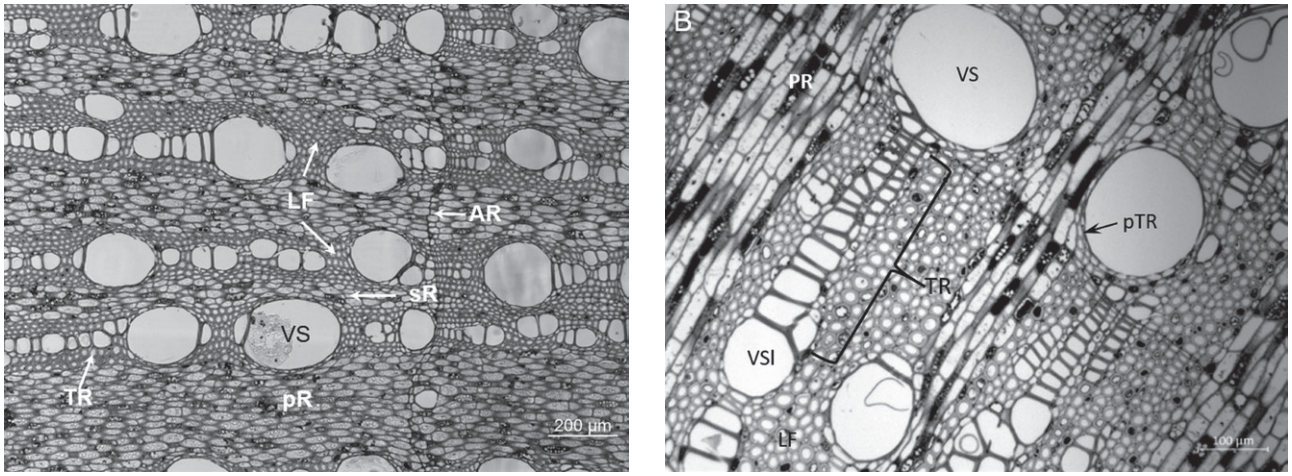

Figure 2. Cross section of intact xylem of *Vitis vinifera* "Mueller-Thurgau". (A) Detail of a wide lumen vessel (VS), paratracheal parenchyma (pTR), tracheids (TR), libriform fibres (LF), parenchyma of a primary wood ray (PR), and parenchyma cells filled with starch grains (ST). Brightfield micrograph, 10× magnification. (B) Series of tracheids within a single annular ring. Wide lumen early wood vessel (VS), and a late wood vessel (VSl). Bright field micrograph, 10× magnification.

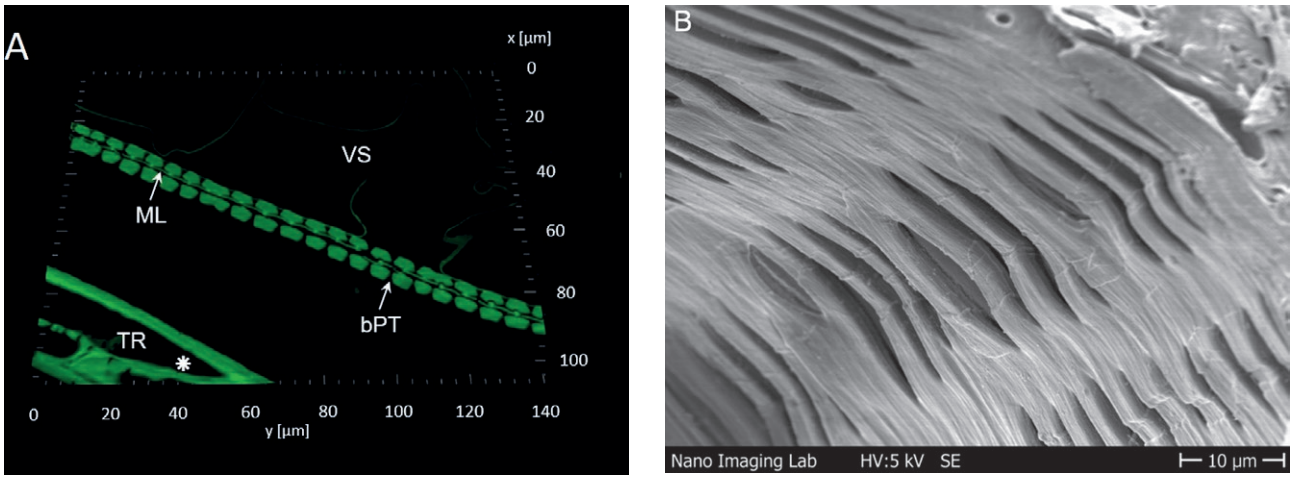

Figure 3. Cross section of asymptomatic xylem of *Vitis vinifera* "Pinot Noir". (A) Scalariform lateral cell wall between tracheids and vessels is formed by bordered pits (bPT). The middle lamella (ML) forms the pit membrane, and a tracheid (TR) with endplate (✱) are indicated. Fluorescence microscopy 3D image, excitation (460–488 nm, emission 500–557 nm). 63× magnification. (B) Vessel with scalariform pitting at the lateral wall. Scanning electron micrograph, 2000× magnification.

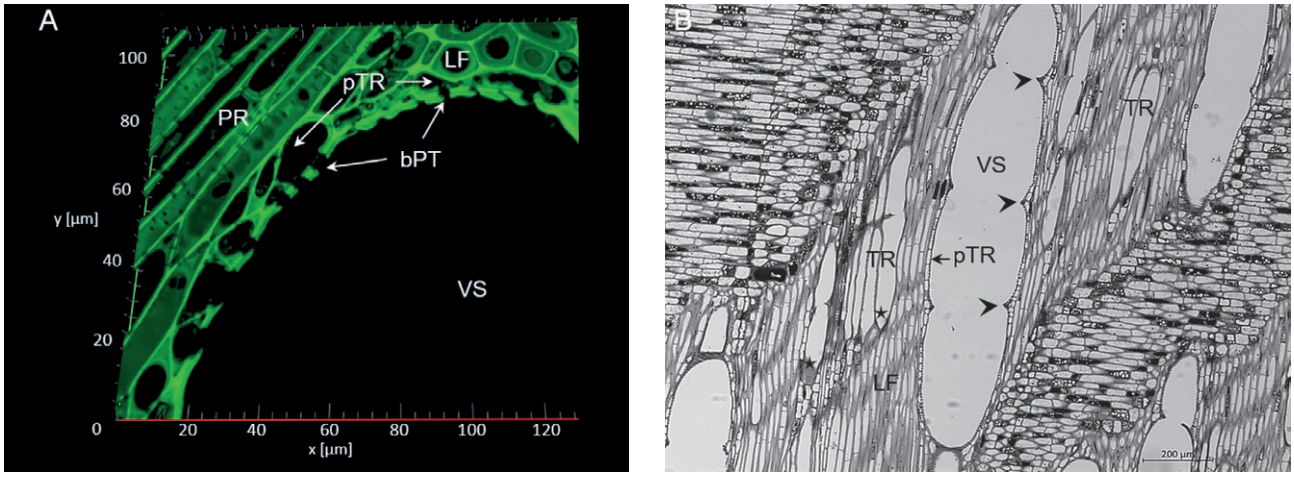

Figure 4. Tracheids (TR) and vessel (VS) from asymptomatic xylem of *Vitis vinifera* "Mueller-Thurgau", longitudinal section. (A) Wide lumen vessel (VS) with semi-bordered pits (bPT), vessels surrounded by a sheath of paratracheal parenchyma (pTR), libriform fibres (LF), and a wood ray (PR) are indicated. Fluorescence microscopy 3D image, 63× magnification. (B) Vessel (VS) with remitted cross walls (arrow heads), tracheids with endplate (★), and paratracheal sheet of parenchyma (pTR). Bright field micrograph, 5× magnification.

composed of the middle lamella, connected the lumina of the libriform fibres to each other and to the adjacent parenchyma cells (Figure 5). The primary and secondary wood rays consisted of elongated parenchymatous cells filled with starch grains (Figures 1; 2 A and B; 4 A; 5).

Trunks with GLSD had different types of lesions in the wood cylinders

In vines with characteristic GLSD canopy symptoms, macroscopically visible necrotic lesions were always evident in longitudinal and cross sections of the trunks. However, plants with GLSD-symptomless canopies also had these lesions. Two different patterns occurred in the trunks: (i) extended lesions with white rot, and (ii) dark brown to black spots in radial sections and streaks in longitudinal sections.

White rot was clearly visible as pale brown zones each with a central ochre amorphous mass (Figure 6). In cross section, black demarcation lines clearly separated the lesions from apparently intact wood (Figures 6; 8 A and B). The lines were more or less concentric, but often showed protuberances with second or third lines, forming distinct compartments (Figure 6). In longitudinal

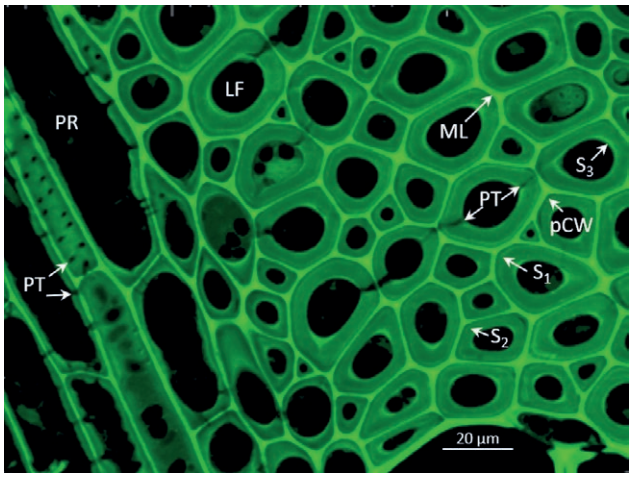

Figure 5. Cross section of libriform fibres (LF) from asymptomatic xylem of *Vitis vinifera* "Mueller-Thurgau". Middle lamella (ML) filling the cell corners, and the primary cell wall (pCW) are indicated. The laminated secondary cell wall, and the exterior S_1-, and the innermost $_3$S- layer enclose the central thick S_2-layer. Pits (PT) connecting fibre cells and parenchyma cells (PR) are also indicated. Fluorescence micrograph 63×, excitation 460-488 nm, emission 500-557 nm.

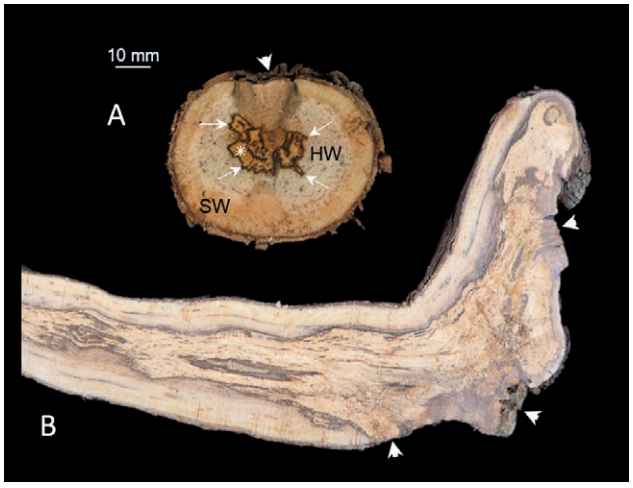

Figure 6. Cross section of a symptomatic (GLSD) xylem of *Vitis vinifera* "Pinot noir" and longitudinal section of a symptomatic (GLSD) *Vitis vinifera* "Mueller-Thurgau" trunk. Xylem with white rot lesions extending from wounds (arrow heads) into the trunk center, protuberances of the demarcation lines (arrows) are clearly visible; in some parts the pathogen has passed the primary demarcation line and colonized further areas of the xylem causing a compartmentalization of the white rot by secondary demarcation lines (✳), sapwood (SW), heartwood (HW). Bright field micrograph 0.8×.

sections, the lesions spread from the top of the trunks to the bases, thinning downwards (Figure 6). The white rot originated from pruning wounds, and from there penetrated into the middle of the trunks (Figure 6).

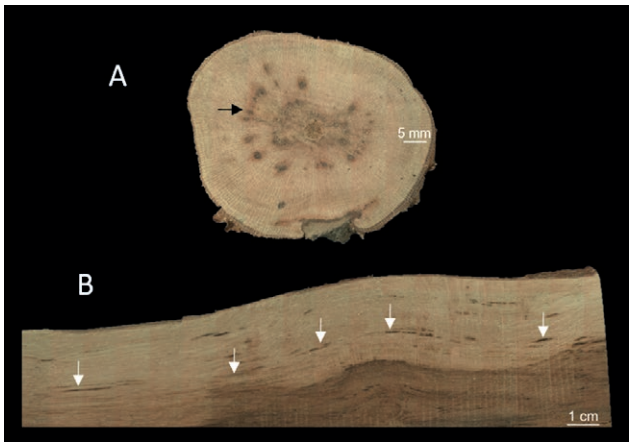

Figure 7. Trunk of a symptomatic (GLSD) *Vitis vinifera* "Mueller-Thurgau". Cross section with a concentric ring of black spots (black arrow); longitudinal section traversed by black streaks visible as a discontinuous line due to the torsional growth (white arrows). Bright field micrograph 0.8×.

In addition, dark brown to black spots were evident in the trunk cross-sections, often arranged in concentric groups or rings. (Figure 7). In longitudinal sections, these spots were as more or less short, dark streaks. However, if an imaginary line was drawn along the dark streaks, they each traversed the trunk in a continuous row for a considerable distance in the longitudinal direction (Figure 7).

Xylem elements naturally affected by white rot had specific decomposition patterns

Light microscopy and SEM visualized the structures of the host tissues and cells in the lesions affected by white rot. In each demarcation zone, the parenchymatic cells and the libriform fibres contained dark inclusions, and the vessels were obstructed by tyloses (Figure 8 A and B). Adjacent to the demarcation line, round cavities were seen in the S_2 layer of each fibre cell wall (Figure 9 A). The pits in the cell walls were frequently dilated and widened toward the unaffected middle lamella (Figure 9 A). These cavities enlarged the closer the cells were to the lesion centres, often became tubular (Figure 9 B). At advanced stages, the entire S_2 layers were decomposed and only the middle lamella and primary cell walls, as well as the S_3 layers, remained (Figure 9 B). In the vessels, vascular tracheids and wood rays resisted degradation until a late stage of decay (Figure 9 C). Observations with Cryo-SEM showed that fungi were evident in affected vessels, in which branched hyphae formed mycelia (Figure 10 A). In the central parts of lesions, a

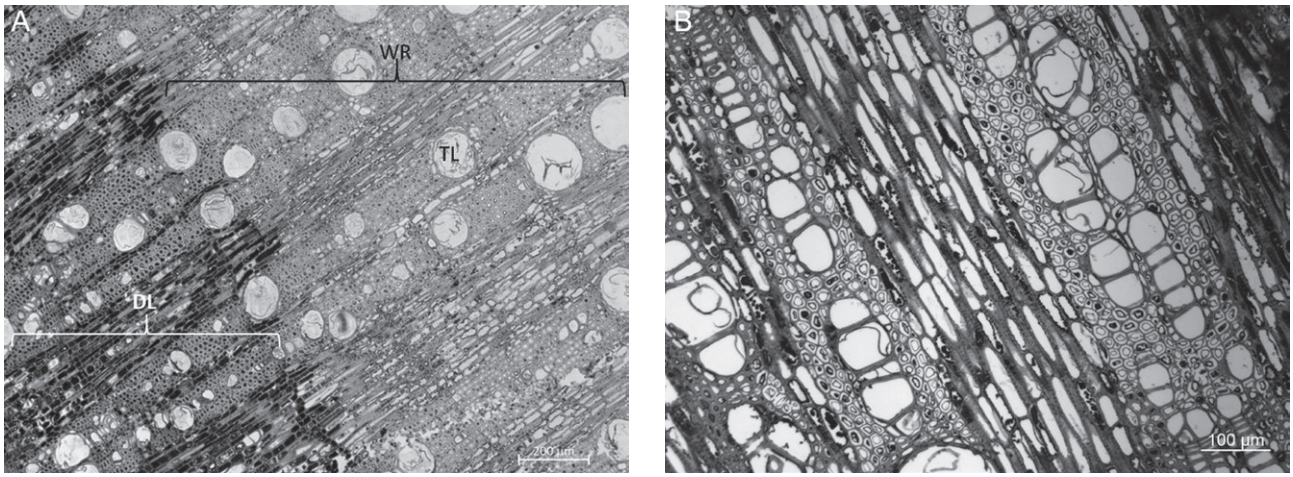

Figure 8. Cross section of the affected by white rot like lesions. (A) Demarcation zone (DL) with darker coloration of xylem elements, inwards with rot like lesion (WR), vessels with tylosis (TL). Bright field 5×. (B) Overview of a white rot like lesion, with decomposed S_2-layer of libriform fibers, the lumen of vessels is filled with tylosis and the parenchyma cells show dark inclusions. Bright field micrograph 10×.

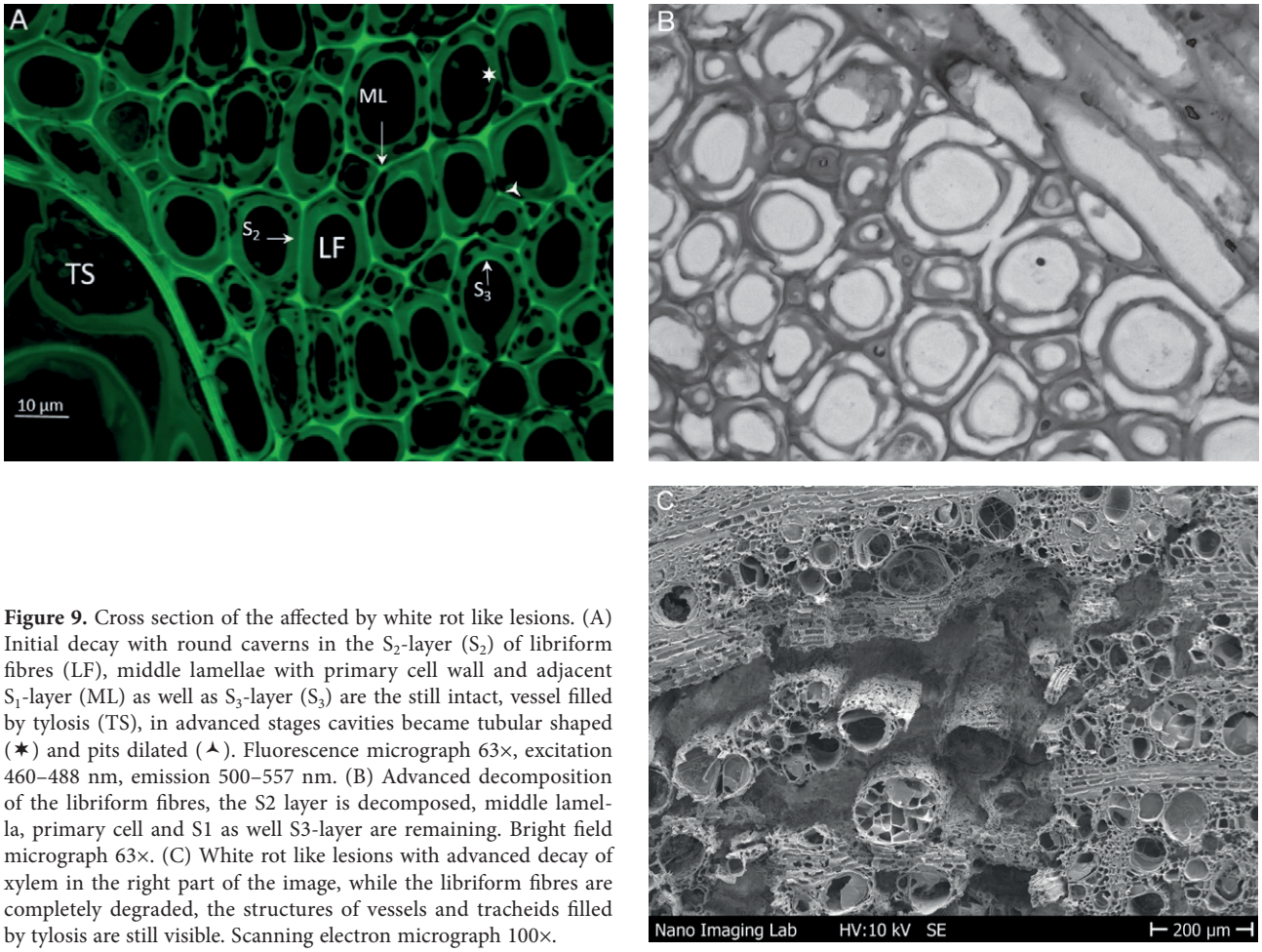

Figure 9. Cross section of the affected by white rot like lesions. (A) Initial decay with round caverns in the S_2-layer (S_2) of libriform fibres (LF), middle lamellae with primary cell wall and adjacent S_1-layer (ML) as well as S_3-layer (S_3) are the still intact, vessel filled by tylosis (TS), in advanced stages cavities became tubular shaped (✶) and pits dilated (⅄). Fluorescence micrograph 63×, excitation 460–488 nm, emission 500–557 nm. (B) Advanced decomposition of the libriform fibres, the S2 layer is decomposed, middle lamella, primary cell and S1 as well S3-layer are remaining. Bright field micrograph 63×. (C) White rot like lesions with advanced decay of xylem in the right part of the image, while the libriform fibres are completely degraded, the structures of vessels and tracheids filled by tylosis are still visible. Scanning electron micrograph 100×.

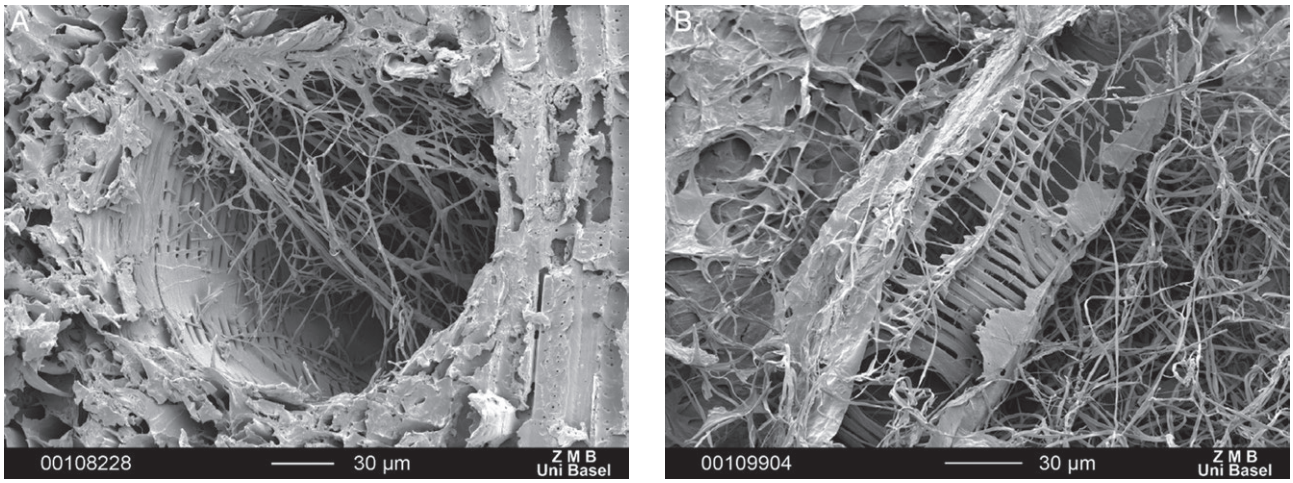

Figure 10. Cross-section of a white rot like lesion, *Vitis vinifera* "Mueller-Thurgau". (A) Vessel with hyphae; Cryo scanning electron micrograph 400×. (B) Mycelium with remains of a vessel. Cryo scanning electron micrograph 500×.

progressive decay of the secondary xylem proceeded, which finally also affected vessels, vascular tracheids and parenchyma. In this final process, a dense mycelium proliferated over the remains of the tissue, and only an amorphous mass remained, from which isolated remnants of the cell walls were recognizable (Figure 10 B). The decomposition patterns of white rot were the same for both *V. vinifera* cultivars.

Brown spots and streaks of naturally infected trunks displayed different decay patterns

In cross-section, the brown spots each consisted of individual groups of vessels with the surrounding tissue located between the wood rays within a growth ring. (Figures 7; 11 A). Examination at higher resolution showed that small spots were also scattered over the entire cross-sections in the secondary xylem, encompassing only one small group of vessels (Figure 11 A and D). Semi-thin sections visualized deposits in the lumina of libriform fibres and parenchyma cells, which caused the dark spots and streaks (Figure 11 A, B and C). In these areas, the vessels were obstructed by tyloses, originating from the VACs and invading through the half-bordered pits of the scalariform cell walls (Supplementary Figure 1). The libriform fibres were partially compressed, and high magnification revealed elongated or crescent-shaped cavities in the cell walls (Figure 12 A and B). In this case, the pits were dilated and often funnel-shaped opened towards the cell lumen (Figure 12 A). Weakly branched hyphae sporadically colonized the vessels and parenchymatic cells of the wood rays (Figure 13 A and B).

Artificial inoculation with Fomitiporia mediterranea *and Phaeomoniella chlamydospora resulted in comparable lesion patterns as in the field*

Within 4 d post inoculation (dpi), Fmed had colonized the plant sample surfaces, and 16 dpi ochercoloured mycelium completely covered the specimen cores. At this stage, fine hyphae permeated the S_2 layers of fibres, which could be distinguished from the pits by their sinuous structure (Figure 14 A). Two months after inoculation, Fmed grew within the cell walls of the libriform fibres and decomposed the S_2 layers, forming round caverns in an identical pattern as seen in the cross sections of samples taken from the field (Figure 14 B). In tangential section, caverns were aligned in a helical pattern at an angle of 50° to 60° in the cell walls of the libriform fibres (Figure 14 C). This alignment was also observed in cross sections when examining round cavities in cell walls at different focal planes (Supplementary Figure 2 Video). Four months after inoculation, advanced decomposition of the S_2 layers occurred (Supplementary Figures 3 A, B, C). In general, the pattern of cell wall decomposition of libriform fibres observed in this study was consistent with that found in white rot lesions of trunks sampled from the field.

In cores inoculated with Pch, isolated hyphae occurred in the secondary xylem two months after inoculation (Figure 15 A). In tangential and cross sections, falciform caverns occurred in each S_2 layer near the middle lamella, and these were similar to those in samples from the field (Figure 15 A; Supplementary Figure 4). In contrast to the cores from plants inoculated with Fmed, the wood inoculated with Pch was only slightly decom-

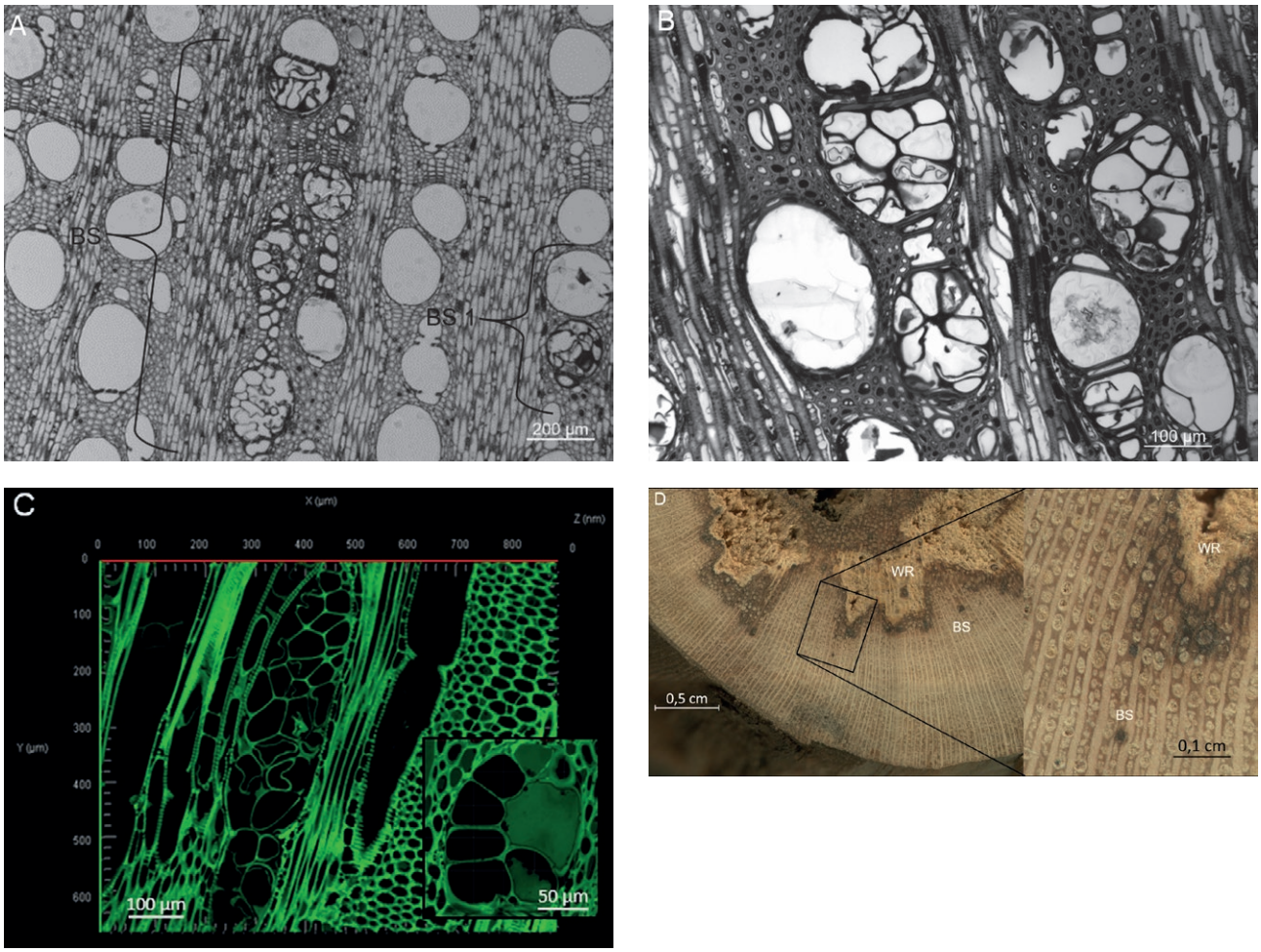

Figure 11. Cross section of black spot, *Vitis vinifera* "Mueller-Thurgau". (A) Wood cylinder, overview with black spots comprising a couple of vascular bundles (BS) and a single vessel interspersed in intact xylem (BS 1); bright field Plan-Neofluar 5×. (B) Vessels obstructed by tylosis in black spots, libriform fibres and parenchyma filled with dark inclusions and slightly deformed. Bright field micrograph 10×. Insert: Cross section of a vessel in a black spot obstructed with tylosis; 3D Fluorescence micrograph 25×. (D) Trunk of a symptomatic *Vitis vinifera* "Mueller-Thurgau", cross section with a small spot encompassing one vessel, whit rot (WR) in the center. Bright field micrograph 0.8×, display window Bright field micrograph 0.8×.

posed, although mycelium had spread on the wood core surfaces, and hyphae had invaded the vessels (Figure 15 B). As in the naturally infected samples, dark deposits filled the libriform fibres and parenchyma cells, and tylosis obstructed the vessels (Supplementary Figure 5).

DISCUSSION

The wide lumen vessels and vascular tracheids of the two grapevine varieties exhibited characteristics of a ring-porous xylem, as described by Carlquist (1985; 2010) and Vazquez-Cooz and Mayer (2004). Vessels and tracheids formed axial continua from top to bottom, which provides high conductivity of plant hydrosystems (Bortolami *et al*., 2021). Plant vessels can reach lengths of several meters in early wood (Hacke and Sperry, 2001). Measurements of vessel length for *Vitis labrusca* by Zimmermann and Jeje (1981) showed a minimum length of 1 m in >70% of samples. The structure of the vessels found in both cultivars in the present study indicates that long open vessel sections also occur in *V. vinifera*. Pronounced primary and secondary wood rays with parenchyma (RP) cells radially traversed the secondary xylem, as is typical of lianas. (Carlquist 1985, 2010; Gallenmüller *et al*., 2001; Rowe and Speck, 2004; Masselter and Speck, 2008; Angyalossy *et al*., 2012). In addition, axial strands of vessel associated parenchy-

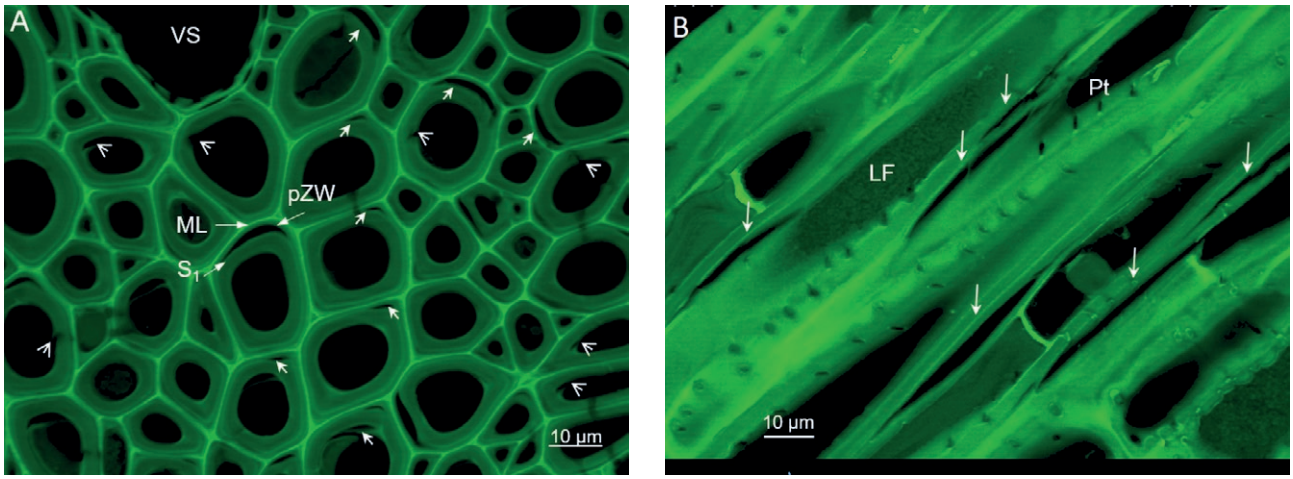

Figure 12. Libriform fibres (LF) in black spots and streaks of *Vitis vinifera* "Mueller-Thurgau". (A) Cross section of libriform fibres with falciform detachments (arrows) of the primary cell wall (pZW) from the S_1-layer and dilated pits (arrow heads), middle lamella (ML) is intact. Fluorescence micrograph 63×, excitation 460–488 nm, emission 500–557 nm. (B) Longitudinal section of libriform fibres, falciform cell wall detachments in axial direction, pits (Pt) interconnect the fibres. Fluorescence micrograph 63×, excitation 460–488 nm, emission 500–557 nm.

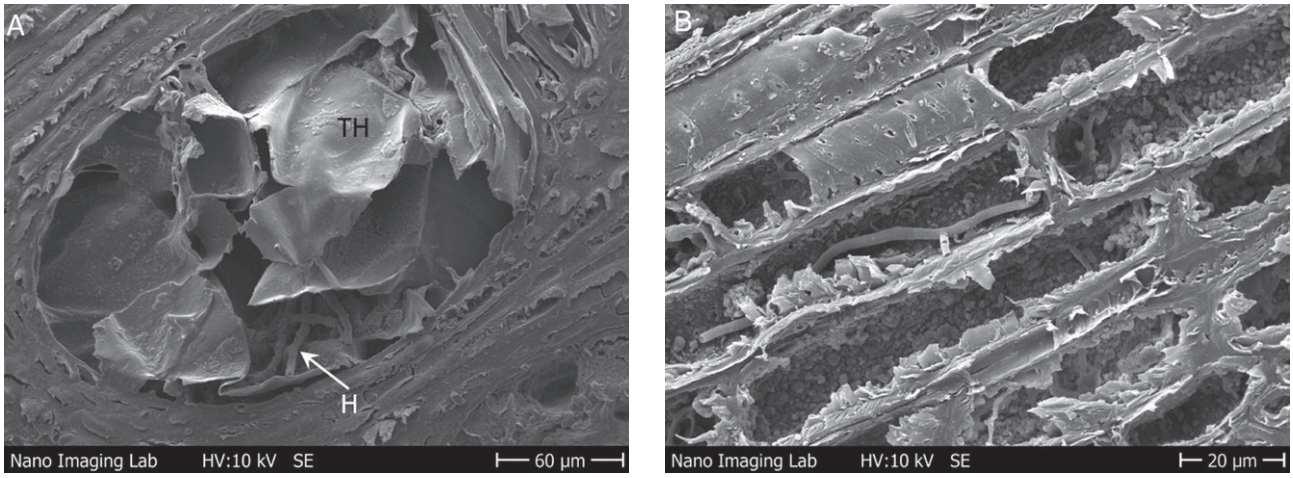

Figure 13. Details of black spots and streaks on *Vitis* vinifera "Mueller-Thurgau"; (A) cross-section, vessel with hyphae (H) and tylosis (TH). Cryo scanning electron micrograph 400×; B longitudinal section, parenchyma cells of the wood ray with hyphae. Cryo scanning electron micrograph 1000×.

ma cells (VACs) formed paratracheal sheaths of living cells, as described in woody plants by Carlquist (2010) and Morris *et al* (2016 a; b; 2018). The parenchyma cells of RP and VACs fulfill important functions in secondary xylem, including: (i) sink and source for assimilates, mainly starch, remobilized in spring; (ii) regeneration into secondary cambium to heal injuries; (iii) refilling vessels; (iv) bidirectional transport of water, ions and organic molecules between the symplastic and the apoplastic elements of the secondary xylem; and (v) defense response after infections by pathogens (Carlquist, 2012; Holbroock and Zwieniecki, 1999; Pfautsch *et al.,* 2015 a; b; Morris *et al*., 2016 a; b; Morris and Jansen 2016; Morris *et al.,* 2018; Secchi *et al*., 2017). Numerous pits interconnect secondary xylem elements and ensure exchange and communication between the living cells of RP and VACs and the apoplastic vessels, tracheids and libriform fibres. Of particular importance are the bordered pits at the lateral scalariform wall of vessels and tracheids and the half-bordered pits at the boundaries with RP and VACs. They form an interface between apoplastic xylem elements and the symplast, constituting a three-dimensional network in the plant trunk that extend to the shoot tips (Kedrov, 2013; Sano *et al*., 2013; Donaldson *et*

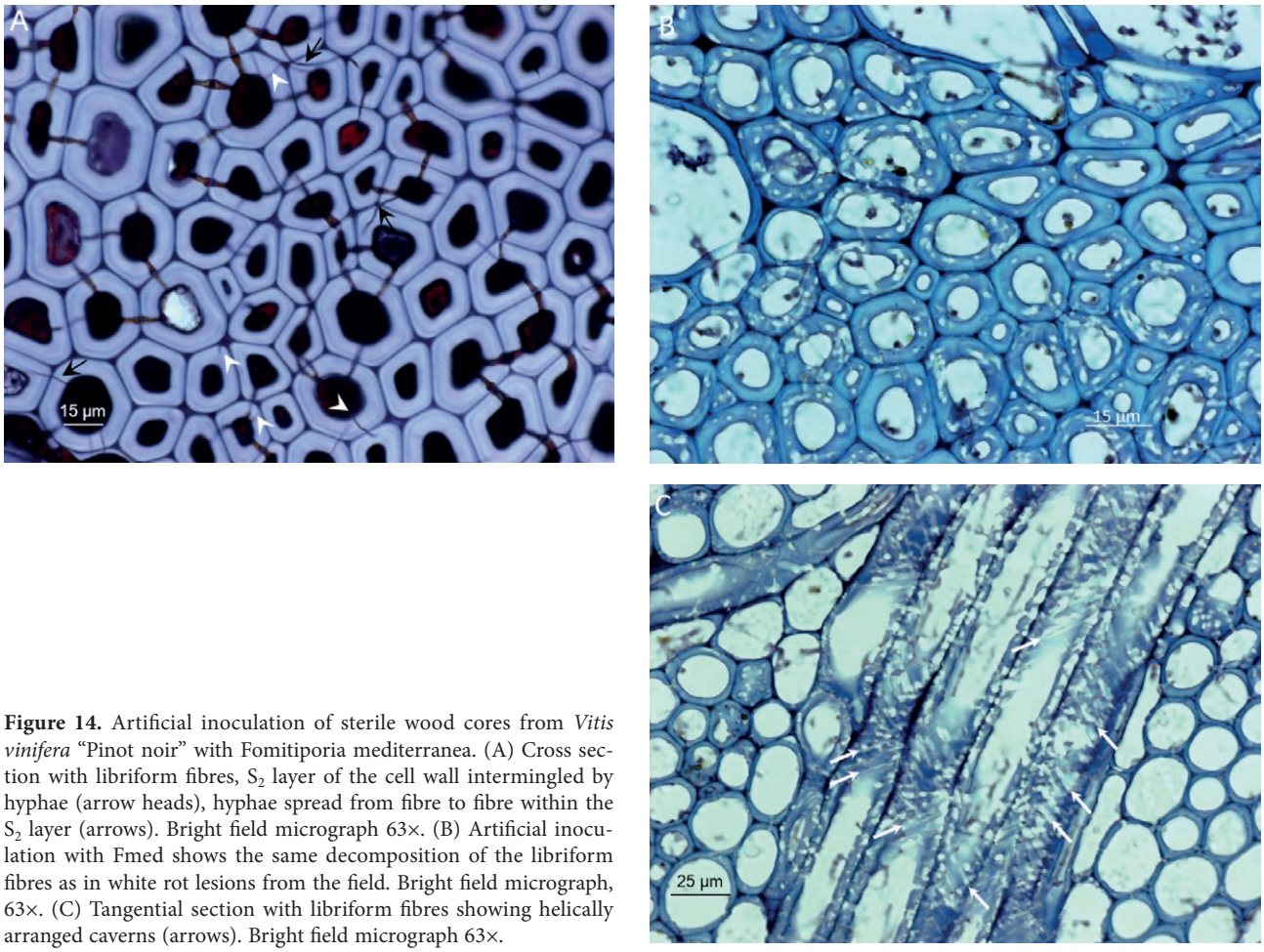

Figure 14. Artificial inoculation of sterile wood cores from *Vitis vinifera* "Pinot noir" with Fomitiporia mediterranea. (A) Cross section with libriform fibres, S_2 layer of the cell wall intermingled by hyphae (arrow heads), hyphae spread from fibre to fibre within the S_2 layer (arrows). Bright field micrograph 63×. (B) Artificial inoculation with Fmed shows the same decomposition of the libriform fibres as in white rot lesions from the field. Bright field micrograph, 63×. (C) Tangential section with libriform fibres showing helically arranged caverns (arrows). Bright field micrograph 63×.

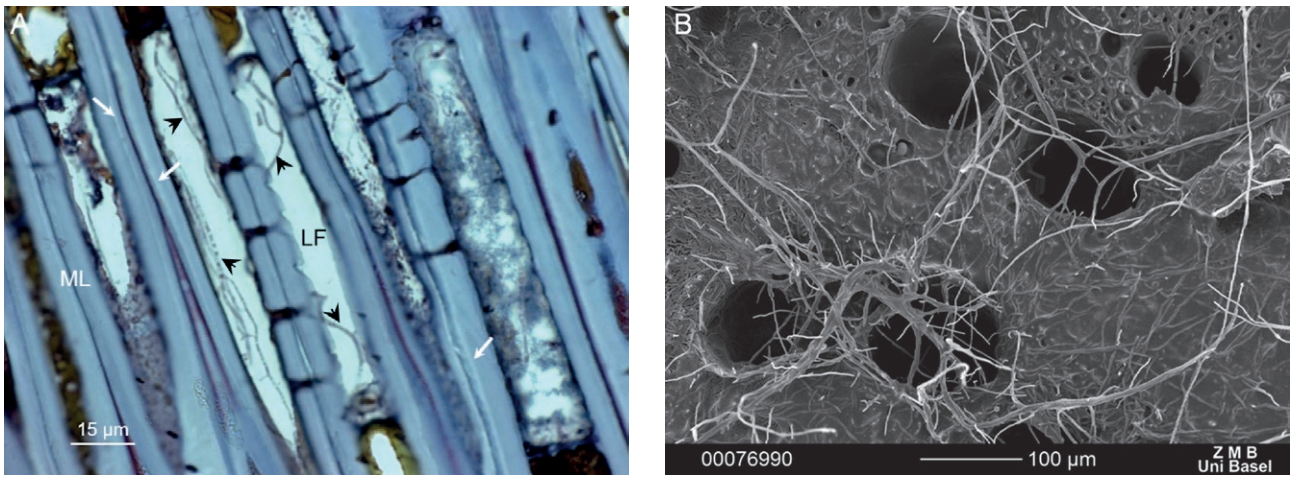

Figure 15. Artificial inoculation of sterile wood cores from *Vitis vinifera* "Pinot noir" with *Phaeomoniella chlamydospora*. (A) Libriform fibres (LF), longitudinal section, growing hypha (arrowheads) in axial direction, beginning detachment of the S_2 layer from the middle lamella (ML) and outer cell wall (arrows), Bright field micrograph 63×. (B) Surface of an inoculated core colonized by Pch, hyphae entering the vessels. Scanning electron micrograph 100×.

al., 2018; Morris *et al*.; 2018; Gao *et al*., 2020; Zhang *et al*., 2020; Kaack *et al*., 2021; Koddenberg *et al*., 2021;).

Structural and functional studies have shown that the vascular architecture of grapevine trunks facilitates dissemination of wood-colonizing pathogens. The wide lumened vessels provide highways for wood-colonizing pathogens to pass axially through trunks (Pouzoulet *et al*., 2014, 2017, 2020; Bruez *et al*., 2020). Longitudinal sections through trunks verified the large-scale colonization of secondary xylem and confirmed that wounds are entry ports for wood-degrading pathogens (Rolshausen *et al*., 2010; Travadon *et al*., 2013; 2016; Claverie *et al*., 2020; Martinez-Diz *et al*., 2020). In addition, the scalariform cell walls facilitate the passage of pathogen hyphae from vessels into adjacent libriform fibres, where the hyphae proliferate laterally via the numerous pits.

The extensive lesions observed in the secondary xylem macroscopically resembled typical white rot of woody plants (Blanchette 1984; Schwarze, 2007; Goodell *et al*., 2008; Daniel et al., 2004; 2014; Hastrup *et al*., 2012). However, greater magnification revealed decomposition patterns in the affected zones of the secondary xylem that were distinctly different from the pattern described for white rot. The first signs of cell wall degradation became evident in the libriform fibres, whose structured walls (middle lamella, primary and secondary cell wall) corresponded to the general pattern of this cell type. Of particular importance for the characterization of the degradation pattern was the thickened secondary cell walls of the libriform fibres, with S_1, S_2, and S_3 layers, generally composed of cross-linked cellulose, hemicellulose, lignin, and pectins in varying ratios (Plomion *et al*., 2001, Schuetz *et al*., 2013, Rathgeber *et al*., 2016; Schneider *et al*., 2017). In the S_2 layers of woody plants, helically arranged cellulose fibrils predominate in most species. The round caverns found here in the S_2 layer of libriform fibres at the periphery of lesions did not correspond either selective delignification or simultaneous degradation of all cell wall components, but were typical of soft rots (Schwarze *et al*., 1995; Worrall *et al*., 1997; Schwarze and Fink, 1998; Schwarze, 2007). In the initial stage of lesions, the cavities extended at an acute angle to the long axis, a conclusive indication that initially the helically oriented cellulose fibrils in the S_2 layers were preferentially degraded, as is typical for soft rot (Schwarze, 2007; Schneider *et al*., 2017). The completely eroded S_2-layers at the advanced stage also indicated soft rot, as the more lignified components of the cell walls such as the middle lamella, the primary cell walls, the S_1 layer and the inner S_3 layer, remained intact. In the final stage, the more lignified parts of the cell walls, such as the middle lamella, the primary and the S_1 and S_3 layers of the secondary cell walls, were also affected, while the vessels and tracheids remained intact for longer. Complete disintegration of all xylem elements including VACs and RP in the centres of lesions can be attributed to simultaneous degradation of lignocellulose in the final stage of white rot, as described by Blanchette (1984) and Schwarze (2007).

The existing classification of Esca affected trunks into white rot does not adequately reflect the decomposition pattern observed in the present study, in particular since the binary classification into white rot and brown rot has recently been further developed in favour of a differentiated classification of wood decay mechanisms. It has been proposed that the molecular patterns of enzymes expressed by wood decomposing fungi, such as carbohydrate active enzymes (CAZymes), peroxidases (PODs), and laccases, should be used to characterize decomposition patterns (Riley *et al*., 2014; Schilling *et al*., 2015, 2020). These current models show a gradient between phenotypes in which lignin degrading PODs with high selectivity for lignin predominate, and those with high activity of CAZymes, which are highly selective for carbohydrates. Based on the enzyme machinery described in publications on lignocellulose-degrading fungi (Bruno and Sparapano 2006a, Alfaro *et al*. 2014, Ohm *et al*. 2014, Riley *et al*. 2014, Floudas *et al*. 2015, Morales-Cruz *et al*. 2015, Massonette *et al*. 2018a; b; Hage and Rosso 2021), and the microscopic analysis of the degradation pattern described in the present paper, it can be concluded that the lesions caused by Fmed are the result of a transition from soft rot to white rot. The sequence of decomposition steps observed here suggests sequential activity of lignocellulose-degrading enzymes in the course of host tissue colonization by Fmed. Future studies should verify whether Fmed and related Esca pathogens first engage CAZymes to utilize the readily degradable cellulose in the S_2 cell wall layer as resources for subsequent depolymerization of the more persistent lignin by PODs and laccases.

A distinctly different pattern was seen in the lesions with brown spots or streaks, which are clearly attributed to brown wood streaking. Microscopic analysis of the spots showed no evidence of intensive degradation in the cell walls of vessels, tracheids, and libriform fibres, even though lignocellulose-degrading enzymes have been found in pathogens that cause brown wood streaking, such as *D. seriata* and *N. parvum* (Czemmel *et al*., 2015; Morales-Cruz *et al*., 2015; Fischer *et al*., 2016; Stempien *et al*., 2017; Massonnet *et al*., 2018 a; b; Garcia *et al*., 2021). These results indicate that the pathogens use the cell wall lignocellulose as a nutrient substrate to a minor extent. Rather, the presence of hyphae

in the parenchyma of the lesions indicates exploitation of alternative carbon sources in living cells. The clusters of putative amylases and plant invertases found in the *N. parvum* genome (Czemmel *et al*., 2015) imply that Pch also abundantly degrades starch stored as a reserve in the parenchyma of wood rays. The extent of brown wood streaking from top to bottom, which is limited to small vessel groups or individual vessels, is evidence that the causing agent spread in the vascular system primarily in an axial direction. These observations are in accordance with those of Bruez *et al*. (2020), who suggested top-to-bottom spread of Pch in grapevine trunks. Vessels are grouped into functional vascular bundles forming individual leaf tracks extending through stems and corresponding shoots into the leaves (Pratt 1974; von Arx *et al*., 2013). Consequently, a vascular bundle with brown wood streaking is in direct contact with a particular shoot and its associated leaves in the host canopy. In this way, toxic or stress-inducing metabolites, and effectors secreted by Esca pathogens in the affected vascular bundles, can be transported *via* the individual leaf track into the corresponding shoots and leaves. This explains the observation, at least in the early stages of GLSD, that symptoms often occur only on single shoots. The scattered single brown stained vessels in secondary xylem can be assigned to brown wood streaking, although they were not visible macroscopically. Lack of visibility also explains the results of Vaz *et al*. (2020), who detected Pch and other agents of brown wood streaking in apparently intact wood, using µ-CT analyses.

The obstruction of vessels by tyloses in both white rot and brown wood streaking has also been described by previous authors (Troccoli *et al*., 2001; Del Rio *et al*., 2001; Edwards *et al*., 2007; Mutawila *et al*., 2011; Fischer and Kassemeyer, 2012; Pouzoulet *et al*., 2014; Gomez *et al*., 2016; Pouzoulet *et al*., 2017; Jacobsen *et al*., 2018; Bortolami *et al*., 2019; 2021; Claverie *et al*., 2020). Tyloses are, among other functions, also respond to abiotic and biotic stress in secondary xylem, and have also been observed in grapevine in response to other vascular colonizing pathogens such as bacteria (Sun et al., 2006; 2008; 2017; Leśniewska *et al*., 2017; Kashyap, 2021). Massonnet *et al*. (2017) showed that infection of grapevine trunks by *Neofusicoccum parvum* triggered a defense response in the leaves, so this may also occur in the secondary xylem colonized by the pathogens.

The dark discoloration of the demarcations encircling white rot, and the vessels affected by brown wood streaks caused by inclusions of phenolics in the cell lumina, can be considered as defense responses in host tissues. Phenols are generally expressed in host-pathogen interactions by inducing transcriptional and biosynthetic machinery of the phenylpropanoid pathway, and these compounds serve a number of functions in plant innate immunity (Boller and Felix 2009; Yadav *et al*., 2021). As a result, numerous hydroxycinnamic acids, stilbenes, and high molecular weight condensation products accumulate in affected xylem (Troccoli *et al*., 2001, Del Rio *et al*., 2004; Bruno and Sparapano, 2006b; 2007; Agrelli *et al*., 2009; Amalfitano *et al*., 2011; Mutawila *et al*., 2011; Lambert *et al*., 2012; 2013; Calzarano *et al*., 2016; Gómez *et al*., 2016; Pierron *et al*., 2016; Rusjan *et al*., 2017; Spagnolo *et al*., 2017; Stempien *et al*., 2017; Khattab *et al*., 2020; Labois *et al*., 2020; 2021). Whether the demarcation lines described here in white rot were solely due to a host response to the pathogen, or whether melanized hyphae of the pathogen also accumulate, could not be clarified.

The present anatomical study of Esca-affected trunks has shown that analysis of structural changes using microscopy contributes to a deeper understanding of the molecular and biochemical processes in Esca host-pathogen interactions. Therefore, for complete elucidation of the etiology of Esca, including GLSD, host and pathogen structural interactions must be considered along with the molecular and biochemical aspects of this pathosystem.

CONCLUSIONS

Comparing the colonization and degradation patterns of the two pathosystems Fmed and Pch in grapevine, fundamental differences between the two emerged. The largely open vascular system in grapevine trunks enables dynamic adaxial pathogen spread direction from top to bottom. In the network of xylem elements, a dense system of pits facilitates lateral spread of Fmed, causing extensive white rot lesions. Cell wall decomposition in the xylem by Fmed indicates an intermediate pattern. Initial soft rot with predominant cellulose decomposition is followed by white rot with simultaneous breakdown of the lignocellulose. Since the final stage of secondary xylem infection by Fmed and related pathogens resembles typical white rot, this term may be further used for this trunk symptom of Esca. In lesions caused by Fmed, there was clear compartmentalization with demarcation zones separating intact secondary xylem from tissues progressively decayed by soft rot first, and then by white rot. This is in accordance with the CODIT model (Compartmentalization of Damage/Dysfunction in Trees), which relates primarily to defense responses against wood-destroying pathogens in the secondary xylem of trees (Shigo 1984, Morris *et al*., 2016b;

2020). Further studies at structural, biochemical and molecular levels are required to clarify this intermediate status of the degradation pattern of Fmed and how it fits into the CODIT model.

The artificial inoculations of wood cores with Pch are evidence for the causal relationship of this pathogen with brown wood streaking. The present study has shown that brown wood streaking in grapevine plants is not a consequence of significant cell wall decomposition, but rather a reaction of host tissues to infection by this pathogen. In order to clarify the role of Pch in the etiology of Esca, particularly GLSD, further in-depth studies are required on the induction of multiple resistance responses in affected xylem areas, and on biosynthesis and acropetal transport of potential stress factors and toxins.

ACKNOWLEDGEMENTS

The authors acknowledge the Michael Fischer Julius-Kühn-Institute for providing the cultures of Fmed and Pch. Sabine Diener of the Albert-Ludwigs-Universität Freiburg, Faculty of Environment and Natural Resources, Forest Botany provided excellent preparation of semithin sections for microscopy. This research was partly funded by a grant of the European Innovation Partnership for Agricultural Productivity and Sustainability (EIP-Agri), and funding from the Baden-Württemberg State Ministry for Rural Areas, Nutrition and Consumer Protection.

LITERATURE CITED

Agrelli D., Amalfitano C., Conte P., Mugnai L., 2009. Chemical and spectroscopic characteristics of the wood of *Vitis vinifera* "Sangiovese" affected by esca disease. *Journal of Agricultural and Food Chemistry* 57 (24): 11469–11475. DOI: 10.1021/jf903561x

Alfaro M., Oguiza J.A., Ramírez L., Pisabarro A.G., 2014. Comparative analysis of secretomes in basidiomycete fungi. *Journal of Proteomics* 102: 28–42. DOI: 10.1016/j.prot.2014.03.001

Amalfitano C., Agrelli D., Arrigo A., Mugnai L., Surico G., Evidente A., 2011. Stilbene polyphenols in the brown red wood of *Vitis vinifera* "Sangiovese" affected by "esca proper" *Phytopathologia Mediterranea* 50: S224–S235. DOI: 10.14601/Phytopathol_Mediterr-9720

Angyalossy V., Angele G., Pace M.R., Lima A.C., Dias-Leme C.L., … Madero-Vega C., 2012. An overview of the anatomy, development and evolution of the vascular system of lianas. *Plant Ecology & Diversity* 5(2): 167–182. DOI: 10.1080/17550874.2011.615574.

Baránek M., Armengol.J., Holleinová V., Pečenka J., Calzarano F., … Eichmeier A., 2018. Incidence of symptoms and fungal pathogens associated with grapevine trunk diseases in Czech vineyards: First example from a north-eastern European grape-growing region. *Phytopathologia Mediterranea* 57(3): 449–458. DOI: 10:14601/Phytopathol_Mediterr-22460.

Bertsch C., Ramírez-Suero. M., Maginin-Robert M., Larignon P., Chong J., … Fontaine F., 2013. Grapevine trunk diseases: Complex and still poorly understood. *Plant Pathology* 62(2): 243–265. DOI: 10.1111/j.1365-3059.2012.02674.x.

Blanchette R.A., 1984. Screening wood decay by white rot fungi for preferential lignin degradation. *Applied and Environmental Microbiology* 48(3): 646–653. DOI: 10.1128/aem.48.3.647-653.1984

Boller T., Felix G., 2009. A renaissance of elicitors: Perception of microbe associated molecular patterns and danger signals by pattern-recognition receptors. *Annual Review of Plant Biology* 60: 379–406. DOI: 10.1146/annurev.arplant.57.032905.105346

Bortolami G., Gambetta G.A., Delzon S., Lamarque L.J., Pouzoulet J., … Delmas C.E.L., 2019. Exploring the hydraulic failure hypothesis of esca leaf symptom formation. *Plant Physiology* 181: 1163–1174. DOI: 10.1104/pp.19.00591

Bortolami G., Farolfi E., Badel E., Burlett R., Cochard H., … Delmas C.E.L., 2021. Seasonal and lon-term consequences of esca grapevine disease on stem xylem integrity. *Journal of Experimental Botany* 72(10): 3914–3928. DOI: 10.1093/jxb/erab117.

Brown A.A., Lawrence D.P., Baumgartner K., 2020. Role of basidiomycete fungi in the grapevine trunk disease esca. *Plant Pathology* 69(2): 205–220. DOI: 10.1111/ppa.13116.

Bruez E., Vallance J., Gerbore J., Lecomte P., Da Costa J.P., … L., Rey P., 2014. Analyses of the temporal dynamics of fungal communities colonizing the healthy wood tissue of esca leaf-symptomatic and asymptomatic vines. *PLoS ONE* 9(5): e5928. DOI: 10.1371/journal.pone.0095928.

Bruez E., Baumgartner K., Bastien S., Travadon R., Guérin-Dubravna L., ReyP., 2016. Various fungal communities colonise the functional wood. *Australian Journal of Grape and Wine Research* 22: 288–295. DOI: 10.1111/ajgw.12209

Bruez E., Vallance J., Gautier A., Laval V., Compant S., … Rey P., 2020. Major changes in grapevine wood microbiota are associated with the onset of esca, a devastating trunk disease. *Environmental Micro-*

biology 22(12): 5189–5206. DOI: 10.1111/1462-2920.15180.

Bruno G., Sparapano L., 2006a. Effects of three esca-associated fungi on *Vitis vinifera* L.: III Enzymes produced by the pathogens and their role in fungus-to-plant or in fungus-to-fungus interactions. *Physiological and Molecular Plant Pathology* 69: 182–194. DOI:10.1016/j.pmpp.2007.04.006

Bruno G., Sparapano L., 2006b. Effects if three esca-associated fungi on *Vitis vinifera* L.: II. Characterization of biomolecules in xylem sap and leaves of healthy and diseased vines. *Physiological and Molecular Plant Pathology* 69: 195–208. DOI: 10.1016/j.pmpp.2007.04.007.

Bruno G., Sparapano L., 2007. Effects if three esca-associated fungi on *Vitis vinifera* L.: V. Changes in the chemical and biological profile of xylem sap from diseased "Sangiovese". *Physiological and Molecular Plant Pathology* 71: 210–229. DOI: 10.1016/j.pmpp.2008.02.005.

Calzarano F., D´Agostino V., Pepe A., Osti F., Della Pelle F., … Di Marco S., 2016. Patterns of phytoalexins in the grapevine leaf stripe (esca complex) / grapevine pathosystem. *Phytopathologia Mediterranea* 55: 410–426. DOI: 10 (3):14601/Phytopathol_Mediterr-18681.

Carlquist S., 1985. Observations on functional wood histology of vine and lianas: Vessel dimorphism, tracheids, narrow vessels and parenchyma. *Aliso* 11(2): 139–157. https://scholarship.claremont.edu/aliso/vol11/iss2/3

Carlquist S., 2010 Comparative wood anatomy. *Systematic, Ecological and Evolutionary Aspects of Dicotyledone Wood*. 2nd ed. Springer series in wood science Springer-Verlag Heidelberg. Germany SSN 1431-8563-0.

Carlquist S., 2012. How wood evolves: a new synthesis. *Botany* 90: 901–940. DOI:10.1139/B2012-048

Claverie M., Notaro M., Fontaine F., Wery J., 2020. Current knowledge on grapevine trunk diseases with complex etiology: A systemic approach. *Phytopathologia Mediterranea* 59(1): 29–53. DOI: 10.14601/Phyto-11150

Chiarappa L., 2000. Esca (black measles) of grapevine. An overview. *Phytopathologia Mediterranea* 39(1): 11–15. DOI: 10.14601/Phytopathol_Mediterr-1537

Cloete M., Mostert L., Fischer M., Halleen F., 2015. Pathogencity of South African *Hymenochaetales* taxa isolated from esca-infected grapevines. *Phytopathologia Mediterranea* 54(2): 368–379. DOI: 10.14601/Phytopatho_lMediterr-16237

Cortesi P., Fischer M., Milgroom M.G., 2000. Identification and spread of *Fomitiporia punctate* associated with wood decay of grapevine showing symptoms of esca. *Phytopathology* 90(9): 967–972. DOI: 10.1094/PHYTO.2000.90.9.967

Crous P.W., Gams W., 2000. Phaeomoniella chlamydospora *gen. et comb. nov*., a causal organism of Petri grapevine decline and esca. *Phytopathologia Mediterranea* 39(1): 112–118. DOI:10.14601/Phytopathol_Mediterr-1530

Crous P.W., Slippers B., Wingfield M.J., Rheeder J., Marasas W.F.O., … Groenewald J.Z., 2006. Phylogenetic lineages in the *Botryosphaeriaceae*. *Studies in Mycology* 55: 235–253.

Czemmel S., Gaarneau E.R., Travadon R., McElrone A.J., Cramer G.R., Baumgartner K., 2015. Genes expressed on grapevine leaves revel latent wood infection by the fungal pathogen *Neofusicoccum parvum*. *PLoS ONE* 10: e0121828. DOI: 10.1371/journal.pone.0121828.

Daniel G., Volc J., Niku-Paavola M.L., 2004. Cryo-Fe-SEM and TEM immuno-techniques reveal new details for understanding white-rot decay of lignocellulose. *Comptes Rendus Biologies* 327: 861–871. DOI: 10.1016/j.crvi.2004.08.003

Daniel G., 2014. Fungal and bacterial biodegradation: White rots, brown rots, soft rots and bacteria. In: *Deterioration and Protection of Sustainable Biomaterial ACS Symposium Series* (Schultz T.P., Godell B., Nocholas D.D., ed.). pp. 24–58. American Chemical Society, Washington DC, 23–58.

Del Frari G., Gobbi A., Aggerbeck M.R., Oliveira H., Hansen L.H., Ferreira R.B., 2019. Characterization of the wood microbiome of *Vitis vinifera* in a vineyard affected by esca. Spatial distribution of fungal communities and their putative relation with leaf symptoms. *Frontier in Plant Science* 10: 910. DOI: 10.3389/fpls.2019.00910.

Del Frari, G., Oliveira, H., Boavida Ferreira, R., 2021. White Rot Fungi (*Hymenochaetales*) and esca of grapevine: Insights from recent microbiome Studies. *Journal of Fungi* 7: 770. DOI: 10.3390/jof7090770

Del Rio J.A., Gómez P., Baidez A., Fuster M.D., Ortuño A., 2001. Tylose formation and changes in phenolic compounds of grape roots infected with *Phaeomoniella chlamydospora* and *Phaeoacremonium* species. *Phytopatholgia Mediterranea.* 40(1): S394–S399. DOI: 10.14601/Phytopathol_Mediterr-1644

Del Rio J.A., Gómez P., Báidez A., Fuster D.M., Ortuño, Frias V., 2004. Phenolic compounds have a role in the defence mechanism protecting grapevine against the fungi involved in Petri disease. *Phytopathologia Mediterranea* 43(1): 87–94. DOI: 10.14601/Phytopathol Mediterr-1736

Donaldson L.A., Cairns M., Hilla S.J., 2018. Comparison of micropore distribution in cell walls of softwood and hardwood xylem. *Plant Physiology* 178: 1142–1153. DOI:10.1104/pp.18.00883

Edwards J., Pascoe. I.G., Salib S., 2007. Impairment of grapevine xylem function by *Phaeomoniella chlamydospora* infection is due to more than physical blockage of vessels with 'goo'. *Phytopathologia Mediterranea* 46(1): 87–90. DOI: 10.14601/Phytopathol_Mediterr-1858

Elena G., Bruez E., Rey P., Luque J., 2018. Microbiota of grapevine woody tissues with or without escafoliar symptoms in northeast Spain. *Phytopathologia Mediterranea* 57(3): 425–438. DOI: 10.14601/Phytopathol_Mediterr-23337

Fischer J., Compant S., Pierron R.J.G., Gorfer M., Jacques A., … Berger H., 2016. Differing alterations of two esca associated fungi, *Phaeoacremonium aleophilum* and *Phaeomoniella chlamydospora* on transcriptomic level, to co-cultured *Vitis vinifera* L. calli. PLoS ONE 11(9): e0163344. DOI:10.1371/journal.pone.0163344

Fischer M., 2001. A new wood-decaying basidiomycete species associated with esca of grapevine: *Fomitiporia mediterranea* (*Hymenochaetales*). *Mycological Progress* 13(3): 315–324. DOI: 10.1007/s11557-006-0029-4

Fischer M., and Kassemeyer H.H., 2003. Fungi associated with esca disease of grapevine in Germany. *Vitis* 42(3): 109–116. DOI: 10.5073/vitis.2003.42.109-116

Fischer M., and Kassemeyer H.H., 2012. Water regime and its possible impact on expression of esca symptoms in *Vitis vinifera*: Growth characters and symptoms in the greenhouse after artificial infection with *Phaeomoniella chlamydospora***.** *Vitis* 51(3): 129–135. DOI 10.5073/vitis.2012.51.129-135

Fischer M., and Peighami Ashnaei S. 2019. Grapevine, esca complex, and environment: The disease triangle *Phytopathologia Mediterranea* 58(1): 17–37. DOI: 10.14601/Phytopathol_Mediterr-25086

Floudas D., Benjamin W., Held B.W., Riley R., Nagy L.G., … Hibbett D.S., 2015. Evolution of novel wood decay mechanisms in *Agaricales* revealed by the genome sequences of *Fistulina hepatica* and *Cylindrobasidium torrendii*. *Fungal Genetics and Biology* 76: 78–92. DOI: 10.1016/j.fgb.2015.02.002

Gallenmüller F. Müller U., Rowe N., Speck T., 2001. The Growth Form of *Croton pullei* (Euphorbiaceae) - Functional Morphology and Biomechanics of a Neotropical Liana. *Plant Biology* 3: 50–61. DOI: 10.1055/s-2001-11750

Gao Y., Yang Z., Wang G., Sun J., Zhang X., 2020. Discerning the difference between lumens and scalariform perforation plates in impeding water flow in single xylem vessels and vessel networks in cotton. *Fronters in Plant Science* 11: 246. DOI: 10.3389/fpls.2020.00246

Garcia J.F., Lawrence D.P., Morales-Cruz A., Travadon R., Minio A., … Cantu D., 2021. Phylogenomics of plant-associated *Botryosphaeriaceae* species. *Frontiers in Microbiology* 12: 652802. DOI: 10.3389/fmicb.2021.652802

Gómez P., Báidez A.G., Ortuño A., Del Río J.A., 2016. Grapevine xylem response to fungi involved in trunk diseases. *European Journal of Plant Pathology*169: 116–124. DOI: 10.1111/aab12285

Goodell B., Quian Y., Jellison J., 2008. Fugal decay of wood: Soft rot-brown rot – white rot. *ACS Symposium Series* 82: 9–31. DOI: 10.1021/bk-2008-0982.ch002

Gramaje D., Úrbez-Torres J.R., Sosnowski M.R., 2018. Managing grapevine trunk diseases with respect to etiology and epidemiology: Current strategies and future prospects. *Plant Disease* 102(1): 12–39. DOI: 10.1094/pdis-04-17-0512-fe

Guerin-Dubrana L., Fontaine F., Mugnai L., 2019. Grapevine trunk disease in European and Mediterranean vineyards: Occurrence, distribution and associated disease-affecting cultural factors. *Phytopathologia Mediterranea* 58(1): 49–71. DOI: 10.14601/Phytopathol_Mediterr-25153

Hacke U.G., SperryJ.S., 2001. Functional and ecological xylem anatomy. *Perspectives in Plant Ecology, Evolution and Systematics* 4(2): 97–115. DOI: 10.1078/1433-8319-00017

Hage H., Rosso M.N., 2021. Evolution of Fungal Carbohydrate-Active Enzyme Portfolios and Adaptation to Plant Cell-Wall Polymers. *Journal of Fungi* 7: 185. DOI: 10.3390/jof7030185

Haidar R., Yacoub A., Vallance J., Compant S., Antonielli L., … Rey P., 2021. Bacteria associated with wood tissues of esca-diseased grapevines: functional diversity and synergy with *Fomitiporia mediterranea* to degrade wood components. *Environmental Microbiology* 23(10): 6104–6121. DOI:10.1111/1462-2920.15676

Hastrup A.C.S., Howell C., Larsen F.H., Sathitsuksanoh N., 2012. Differences in crystalline cellulose modification due to degradation by brown and white rot fungi. *Fungal Biology* 116: 1052–1063. DOI: 10.1016/j.funbio.2012.07.009.

Hess J., Balasundaram S.V., Bakkemo R.I., Drula E., Henrissat B., … Skrede I., 2020. Niche differentiation and evolution of the wood decay machinery in the invasive fungus *Serpula lacrymans*. *The ISEM Journal* 15: 592–604. DOI: 10.1038/s41396-020-00799-5

Hofstetter V., Buyck B., Croll D., Viret O., Couloux A., Gindro K., 2012. What if esca disease of grapevine were not a fungal disease? *Fungal Diversity* 54: 51–67. DOI 10.1007/s13225-012-0171-z

Holbroock N.M., Zwieniecki M.A., 1999. Embolism repair and xylem tension: Do we need a miracle. *Plant Physiology* 120: 7–10. DOI: 10.1104/pp.120.1.7

Hrycan J., Hart M., Bowen P., Forge T., Úrbez-Torres J.R., 2020. Grapevine trunk disease fungi: Their roles as latent pathogens and stress factors that favour disease development and symptom expression. *Phytopathologia Mediterranea* 59(3): 395–424. DOI: 10.14601/Phyto-11275

Jacobsen A. L., Valdovinos-Ayala J., Pratt R.B., 2018. Functional lifespans of xylem vessels: Development, hydraulic function, and post-function of vessels in several species of woody plants. *American Journal of Botany* 105(2): 142–150. DOI:10.1002/ajb2.1029

Kaack L., Weber M., Isasa E., Karimi Z., Li S., … Jansen S., 2021. Pore constrictions in intervessel pit membranes provide a mechanistic explanation for xylem embolism resistance in angiosperms. *New Phytologist* 230: 1829–1843. DOI: 10.1111/nph.17282

Kashyap A., Planas-Marques M., Capellades M., Valls M., Coll N.S., 2021. Blocking intruders: inducible physico-chemical barriers against plant vascular wilt pathogens. *Journal of Experimental Botany* 72(2): 184–198. DOI:10.1093/jxb/eraa444

Khattab I.M., Sahi V.P., Baltenweck R., Maia-Grondard A., Hugueney P., … Nick P., 2020. Ancestral chemotypes of cultivated grapevine with resistance to *Botryosphaeriaceae*-related dieback allocate metabolism towards bioactive stilbenes. *New Phytologist* 229: 1133–1146. DOI: 10.1111/nph.16919

Kedrov G.B., 2013. Scalariform tracheids in secondary xylem of woody dicotyledons: Distribution, function and evolutionary significance. *Wulfenia* 20: 43–54

Koddenberg T., Greving I., Hagemann J., Flenner S., Krause A., … Nopens M., 2021. Threedimensional imaging of xylem at cell wall level through near field nano holotomography. *Nature Scientific Reports* 11: 4574. DOI: 10.1038/s41598-021-83885-8

Koyani R.D., Sanghvi G.V., Bhatt I.M., Rajput K.S., 2010. Pattern of delignification in *Ailanthus excelsa* Roxb. Wood by *Inonotus hispidus* (Bull.: Fr.) Karst. *Mycology* 1(3): 204–211. DOI 10.1080/21501203.2010.5.516409

Labois C., Wilhelm K., Laloue H., Tarnus C., Bertsch C., Goddart M.L., Chong J., 2020. Wood metabolomics response of wild and cultivated grapevine to infection with *Neofusicoccum parvum*, a trunk disease pathogen. *Metabolites* 10: 232. DOI: 10.3390/metabo10060232

Labois C., Stempien E., Schneider J., Schaeffer-Reiss C., Bertsch C., Goddard M.-L., Chong J., 2021. Comparative study of secreted proteins, enzymatic activities of wood degradation and stilbene metabolization in grapevine *Botryosphaeria* dieback fungi. *Journal of Fungi* 7: 568. DOI10.3390/jof7070568

Lambert C., Bisson J., Waffo-Téguo P., Papastamoulis Y., Richard T., … Cluzet S., 2012. Phenolics and their antifungal role in grapevine wood decay: Focus on the *Botryosphaeriaceae* family. *Journal of Agricultural and Food Chemistry* 60: 11859–11868dx. DOI: 10.1021/jf303290g

Lambert, C., Khiook, I. L. K., Lucas, S., Télef-Micouleau, N., Mérillon, J.-M., Cluzet, S., 2013. A faster and a stronger defense response: One of the key elements in grapevine explaining its lower level of susceptibility to esca? *Phytopathology* 103: 1028–1034. DOI: 10.1094/PHYTO-11-12-0305-R

Larignon P., Dubos B., 1997. Fungi associated with esca disease in grapevine. *European Journal of Plant Pathology* 103: 147–157. DOI: 10.1023/A:1008638409410

Larsson K.H., Parmasto E., Fischer M., Langer E., Nakasone K.K., Redhead S.A., 2006. *Hymenochaetales*: a molecular phylogeny for the hymenochaetoid clade. *Mycologia* 98(6): 926–936. DOI: 10.3852/mycologia.98.6.926

Lecomte P., Darrieutort G., Liminana J.-M., Comont G., Muruamendiaraz A., … Fermaud, M., 2012. New insights into esca of grapevine: The development of foliar symptoms and their association with xylem discoloration. *Plant Diseases* 96: 924–934. DOI: 10.1094/PDIS-09-11-0776-RE

Leśniewska J., Öhmann D., Krzesłowskka M., Kushwa S., Barciszewska-Pacak M., … Mellerowicz E.J., 2017. Defense response in aspen with altered pectin methylesterase activity reveal the hormonal inducers of tylosis. *Plant Physiology* 173: 1409–1419. DOI: 10.1104/pp.16.01443

Li S., Bonneu F., Chadoeuf J., Picart D., Gégout-Petit A., Guérin-Dubrana L., 2017. Spatial and temporal pattern analyses of esca grapevine disease in vineyards in France. *Phytopathology* 107: 59–69. DOI: 10.1094/PHYTO-07-15-0154-R

Liers C., Arnstadt T., Ullrich R., Hofrichter M., 2011. Patterns of lignin degradation and oxidative enzyme secretion by different wood- and litter-colonizing B*asidiomycetes* and *Ascomycetes* grown on beech-wood. *FEMS Microbiology Ecology* 78: 91–102. DOI:10.1111/j.1574-6941.2011.01144.x

Lima M.R.M., Machado A.F., Gubler W.D., 2017. Metabolomic studies of “Chardonnay” grapevine double

stressed with esca-associated fungi and drought. *Pytopathology* 107: 669–680. DOI: 10.1094/PHYTO-11-26-0410-R

Troccoli T., Calamassi R., Mori B., Mugnai L., Surico G., 2001. *Phaeomoniella chlamydospora*-grapevine interaction: Histochemical reactions to fungal infection. *Phytopathologia Mediterranea* 40: S400–S406. DOI: 10.14601/Phytopathol_Mediterr-1610

Maher N., Piot J., Bastien S., Vallance J., Rey P., Guérin-Dubrana J., 2011. Wood necrosis in esca-affected vnes. Types, relationship and possible links with foliar symptom expression. *Journal International des Sciences de la Vigne et du Vin* 46(1):15–27. DOI:10.20870/oeno-one.2012.46.1.1507

Martinez-Diz M.P., Eichmeier A., Spetik M., Bujanda R., Díaz-Fernández A., … Gramaje D., 2020. Grapevine pruning time affects natural wound colonization by wood invading fungi. *Fungal Ecology* 48: 1–13. DOI: 10.1016/j.funeco.2020.100994

Masi M., Cimmino A., Reveglia P., Mugnai L., Surico G., Evidente A., 2018. Advances on fungal phytotoxins and their role in grapevine trunk diseases. *Journal of Agricultural and Food Chemistry* 66(5): 948–958. DOI: 10.1021/acs.jafc.8b00773.

Masselter T., Speck T., 2008. Quantitative and qualitative changes in primary and secondary stem organization of *Aristolochia macrophylla* during ontogeny: Functional growth analysis and experiments. *Journal of Experimental Botany* 59(11): 2955–2967. DOI:10.1093/jxb/ern151

Massonnet M., Figueroa-Balderas R., Galarneau E.R.A., Miki S., Lawrence D.P., … Cantu D., 2017. *Neofusicoccum parvum* colonization of the grapevine woody stem triggers asynchronous host responses at the site of infection and in the leaves. *Frontier in Plant Science* 8: 1117. DOI: 10.3389/fpls.2017.01117

Massonnet M., Morals-Cruz A., Figueroa-Balderas R., Lawrence D.P., Baumgartner K., Cantu D., 2018a. Condition-dependent co-regulation of genomic clusters of virulence factors in the grapevine trunk pathogen *Neofusicoccum parvum*. *Molecular Plant Pathology* 19: 21–34 DOI: 10.1111/mpp.12491

Massonnet M., Morales-Cruz A., Minio A., Figueroa-Balderas R., Lawrence D.P., … Cantu D., 2018b. Whole-genome resequencing and pan-transcriptome reconstruction highlight the impact of genomic structural variation on secondary metabolite gene clusters in the grapevine esca pathogen *Phaeoacremonium minimum*. *Frontiers in Microbiology* 9: 1784. DOI: 10.3389/fmicb.2018.01784

Miedes E., Vanholme R., Boerjan W., Molina A., 2014. The role of the secondary cell wall in plant resistance to pathogens. *Frontiers in Plant Science* 5: 358. DOI: 10.3389/fpls.2014.00358

Mondello V., Songy A., Battiston E., Pinto C., Coppin C., … Fontaine F., 2018. Grapevine trunk diseases: A review of fifteen years of trials for their control with chemicals and biocontrol agents. *Plant Disease* 10: 1189–1217. DOI: 10.1094/PDSI-08-17-1181-FE

Morales-Cruz A., Amrine K.C.H., Blanco-Ulate B., Lawrence D.P., Travadon R., … Cantu D., 2015. Distinctive expansion of gene families associated with plant cell wall degradation, secondary metabolism, and nutrient uptake in the genomes of grapevine trunk pathogens. *BMC Genomics* 16: 469. DOI 10.1186/s12864-015-1624-z

Moretti S., Pacetti A., Pierron R., Kassemeyer H.H., Fischer M., … Farine S., 2021. *Fomitiporia mediterranea* M. Fisch., the historical esca agent: A comprehensive review on the main grapevine wood rot agent in Europe. *Phytopathologia Mediterranea* 60 (2): 357–385. DOI: 10.14601/Phyto-13021

Morgenstern I., Robertson D.L., Hibbett D.S., 2010. Characterization of three *mnp* genes of *Fomitiporia mediterranea* and report of additional class II peroxidases in the order *Hymenochaetales*. *Applied and Environmental Microbiology* 76(19): 6431–6440. DOI:10.1128/AEM.00547-10

Morris H., Jansen S., 2016. Secondary xylem parenchyma – From classical terminology to functional traits. *IAW Journal* 37(1): 1–13. DOI: 10.1163/22941932-201160117

Morris H., Plavcová L., Cvecko P., Fichtler E., Gillingham M.A.F., … Jansen S., 2016 a. A global analysis of parenchyma tissue fractions in secondary xylem of seed plants. *New Phytologist* 209: 1553–1565. DOI: 10.1111/nph.13737

Morris H., Brodersen C., Schwarze F.W.M.R., Jansen S., 2016b. The parenchyma of secondary xylem and its critical role in tree defense against fungal decay in relation to the CODIT model.*iers in Plant Science* 7: 1665. DOI: 10.3389/fpls.2016.01665

Morris, H., Plavcova L., MGorai M., Klepsch M., Kotowska M., … Jansen S., 2018. Vessel-associated cells in angiosperm xylem: Highly specialized living cells at the symplast–apoplast boundary. *American Journal of Botany* 105(2): 151–160. DOI:10.1002/ajb2.1030

Morris H., Hietala A.M., Jansen S., Ribera J., Rosner S., … Schwarze F.W.M.R., 2020. Using the CODIT model to explain secondary metabolites of xylem in defence systems of temperate trees against decay fungi. *Annals of Botany* 125(5): 701–720. DOI: 10.1093/aob/mcz138

Mugnai L., Graniti A., Surico G., 1999. Esca (Black measles) and brown wood-streaking: Two old and elusive

diseases of grapevine. *Plant Disease* 83(5): 404–418. DOI: 10.1094/PDIS.1999.83.5.404

Mutawila C., Fourie P., Halleen F., Mostert L., 2011. Histo-pathology study of the growth of *Trichoderma harzianum*, *Phaeomoniella chlamydospora* and *Eutypa lata* on grapevine pruning wounds. *Phytopathologia Mediterranea* 50: S46–S60.

Ohm R.A., Riley. R., Salamov A., Min B., Choi I.G., Grigoriev I.V., 2014. Genomics of wood-degrading fungi. *Fungal Genetics and Biology* 72: 82–90. DOI: 10.1016/j.fgb2014.05.001

Pacetti A., Moretti S., Pinto C., Compant S., Farine S., … Mugnai L., 2021. Trunk surgery as a tool to reduce foliar symptoms in diseases of the esca complex and its influence on vine wood microbiota. *Journal of Fungi*: 7(7), 521. DOI: 0.3390/jof7070521

Pacetti A., Moretti S., Perrin C., Gelhaye E., Bieler E., … Bertsch C., 2022. Grapevine wood-wegrading activity of *Fomitiporia mediterranea* M. Fisch.: A focus on the enzymatic pathway regulation. *Frontiers in Microbiology* 13: 844264. DOI: 10.3389/fmicb.2022.844264. PMID: 35369524; PMCID: PMC8971955.

Pacifico D., Squartini A., Crucitti D., Barizza E., Lo Schiavo F., … Zottini M., 2019. The role of the endophytic microbiome in the grapevine response to environmental triggers. *Frontiers in Plant Science* 10: 1256. DOI: 10.3389/fpls.2019.01256

Pfautsch S., Hölttä T., Mencuccini M., 2015 a. Hydraulic functioning of tree stems - fusing ray anatomy, radial transfer and capacitance. *Tree Physiology* 35: 706–722. DOI:10.1093/treephys/tpv058

Pfautsch S., Renard J., Tjoelker M.G., Salih A., 2015 b. Phloem as capacitor: Radial transfer of water into xylem of tree stems occurs via symplastic transport in ray parenchyma. *Plant Physiology* 167: 963–971. DOI: 10.1104/pp.114.254581

Pierron R.J.G., Pouzoulet J., Couderc C., Judic E., Compant S., Jacques A., 2016. Variations in early response of grapevine wood depending on wound and inoculation combinations with *Phaeoacremonium aleophilum* and *Phaeomoniella chlamydospora*. *Frontiers- in. Plant Sciience* 7: 268. DOI: 10.3389/fpls.2016.00268

Plomion C., Leprovost G., Stokes A., 2001. Wood formation in trees. *Plant Physiology* 127: 1513–1523. DOI: 10.1104/pp.010816

Pouzoulet J., Pivovaroff A.L., Santiago L.S., Rolshausen P.E. 2014. Can vessel dimension explain tolerance toward fungal vascular wilt diseases in woody plants? Lessons from Dutch elm disease and esca disease in grapevine. *Frontiers in Plant Sci*ence 5: 253. DOI: 10.3389/fpls.2014.00253

Pouzoulet J., Scudiero E., Schiavon M., Rolshausen P.E. 2017. Xylem vessel diameter affects the compartmentalization of the vascular pathogen *Phaeomoniella chlamydospora* in grapevine. *Front. Plant Sci*. 8: 1442. DOI: 10.3389/fpls.2017.01442

Pouzoulet J., Rolshausen P.E., Charbois R., Chen J., Guillaumie S., … Delmas C.E.L., 2020. Behind the curtain of the compartmentalization process: Exploring how xylem vessel diameter impacts vascular pathogen resistance. *Plant Cell & Environ*men 43: 2782–2796. DOI: 10.1111/pce.13848

Pratt C. 1974. Vegetative anatomy of cultivated grapes – A review. *American Journal of. Enology and Viticulture* 25(3): 131–149.

Rathgeber C.B.K., Cuny H.E., Fonti P., 2016. Biological basis of tree-ring formation: A crash course. *Frontiers in Plant Science* 7: 734. DOI: 10.3389/fpls.2016.00734

Reis P., Pierron R., Larignon P., Lecomte P., Abou-Mansour E., … Fontaine F., 2019. *Vitis* methods to understand and develop strategies for diagnosis and sustainable control of grapevine trunk diseases. *Phytopathology* 109: 916–931. DOI: 10.1094/PHYTO-09-18-0349-RVW

Riley R., Salamov A.A., Brown D.W., Nagy L.G., Floudas D., … Grigoriev I.V., 2014. Extensive sampling of basidiomycete genomes demonstrates inadequacy of the white-rot/brown-rot paradigm for wood decay fungi. Proceedings of the National Academy of Sciences (*PNAS*) 111(27): 9923–9928. DOI: 10.1073/pnas.1400592111

Rolshausen P., Úrbez-Torres J.R., Rooney-Latham S., Eskalen A., Smith R.J., Gubler W.G., 2010. Evaluation of pruning wound susceptibility and protection against fungi associated with grapevine trunk diseases. *American Journal o. Enology and Viticulture* 61: 113–119.

Rowe N., Speck T., 2004. Plant growth forms: An ecological and evolutionary perspective. *New Phytologist* 166: 61–72. Doi: 10.1111/j.1469-8137.2004.01309.x

Rusjan D., Persic M., Likar M., Biniari K. Mikulic-Petkovsek M., 2017. Phenolic responses to esca-associated fungi in differently decayed grapevine woods from different trunk parts of 'Cabernet Sauvignon'. *Journal of Agricultural and Food Chemistry* 65: 6615–6624 DOI: 10.1021/acs.jafc.7b02188

Sano Y., Utsumi Y., Nakada R., 2013. Homoplastic occurrence of perforated pit membranes and torus-bearing pit membranes in ancestral angiosperms as observed by field-emission scanning electron microscopy. *Journal* of *Wood Science* 59: 95–103. DOI: 10.1007/s10086-012-1304-4

Schilling J.S., Kaffenberger J.T., Liew F.J., Song Z., 2015. Signature wood modifications reveal decomposrer

community history. *PLoSONE* 10: e0120679. DOI: 10.1371/journal.pone.0120679

Schilling J.S., Kaffenberger J.T., Held B.W., Ortiz R., Blanchette R.A., 2020. Using wood rot phenotypes to illuminate the "Gray" among decomposer fungi. *Frontiers in Microbiolology* 11: 1288. DOI: 10.3389/fmicb.2020.01288

Schneider R., Tang L., Lampugnani E.R., Barkwill S., Lathe R., … Perssona A., 2017. Two complementary mechanisms underpin cell wall patterning during xylem vessel development. *The Plant Cell* 29: 2433–2449. DOI: 10.1105/tpc.17.00309

Schuetz M., Smith R., Ellis B., 2013. Xylem tissue specification, patterning, and differentiation mechanisms. *Journal of Experimental Botany* 64(1): 11–31. DOI: 10.1093/jxb/ers287

Schwarze F.W.M.R., 2007. Wood decay under the microscope. *Fungal Biology Reviews* 21(4): 133–170. DOI: 10.1016/j.fbr.2007.09.001

Schwarze F. W. M. R., Fink S. 1998. Host and cell type affect the mode of degradation by *Meripilus giganteus*. *New Phytol*ogist 139: 721–731. DOI: 10.1046/j.1469-8137.1998.00238.x

Schwarze F. W. M. R., Lonsdale D., Fink S., 1995. Soft rot and multiple T-branching by the basidiomycete *Inonotus hispidus* in ash and London plane. Mycological Research. 99: 813–820. DOI:_10.1016/S0953-7562(09)80732-6

Secchi F., Pagliarani C., Zwieniecki M.A., 2017. The functional role of xylem parenchyma cells and aquaporins during recovery from severe water stress. *Plant, Cell and Environment* 40: 858–871. DOI: 10.1111/pce.12831

Shigo A.L., 1984. Compartmentalization: A conceptual framework for understanding how trees grow and defend themselves. *Annual Review* of *Phytopathology* 22: 189–214.

Spagnolo A., Mondello V., Larignon P., Villaume S., Rabenoelina F., … Fontaine F., 2017. Defense responses in grapevine ("Mourvèdre") after inoculation with the *Botryosphaeria* dieback pathogens *Neofusicoccum parvum* and *Diplodia seriata* and their relationship with flowering. *International Journal of Molecular Scie*ince 18: 393. DOI: 10.3390/ijms18020393

Stempien E., Goddard M.L., Wilhelm K., Tarnus C., Bertsch C., Chong J., 2017. Grapevine *Botryosphaeria* dieback fungi have specific aggressiveness factor repertory involved in wood decay and stilbene metabolization. *PLoS ONE* 12. DOI: 10.1371/journal.pone.0188766

Sun Q., Rost T.L., Matthews M.A., 2006. Pruning-induced tylose development in stems of current-year shoots of *Vitis vinifera* (Vitaceae). *American Journal of Botany* 93(11): 1567–1576. DOI: 10.3732/ajb.93.11.1567

Sun Q., Rost T.L., Matthews M.A., 2008. Wound-induced vascular occlusions in *Vitis vinifera* (Vitaceae). *American Journal of Botany* 95(12): 1498–1505. DOI: 10.3732/ajb.0800061

Sun Q., Sun Y., Juzenas K., 2017. Immunogold scanning electron microscopy can reveal the polysaccharide architecture of xylem cell walls. *Journal of Experimental Botany*, 68(9): 2231–2244. DOI: 10.1093/jxb/erx103

Surico G., Marchi G., Braccini P., Mugnai L., 2000. Epidemiology of esca in some vineyards in Tuscany (Italy). *Phytopathologia Mediterranea* 39(1): 190–205. DOI: 10.14601/Phytopathol_Mediterr-1536

Surico G., 2009. Towards a redefinition of the diseases within the esca complex of grapevine. *Phytopathologia Mediteranea*. 48(1): 5–10. DOI:10.14601/Phytopathol_Mediterr-2870

Travadon, R., Rolshausen, P. E., Gubler, W. D., Cadle-Davidson, L., Baumgartner, K., 2013. Susceptibility of cultivated and wild *Vitis* spp. to wood infection by fungal trunk pathogens. *Plant Disease*. 97: 1529–1536. DOI: 10.1094/PDIS-05-13-0525-RE

Travadon R., Lecomte P., Diarra B., Lawrence D.P., Renault D., … Baumgartner K., 2016. Grapevine pruning systems and cultivars influence the diversity of wood-colonizing fungi. *Fungal Ecology* 24: 82–93 DOI: 10.1016/j.funeco.2016.09.003

Úrbez-Torres, J. R., Leavitt, G. M., Guerrero, J. C., Guevara, J., Gubler, W. D., 2008. Identification and pathogenicity of *Lasiodiplodia theobromae* and *Diplodia seriata*, the causal agents of bot canker disease of grapevines in Mexico. *Plant Disease* 92: 519–529. DOI: 10.1094/PDIS-92-4-0519

Úrbez-Torres J. R., 2011. The status of Botryosphaeriaceae species infecting grapevines. *Phytopathologia Mediteranea* 50: S5–S45. DOI:10.14601/Phytopathol_Mediterr-9316

Vaz A.T., Del Frari G., Chagas R., Ferreira A., Oliveira H., Boavida Ferreira R., 2020. Precise nondestructive location of defective woody tissue in grapevines affected by wood diseases. *Phytopathologia Mediterranea* 59(3): 441–451. DOI: 10.14601/Phyto-11110

Vazquez-Cooz I., Mayer R.W., 2004. Occurrence and lignification of libriform fibers in normal and tension wood of red sugar maple. *Wood and Fibers Science* 36: 56–70.

Viala P., 1926. Recherches sur les maladie de la vigne - esca. *Annales des Epiphyties*, Fasc. 1 et 2. Paris Institut des Recherches Agronomique.

von Arx G., Kueffer C., Fonti P., 2013. Quantifying plasticity in vessel grousing – Added value from the

image analysis tool ROXAS. *IAWA Journal* 34: 433–445. DOI: 10.1163/22941932-00000035

Worrall J.J., Anagnost S.E., Zabel R.A., 1997. Comparison of wood decay among diverse lignicolous fungi. *Mycologia* 89(2): 199–219. DOI: 10.1080/00275514.1997.12026772

Yadav V., Wang Z., Wie C., Amo A., Ahmed B., … Zhang X., 2021.Phenylpropanoid pathway engineering: An emerging approach toward plant defense. *Pathogens* 9: 312. DOI: 10.3390/pathogens.9040312

Yadeta K.A., Thomma B.P.H.J,. 2013. The xylem as battleground for plant host and vascular wilt pathogens. *Frontiers in Plant Science* 4: 97. DOI:10.3389/fpls.2013.00097

Ye Q., Jia J., Manawasinghe I.S., Li X., Zhang W., … Yan J., 2021. *Fomitiporia punicata* and *Phaeoacremonium minimum* associated with esca complex of grapevine in China. *Phytopathology Research* 3: 11. DOI: 10.1186/s42483-021-00087-w

Zhang Y., Carmesin C., Kaack L., Klepsch M.M., Kotowska M., … Jansen S., 2020. High porosity with tiny pore constrictions and unbending pathways characterize the 3D structure of intervessel pit membranes in angiosperm xylem. *Plant Cell Environ*. 43(1):116–130. DOI: 10.111/pce.13654

Zimmermann M.H., Jeje A.A., 1981. Vessel-length distribution in stems of some American woody plants. *Canadian Journal of Botany* 59: 1882–1892. DOI: 10.1139/b81-248

Phytopathologia Mediterranea
The international journal of the
Mediterranean Phytopathological Union

Firenze University Press
www.fupress.com/pm

Research Papers

Recovery after curettage of grapevines with esca leaf symptoms

Pascal LECOMTE[1,*], Céline CHOLET[2], Emilie BRUEZ[2], Tommaso MARTIGNON[3], Massimo GIUDICI[3], Marco SIMONIT[3], Adeline ALONSO UGAGLIA[4], Dominique FORGET[5], Jerôme MIRAMON[5], Matthieu ARROYO[5], Denis DUBOURDIEU[2,6], Laurence GENY-DENIS[2], Patrice REY[4]

[1] *INRAE, Université de Bordeaux, UMR SAVE, ISVV, 71 avenue Edouard Bourleaux, BP81, 33883 Villenave d'Ornon, France*
[2] *Université de Bordeaux, UR Œnologie, ISVV, 210 Chemin de Leysotte, 33882 Villenave d'Ornon, France*
[3] *Simonit & Sirch France, 1 rue Porte des Benauges, 33410 Cadillac, France*
[4] *Université de Bordeaux, Bordeaux Sciences Agro, UMR SAVE, ISVV, 33883 Villenave d'Ornon, France*
[5] *INRAE, Unité Expérimentale Château Couhins, Chemin de la Gravette, 33140 Villenave d'Ornon, France*
[6] *Château Reynon - Domaines Denis Dubourdieu, 21 Route de Cardan, 33040 Béguey, France*
*Corresponding author. E-mail: pascal.lecomte@inrae.fr

Summary. Grapevine curettage was re-introduced in France in the early 2000s, and is important for facilitating recovery of plants from esca disease. This surgical practice involves removal of deadwood of vines with leaf symptoms, focusing on white rot generally observed at the centres of grapevine trunks. Assessment of the efficacy of this practice was initiated in the Bordeaux region in 2014. One 'Sauvignon Blanc' vineyard severely affected by esca was initially surveyed in the summer of 2014, to identify and treat vines with esca foliar symptoms. Annually thereafter, from 2014 to 2018, selected vine stocks were curetted. Two other 'Sauvignon Blanc' vineyards also displaying high levels of esca damage were added to the study in 2015 and 2016. Curettage treatments ceased in 2018, resulting in 11 trials (vineyard × year combinations). In total, 856 vines (422 curetted and 434 control vines) were then surveyed annually up to 2021, for assessments and comparisons of esca development. At each site, plants with esca symptoms recovered well after curettage: on average 85% of all curetted vines became asymptomatic the year immediately after the treatment. Six years after treatment, for curettage campaigns carried out in 2014 and 2015, more than half of the curetted vines were symptom-free, whereas <12% of the control vines were asymptomatic, and gradual loss of efficacy was observed at each site. The mean annual proportion of efficacy erosion was approx. 8% per year. This study highlights the possible short- and mid-term benefits of trunk surgery to enable recovery of esca-affected vines, and for them to recover and remain leaf-asymptomatic for several years.

Keywords. Trunk surgery, plant health recovery, *Vitis vinifera* L., white rot.

OPEN ACCESS

Citation: P. Lecomte, C. Cholet, E. Bruez, T. Martignon, M. Giudici, M. Simonit, A. Alonso Ugaglia, D. Forget, J. Miramon, M. Arroyo, D. Dubourdieu, L. Geny-Denis, P. Rey (2022) Recovery after curettage of grapevines with esca leaf symptoms. *Phytopathologia Mediterranea* 61(3): 473-488. doi: 10.36253/phyto-13357

Accepted: October 17, 2022

Published: November 25, 2022

Data Availability Statement: All relevant data are within the paper and its Supporting Information files.

Competing Interests: The Author(s) declare(s) no conflict of interest.

Editor: Hanns-Heinz Kassemeyer, Staatliches Weinbauinstitut Freiburg, Germany.

ORCID:
PL: 0000-0002-0479-0295
CC: 0000-0002-9268-3835
EB: 0000-0003-4363-4284
AAU: 0000-0003-4520-3330
LG-D: 0000-0002-7663-7927
PR: 0000-0002-7250-0114

INTRODUCTION

Grapevine trunk diseases (GTDs) are a major cause of grapevine decline and death in many grape-growing regions, including the vineyards of European wine-producing countries (Guérin-Dubrana *et al*., 2019). These fungal diseases affect the perennial parts of vines, causing diverse types of damage in established vineyards (Lecomte *et al*., 2018). The principal GTDs in mature vineyards are Botryosphaeria dieback, esca disease, Eutypa dieback, and Phomopsis dieback (Larignon and Dubos, 1997; Mugnai *et al*. 1999; Úrbez-Torres, 2011; Baumgartner *et al.* 2013; Gramaje *et al.,* 2018). Esca, in particular, causes major economic losses in France (Bruez *et al*., 2013). Pruning wounds are the main entry sites for pathogenic fungi, and slow and progressive extension of the infections within the grapevine wood leads to permanent infections of different degrees of latency (Hrycan *et al*., 2020). These may result in development of cankers or inner necroses of variable size, shape and discolouration (Larignon and Dubos, 1997; Mugnai *et al*., 1999; Maher *et al*., 2012, Úrbez-Torres, 2011).

Eutypa, Botryosphaeria and Phomopsis (or Diaporthe) diebacks are generally associated with one or several related xylem-inhabiting fungi (Hrycan *et al*., 2020). Esca on mature vines is associated, following the definition of Larignon and Dubos (1997), with a large complex of vascular fungi as primary and secondary pathogens, including *Ascomycota* and *Basidiomycota*. The ascomycetes *Phaeomoniella chlamydospora*, *Phaeoacremonium minimum* and other *Phaeoacremonium* spp. were reported as the pioneering pathogens (Larignon and Dubos, 1997), but the other ascomycetes involved in the three dieback diseases (above) may also act as precursors, or co-colonizing fungi, as reported for *Eutypa lata* in temperate climates (Larignon and Dubos, 1997) and *Botryosphaeria* species in dry (e.g. Mediterranean) regions (Luque *et al*., 2009; Ammad *et al*., 2014; Choueiri *et al*., 2014). These fungi can be isolated from wood lesions on the trunks or cordons of esca-infected grapevines (Larignon and Dubos, 1997; Choueiri *et al*., 2014; Elena *et al*., 2018). Communities of wood-inhabiting microorganisms, including other fungi or bacteria, can also be identified in individual samples (Larignon and Dubos, 1997, Bruez *et al*., 2014, 2015), but their roles in host degradation remain unclear. As vines and their necroses age, the basidiomycete *Fomitiporia mediterranea,* which causes white rot ('amadou'), may develop in grapevine wood. Presence of white rot and its progressive development are associated with foliar symptoms of esca, or sudden vine collapse in the summer (Arnaud and Arnaud, 1931; Maher *et al*., 2012; Ouadi *et al*., 2019).

In the summer, leaf symptoms of esca, such as gradual discolouration, drying, wilting or leaf fall and collapse, differ between grapevine cultivars. Appearance of orangish longitudinal stripes just under the bark is another typical feature of esca, and is indicative of a probable vascular disorder (Lecomte *et al*., 2012). This peculiar symptom was first described by Arnaud and Arnaud (1931), but the underlying mechanism remains unknown. Several hypotheses have been proposed, including association of leaf stripe symptoms with sudden xylem disruption in summer, a period generally marked by high temperatures and water deficits (Lecomte *et al*., 2012), or the presence of vessel occlusions (Pouzoulet *et al*., 2019).

Eradicative pruning is a classical practice in plant protection (Svihra, 1994; Clark and Matheny, 2010), and removal of infected host branches or wood by cutting has been recommended for the control of many plant diseases or decay (Shigo, 1982). This technique has been used, with various degrees of success, for the management of Dutch elm disease (Gregory and Allison, 1979), oak wilt (Camilli *et al*., 2007), and played a strategic role in the control of fire blight (Paulin, 1996). In viticulture, trunk renewal is a common method for removing infected vine parts (Sosnowski *et al*., 2004; Smart, 2015), and involves the re-training of vines from suckers growing at trunk base. Excising cankers with pruning knives is another surgical approach suitable for treating diseases such as anthracnose (Garton *et al*., 2018) or European canker (Zeller, 1926). In viticulture, the surgical method known as 'curettage' has been used for centuries, as reported by Larignon and Yobregat (2016). This involves removing rotten tissues from trunk wood of diseased vines. Curettage of grapevines has played a key historical role, and was described by Columelle, Pline the Elder, and Palladius in Roman times. Use of curettage was subsequently mentioned by Pierre de Crescens in the Middle Ages, and then by Bidet and Duhamel du Monceau in the 18th Century. It was also an ancient oriental method (Pavlou, 1906; Gaudineau 1959). Curettage was historically performed with metal tools, including pruning or farrier's knives, small hatchets, billhooks or 'gouges', used to remove the necrotic parts of the diseased vines. Given the very long period over which curettage has been used, the practices covered by this term have been highly diverse.

Efficacy of curettage has been little studied, despite its use over many centuries and the likely beneficial effects that such long-term use implies. Some information was provided by Eugène Poussard (Lafon, 1921), a viticulturist who regularly applied the curettage technique (Figure 1) to his vineyards. He reported a high

Figure 1. Illustration of a grapevine curetted in 1919, as shown by Lafon (1921).

degree of efficacy because 90 to 95% of the curetted plants were resilient. However, curettage remained a minority practice until its modernization and reintroduction in France at the beginning of the 21st Century (Larignon and Yobregat, 2016). This return has been associated with a combination of factors, including the ban of sodium arsenite, the only curative pesticide previously used to control esca (Bruez *et al*., 2021a), that was forbidden in Europe in the first decade of the 21st century. Development of tools, such as lightweight chain saws, has also opened new possibilities for the use of curettage. Nowadays, necrotic wood is removed with thermal and/or electric saws, and an increasing number of operators are proposing curetting services to vine growers.

Despite the renewed development of curettage, questions about the efficacy of the technique remain unanswered, because very few experiments have been performed to assess curettage efficacy (Mondello *et al*., 2018; Pacetti *et al*., 2021). The present study has provided relevant information about the short and mid-term efficacy of curettage, based on results obtained over 3 to 7 years in three Bordeaux vineyards in which the development of esca-leaf-symptomatic vines was monitored, with or without curettage. The study was undertaken over a long period to ensure that the results were robust. Advantages and limitations of curettage are discussed. Some preliminary results of this study have also been used to assess effects of curettage on vine physiology and berry quality (Cholet *et al*., 2021; Bruez *et al*., 2021b).

MATERIALS AND METHODS

Field study

This study was based on comparisons of esca development in curetted or non-curetted grapevines in three vineyards in the Bordeaux region of France (Table 1). First assessments of the effects of curettage on the grapevines with esca began in 2014 at a commercial and conventional farm in Béguey (Gironde). An initial vineyard of Sauvignon Blanc vines, named 'Cyprès East', was selected for study, based on its high susceptibility to GTDs (Experiment 1). This vineyard had sandy gravel soil, and was planted in 1994 with vines omega-grafted onto 101-14 rootstocks (row width × inter-vine distance = 1.8 × 1 m). The trellising system was typical of the region, with an 'Espalier' Guyot vine form comprising short trunks (60–70 cm) each with two lateral cordons. The vines were trained according to a 'Guyot-double' pruning regime. Experiment 2 was carried out on the same farm and began in 2015, in a second and adjacent vineyard, named 'Cyprès West' with very similar characteristics (Table 1). These two vineyards were located at the bottom of a hill and the vine rows were arranged to follow the topography slope. A third vineyard with the same vine training system was integrated into the study in 2016, at another commercial and conventional farm, Château Couhins at Villenave d'Ornon, close to Bordeaux, on a clay-limestone and soil with flat topography (Experiment 3). There was no known soil-related heterogeneity factor at this location. For all three sites, curettage campaigns were carried out annually and ceased in 2017 or 2018. This gave a total of 11 trials (vineyard × year combinations), and 53 comparisons between treated (curetted) and control vines from 2014 onwards.

Study design

The experimental designs differed between vineyards and years. In 2014, in the 'Cyprès East' vineyard at Béguey (Exp. 1), control and curetted vines were randomly selected in the same part of the vineyard. In 2015, for practical reasons, this vineyard was divided into two equal parts, one for the curetted vines and the other for non-curetted vines (controls). The 'Cyprès west' vineyard (Exp. 2) was also divided in two equal parts. At Villenave d'Ornon (Exp. 3; 'Couhins III-7'), curetted or control vines were randomly selected from vines displaying

Table 1. Main cropping characteristics of the three 'Sauvignon blanc' vineyards used for assessment of 'curettage' effects.

Site Winery	Experiment and *vineyard name*	Rootstock	Date of planting	Trellising system and vine intervals[a] (m)	No. of rows	Total No. of vines	'Curettage' Year(s)	Rows used for control ( )[b]	Rows used for curettage ( )[b]
Béguey Château Reynon	Experiment 1 *Cyprès East*	101-14	1994	Espalier Guyot double 1.8 × 1	25	914	2014	16-25 914 vines	
						2424	2015 to 2018	1-13 (1105 vines)	14-25 (1319 vines)
	Experiment 2 *Cyprès West*	101-14	1996	Espalier Guyot double 1.8 × 1	14	1409	2015 to 2017	1-7 (717 vines)	8-14 (692 vines)
Villenave d'Ornon, Château Couhins	Experiment 3 *Couhins III-7*	Fercal	2000	Espalier Guyot double 1.5 × 1	20	940	2016 and 2017a	1-10 Random selection	
						940	2017b	16-20 (470 vines)	11-15 (470 vines)

[a] Distances between and within rows (m). [b] Total number of vines surveyed.

symptoms, within a ten-row sample, in 2016 and for one trial in 2017 (2017a). For another trial in 2017 (2017b), an additional ten new rows were split into two equal parts, as at Béguey. The rows studied in each vineyard and the number of vines surveyed in each part are indicated in Table 1. All vineyards were managed under conventional sanitary programmes in accordance with IPM guidelines. Esca was the most widely reported disease in these vineyards. Any damage to vine wood was therefore assumed to be mostly due to this trunk disease.

Esca symptom assessment

Esca symptoms on wood and leaves were recorded in late August before harvest: i) to assess the sanitary status of each part of the vineyards, and ii) to select diseased vines with symptoms of similar severity for use in comparisons of the control and curettage treatments. All vines were mapped and symptoms were recorded until 2021, for 2 to 7 years after the first curettage treatment. Symptoms were assessed with severity scales used in previous similar studies (Darrieutort and Lecomte, 2007; Lecomte *et al.*, 2012; Lecomte *et al.*, 2018). Leaf symptoms were assigned to five classes according to severity and position on each vine (Table 2): S1 and S2, corresponding to mild symptoms, limited to the leaves, mostly discolourations, affecting one (S1) or two (S2) cordons, or corresponding to severe symptoms, with many drying zones (S3), wilting (S4) or leaf fall (S5) on one or two cordons. Apoplectic vines (APO) were also observed but were not analyzed in detail in this study. For assessment of the sanitary status of each part of each vine plot, the original vines were grouped into three severity categories: asymptomatic, unproductive (trunk-affected: retrained, restored, replanted, dead, absent or with dead or missing arm, as detailed in Table 2), and leaf-symptomatic vines, as in a previous study comparing trellising systems (Lecomte *et al.*, 2018). For assessments of the recovery from esca of curetted vines, and comparison with the control vines, vines were again assigned to three categories: asymptomatic, symptomatic (on leaves or on wood), or dead vines. Differences between the proportions (%) of all asymptomatic curetted vines observed in each year and those observed the previous year were calculated, and these were used to estimate the annual losses of curettage efficacy.

Curettage

All annual curettage operations were carried out by specialist operators from Simonit & Sirch, France (Table 1). With the exception of one trial at Villenave d'Ornon established in 2017 (Exp. 3, Couhins III-7 vineyard, trial 2017b) with vines identified in summer but curetted in spring 2018, the selected symptomatic vines were curetted in late August, after most esca symptoms had appeared. The objective was a complete decay removal by avoiding weakening the vine structures to support mechanized working. Degraded wood (generally with white rot and dark-brown necroses) was gradually removed with a thermal chainsaw from the tops of trunks or cordons down to the base of the visible necroses. A smaller electric chain saw with a sharpened tip was used to refine the removal of discoloured wood. A small gutter was fitted to direct the flow of rainwater on the base of each open cavity to avoid any waterlog-

Table 2. Esca disease severity indices used to assess the status of each original 'Espalier' grapevine surveyed in this study (from Lecomte *et al*., 2018).

Code	Meaning
V	Original vine with no damage (leaves and wood)
S	Symptomatic vine with leaf symptoms[a]: S1 = light symptoms (mostly discolorations) on one cordon only S2 = light symptoms (mostly discolorations) on both cordons S3 = severe symptoms (discolorations, drying and some wilting) on one cordon only S4 = severe symptoms (discolorations, drying and some wilting) on both cordons S5 = very severe symptoms of wilting affecting a large number of leaves and grapes on both cordons
APO1 - APO2	Vine showing complete wilting on one or two cordons (apoplexy)
DA[b]	Vine showing portion of dead wood (often a dead cordon)*
U[b]	Vine trained with only one cordon (a dead cordon had been removed)
R[b]	Retrained or restored vine*
D or A[b]	Dead or absent vine
Y[b]	Replanted, regrafted, marcotte, or young vine (any vine planted after the original planting date)

[a] Other or intermediate categories of leaf symptoms were possible, as for example, S1 + S3 for a vine with mild symptoms on one cordon and severe symptoms on the other.
[b] The categories DA, U, R, D or A, and Y refer to all original vines with GTD-affected trunks, and can be grouped into a one category, ("unproductive").

ging. Depending on the robustness of the vine stocks, one or two wooden stakes were positioned at each treatment site to provide support and protection, particularly when the soil was regularly tilled, as at Béguey. Correct curetted vines had as little darkened necrotic areas as possible, each with mostly functional wood exposed to oxidation (Figures 2 and 3).

Statistical analyses

Chi-squared tests were performed on three categories of vines (two degrees of freedom) for all annual comparisons of vine distributions for the assessment of the sanitary status of selected vines prior to treatment or recovery (P = 0.05, 0.01, or 0.001).

Figure 2. Examples of 'Sauvignon Blanc' vines curetted in the Couhins III-7 vineyard.

Figure 3. Illustration of the curettage technique, performed on a grapevine stock with a small chain saw (Photograph Francesco Cecconi).

RESULTS

Sanitary status of vineyards

The numbers of vines examined in each part of each vineyard (control or curettage) ranged from 470 to 1319 (Table 1). In total, 5713 different vine stocks were examined. The proportions of unproductive and esca-symptomatic vines varied from 20 to 66%, depending on the year and the vineyard considered (Suppl. Table 1). These high disease levels facilitated the selection of vines for the experiments. At Béguey, the proportions of unproductive vines were particularly high in the 'Cyprès East' (Exp. 1) and 'Cyprès West' (Exp.2) vineyards, at greater than 50%, about four times the national (French) average (Bruez *et al*., 2013). Annual statistical comparisons of the distributions of percentages of vines in each symptom category showed that the parts of the vineyards used for control and curettage treatments had similar levels of disease development (Suppl. Table 1).

The esca disease status of the vines randomly selected each year for control or curettage treatments in each part of the vineyards is shown in Table 3. The number of vines in the sample displaying very severe symptoms was generally small, except in Exp. 3 for two treatments (curettage sample in the 2016 trial, and control sample in the 2017a trial). Annual statistical comparisons of the distributions of the numbers of vines in each symptom severity category between the control and curettage treatments showed no statistically significant differences ($P > 0.05$) in all the trials except one (Exp. 1, 2015 trial).

Vine recovery

Esca development, recorded each year for the control and curettage treatments, is summarized in Table 4. In total, 422 vines were curetted and examined from 2014 onwards. They were compared to 434 vines used as experimental controls. One year after symptom expression and treatment (y + 1), most of the vines curetted in all 11 trials (358 out of 422), regardless of vineyard site, displayed general decreases in esca expression after curettage treatment relative to the controls. Percentages of curetted vines that became asymptomatic in the year after treatment ranged from 73 to 96% for vines treated just after the appearance of leaf symptoms (ten trials). The exception was in the 2017b trial in the 'Couhins III-7' vineyard (Exp. 3), where only 64% of the vines that were symptomatic in summer 2017 but treated in April 2018 remained symptomatic. For each annual distribution of curetted vines in three severity categories, the category with the greatest number of vines was asymptomatic, for all years of observations except two, for the seventh year after treatment in the oldest trial (Exp. 1, 2014 trial at 'Cyprès East') and for the fourth year after treatment in the 2017b trial in the Couhins III-7 vineyard (Exp. 3). This indicates a decrease in efficacy of curettage over time. Conversely, for control vines, the severity category with the largest number of vines generally corresponded to symptomatic or dead vines. One year after treatment, only 33% of control vines (144 out of 434) were asymptomatic. From 2014 to 2021, the annual records provided 53 comparisons of distributions between control and curettage treatments. Significant differences were observed in all comparisons: 42 of the 53 comparisons revealed highly significant differences at $P = 0.001$, and six of comparisons were significant at $P = 0.01$. The mean annual loss of efficacy of the curettage treatment was almost 7.6%, indicating a gradual decrease in health recovery over time.

Figure 4 summarizes the data for Béguey only (Experiments 1 and 2), a site at which there was a 6-7 year history of treatment. This provides a graphical representation of the fate of vines after curettage treatment, using proportions calculated for the three symptom categories. Despite the variability between years, these data clearly indicate that more than 70% curetted vines did not develop esca symptoms for at least 3 years after curettage. In contrast, despite the well-known variability of esca leaf symptoms between years (Marchi *et al*., 2006), most of the control vines continued to display

Table 3. Esca status of the control and curetted vines used in this study (11 trials). Distributions of vines between the three leaf symptom categories indicated in Table 2. The distributions were compared by pair-wise Chi-square tests ($P = 0.05$).

Experiment *Vineyard*	Year	Treatment	No. of vines	No. of vines per category			Chi-squared test result
				Mild symptoms S1 + S2	Severe symptoms S3 + S4	Very severe symptoms S5 + APO	
Experiment 1 *Cyprès East*	2014	*Control*[a]	*52*	*n. a.*	*n. a.*	*n. a.*	-
		Curettage	79	46	29	4	
	2015	*Control*	*26*	*9*	*16*	*1*	S
		Curettage	28	20	7	1	
	2016	*Control*	*32*	*20*	*10*	*2*	NS
		Curettage	29	25	3	1	
	2017	*Control*	*51*	*26*	*22*	*3*	NS
		Curettage	*36*	12	21	3	
	2018	*Control*	*21*	*10*	*11*	*0*	NS
		Curettage	19	10	8	1	
Experiment 2 *Cyprès West*	2015	*Control**	*16*	*n. a.*	*n. a.*	*n. a.*	-
		Curettage*	25	n. a.	n. a.	n. a.	
	2016	*Control*	*35*	*17*	*13*	*5*	NS
		Curettage	26	13	11	2	
	2017	*Control*	*33*	*11*	*16*	*6*	NS
		Curettage	25	10	14	1	
Experiment 3 *Couhins III-7*	2016	*Control*	*45*	*4*	*35*	*6*	NS
		Curettage	37	4	23	10	
	2017a	*Control*	*93*	*34*	*42*	*17*	NS
		Curettage	88	25	55	8	
	2017b	*Control*	*34*	*0*	*34*	*0*	NS
		Curettage in 2018	30	0	30	0	

[a] In this treatment, symptom severity on the selected symptomatic vines used was not assessed (n.a.).
Control plots are indicated in italics.

esca or died. The recovery of vines treated from 2014 onwards in the three vineyards is further highlighted in Figure 5. The total percentage of curetted vines (all trials combined) that became asymptomatic the year after curettage treatment was nearly 85%. The percentage of asymptomatic vines subsequently decreased to 39%, 7 years after treatment, for vines that were curetted in 2014. In contrast, for vines used as controls in 2014, the proportion that were symptomatic or died remained high: 60% the year after treatment and 96% 7 years later.

DISCUSSION

Curettage has a long history and was used to control GTDs a century ago, as reported by Lafon (1921). Use of this disease management strategy subsequently declined, but interest in the technique has increased in France over the last 20 years. Viticulturists and extension workers from the Loire Valley, around Sancerre (Thibault, 2015), Alsace and the South-West of France have promoted the use of curettage. Over the same period, this curative treatment has also been used in a number of other European countries, including Italy, Spain, Portugal, Germany, Croatia and Hungary (AA.VV., 2017; Mondello *et al.*, 2018). Since 2011, under the impetus of the late Professor Denis Dubourdieu, this technique has been progressively employed in many vineyards in the Bordeaux region. However, no research data were available on the duration of curettage efficacy and on the limitations of this rehabilitated technique. One recent publication (Cholet *et al.*,

Table 4. Fates of curetted and control vines (in italics), by year, after surgical treatment, in three experiments. The bold figures in gray cells indicate the greatest numbers (or percentages) of vines in each annual distribution. All distributions of numbers of vines per symptom category were significantly different using Chi-squared tests: *P* values are indicated as superscripts above the numbers of asymptomatic vines for each annual distribution of curetted vines: $P = 0.05$ (*), $P = 0.01$ (**) and $P = 0.001$ (***). Percentages values were rounded.

Experiment *Vineyard*	Year	Treatment	No. of vines	Esca health status by year after treatment; No. and % of vines per category[a]																				
				y + 1			**y + 2**			**y + 3**			**y + 4**			**y + 5**			**y + 6**			**y + 7**		
				As	S	D	As	S	D	As	S	D	As	S	D	As	S	D	As	S	D	As	S	D
Experiment 1 *Cyprès East*	2014	Curettage	79	**61***** **77%**	16 20%	2 3%	**59***** **75%**	18 23%	2 2%	**50***** **63%**	22 28%	7 9%	**46***** **58%**	26 33%	7 9%	**41***** **52%**	28 35%	10 13%	**38***** **48%**	30 38%	11 14%	31*** 39%	**33** **42%**	15 19%
		Control	*52*	*21 40%*	***28*** ***54%***	*3 6%*	*22 42%*	***25*** ***48%***	*5 10%*	*10 19%*	***32*** ***62%***	*10 19%*	*8 15%*	***24*** ***46%***	*20 39%*	*9 17%*	*18 35%*	***25*** ***48%***	*5 9%*	*17 33%*	***30*** ***58%***	*2 4%*	*14 27%*	***36*** ***69%***
	2015	Curettage	28	**27***** **96%**	1 4%	0	**25***** **89%**	1 4%	2 7%	**20***** **72%**	4 14%	4 14%	**21***** **75%**	2 7%	5 18%	**19***** **68%**	4 14%	5 18%	**15***** **54%**	7 25%	6 21%			
		Control	*26*	*3 12%*	***23*** ***88%***	*0*	*3 12%*	***22*** ***85%***	*1 4%*	*5 19%*	***14*** ***54%***	*7 27%*	*5 19%*	***13*** ***50%***	*8 31%*	*2 8%*	*10 38%*	***14*** ***54%***	*1 4%*	*7 27%*	***18*** ***69%***			
	2016	Curettage	29	**21***** **73%**	3 10%	5 17%	**23***** **79%**	1 4%	5 17%	**22***** **76%**	2 7%	5 17%	**20***** **69%**	4 14%	5 17%	**18***** **62%**	5 17%	6 21%						
		Control	*32*	*11 34%*	***21*** ***66%***	*0*	*10 31%*	***20*** ***63%***	*2 6%*	*11 34%*	***17*** ***53%***	*4 13%*	*8 25%*	***15*** ***47%***	*9 28%*	*4 12%*	***15*** ***47%***	*13 41%*						
	2017	Curettage	36	**29***** **81%**	4 11%	3 8%	**33***** **92%**	0	3 8%	**30***** **84%**	3 8%	3 8%	**25***** **70%**	8 22%	3 8%									
		Control	*51*	*20 39%*	***28*** ***55%***	*3 6%*	*15 29%*	***30*** ***59%***	*6 12%*	*14 27%*	***25*** ***49%***	*12 24%*	*4 8%*	***34*** ***67%***	*13 25%*									
	2018	Curettage	19	**16***** **84%**	2 11%	1 5%	**13**** **69%**	5 26%	1 5%	**10*** **53%**	8 42%	1 5%												
		Control	*21*	*3 14%*	***18*** ***86%***	*0*	*4 19%*	***16*** ***76%***	*1 5%*	*3 14%*	***15*** ***72%***	*3 14%*												
Experiment 2 *Cyprès West*	2015	Curettage	25	**24**** **96%**	1 4%	0	**23***** **92%**	2 8%	0	**21***** **84%**	3 12%	1 4%	**20**** **80%**	4 16%	1 4%	**19**** **76%**	3 12%	3 12%	**18*** **72%**	4 16%	3 12%			
		Control	*16*	***8*** ***50%***	*7 44%*	*1 6%*	*4 25%*	***11*** ***69%***	*1 6%*	*4 25%*	***10*** ***62%***	*2 13%*	*4 25%*	***10*** ***62%***	*2 13%*	*5 31%*	***6*** ***38%***	*5 31%*	*5 31%*	*3 19%*	***8*** ***50%***			
	2016	Curettage	26	**23***** **88%**	1 4%	2 8%	**22***** **84%**	2 8%	2 8%	**22***** **84%**	2 8%	2 8%	18*** **70%**	4 15%	4 15%	**17***** **66%**	5 19%	4 15%						
		Control	*35*	*11 31%*	***23*** ***66%***	*1 3%*	*7 20%*	***26*** ***74%***	*2 6%*	*8 23%*	***21*** ***60%***	*6 17%*	*2 6%*	***18*** ***51%***	*15 43%*	*2 6%*	*13 37%*	***20*** ***57%***						
	2017	Curettage	25	**21***** **84%**	1 4%	3 12%	**20***** **80%**	2 8%	3 12%	**14***** **56%**	6 24%	5 20%	**15***** **60%**	4 16%	6 24%									
		Control	*33*	*9 27%*	***23*** ***70%***	*1 3%*	*5 15%*	***23*** ***70%***	*5 15%*	*3 9%*	***18*** ***55%***	*12 36%*	*2 6%*	***17*** ***52%***	*14 42%*									

(Continued)

Table 4. (Continued).

Experiment *Vineyard*	Year	Treatment	No. of vines	Esca health status by year after treatment; No. and % of vines per category[a]																				
				y + 1			**y + 2**			**y + 3**			**y + 4**			**y + 5**			**y + 6**			**y + 7**		
				As	S	D	As	S	D	As	S	D	As	S	D	As	S	D	As	S	D	As	S	D
Experiment 3 *Couhins III-7*	2016	Curettage	37	**34***** **92%**	3 8%	0	**33***** **89%**	3 8%	1 3%	**29***** **79%**	6 16%	2 5%	**26***** **70%**	8 22%	3 8%	**24***** **65%**	9 24%	4 11%						
		Control	*45*	*16 36%*	***27 60%***	*2 4%*	*13 29%*	***24 53%***	*8 18%*	*8 18%*	***23 51%***	*14 31%*	*5 11%*	***24 53%***	*16 36%*	*2 4%*	*17 38%*	***26 58%***						
	2017a	Curettage	88	**83***** **94%**	2 2%	3 4%	**75***** **85%**	9 10%	4 5%	**62***** **70%**	22 25%	4 5%	**52***** **59%**	28 32%	8 9%									
		Control	*93*	*35 38%*	***40 43%***	*18 19%*	*23 25%*	***42 45%***	*28 30%*	*18 14%*	***45 54%***	*30 32%*	*1 1%*	***46 49.5%***	***46 49.5%***									
	2017b	Curettage	30	**19**** **64%**	10 33%	1 3%	**14*** **47%**	12 40%	4 13%	**14*** **47%**	10 33%	6 20%	8* 27%	**13 43%**	9 30%									
		Control	*30*	*7 23%*	***22 74%***	*1 3%*	*7 23%*	***22 74%***	*1 3%*	*8 27%*	***20 67%***	*2 6%*	*1 3%*	***17 57%***	*12 40%*									
Total		Curettage	*422*	**358 85%**	44 10%	20 5%	**340 81%**	55 13%	27 6%	**296 70%**	87 21%	39 9%	**254 62%**	99 25%	50 13%	**139 62%**	53 24%	32 14%	**73 54%**	39 31%	20 15%	31 39%	**33 42%**	15 19%
		Control	*434*	*144 33%*	***260 60%***	*30 7%*	*113 26%*	***261 60%***	*60 14%*	*87 20%*	***245 56%***	*102 24%*	*40 10%*	***218 53%***	*155 37%*	*24 12%*	*79 38%*	***103 50%***	*11 12%*	*27 29%*	***56 59%***	*2 4%*	*14 27%*	***36 69%***

[a] Vines were classified into three categories: As = Asymptomatic; S = Symptomatic (foliar and wood symptoms); D = Dead.

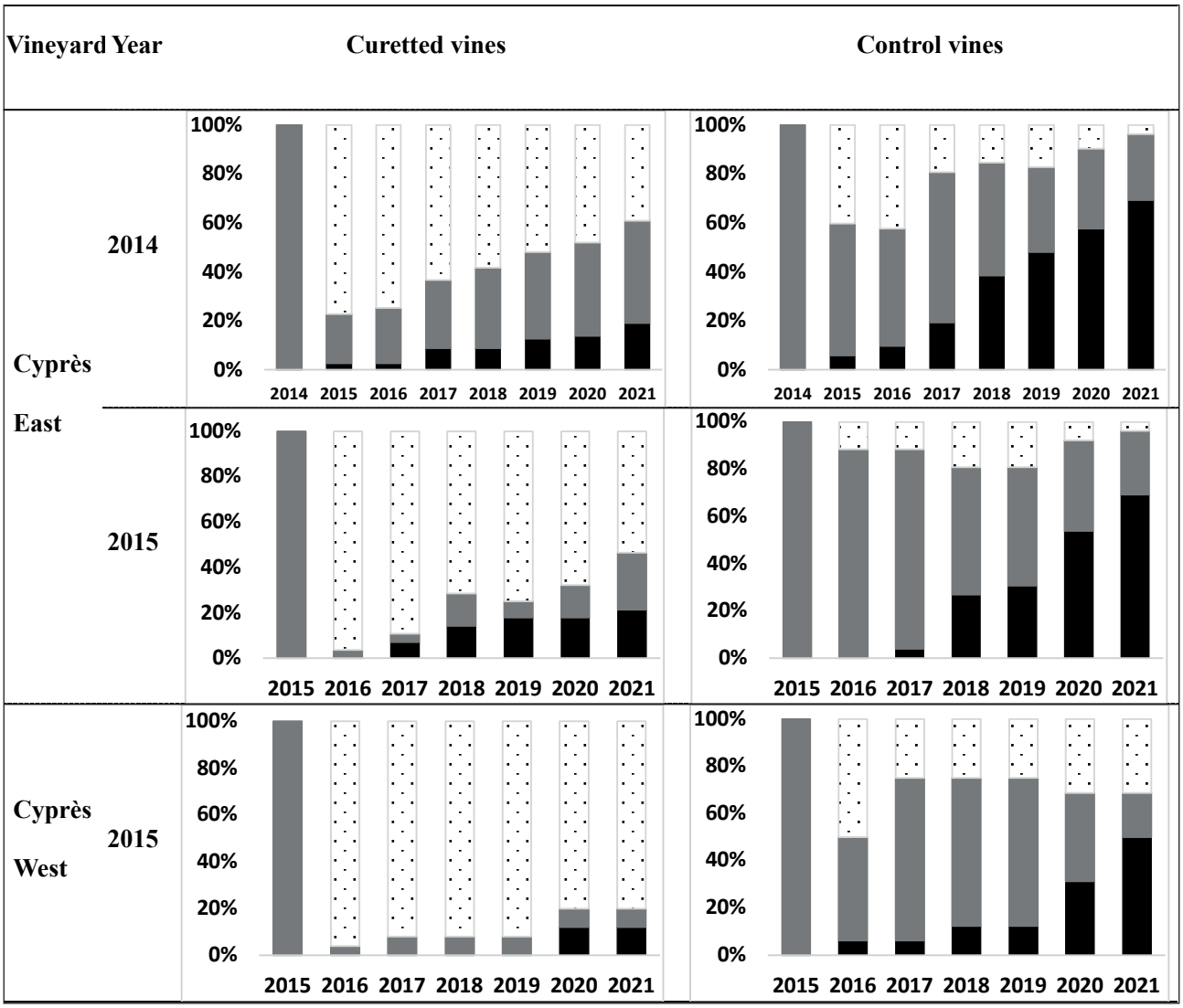

Figure 4. Percent of curetted and control vines, by year, for up to 6 and 7 years after the curettage treatment. The vines concerned were those curetted in 2014 and 2015 at Cyprès East (Exp. 1) and Cyprès West (Exp. 2). The X-axis relates to the rating years and the Y-axis relates to the % in each symptom category: asymptomatic vines are shown in white with black dots, esca-symptomatic are shown in dark gray and dead vines are shown in black.

2021) on data from the present study (Exp.1, in 2014 and 2016) focused on vine vigour, soil fertility, berry quality, and year-to-year plant recovery over a 4-year period. The study presented here is the first report on the short and mid-term recovery of curetted vines with symptomatic esca, and is based on 11 trials.

The annual esca development comparisons between curetted and non-curetted vines began in 2014 in three local vineyards. However, the study was initiated in 2012 in the vineyard 'Cyprès East' at Béguey, in which two preliminary trials were carried out in 2012 and 2013, to establish the curettage technique (results not shown). In 2012, 35 esca leaf-symptomatic vines were curetted but were not compared with control vines. Most of the curetted vines had severe esca leaf symptoms (none of the vines were classified S1 + S2), and were either dead or displaying trunk damage or were symptomatic in the year after treatment. The failure of the treatment in this trial was explained by overthinning of the trunks, lack of support stakes, and high severity of leaf symptoms. Another possible explanation was that, among the vines that were curetted at the start of the curettage campaigns, most would exhibit foliar symptoms with long esca histories. As experiments progress, treated vines

Years after treatment (T)	Curetted	Control
T + 1	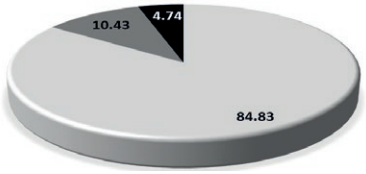	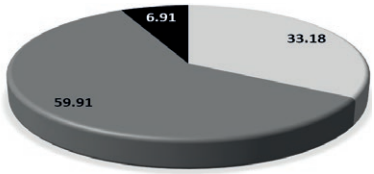
	422 vines curetted in 2014, 2015, 2016, 2017 and 2018	434 vines used as controls in 2014, 2015, 2016, 2017 and 2018
T + 2	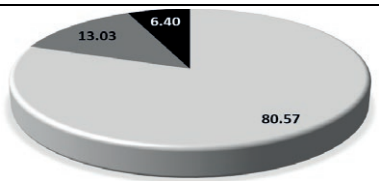	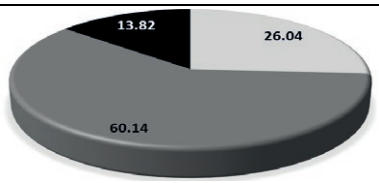
	422 vines curetted in 2014, 2015, 2016, 2017 and 2018	434 vines used as controls in 2014, 2015, 2016, 2017 and 2018
T + 3	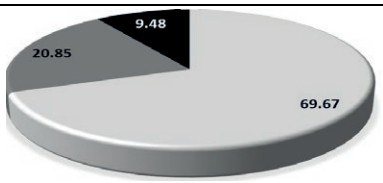	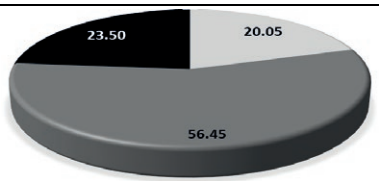
	422 vines curetted in 2014, 2015, 2016, 2017 and 2018	434 vines used as controls in 2014, 2015, 2016, 2017 and 2018
T + 4	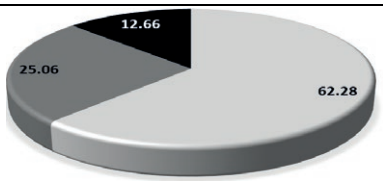	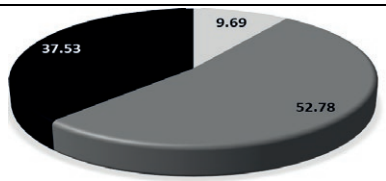
	406 vines curetted in 2014, 2015, 2016 and 2017	413 vines used as controls in 2014, 2015, 2016 and 2017
T + 5	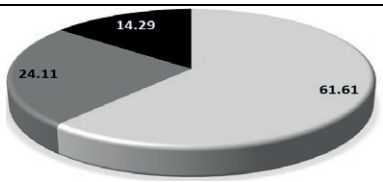	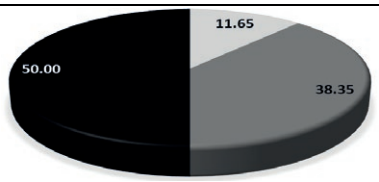
	224 vines curetted in 2014, 2015 and 2016	206 vines used as controls in 2014, 2015 and 2016
T + 6	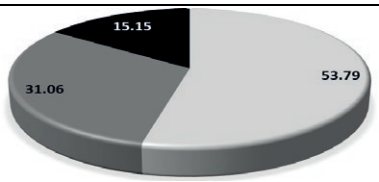	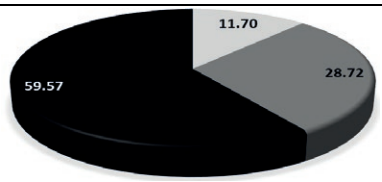
	132 vines curetted in 2014 and 2015	94 vines used as controls in 2014 and 2015
T + 7	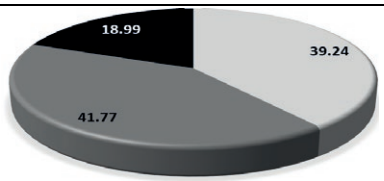	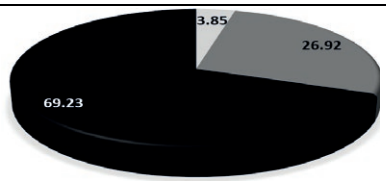
	79 vines curetted in 2014	52 vines used as controls in 2014

Figure 5. Health status, with respect to esca, for all vines that were curetted or used as experimental controls since 2014 (all experiments combined), 1 to 7 years after curettage treatment (T). Percentages of asymptomatic vines are shown in light gray, those of symptomatic vines are in dark gray, and those of dead vines are shown in black.

could previously have not, or infrequently, expressed symptoms. These explanations are consistent with the observations of Thibault (2015) in the Loire Valley and the outcomes of the "Winetwork" project (AA. VV., 2017). In 2013, a second preliminary trial without experimental controls, carried out on 62 curetted vines with 52 vines showing mild (26 vines) or moderately severe symptoms (26), 81% recovered the year after treatment. After these trials, it was decided to apply curettage primarily on vines with mild or moderately severe symptoms and to protect them with small wooden posts. However, further experiments are required, such as the 2017b trial at Couhins on vines showing uniform disease levels, to establish precise limits of the technique.

The experimental designs of the present study were dependent on curettage operators requiring simple, non-time-consuming procedures with easy-to-use equipment, so it was not possible to set up experiments with blocks within each vineyard. For eight of the trials, vineyards were split into two areas, one for the curettage treatment, and the other as a control. This experimental design was possible due to the severe GTD damage and its relative homogeneity at the sites. The high levels of GTD affected vines facilitated identification of symptomatic vines for the experiments in each year. For three trials, at Béguey in 2014 (Exp. 1) and at Villenave d'Ornon (Exp. 3) in 2016 and in 2017 for the 2017a trial, vines were selected at random within the same rows. Clear, highly consistent trends emerged from the results obtained from both study designs.

From 2014 onwards, curettage led to immediate recovery in symptomatic vines the year after treatment. All annual comparisons showed a general and positive effect of curettage on esca control. Conversely, most of the control vines steadily declined and eventually died. The high mean percent efficacy the year immediately after curettage (close to 85%) was consistent with other reports (Lafon, 1921; Thibault, 2015; De Montaignac, 2019; Pacetti *et al*., 2021). The gradual loss of efficacy that was subsequently observed indicates that curettage can delay vine decline due to esca, but does not completely control the disease. Additional long-term experiments focusing on the durability of vine recovery induced by curettage would be useful, to determine the value this technique over total vineyard lifespans.

Based on the present study, several hypotheses can be formulated to explain curettage-induced recovery of vines with esca symptoms. A high proportion of curetted vines displayed no esca symptoms in the years following treatments. The mechanism(s) involved cannot only be related to the well-known year-to-year variability of esca leaf symptoms (Surico *et al*., 2000; Marchi *et al*., 2006). Mondello *et al.* (2018) showed that suppression of GTD foliar symptoms may reflect temporary increases in oxygenation, the action of elicitors inducing host resistance, or possible interactions with saprobes. However, these studies did not focus on the effect of the removal of dead wood and rotten tissues, including white rot in particular. The hypotheses were based on a study of Calzarano and Di Marco (2007), where no correlation was found between the volume of white rot or wood discolouration in vine trunks and foliar symptoms in esca-affected vines. However, other studies have reported that the volume of degraded wood may be a key factor, at least partly explaining grapevine decline and the expression of esca leaf symptoms (Lecomte *et al*., 2008 a; b; Liminana *et al*., 2009; Maher *et al*., 2012; Travadon *et al.* 2016; Lecomte *et al*., 2018; Bénétreau *et al*., 2019). By removing white rot, curettage eliminates much of the tissue colonized by pathogenic basidiomycetes, including *Fomitiporia mediterranea* in particular, a fungus already reported to play a major role in esca (Maher *et al*., 2012; Bruez *et al*., 2017). Ouadi *et al*. (2019) also suggested that a threshold of at least 10% white rot was potentially a is a potentially good descriptor of the chronic form of esca, and Pacetti *et al.* (2021) observed a significant decrease in the abundance of *Fomitiporia mediterranea* after trunk surgery. Two reviews (Del Frari *et al*., 2021; Moretti *et al*., 2021) have also underlined the key role of *Fomitiporia mediterranea* in esca leaf expression. Curettage surgically removes white rot and part of dead wood, thereby eliminating the GTD pathogens present in damaged wood, mostly caused by *Fomitiporia mediterranea*. This probably leads to decreasen the inoculum pressure of this pathogen, and improves the balance between functional and non-functional wood structures. This physiological and pathological context may explain the remission of leaf symptoms, which may also be related to decreased water or nutrient demands by the remaining pathogens.

Curettage is a technique that should be used as soon as the first esca symptoms are expressed, or on asymptomatic vines before disease expression, such as those with external dead wood 10 years after planting. In practical terms for each vine, curettage first involves identifying a large wound or a necrotic sectoral wood zone as a starting point for opening up the trunk or cordons. The operator then removes the damaged wood, while avoiding interference with functional wood. At the start of the 20th Century, the removal of all dead wood was recommended (Ravaz, 1909; Lafon, 1921), but some operators now consider that the principal objective of curettage is specific removal of white-rot tissues (often in trunk centres), rather than removal of all dead wood.

This procedure is more rapid, is just as effective and does not greatly weaken the stocks (Thibault, 2015). In practice, it is not possible to remove all the dead wood. Curettage may leave some hard wood in place, and cannot eliminate vascular pathogens, such as *Phaeoacremonium minimum* and *Phaeomoniella chlamydospora*, which are also involved in the esca complex. These two fungi, and many others, are also often present in functional wood (Bruez *et al*., 2014), and possibly cause the foliar symptoms through the action of metabolites (Andolfi *et al*., 2011), although this view remains controversial. Despite the presence of these fungi and their putative toxic activity, most curetted vines display no leaf symptoms of esca for several years after treatment. This observation is consistent with *Fomitiporia mediterranea* being involved in the mechanism of foliar symptom expression, and lends weight to the theory that toxins (from *Phaeoacremonium minimum* and *Phaeomoniella chlamydospora*) are probably not the only elements involved in the development of esca leaf symptoms (Moretti *et al*., 2021).

Esca symptoms are also observed only in the summer, when temperatures are high and water constraints can be strong (Lecomte *et al*., 2012). Beside leaf symptoms, longitudinal stripes affecting host vessels just below the bark have also been observed. These stripes were associated with sudden disruptions of sap routes during a period in which competition for water can be strong, particularly if there are large volumes of necroses and an imbalance between the amounts of functional and non-functional wood (Maher *et al*., 2012). Removal of the white rot helps to decrease inoculum pressure and competition for water and nutrients. This hypothesis is consistent with the general rationale of curative control. Curettage may have other consequences, such as improvements in vine capacity to compartmentalize necroses, or reductions in host energy required for defenses. By opening trunks and removing the tender and spongy tissues characteristic of white rot, curettage may also decrease the amount of water available to mycelia of esca pathogens, particularly of *Fomitiporia medirerranea*, thereby decreasing colonization of functional wood during rainy periods. Curettage should be accompanied by insertion of gutter in the lower parts of curetted wood, to facilitate water flow.

Decreases in inoculum pressure and recovery plant health are not the only benefits of curettage. Cholet *et al.* (2021) showed that curetted grapevines rapidly regained growth capacity similar to that of asymptomatic vines. By extending vine lifespan, this technique enables them to continue to produce high quality grapes, which is essential for wine production. However, previous studies on curettage have shown that this technique is not suitable for all vineyards. The most suitable vine training systems for this technique are those in which the vines have large trunks, such as the 'Espalier Guyot' forms. Other limitations are the costs which have not been economically analysed. Growers may be reluctant to adopt curettage because the increases in lifespan and net returns afforded by this technique have yet to be quantified. The equipment required is not expensive, but the technique is time-consuming and highly dependent on operator skills. Curettage takes at least 10-15 min per vine, with estimated cost of between 18 and 35 euro per h, depending on the operator. Depending on region, the time spent by the operators and the type of operator (company employee or external service provider), the additional cost of curettage ranges from 2.5 to 15 euro per vine (Thibault, 2015; De Montaignac, 2019). However, as curettage results in vine recovery for several years, the net returns are increased before vines need to be uprooted. There are also time lags between the cost and the benefits of curettage procedures. Annual costs must therefore be considered in light of long-term outcomes. Based on this 7-year study, simulations may be able to show whether no action results in significant economic losses, or whether a given investment in curettage is profitable, as was reported by Kaplan *et al.* (2016) for preventative techniques.

The rehabilitation of curettage extends the array of methods available for esca control. Curettage is particularly suitable for grapevines with moderate esca symptoms or for vines with external dead wood. Eugène Poussard recommended performing curettage as soon as leaf symptoms appear, and Lafon (1921) performed this operation in winter. The reduced efficacy of the technique recorded in the present study for Experiment 3 trial 2017b, with vines curetted later than the others, also indicates early implementation of this control strategy. In cases of moderate symptoms not affecting the grapes, curettage may also save part of the harvest. For vines with very severe symptoms, other alternatives must be used, such as trunk renewal (Smart, 2015), trunk renewal plus curettage (cutting off the cordons), or re-grafting (Dal *et al*., 2013). A feature of this mutilating technique is the absence of protection after exposure of the functional wood to the open air. The opened trunks, with their large wounds, would be expected to facilitate new infections and/or development of latent pathogens, which would limit vine longevity. In the past, Ravaz (1909) advised application of tar products on wounded tissues, and Eugène Poussard painted curetted vines with a solution of copper salts (Lafon, 1921). Protection products currently are not applied to the curetted vine tissues, and further research

is required to determine if application of these products increases the lifespan of the curetted vines.

In the present study, curettage reduced vine mortality due to GTDs. This practice is a useful GTD control strategy, for vineyards with low training systems, such as 'Espalier Guyot' forms (Pacetti *et al*., 2021), and for vineyards producing wines with high added value or with high expected longevity. Increased understanding of the mechanisms of esca symptom expression will help explain symptom suppression after curettage. This is the first report on the efficacy of this technique based on a mid-term study over 7 years.

ACKNOWLEDGMENTS

This study is dedicated to the memory of the late Professor Denis Dubourdieu, who initiated the research. The study was within the framework of the COTE cluster of excellence and the GTDfree Industrial Chair, jointly funded by the French National Research Agency (*Agence Nationale de la Recherche*, ANR) and Hennessy (Cognac, France). Technical assistance was provided by Barka Diarra, Léocadie Benech, Guillaume Bonneau and Lucille Gendre. The authors also thank Chateau Couhins and Chateau Reynon - Denis & Florence Dubourdieu EARL, for providing the experimental plots, with particular thanks to Jean-Claude Delmas, and Fabrice and Jean-Jacques Dubourdieu.

LITERATURE CITED

AA.VV., 2017. Le Curetage. Une pratique appliquée au vignoble pour limiter l'expression des symptômes des maladies du bois. Fiche Technique, Winetwork. Available on line: http://www.winetwork-data.eu/fr/fiches_techniques/le_curetage_sc_16484.htm (accessed June 28, 2021).

Andolfi A., L. Mugnai, J. Luque, G. Surico, A. Cimmino, A. Evidente, 2011. Phytotoxins produced by fungi associated with grapevine trunk diseases. *Toxins* 3: 1569–1605. DOI: 10.3390/toxins3121569

Ammad F., M. Benchabane, M. Toumi, N. Belkacem, A. Guesmi, … O. Merah, 2014. Occurrence of Botryosphaeriaceae species associated with grapevine dieback in Algeria. *Turkish Journal of Agriculture and Forestry* 38(6): 965–976. DOI: 10.3906/tar-1404-15

Arnaud G. and M. Arnaud, 1931. Esca, polypores et maladies fongiques diverses du tronc. In : *Traité de Pathologie Végétale - Encyclopédie Mycologique III* (Lechevalier et Fils, ed.) Paris, 428–444.

Baumgartner K., P.T. Fujiyoshi, R. Travadon, L.A. Castlebury, W.F. Wilcox, and P.E. Rolshausen, 2013. Characterization of species of *Diaporthe* from wood cankers of grape in eastern North American vineyards. *Plant Disease* 97: 912–920.

Bénétreau C., P. Lecomte, B. Diarra, J. Vallance, M.-C. Dufour, … P. Rey, 2019. Esca and training systems in the viticulture region of Charentes, France. Abstracts of oral and poster presentations given at the 11th International Workshop on Grapevine Trunk Diseases, Penticton, British Columbia, Canada, July 7–12, 2019. *Phytopathologia Mediterranea* 58(2): 445.

Bruez E., P. Lecomte., J. Grosman, B. Doublet, C. Bertsch, … P. Rey, 2013. Overview of grapevine trunk diseases in France in the early 2000s. *Phytopathologia Mediterranea* 52(2): 262–275.

Bruez E., J. Vallance, J. Gerbore, P. Lecomte, J.-P. Da Costa, L. Guérin-Dubrana, P. Rey, 2014. Analyses of the temporal dynamics of fungal communities colonizing the healthy wood tissues of Esca leaf-symptomatic and asymptomatic vines. *PLoS ONE* 9(5): e95928. DOI: -10.1371/-journal.pone.0095928

Bruez E., R. Haidar, M.T. Alou, J. Vallance, C. Bertsch, … P. Rey, 2015. Bacteria in a wood fungal disease: characterization of bacterial communities in wood tissues of esca-foliar symptomatic and asymptomatic grapevines. *Frontiers in Microbiology* 6: 1137. DOI: 10.3389/fmicb.-2015.01137

Bruez E., P. Larignon, C. Bertsch, P. Rey, F. Fontaine, 2017. Comparison of the wood-microbiome from grapevine trunk disease-plants, treated or not with sodium arsenite. In: Abstracts of oral and poster presentations given at the 10th International Workshop on Grapevine Trunk Diseases, Reims, France, 4–7 July 2017. *Phytopathologia Mediterranea* 56(3): 560–561.

Bruez E, P. Larignon, C. Bertsch, G. Robert-Siegwald, M. H. Lebrun, … F. Fontaine, 2021a. Impacts of sodium arsenite on wood microbiota of esca-diseased grapevines. *Journal of Fungi* 7: 498. DOI: 10.3390/jof7070498

Bruez E., C. Cholet., C. Thibon, P. Redon, S. Lacampagne, … L. Gény, 2021b. Influence of curettage on esca-diseased Vitis vinifera L. cv Sauvignon blanc plants on the quality of musts and wines. *OENO One*. 55(1), 171–182. DOI: 10.20870/oeno-one.2021.55.1.4479

Calzarano F., S. Di Marco., 2007. Wood discoloration and decay in grapevines with esca proper and their relationship with foliar symptoms. *Phytopathologia Mediterranea* 46(1): 96–101.

Camilli K., D. Appel, W. Watson, 2007. Studies on pruning cuts and wound dressings for oak wilt control. *Arboriculture and Urban Forestry* 33(2): 132–130.

Choueiri E., F. Jreijiri, P. Chlela, V. Mayet, G. Comont., … P. Lecomte, 2014. Fungal community associated with grapevine wood lesions in Lebanon. *Journal International des Sciences de la Vigne et du Vin* 48: 293–302.

Cholet C., E. Bruez., P. Lecomte, A. Barsacq., T. Martignon, ... L. Gény, 2021. Plant resilience and physiological modifications induced by curettage of Esca-diseased grapevines. *OENO One 55*(1): 153–169. DOI: 10.20870/-oeno-one.2021.55.1.4478

Clark J.R., N. Matheny, 2010. The Research Foundation to Tree Pruning: a review of the literature. *Arboriculture & Urban Forestry* 36(3): 110–120.

Dal F. *et al*., 2013. Manuel des pratiques viticoles contre les maladies du bois. Sicavac et Bivc eds, Imprimerie Paquereau, Angers, France, 120 pp.

Darrieutort G., P. Lecomte, 2007. Evaluation of a trunk injection technique to control grapevine wood diseases. *Phytopathologia Mediterranea* 46(1): 50–57.

Del Frari G., H. Oliveira, R. Boavida Ferreira, 2021. White Rot Fungi (*Hymenochaetales*) and Esca of grapevine: insights from recent microbiome studies. *Journal of Fungi* 7: 770. DOI: 10.3390/jof7090770

De Montaignac H., 2019. Le curetage porte ses fruits. *La Vigne* 316: 32–33.

Elena G., E. Bruez., P. Rey, J. Luque, 2018. Microbiota of grapevine woody tissues with or without escafoliar symptoms in northeast Spain. *Phytopathologia Mediterranea* 57(3): 425–443. DOI: 10.14601/Phytopathol_Mediterr-23337

Garton W.J., M. Mazzola, N. Dasgupta, R. Travis, T.R. Alexander, C.A. Miles., 2018. Efficacy of excision, cauterization, and fungicides for management of apple anthracnose canker in maritime climate. *HortTechnology* 28(6): 728–736. DOI: /10.21273/horttech04148-18

Gramaje D., J.R. Úrbez-Torres, M.R. Sosnowski., 2018. Managing grapevine trunk diseases with respect to etiology and epidemiology: current strategies and future prospects. *Plant Disease* 102(1): 12–39.

Gaudineau M., 1959. L'esca ou Apoplexie parasitaire. Rapport national. VIII° Congrès International de la Vigne et du Vin. *Bulletin de l'Office International de la Vigne et du Vin*, 4–8.

Gregory G., J. Allison, 1979. The comparative effectiveness of pruning versus pruning plus injection of trunk and/or limb for therapy for Dutch elm disease in American elms. *Journal of Arboriculture* 5: 1–4.

Guérin-Dubrana L., F. Fontaine, L. Mugnai, 2019. Grapevine trunk disease in European vineyards: occurrence, distribution and associated disease-affecting cultural factors. *Phytopathologia mediterranea* 58(1): 49–71. DOI: 10.13128/Phytopathol_Mediterr-25153

Hrycan J., M. Hart, P. Bowen, T. Forge, J.R. Úrbez-Torres., 2020. Grapevine trunk disease fungi: their roles as latent pathogens and stress factors that favour disease development and symptom expression. *Phytopathologia Mediterranea* 59(3): 395–424. DOI: 10.14601/PHYTO-11275

Kaplan J., R. Travadon, M. Cooper, V. Hillis, M. Lubell, K. Baumgartner, 2016. Identifying economic hurdles to early adoption of preventative practices: the case of trunk diseases in California winegrape vineyards, *Wine Economics and Policy* 5: 127–141.

Lafon R., 1921. Modifications à apporter à la taille de la vigne des Charentes, taille Guyot-Poussart mixte et double : l'apoplexie, traitement préventif (méthode Poussard), traitement curatif. Roumégous et Déhan Impr., Montpellier, 96 pp.

Larignon P., B. Dubos, 1997. Fungi associated with esca disease in grapevine. *European Journal of Plant Pathology* 103: 147–157.

Larignon P., O. Yobregat, 2016. Cahier pratique: comment lutter contre les maladies du bois de la vigne? Institut Français de la Vigne et du Vin ed., 7 pp.

Lecomte P., G. Darrieutort, J.-M. Limiñana, G. Louvet, L. Guérin, … D. Blancard, 2008a. (I) Eutypiose et Esca - Eléments de réflexion pour mieux appréhender ces phénomènes de dépérissement. *Phytoma - La Défense des Végétaux* 615: 42–48.

Lecomte P., G. Darrieutort, J.-M. Limiñana, G. Louvet, L. Guérin, … D. Blancard, 2008b. (II) Esca de la vigne - Vers une gestion raisonnée des maladies de dépérissement. *Phytoma - La Défense des Végétaux* 616: 37–41.

Lecomte P., G. Darrieutort, J.-M. Limiñana, G. Comont, A. Muruamendiaraz, … M. Fermaud, 2012. New insights into Esca of grapevine: the development of foliar symptoms and their association with xylem discoloration. *Plant Disease* 96 (7): 924–934.

Lecomte P., B. Diarra, A. Carbonneau, P. Rey, C. Chevrier, 2018. Esca of grapevine and training practices in France: results of a 10-year survey. *Phytopathologia Mediterranea* 57(3): 472–487. DOI: 10.14601/Phytopathol_Mediterr-22025

Liminana J.-M., G. Pacreau, F. Boureau., E. Menard., S. David., … V. Dumot, 2009. Inner necrosis in grapevine rootstock mother plants in the Cognac area (Charentes, France). *Phytopathologia Mediterranea* 48(1): 92–100.

Luque J., S. Martos, A. Aroca, R. Raposo, F. Garcia-Figueres, 2009. Symptoms and fungi associated with declining mature grapevine plants in northeast Spain. *Journal of Plant Pathology* 91(2): 381–390.

Maher N., J. Piot, S. Bastien, J. Vallance., P. Rey, L. Guérin-Dubrana, 2012. Wood necrosis in esca-affected

vines: types, relationships and possible links with foliar symptom expression. *Journal International des Sciences de la Vigne et du Vin* 46(1): 15–27.

Marchi G., F. Peduto, L. Mugnai, S. Di Marco., F. Calzarano, G. Surico, 2006. Some observations on the relationship of manifest and hidden Esca to rainfall. *Phytopathologia Mediterranea* 45(Supplement): 117–126. DOI: 10.14601/Phytopathol_Mediterr-1841

Mondello V., P. Larignon., J. Armengol, K. Kortekamp, K. Vaczy, … F. Fontaine, 2018. Management of gravevine trunk diseases: knowledge transfer, current strategies and innovative strategies adopted in Europe. *Phytopathologia Mediterranea* 57(3): 369-383. DOI: 10.14601/Phytopathol_Mediterr-23942

Moretti S., A. Pacetti, R. Pierron, H.-H. Kassemeyer, M. Fisher, ... S. Farine, 2021. "*Fomitiporia mediterranea* M. Fisch., the historical Esca agent: a comprehensive review on the main grapevine wood rot agent in Europe". *Phytopathologia Mediterranea* 60(2): 351–379. DOI: 10.36253/phyto-13021

Mugnai. L., A. Graniti, G. Surico, 1999. Esca (black measles) and brown wood-streaking: two old and elusive diseases of grapevines. *Plant Disease* 83(5): 404–418. DOI: /10.1094/PDIS.-1999.83.5.404

Ouadi L., E. Bruez, S. Bastien, J.-C. Domec, P. Rey, 2019. Ecophysiological impacts of esca, a devastating grapevine trunk disease, on *Vitis vinifera* L. *PLoS One* 14(9), e0222586. DOI: 10.1371/journal-.pone.0222586

Pacetti A., S. Moretti, C. Pinto, S. Compant, S. Farine, C. Bertsch, L. Mugnai, 2021. Trunk surgery as a tool to reduce foliar symptoms in diseases of the Esca complex and its influence on vin wood microbiota. *Journal of Fungi* 7, 521. DOI: 10.3390/jof7070521

Paulin J.-P., 1996. Control of fireblight in European pome fruits. *Outlook on Agriculture* 25(1): 49-55.

Pavlou C.H., 1906. Lettre à M. Ravaz. *Progrès Agricole et Viticole* 46: 690.

Pouzoulet J., E. Scudiero, M. Schiavon, L. S. Santiago, P. E. Rolshausen, 2019. Modeling of xylem vessel occlusion in grapevine. *Tree Physiology* 39: 1438–1445. DOI: 10.1093/-treephys/tpz036

Ravaz L., 1909. Sur l'apoplexie de la vigne. *Progrès Agricole et Viticole* 52: 574–579.

Rolshausen P., M. Sosnowski, F.P. Trouillas, W.D. Gubler, 2015. Eutypa dieback. In *Compendium of Grape Diseases, Disorders and Pests* (2nd Ed), (W. F. Wilcox, W. D. Gubler and J. K. Uyemoto, ed.), APS Press, Saint Paul, MN, USA, 57–61.

Shigo A. L., 1982. Tree decay in our urban forests: What can be done about it. *Plant Disease* 66 (9): 763-768.

Smart R., 2015. Timely trunk renewal to overcome trunk disease. *Practical Winery & Vineyard* October, 64–70.

Sosnowski M., M. Creaser., T. Wicks, 2004. Managing eutypa dieback of grapevines by remedial surgery. *The Australian and New Zealand Grapegrower and Winemaker* 488: 35–39.

Surico G., G. Marchi, Bracini P., L. Mugnai., 2000. Epidemiology of Esca in some vineyards in Tuscany (Italy). *Phytopathologia Mediterranea* 39(1): 190–205.

Svihra P., 1994. Principles of eradicative pruning. *Journal of Arboriculture* 20: 262–271.

Thibault M., 2015. Le curetage. *Proceedings of the «Journées Maladies du bois»*, 17-18 November 2015, Institut Français de la Vigne-Université de Haute-Alsace, 55-57.

Travadon R., P. Lecomte P., B. Diarra, D.P. Lawrence., D. Renault, … Baumgartner, 2016. Grapevine pruning systems and cultivars influence the diversity of wood-colonizing fungi. *Fungal Ecology* 24: 82–93.

Úrbez-Torres J.R., 2011. The status of Botryosphaeriaceae species infecting grapevines. *Phytopathologia Mediterranea* 50(4): S5–S45. DOI: 10.14601/Phytopathol_Mediterr-9316

Zeller S.M., 1926. Cankers of apple and pear in Oregon and their control. *Oregon Agriculture College Experiment Station Bulletin* 222, 52 pp.

Phytopathologia Mediterranea
The international journal of the
Mediterranean Phytopathological Union

Firenze University Press
www.fupress.com/pm

Research Papers

Nanoplate digital PCR assays for detection and quantification of *Xylella fastidiosa*

Alessandro PASSERA[1], Valentina GROSSO[2], Niccolò MIOTTI[1], Marzia ROSSATO[2], Francesca GAFFURI[3], Paola CASATI[1], Massimo DELLEDONNE[2,4], Piero Attilio BIANCO[1,5,*]

[1] *Department of Agricultural and Environmental Sciences – Production, Landscape, Agroenergy, University of Milan, Milan, Italy*
[2] *Department of Biotechnology, University of Verona, Verona, Italy*
[3] *Laboratorio del Servizio Fitosanitario, Servizio Fitosanitario Regione Lombardia, Fondazione Minoprio, Vertemate con Minoprio, Italy*
[4] *Genartis s.r.l., Verona, Italy*
[5] *Institute for Sustainable Plant Protection, National Research Council (IPSP-CNR), Turin, Italy*
*Corresponding author. E-mail: piero.bianco@unimi.it

Summary. *Xylella fastidiosa* is a fastidious Gram-negative bacterium that is associated with several important plant diseases, and is regulated as a quarantine pest in many countries where strategies are implemented to prevent its introduction and spread. To enact efficient quarantine measures, effective and early detection of the pathogen are essential, especially because global trade of goods increases the risks of introduction of alien pathogens. this study aimed to adapt two qPCR-based diagnostic methods (SYBR Green and Probe based qPCR), already in use to detect *X. fastidiosa*, for use with a nanoplate based digital PCR assay. Detection of the pathogen using the two digital PCR assays (EvaGreen- and Probe-based) was similar to standard qPCR, giving 100% sensitivity, specificity, and accuracy, while providing accurate absolute quantification of the pathogen when using experimental samples that had low concentrations of host DNA. Using undiluted plant DNA added with low concentrations of *X. fastidiosa*, only the TaqMan method maintained satisfactory performance and quantification, and is therefore preferred. These results are a first step demonstrating the usefulness of nanoplate-based digital PCR for detection of plant pathogens, which allows greater throughput than qPCR, reducing the time and cost of diagnostic assays.

Keywords. qPCR, *Nerium oleander*, TaqMan, EvaGreen, dPCR.

OPEN ACCESS

Citation: A. Passera, V. Grosso, N. Miotti, M. Rossato, F. Gaffuri, P. Casati, M. Delledonne, P.A. Bianco (2022) Nanoplate digital PCR assays for detection and quantification of *Xylella fastidiosa*. *Phytopathologia Mediterranea* 61(3): 489-503. doi: 10.36253/phyto-13803

Accepted: December 9, 2022

Published: January 13, 2023

Data Availability Statement: All relevant data are within the paper and its Supporting Information files.

Competing Interests: The Author(s) declare(s) no conflict of interest.

Editor: Anna Maria D'Onghia, CIHEAM/Mediterranean Agronomic Institute of Bari, Italy.

ORCID:
AP: 0000-0001-6928-453X
VG: 0000-0002-2983-728X
NM: 0000-0002-7633-4053
MR: 0000-0002-6101-1550
FG: 0000-0002-2132-4093
PC: 0000-0001-6152-8712
MD: 0000-0002-7100-4581
PAB: 0000-0002-9541-1923

INTRODUCTION

Xylella fastidiosa (Xf) is an important plant pathogen (Mansfield *et al.*, 2012). Xf is a Gram-negative bacterium that colonizes plants, particularly their xylem vessels, as well as insects. This pathogen is difficult to culture, which led to the species name of *fastidiosa* (Wells *et al.*, 1987). Xf can cause severe damage when introduced in new environments. The pathogen was

initially known in North and South America, associated with grapevine Pierce's disease (Davis *et al.*, 1978). However, Xf has been identified in numerous outbreaks, and many studies have determined that Xf has a wide host range, including 655 plant species in 88 families (EFSA, 2022). To date, the main crops affected by Xf are olive trees (*Olea* spp.), grapevine (*Vitis* spp.), citrus (*Citrus* spp.), coffee (*Coffea* spp.), peach (*Prunus persica*) and almond (*Prunus dulcis*) (Chang *et al.*, 1993; Rodriguez *et al.*, 2007; Saponari *et al.*, 2013; EFSA 2022), but the pathogen has also been found in forest trees, including American elm (*Ulmus americana*), American sycamore (*Platanus occidentalis*) and northern red oak (*Quercus rubra*) (Desprez-Loustau *et al.*, 2020), as well as in common ornamental, wild and crop plants including fleabane (*Erigeron* sp.), *Helichrysum stoechas*, pistachio (*Pistacia vera*), and persimmon (*Diospyros kaki*) (EFSA 2022). This host list is being often updated, as EFSA has been mandated by the European Commission to publish biannual updates of *Xylella* hosts species during 2021 to 2026.

Many asymptomatic hosts of Xf have been discovered, because the pathogen is commensalist with its host plants, and only a subset of interactions between specific hosts and clades of Xf can result in the disease development (Sicard *et al.*, 2018). This phenomenon is also because Xf is genetically diverse, and its classification has been a matter of opinion with as few as two and as many as five subspecies being recognized. Among these, three subspecies are widely supported: *Xylella fastidiosa* subsp. *fastidiosa*, *Xylella fastidiosa* subsp. *multiplex*, and *Xylella fastidiosa* subsp. *pauca* (Potnis *et al.*, 2019; Vanhove *et al.*, 2019). *Xylella fastidiosa* subsp. *pauca* is gaining importance in Europe as the cause of olive quick decline syndrome in Apulia (Saponari *et al.*, 2013; 2017).

As well as high genetic variability and wide host range, management of Xf is further complicated because the pathogen is transmitted by insect vectors, which harbour the bacterium in their foreguts (Purcell, 1979, Backus and Morgan, 2011). This is different from most other pathogens transmitted persistently, that instead perform complex molecular interactions with their insect vectors and have limited host ranges (Redak *et al.*, 2004). In practical terms, this means that sharpshooter leafhoppers (Hemiptera, Cicadellidae, Cicadellinae) or spittlebugs (Hemiptera, Cercopoidea, Aphrophoridae, Cercopidae, Clastopteridae), which are xylem-sap feeders, could potentially be Xf vectors (Frazier, 1965). The most important known vectors of Xf are *Homalodisca vitripennis* (Hemiptera, Cicadellidae) in America, and *Philaenus spumarius* (Hemiptera, Aphrophoridae) in Europe (Cornara *et al.*, 2016).

Taking these biological features of Xf into consideration, which are further complicated by ecological, social, and economic factors, introduction of Xf into new areas where novel vectors and hosts occur, can have severe consequences, leading to inclusion of Xf into the quarantine pest category (NAPPO, 2004; EPPO, 2021). The European Commission has published a list of priority regulated quarantine pests, including Xf, which every Member State must implement all possible actions to avoid introduction and spread of this organism, and formulate contingency plans, simulation exercises, and action plans for the eradication of these pests (Regulation (EU) 2016/2031).

For this reason, early and precise diagnoses of the presence of Xf are important, particularly because this pathogen causes non-specific symptoms which can be mistaken for abiotic stresses (Thorne *et al.*, 2006), particularly water or nutrient stress, and these symptoms develop months after infections (Baldi and La Porta, 2017). In the periods between infection and symptom development, the pathogen can be acquired by vectors and transmitted to new hosts, so diagnoses based on symptom observation are inefficient for the containment of the pathogen. However, Xf can be detected by molecular assays before host symptoms develop, so molecular assays have dominated diagnosis of this pathogen. These methods include traditional assays such as ELISA and conventional PCR, as well as more modern approaches such as real-time PCR (qPCR) and LAMP. The main methods for the detection of the pathogen are indicated in the standard EPPO PM 7/24 (EPPO, 2019), while in Regulation EU 2020/1201 (Annex IV) official test methods are indicated that must be used by laboratories for the identification of *X. fastidiosa* and its subspecies.

Despite being accurate and efficient, the current methods used for detection of Xf suffer from low throughput rates and being time-consuming and labour-intensive. These methods also allow precise pathogen quantification only when using standards of known concentration as references. Digital PCR (dPCR) can increase analysis throughput by removing the need for technical replicates and allowing absolute pathogen quantification without the need for reference material or standards (Selvaraj *et al.*, 2019). This reduces pathogen detection times. Early pathogen detection is important in areas where the pathogen is yet to establish, and at important entry points of plant material into a country, such as harbours and airports. In global trade, the availability of fast, reliable, and quantitative diagnostic assays for pathogens and pests has become are urgently required (Faino *et al.*, 2021), as testified by the reports of impor-

tant pests being recently found in new areas, for example *Erwinia amylovora*, another relevant bacterial pathogen, reported in Tuscany in 2020 (Migliorini et al., 2021).

The present study aimed to evaluate the performance of primers and probes currently employed for diagnosis of Xf through qPCR when used in a nanoplate-based dPCR assay, and to determine if the qPCR methods could be directly transposed to this new dPCR technology. Similar studies have been carried out to test these methods in droplet-based dPCR (Dupas *et al.*, 2019), but considering the technical differences between droplet- and nanoplate-based dPCR, an entirely separate set of tests for initial validation of these methods in nanoplate-based dPCR was necessary. All tests were carried out on experimental samples obtained by adding known quantities of DNA from Xf subsp. *fastidiosa*, Xf subsp. *multiplex*, or Xf subsp. *pauca* in the nucleic acid extracts from healthy plants of *Nerium oleander,* an ornamental host of Xf. These tests underwent preliminary validation by comparison with the current qPCR assays.

MATERIALS AND METHODS

Bacterial strains and DNA used in this study

Total nucleic acids from three *X. fastidiosa* strains and one strain of a non-target, non-pathogenic *Pseudomonas syringae* pv. *syringae,* belonging to a genus commonly found in healthy plant tissues, were used in this study.

The nucleic acids of pure cultures of *X. fastidiosa* subsp. *fastidiosa* strain DSM 10026 (indicated hereafter as Xff) and *X. fastidiosa* subsp. *multiplex* strain DSM 103418 (Xfm) were supplied by DSMZ GmbH. The nucleic acids of *X. fastidiosa* subsp. *pauca* strain ST53 (Xfp) were kindly provided by the Phytosanitary Service of Lombardy region.

Nucleic acids from *P. syringae* strain 260-02 (indicated hereafter as 260-02) were extracted using GenElute™ Bacterial Genomic DNA Kit (Sigma-Aldich), following the manufacturer's instructions, as previously reported by Passera *et al.*, (2019).

After acquisition or extraction, all bacterial nucleic acids were stored at -30°C.

Nucleic acids from oleander (*Nerium oleander*) were extracted from asymptomatic whole leaf samples or midribs (0.5–1 g) using a CTAB method, described in EPPO standard 7/24 (EPPO, 2019). Oleander leaves were sampled in spring 2020 from three different asymptomatic plants, the samples were pooled together, and then kept frozen at -30°C until extraction in September 2020. Three samples of whole leaves were obtained and pooled together, while 4 samples of midribs only were obtained and assessed individually, as reported in the following paragraphs and Tables 1 and 2. Absence of *X. fastidiosa* in these samples was confirmed by including the nucleic acids from the plants, without spike of any kind, in all subsequent molecular assays: no amplification due to *X. fastidiosa* presence was detected in any of the nucleic acid samples extracted from asymptomatic *N. oleander* plants used in this study.

All quantifications of nucleic acids were carried out using a Nanodrop 1000 spectrophotometer.

Preparation of experimental samples and controls

Two sets of experimental samples and controls were prepared.

The first set was prepared by adding nucleic acids from oleander (using samples obtained from whole leaves, final concentration = 10 ng μL^{-1}) with nucleic acids from one of the three *X. fastidiosa* strains (final concentrations down to ten copies per µL, as shown in Table 1), or the 260-02 strain (final concentration = 10^5 copies per µL). The theoretical copy numbers of the bacterial genomes were estimated using concentration of the nucleic acids, the size of the genome, and the average molecular weight of a DNA base pair to calculate molarity, and, therefore, the number of molecules in the volume. Positive controls included nucleic acids from one of the three *X. fastidiosa* strains at different final concentrations, as shown in Table 1. Negative controls included nucleic acids either from the 260-02 strain, only from oleander, from oleander with 260-02 added, or no nucleic acids (NTC), as shown in Table 1.

The second set of samples and controls was prepared to further assess possible interference from the plant matrix in a sample more closely resembling those obtained during actual surveys for *X. fastidiosa* diagnoses. DNA was extracted from four samples each of 0.5 g of midribs from asymptomatic oleander plants. Each of the three Xf subspecies was added to each DNA sample at the following concentrations: Xff approx. 250 or 125 copies per µL, Xfm approx. 150 or 75 copies per µL, Xfp approx. 275 or 140 copies per µL, for a total of 6 experimental samples from each single starting DNA. DNA samples without added Xf DNA were also employed as negative controls in this experiment. All the samples and controls included in this second set are reported in Table 2.

Xylella fastidiosa *detection using qPCR*

The presence of Xf in the samples was determined using the SYBR Green assay (Francis *et al.*, 2006), and

Table 1. List of samples, positive controls, and negative controls included in the first set of analyzed material. The table reports for each sample/control the name, composition of host DNA and the source of added DNA. The concentration of the nucleic acids is expressed either as ng μL^{-1} or copy number per µL, depending on which parameter was more relevant during the preparation of the sample. This concentration value is an approximation used to express the order of magnitude of the target (for copies per µL) or rounded to the nearest multiple of 5 (for ng μL^{-1}).

Sample	Host DNA		Added DNA		Category
	Host	Concentration	Bacterium	Concentration	
OXFM_4	*N. oleander*	10 ng/µL	*X. fastidiosa* subsp. *multiplex*	10^4 copies/µL	Sample
OXFM_3	*N. oleander*	10 ng/µL	*X. fastidiosa* subsp. *multiplex*	10^3 copies/µL	Sample
OXFM_2	*N. oleander*	10 ng/µL	*X. fastidiosa* subsp. *multiplex*	10^2 copies/µL	Sample
OXFM_1	*N. oleander*	10 ng/µL	*X. fastidiosa* subsp. *multiplex*	10^1 copies/µL	Sample
OXFF_4	*N. oleander*	10 ng/µL	*X. fastidiosa* subsp. *fastidiosa*	10^4 copies/µL	Sample
OXFF_3	*N. oleander*	10 ng/µL	*X. fastidiosa* subsp. *fastidiosa*	10^3 copies/µL	Sample
OXFF_2	*N. oleander*	10 ng/µL	*X. fastidiosa* subsp. *fastidiosa*	10^2 copies/µL	Sample
OXFF_1	*N. oleander*	10 ng/µL	*X. fastidiosa* subsp. *fastidiosa*	10^1 copies/µL	Sample
OXFP_3	*N. oleander*	10 ng/µL	*X. fastidiosa* subsp. *pauca*	10^3 copies/µL	Sample
OXFP_2	*N. oleander*	10 ng/µL	*X. fastidiosa* subsp. *pauca*	10^2 copies/µL	Sample
OXFP_1	*N. oleander*	10 ng/µL	*X. fastidiosa* subsp. *pauca*	10^1 copies/µL	Sample
XFM-2	None	-	*X. fastidiosa* subsp. *multiplex*	0.5 ng/µL	Positive Control
XFM-3	None	-	*X. fastidiosa* subsp. *multiplex*	0.05 ng/µL	Positive Control
XFM-4	None	-	*X. fastidiosa* subsp. *multiplex*	0.005 ng/µL	Positive Control
XFM-5	None	-	*X. fastidiosa* subsp. *multiplex*	0.0005 ng/µL	Positive Control
XFF-2	None	-	*X. fastidiosa* subsp. *fastidiosa*	0.5 ng/µL	Positive Control
XFF-3	None	-	*X. fastidiosa* subsp. *fastidiosa*	0.05 ng/µL	Positive Control
XFF-4	None	-	*X. fastidiosa* subsp. *fastidiosa*	0.005 ng/µL	Positive Control
XFF-5	None	-	*X. fastidiosa* subsp. *fastidiosa*	0.0005 ng/µL	Positive Control
XFP-2	None	-	*X. fastidiosa* subsp. *pauca*	0.05 ng/µL	Positive Control
XFP-3	None	-	*X. fastidiosa* subsp. *pauca*	0.005 ng/µL	Positive Control
XFP-4	None	-	*X. fastidiosa* subsp. *pauca*	0.0005 ng/µL	Positive Control
XFP-5	None	-	*X. fastidiosa* subsp. *pauca*	0.00005 ng/µL	Positive Control
Oleander	*N. oleander*	10 ng/µL	None	-	Negative Control
OPSS_5	*N. oleander*	10 ng/µL	*P. syringae* strain 260-02	10^5 copies/µL	Negative Control
PSS	None	-	*P. syringae* strain 260-02	85 ng/µL	Negative Control
NTC	None	-	None	-	Negative Control

a TaqMan assay (Harper *et al.* (2010), erratum 2013). The methods for these two assays are outlined in EPPO standard PM 7/24 (EPPO, 2019).

The first method uses a pair of specific primers for XF, that was designed on the sequence of a conserved hypothetical protein gene: HL5 (5'-AAGGCAATAAACGCG-CACTA-3') and HL6 (5'-GGTTTTGCTGACTG-GCAACA-3'). This primer pair amplifies a segment of length 221 bp. The reaction mix was prepared as indicated in the EPPO standard PM 7/24 (4) (Francis *et al.*, 2006; EPPO, 2019), modified as follows: the volume of template nucleic acids was doubled and the total reaction volume was raised to 12 µL. The final composition of the mix was as follows: PowerSYBR master mix (Applied Biosystems) 1×, primer HL5 0.28 µM, primer HL6 0.28 µM, DNA template 2 µL, and water up to a volume of 12 µL.

The second method uses a specific primer pair which amplifies a sequence located in the *rimM* gene coding for a 16S rRNA processing protein: XF-F (5'-CACG-GCTGGTAACGGAAGA-3') and XF-R (5'-CACGGCTG-GTAACGGAAGA-3'), and the probe XF-P (5'-6-FAM-TCGCAT CCCGTGGCTCAGTCC-BHQ-1-3').

Each reaction mix was prepared as indicated in the EPPO standard PM 7/24 (Harper *et al.*, 2010; EPPO, 2019), modified as follows: the total reaction volume was reduced to 12 µL. The final composition of the mix was: TaqMan Universal Master Mix No Amperase (Applied Biosystems) 1×, primer XF-F 0.3 µM, primer XF-R 0.3 µM, probe XF-P 0.1 µM, BSA 0.3 µg μL^{-1}, DNA template 2 µL, and water up to volume of 12 µL.

For both methods, the changes in volumes of the reactions in comparison with that described in the

Table 2. List of samples, positive controls, and negative controls included in the second set of analyzed material. The table reports for each sample/control the name, composition of host DNA and the source of added DNA. The concentration of the nucleic acids is expressed as copy number per μL.

Sample	Host DNA		Added DNA		Category
	Host	Concentration	Bacterium	Concentration	
O1_XFM_2	*N. oleander*	418 ng/μL	*X. fastidiosa* subsp. *multiplex*	150 copies/μL	Sample
O1_XFM_1	*N. oleander*	418 ng/μL	*X. fastidiosa* subsp. *multiplex*	75 copies/μL	Sample
O1_XFF_2	*N. oleander*	418 ng/μL	*X. fastidiosa* subsp. *fastidiosa*	250 copies/μL	Sample
O1_XFF_1	*N. oleander*	418 ng/μL	*X. fastidiosa* subsp. *fastidiosa*	125 copies/μL	Sample
O1_XFP_2	*N. oleander*	418 ng/μL	*X. fastidiosa* subsp. *pauca*	275 copies/μL	Sample
O1_XFP_1	*N. oleander*	418 ng/μL	*X. fastidiosa* subsp. *pauca*	140 copies/μL	Sample
O1_C	*N. oleander*	418 ng/μL	None	-	Negative Control
O2_XFM_2	*N. oleander*	378 ng/μL	*X. fastidiosa* subsp. *multiplex*	150 copies/μL	Sample
O2_XFM_1	*N. oleander*	378 ng/μL	*X. fastidiosa* subsp. *multiplex*	75 copies/μL	Sample
O2_XFF_2	*N. oleander*	378 ng/μL	*X. fastidiosa* subsp. *fastidiosa*	250 copies/μL	Sample
O2_XFF_1	*N. oleander*	378 ng/μL	*X. fastidiosa* subsp. *fastidiosa*	125 copies/μL	Sample
O2_XFP_2	*N. oleander*	378 ng/μL	*X. fastidiosa* subsp. *pauca*	275 copies/μL	Sample
O2_XFP_1	*N. oleander*	378 ng/μL	*X. fastidiosa* subsp. *pauca*	140 copies/μL	Sample
O2_C	*N. oleander*	378 ng/μL	None	-	Negative Control
O3_XFM_2	*N. oleander*	316 ng/μL	*X. fastidiosa* subsp. *multiplex*	150 copies/μL	Sample
O3_XFM_1	*N. oleander*	316 ng/μL	*X. fastidiosa* subsp. *multiplex*	75 copies/μL	Sample
O3_XFF_2	*N. oleander*	316 ng/μL	*X. fastidiosa* subsp. *fastidiosa*	250 copies/μL	Sample
O3_XFF_1	*N. oleander*	316 ng/μL	*X. fastidiosa* subsp. *fastidiosa*	125 copies/μL	Sample
O3_XFP_2	*N. oleander*	316 ng/μL	*X. fastidiosa* subsp. *pauca*	275 copies/μL	Sample
O3_XFP_1	*N. oleander*	316 ng/μL	*X. fastidiosa* subsp. *pauca*	140 copies/μL	Sample
O3_C	*N. oleander*	316 ng/μL	None	-	Negative Control
O4_XFM_2	*N. oleander*	344 ng/μL	*X. fastidiosa* subsp. *multiplex*	150 copies/μL	Sample
O4_XFM_1	*N. oleander*	344 ng/μL	*X. fastidiosa* subsp. *multiplex*	75 copies/μL	Sample
O4_XFF_2	*N. oleander*	344 ng/μL	*X. fastidiosa* subsp. *fastidiosa*	250 copies/μL	Sample
O4_XFF_1	*N. oleander*	344 ng/μL	*X. fastidiosa* subsp. *fastidiosa*	125 copies/μL	Sample
O4_XFP_2	*N. oleander*	344 ng/μL	*X. fastidiosa* subsp. *pauca*	275 copies/μL	Sample
O4_XFP_1	*N. oleander*	344 ng/μL	*X. fastidiosa* subsp. *pauca*	140 copies/μL	Sample
O4_C	*N. oleander*	344 ng/μL	None	-	Negative Control
N_XFM_2	None	-	*X. fastidiosa* subsp. *multiplex*	150 copies/μL	Positive Control
N_XFM_1	None	-	*X. fastidiosa* subsp. *multiplex*	75 copies/μL	Positive Control
N_XFF_2	None	-	*X. fastidiosa* subsp. *fastidiosa*	250 copies/μL	Positive Control
N_XFF_1	None	-	*X. fastidiosa* subsp. *fastidiosa*	125 copies/μL	Positive Control
N_XFP_2	None	-	*X. fastidiosa* subsp. *pauca*	275 copies/μL	Positive Control
N_XFP_1	None	-	*X. fastidiosa* subsp. *pauca*	140 copies/μL	Positive Control
NTC	None	-	None	-	Negative Control

EPPO standard (EPPO, 2019) were carried out to be more similar to the operative conditions of the dPCR assay, which uses a total volume of 12 μL, as reported in the handbook for the reaction mixes. Using the same total reaction and experimental sample volumes assures that the concentration of target DNA is the same in both assays, making the results directly comparable.

These reactions were carried out in StepOnePlus Real-Time PCR thermocycler (Thermo Fisher Scientific). The thermal cycling profile used for both methods was as described in the EPPO standard (EPPO, 2019).

All the samples reported in Table 1 were tested with both methods. Each sample and control were analysed in triplicate.

For assessing the results obtained, in accordance with two methods described in the EPPO standard (EPPO, 2019), the quantification cycle (Cq) was evaluated for both the Taqman and SYBR Green methods,

and the melting temperature (Tm) was evaluated for the SYBR Green method.

Xylella fastidiosa *detection and quantification using dPCR*

The presence and quantity of XF in the samples and controls were assessed in nanoplate-based dPCR, using the QIAcuity instrument (Qiagen). The results obtained were analyzed using the QIAcuity Software Suite version 2.0.20.

The methods of Francis *et al.* (2006) and Harper *et al.* (2010) were carried out in dPCR. The reaction mixes were set up with the same composition as the corresponding mixes used for the qPCR assays, but using the EG PCR Master Mix 3× (Qiagen) in place of the PowerSYBR mix, and QIAcuity Probe PCR Master Mix 4× (Qiagen) in place of TaqMan Universal Master Mix No Amperase. Both master mixes were used at final concentrations of 1×.

To keep these reactions as close as possible to the original methods used in qPCR, no restriction enzyme was added to the mixes, although use of a restriction enzyme is normally suggested in instructions for the master mixes used in dPCR.

The reactions were carried out in 96 well QIAcuity Nanoplates, with 8.5K partitions per well. All the samples and controls reported in Table 1 were assayed with both methods. Each sample and control were tested in duplicate. All the samples and controls reported in Table 2 were assayed with both methods, without carrying out technical replicates, with the exception of NTC, which was assayed in triplicate.

For the Eva Green (EG) protocol, thermal cycling was as follows: one cycle of incubation at 95°C for 2 min; 40 cycles of 95°C for 15 sec, 60°C for 15 sec, and 72°C for 15 sec; then incubation at 40°C for 5 min. This cycle followed instructions in the EG PCR Master Mix 3× (Qiagen) handbook, changing only the annealing temperatures to match that of the primers employed. Imaging was carried out with 700 ms of exposure and a gain value of 8.

For the Probe protocol, thermal cycling was as follows: one cycle of incubation at 95°C for 2 min; 40 cycles of 95°C for 15 sec, and 62°C for 30 sec. This followed the instructions of the Probe PCR Master Mix 4× (Qiagen) handbook, changing only the annealing temperature to match that for the primers employed. Imaging was carried out with 500 ms of exposure and a gain value of 6.

Evaluation of diagnostic performance parameters

For each test, parameters were calculated as follows:
Accuracy = 100 × (PA + NA) / (PA + NA + PD + FD);
Sensitivity = 100 × PA / (PA + ND);
Specificity = 100 × NA / (NA + PD);
where PA was positive agreement (a positive result is obtained when a positive result is expected), NA is negative agreement (a negative result is obtained when a negative result is expected), PD is positive deviation (a positive result is obtained when a negative result is expected), and ND is negative deviation (a negative result is obtained when a positive result is expected).

RESULTS

Xylella fastidiosa *detection through qPCR*

The qPCR assays correctly detected the presence of Xff, Xfm and Xfp in all the experimental samples and positive controls (Table 1, Figure 1), regardless of the primer pairs employed. For all samples and positive controls, the qPCR assays yielded the expected results, with Cq increasing as the concentration of pathogen decreased and, for the SYBR Green assay, giving a single, recognizable Tm peak for each sample. The assays therefore detected the pathogen at an order of magnitude as low as ten copies per µL.

The TaqMan assay gave an expected result of "undetected" for all the negative controls. On the other hand, the SYBR Green assay gave as result a Cq also on negative samples and controls. The NTC gave an average Cq of 37.32, which is indicated as an undetermined result, but did not show exponential amplification nor the correct Tm of the amplicon and are therefore considered as negative results as indicated in the protocol (EPPO, 2019). However, other negative controls gave results that could be mistaken as positive based on Cq alone. These included *N. oleander* with added *P. syringae* nucleic acids (OPSS_5), or without these nucleic acids (Oleander), gave Cq values between 32 and 34, regardless of the presence of added nucleic acids, while nucleic acids from *P. syringae* pure culture (PSS) gave an average Cq of 33.82. Analysis of the melting curves showed that these results were due to non-specific amplification: Tm was consistent between samples with added Xf subspecies (average 83.15°C), while in the samples without Xf DNA the Tm varied between 61–93°C, without clear, defined peaks in the melting curves.

Xylella fastidiosa *detection through dPCR*

Results of dPCR assays from the Eva Green (EG) and the Probe methods for each control and sample reported in Table 1 indicated that both primer pairs

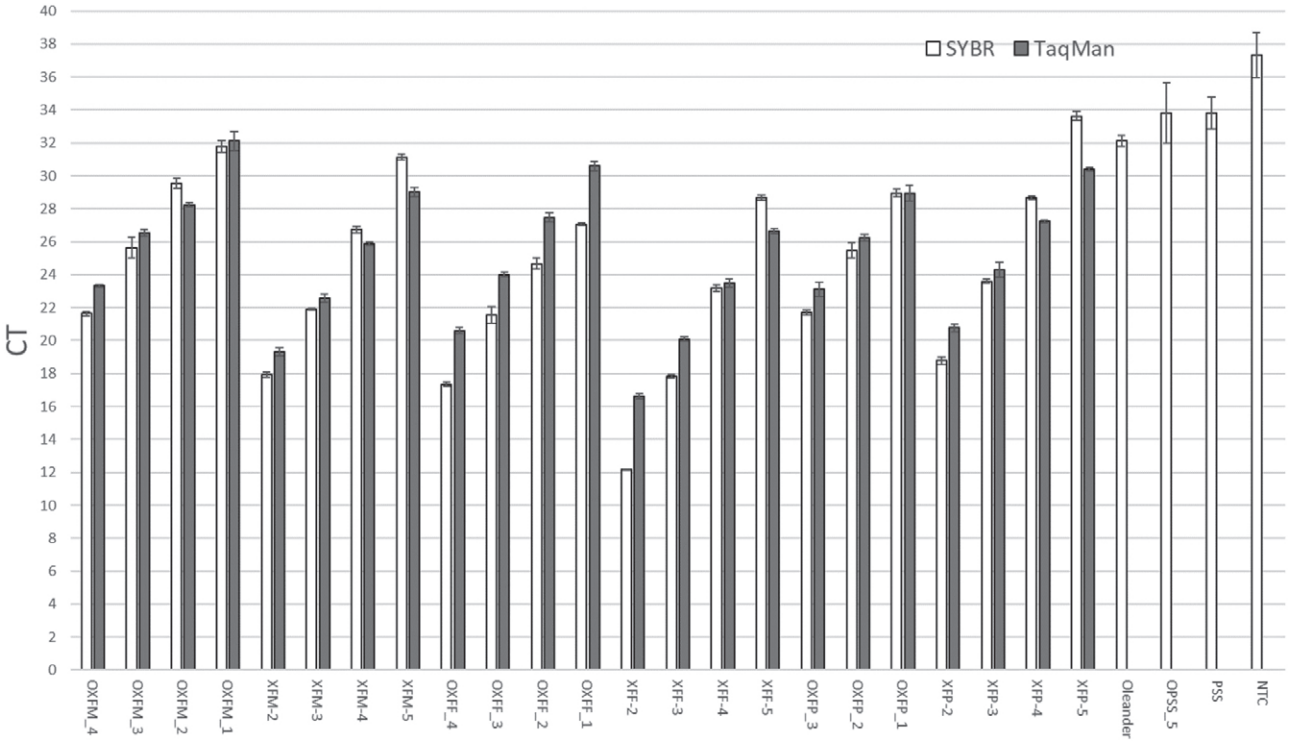

Figure 1. Results from qPCR *Xylella fastidiosa* detection assays. The graph shows different samples (Table 1) on the X-axis, and quantification cycles (Cq) obtained on the Y-axis. For each sample, the grey bars are results of TaqMan assays (Harper *et al.*, 2010) while the white bars are results of the SYBR Green assay (Francis *et al.*, 2006). The represented number for each Cq is the average obtained from three replicates, and the error bar represents the standard deviation. Where no bar is present, the result of the assay was "undetected".

amplified as intended. Some examples of the outputs produced by the dPCR are presented in Supplementary Figures 1 and 2.

For the EG method, a strong background fluorescence was detected, with a fluorescence for negative partitions ranging from 50 to 135 RFU, while the positive partitions had intensity of 200 to 250 RFU (Figure 2A). It is important to note that the RFUs for negative controls are different between the NTC or *P. syringae* DNA, and those that contain DNA of *N. oleander*, being greater for *N. oleander* DNA. This could be due to some non-specific annealing of the primers producing some DNA amplicons, in line with the results obtained with qPCR. Also, there is likely presence of some 'rain' in the samples and positive controls, defined as partitions that give intermediate fluorescence between negative and positive (in this case 135-200 RFU), which were found with high frequency in the XFM samples and controls. To determine the effect of the threshold level on detection and quantification of XF, results include two different thresholds. The first threshold was set just above the RFU of the negative cloud (dMIQE group, 2020) which is presented under the code EG_135, since the threshold is at 135 RFU. The second threshold was set at the lowest border of the positive cloud, effectively removing the 'rain' partitions, which is presented under the code of EG_200, since the threshold is set at 200 RFU (Table 3). The Probe method showed an overall lower level of fluorescence, both for negative and positive partitions: negative partitions had fluorescence of 10 to 20 RFU, while the positive partitions ranged from approx. 40 to 60 RFU (Figure 2B). This result is in line with the lower exposition time and gain utilized for the imaging. Although less common than in the EG method, also in this assay there was some 'rain', with fluorescence between 20 and 40 RFU. In order to determine the effects of the threshold level on detection and quantification of XF, results include two different thresholds: one set just above the RFU of the negative cloud (dMIQE group, 2020) which is presented under the code of Probe_20, since the threshold is at 20 RFU; the second threshold was set at the lowest border of the positive cloud, effectively removing the 'rain' partitions, which is presented under the code of Probe_40, since the threshold is set at 40 RFU (Table 3).

Detection and quantification of the pathogen was possible in all samples and positive controls (Table 3),

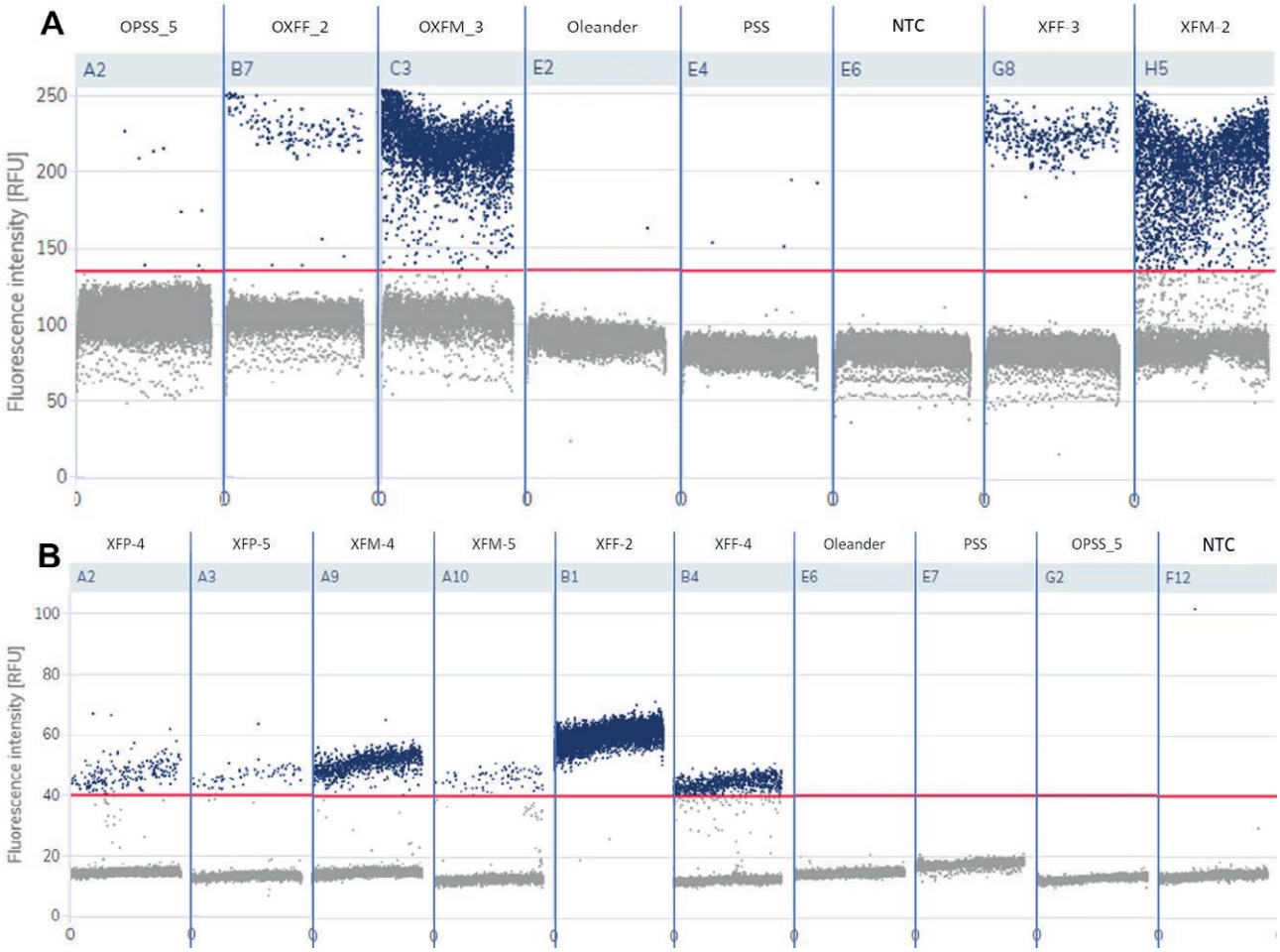

Figure 2. 1-D Scatterplots of representative samples for dPCR assays. Each box represents the fluorescence value (expressed as RFU) for each partition, the red line shows the threshold. Each partition above the threshold (in blue) is considered positive, while each below the threshold (in grey) is considered negative. A) Representative samples for the EG method, with threshold set at 135 RFU. This same dataset was also analysed with the threshold set at 200 RFU. B) Representative samples for the Probe method, with threshold set at 40 RFU. This same dataset was also analysed with the threshold set at 20 RFU.

regardless of the threshold setting, for both the EG and Probe methods. Taking into consideration that there was no standardized protocol to follow for these methods for nanoplate-based dPCR, and that the present study was carried out only on experimental samples and controls of known status (positive and negative), also certified by two different qPCR diagnostic methods, the parameters to discriminate between positive or negative results were not decided beforehand, but were instead formulated by analyzing the present results. For copy numbers of targets per µL and confidence intervals, it was possible to discriminate between positive and negative results by setting threshold copy number for a positive result as greater than the average target copy number detected in negative controls, taking into consideration the greatest bounds of the confidence intervals. Due to the rare cases of amplification in the negative controls, this threshold was calculated as 12 for EG_135, 2 for EG_200, 3 for Probe_20, and 2 for Probe_40 (Table 3). The numbers of copies to consider a sample positive were greater in the cases of lower thresholds (EG_135 and Probe_20), as there was presence of 'rain' partitions in the negative controls, but there was negligible influence of the threshold setting in the Probe method. Also when considering 'rain' partitions as positive, in line with dMIQE guidelines, in no case was there a copy number of target sequence greater than 10 for negative controls, or less than 10 for samples and positive controls (Table 3). Nevertheless, considering that ten target copies is close to the greatest registered also for negative controls, an order of magnitude of ten copies of target per µL of sample was the limit of detection for these assays.

Table 3. Results of dPCR assays on the first set of samples, positive and negative controls. The table reports the target copy number/μL for each sample, the error is calculated as a CI of 95%. The columns report the results obtained with either the EG or Probe method with the two considered thresholds. Copy number was rounded to the closest unit. The error is rounded to the closest decimal.

Sample	Digital PCR results (copies/μL of template)			
	EG (Francis *et al.*, 2006)		Probe (Harper *et al.*, 2010)	
	EG_135	EG_200	Probe_20	Probe_40
OXFM_4	16,469 ± 2.1%	13,404 ± 2.6%	14,783 ± 2.2%	13,254 ± 2.6%
OXFM_3	1,602 ± 7.2%	1,303 ± 7.9%	1,730 ± 7.7%	1,556 ± 7.9%
OXFM_2	152 ± 23.6%	133 ± 25.1%	158 ± 25.9%	148 ± 26.1%
OXFM_1	24 ± 61.5%	19 ± 67.5%	13 ± 94.5%	10 ± 95.2%
OXFF_4	22,420 ± 2.2%	22,419 ± 2.1%	19,815 ± 2.1%	17,830 ± 2.2%
OXFF_3	2,215 ± 6.1%	2,188 ± 6.1%	2,756 ± 6.0%	2,437 ± 6.0%
OXFF_2	306 ± 16.5%	294 ± 16.9%	279 ± 19.3%	242 ± 19.7%
OXFF_1	17 ± 73.3%	16 ± 75.6%	16 ± 84.6%	14 ± 84.5%
OXFP_3	5,054 ± 4.2%	5,025 ± 4.2%	4,556 ± 4.6%	4,096 ± 4.6%
OXFP_2	600 ± 12.6%	579 ± 12.9%	585 ± 13.1%	525 ± 13.1%
OXFP_1	84 ± 33.7%	81 ± 34.0%	81 ± 36.4%	72 ± 36.5%
XFM-2	N/A (oversaturated)	N/A (oversaturated)	N/A (oversaturated)	N/A (oversaturated)
XFM-3	88,351 ± 0.7%	67,076 ± 1.0%	26,173 ± 1.9%	24,891 ± 1.9%
XFM-4	8,370 ± 3.2%	4,285 ± 4.9%	2,682 ± 5.6%	2,656 ± 5.6%
XFM-5	955 ± 8.2%	427 ± 14.5%	208 ± 24.2%	161 ± 24.7%
XFF-2	N/A (oversaturated)	N/A (oversaturated)	N/A (oversaturated)	N/A (oversaturated)
XFF-3	41,228 ± 1.8%	41,226 ± 1.8%	33,491 ± 1.9%	30,160 ± 1.60%
XFF-4	2,272 ± 6.6%	2,189 ± 6.6%	2,266 ± 6.2%	2,039 ± 6.6%
XFF-5	152 ± 24.2%	150 ± 24.3%	145 ± 26.7%	123 ± 27.8%
XFP-2	13,429 ± 2.2%	13,428 ± 2.2%	12,377 ± 1.6%	11,152 ± 2.7%
XFP-3	2,015 ± 6.8%	2,012 ± 6.8%	1,648 ± 7.61%	1,465 ± 7.9%
XFP-4	184 ± 23.9%	181 ± 24.0%	162 ± 25.7%	142 ± 26.0%
XFP-5	35 ± 57.9%	32 ± 58.7%	29 ± 61.9%	25 ± 63.8%
Oleander	3 ± 274.4%	0	0	0
OPSS_5	3 ± 171.6%	1 ± 109.1%	0	0
PSS	8 ± 138.8%	0	0	0
NTC	0	0	1 ± 275.4%	1 ± 168.6%
Threshold	>12	>2	>3	>2

The results obtained with both assays confirmed the theoretical concentration of Xf in the experimental samples and positive controls, as the concentration of target was always in the expected order of magnitude. The positive controls with the greatest concentrations of target, namely XFM-2 and XFF-2, caused the respective wells to be oversaturated. This result, while positive, did not allow quantification of the target concentrations, so was not optimal. While the order of magnitude of target copy number in the samples and positive controls was confirmed by the two different assays, there were differences in the results. samples and positive controls containing Xfm gave much greater copy numbers per μL when tested with the EG method than with the Probe method. This result is partially explained by the high number of 'rain' partitions in the Xfm samples tested with the EG dPCR method. The overestimation in this sample type was exemplified by the XFM-3 positive control. The Probe_20 and Probe_40 results were similar, with, respectively, 26,173 and 24,891 copies per μL. In contrast the results for EG_135 were 88,351 copies per μL, and 67,076 for EG_200. While the higher threshold caused overestimation of the target's quantity by 2.7 times, the lower threshold raised this error further to around 3.5

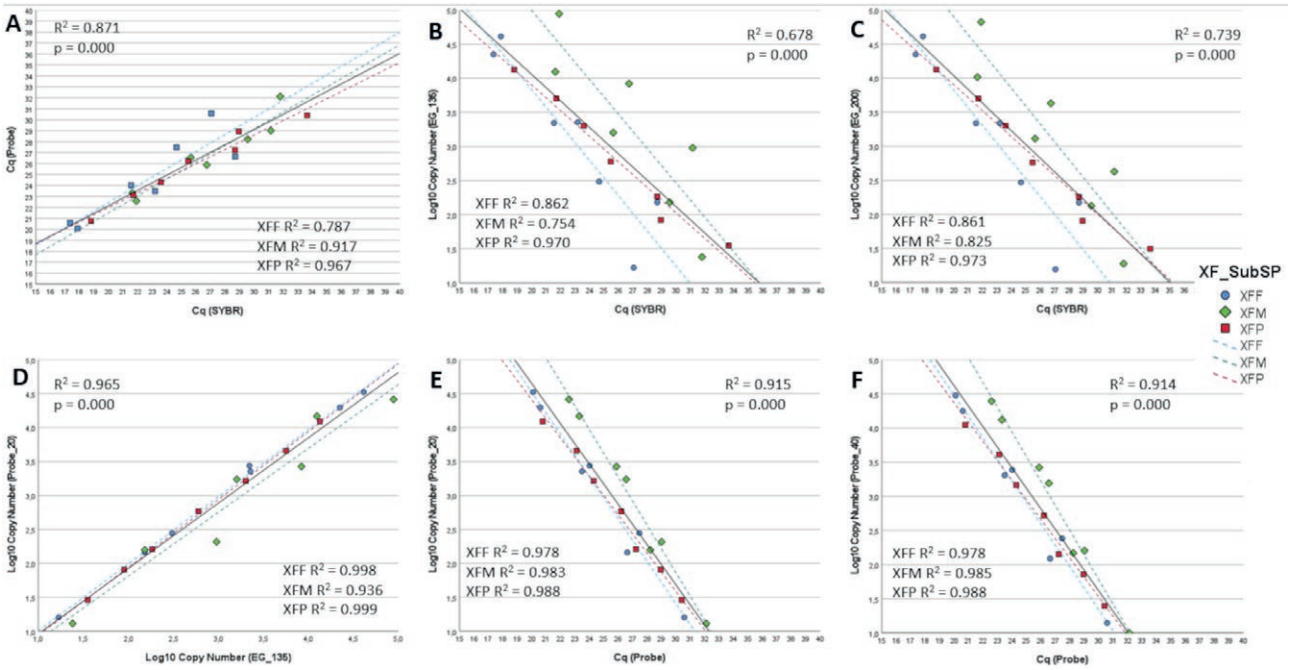

Figure 3. Scatterplots showing the correlations between results obtained by different diagnostic assays in the following pairs: (A) qPCR with SYBR Green on the X-axis and qPCR with Probe on the Y-axis; (B) qPCR with SYBR Green on the X-axis and dPCR with EG, threshold set at 135 RFU, on the Y-axis; (C) qPCR with SYBR Green on the X-axis and dPCR with EG, threshold set at 200 RFU, on the Y-axis; (D) dPCR with EG, threshold set at 135 RFU, on the X-axis and dPCR with Probe, threshold set at 20 RFU, on the Y-axis; (E) qPCR with Probe on the X-axis and dPCR with Probe, threshold set at 20 RFU, on the Y-axis; and (F) qPCR with Probe on the X-axis and dPCR with Probe, threshold set at 40 RFU, on the Y-axis. Markers on the plots indicate single samples, and their colours and shapes indicate the subspecies of *Xylella fastidiosa* they belong to, as reported in the legend. Each graph contains three dashed trendlines, which are calculated on samples belonging to a single subspecies, and a solid-line trendline, calculated on all the samples for each combination of the diagnostic assays. Each graph also reports the overall R^2 value and the *P* value obtained from linear regression analysis, as well as the R^2 value for each *X. fastidiosa* subspecies.

times greater. The positive control XFM-4 gave a similar result, with EG_200 giving a result two times greater than that obtained with the Probe method, and with EG_135 giving a result four times greater. For the samples and positive controls containing Xff and Xfp, these differences were not as pronounced, especially when the copy number was at 10^3 or less. While this overestimation of the target abundance for XFM did not interfere with detection of the pathogen, it would become an issue when accurate quantification is necessary.

Comparison between different diagnostic methods

All four methods employed in the study (qPCR SYBR Green, qPCR Probe, dPCR EG, dPCR Probe) detected presence of the target pathogens in the samples and positive controls, and did not detect the target pathogens in the negative controls. Having detected no differences between the expected results and experimental results, all four methods showed a 100% accuracy, diagnostic sensitivity, and specificity. All the methods also detected *X. fastidiosa* at all the tested concentrations, down to an order of magnitude of ten target copies per µL.

Since both the qPCR and dPCR approaches are quantitative, a direct comparison of the results obtained by the methods is possible. Linear regression analyses showed, that there was strong statistical significance ($P = 0.000$) for the correlations between results from the different diagnostic assays (Figure 3). Correlations for the different methods were especially high when comparing the two dPCR methods (Figure 3D), and the qPCR and dPCR using probes (Figures 3E and 4F), and with overall R^2 values greater than 0.9 and close to 1 when considering the individual Xf subspecies. The least correlations were measured for the comparisons between the qPCR with SYBR Green, and the dPCR with EG and threshold of 135 (Figure 3B). This was due to two distinct forms of bias that have been highlighted by the comparison of distinct methods. Firstly, Cq registered for Xff using the SYBR Green method was slightly less than those for the other two subspecies at equal concentrations of target. Secondly, the dPCR quantification for

Table 4. Results of dPCR assays on the second set of samples, positive and negative controls. The table reports the target copy number/μL for each sample, the error is calculated as a CI of 95%. The columns report the results obtained with either the Probe method with the two considered thresholds, or with EG with threshold at 200. Copy number was rounded to the closest unit. The error is rounded to the closest decimal.

Sample	Digital PCR results (copies/μL of template)		
	EG_200	Probe_20	Probe_40
O1_XFM_2	N/A (Oversaturated)	142 ± 26.9%	145 ± 26.6%
O1_XFM_1	N/A (Oversaturated)	79 ± 34.0%	76 ± 34.6%
O1_XFF_2	N/A (Oversaturated)	303 ± 17.3%	299 ± 17.5%
O1_XFF_1	N/A (Oversaturated)	129 ± 25.3%	125 ± 26.1%
O1_XFP_2	N/A (Oversaturated)	352 ± 16.1%	343 ± 16.3%
O1_XFP_1	N/A (Oversaturated)	154 ± 23.8%	152 ± 23.9%
O1_C	N/A (Oversaturated)	0	0
O2_XFM_2	N/A (Oversaturated)	120 ± 27.4%	120 ± 27.4%
O2_XFM_1	N/A (Oversaturated)	75 ± 38.3%	72 ± 39.1%
O2_XFF_2	N/A (Oversaturated)	258 ± 17.9%	251 ± 18.1%
O2_XFF_1	N/A (Oversaturated)	119 ± 27.1%	115 ± 27.9%
O2_XFP_2	N/A (Oversaturated)	275 ± 17.8%	269 ± 18.0%
O2_XFP_1	N/A (Oversaturated)	139 ± 25.7%	136 ± 25.8%
O2_C	N/A (Oversaturated)	0	0
O3_XFM_2	N/A (Oversaturated)	114 ± 27.9%	114 ± 27.9%
O3_XFM_1	N/A (Oversaturated)	97 ± 30.9%	90 ± 32.2%
O3_XFF_2	N/A (Oversaturated)	170 ± 22.0%	166 ± 22.3%
O3_XFF_1	N/A (Oversaturated)	130 ± 25.7%	123 ± 26.4%
O3_XFP_2	N/A (Oversaturated)	195 ± 21.5%	188 ± 21.3%
O3_XFP_1	N/A (Oversaturated)	102 ± 33.1%	138 ± 25.7%
O3_C	N/A (Oversaturated)	3 ± 274.0%	0
O4_XFM_2	N/A (Oversaturated)	142 ± 26.9%	144 ± 26.1%
O4_XFM_1	N/A (Oversaturated)	74 ± 38.7%	74 ± 38.7%
O4_XFF_2	N/A (Oversaturated)	266 ± 17.4%	254 ± 17.8%
O4_XFF_1	N/A (Oversaturated)	89 ± 30.5%	89 ± 30.5%
O4_XFP_2	N/A (Oversaturated)	188 ± 21.3%	188 ± 21.3%
O4_XFP_1	N/A (Oversaturated)	137 ± 25.9%	138 ± 25.7%
O4_C	N/A (Oversaturated)	0	0
N_XFM_2	13 ± 86.2%	120 ± 26.9%	117 ± 27.1%
N_XFM_1	2 ± 274.4%	65 ± 38.3%	65 ± 38.3%
N_XFF_2	174 ± 21.5%	278 ± 18.1%	262 ± 18.6%
N_XFF_1	124 ± 25.9%	121 ± 26.9%	118 ± 27.1%
N_XFP_2	366 ± 15.1%	323 ± 16.1%	323 ± 16.1%
N_XFP_1	20 ± 68.7%	150 ± 24.1%	148 ± 24.2%
NTC	2 ± 274.4%	1 ± 274%	0

Xfm gave greater copy number per μL than expected, mostly due to presence of many 'rain' partitions. These two effects reduced the R^2 values for the subspecies in which they were identified by small amounts (to 0.862 for Xff and 0.754 for Xfm). Overall, when both effects are considered together by evaluating all three Xf subspecies at the same time, they caused high reductions in correlations between the two methods, with an R^2 value of 0.678. The same analysis with the threshold at 200, ignoring the effect of the 'rain' partitions on Xfm, gave greater correlation with the qPCR results, with an R^2 values of 0.861 for Xff and 0.826 for Xfm, and an overall correlation of 0.739 (Figure 3C). Xfp gave consistently greater correlation values compared to other Xf subspecies, regardless of which two methods were being compared. A list of all R^2 values for the correlations of each pair of methods is presented in Supplementary Table 1.

Evaluation of plant matrix effect on detection through dPCR

The methods previously described and tested on samples that contained *N. oleander* DNA diluted to 10 ng μL^{-1} were tested on a set of samples and controls that resembled real samples that could be obtained by DNA extraction from infected host material. Results of dPCR EG and dPCR Probe from this set of samples and controls are shown in Table 4.

dPCR EG failed to provide useful information for this set of samples. The positive controls that contained only Xf were correctly amplified, but all samples and negative controls that contained undiluted *N. oleander* DNA resulted in oversaturation, probably caused by the high quantity of DNA that can bind to the non-specific EvaGreen reporter.

In contrast, the dPCR Probe method correctly detected the presence of Xf subspecies in all samples and positive controls, while giving negative results for the negative controls. The negative control O3_C with the threshold set at 20 had a total of three copies per μL. However, as the positive threshold was determined to be more than three for the Probe_20 method, it was still considered negative. With the threshold set at 40, all negative controls returned a concentration of zero copies of the targets.

Quantification of the pathogen concentrations was adequate with the dPCR Probe method, as the results were in line with the expected orders of magnitude for each sample and control.

DISCUSSION

Digital PCR (dPCR) is a technique that is recently being adopted in research laboratories and will probably not rapidly become widespread for diagnostic applications. Nevertheless, its potential benefits for detection and quantification of pathogens are many, and rapid

integration of this molecular technique in diagnostics could prove beneficial for early detections of pathogens, particularly for quarantine pests. Several examples of the use of dPCR as diagnostic tools are available in human medicine (Sedlak *et al.*, 2014; Mangolini *et al.*, 2015; Devonshire *et al.*, 2016), indicating the benefits that can be obtained from the use of this technique. While it is still a budding technology in plant health, there are some studies that have showed adaptation of qPCR assays to dPCR (Dreo *et al.*, 2014; Lu *et al.*, 2019; Maheshwari *et al.*, 2017; Zhao *et al.*, 2016; Dupas *et al.*, 2019). These studies utilized the droplet-based dPCR technology, which uses oil emulsions to create partitions as small droplets, which then each undergo amplification and analysis. This technology needs additional steps in adaptation of qPCR protocols, due to different working environments caused by the use of oil, and the available systems for droplet-based dPCR suffer from lower throughput compared to qPCR while requiring more steps for sample preparation (Dupas *et al.*, 2019). The system used in the present study was a nanoplate-based dPCR, which obtained the partition of the reaction mixture through the physical conformation of the reaction plate. This allowed direct adaptation of qPCR protocols, and could process a high number of samples at once.

The present study used qPCR and dPCR which gave comparable results for detection of *X. fastidiosa.* Both approaches showed high performance criteria, with accuracy, specificity, and diagnostic sensitivity equal to 100% in the first set of experimental samples. While some differences based on the pathogen subspecies were highlighted in these analyses, all the methods detected the pathogen, regardless of subspecies. All the results confirmed that dPCR and qPCR had similar performance criteria for detection of Xf, which was in accordance with a previous reported by Dupas *et al.* (2019). That study compared the qPCR diagnostic method of by Harper *et al.* (2010) for Xf with droplet-based dPCR. Both methods were effective for detection of the pathogen, and there was high correlation between copy numbers detected by droplet-based dPCR and the Cq values from qPCR. Since it is reported that the benefits obtained from the use of dPCR can be dependent on the studied pathosystem (Dreo *et al.*, 2014), it is significant that the present results confirm that dPCR can be suitable for the detection of Xf, using different plant matrices and dPCR technology than those tested by Dupas *et al.* (2019). Quantification of Xf through dPCR was an improvement compared with qPCR, which would result in increased throughput in the pathogen diagnoses. Since qPCR can only achieve relative quantifications in comparison to reference material, using this technique to quantify target copy numbers requires the inclusion of standards with known concentrations, which uses up several wells in each assay plate. Obtaining accurate, absolute pathogen quantification without using such standards allows the processing of large numbers of samples per reaction. Such standards may not always be available. For Xf, axenic culturing is possible, so standards of known quantity can be developed to make absolute quantifications through qPCR. This is not the case for many other plant pathogens, for which the use of dPCR for quantitative assays offers benefit (Gutierrez-Aguire *et al.*, 2015). Considering that standard qPCR procedures analyze two or three replicates for each sample, use of dPCR, with results from thousands of repetitions in each well, can increase the numbers of samples processed per reaction, removing the limitation of employing several wells per sample. The increase of throughput can translate into shortening of the technical time needed to carry out diagnoses for many samples and also in reduced per sample analysis costs.

As dPCR is a quantitative and highly sensitive assay, it rarely gives exclusively negative results (zero positive partitions), and could also show some partitions with fluorescence from negative samples, in a way similar to how qPCR can give late Cq values greater than 37 for negative samples. Therefore, it is necessary to set thresholds to discriminate between positive and negative results, especially for EG methods that do not use specific probes. In the present analyses, setting the threshold at the highest copy number per µL detected in a known negative control (adjusted to the highest range of the confidence interval) allowed discrimination between positive and negative samples. This result will need further confirmation and validation before it can be used as a threshold for true diagnostic tests, especially considering that for EG_135 the threshold was high, at 12 copies per µL and could theoretically cause positive samples with ten copies per µL to be incorrectly classified as negatives. Also, the possibility of adding more negative and non-template controls to each plate could be considered, to more precisely estimate how many positive partitions are detected in negative samples when working with environmental samples.

In conclusion, EG and Probe dPCR methods, with either low thresholds set just above the cloud of negative partitions or higher thresholds set just below the cloud of positive partitions, were able to detect the presence of three different Xf subspecies in the analyzed samples. For the quantification, the EG method was not reliable for Xfm, and, especially with the lower threshold (EG_135), it detected several positive partitions in negative controls. Concern regarding fluorescence derived from non-specific amplification was more relevant in EG

dPCR. as, compared to SYBR Green assays carried out on qPCR, the lack of a melting curve step might contribute to incorrect positive detections in samples that do not contain the targets organisms. This concern was a major downfall of the method for the second set of samples containing large quantities of non-target DNA, in line with what would be obtained from extractions from infected plant material. This caused oversaturation of the wells even in the negative controls. Also, this method showed relevant production of 'rain', in particular for Xfm, that could contribute to uncertainty in the data analyses. In contrast, having lower values for positive partitions in the negative controls, guaranteed by using specific primers and a specific probe, the present study results suggest that using the protocol described by Harper *et al.* (2010) could give more reliable results. These considerations, in particular the completely unreliable results obtained when using samples that contained 300-600 ng per µL of host plant DNA, suggest that the EG method should not be employed for actual diagnostics, while the Probe dPCR method was reliable.

This study indicates the potential benefits of using nanoplate-based dPCR as a technique that can substitute traditional qPCR assays for detection of Xf, offering comparable performance criteria and the possibility of increased sample throughput, lowering the time and cost of analyses. This study is a first step demonstrating the possibility of using this technique for diagnostic applications in plant pathology. Before being utilized in actual diagnoses, these results should be validated by accredited laboratories, using more samples and including naturally infected plants.

ACKNOWLEDGMENTS

The authors gratefully acknowledge Vivai Nord s.n.c. for providing *Nerium oleander* plant tissues, and Bachelor Student Anna Leone for the support with DNA extraction and preparation of experiment reactions. The Department of Agricultural and Environmental Sciences of the University of Milan, with the REE initiative, allowed acquisition of the digital PCR instrument used in this study. This research was funded by Regione Lombardia, GARDING project (prot. dom. M1.2018.0067306).

DATA AVAILABILITY STATEMENT

All relevant data are within the paper and its Supporting Information files.

LITERATURE CITED

Backus E.A., Morgan D.J.W., 2011. Spatiotemporal colonization of *Xylella fastidiosa* in its vector supports the role of egestion in the inoculation mechanism of foregut-borne plant pathogens. *Phytopathology* 101: 869–884.

Baldi P., La Porta N., 2017. *Xylella fastidiosa*: host range and advance in molecular identification techniques. *Frontiers in Plant Sciences* 8: 944. DOI: 10.3389/fpls.2017.00944

Chang C.J., Garnier M., Zreik L., Rossetti V., Bové J.M., 1993. Culture and serological detection of the xylem-limited bacterium causing citrus variegated chlorosis and its identification as a strain of *Xylella fastidiosa*. *Current Microbiology* 27: 137–142. DOI: 10.1007/BF01576010

Cornara D., Sicard A., Zeilinger A.R., Porcelli F., Purcell A.H., Almeida R.P.P., 2016. Transmission of *Xylella fastidiosa* to grapevine by the meadow spittlebug. *Phytopathology* 106: 1285–1290.

Davis M.J., Purcell A.H., Thomson S.V., 1978. Pierce's disease of grapevines: isolation of the causal bacterium. *Science* 199: 75–77. DOI: 10.1126/science.199.4324.75

Desprez-Loustau M.L., Balci Y., Cornara D., Gonthier P., Robin C., Jacques M.A., 2020. Is Xylella fastidiosa a serious threat to European forests? *Forestry* 94: 1–17. DOI: 10.1093/forestry/cpaa029

Devonshire A.S., O'Sullivan D.M., Honeyborne I., Jones G., Karczmarczyk M., (…), Huggett J.F., 2016. The use of digital PCR to improve the application of quantitative molecular diagnostic methods for tuberculosis. *BMC Infectious Diseases* 16: 366. DOI: 10.1186/s12879-016-1696-7

dMIQE group, 2020. The Digital MIQE guidelines update: minimum information for publication of quantitative digital PCR experiments for 2020. *Clinical Chemistry* 66: 1012–1029. DOI: 10.1093/clinchem/hvaa125

Dreo T., Pirc M., Ramsak Z., Pavsic J., Milavec M., Zel J., Gruden K., 2014. Optimising droplet digital PCR analysis approaches for detection and quantification of bacteria: a case study of fire blight and potato brown rot. *Analytical and Bioanalytical Chemistry* 406: 6512–6528. DOI: 10.1007/s00216-014-8084-1

Dupas E., Legendre B., Olivier V., Poliakoff F., Manceau C., Cunty A., 2019. Comparison of real-time PCR and droplet digital PCR for the detection of Xylella fastidiosa in plants. *Journal of Microbiological Methods* 162: 86–95. DOI: 10.1016/j.mimet.2019.05.010

EFSA (European Food Security Authority), 2022. Update of the *Xylella* spp. host plant database–systematic lit-

erature search up to 30 June 2021. 12 January 2022. *EFSA Journal* 20: 7039. DOI: 10.2903/j.efsa.2022.7039

Faino L., Scala V., Albanese A., Modesti V., Grottoli A., (…), Loreti S., 2021. Nanopore sequencing for the detection and identification of *Xylella fastidiosa* subspecies and sequence types from naturally infected plant material. *Plant Pathology* 70: 1860–1870. DOI: 10.1111/ppa.13416

Francis M., Lin H., Cabrera-La Rosa J., Doddapaneni H., Civerolo E.L., 2006. Genome-based PCR primers for specific and sensitive detection and quantification of *Xylella fastidiosa*. *European Journal of Plant Pathology* 115: 203–213.

Frazier N.W., 1965. Xylem viruses and their insect vectors. In: *Proceeding of the International Conference of Virus Vectors Perennial Hosts Special Ref. Vitis*. Ed. WB Hewitt, pages 91-99. Davis, CA: Division of Agricultural Science, University of California.

Gutierrez-Aguirre I., Racki N., Dreo T., Ravniakr M., 2015. Droplet digital PCR for absolute quantification of pathogens. *Methods in Molecular Biology* 1302: 331–347. DOI: 10.1007/978-1-4939-2620-6_24

Harper S.J., Ward, L.I. Clover G.R.G., 2010. Development of LAMP and real-time PCR methods for the rapid detection of *Xylella fastidiosa* for quarantine and field applications. *Phytopathology* 100: 1282–1288.

Lu Y., Zhang H., Wen C., Wu P., Song S., (…), Xu X., 2019. Application of droplet digital PCR in detection of seed-transmitted pathogen *Acidovorax citrulli*. *Journal of Integrative Agriculture* 19: 561–569. DOI: 10.1016/S2095-3119(19)62673-0

Maheshwari Y., Selvaraj V., Hajeri S., Yokomi R., 2017. Application of droplet digital PCR for quantitative detection of *Spiroplasma citri* in comparison with real time PCR. *PLoS One* 12: e0184751. DOI: 10.1371/journal.pone.0184751

Mangolini A., Ferracin M., Zanzi M.V., Saccenti E., Ebnaod S.O., (…), Negrini M., 2015. Diagnostic and prognostic microRNAs in the serum of breast cancer patients measured by droplet digital PCR. *Biomarker Research* 6: 3–12. DOI: 10.1186/s40364-015-0037-0

Mansfield J., Genin S., Magori S., Citovsky V., Sriariyanum M., (…), Foster G.D., 2012. Top 10 plant pathogenic bacteria in molecular plant pathology. *Molecular Plant Pathology* 13: 614–629. DOI: 10.1111/j.1364-3703.2012.00804.x

Migliorini D., Pecori F., Raio A., Luchi N., Rizzo D., (…), Santini A., 2021. First report of *Erwinia amylovora* in Tuscany, Italy. *Phytopathologia Mediterranea* 60: 253-257. DOI: 10.36253/phyto-12817

NAPPO, Guidelines for the Movement of Propagative Plant Material of Stone Fruit, Pome Fruit, and Grapevine into a NAPPO Member Country. 2004.

OEPP/EPPO, 2019. PM 7/24 (4) *Xylella fastidiosa*. *Bulletin OEPP/EPPO Bulletin* 49(2): 175–227 DOI:10.1111/epp.12575

OEPP/EPPO, 2021 EPPO standard PM 1/2 (30) EPPO A1 and A2 lists of pests recommended for regulation as quarantine pests. 2021.

Passera A., Compant S., Casati P., Maturo M.G., Battelli G., (…), Mitter B., 2019. Not just a pathogen? Description of a plant-beneficial *Pseudomonas syringae* strain. *Frontiers in Microbiology* 10:1409. DOI: 10.3389/fmicb.2019.01409

Potnis N., Kandel P.P., Merfa M.V., Retchless A.C., Parker J.K., (…), De La Fuente L., 2019. Patterns of inter- and intrasubspecific homologous recombination inform eco-evolutionary dynamics of *Xylella fastidiosa*. *ISME Journal* 13: 2319–2333. DOI: 10.1038/s41396-019-0423-y

Purcell A.H., 1979. Control of the blue-green sharpshooter and effects on the spread of Pierce's disease of grapevines. *Journal of Economical Entomology* 72: 887–892.

Redak P.A., Purcell A.H., Lopes J.R.S., Blua M.J., Mizell III R.F., Andersen P.C., 2004. The biology of xylem fluid-feeding insect vectors of *Xylella fastidiosa* and their relation to disease epidemiology. *Annual Review of Entomology* 49: 243–270.

Regulation (EU) 2016/2031 of the European Parliament of the Council on protective measures against pests of plants, amending Regulations (EU) No 228/2013, (EU) No 652/2014 and (EU) No 1143/2014 of the European Parliament and of the Council and repealing Council Directives 69/464/EEC, 74/647/EEC, 93/85/EEC, 98/57/EC, 2000/29/EC, 2006/91/EC and 2007/33/EC. 26 October 2016

Rodriguez C.M., Obando J.J., Villalobos W., Moreira L., Rivera C., 2007. First report of *Xylella fastidiosa* infecting coffee in Costa Rica. *Plant Disease* 85: 1027. DOI: 10.1094/PDIS.2001.85.9.1027A

Saponari M., Boscia D., Nigro F., Martelli G.P., 2013. Identification of DNA sequences related to *Xylella fastidiosa* in oleander, almond and olive trees exhibiting leaf scorch symptoms in Apulia (Southern Italy). *Journal of Plant Pathology* 94: 688. DOI: 10.4454/JPP.V95I3.035

Saponari M., Boscia D., Altamura G., Loconsole G., Zicca S., (…), Martelli G.P., 2017. Isolation and pathogenicity of *Xylella fastidiosa* associated to the olive quick decline syndrome in southern Italy. *Scientific Reports* 7: 17723.

Sedlak R.H., Kuypers J., Jerome K.R., 2014. A multiplexed droplet digital PCR assay performs better than qPCR

on inhibition prone samples. *Diagnostic Microbiology and Infectious Diseases* 80: 285–286. DOI: 10.1016/j.diagmicrobio.2014.09.004

Selvaraj V., Maheshwari Y., Hajeri S., Yokomi R., 2019. Droplet Digital PCR for absolute quantification of plant pathogens. Pages 583-585 In: *Plant Biotechnology: Progress in Genomic Era*, (Khurana, S.M.P. and Gaur, R.K. ed.), Springer Nature, Singapore.

Sicard A., Zeilinger A.R., Vanhove M., Schartel T.E., Beal D.J., Daugherty M.P., Almeida R.P.P., 2018. *Xylella fastidiosa*: insights into an emerging plant pathogen. *Annual Review of Phytopathology* 56: 181–202. DOI: 10.1146/annurev-phyto-080417-045849

Thorne E.T., Stevenson J.F., Rost T.L., Labavitch J.M., Matthews M.A., 2006. Pierce's disease symptoms: comparison with symptoms of water deficit and the impact of water deficits. *American Journal of Enology and Viticulture* 57: 1–11.

Vanhove M., Retchless A.C., Sicard A., Rieux A., Coletta-Filho H.D., (…), Almeida R.P.P., 2019. Genomic diversity and recombination among *Xylella fastidiosa* subspecies. *Applied and Environmental Microbiology* 85: e02972-18. DOI: 10.1128/AEM.02972-18

Wells J.M., Raju B.C., Hung H.Y., Weisburg W.G., Mandelco-Paul L., Brenner D.J., 1987. *Xylella fastidiosa* gen. nov., sp. Nov: Gram-negative, xylem-limited, fastidious plant bacteria related to *Xanthomonas* spp. *International Journal of Systematic and Evolutionary Microbiology* 37: 136–147. DOI: 10.1099/00207713-37-2-136

Zhao Y., Xia Q., Yin Y., Wang Z., 2016. Comparison of droplet digital PCR and quantitative PCR assays for quantitative detection of *Xanthomonas citri* Subsp. *citri*. *PLoS One* 11: e0159004. DOI: 10.1371/journal.pone.0159004

Phytopathologia Mediterranea
The international journal of the
Mediterranean Phytopathological Union

Firenze University Press
www.fupress.com/pm

New or Unusual Disease Reports

Identification of grapevine virus G and grapevine virus H in Sardinia, Italy

Nicola SCHIANCHI[1,*], Sandro FLORE[1], Martin JAGUNIĆ[2], Salvatorica SERRA[1], Vanda Assunta PROTA[1], Darko VONČINA[2,3]

[1] *Department of Agriculture, Section of Plant Pathology, University of Sassari, Viale Italia 39, 07100 Sassari, Italy*
[2] *University of Zagreb Faculty of Agriculture, Department of Plant Pathology, Svetošimunska cesta 25, 10000 Zagreb, Croatia*
[3] *Centre of Excellence for Biodiversity and Molecular Plant Breeding (CroP-BioDiv), Svetošimunska cesta 25, Zagreb 10000, Croatia*
*Corresponding author. E-mail: nschianchi@uniss.it

Summary. Grapevine virus G (GVG) and grapevine virus H (GVH) (genus *Vitivirus*) are recently discovered viruses. Analysis of 38 samples from Sardinian grapevine cultivars for the presence of GVG and GVH was carried out using RT-PCR. All samples were also tested for grapevine Pinot gris virus (GPGV) using RT-PCR, and for grapevine leafroll virus -1, -2 and -3, grapevine virus A (GVA) and B (GVB), arabis mosaic virus (ArMV), grapevine fanleaf virus (GFLV) and grapevine fleck virus (GFkV) using multiplex RT-PCR. GVG was confirmed in four vines, and GVH was detected in only one sample. In phylogenetic analyses of the coat protein (CP) region, the Sardinian GVG isolates clustered separately from isolates from Croatia and New Zealand. The Sardinian GVH isolate clustered with most sequences from other countries, but with greater affinity to isolates from California (USA) for the CP region, whereas it clustered with isolates from Croatia in the RNA-dependent RNA polymerase (RdRp) region. In addition to GVG and GVH, many samples were coinfected with GVA, viruses from the leafroll complex, and GPGV. This is the first record of GVG and GVH occurring in Italy.

Keywords. RT-PCR, sequencing, grapevine viruses, vitiviruses.

OPEN ACCESS

Citation: N. Schianchi, S. Flore, M. Jagunić, S. Serra, V.A. Prota, D. Vončina (2022) Identification of grapevine virus G and grapevine virus H in Sardinia, Italy. *Phytopathologia Mediterranea* 61(3): 505-511. doi: 10.36253/phyto-13619

Accepted: December 2, 2022

Published: January 13, 2023

Data Availability Statement: All relevant data are within the paper and its Supporting Information files.

Competing Interests: The Author(s) declare(s) no conflict of interest.

Editor: Nihal Buzkan, Kahramanmaraş Sütçü Imam University, Turkey.

ORCID:
NS: 0000-0003-2432-3800
SF: 0000-0002-6666-4921
MJ: 0000-0003-0959-6296
SS: 0000-0001-5663-318X
VAP: 0000-0002-5848-5632
DV: 0000-0001-6093-5471

More than 80 viruses have been identified in grapevine, which is the greatest number of intracellular pathogens reported in one economic crop host (Martelli, 2014; Martelli, 2018; Fuchs, 2020). The genus *Vitivirus* (family *Betaflexiviridae*) contains plant-infecting viruses (Adams *et al*., 2012). The known *Vitivirus* species infecting grapevines are: grapevine virus A (GVA), grapevine virus B (GVB), grapevine virus D (GVD), grapevine virus E (GVE), and grapevine virus F (GVF) (Minafra *et al*., 2017). Recently, new vitiviruses have been identified and named: grapevine virus G (GVG) (Blouin *et al*., 2018a), grapevine virus H (GVH) (Candresse *et al*., 2018), grapevine virus I (GVI) (Blouin *et al*., 2018b), grapevine virus J (GVJ) (Diaz-Lara *et al*., 2018), grapevine virus L (GVL) (Debat *et al*., 2019), grapevine

virus N (GVN), and grapevine virus O (GVO) (Read *et al*., 2022). Currently, GVG has been reported in New Zealand (Blouin *et al*., 2018a), the United States of America (Diaz-Lara *et al*., 2019), and Croatia (Vončina and Almeida, 2018), while GVH has been reported in Portugal (Candresse *et al*., 2018), the United States of America (Diaz-Lara *et al*., 2019), Greece (Panailidou *et al*., 2021), and Croatia (Jagunić *et al*., 2021).

In Italy, only GVA (Conti *et al*., 1980), the cause of Kober Stem Grooving (KSG) (Garau *et al*., 1994), GVB, the cause of Corky Bark (Boscia *et al*., 1993), and GVD associated with Grapevine Rugose Wood Disease (Abou-Ghanem *et al*., 1997) have been reported to date.

To verify occurrence of new grapevine viruses in Sardinia (Italy), particularly GVG and GVH, a survey was conducted of several grapevine varieties randomly collected from different vineyards in this region.

During winter of 2020 and spring of 2021, a total of 38 grapevine samples/vines were analyzed for the presence of grapevine Pinot gris virus (GPGV), GVG, GVH, grapevine leafroll associated virus 1, 2 and 3 (GLRaV-1, GLRaV-2, GLRaV-3), GVA, GVB, arabis mosaic virus (ArMV), grapevine fanleaf virus (GFLV) and grapevine fleck virus (GFkV). Of the vines analyzed, eight were 'Cannonau' from a vineyard near Alghero, ten were 'Vermentino' from a vineyard near Olmedo, and five each were of 'Cannonau', 'Vermentino' 'Vernaccia', and 'Carignano' from a vineyard near Narbolia. For each sampling, five to six 10 cm canes were taken from different parts of the vine canopy to assess for presence of the viruses using molecular assays.

To extract total RNA, 100 mg of phloem tissue from each sample was macerated in liquid nitrogen using a pestle and mortar, and then transferred to a 2.0 mL capacity tube containing on of 1.8 mL of grinding buffer (15 mM Na_2CO_3, 35 mM $NaHCO_3$, 2% (w/v) PVP40, 0.2% (w/v) BSA, 0.05% (v/v) Tween 20, pH 9.6), and vortexed briefly. After centrifugation for 10 min at 13,200 g using a high-speed Centrifuge 5415 R (Eppendorf) , 8 µL of clear supernatant was added to 0.1 mL of GES buffer (0.1 M glycine-NaOH pH 9.0, 50 mM NaCl, 1 mM EDTA pH 9.0, 0.5% (v/v) Triton X-100) (La Notte *et al*., 1997), containing 1% β-mercaptoethanol in a 0.2 mL PCR reaction tube. The sample tubes were then incubated in a Mastercycler (Eppendorf) at 95°C for 10 min.

All samples were tested for the presence of GVG and GVH using the OneStep RT-PCR kit (Qiagen), with 0.5 µM of each specific primer (Supplementary Table 1) and the supplied mastermix, following the manufacturer's recommendations. The RT-PCR conditions applied in the Mastercycler (Eppendorf) included the reverse transcription step at 52°C for 30 min, an initial activation step at 95°C for 15 min, 35 cycles at 94°C for 30 s, 55°C for 45 s, and 72°C for 1 min, followed by a final extension at 72°C for 7 min. In addition, all samples were tested for GPGV by RT-PCR using specific primers (Supplementary Table 1), and by multiplex RT-PCR, to simultaneously test the samples for the presence of GLRaV-1, GLRaV-2, GLRaV-3, GVA, GVB, ArMV, GFLV and GFkV. Multiplex PCR was carried out according to published protocols (Faggioli *et al*., 2012).

The PCR products obtained, including partial coat protein (CP) and partial RNA-dependent RNA polymerase (RdRp) genes, were Sanger sequenced in both directions at Macrogen Europe (Amsterdam, The Netherlands), and analyzed using MEGA X (Kumar *et al*., 2018) and BioEdit software, version 7.2.5 (Hall, 1999).

Phylogenetic trees for GVG and GVH were generated using the sequences from the Sardinian isolates and sequences available in GenBank, including the GVN isolate (GenBank. MZ68235) for rooting the GVG tree and the GVM isolate (GenBank. MK492703) for rooting the GVH trees (Supplementary Table 2). Phylogenetic analyses were carried out using the aligned sequences, and trees were generated using the maximum likelihood method with the MEGA X program. A bootstrap analysis with 1,000 replicates was performed to estimate statistical support for the different tree branches, using a minimum of 50% as a threshold.

Four of the 38 grapevines/samples tested were positive for GVG, and one sample was positive for GVH (Table 1). The four GVG-positive samples were detected only with primers specific to the CP region, whereas the same samples were negative with primer pairs targeting the RdRp region. The failure to detect the virus was probably due to the genetic variability of the Sardinian isolates in the respective regions of the genomes.

In several studies investigating the effects of GVA, GVB, and GVD on plants (Sciancalepore *et al*., 2006; Blouin *et al*., 2018b; Rosa *et al.* 2011), combined infections were found to have greater negative effects on symptoms than single virus infections. Sardinian grapevines positive for GVG were coinfected with GVA in two samples, GLRaV-1 in one sample, GLRaV-2 in one sample, and GPGV in three samples, whereas coinfections with GLRaV-3 were present in all the samples (Table 1). Presence of other viruses included in the study was not confirmed in the vine infected with GVH.

Phylogenetic analyses indicated that all Sardinian GVG CP sequences formed a separate clade. The four Sardinian GVG isolates had nucleotide similarities from 98.3% to 100%. In addition, CP sequences clustered in separate clades based on the location of the vineyards, in Narbolia and Olmedo (Figure 1).

Table 1. RT-PCR detection of different viruses in different grapevine in Sardinia, in cvs. 'Cannonau'(CN) located in Alghero (AHO) and Narbolia (NAR), 'Vermentino' located in Olmedo (OLM) and Narbolia (NAR), and 'Vernaccia' (VRN) and 'Carignano' (CRG) located in Narbolia (NAR). Vines positives for GVG and GVH are indicated in bold font.

Samples	Cultivar	Site	GVG	GVH	GPGV	GLRaV 1	GLRaV 2	GLRaV 3	GVA	GFkV
AHO_1_CN	Cannonau	Alghero	-	-	+	-	-	+	-	-
AHO_2_CN	Cannonau	Alghero	-	-	+	-	-	+	+	+
AHO_3_CN	Cannonau	Alghero	-	-	+	-	+	+	-	+
AHO_4_CN	Cannonau	Alghero	-	-	+	-	+	+	+	+
AHO_5_CN	Cannonau	Alghero	-	-	+	-	+	+	-	+
AHO_6_CN	Cannonau	Alghero	-	-	+	-	-	-	-	+
AHO_7_CN	Cannonau	Alghero	-	-	+	-	-	+	+	-
AHO_8_CN	Cannonau	Alghero	-	-	-	-	-	-	+	+
OLM_9_VRM	Vermentino	Olmedo	-	-	+	-	-	+	+	-
OLM_10_VRM	Vermentino	Olmedo	-	-	+	-	-	-	-	-
OLM_11_VRM	Vermentino	Olmedo	-	-	+	-	-	+	+	-
OLM_12_VRM	Vermentino	Olmedo	-	-	+	-	-	+	-	-
OLM_13_VRM	Vermentino	Olmedo	-	-	+	-	-	-	-	-
OLM_14_VRM	Vermentino	Olmedo	+	-	+	-	-	+	+	-
OLM_15_VRM	Vermentino	Olmedo	-	-	+	-	-	+	+	-
OLM_16_VRM	Vermentino	Olmedo	-	-	+	-	-	+	-	-
OLM_17_VRM	Vermentino	Olmedo	+	-	+	-	-	+	-	+
OLM_18_VRM	Vermentino	Olmedo	-	-	+	-	-	+	-	-
NAR_19_CN	Cannonau	Narbolia	-	-	-	-	-	+	-	-
NAR_20_CN	Cannonau	Narbolia	-	-	+	-	-	+	-	-
NAR_21_CN	Cannonau	Narbolia	-	-	+	-	-	+	-	-
NAR_22_CN	Cannonau	Narbolia	-	-	+	-	-	+	-	-
NAR_23_CN	Cannonau	Narbolia	-	-	-	-	-	+	-	-
NAR_24_VRN	Vernaccia	Narbolia	-	-	-	-	-	-	-	-
NAR_25_VRN	Vernaccia	Narbolia	-	-	+	-	-	-	-	-
NAR_26_VRN	Vernaccia	Narbolia	-	-	+	-	-	+	-	-
NAR_27_VRN	Vernaccia	Narbolia	-	-	-	-	-	-	-	-
NAR_28_VRN	Vernaccia	Narbolia	-	-	-	-	-	-	-	-
NAR_29_VRM	Vermentino	Narbolia	-	-	+	-	-	-	-	-
NAR_30_VRM	Vermentino	Narbolia	-	-	+	-	-	-	-	-
NAR_31_VRM	Vermentino	Narbolia	-	-	+	-	-	-	-	-
NAR_32_CRG	Carignano	Narbolia	-	-	+	+	-	-	-	-
NAR_33_CRG	Carignano	Narbolia	-	-	-	-	-	-	-	-
NAR_34_CRG	Carignano	Narbolia	-	-	+	+	-	+	+	-
NAR_35_CRG	Carignano	Narbolia	-	-	+	-	-	+	+	-
NAR_36_CRG	Carignano	Narbolia	+	-	+	+	+	+	-	-
NAR_37_CRG	Carignano	Narbolia	+	-	-	-	-	+	+	-
NAR_38_CRG	Carignano	Narbolia	-	+	-	-	-	-	-	-

Sardinian GVG isolates showed the greatest nt identity (93.57%) with the Croatian VD-102 isolate (Vončina and Almeida 2018).

The GVH phylogenetic trees (Figures 2 and 3) generated using the partial CP and RdRp sequences showed the greatest CP nucleotide similarity of 99.72% with isolate GC5462 (GenBank acc. no. MK838926) from the United States of America, but a grapevine accession originating from Romania (Diaz-Lara *et al*., 2019). In the RdRp region, the Sardinian GVH isolate showed greatest nucleotide identity (98.31%) with the Babica plosnata isolate from Croatia (Jagunić *et al*., 2021).

This study is the first to record the presence of GVG and GVH in Italy. GVG was found in two different areas of Sardinia, in one area in the red grape 'Carignano', and one in the white grape 'Vermentino'. GVH

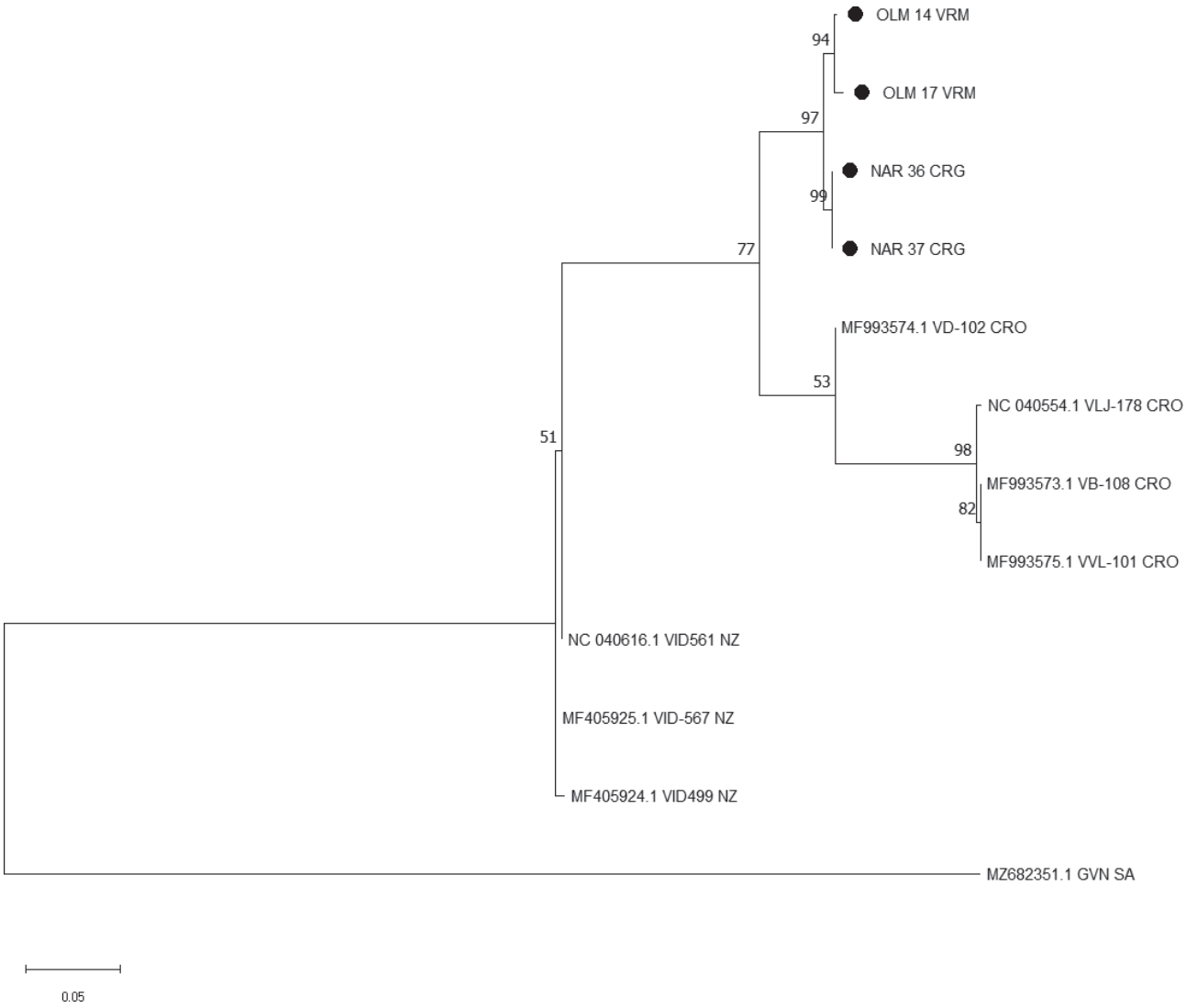

Figure 1. Phylogenetic tree generated from partial nucleotide sequences of the CP region of GVG isolates. Bootstrap values were obtained using 1000 replicates. Only branches with support greater than 50% are indicated. Sardinian isolates detected in this study are indicated by black dots. The phylogenetic tree was reconstructed using the maximum likelihood algorithm implemented in MEGA X software. Four isolates from Croatia (CRO) and three from New Zealand (NZ) were selected from the GenBank database. The GVN sequence (MZ682351) was used as the rooting outgroup.

was detected only in one sample of 'Carignano'. As mentioned by Diaz-Lara *et al*. (2019), none of the novel grapevine vitiviruses have been associated with diseases. It may be important, however, to monitor infection by these viruses in grapevines, to check for any impacts on vine performance and production.

ACKNOWLEDGMENTS

This research was supported by a project grant from the University of Sassari (Fondo di Ateneo per la ricerca 2020). Part of this research received funds from the Croatian Science Foundation, grant number IP-2018-01-1305 project "Ecology and characterization of two novel viruses infecting grapevine—ENVISaGE".

LITERATURE CITED

Abou-Ghanem N., Saldarelli P., Minafra A., Buzkan N., Castellano M.A, Martelli G.P., 1997. Properties of grapevine virus D, a novel putative trichovirus. *Journal of Plant Pathology* 79(1): 15-25.

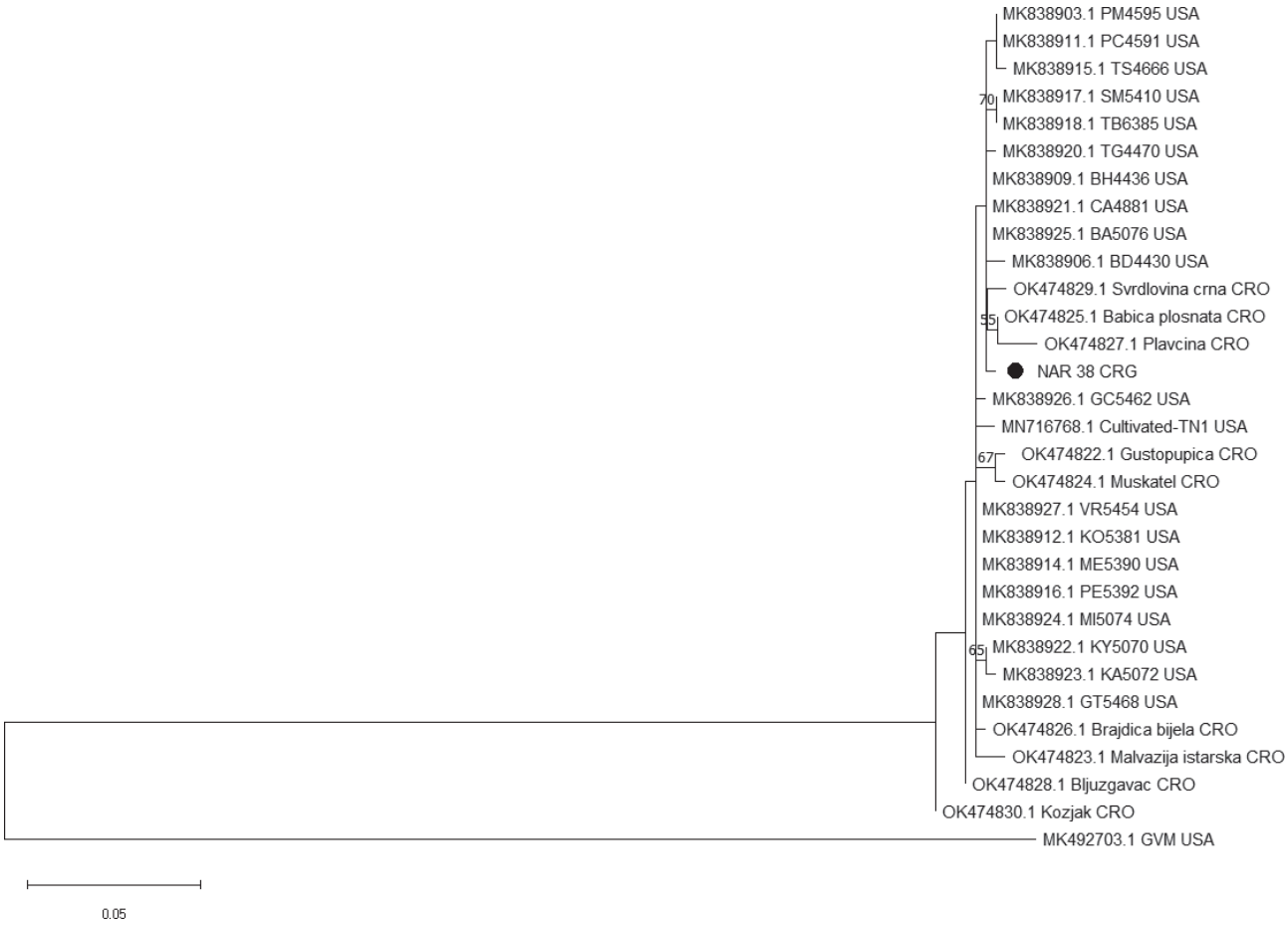

Figure 2. Phylogenetic tree generated from partial nucleotide sequences of the GVH CP region. Bootstrap values were obtained using 1000 replicates. Only branches having a support greater than 50% are indicated. The Sardinian isolate detected in this study is indicated by a black dot. The phylogenetic tree was reconstructed using the maximum likelihood algorithm implemented in the MEGA X software. Nineteen isolates from different countries located in the collection in the United States of America (USA) and eight isolates from Croatia (CRO) were selected from GenBank and used to construct the tree. The GVM sequence (MK492703) was used as the rooting outgroup.

Adams M.J., Candresse T., Hammond J., Kreuze J.F., Martelli G.P., …Yoshikawa N., 2012. Family—Betaflexiviridae. In: (King A.M.Q., Adams M.J., Carstens E.B., Lefkowitz E.J., ed.) *Virus Taxonomy*. *Ninth report of the International Committee on Taxonomy of Viruses*, pp. 920-941.

Alabi O.J., McBride S., Appel D.N., Al Rwahnih M., Pontasch F.M., 2019. Grapevine virus M, a novel vitivirus discovered in the American hybrid bunch grape cultivar Blanc du Bois in Texas. *Archives of Virology* 164(6): 1739-1741. doi: 10.1007/s00705-019-04252-7. https://doi.org/10.1007/s00705-019-04252-7

Blouin A.G., Keenan S., Napier K.R., Barrero R.A., MacDiarmid R.M., 2018a. Identification of a novel vitivirus from grapevines in New Zealand. *Archives of Virology* 163(1): 281-284. https://doi.org/10.1007/s00705-017-3581-0

Blouin A.G., Chooi, K.M., Warren B., Napier K.R., Barrero R.A., MacDiarmid R.M., 2018b. Grapevine virus I, a putative new vitivirus detected in co-infection with grapevine virus G in New Zealand. *Archives of Virology* 163(5): 1371-1374. https://doi.org/10.1007/s00705-018-3738-5

Boscia D., Savino V., Minafra A., Namba S., Elicio V., ... Martelli G.P., 1993. Properties of a filamentous virus isolated from grapevines affected by corky bark. *Archives of Virology* 130 (1-2): 109-120. https://doi.org/10.1007/BF01319000

Candresse T., Theil S., Faure C., Marais A., 2018. Determination of the complete genomic sequence of grapevine virus H, a novel vitivirus infecting grapevine. *Archives of Virology* 163(1): 277-280. https://doi.org/10.1007/s00705-017-3587-7

Conti M., Milne R.G., Luisoni E., Boccardo G., 1980. A

Figure 3. Phylogenetic tree generated from partial nucleotide sequences of the GVH RdRp region. Bootstrap values were obtained using 1000 replicates. Only branches having a support above 50% are indicated. The Sardinian GVH isolate detected in this study is indicated by a black dot. The phylogenetic tree was reconstructed using the maximum likelihood algorithm implemented in the MEGA X software. Seventeen isolates from different countries (United States of America - USA, Portugal - PT and Croatia - CRO) were selected from GenBank and used to construct the tree. A GVM sequence (MK492703) was used as the rooting outgroup.

closterovirus from a stem-pitting-diseased grapevine. *Phytopathology* 70(5): 394-399. https://doi.org/10.1007/10.1094/Phyto-70-394

Debat H., Zavallo D., Brisbane R.S., Vončina D., Almeida R.P., ... Asurmendi S., 2019. Grapevine virus L: a novel vitivirus in grapevine. *European Journal of Plant Pathology* 155(1): 319-328. https://doi.org/10.1007/s10658-019-01727-w

Diaz-Lara A., Brisbane R.S., Aram K., Golino D., Al Rwahnih M., 2019. Detection of new vitiviruses infecting grapevine in California. *Archives of Virology* 164(10): 2573-2580. https://doi.org/10.1007/s00705-019-04355-1

Diaz-Lara A., Golino D., Al Rwahnih M., 2018. Genomic characterization of grapevine virus J, a novel virus identified in grapevine. *Archives of Virology* 163(7): 1965-1967. https://doi.org/10.1007/s00705-018-3793-y

Faggioli F., Anaclerio F., Angelini E., Antonelli M.G., Bertazzon N., Barba M., 2012. Validation of diagnostic protocols for the detection of grapevine viruses covered by phytosanitary rules. In: *Proceedings of the 17th Congress of the International Council for the Study of Virus and Virus-like Diseases of the Grapevine (ICVG)*, October 7–14, 2012, Davis, California, USA. http://hdl.handle.net/10449/23674

Fuchs M., 2020. Grapevine viruses: A multitude of diverse species with simple but overall poorly adopted management solutions in the vineyard. *Journal of Plant Pathology* 102(3): 643-653. https://doi.org/10.1007/s42161-020-00579-2

Garau R., Prota V.A., Piredda R., Boscia D., Prota U., 1994. On the possible relationship between Kober stem grooving and grapevine virus A. *Vitis* 33(3): 161-163.

Hall T.A., 1999. BioEdit: A user-friendly biological sequence alignment editor and analysis program for Windows 95/98/NT. *Nucleic Acids Symposium Series* 41: 95-98.

Hu R., Dias N.P., Soltani N., Vargas-Asencio J.A., Hensley D., … Hajimorad M.R., 2021. Cultivated and wild grapevines in Tennessee possess overlapping but distinct virus populations. *Plant Disease* 105(10): 2785–2791. https://doi.org/10.1094/PDIS-11-20-2483-SC

Jagunić M., Lazarević B., Nikolić K., Stupić D., Preiner D., Vončina D., 2021. Detection, Transmission, and Characterization of Grapevine Virus H in Croatia. *Pathogens* 10(12): 1578. https://doi.org/10.3390/pathogens10121578

Kumar S., Stecher G., Li M., Knyaz C., Tamura K., 2018. MEGA X: Molecular Evolutionary Genetics Analysis across computing platforms. *Molecular Biology and Evolution* 35: 1547-1549. https://doi.org/10.1093/molbev/msy096

La Notte P., Minafra A., Saldarelli P., 1997. A spot-PCR technique for the detection of phloem-limited grapevine viruses. *Journal of Virological Methods* 66(1): 103-108. https://doi.org/10.1016/S0166-0934(97)00038-4

Martelli G.P., 2014. Directory of virus-like diseases of the Grapevine an their agents. *Journal Plant Pathology* 96(1): 1-136. http://dx.doi.org/10.4454/JPP.V96I1SUP

Martelli G.P., 2018. Where Grapevine Virology is Heading to. In: *Proceedings of the 19th Congress of the International Council for the Study of Virus and Virus-Like Diseases of the Grapevine (ICVG)*', Santiago, Chile, 9-12 April, 2018.

Minafra A., Mawassi M., Goszczynski D., Saldarelli P., 2017. Grapevine Vitiviruses. In: *Grapevine Viruses: Molecular Biology, Diagnostics and Management* (Meng B., Martelli G., Golino D., Fuchs M., ed.), Springer, Cham. https://doi.org/10.1007/978-3-319-57706-7_11

Panailidou P., Lotos L., Sassalou C.L., Gagiano E., Pietersen G., Maliogka V.I., 2021. First Report of Grapevine Virus H in Grapevine in Greece. *Plant Disease* 105(9): 2738. https://doi.org/10.1094/PDIS-01-21-0179-PDN

Read D.A., Thompson G.D., Cordeur N.L., Swanevelder D., Pietersen G., 2022. Genomic characterization of grapevine viruses N and O: novel vitiviruses from South Africa. *Archives of Virology* 167: 611-614. https://doi.org/10.1007/s00705-021-05333-2

Rosa C., Jimenez J.F., Margaria P., Rowhani A., 2011. Symptomatology and effects of viruses associated with rugose wood complex on growth of four different rootstocks. *American Journal of Enology and Viticulture* 62: 207-213. https ://doi.org/10.5344/ajev.2011.10104

Saldarelli P., Giampetruzzi A., Morelli M., Malossini U., Pirolo C., … Gualandri V., 2015. Genetic variability of Grapevine Pinot gris virus and its association with grapevine leaf mottling and deformation. *Phytopathology* 105(4): 555-563. https://doi.org/10.1094/PHYTO-09-14-0241-R

Sciancalepore A., Pio Ribeiro G., Turturo C., Dell'Orco M., Minafra A., Martelli G.P., 2006. Molecular variability of GVA and GVB coat protein genes in naturally infected grapevine accessions. In: *Extended abstracts of the 15th meeting of ICVG*, 3-7 April 2006, Stellenbosch, South Africa, 81–82.

Vončina D., Almeida R.P.P., 2018. Screening of some Croatian autochthonous grapevine varieties reveals a multitude of viruses, including novel ones. *Archives of Virology* 163(8): 2239–2243. https://doi.org/10.1007/s00705-018-3850-6

Phytopathologia Mediterranea
The international journal of the
Mediterranean Phytopathological Union

Firenze University Press
www.fupress.com/pm

Short Notes

Response of carrot seed germination to heat treatment, the emergency measure to reduce the risk of '*Candidatus* Liberibacter solanacearum' seed transmission

Lorenza TIZZANI, Andrea GENTILI, Anna TAGLIENTI, Sabrina BERTIN, Vincenza ILARDI*

Research Centre for Plant Protection and Certification, Council for Agricultural Research and Economics (CREA-DC) Via C.G. Bertero, 22, 00156 Rome, Italy
*Corresponding author: vincenza.ilardi@crea.gov.it

Summary. In Europe and the Mediterranean region, '*Candidatus* Liberibacter solanacearum' (Lso) is associated with emerging diseases of *Apiaceae* crops, mainly carrot. Emergency measures for import of carrot seed were set, requiring seed to be heat-treated at 50°C or tested as Lso-negative by PCR. The germination response to heat treatment was assessed for 24 carrot cultivar and hybrid seed lots. Ten parsley, five fennel, and two celery seed lots were also analysed. Of these 41 seed lots, 21 were Lso-infected. Water heat treatment significantly decreased germinability compared to dry heat treatment, indicating that dry heat treatment is a cheaper and less detrimental procedure. However, the dry heat treatment significantly decreased seed germination compared to untreated controls in four of 24 seed lots of carrot, four of ten parsley seed lots, three of five fennel seed lots, and one of two celery seed lots. For parsley, the heat treatment reduced germinability to a lesser extent in Lso-infected than Lso-free seed lots. These data show that heat treatment can affect the germination of *Apiaceae* seeds to varying degrees, depending on species or variety, the type of heat treatment, and the sanitary status of the seeds.

Keywords. *Apiaceae*, *Daucus carota*, 50°C, seed import-export, FAO-IPPC emergency action.

Citation: L. Tizzani, A. Gentili, A. Taglienti, S. Bertin, V. Ilardi (2022) Response of carrot seed germination to heat treatment, the emergency measure to reduce the risk of '*Candidatus* Liberibacter solanacearum' seed transmission. *Phytopathologia Mediterranea* 61(3): 513-522. doi: 10.36253/phyto-13958

Accepted: December 9, 2022

Published: January 13, 2023

Data Availability Statement: All relevant data are within the paper and its Supporting Information files.

Competing Interests: The Author(s) declare(s) no conflict of interest.

Editor: Assunta Bertaccini, Alma Mater Studiorum, University of Bologna, Italy.

ORCID:
LT: 0000-0003-0609-9876
AG: 0000-0002-7728-3139
AT: 0000-0002-1637-5291
SB: 0000-0001-7817-0710
VI: 0000-0003-3657-1158

INTRODUCTION

'*Candidatus* Liberibacter solanacearum' (Lso) is a Gram-negative α proteobacterium, limited to the host plant phloem and psyllid vector haemolymph. Lso is associated with several severe plant diseases (Ilardi and Catara, 2013). The pathogen was first identified as associated with zebra chip in potato (*Solanum tuberosum*) (Munyaneza *et al*., 2007), and then with other diseases of solanaceous crops in Central and North America and Oceania. In Europe and the Mediterranean region, Lso was associated with vegetative disorders in *Apiaceae* crops, mainly carrot (*Daucus carota*) but also parsley (*Petroselinum*

crispum), celery (*Apium graveolens*), and fennel (*Foeniculum vulgare*) (EFSA, 2019; EPPO, 2020a; and references therein). In addition, Lso was detected in several commercial *Apiaceae* seeds marketed in Italy and the United Kingdom (Ilardi *et al*., 2016; Monger and Jeffries, 2016); in the United Kingdom, Lso was also found in seeds from an historical collection (Monger and Jeffries, 2018).

Twelve haplotypes of Lso have been described (EPPO, 2020a; Haapalainen *et al*., 2020 and references therein; Sumner-Kalkun *et al*., 2020). Haplotypes A and B are associated with diseases of potato and other solanaceous crops in the Americas and Oceania, and are included in the European Plant Protection Organization (EPPO) A1 quarantine list (EPPO, 2020b). Haplotypes C, D, E and H infect apiaceous hosts in Europe and the Mediterranean area, while haplotypes H(Con) and U mainly infect weeds. Cras1 and Cras2 are novel haplotypes recently found in psyllid *Craspedolepta* spp. (Sumner-Kalkun *et al*., 2020).

Lso is transmitted by psyllids (superfamily *Psylloideae*) in a persistent-propagative manner (Haapalainen, 2014), and species of *Trioza* and *Bactericera* (*Triozidae*) are known to transmit the most economically relevant Lso haplotypes worldwide (reviewed in Haapalainen, 2014). Recently, also *Craspedolepta* spp., in the family *Aphalaridae* were reported as vectors of Lso in Europe (Sumner-Kalkun *et al*., 2020). Transmission of Lso in true seed was suggested in carrot by Bertolini and colleagues (2015). This finding triggered activation of an emergency action by the Food and Agriculture Organization of the United Nations (FAO) - International Plant Protection Convention (IPPC) (FAO-IPPC Emergency actions, 2016). This measure requires carrot seed to be confirmed as Lso-negative by PCR, or to be heat-treated to inactivate the pathogen. Heat treatments are specified to be performed either in dry conditions, at a minimum temperature of 50°C for at least 72 continuous hours, or with hot water at a minimum temperature of 50°C for at least 20 continuous minutes. Other studies have reported that Lso seed transmission in carrot is not observed (Haapalainen *et al.* 2017; Oishi *et al*., 2017; Mawassi *et al*., 2018; Carminati *et al*., 2019; Fujikawa *et al*., 2020b; Nissinen *et al*., 2021). Based on these findings, Australia recently revised import conditions for apiaceous seeds, removing the requirement of heat treatment or Lso negative test (Australian Government, 2021). Nonetheless, some countries (e.g., Japan) still impose emergency measures and import restrictions for carrot and other *Apiaceae* seeds, and many countries reject imported *Apiaceae* Lso-infected seed lots (Italian National Plant Protection Organization, personal communication, 2022). Such measures have negative impacts on import stakeholders and seed producers. Moreover, the effect of heat treatment on the germinability of *Apiaceae* seeds has not been fully ascertained. Literature on this is limited, and the results have been contradictory.

Since a considerable share of carrot seed production is concentrated in the Mediterranean basin (Nissinen *et al*., 2021; Carosem GmbH, 2022), it is important to know the extent of heat treatment effects on carrot seed germination, for the varieties/hybrids cultivated in this area. The present study investigated the response to heat treatment of 24 carrot seed lots, including examples that were Lso-free and Lso-infected, and some relevant varieties (e.g., Nantese, Berlicum, Flakkée) which are extensively used by commercial growers and have major shares of the carrot seed market. In addition, parsley, fennel, and celery seed lots were also tested; the parsley seed lots included Lso-free and Lso-infected samples, while the fennel and celery seed lots were all Lso-free.

MATERIALS AND METHODS

Apiaceae *seed lots*

A total of 41 *Apiaceae* seed lots were used in this study (Table 1). These included: 24 carrot seed lots, belonging to six cultivars and two hybrids, plus 12 lots as blind samples; ten parsley seed lots, belonging to five cultivars, plus two seed lots as blind samples; five fennel seed lots, belonging to three cultivars and one hybrid; and two celery seeds lots of different cultivars. The commercial batches of seeds were purchased from nursery gardens, supermarkets, or plant shops. The blind seed lots were provided by the Plant Protection Service of Emilia Romagna region, Italy (SF-ER).

DNA extraction from Apiaceae *seeds and quantitative PCR for '*Candidatus *Liberibacter solanacearum' detection*

DNA extraction procedure and quantitative PCR test described by Li *et al.* (2009) and validated by Ilardi *et al.* (2019) were used to detect Lso in seeds. For each seed sample, the seeds were shaken for 30 min in 0.5% Triton X-100, rinsed and then left to soften in water overnight. The seeds were then crushed with a mechanical homogenizer (Interscience Bagmixer) for 10 min at maximum speed in plastic bags (Bioreba) with 1:10 (w/v) modified trimethylammonium bromide (CTAB) buffer (2.5% CTAB; 1.4 M NaCl; 0.1 M Tris-HCl, pH 8.0; 0.02 M EDTA, pH 8.0; 1% PVP-40; 0.53% ascorbic acid). 400 µg of RNase A were added to 500 µL of homogenate and, after incubation at 65°C for 30 min, genomic DNA was extracted using DNeasy Plant Mini Kit (Qiagen), follow-

Table 1a. Seed lots used in experiments, their germination rates after treatments (n.t. = no treatment, dry = dry heat treatment, water = water heat treatment), Chi-square and *P* values obtained by Chi-square tests. Germinability values are expressed as means ± standard deviations of n = 400 seeds. Significant differences (Chi-square tests) are indicated by * = $P < 0.05$, ** = $P < 0.01$, *** = $P < 0.001$, **** = $P < 0.0001$, *****= $P < 0.00001$, ns = not significant.

#	SPECIES (No. of analyzed lots) / Variety	Lso	Treatment	Germinability (%)	Chi-square value	*P* value	Significance
	CARROT (24 lots)						
7	Flakkée 2	+	n.t.	84.5 ± 1.73	11.46	0.000709	***
			dry	80.75 ± 4.79			
6	Berlicum 2	+	n.t.	86.75 ± 0.50	0.28	0.594553	ns
			dry	88.00 ± 2.16			
9	Nantese 2	+	n.t.	75.50 ± 5.74	11.52	0.000687	***
			dry	64.50 ± 1.73			
10	Flakkée 2	+	n.t.	80.25 ± 2.22	0.07	0.788421	ns
			dry	81.00 ± 1.41			
5	Nantese Migliorata 2	+	n.t.	82.25 ± 2.75	0.91	0.340838	ns
			dry	84.75 ± 1.71			
19	Parijse markt	-	n.t.	72.75 ± 4.79	10.99	0.000917	***
			dry	61.75 ± 4.43			
20	Nantese Clodia 2	+	n.t.	91.00 ± 3.74	11.32	0.000768	***
			dry	83.00 ± 3.56			
29	Kamilla F1	-	n.t.	90.75 ± 2.87	0.13	0.719126	ns
			dry	90.00 ± 1.41			
31	Rainbow F1	-	n.t.	39.50 ± 4.51	16.32	0.000054	****
			dry	53.75 ± 5.50			
5E	5E	+	n.t.	93.75 ± 1.26	0.56	0.757277	ns
			dry	93.50 ± 1.29			
			water	92.50 ± 1.91			
6F	6F	+	n.t.	92.00 ± 1.41	1.25	0.535037	ns
			dry	89.75 ± 3.86			
			water	90.50 ± 2.65			
38	Flakkèe 2	-	n.t.	88.75 ± 2.22	5.72	0.057303	ns
			dry	86.75 ± 2.99			
			water	83.00 ± 1.41			
39	Nantese 2	+	n.t.	89.50 ± 1.73	0	1	ns
			dry	89.50 ± 3.11			
40	Berlicum 2	+	n.t.	92.75 ± 0.96	2.99	0.083705	ns
			dry	89.25 ± 2.50			
196	196 (SF-ER)	-	n.t.	14.50 ± 4.36	2.2	0.137799	ns
			dry	11.00 ± 2.16			
198	198 (SF-ER)	-	n.t.	29.25 ± 4.65	0.48	0.488987	ns
			dry	31.50 ± 5.57			
199	199 (SF-ER)	-	n.t.	30.25 ± 3.86	2.49	0.114292	ns
			dry	25.25 ± 5.97			
201	201 (SF-ER)	-	n.t.	12.25 ± 1.71	0.05	0.827743	ns
			dry	11.75 ± 3.59			
202	202 (SF-ER)	-	n.t.	24.50 ± 5.32	3.55	0.059374	ns
			dry	19.00 ± 1.83			
204	204 (SF-ER)	+	n.t.	72.00 ± 1.15	0.01	0.937152	ns
			dry	72.25 ± 3.86			

(Continued)

Table 1a. (Continued).

#	SPECIES (No. of analyzed lots) Variety	Lso	Treatment	Germinability (%)	Chi-square value	*P* value	Significance
205	205 (SF-ER)	+	n.t.	89.25 ± 1.71	74.16	<0.00001	*****
			dry	89.25 ± 2.63			
			water	69.25 ± 5.44			
942	942 (SF-ER)	+	n.t.	87.25 ± 2.22	103.82	<0.00001	*****
			dry	88.25 ± 4.03			
			water	62.50 ± 3.51			
943	943 (SF-ER)	+	n.t.	81.75 ± 5.79	2.76	0.096867	ns
			dry	77.00 ± 2.71			
944	944 (SF-ER)	+	n.t.	81.50 ± 0.58	0.01	0.927261	ns
			dry	81.75 ± 2.50			
	PARSLEY (10 lots)						
P2	P2 (SF-ER)	+	n.t.	96.5 ± 2.65	21.47	0.000022	****
			dry	92.5 ± 1.91			
			water	87.75 ± 1.71			
P3	P3 (SF-ER)	+	n.t.	95.00 ± 1.15	1.79	0.408199	ns
			dry	92.75 ± 5.19			
			water	93.50 ± 1.29			
12	Gigante di Napoli - A	+	n.t.	62.75 ± 6.70	15.89	0.000067	****
			dry	48.75 ± 6.50			
18	Gigante di Napoli - B	-	n.t.	84.75 ± 2.63	0.04	0.843022	ns
			dry	85.25 ± 1.50			
22	Nano Ricciuto 2	+	n.t.	61.00 ± 3.56	54.17	<0.00001	*****
			dry	35.00 ± 4.24			
23	Comune 2	+	n.t.	92.75 ± 1.50	1.06	0.303925	ns
			dry	90.75 ± 4.57			
25	Comune	-	n.t.	94.50 ± 2.65	0.35	0.551515	ns
			dry	93.50 ± 2.52			
26	Halflange	-	n.t.	83.00 ± 3.16	0.68	0.408801	ns
			dry	80.75 ± 2.06			
27	Gigante di Napoli	-	n.t.	91.25 ± 1.71	5.47	0.019366	*
			dry	86.00 ± 5.35			
28	Nano Ricciuto 2	+	n.t.	90.00 ± 2.58	1.5	0.22062	ns
			dry	87.25 ± 1.50			
	CELERY (2 lots)						
17	d'Elne	-	n.t.	96.00 ± 0.82	3.46	0.062749	ns
			dry	93.00 ± 3.16			
24	Dorato d'Asti	-	n.t.	76.00 ± 2.16	239.99	<0.00001	*****
			dry	21.25 ± 4.99			
	FENNEL (5 lots)						
21	Romanesco	-	n.t.	86.00 ± 1.83	151.91	<0.00001	*****
			dry	44.50 ± 7.33			
30	Romanesco	-	n.t.	86.50 ± 3.42	256.27	<0.00001	*****
			dry	30.75 ± 5.68			
32	Selvatico	-	n.t.	64.25 ± 4.27	0.14	0.711143	ns
			dry	65.50 ± 6.45			
33	Waden Romen	-	n.t.	90.25 ± 0.50	12.62	0.000381	***
			dry	81.50 ± 5.80			
34	Amedeus F1	-	n.t.	84.00 ± 3.74	0.32	0.569983	ns
			dry	82.50 ± 3.32			

ing the manufacturer's instructions. Quantitative PCR tests was carried out according to Ilardi *et al*. (2019) and using TaqMan Universal Master Mix II no UNG (Applied Biosystem). After 45 cycles, samples were considered positive if an exponential amplification curve was produced with a cycle threshold (Ct) value <40. For each amplification event, the following controls were included: a negative extraction control, represented by a sample of uninfected matrix; a positive amplification control, represented by DNA extracted from infected carrot; and a negative amplification control, i.e., nuclease-free water. All samples were tested in two technical repetitions.

Heat treatments of Apiaceae *seeds*

Dry heat treatment is generally considered as more feasible by seed producers and seed companies than water heat treatment. Dry treatments avoid the need for subsequent drying step and the risk of mould development. For this reason, the *Apiaceae* seed lots analysed in the present study were mainly tested by dry heat treatment. Comparisons of dry and water treatments were also carried out on a smaller scale, for five carrot seed lots (# 5E, 6F, 38, 205 and 942) and two parsley seed lots (# P2 and P3) (Table 1, Figure 1). For dry treatment, the seed samples (10 g, corresponding to approx. 10,000 seeds) were placed in 50 mL capacity polypropylene tubes, and these were heated in an oven at 50°C for 72 continuous hours. After heating, seed samples were stored at 4°C until used.

For water treatment, the seed samples (each of 10 g each contained in a woven cotton bag) were immersed in a 50°C water bath for 20 min, and then immediately cooled with cold tap water. The seeds were then air-dried on filter paper and then stored at 4°C until used.

Germination of Apiaceae *seeds*

For each lot, 400 heat-treated and 400 untreated control seeds (four biological replicates, each of 100 seeds) were germinated, using the Italian rule DM 22 /12/ 1992 for official methods for seed analyses (https://www.gazzettaufficiale.it/eli/gu/1993/01/04/2/so/1/sg/pdf) and according to the International Seed Testing Association (ISTA 2020).

Statistical analyses

Statistical analyses were carried out using software R version 4.1.1 (R Core Team, 2021). Dry heat-treated and untreated germination rates for each lot were compared by Chi-square tests. Germination data from dry heat-treated, water heat-treated and untreated groups on five carrot seed lots (# 5E, 6F, 38, 205, and 942) and two parsley seed lots (# P2 and P3) were compared by Chi-square tests; when significant, *post-hoc* multiple comparison tests were carried out to establish statistical significance of differences between each pair of groups.

Lso-free/heat-treated, Lso-free/untreated, Lso-infected/heat-treated and Lso-infected/untreated groups were analysed by Chi-square tests, followed by *post-hoc* multiple comparisons. This analysis was carried out for carrot and parsley seed lots whose germinability was above the limit for marketable seeds (Council Directive 2002/55/EC). For fennel and celery, this comparison was not feasible because no infected lots were available.

Table 1b. *Post-hoc* multiple comparison test results following Chi-square test with more than two treatments, when significant difference among groups was indicated in the first test (Table 1a).

#	Multiple comparison test			
	Comparison	Chi-square	*P* value	Significance
Carrot 205	n.t. vs dry	0	1	ns
	n.t. vs water	48.65	<0.00001	*****
	dry vs water	48.65	<0.00001	*****
Carrot 942	n.t. vs dry	0.19	0.666219	ns
	n.t. vs water	65.12	<0.00001	*****
	dry vs water	71.45	<0.00001	*****
Parsley P2	n.t. vs dry	6.16	0.013091	*
	n.t. vs water	21.11	<0.00001	*****
	dry vs water	5.07	0.024339	*

RESULTS

High levels of Lso infection were observed in carrot and parsley seeds, with 15 of 24 carrot seed lots positive for Lso, and six of ten parsley seed lots positive for Lso. All the fennel and celery lots were Lso-free (Table 1a). Table 1a reports germination rates of all the tested seed lots after treatments, as well as Chi-square test results (Chi-square value, *P* value, and statistical significance). When more than two treatments were compared (*i.e.,* no treatment, dry treatment and water treatment), and a Chi-square test indicated a statistically significant difference among them, *post-hoc* multiple comparison test results are reported (Table 1b).

Six Lso-free carrot seed lots showed low germination rate (i.e., # 31, 196, 198, 199, 201 and 202), and five of them were blind samples provided by SF-ER. They were

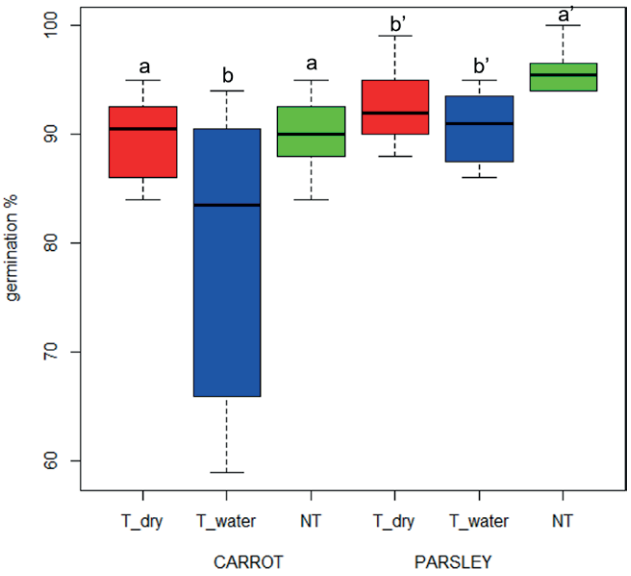

Figure 1. Mean germination rates (%) for carrot and parsley seeds after different treatments. Left: rates for dry heat-treated (T_dry), water heat-treated (T_water) and untreated (NT) carrot seed lots. Means and standard deviations were calculated for n = 2000 seeds from five seed lots. Right: germination rates for dry heat-treated (T_dry), water heat-treated (T_water) and untreated (NT) groups of parsley seed lots. Means and standard deviations were calculated for n = 800 seeds from two seed lots. Statistical significance of differences was determined using Chi-square *post-hoc* multiple comparison tests: different letters indicate significantly different treatments.

official samples whose storing conditions and expiry date were unknown.

The germination rates of carrot seeds decreased after dry heat treatment in four of 24 seed lots, of at least six cultivars and two 2 hybrids, while germination increased in the treated hybrid Rainbow F1 (Table 1a). For the other *Apiaceae* seed lots, reductions of germination were detected for four of ten parsley seed lots from five cultivars, three of five fennel seed lots of three cultivars, and one hybrid and one of two celery seed lots of two cultivars (Table 1a).

The experiment using five carrot seed lots (# 5E, 6F, 38, 205, and 942) and two parsley seed lots (# P2 and P3), which were selected among those having germination rates greater than the limit of marketable seeds (Council Directive 2002/55/EC), was carried out applying dry and water treatments. For the carrot seed lots # 205 and 942, dry heat treated and untreated seeds had similar germination rates while the water treatment reduced germination. The germination rates for the other three carrot seed lots were not significantly different for all the treatments (Table 1, a and b). For parsley, the seed lot P2 gave differences between each pair of treatments, with greatest germination (96.5%) for the untreated seeds, and the least (87.8%) for water treated seeds (Table 1, a and b). Overall, for carrot, the comparison of treatments showed decreases ($P < 0.00001$) of germinability for water treated seeds compared to dry treated or untreated seeds, which were comparable to each other (Figure 1, Table S1). The same experiment for parsley seed (Figure 1, Table S1) showed that germinability decreased after both types of treatment ($P < 0.001$).

The effects of heat treatments were also evaluated by comparing the germination rates for Lso-infected and Lso-free seed lots of carrot and parsley. The seed lots were chosen among those with germination rates above the limit for marketable seeds (Council Directive 2002/55/EC). For carrot seed, heat treatment decreased the germinability of both Lso-infected and Lso-free seed groups compared to their untreated controls (Figure 2 A, Table S2); for parsley, the heat treatment only decreased germinability of Lso-infected seeds (Figure 2B, Table S2). Overall, Lso-infected seeds had greater germinability than Lso-free seeds, either with or without treatments.

Similar comparisons were not carried out for celery and fennel seeds, since no Lso-infected seed lots were available.

DISCUSSION

Carrot is one of the most important root vegetables and it is cultivated in many countries (Que *et al.*, 2019). Carrot seeds and phloem sieve tubes within the seed coats are known to transmit several pathogens (Kuan *et al.*, 1985; Zhang *et al.*, 2020), including Lso (Bertolini *et al.*, 2015), which has been detected in infected seed lots to produce approx. 12-24% of infected seedlings. Two other distinct experimental replications did not show any Lso seed transmission (Loiseau *et al.* 2017a; 2017b; Carminati *et al.,* 2019), and further studies did not find evidence of Lso seed transmission in carrot (Haapalainen *et al.* 2017, Oishi *et al.*, 2017; Mawassi *et al.*, 2018; Fujikawa *et al.*, 2020b; Nissinen *et al.*, 2021). Based on these results, some seed import restrictions have been eased.

As Lso has been widespread in commercial *Apiaceae* seed lots (Ilardi *et al.*, 2016; Monger and Jeffries, 2016), heat treatment is the only procedure for ensuring seed importation.

In the present study experiments, six Lso-free carrot seed lots had low germination rates, and five of them were official samples whose storage conditions and expiry dates were unknown. The age of these lots and/or storage conditions may be a reason for such reduced germinability. The presence of other pathogens in the samples may have also caused low germinability. These

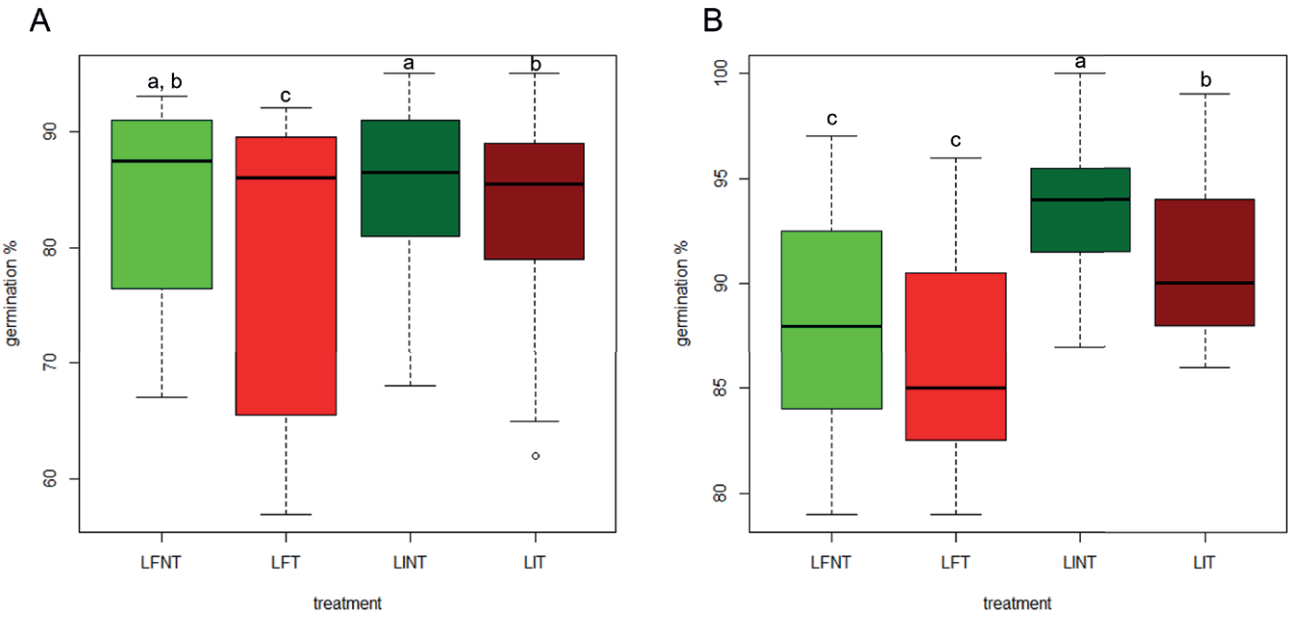

Figure 2. Mean germination rates (%) of Lso-free untreated (LFNT), Lso-free dry treated (LFT), Lso-infected untreated (LINT) and Lso-infected dry treated (LIT) seeds of carrot (A) or parsley (B). In boxplot A, the values are each expressed as mean ± standard deviation for n = 6000 Lso-infected seeds from 15 seed lots, and n = 1200 Lso-free seeds from three lots. In boxplot B, n = 1600 seeds from four seed lots. Different letters accompanying each treatment indicate statistically significant differences between treatments (Chi-square *post-hoc* multiple comparison tests).

factors were not assessed, but, during the germination experiments, no fungal contamination was observed when the germination dishes were inspected.

Dry heat treatment of seeds has been commonly described for disinfection from many pathogens (fungi, bacteria). Exposure to temperatures between 55 and 75°C was reported to be lethal for seeds of conifer (Baker, 1929), bunch grass (Wright, 1970; Koppenaal and Colombo, 1988) and bottle gourd (Nakamura, 1982). More recently, a comprehensive study on 66 wild species from 22 plant families (but not *Apiaceae*) reported that dry heat treatment at 60°C for 1 h did not cause significant decreases in seed germinability, and germination was increased for ten species (Godefroid *et al*., 2017). Grondeau *et al*. (1992) suggested that rehydration of seeds after dry treatments could be necessary to achieve germination. These reports are therefore contradictory, showing lethal and no effects of heat treatments on seed germination, depending on the species, the thermal protocol and rehydration procedures.

The present study showed that germination rates decreased after dry heat treatments for four of 24 carrot seed lots. The effect was even more evident for parsley and fennel, where germination was reduced for four of ten parsley seed lots and three of five fennel seed lots. These data indicate slight to moderate impacts of dry heat treatments on *Apiaceae* seed germinability, depending on the species. In carrot, three of the four varieties showing germination reductions (*i.e*., Flakkée, Nantese, Berlicum) are extensively used by commercial growers, and represent a major share of the carrot market. Therefore, the impacts of heat treatments on seed producers and importers are likely to be relevant. Only for the carrot hybrid Rainbow F1 did heat treatment improve the germinability of seeds. This could be related to the low germination percentage of the untreated seed lot, which was below the minimum germination rate standards required for commercialization (65% for carrot seed, Council Directive 2002/55/EC). However, other carrot seed lots with germination percentages below the minimum standards (*i.e*., lots 196, 198, 199, 201 and 202) did not show significant differences in germinability between treated and untreated samples (Table 1 a).

Hot water treatment is the oldest type of heat treatment for seeds. For carrot seeds, it is used for disinfection from *Xanthomonas campestris* pv. *carotae* (Ark and Gardner, 1944). Ten min at 52°C are sufficient to inactivate the bacterium. Studies on germination of seeds after hot water disinfection indicate variability among plant species from temperate ecosystems, and but this topic has not been widely studied. Some authors have indicated that carrot seed disinfection procedures using hot water, as well as hypochlorite treatment, did not affect germinability, but chemical treatments with ethanol or

oxytetracycline greatly decreased germination (Fujikawa *et al*., 2020a). Other studies have reported decreased germination of carrot seeds after hot water treatments, indicating the thermal treatment limit was 50°C for 40 min. For higher temperatures or longer exposure times, germinability decrease has been observed (Merfield, 2005). Strandberg and White (1989) reported that ten of 25 carrot hybrids had reduced seedling emergence in greenhouse experiments after hot water treatments of seeds at 50°C for 20 min. Fourteen hybrids were not affected, and one had increased seedling emergence after treatment. Injurious effects on germination induced by hot water seed treatments were also reported by Grondeau *et al.* (1994), depending on exposure time. Bolton *et al.* (2019) reported that heat water treatment at 35°C applied to 293 carrot accessions reduced germination from a mean of 63.8% to 33.0%. Data from the present study showed that germination of two of five carrot varieties and one of two parsley varieties decreased after hot water treatments, confirming previous literature, and supporting dependence of this effect on plant variety. In carrot, the hot water treatment reduced germination more than dry treatment, whereas in parsley, germination decreased after both treatments compared to no treatment. As reported above, use of water for heat treatment is not considered suitable by stakeholders. For carrot seed, the results achieved support the use of dry heat rather than water.

The decrease in germination rates after heat treatments, which involved Lso-free and infected seeds of carrot and only Lso-infected parsley seeds, further confirms that impacts of heat treatments of seeds is strongly dependent on species. The data obtained in the present study indicate that heat treatments of seeds can have economic impacts, from the direct costs of the procedures, and from resulting decreases in seed germinability of some cultivars of *Apiaceae* species. Carrot seed germinability decrease after heat treatment in some economically important cultivars, and the same trend was found in other *Apiaceae* species.

ACKNOWLEDGEMENTS

This research was supported by Proteggo project founded by MiPAAF, and carried out within the frame of Euphresco PhyLib III project. The authors thank Mario Tavazza for critical revision of the manuscript of this paper.

LITERATURE CITED

Ark P.A., Gardner M.W., 1944. Carrot bacterial blight as it affects the roots. *Phytopathology* 34: 416–420.

Australian Government, 2021. Revised import conditions for CaLso on apiaceous seed – Information sheet. URL: https://www.agriculture.gov.au/sites/default/files/documents/revised-import-conditions-calso-apiaceous-seed-information-sheet.pdf accessed on 14/11/2022.

Baker F.S., 1929. Effect of excessively high temperatures on coniferous reproduction. *Journal of Forestry* 27: 949–975. https://doi.org/10.1093/jof/27.8.949

Bertolini E., Teresani G.R., Loiseau M., Tanaka F.A.O., Barbé S., Martinez C., Gentit P., Lopez M., Cambra M., 2015. Transmission of '*Candidatus* Liberibacter solanacearum' in carrot seeds. *Plant Pathology* 64: 276–285. https://doi.org/10.1111/ppa.12245

Bolton A., Nijabat A., Mahmood-ur-Rehman M., Naveed N.H., Majharul Mannan A.T.M., … Simon P., 2019. Variation for Heat Tolerance During Seed Germination in Diverse Carrot [*Daucus carota* (L.)] Germplasm. *Horticultural Science* 54(9): 1470–1476. https://doi.org/10.21273/HORTSCI14144-19

Carminati G., Satta E., Paltrinieri S., Bertaccini A., 2019. Simultaneous evaluation of '*Candidatus* Phytoplasma' and '*Candidatus* Liberibacter solanacearum' seed transmission in carrot. *Phytopathogenic Mollicutes* 9(1): 141–142.

Carosem GmbH, 2022. Commercial production of carrot seed. Available at: https://carosem.eu/seed-production/

Council Directive 2002/55/EC of 13 June 2002 on the marketing of vegetable seed. Available at: https://eur-lex.europa.eu/legal-content/EN/TXT/PDF/?uri=CELEX:32002L0055&from=EN

European Food Safety Authority (EFSA), Loiseau M., Schrader G., Camilleri M., Diakaki M., Vos S., 2019. Pest survey card on '*Candidatus* Liberibacter solanacearum'. *EFSA Supporting Publications* 16(6): 1632E. https://doi.org/10.2903/sp.efsa.2019.EN-1632

European Plant Protection Organization (EPPO) PM 7/143 (1) 2020a. '*Candidatus* Liberibacter solanacearum'. *EPPO Bulletin* 50: 49–68. https://doi.org/10.1111/epp.12611

European Plant Protection Organization (EPPO), 2020b. Available at: https://www.eppo.int/ACTIVITIES/plant_quarantine/A1_list

FAO/IPPC Emergency Action (2016). Proposed revision of List of the plants subject to Specific Phytosanitary Measures to be carried out in Exporting Countries (Annexed Table 2–2 of the Ordinance for Enforce-

ment of the Plant Protection Act). Available at: http://www.maff.go.jp/j/syouan/keneki/kikaku/pdf/04_at2_2_specific_measures.pdf

Fujikawa T., Taguchi M., Kido K., Kusano S., Enya J., … Sato M., 2020a. Evaluation of an RNA-based PCR assay to detect viable '*Candidatus* Liberibacter solanacearum' (Lso) in Lso-contaminated carrot seeds using different disinfection methods. *Journal of Plant Pathology* 102: 205–211. doi: https://doi.org/10.1007/s42161-019-00405-4

Fujikawa T., Yamamura K., Osaki K., Onozuka N., Taguchi M., … Sato M., 2020b. Seed transmission of '*Candidatus* Liberibacter solanacearum' is unlikely in carrot. *Journal of General Plant Pathology* 86(4): 266–273. https://doi.org/10.1007/s10327-020-00927-1

Godefroid S., Van der Vyver A., Stoffelen P., Vandeborght B., 2017. Effectiveness of dry heat as seed sterilisation technique: Implications for ex situ conservation. *Plant Biosystems* 151(6): 1054–1061. doi: https://doi.org/10.1080/11263504.2016.1231140

Grondeau C., Ladonne F., Fourmond A., Poutier F., Samson R., 1992. Attempt to eradicate *Pseudomonas syringae* pv. *pisi* from pea seeds by heat treatments. *Seed Science and Technology* 20: 515–525.

Grondeau C., Samson R., Sands D.D.C., 1994. A Review of Thermotherapy to Free Plant Materials from Pathogens, Especially Seeds from Bacteria. *Critical Reviews in Plant Sciences* 13(1): 57–75. https://doi.org/10.1080/07352689409701908

Haapalainen M., 2014. Biology and epidemics of '*Candidatus* Liberibacter' species, psyllid-transmitted plant-pathogenic bacteria. *Annals of Applied Biology* 165(2): 172–198. https://doi.org/10.1111/aab.12149

Haapalainen M., Kivimäki P., Latvala S., Rastas M., Hannukkala A., … Nissinen A. I., 2017. Frequency and occurrence of the carrot pathogen '*Candidatus* Liberibacter solanacearum' haplotype C in Finland. *Plant Pathology* 66: 559–570. https://doi.org/10.1111/ppa.12613

Haapalainen M., Latvala S., Wickström A., Wang J., Pirhonen M., Nissinen A. I., 2020. A novel haplotype of '*Candidatus* Liberibacter solanacearum' found in *Apiaceae* and *Polygonaceae* family plants. *European Journal of Plant Pathology* 156(2): 413–423. https://doi.org/10.1007/s10658-019-01890-0

International Seed Testing Association, 2020. The germination test. In: *International Rules for Seed Testing*. Chapter 5: 1–57. https://doi.org/10.15258/istarules.2022.05

Ilardi V., Catara V., 2013. '*Candidatus* Liberibacter' spp. Emerging Threats for Agriculture in the European and Mediterranean Region. *Biosafety* 2: E135. https://doi.org/10.4172/2167-0331.1000e135

Ilardi V., Di Nicola E., Tavazza, M., 2016. First report of '*Candidatus* Liberibacter solanacearum' in commercial carrot seeds in Italy. *Journal of Plant Pathology* 98(2). DOI: http://dx.doi.org/10.4454/JPP.V98I2.040

Ilardi V., Lumia V., Di Nicola E., Tavazza M., 2019. Identification, intra-and inter-laboratory validation of a diagnostic protocol for '*Candidatus* Liberibacter solanacearum' in carrot seeds. *European Journal of Plant Pathology* 153(3): 879–890. https://doi.org/10.1007/s10658-018-01606-w

Koppenaal, R.S., Colombo, S.J., 1988. Heat tolerance of actively growing bud-initiated, and dormant black spruce seedlings. *Canadian Journal of Forest Research* 18: 1103–1105. https://doi.org/10.1139/x88-169

Kuan T. L., Minsavage G. V., Gabrielson R. L.,1985. Detection of *Xanthomonas campestris* pv. *carotae* in carrot seed. *Plant Disease* 69(9): 758–760. https://doi.org/10.1094/PD-69-758

Li W., Abad J.A., French-Monar R.D., Rascoe J., Wen A., … Levy L., 2009. Multiplex real-time PCR for detection, identification and quantification of '*Candidatus* Liberibacter solanacearum' in potato plants with zebra chip. *Journal of Microbiological Methods* 78: 59–65. https://doi.org/10.1016/j.mimet.2009.04.009

Loiseau M., Renaudin I., Cousseau-Suhard P., Poliakoff F., Gentit P., 2017a. Transmission tests of '*Candidatus* Liberibacter solanacearum' by carrot seeds. *Acta Horticolturae* 41–46. https://doi.org/10.17660/ActaHortic.2017.1153.7

Loiseau M., Renaudin I., Cousseau-Suhard P., Lucas P.-M., Forveille A., Gentit P., 2017b. Lack of evidence of vertical transmission of '*Candidatus* Liberibacter solanacearum' by carrot seeds suggests that seed is not a major transmission pathway. *Plant Disease* 101: 2104–2109. https://doi.org/10.1094/PDIS-04-17-0531-RE

Mawassi M., Dror O., Bar-Joseph M., Piasezky A., Sjolund J.M., … Bahar O., 2018. '*Candidatus* Liberibacter solanacearum' is Tightly Associated with Carrot Yellows Symptoms in Israel and Transmitted by the Prevalent Psyllid Vector Bactericera trigonica. *Phytopathology* 108(9): 1056–1066. https://doi.org/10.1094/PHYTO-10-17-0348-R

Merfield C., Hampton J., Hill M., Wratten S.,. The effect of seed moisture content and the duration and temperature of hot water treatment on carrot seed viability and the control of *Alternaria radicina*. *Proceedings of the First Scientific Conference of the International Society of Organic Agriculture Research (ISOFAR)*, 2005 Adelaide, Australia.

Monger W.A., Jeffries C.J, 2016. First report of '*Candidatus* Liberibacter solanacearum' in parsley (*Petroseli-*

num crispum) seed. *New Disease Reports* 34: 31. doi: http://dx.doi.org/10.5197/j.2044-0588.2016.034.031

Monger W.A., Jeffries C.J., 2018. A survey of '*Candidatus* Liberibacter solanacearum' in historical seed from collections of carrot and related *Apiaceae* species. *European Journal of Plant Pathology* 150: 803–815. https://doi.org/10.1007/s10658-017-1322-6

Munyaneza J.E., Crosslin J.M., Upton, J.E., 2007. Association of Bactericera cockerelli (Homoptera: Psyllidae) with zebra chip, a new potato disease in southwestern United States and Mexico. *Journal of Economic Entomology* 100(3): 656–663. https://doi.org/10.1603/0022-0493(2007)100[656:aobchp]2.0.co;2

Nakamura H., 1982. Effects of Dry Heat Treatment for Seed Disinfection on Germination in Vegetables. *Japan Agricultural Research Quarterly* 15(4): 243–247.

Nissinen A.I., Haapalainen M., Ojanen H., Pirhonen M., Jauhiainen, L., 2021. Spreading of Trioza apicalis and development of '*Candidatus* Liberibacter solanacearum' infection on carrot in the field conditions. *Annals of Applied Biology* 178(1): 39–50. https://doi.org/10.1111/aab.12644

Oishi M., Hoshino S., Fujiwara Y., Ushiku S., Kobayashi Y., Namba I., 2017. A Comparison of Protocols to Detect Candidatus Liberibacter solanacearum from Carrot Seeds. Research on the Effectiveness of Propidium Monoazide Treatment and Evaluation of Seed Transmission in Carrot. *Research Bulletin of the Plant Protection Service* 53: 111–117. doi: http://www.maff.go.jp/pps/j/guidance/r_bulletin/pdf/rb053_016.pdf

Que F., Hou X. L., Wang G. L., Xu Z. S., Tan,G. F., Xiong A. S., 2019. Advances in research on the carrot, an important root vegetable in the *Apiaceae* family. *Horticulture Research* 6. https://doi.org/10.1038/s41438-019-0150-6

R Core Team, 2021. *R: A language and environment for statistical computing. R Foundation for Statistical Computing*, Vienna, Austria. URL https://www.R-project.org/

Strandberg J.O., White J.M., 1989. Response of carrot seeds to heat treatments. *Journal of the American Society for Horticultural Science* 114(5): 766–769. https://doi.org/10.21273/JASHS.114.5.766

Sumner-Kalkun J.C., Highet F., Arnsdorf Y.M., Back E., Carnegie M., … Kenyon D., 2020. '*Candidatus* Liberibacter solanacearum' distribution and diversity in Scotland and the characterisation of novel haplotypes from *Craspedolepta* spp. (Psyllidae: Aphalaridae). *Scientific Reports* 10: 1–11. https://doi.org/10.1038/s41598-020-73382-9

Wright H.A., 1970. A method to determine heat-caused mortality in bunchgrasses. *Ecology* 51: 582–587. https://doi.org/10.2307/1934038

Zhang X., Wang R., Ning H., Li W., Bai Y., Li, Y., 2020. Evaluation and management of fungal-infected carrot seeds. *Scientific Reports* 10(1): 1–8. https://doi.org/10.1038/s41598-020-67907-5

Phytopathologia Mediterranea
The international journal of the
Mediterranean Phytopathological Union

Firenze University Press
www.fupress.com/pm

60th MPU Anniversary Special Section

Preface

This Special Section of *Phytopathologia Mediterranea* is dedicated to the 60th Anniversary of the foundation of the Mediterranean Phytopathological Union (MPU).

On 7 August, 1962, six Italian researchers, three from the University of Bari and Bologna (Vincenzo Grasso, Gilberto Govi and Antonio Graniti) and three from the Plant Pathology Station of the Ministry of Agriculture in Rome (Anna Saponaro, Anna Luisa Madaluni and Maria Benetti) presented before Alfredo Tassitani Farfaglia, a Notary in Rome, to sign the deed of incorporation of a new Scientific Association, the "Mediterranean Phytopathological Union". The registered location of this Association was the Plant Pathology Station at Via Casal de' Pazzi, n. 280, Rome, Italy. The first appointments in this Society, pending regular elections, were Prof. Cesare Sibilia as President, Jean Barthelet and Umberto Francisco Diaz as Vice Presidents, and Vincenzo Grasso as Secretary-Treasurer.

The MPU was founded as a regional Society of plant pathologists, in response to the invitation of Professor Israel Reichert ("On research and co-operation of Mediterranean Phytopathologists") published in the first issue of *Phytopathologia Mediterranea* (Reichert, 1960).

This journal was devoted to plant diseases in the Mediterranean region with a mission to assist the development of agriculture and agricultural research in the region. It had been founded in 1960 by Prof. A. Ciccarone and Prof. G. Goidanich, and started its work with an Editorial Board from several Mediterranean countries, including: J. Barthelet, C. Catsimbas, H. Dias, A.F. El-Helaly, G. Karel, L. Ling, G. Malençon, I. Reichert, J.R. Sardiña and M. Yossifovitch. As soon as MPU was funded Phytopathologia Mediterranea became the MPU official organ.

Paragraphs 1 and 2, of the Article 1 of the first Statute of the MPU, clearly stated the objectives of this research association, which were:

– to disseminate and increase phytopathological knowledge referring to the Mediterranean region, considered as an ecological unit;
– to establish a meeting point between plant pathologists and those in general who carry out technical activities in the region in phytopathology, so that they can make personal contacts, collaborate with each other and exchange news and information.

With these intentions, the active members of the Association, including Antonio Ciccarone, Gabriele Goidanich from Italy, Jean Barthelet and G. Viennot-Bourgin from France, I. Reichert from Israel, H. Dias and A.L. Branquiñho De Oliveira from Portugal, among many others, aimed to give the MPU high scientific and social values. Activities of the MPU commenced, and continued under guidance of multiple term Presidents including; A. Ciccarone, G. Viennot-Bourgin, A. Graniti, E.C. Tjamos, F. Lamberti, K.M. Makkouk, A. Phillips, A. Logrieco, and presently D. Tsitsigiannis. These people were assisted by Boards and Councils with members from different countries.

Congresses of the MPU have been held in Italy (Bari and Naples) in 1966; France (Montpellier and Avignon) in 1969; Portugal (Oeiras) in 1972; Yugoslavia (Zadar) in 1975; Greece (Patras) in 1980; Egypt (Cairo) in 1984; Spain (Granada) in 1987; Morocco (Agadir) in 1990; Turkey (Kusadasi) in 1994; France (Montpellier) in 1997; Portugal (Evora) in 2001; Greece (Rodos) in 2006; Italy (Rome) in 2010; Turkey (Istanbul) in 2014; in Spain (Cordoba) in 2017, and in Cyprus (Limassol) in 2022.

The MPU Statute is currently being revised to reinforce collaboration with all associations dealing with Plant Pathology. This revision aims to promote and expand the networks of plant and crop protection, and for food safety and environmental sustainability.

The 60th Anniversary of the MPU was celebrated in April 2022, during the 14th MPU Congress in Limassol, Cyprus (AA.VV., 2022). This Special Section of the journal contains four papers from the Congress, including a current topic paper and three reviews. These papers outline modern challenges to plant protection in Mediterranean crops, continuing the long-established traditions of the MPU and *Phytopathologia Mediterranea*.

ISSN 0031-9465 (print) | ISSN 1593-2095 (online) | DOI: 10.36253/phyto-14192

The first of these papers, by Giovani *et al*. (2022) underlines what was a major motivation for establishing *Phytopathologia Mediterranea* in 1960 (Graniti *et al*., 2010) and the MPU in 1962: the need to strengthen plant health research through coordination and collaboration in research, and to maximise outputs from limited research funding. The paper introduces and presents the relevance of the 'Plant health research priorities for the Mediterranean region' initiative.

The second paper, by Velasco-Amo *et al*. (2022),is a review focused on *X. fastidiosa*, a invasive transboundary and emerging plant pathogen, that is ranked as the first priority pest for the Europe Union. The review summarises knowledge on modern detection of *Xylella fastidiosa*, emphasising that surveillance and monitoring are essential for preventing spread of this harmful plant pathogen.

The review by Guarnaccia *et al*. (2022) outlines the spread of wood colonizing pathogens affecting fruit crop trees and other woody hosts in the Mediterranean region. After the increasing importance of grapevine trunk diseases, a topic frequently addressed in *Phytopathologia Mediterranea*, this review summarizes the situation affecting many economically important Mediterranean crops.

The third review paper, by Mellikeche *et al*. (2022), concerns the rapid and efficient diagnosis of decay-inducing pathogens using Loop-mediated isothermal amplification (LAMP) molecular assays. Early detection of these pathogens, that can be performed *in situ*, is essential for food safety and to reduce food waste. The LAMP assay provides a simple way to test products at production sites and borders, thus facilitating rapid treatment decisions to avoid the risk posed by the presence of harmful postharvest pathogens.

The efforts of members of the MPU, including all affiliated national plant pathology and protection organisations and individual researchers, will continue to promote MPU activities and *Phytopathologia Mediterranea*. These will be valuable avenues for knowledge exchange, building open, inclusive and safe environments, and contributing to food safety and security for Mediterranean countries and elsewhere.

Laura Mugnai, Richard Falloon

LITERATURE CITED

AA.VV., 2022. *Abstracts of invited, oral and poster papers given at the 16th Congress of the Mediterranean Phytopathological Union*", April 4–8, 2022, Limassol, Cyprus. *Phytopathologia Mediterranea* 61(1): 181–239. https://doi.org/1036253/phyto-13613

Giovani B., Boutigny A.L., Djelouah K., Fox A., D'Onghia A.M., 2022. Plant Health research collaboration in the Mediterranean region: case studies on citrus tristeza virus, tomato brown rugose fruit virus and *Xylella fastidiosa. Phytopathologia Mediterranea* 61(3): 491–496. https://doi.org/10.36253/phyto-14085

Graniti A., Surico G., Mugnai L., Falloon R., 2010. *Phytopathologia Mediterranea*: 50 years of plant pathology communication for the Mediterranean region. *Phytopathologia Mediterranea* 49(2): 139–142. https://doi.org/10.14601/Phytopathol_Mediterr-8724

Guarnaccia V., Kraus C., Markakis E., Alves A., Armengol J., Eichmeier A., Compant S., Gramaje D., 2022. Fungal trunk diseases of fruit trees in Europe: pathogens, spread and future directions. *Phytopathologia Mediterranea* 61(3): 563–599. https://doi.org/10.36253/phyto-14167

Mellikeche W., Casini G., Ricelli A., Colelli G., Gallo M., D'Onghia A.M., 2022. Detection of post-harvest pathogens by loop-mediated isothermal amplification: a review. *Phytopathologia Mediterranea* 61(3): 533–549. https://doi.org/10.36253/phyto-14093

Reichert I., 1960. On research and co-operation of Mediterranean Phytopathologists. *Phytopathologia Mediterranea* 1(1), 1–4. JSTOR, http://www.jstor.org/stable/42683833

Velasco-Amo M.P., Vicent A., Zarcotejada P.J., Navas-Cortes J.A., Landa B.B., 2022. Recent research accomplishments on early detection of *Xylella fastidiosa* outbreaks in the Mediterranean Basin. *Phytopathologia Mediterranea* 61(3): 549–561. https://doi.org/10.36253/phyto-14171

Phytopathologia Mediterranea
The international journal of the
Mediterranean Phytopathological Union

Firenze University Press
www.fupress.com/pm

60th MPU Anniversary Special Section - Current topics

Plant Health research collaboration in the Mediterranean region: case studies on citrus tristeza virus, tomato brown rugose fruit virus and *Xylella fastidiosa*

Baldissera GIOVANI[1,*], Anne-Laure BOUTIGNY[2], Khaled DJELOUAH[3], Adrian FOX[4], Anna Maria D'ONGHIA[3]

[1] *Euphresco network for phytosanitary research coordination and funding, France*
[2] *French Agency for Food, Environmental and Occupational Health and Safety, France*
[3] *International Centre for Advanced Mediterranean Agronomic Studies of Bari, Italy*
[4] *Fera Science Limited, United Kingdom*
*Corresponding author. E-mail: bgiovani@euphresco.net

Summary. Strengthening Plant Health research is a major challenge for Mediterranean countries. The diversity and fragmentation of the research landscape in this region have weakened the impacts of national efforts. Mediterranean countries can benefit from coordination of research activities to increase efficiency and impacts. The initiative 'Plant health research priorities for the Mediterranean region', led by the International Centre for Advanced Mediterranean Agronomic Studies (CIHEAM Bari)[1] and the Euphresco network for phytosanitary research coordination and funding[2] can promote convergence of national programmes and optimize the use of the scarce funding available to plant health, thus strengthening international cooperation and increasing the excellence and relevance of research.

Keywords. Research coordination, international collaboration, science diplomacy.

OPEN ACCESS

Citation: B. Giovani, A.-L. Boutigny, K. Djelouah, A. Fox, A.M. D'Onghia (2022) Plant Health research collaboration in the Mediterranean region: case studies on citrus tristeza virus, tomato brown rugose fruit virus and *Xylella fastidiosa*. *Phytopathologia Mediterranea* 61(3): 525-530. doi: 10.36253/phyto-14085

Accepted: December 14, 2022

Published: January 13, 2023

Data Availability Statement: All relevant data are within the paper and its Supporting Information files.

Competing Interests: The Author(s) declare(s) no conflict of interest.

Editor: Giuseppe Surico, University of Florence, Italy.

ORCID:
BG: 0000-0001-9217-3555
A-LB: 0000-0001-8999-2314
KD: 0000-0002-4806-122X
AF: 0000-0003-1280-1836
AMD'O: 0000-0002-1817-4637

INTRODUCTION

Approximately 25,000 plant species inhabit the Mediterranean region, and of these 13,000 are endemic. The region has been recognised as a biodiversity hotspot that is suffering unprecedented loss of habitat (Myers *et al*., 2000).

[1] CIHEAM Bari, International Center for Advanced Mediterranean Agronomic Studies, (https://www.iamb.it/), is an intergovernmental organization for high education, applied scientific research and planning of partnership actions in the field of research and international cooperation in the Mediterranean region.

[2] Euphresco, Network for phytosanitary research coordination and funding (https://www.euphresco.net/), is an international network of research programme owners, programme managers, policy makers, regulators and research and educational organizations from ca. 60 countries in 5 continents.

Mediterranean agriculture, forests and other environments are threatened by numerous quarantine and emerging pests. The negative impacts of these organisms have increased due to global trade and climate change that favour their movement over long distances and facilitate their survival in previously unfavourable environments. The EU Farm to Fork strategy, with its target to reduce by 50% the use and risk of chemical and hazardous pesticides by 2030, and the rise of biological crop products market, have also reduced the availability (if any) of control measures for some quarantine or emerging pathogens. In the face of these challenges, the Mediterranean region is particularly vulnerable.

The political and cultural diversity that are a characteristic of the Mediterranean region are its strength and its weakness. Diversity creates fragmentation, is an obstacle to collaboration, and reduces opportunities for concerted actions, which can result in individual countries having to deal alone with problems. The International Centre for Advanced Mediterranean Agronomic Studies of Bari (CIHEAM Bari) and the Euphresco network for phytosanitary research coordination and funding joined forces in 2016 to help Mediterranean countries to rethink organization of research activities and their coordination, to increase the efficiency and impacts of national efforts.

The benefits of research coordination and international collaboration are diverse. Identifying research priorities (important pests, infrastructure and capabilities) at the supra-national level will enhance convergence of national and regional programmes and will allow research funders to take advantage of the optimization of the scarce funds dedicated to plant health. Regulators will benefit from reinforced links with research funders and researchers, and from research support for policy development. Scientists will benefit from international knowledge exchange projects, from opportunities for enhancing their science capability and from increased relevance and visibility of plant health (research) activities.

THE CIHEAM BARI AND EUPHRESCO INITIATIVE

The approach followed by the CIHEAM Bari and Euphresco to identify the plant health research priorities for the Mediterranean region merged research experience and national guidance. A survey collected opinions of national experts from Mediterranean countries. The survey resulted in lists of pests, research priorities, infrastructures and research capacity that are considered important for the region. The priorities from the survey were refined and complemented by taking into account the short- and medium-term (up to 5 years) national research programmes, which provided information on the more urgent research topics planned for funding in each country. The views of national regulators provided additional guidance for selecting the most relevant priorities (Table 1).

Table 1. Priority pests for the Mediterranean region, identified through a survey.

Selected pests (in alphabetical order)
Anoplophora chinensis
Bursaphelenchus xylophilus
'*Candidatus* Liberibacter africanus'
'*Candidatus* Liberibacter americanus'
'Candidatus Liberibacter asiaticus'
'*Candidatus* Liberibacter solanacearum'
Citrus tristeza virus
Drosophila suzukii
Erwinia amylovora
Fusarium oxysporum f.sp. *albedinis*
Phyllosticta citricarpa
Plum pox virus
Rhynchophorus ferrugineus
Spodoptera frugiperda
Tomato brown rugose fruit virus
Xylella fastidiosa

Workshops and consultations were organised to involve and seek the endorsement of high-level representatives from Mediterranean countries, international organizations, and initiatives, that represent research funders, policy makers and research organizations in the Mediterranean region, including the Arab Society for Plant Protection (ASPP)[3] and the Mediterranean Phytopathological Union (MPU)[4] (D'Onghia *et al*., 2022; Giovani *et al*., 2022). Given the large number of priorities and the limited human and financial resources available, it was agreed that the research effort would focus on a small number of research topics. These shortlisted topics were those that received the largest number of expressions of interest from organizations in the four Mediterranean regions of Balkan-Mediterranean, Eastern Mediterranean, Maghreb, and Western Mediterranean. The three projects are outlined below.

[3] ASPP, Arab Society for Plant Protection (https://www.arabspp.org/), is an organization of scientists from public and private academic institutions and from industry that promotes research, education, and extension activities related to pests in Arab speaking countries

[4] MPU, Mediterranean Phytopathological Union (http://www.mpunion.eu/), is a regional not-for-profit organization that aims to advance and disseminate knowledge on phytopathology and closely related fields relevant to Mediterranean agro-ecological regions, and to establish and foster research relationships among scientific societies, academia, scientists and stakeholders

Rapid and efficient detection and identification of citrus tristeza virus (CTV) isolates that induce severe symptoms on Citrus

This research initiative aims to simplify the diagnosis of CTV isolates that cause severe symptoms on *Citrus*. To date, six major CTV phylogenetic groups have been described, including: T36 (Karasev *et al*., 1995), T3 (Hilf and Garnsey, 2002), VT (Mawassi *et al*., 1996), T68 (Harper, 2013), T30 (Albiach-Marti *et al*., 2000), and RB (Harper *et al*., 2010). These groups are mainly based on their genomic features. Virus genotype variation may occur after the passage through different hosts and CTV genotype populations may influence the success of virus transmission by the vector *Aphis gossypii* (Camps *et al*., 2022). Some of CTV genotypes are known to cause severe symptoms in *Citrus* orchards and have restricted distribution in the EPPO region. As molecular tests alone are of limited value for the prediction of pathogenic properties of CTV isolates (Bar-Joseph *et al*., 2010; Harper, 2010), the diagnosis of CTV isolates that induce severe symptoms on *Citrus* has been classically performed using a combination of molecular, serological and/or biological tests. This protocol is lengthy and difficult to perform. Moreover, the monoclonal antibodies MCA13 (Permar *et al*., 1990) used to diagnose CTV isolates that cause severe symptoms are no longer commercially available, which negatively impacts the diagnostic protocol currently in use. During this project, information on the diagnostic molecular tests available or in development will be collected, and plant material from the field (infected, healthy, symptomatic, asymptomatic) will be sampled, following a common methodology for monitoring. In addition, relevant plant material from reference CTV collections will also be collected. The CTV isolates will be molecularly characterized, and sequence data will be used to design the primers and the probes. A test performance study will be organized to validate the tests available or in development, and the test developed in the framework of the project. Several countries have expressed interest in participating in the project, including Australia, Austria, Croatia, Egypt, France, Greece, Israel, Italy, Morocco, Palestine, Portugal, Spain, Switzerland, and Tunisia.

Insights into the biology of tomato brown rugose fruit virus: virus survival in soil

Tomato brown rugose fruit virus has rapidly emerged from initial outbreaks in Jordan and Israel (Salem *et al*., 2016; Luria *et al*., 2017), and has now been reported from multiple countries across the Northern Hemisphere (EPPO, 2022). The virus particles are stable and can survive for months outside hosts on inert and biological surfaces as well as in nutrient film solutions and soil, without losing their virulence (Skelton *et al*., 2021). Studies on the survival of this virus have been ongoing in Israel (Dombrovsky *et al*., 2022), but additional information is required, including effects of soil type, environmental conditions, crops cultivated and the management practices. The project aims to develop new knowledge on survival of the virus in soil in different agro-ecological and pedoclimatic conditions. Survival during composting for bioremediation will also be considered within the project. Tests will be validated for the diagnosis of the Tobamovirus in soil and compost (including eDNA approaches), considering approaches to confirm infectivity of detected viral nucleic acids. These data will support development of guidelines for management of the virus. Several countries have expressed interest to participate in the project, including Australia, Austria, Chile, Germany, United Kingdom, Ireland, Israel, Italy, the Netherlands, New Zealand, Palestine, Russia, Slovenia, Switzerland, and Turkey.

Diagnosis of Xylella fastidiosa*: detection on dormant plant species which are important for Mediterranean countries*

Several research projects on *Xylella fastidiosa* have been commissioned since 2015, by national and regional funders in Europe. This has allowed development of knowledge on the bacterium, which has been useful for developing guidelines for sampling and diagnostics. Hopkins (1981) concluded that sampling should be performed during the period of active plant growth to maximize the likelihood of detection. However, recent experiments have shown that in Mediterranean countries, *X. fastidiosa* can be detected in plants (such as olive, almond and cherry) throughout the year, and especially during the asymptomatic phases or host dormancy, the period with the lowest bacterial concentrations (D'Onghia *et al*., 2022). The Euphresco project aims to evaluate the distribution dynamics of *X. fastidiosa* within dormant Mediterranean plant species and matrices that are commercially important throughout the year and during dormancy on woody host stems. During the project, samples from dormant Mediterranean plant species that are hosts of *X. fastidiosa* will be collected. An inventory will be made of tests (sampling, DNA extraction, diagnostic tests) used by different laboratories to detect *X. fastidiosa* in dormant plants. Selected tests will be validated on spiked and naturally infected host samples at low bacterial concentrations. Distribution dynamics of the pathogen within natu-

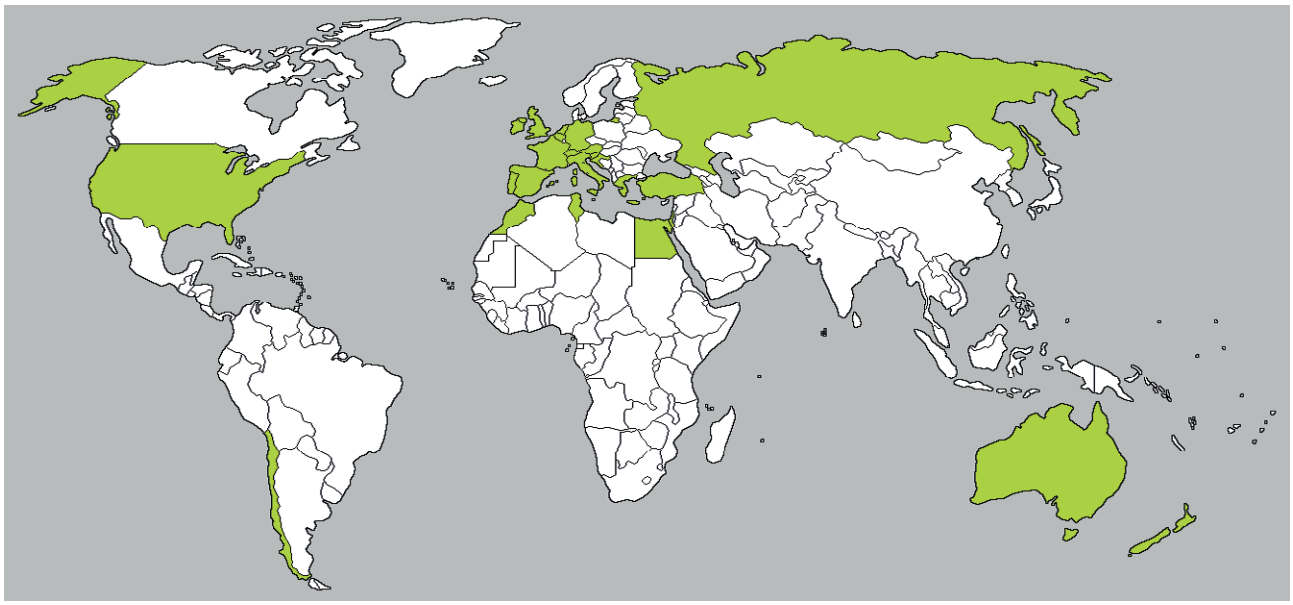

Figure 1. Countries that have expressed interest to participate in at least one of the research projects commissioned through Euphresco on research priorities for the Mediterranean region.

rally infected woody stems will be assessed throughout the year (including during dormancy), if plant material is available. Several countries have expressed interest to participate in the project, including Australia, Belgium, Egypt, France, United Kingdom, Israel, Ireland, Italy, Morocco, the Netherlands, Slovenia, Spain, Switzerland and Turkey.

GEOGRAPHIC EXTENT OF THE PROJECTS

The geographic coverage of the three research consortia is presented in Figure 1.

CONCLUSIONS

The Strategic Framework 2020–2030 of the International Plant Protection Convention (IPPC)[5], adopted at the 15th Session of the Commission on Phytosanitary Measures (CPM-15) in April 2021, includes global phytosanitary research coordination as one of the eight development agenda items to be addressed by the global Plant Health community over the current decade. Euphresco and CIHEAM Bari have concluded that the inclusive and participatory approach used to strengthen plant health research coordination and transnational collaboration for the Mediterranean region can be used for other regions, and also for global research coordination. Regional consultations may be part of processes that will allow transition from local needs (e.g., reduction of particular pests) to shared global priorities (e.g., prevention of pest spread). Opportunities will be created for scientific communities from less research-intense countries to reduce their isolation and increase their international exposure. In this context, involvement is essential of organizations and initiatives that are deeply rooted locally and that have leading regional roles. A workshop was organized by Euphresco, Better Border Biosecurity (B3; New Zealand) and the Plant Biosecurity Research Initiative (Australia), and was held on the 20th of September, 2022 in London. This workshop gathered representatives from the Australian Centre for International Agricultural Research (ACIAR), the Centre for Agriculture and Biosciences International (CABI), CIHEAM Bari, the Department for Environment, Food and Rural Affairs (Defra), the Consultative Group on International Agricultural Research (CGIAR), and the National Institute for Agricultural Research and Food Technology, National Research Council (INIA-CSIC). The workshop participants discussed the structures, operations and resources for international research coordination. This started from the models developed in the framework of ongoing Euphresco

[5] The IPPC, International Plant Protection Convention (https://www.ippc.int/en/), is an intergovernmental treaty signed by over 180 countries worldwide that aims to protect the world's plant resources from the spread and introduction of pests, and to promote safer trade.

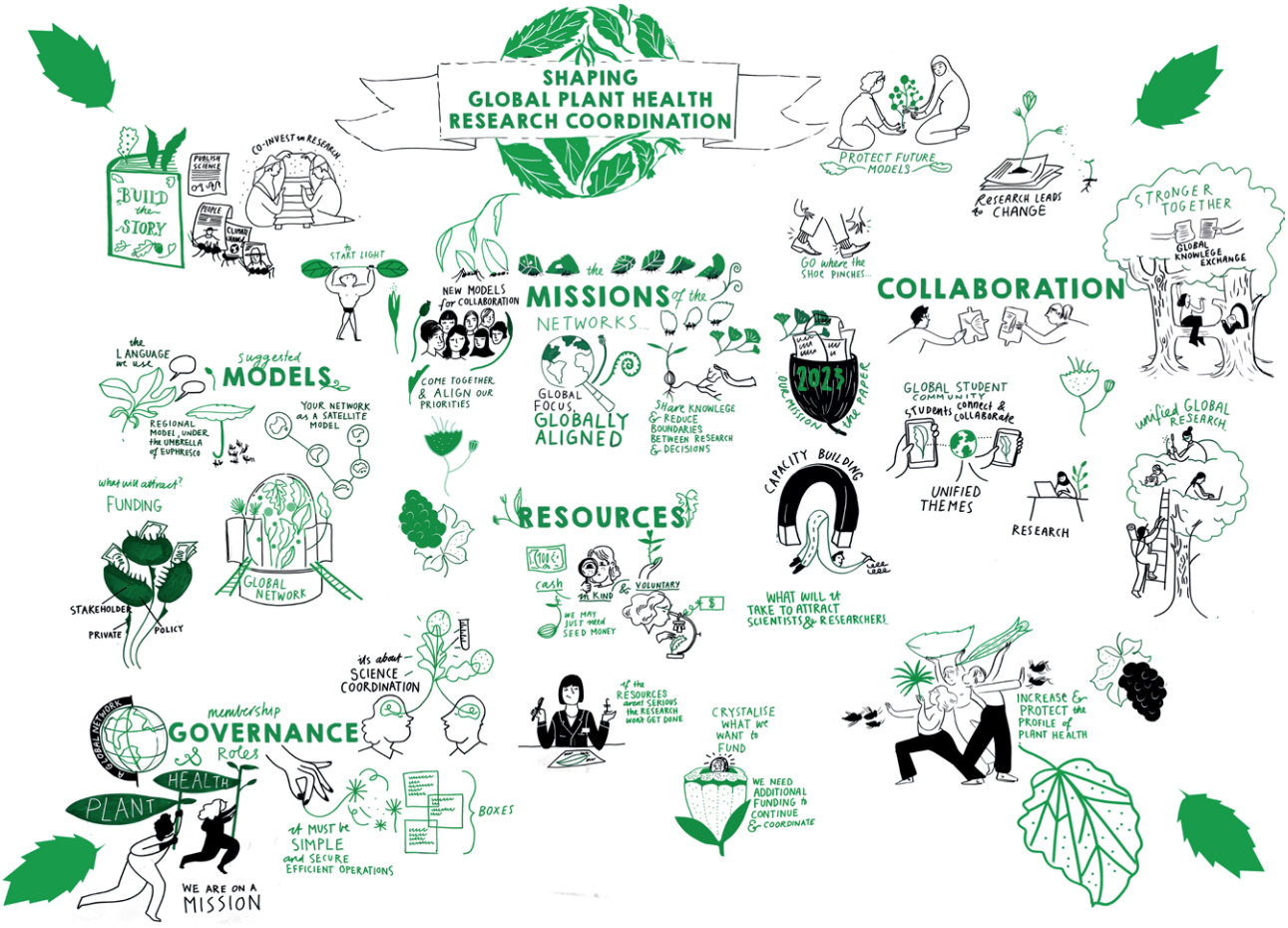

Figure 2. Transcription and illustration (by Josephine Ford) of the main topics discussed during the Euphresco B3 PBRI workshop, held in London (United Kingdom), on 20 September, 2022.

activities, taking into account the specificities of other international initiatives and organizations (Figure 2). Work will continue throughout 2023, with contributions from policy makers, research funders and research organizations that operate in plant health and are interested in joining this initiative.

LITERATURE CITED

Albiach-Marti M.R., Mawassi M., Gowda S., Satyanarayana T., Hilf M.E., Shanker S., … Dawson W.O., 2000. Sequences of Citrus tristeza virus separated in time and space are essentially identical. *Journal of Virology* 74: 6856–6865.

Bar-Joseph M., Batuman O., Roistacher C. 2010. The history of Citrus tristeza virus—Revisited. In: Karasev AV and Hilf ME (eds.). *Citrus Tristeza Virus Complex and Tristeza Diseases*. APS Press, St Paul, MN, USA, 3–26.

Camps R., Fiore N., Riquelme N., Barros-Parada W., Besoain X., 2022. Genotype variation of citrus tristeza virus after passage on different hosts, and changes in the virus genotype populations by the vector Aphis gossypii. *Phytopathologia Mediterranea* 61(1): 55–63. https://doi.org/10.36253/phyto-12965

Dombrovsky A., Mor N., Gantz S., Lachman O., Smith E., 2022. Disinfection efficacy of Tobamovirus-contaminated soil in greenhouse-grown crops. *Horticulturae* 8(7): 563.

D'Onghia A.M., 2022. CIHEAM policy in plant health to enhance food security in the Mediterranean region. In: Abstracts of invited, oral and poster papers presented at the 16th Congress of the Mediterranean Phytopathological Union, April 4–8, 2022, Limassol, Cyprus. *Phytopathologia Mediterranea* 61(1): 181–239. https://doi.org/1036253/phyto-13613

D'Onghia A.M., Santoro F., Minutillo S.A., Frasheri D., Gallo M., … Valentini F., 2022. Optimisation of

sampling and testing for asymptomatic olive trees infected by *Xylella fastidiosa* in Apulia region, Italy. *Phytopathologia Mediterranea* 61(3): 439–449. doi: 10.36253/phyto-13732

EPPO (2022). EPPO Global Database https://gd.eppo.int/taxon/TOBRFV [accessed on 2022-11-28].

Harper S.J., Dawson T.E., Pearson M.N., 2010. Isolates of Citrus tristeza virus that overcome *Poncirus trifoliata* resistance comprise a novel strain. *Archives of Virology* 155: 471–480.

Harper S.J., 2013. Citrus tristeza virus: evolution of complex and varied genotypic groups. *Frontiers in Microbiology* 93: 1–18.

Hilf M.E., Garnsey S.M., 2002. Citrus tristeza virus in Florida: a synthesis of historical and contemporary biological, serological, and genetic Data. In *Proceedings 15th International Conference of the Organization of Citrus Virologists*: 13–20. https://escholarship.org/uc/item/0v8463sn [accessed on 2022-11-28].

Hopkins DL, 1981. Seasonal concentration of pierce's disease bacterium in grapevine stems, petioles, and leaf veins. *The American Phytopathological Society* 71: 415–418.

Karasev A.V., Boyko V.P., Gowda S., Nikolaeva O.V., Hilf M.E. … Dawson W.O., 1995. Complete sequence of the Citrus tristeza virus RNA genome. *Virology* 208: 511–520.

Luria N., Smith E., Reingold V., Bekelman I., Lapidot M. … Ezra N., 2017. A new Israeli Tobamovirus isolate infects tomato plants harboring Tm-22 resistance genes. *PloS one* 12(1): p.e0170429.

Mawassi M., Mietkiewska E., Gofman R., Yang G., Bar J.M., 1996. Unusual sequence relationships between two isolates of citrus tristeza virus. *Journal of General Virology* 77: 2359–2364.

Myers N., Mittermeier R.A., Mittermeier C.G., da Fonseca G.A., Kent J., 2000. Biodiversity hotspots for conservation priorities. *Nature* 403(6772): 853–858.

Permar T.A., Garnsey S.M., Gumpf D.J., Lee R., 1990. A monoclonal antibody that discriminates strains of Citrus tristeza virus. *Phytopathology* 80: 224–228.

Salem N., Mansour A., Ciuffo M., Falk B.W., Turina M., 2016. A new Tobamovirus infecting tomato crops in Jordan. *Archives of Virology* 161(2): 503–506.

Skelton A., Frew L., Buxton-Kirk A., Ward R., Forde S. … Fox A., 2021. Tomato brown rugose fruit virus: survival of the virus and efficacy of disinfection approaches. Final report of the research project PE033a 'ToBRFV: survival of the virus and efficacy of disinfection approaches, accessible from https://projectbluearchive.blob.core.windows.net/media/Default/Research%20Papers/Horticulture/PE%20033a_Report_Final_2021.pdf [accessed on 2022-11-28].

Phytopathologia Mediterranea
The international journal of the
Mediterranean Phytopathological Union

Firenze University Press
www.fupress.com/pm

60th MPU Anniversary Special Section - Review

Detection of post-harvest pathogens by loop-mediated isothermal amplification: a review

Wanissa MELLIKECHE[1], Giulia CASINI[2], Alessandra RICELLI[3,*], Giancarlo COLELLI[1], Marilita GALLO[4], Anna Maria D'ONGHIA[4]

[1] *Dipartimento di Scienze Agrarie, degli Alimenti e dell'Ambiente, Università di Foggia, Via Napoli 25, 71122 Foggia, Italy*
[2] *Enbiotech S.r.l., Via Quarto dei Mille, 6, 90129 Palermo, Italy*
[3] *Istituto di Biologia e Patologia Molecolari (IBPM-CNR) P.le A. Moro 5, 00185, Roma, Italy*
[4] *Centre International de Hautes Etudes Agronomiques Méditerranéennes Bari (CIHEAM Bari), Via Ceglie 9, 70010 Valenzano, Bari, Italy*
*Corresponding author. E-mail: alessandra.ricelli@cnr.it

Summary. Postharvest losses, which occur between harvest and consumption of agricultural commodities, are major causes of food waste. Minimizing food loss helps provide nutritious food for animals and humans, and alleviate adverse environmental effects on food production. These losses are often related to the presence of postharvest pathogens, including fungi and bacteria, which typically start by infecting crops in the field as well as during postharvest chain. Control of these pathogens relies on development of tools that ensure their early and accurate detection. Among these is loop-mediated isothermal amplification (LAMP), a molecular method for pathogen detection. LAMP characteristics of rapidity, specificity and simplicity have encouraged development of a number of LAMP assays for detection of postharvest pathogens. Each LAMP assay allows to detect a specific genetic region of the target microorganism, which can be directly related to mycotoxin production, fungicide resistance and phytotoxicity. The LAMP amplicons are rapidly visualized, either at a specific timepoint, or in real-time by taking measurements throughout reaction, thereby necessitating less sophisticated facilities than those needed for PCR assays. In addition, many studies have developed simple protocols for the direct detection of pathogens on fresh produce. This paper explains the LAMP reaction, and its importance for postharvest detection of fungi and bacteria. Previous studies that have developed LAMP assays are also discussed.

Keywords. Food losses, microorganism contamination, mycotoxins, LAMP.

OPEN ACCESS

Citation: W. Mellikeche, G. Casini, A. Ricelli, G. Colelli, M. Gallo, A.M. D'Onghia (2022) Detection of post-harvest pathogens by loop-mediated isothermal amplification: a review. *Phytopathologia Mediterranea* 61(3): 531-547. doi: 10.36253/phyto-14093

Accepted: December 28, 2022

Published: January 13, 2023

Data Availability Statement: All relevant data are within the paper and its Supporting Information files.

Competing Interests: The Author(s) declare(s) no conflict of interest.

Editor: Lluís Palou, Valencian Institute for Agricultural Research, Valencia, Spain.

ORCID:
WM: 0000-0001-6383-4094
GC: 0000-0001-7224-7158
AR: 0000-0002-1151-6120
GCo: 0000-0001-8619-3541
MG: 0000-0003-4981-485X
MD'O: 0000-0002-1817-4637

INTRODUCTION

Human population growth has created major concerns about food security. By 2050, global food production will have to increase by an estimated 70% to adequately feed humans and avoid an unprecedented food crisis (Mvumi and Stathers, 2015). Although intensifying food production seems an obvious solution, this is unpractical due to the challenges of cli-

mate change and the role of intensive agriculture in their escalation (Giovani *et al.,* 2022). A good way to improve this situation while protecting the environment would be to reduce the important amounts of wasted commodities (Parfitt *et al.*, 2010). Approximately one-third of all food produced for human consumption is lost or wasted along supply chains (FAO, 2011), thereby rendering postharvest food losses a leading cause of food insecurity. These losses occur between harvest and consumption, at rates of 20% to 50% in developing countries and 5% to 25% in developed ones, depending on product type, cultivar, environmental factors, and postharvest conditions (Kader, 2003; Yahia *et al.*, 2019). Presence of postharvest pathogens on produce, whether in the field or during product handling, are major factors in product commodity deterioration. For each fruit or vegetable species, pathogenic bacteria, fungi and yeasts can cause many postharvest diseases (Antunes and Cavaco, 2010). Several bacterial pathogens such as *Bacillus, Pseudomonas, Pectobacterium* and *Xanthomonas* can cause important losses in the field and postharvest. Nevertheless, fungi are considered the most important degrading agents that affect foods during storage, making the food products unfit for human consumption by decreasing their nutritive value. Many of these pathogens are also able to produce carcinogenic mycotoxins. The health hazards posed by these compounds for humans have led most countries to issue regulations of their consumption, which target the mycotoxins or, in some cases, the toxigenic agent (Wenderoth *et al.,* 2019). In addition, agricultural exports are subjected to maximum tolerated mycotoxin levels. In some cases, these have reshaped the trade patterns of economically important crops (Bui-Klimke *et al.*, 2014).

For a long time, synthetic fungicides were the primary means of controlling postharvest decays (Spadaro and Gullino, 2005). However, their use has decreased due to their potentially hazardous effects on human health and environments, as well as the development of fungicide-resistant strains of postharvest pathogens (Baibacova *et al.*, 2019). These factors have restricted the approval of many products and motivated researchers to find alternative ways to control postharvest pathogens. Consequently, new technologies, substances and practices have emerged for fresh produce storage which target these pathogens, to preserve agricultural products and extend their shelf-lives (Tripathi and Dubey, 2004).

Most postharvest pathogens start infection processes in the field and often remain latent in fresh produce before causing serious damage during storage (Suarez *et al.*, 2005; Wenneker and Thomma, 2020). Many farmers therefore apply treatments on their crops to avoid these contaminations. However, in some cases, these treatments may be unnecessary since they are applied without accurate verification of the presence of pathogens. This random decision-making contradicts the principles of precision agriculture, and can have severe effects on the environment. Furthermore, they are often costly. Successful treatment depends on early detection and accurate identification of spoilage agents. This relies on several methods, traditionally including morphological characterization after growth on agar media (Samson *et al.*, 2007). However, these methods are time-consuming and require laboratory facilities and mycological expertise (Luo *et al.*, 2012).

Molecular methods such as PCR and real-time PCR are more rapid, sensitive and specific than culturing techniques (Schaad *et al.*, 2002; Rodríguez *et al.*, 2012). They can be used to identify mycotoxigenic strains by targeting the genes linked to toxin production (Stakheev *et al.*, 2011). However, they are costly and require suitably trained personnel and well equipped laboratories. As an alternative technology, Loop-mediated isothermal AMPlification (LAMP) reaction was described as a specific, rapid, cost-effective, and easy-to-use method by Notomi *et al.* (2000). This method uses four to six primers from the target region of each organism which is amplified at a fixed temperature. The high levels of specificity and sensitivity obtained with LAMP, coupled with its robustness to inhibition substances and its user-friendliness, have encouraged researchers to improve this method by developing real-time way to visualize the amplification products such as real-time LAMP. This method is largely used for the detection of several pathogens in preharvest among viruses (Bhat *et al.*, 2022), fungi (Abderraouf *et al.*, 2022) and bacteria (Yaseen *et al.*, 2015; Valentini *et al.*, 2022). Previous studies that developed specific LAMP primer sets for the identification of postharvest pathogens also assessed the possibility to apply LAMP-based assays to rapidly detect pathogens directly from infected commodities (Niessen *et al.*, 2018). In these protocols, simplicity is often researched throughout all the steps of the analysis, from the nucleic acid extraction to the amplification and detection of results. This paper reviews these studies and offers insights on LAMP and its potential effects on the management of postharvest pathogens.

POSTHARVEST PATHOGENS

Plant protection for economically important species is based on two essential pillars: the first is protection of plants throughout production stages to maximize yields by avoiding losses due to pest attacks; the second is pro-

tection of agricultural produce after their harvest to preserve food security and reduce waste due to postharvest pathogens. It is estimated that, in some cases, postharvest losses can be up to 50% of potential production (Kasso and Bekele, 2018; Kader, 2003; Yahia *et al.*, 2019). This can especially be the case when postharvest management lacks advanced technologies, such as continuous cold storage (Kitinoja *et al.*, 2019). Harvesting is the detachment of product from living plants, which renders products vulnerable to opportunistic spoilage agents that enter through wounds caused by agricultural practices, feeding animals, or the handling processes. These agents, such as *Ralstonia solanacearum* (Lemma *et al.*, 2014), *Erwinia carotovora* (Zhao *et al.*, 2013) and *Botrytis cinerea* (Suarez *et al.*, 2005), are often encountered in the field, and many can also cause damage at preharvest stages.

Several taxonomic groups of pathogens can cause postharvest infections. These include bacteria, yeasts and filamentous fungi. The most important filamentous fungi are species of *Alternaria, Aspergillus, Botrytis, Fusarium, Geotrichum, Gloeosporium, Monilinia, Penicillium, Mucor* and *Rhizopus* (Barkai-Golan, 2001). These are responsible for decay of agricultural commodities, they break barriers that would otherwise protect against other microorganisms such as bacteria and human pathogens, and many produce mycotoxins (Dukare *et al.*, 2019). Mycotoxins are secondary metabolites that can be highly toxic and carcinogenic, mutagenic and teratogenic to humans and animals (Omotayo *et al.*, 2019). They are mainly produced by species of *Aspergillus*, *Penicillium*, *Fusarium* and *Alternaria* (Table 1). Due to the hazardous effects of these fungi, many countries have issued regulations to control the importation of mycotoxin-susceptible commodities (van Egmond *et al.*, 2007). In some cases, the costs imposed by these regulations have caused important economic losses to exporting countries. For example, in 1997, the EU banned pistachio nut imports from Iran due to high aflatoxin levels. This decision shifted the trade patterns when the United States of America became the main exporter of this crop to countries with strict aflatoxin tolerance regulations (Bui-Klimke *et al.*, 2014).

DETECTION METHODS FOR POSTHARVEST PATHOGENS

Successful management of postharvest pathogens is directly related to their early and accurate detection. Therefore, many detection methods have been developed and improved. These methods can be either microbiological, serological or molecular.

Table 1. The most important postharvest pathogens, the symptoms they cause, and the main mycotoxins they produce.

Pathogen group	Main species	Symptom	Main mycotoxins	Reference
Aspergillus section *flavi*	*A. flavus* *A. parasiticus*	Green mold	Aflatoxins	Varga *et al.*, 2011
Aspergillus section *nigri*	*A. carbonarius* *A. niger*	Black mold	Ochratoxin A Fumonisin B_2	Astoreca *et al.*, 2010 Palumbo *et al.*, 2011
Penicillium	*P. verrucosum* *P. expansum* *P. italicum*	Blue mold	Ochratoxin A Patulin	Perrone and Susca, 2017
Alternaria	*A. alternata*	Black spots	Alternariol Tenuazonic acid Altertoxins I, II, III	Ostry, 2008
Fusarium	*F. verticillioides* *F. moniliforme* *F. graminearum*	Dark to brown rot	Fumonisin	Duvick *et al.*, 2001
Colletotrichum	*C. acutatum* *C. gloeosporioides* *C. boninense*	Anthracnose	—	Shi *et al.*, 2020a
Geotrichum	*G. candidum*	Sour rot	—	Talibi *et al.*, 2012
Botrytis	*B. cinerea*	Gray mold	—	
Monilinia	*M. fructicola* *M. laxa* *M. fructigena*	Brown rot on stone fruit	—	Côté *et al.*, 2004
Rhizopus	*R. microsporus* *R. stolonifer*	Rhizopus rot, Black bread mold	Rhizonin	Partida-Martinez *et al.*, 2007

Microbiological methods

Microbiological methods are the traditional ways of identifying and differentiating postharvest pathogens. They are based on pathogen cultivation on agar media followed by the observation of microorganism macro and micro-morphological characteristics (Klich and Pitt, 1988). Microbial growth manifests differently depending on the medium and environmental conditions (Cotty, 1994). In addition, some media are selective or semi-selective, encouraging growth and/or sporulation of particular fungus species while preventing development of others. For example, Samson *et al.* (2007) described the boscalid MEA medium, which only allowed the sporulation of *Aspergillus carbonarius* amongst all other black aspergilli. Other media, such as coconut cream agar (CCA) (Dyer and McCammon, 1994) and *A. flavus* and *A. parasiticus* agar (AFPA) (Pitt *et al.*, 1983) are particularly suitable for the growth of toxigenic strains.

Although these methods have played important roles in improving microbiological analyses, they are inadequate for current challenges, even though they are still needed if the pathogen is new and other kind of methods are still not available. They are time-consuming and require high levels of laboratory expertise and mycological knowledge in order to provide accurate diagnoses. Furthermore, these methods cannot be applied for every species and strain, and their results are strictly dependent on appropriate incubation conditions (Balajee *et al.*, 2007a; b). These methods also do not ensure high sensitivity due to low survival of fungal propagules under stressful conditions of selective and semi-selective media (Beuchat, 1993).

Serological methods

Serological diagnostic methods, such as Enzyme-Linked Immunosorbent Assay (ELISA), are based on detection of antibodies against pathogens and constitute a group of sensitive, rapid, specific and cost-effective tests (Clarck *et al.*, 1986). ELISA targets specific proteins based on the interaction between antigens specific to each pathogen, and their specific antibodies (Crowther, 1995). ELISA methods have been widely used to detect plant pathogens (Le and Vu, 2017), and were tested for the detection of pathogens in food products (Tsai and Cousin, 1990). Some researchers were interested in using ELISA for postharvest analyses, such as in the quantification of *B. cinerea* (Fernàndez-Baldo *et al.*, 2011) and for the detection of mycotoxins (Pei *et al.*, 2009). As field test, the lateral flow assay is applied for the rapid, equipment-free detection of different pathogens, e.g., *Phytophthora* spp. (Lane *et al.*, 2007). Nevertheless, sensitivity of these methods remains low compared to molecular methods, which are the most trusted tools for pathogen identification.

Molecular methods

Molecular methods are based on detection and amplification of target sequences from reference genes in pathogen nucleic acids. Therefore, they are used for species and strain differentiation and in phylogenic studies (Luo *et al.*, 2012). Among these methods, PCR is most commonly used. It amplifies target regions using polymerase and two specific primers throughout a series of repeated thermal cycles. PCR-based methods (PCR, real-time PCR, qPCR, multiplex qPCR) are powerful tools that provide high levels of specificity and sensitivity for detection of postharvest pathogens (Suarez *et al.*, 2005; Samson *et al.*, 2007). These methods have also been applied for amplification of genes relevant to mycotoxin biosynthesis (Shapira *et al.*, 1996) which, in some cases, can also be involved in pathogenicity (Sanzani *et al.*, 2012). However, PCR-based methods are costly due to the necessity for expensive reagents and high technology equipment such as thermocyclers. They also require advanced laboratory training and long DNA or RNA clean-up steps before amplification procedures. Therefore, these methods do not detect contaminants *in situ*. As an alternative molecular technology, LAMP was described by Notomi *et al.* (2000) as a specific, rapid, cost-effective, and easy-to-use method.

LAMP

LAMP is a molecular detection technique that amplifies DNA or RNA fragments using a strand displacing DNA polymerase (usually the Bst DNA polymerase from *Bacillus stearothermophilus*). This allows production of high amounts of DNA in a short time (Luo *et al.*, 2014). LAMP works under isothermal conditions (operating at a constant temperature), and can be highly specific since it uses four to six primers able to hybridize from six to eight regions of the target sequence. Usually, this technique requires no post-reaction processing because results can be quickly observed using indicators. Consequently, it can speed up the diagnostic process in comparison to a PCR-based method. LAMP is also highly tolerant to sample inhibitors, allowing it to be used directly on crude DNA extracted from infected or infested commodities (King *et al.*, 2019).

LAMP primer design

The most popular softwares to design LAMP primers are: Primer Explorer, a free, online tool with five versions released to date (the latest version is available at https://primerexplorer.jp/e/), OptiGene Limited (Horsham, UK) using Genie platforms, and "LAMP Designer" by PREMIER Biosoft (USA) (Le and Vu, 2017). While taking into consideration the four key factors in LAMP primer design (melting temperature, stability at the end of each primer, GC content, and secondary structure), these tools facilitate the design of the following primers (Figure 1): Forward inner primer (FIP), which consists of an F2 region complementary to the F2c region at the 3' end of the target sequence; whereas at the 5' end, it consists of an F1c region identical to the F1 region of the target sequence. Forward outer primer (F3), which is complementary to the F3c region of the target sequence. Backward inner primer (BIP), which consists of a B2 region complementary to the B2c region at 3' end of the target sequence; whereas at 5' end, it consists of the B1c region identical to the B1 region of the target sequence. Backward outer primer (B3), which is complementary to the B3c region of the template sequence. Forward loop primer (LF) which is complementary to the region between F1 and F2. Backward loop primer (LB) which is complementary to the region between B1 and B2.

The loop primers reduce the reaction time and increase the rate of amplification by binding the loops that are incorrectly oriented to bind to internal primers (Nagamine *et al.*, 2002).

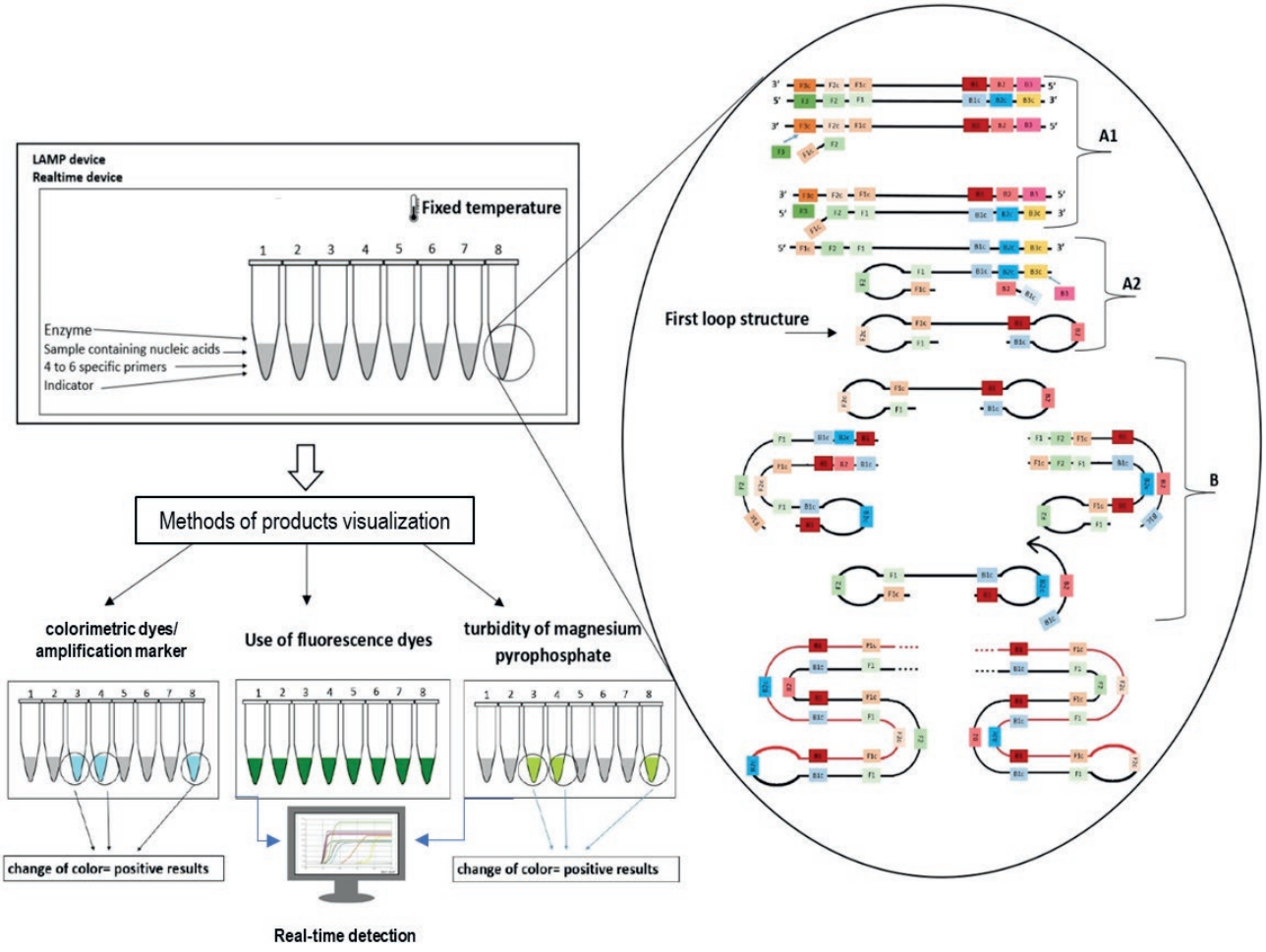

Figure 1. LAMP reaction and amplicon detection. Loop structure production: (A1) annealing and elongation of primer F2 (on primer FIP), followed by annealing and elongation of primer F3 which allows the first strand displacement and first loop formation through the annealing of F1(on primer FIP); and (A2) the annealing of primer B2 (on primer BIP), followed by annealing and elongation of primer B3 with the displacement of the polymerized strand and the formation of the second loop through B1 (on primer BIP). Target amplification (B): repetition of the annealing and elongation cycles on the produced loop and primer sites.

LAMP reaction

Two main steps can be differentiated in the LAMP reaction: loop structure production (Figure 1, A1 and A2) and amplification (Figure 1, B).

Loop structure production begins when FIP anneals the target sequence and separates the amplified sequence from the template by extending the primer, thereby forming the first product. This product is then displaced by synthesis when F3 anneals to an upstream target region (F3c), and the end of it forms a self-hybridizing loop structure due to the presence of the reverse complementary sequence F1c (Figure 1, A1). The same cycle repeats on the other end of the target sequence by the backward primers (BIP and B3) to form the first loop dumbbell structure (Figure 1, A2).

During elongation and amplification, the nucleic acid structure resulting from the previous step serves as a template for carrying on the amplification. It contains several sites from which the synthesis can initiate including the 3' end of the loop and the annealing sites of FIP and BIP. This allows the distinction of two elongation cycles: self-elongation from the loop and binding elongation of the inner region (Notomi *et al*., 2015) (Figure 1, B). The amplification step allows synthesis of complex structures with multiple loop sites that allow for exponential amplification of the sequence chosen as target.

Detection of LAMP products

Detection of LAMP amplicons can be accomplished by agarose gel electrophoresis. However, the most widely used methods are those that can ensure rapid observation of results without requiring further experimental steps (Figure 1). These methods can be either end-point tests (measured at specific timepoints) or real-time tests (measurement of amplification progress throughout the reactions). These methods can be classified into two groups (Moore *et al*., 2021). Sequence-independent methods rely on the detection of concentration changes of substrates or products produced throughout the reaction related to the amplification of the target sequences, and include changes in turbidity pH reactive dyes, intercalating fluorescent dyes, or bioluminescence. Conversely, sequence-dependent methods generate a signal directly dependent on the specific sequence targeted and allow the multiple target detection in a single tube; they include Quenching of Unincorporated Amplicon Signal Reporters (QUASR), Detection of Amplification by Releasing of Quenching (DARQ), CRISPR-Cas cleavage systems, one step strand displacement, and molecular beacons.

LAMP assays for postharvest molds

The review of Niessen (2018) identified 23 research publications describing development of LAMP assays to detect mycotoxigenic fungal pathogens on food matrices. Among these, two assays were panfungal, detecting presence of any fungal contamination in samples (Zhang *et al.,* 2017). Since then, similar studies have shown increased interest in LAMP as effective for distinguishing mycotoxigenic pathogens. However, other fungi, such as *Botrytis* spp. and *Monilinia* spp., which are unknown for mycotoxin production, can also severely damage harvested commodities. Therefore, these fungi have been the subject of several LAMP assays. In addition, some important postharvest bacterial pathogens have been subjects for development of rapid LAMP detection assays. In total, the present review lists 42 articles for fungi, and many of the studies provide simple and rapid protocols for detection of postharvest fungal contaminants directly from food. Since these pathogens are often present in preharvest as latent infections (Sanzani *et al*., 2012), the assays conducted on plant parts or seedlings have also been taken into consideration in the present review (Table 2).

Aspergillus

Among postharvest fungal pathogens, *Aspergillus* spp. are the most studied for development of rapid detection LAMP assays. Luo *et al.* (2012) were the first to aim to detect aflatoxigenic *Aspergillus* spp. directly from food samples, including Brazil nuts, peanuts and coffee beans. Their assay targeted the *acl1*-gene of *A. flavus* and *amy1*-genes of *A. nomius* and *A. parasiticus,* and positive results were detected by bright green fluorescence under UV 366 nm light. The detection limits were 2.4, 7.6 and 20 pg of pure DNA per reaction, respectively, for *A. flavus, A. nomius* and *A. parasiticus*. Specificity of the assays was also high with the *A. nomius* primer set not detecting any non-target isolate, and the other two primer sets detecting only some *Aspergillus* spp., which are very closely related to the targets.

The same primers were further tested by Luo *et al.* (2014) as parts of species-specific turbidimeter-based real-time LAMP assays, where turbidity was measured at 600 nm at intervals of 6s. These assays attempted to define contamination levels in samples of shelled Brazil nuts, maize, and peanuts. The detection limit was 10 conidia g^{-1} for *A. flavus* and *A. nomius* in Brazil nuts. The assay detection limits for *A. flavus* were 10^2 conidia g^{-1} for peanuts, and 10^4 conidia g^{-1} for maize, and for *A. parasiticus* were 10^5 conidia g^{-1} for peanuts and 10^4 conidia g^{-1} for maize.

Table 2. LAMP assays developed for the detection of postharvest fungal pathogens.

Pathogen	Target gene	Sensitivity	Food matrix	Reference
Aspergillus flavus *A. nomius* *A. parasiticus*	Alpha amylase (*amy1*) *amy1* ATP citrate lyase subunit 1	2.4 pg of pure DNA/ reaction 7.6 pg of pure DNA/ reaction 20 pg of pure DNA/ reaction	Brazil nuts, peanuts, green coffee beans	Luo *et al.*, 2012
A. flavus *A. nomius* *A. parasiticus*	a*my1* *amy1* ATP citrate lyase subunit 1	10 spores 100 spores 100 spores (sensitivity according to matrix and pathogen)	Brazil nuts, peanuts, maize	Luo *et al.*, 2014
A. flavus, *A. flavus* (toxygenic strains)	ITS1–5.8S–ITS2 rDNA region aflatoxin-encoding gene *aflP*	10 fg 1 pg of pure DNA	Peanuts, maize	Luo *et al.*, 2014
Aflatoxigenic Aspergilli	*nor1*	9.03 pg of DNA 211 conidia	Rice, nuts, raisins, dried figs	Niessen *et al.*, 2018
A. flavus, *A. parasiticus*	Aflatoxin efflux pump gene *aflT*	100-999 pg of DNA	Hazelnuts	Ortega *et al.*, 2020
A. carbonarius *A. niger* (ochratoxigenic)	polyketide synthase genes *pks*	Between 0.01 and 0.1 ng	Grapes	Storari *et al.*, 2013 Storari and Broggini, 2017
Ochratoxigenic strains of *Aspergillus* spp.	*pks*	Not mentioned	Peanuts	Al-Sheikh, 2015
A. niger *A. welwistchiae*	*fum10* (Fumonisin production)	10 conidia g^{-1} of maize	Maize	Ferrara *et al.*, 2020
A. caelatus *A. flavus* *A. nominus*	*acl1*	10^1 for *A. nomius*, 10^2 for *A. flavus*	Brazil nuts	Luo *et al.*, 2012
Botrytis cinerea	*bcos5*	10^{-3} ng μL^{-1}	Tomato and strawberry petals	Duan *et al.*, 2014a
B. cinerea	β-tubulin gene (*tub2*) mutation that causes resistance to benzimidazole	2×10^5 copies per μL of the plasmid	_____	Fan *et al.*, 2019
B. cinerea	Intergenic spacer (IGS) of nuclear ribosomal DNA	65 pg *B. cinerea* DNA	Detached rose petals, pelargonium leaves	Tomlinson *et al.*, 2010
B. cinerea	β-tubulin gene (*tub2*) mutation that causes resistance to benzimidazole	2×10^3 copies per μL of the plasmid	_____	Duan *et al.*, 2018
Penicillium expansum	*pex2_044840*	25 pg genomic DNA of *P. expansum*	Apples, grapes, apple juice, apple puree, grape juice	Frisch *et al.*, 2021
Patulin producing *Penicillium* spp.	isoepoxydon dehydrogenase *idh*	2.5 pg of purified genomic DNA	Grapes, apples	Frisch and Niessen, 2019
P. oxalicum	*pde_07106*	100 pg genomic DNA	Grapes	Vogt *et al.*, 2017
Monilinia laxa; M. fructicola	Intron in the cytochrome b, 166 associated with the *qoi* fungicides resistance	100-999 fg of DNA (*M. fructicola)*, 100-999 fg of DNA (*M. laxa)*	Nectarines	Ortega *et al.*, 2019
Fusarium graminearum	F167Y mutation of carbendazim-resistance of the b2-tubulin gene	Not mentioned	Perithecia produced on rice, infected wheat spikelets	Duan *et al.*, 2014b
Fusarium fujikuroi	*nrps31*	1 to 10 fg of DNA extracted from pure culture	Rice seeds and seedlings	Zhang *et al.*, 2019
Fumonisin-producing *Fusarium* spp.	*fum1* polyketide synthase involved in the biosynthesis of fumonisins	5 pg of genomic DNA 10^3 spores per reaction	Maize	Wigmann *et al.*, 2020

(Continued)

Table 2. (Continued).

Pathogen	Target gene	Sensitivity	Food matrix	Reference
F. graminearum	galactose oxidase gene *gaoA* of *F. austroamericanum*		Cereal	Niessen, 2013
Fusarium spp. *F. graminearum*	*hyd5*	0.74 pg of DNA	Barley	Denschlag *et al.*, 2012
Fusarium spp	hyd5	27 gene copies	Barley	Denschlag *et al.*, 2013
Fusarium spp.	*tri6*, *tri5* combination of the two sets	1.7 pg of DNA	_____	Denschlag *et al.*, 2014
A. carbonarius *A. niger* *A. awamori*	polyketide synthase genes	100 and 10 pg of DNA	Grapes	Storari *et al.*, 2013
Alternaria alternata	*actts2*	15 pg of DNA		Moghimi *et al.*, 2016
Alternaria spp.	cytochrome b (*cytb*)	15 pg	Pears	Yang *et al.*, 2019
Monilinia fructicola	*mfcyp51*	10 fg of purified target DNA	Peaches	Chen *et al.*, 2019
Phomopsis longicolla	1-α (tef1-α)	100 pg μL^{-1}	Soybeans	Dai *et al.*, 2016
Venturia carpophila	rDNA-ITS	56.6 Fg μL^{-1}	Peaches	Zhou *et al.*, 2021
A. fumigatus *P. expansum* *P. marneffei* *Histoplasma capsulatum*	rRNA-28S	20 copies of plasmid DNA for *A. fumigatus*	Mycelium culture	Tone *et al.*, 2017
F. graminearum	gaoA	2 pg of DNA	Wheat grains	Niessen and Vogel., 2010 Abd-elsalam *et al.*, 2011 Almoammar *et al.*, 2013
F. asiaticum	cyp51C	100 pg of DNA	Wheat grain	Xu *et al.*, 2017
F. culmorum	cyp51C	100 pg of DNA	Soybeans	Zeng *et al.*, 2017
F. equiseti	cypP51C	10 pg μL^{-1} 4 conidia per g of soil	Soybean roots	Lu *et al.*, 2015
Aflatoxin producers section *Flavi*	nor1	9 pg gDNA per rxn 211 conidia per rn after disruption	Rice, maize, raisins, figs, hazelnuts, almonds, paprika, ginger	Niessen *et al.*, 2018
Claviceps purpurea	cpn60	50 genome copies per rxn	Cereal grains	Comte *et al.*, 2017

Ferrara *et al.* (2020) aimed for rapid detection by targeting the *fum10* gene of *A. niger* and *A. welwitshiae,* which can produce the mycotoxin fumonisin (FB2) in maize kernels. The amplification was carried out in a portable thermal block, and the results were detected using phenol red according to colour change from red (negative) to yellow (positive). These assays were highly specific when tested using the nucleotide BLAST search tool on the NCBI sequence database. The detection limit was as low as 10 conidia per reaction. Ferrara *et al.* (2020) also developed a user-friendly "in field" analysis protocol based on extraction of crude DNA from contaminated maize kernels using a programmable, portable device with long-life battery. Since *Aspergillus* spp. have wide host ranges, matrix-specific assays must be developed, especially for species/host combinations targeted by regulations. Currently, the present authors are developing specific real-time LAMP assays for detection of *A. carbonarius, A. flavus* and aflatoxigenic aspergilli, on pistachios and almonds which are some of the most susceptible commodities to mycotoxigenic contamination. These assays are based on detection of the pathogens directly from samples, without laborious DNA purification steps, aiming to offer simple product tests for growers.

Penicillium

The study of Sun *et al.* (2010) was the first to focus on detecting *Penicillium* species by LAMP, targeting the human pathogen *P. marneffei* in archived human tissues. Later, LAMP assays were developed to detect *Penicillium* spp. in food samples (Tone *et al.*, 2017; Frisch and Niessen, 2019). Frisch and Niessen (2019) focused on rapid detection of *P. expansum,* which causes blue

mold decay, an important postharvest fruit disease. This assay targeted the *pex2_044840* gene, and was able to detect *P. expansum* DNA at high specificity and sensitivity of 25 pg per reaction. Results were visualized using neutral red as indicator. The assay was further tested on artificially contaminated food samples including apples, grapes, apple juices, apple puree and grape juice. The protocol required different DNA preparations depending on the type of sample; for grapes and apples, detectable amounts of DNA were obtained after simple steps of washing and mechanical treatment. For juices and purees, extraction of pure DNA was necessary for LAMP amplification. Despite the importance of *Penicillium* spp. as dominant food pathogens which produce hazardous mycotoxins, only a few LAMP assays targeting these fungi have been developed, compared to other important toxigenic postharvest pathogens such as *Aspergillus* and *Fusarium*. Development of rapid species-specific real-time LAMP assays would facilitate detection and treatment of these common mold fungi.

Botrytis

LAMP assays were developed both for toxigenic postharvest fungi and those such as *Botrytis cinerea*, whose damaging effects are unrelated to mycotoxin production. This pathogen causes grey mold, an important pre- and postharvest disease on many high value crops such as grapes, strawberries and kiwifruit (Droby *et al.*, 2007; Williamson *et al.*, 2007). This pathogen is often present as latent infection, and causes damage on fresh produce after periods of quiescence. For this reason, the fungus must be detected in early stages on plant material, rather than later, when the damage has occurred. The first rapid LAMP protocol for *B. cinerea* detection was published by Tomlinson *et al.* (2010), detecting the pathogen on plant material. Their study compared this protocol with the two previously used detection methods, TaqMan real time PCR and lateral flow devices. The LAMP assay targeted the intergenic spacer (IGS) of the *B. cinerea* nuclear ribosomal DNA (rDNA) sequence, which was the same sequence targeted by the Taq-Man real time PCR assay of Suarez *et al.* (2005). LAMP was carried out on DNA extracted from inoculated rose and pelargonium, and the results were visualized by electrophoresis on 1.4% agarose gels, followed by staining with ethidium bromide. The assay was further optimized and tested in real time, with sensitivity of 6.5 pg of DNA. Comparison of LAMP and TaqMan PCR showed that both methods were very specific by only detecting *B. pelargonii* among other closely related species. When tested directly on inoculated rose petals, only real-time PCR gave results 5 h after inoculation. Both methods detected the pathogen 29 h after inoculation. *Botrytis cinerea* is an important pathogen that often commences infection in the field and spreads rapidly at postharvest stages. However, few LAMP studies have been carried out with this fungus, but two have targeted the b-tubulin gene (*tub2*) mutation that causes resistance to benzimidazole (Duan *et al.,* 2014). While those studies are important for the detection of fungicide-resistant strains, further research is required to develop protocols for field detection and identification of this pathogen.

LAMP assays developed for the detection of postharvest bacteria

Postharvest bacteria often begin infections in the field and continue to cause damage on products after harvest. They mostly cause rotting which makes pathogen differentiation difficult from symptoms. Management of these pathogens is complicated and often requires extreme measures such crop eradication. Regular monitoring for presence of these organisms in susceptible crops is mandatory. In addition, these pathogens are strictly regulated by countries which classify them in quarantine lists. Development of new, rapid and sensitive tools for detection of postharvest bacteria will ease monitoring processes and border surveillance. Several studies have aimed to develop simple LAMP protocols for the detection of postharvest bacterial pathogens (Table 3).

Kubota *et al.* (2008) were the first to attempt to develop a LAMP assay on a postharvest bacterial pathogen, for *Ralstonia solanacearum*. This pathogen is important because of its wide host range (at least 200 plants, including economically important potato, tomato and peanuts). *R. solanacearum* is also of quarantine importance in several countries, so susceptible imported crops are often tested for this pathogen at borders, making it important to develop rapid and simple detection. Kubota *et al.* (2008) targeted the *fliC* sequence of the *R. solanacearum* genome to design specific LAMP primers. They also developed an assay for direct detection from edible ginger plants. The amplification results were electrophoresed at 85V for 90 min through 2% agarose gel (1× Tris-acetate-EDTA), followed by staining with ethidium bromide. Detection was by observation of white turbidity in reaction mixtures using magnesium pyrophosphate (Mori *et al.,* 2001). This assay was highly specific when tested on other soil-borne bacteria, but sensitivity varied according to the *R. solanacearum* strain. Efficacy of the same primers was also tested by Kubota *et al.* (2008) on potato tubers in a real-time LAMP assay, that

Table 3. LAMP assays for postharvest bacterial pathogens.

Pathogen	Gene	Sensitivity	Food matrices	Reference
Pectobacterium parmentieri	*petF1* gen	10 CFU mL^{-1} 100 fg of DNA	Potato plants and tubers	Domingo *et al*., 2021
P. atrosepticum	*sorA* *cfa6*	2.5×10^2 CFU mL^{-1}	Edible ginger plants	Li *et al*., 2011
P. carotovorum	(*p4h*) (α subunit)	1 ng μL^{-1} – 5 fg μL^{-1}	Potato	Yasuhara-Bell *et al*., 2016
P. atrosepticum	*gyr*B	3 CFU/reaction from pure cultures 22 CFU/reaction from samples	Potato tubers	Hu *et al*., 2016
Dykeya spp.	*mglC*	5 pg/reaction	Pineapple, Potato	Yasuhara-Bell *et al*., 2017
P. carotovorum	*pmrA*	10^4 CFU mL^{-1}	Celery	Shi *et al*., 2020b
Xanthomonas euvesicatoria	*recG*	100 fg of pure DNA 1,000 fg of DNA in samples spiked with tomato DNA	Tomato plants	Larrea-Sarmiento *et al*., 2018
X. arboricola pv. pruni	ABC transporter ATP-binding protein	1.8 ng μL^{-1} of genomic DNA	Peach orchards	Li *et al*., 2019
Ralstonia solanacearum	*fliC*	10^4 to 10^6 CFU mL^{-1}	Edible ginger plants	Kubota *et al*., 2008
R. solanacearum	*egl*	10^4 cells mL^{-1} (25 cells per LAMP reaction) for strains of phylotypes I and III 10^5–10^6 cells mL^{-1} for strains of phylotypes II	Tomato plants, potato plants and tubers	Lenarčič *et al*., 2014
R. solanacearum	*orf428*	100 fg mL^{-1} of DNA 10^3 CFU mL^{-1} of bacterial fluid	Sweet potato	Li *et al.,* 2021

gave a detection limit of 1.25×10^5 CFU g^{-1}. This is low sensitivity, compared to results previously reported from PCR, which amplified the gene at 2×10^2 CFU g^{-1} (Horita *et al*., 2004). Improvements of LAMP techniques have allowed development of more sensitive LAMP protocols, with lower detection limits. For example, Li *et al.* (2021) designed a LAMP primer set targeting the *orf428* gene, with a detection limit of 100 fg mL^{-1} of DNA and 10^3 CFU mL^{-1} of bacterial fluid.

In addition to *Ralstonia* spp., *Pectobacterium* spp. have also been subjects for development of rapid LAMP assays. Li *et al.* (2011) developed a LAMP assay for the detection of *Pectobacterium atrosepticum* (*Erwinia carotovora* subsp. *atrosepticum*), which causes potato blackleg associated with pre- and postharvest losses in potato crops. The assay targeted the gene cluster encoding a pathogenicity-related phytotoxin, specifically PKS *cfa6* and *Polyangium cellulosum* soraphen polyketide synthase A (*sorA*) genes. The assay had a specificity and a low detection limit of 2.5×10^2 CFU mL^{-1}. However, the assay described by Hu *et al.* (2016) for the same pathogen, which targeted the *gyr*B gene, had a detection limit of 3 CFU per reaction from pure cultures, and 22 CFU per reaction from samples of contaminated potato tubers. Improvement of LAMP has resulted in assays with greater specificity and simpler detection protocols. Domingo *et al.* (2021) aimed to specifically detect among *Pectobacterium* spp. and *Dickeya* spp. that can cause the soft rot of potato. This highly specific real-time LAMP assay allowed detection of the target species, and no other very closely related species. This is due to the signature region within the *petF1* gene that was not found in other *Pectobacterium* spp.. In addition to real-time measurement, results were also observed from orange to bright green colour change after adding SYBR green before the reaction. Domingo *et al.* (2021) also developed a simple and effective protocol for the detection of *P. parmentieri* from potato plants and tubers. Several LAMP assays have been developed for food-borne bacteria such as *Salmonella* spp. and *Escherichia coli*, in association with foods such as meat, milk and juice. Some studies tested LAMP on fresh agricultural produce, such as that targeting the *invA* gene of *Salmonella* spp. (Zhang *et al*., 2011). This assay had a detection limit of 2 CFU per 25 g and was tested on coriander, lettuce, parsley, spinach, tomato, jalapeno

and pepper. Yokoyama *et al.* (2010) developed a LAMP assay for *E. coli* associated with radish sprouts, broccoli sprouts, ready-to-eat salads, ground pork and beef, which targeted the *aggR* gene of this bacterium, and was able to detect 6.3 CFU per reaction.

CONCLUSIONS

Postharvest waste threatens food security, and is mainly caused by decay-inducing pathogens. Protection of harvested commodities relies heavily on the early detection of these pathogens, which often commence host infections in the field (Logrieco, 2022). LAMP is a rapid, sensitive and specific method for detecting and accurately identifying these pathogens, even in the field. Indeed, LAMP is easily performed as requires no special expertise, is less expensive than other molecular identification tools. To amplify a target sequence of target nucleic acid, LAMP uses four to six primers designed specifically according to the relevant DNA. Many assays have been developed to detect postharvest fungi using this method as reported in Table 3. These assays have targeted several mold species, particularly *Aspergillus* and *Fusarium* spp. For postharvest bacteria, however, assays have been designed for only a few agricultural product hosts, and tests for this general group of products should be more widely developed. This can be achieved utilizing the current revolution in molecular biology, specifically in gene sequencing, which provides material to design specific and functional LAMP primer sets. The continuous improvement of real-time LAMP using simple extraction methods, with crude extract instead of highly purified DNA (Kogovšek *et al.,* 2017; Yaseen *et al.,* 2015), in combination with lyophilized primers contribute to the suitability of this technique for *in situ* detection of postharvest pathogens.

Since most of these pathogens and their mycotoxins are regulated by many countries, LAMP represents an easy way of testing commodities at production sites, to facilitate future treatment decisions at borders and to alert importing countries about the presence of potentially harmful and damaging pathogens.

LITERATURE CITED

Abd-Elsalam K., Bahkali A., Moslem M., Amin O.E., Niessen L., 2011. An optimized protocol for DNA extraction from wheat seeds and loop-mediated isothermal amplification (LAMP) to detect *Fusarium graminearum* contamination of wheat grain. *International Journal of Molecular Sciences* 12: 3459–3472. https://doi.org/10.3390/ijms12063459

Abderraouf S., Minutillo S.A., Valentini F., Raimondo M.L., Lops F.,…D'Onghia A.M., 2022. A real time loop-mediated amplification (RealAmp) assay for rapid detection of *Pleurotus richardsiae* in declining olive plants. *Phytopathologia Mediterranea* 61: 259–267. 10.36253/phyto-12748

Almoammar H., Bahkali A.H., Abd-Elsalam K.A., 2013. One-hour loop-mediated isothermal amplification assay for the detection of quarantinable toxigenic *Fusarium graminearum*. *African Journal of Microbiology Research* 7: 1179–1183. https://doi.org/10.5897/AJMR2012.2346

Al-Sheikh H.M., 2015. LAMP-PCR detection of ochratoxigenic Aspergillus species collected from peanut kernel. *Genetics and Molecular Research* 14: 634–44. https://doi.org/10.4238/2015.January.30.5

Antunes M.D.C., Cavaco A.M., 2010. The use of essential oils for postharvest decay control. a review. *Flavour and Fragrance Journal* 25: 351–366. https://doi.org/10.1002/ffj.1986

Astoreca A.L., Magnoli C.E., Dalcero A.M., 2010. Ecophysiology of Aspergillus section nigri species potential ochratoxin A producers. *Toxins* 2: 2593–2605. https://doi.org/10.3390/toxins2112593

Baibakova E.V., Nefedjeva E.E., Suska-Malawska M., Wilk M., Sevriukova G.A., Zheltobriukhov V.F., 2019. Modern fungicides: mechanisms of action, fungal resistance and phytotoxic effects. *Annual Research & Review in Biology* 32: 1–16. https://doi.org/10.9734/arrb/2019/v32i330083

Balajee S.A., Sigler L., Brandt M.E., 2007a. DNA and the classical way: identification of medically important molds in the 21st century. *Medical Mycology* 45: 475–490. https://doi.org/10.1080/13693780701449425

Balajee S.A., Houbraken J., Verweij P.E., Hong S.B., Yaghuchi T., Varga J., Samson R.A., 2007b. Aspergillus species identification in the clinical setting. *Studies in Mycology* 59: 39–46. https://doi.org/10.3114/sim.2007.59.05

Barkai-Golan R., 2001. Postharvest Diseases of Fruits and Vegetables. In: *Postharvest Diseases of Fruits and Vegetables: Development and Control* (R. Barkai-Golan, ed.), Elsevier, Amsterdam, 1–418, ISBN 0-444-50584-9.

Beuchat L.R., 1993. Selective media for detecting and enumerating foodborne yeasts. *International Journal of Food Microbiology* 19: 1–14. https://doi.org/10.1016/0168-1605(93)90119-2

Bhat A.I., Aman R., Mahfouz M., 2022. Onsite detection of plant viruses using isothermal amplification assays.

Plant Biotechnology Journal 20: 1859–1873. https://biblioproxy.cnr.it:2481/10.1111/pbi.13871

Bui-Klimke T.R., Guclu H., Kensler T.W., Yuan J.M., Wu F., 2014. Aflatoxin regulations and global pistachio trade: Insights from social network analysis. *PLoS ONE* 9(3): e92149. https://doi.org/10.1371/journal.pone.0092149

Chen S., Schnabel G., Yuan H., Luo C., 2019. LAMP detection of the genetic element 'Mona' associated with DMI resistance in *Monilinia fructicola*. *Pest Management Science* 75: 779–786. https://doi.org/10.1002/ps.5178

Clark M.F., Lister R.M., Bar-Joseph M., 1986. ELISA techniques. In: Plant Molecular Biology, (Weissbach A., Weissbach H., ed.), *Methods in Enzymology* 118: 742–766. https://doi.org/10.1016/0076-6879(86)18114-6

Comte A., Gräfenhan T., Links M.G., Hemmingsen S.M., Dumonceaux T.J., 2017. Quantitative molecular diagnostic assays of grain washes for *Claviceps purpurea* are correlated with visual determinations of ergot contamination. *PloS ONE* 12: e0173495. https://doi.org/10.1371/journal.pone.0173495

Côté M.J., Tardif M.C., Meldrum A.J., 2004. Identification of *Monilinia fructigena*, *M. fructicola*, *M. laxa*, and *Monilia polystroma* on inoculated and naturally infected fruit using Multiplex PCR. *Plant Disease* 88: 1219–1225. https://doi.org/10.1094/PDIS.2004.88.11.1219

Cotty P.J., 1994. Comparison of four media for the isolation of *Aspergillus flavus* group of fungi. *Mycopathologia* 125: 157–162. https://doi.org/10.1007/BF01146521

Crowther J.R., 1995. ELISA. Theory and practice. *Methods in Molecular Biology* 42: 1–218. https://doi.org/10.1385/0-89603-279-5:1

Dai T.T., Shen H., Zheng X.B., 2016. Establishment and evaluation of a TEF1-α based loop-mediated isothermal amplification assay for detection of *Phomopsis longicolla*. *Australasian Plant Pathology* 45: 335–337. https://doi.org/10.1007/s13313-016-0415-6

Denschlag C., Vogel R.F., Niessen L., 2012. Hyd5 gene-based detection of the major gushing-inducing Fusarium spp. in a loop-mediated isothermal amplification (LAMP) assay. *International Journal of Food Microbiology* 156: 189–196. https://doi.org/10.1016/j.ijfoodmicro.2012.03.009

Denschlag C., Vogel R.F., Niessen L., 2013. Hyd5 gene based analysis of cereals and malt for gushing-inducing Fusarium spp. by real-time LAMP using fluorescence and turbidity measurements. *International Journal of Food Microbiology* 162: 245–251. https://doi.org/10.1016/j.ijfoodmicro.2013.01.019

Denschlag C., Rieder J., Vogel R.F., Niessen L., 2014. Real-time loop-mediated isothermal amplification (LAMP) assay for group specific detection of important trichothecene producing Fusarium species in wheat. *International Journal of Food Microbiology* 177: 117–127. https://doi.org/10.1016/j.ijfoodmicro.2014.02.010

Domingo R., Perez C., Klair, D., Vu H., Candelario-Tochiki A., Arif M., 2021. Genome-informed loop-mediated isothermal amplification assay for specific detection of *Pectobacterium parmentieri* in infected potato tissues and soil. *Scientific Reports* 11: 21948. https://doi.org/10.1038/s41598-021-01196-4

Droby S., Licher A., 2007. Postharvest Botrytis infection: Etiology, Development and Management. In: *Botrytis: Biology, Pathology and Control*. (Y. Eiad, B. Williamson, P. Tudzynski, P. Delen, ed.), Springer, Dordrecht. https://doi.org/10.1007/978-1-4020-2626-3_19

Duan Y.B., Ge C.Y., Zhang X.K., Wang J.X., Zhou M.G., 2014a. Development and evaluation of a novel and rapid detection assay for *Botrytis cinerea* based on loop-mediated isothermal amplification. *PLoS One* 9: e111094 https://doi.org/10.1371/journal.pone.0111094.

Duan Y., Zhang X., Ge C. Y., Wang Y., Cao J., Zhou M., 2014b. Development and application of loop-mediated isothermal amplification for detection of the F167Y mutation of carbendazim-resistant isolates in *Fusarium graminearum*. *Scientific Reports* 4: 7094. https://doi.org/10.1038/srep07094

Duan Y.B., Yang Y., Wang J.X., Chen C.J., Steinberg G., Zhou M.G., 2018. Simultaneous detection of multiple benzimidazole-resistant β-tubulin variants of *Botrytis cinerea* using loop-mediated isothermal amplification. *Plant Disease* 102: 2016–2024. https://doi.org/10.1094/PDIS-03-18-0542-RE

Dukare A.S., Paul S., Nambi V.E., Gupta R.K., Singh R., Vishwakarma R.K., 2019. Exploitation of microbial antagonists for the control of postharvest diseases of fruits: a review. *Critical Reviews in Food Science and Nutrition* 59: 1498–1513. https://doi.org/10.1080/10408398.2017.1417235

Duvick J., 2001. Prospects for reducing fumonisin contamination of maize through genetic modification. *Environmental Health Perspectives* 109: 337–342. https://doi.org/10.1289/ehp.01109s2337

Dyer S.K., McCammon S., 1994. Detection of toxigenic isolates of *Aspergillus flavus* and related species on coconut cream agar. *Journal of Applied Microbiology* 76: 75–78. https://doi.org/10.1111/j.1365-2672.1994.tb04418.x

Fan F., Hahn M., Li G.Q., Lin Y., Luo, C.X., 2019. Rapid detection of benzimidazole resistance in *Botry-*

tis cinerea by loop-mediated isothermal amplification. *Phytopathology Research* 1: 1–10. https://doi.org/10.1186/s42483-019-0016-8

FAO, 2011. *Global Food Losses and Food Waste–Extent, Causes and Prevention*. Rome: Food and Agriculture Organisation of the United Nations (FAO). Available at: https://www.fao.org/3/i2697e/i2697e.pdf. Accessed November 20, 2022.

Fernández-Baldo M.A., Fernández J.G., Pereira S.V., Messina G.A., Salinas E., Sanz Ferramola M.I., 2011. Development of an indirect competitive enzyme-linked immunosorbent assay applied to the *Botrytis cinerea* quantification in tissues of postharvest fruits. *BMC Microbiology* 11: 220. https://doi.org/10.1186/1471-2180-11-220

Ferrara M., Logrieco A.F., Moretti A., Susca A., 2020. A loop-mediated isothermal amplification (LAMP) assay for rapid detection of fumonisin producing Aspergillus species. *Food Microbiology* 90: 103469. https://doi.org/10.1016/j.fm.2020.103469

Frisch L.M., Mann M.A., Marek D.N., Niessen, L., 2021. Development and optimization of a loop-mediated isothermal amplification (LAMP) assay for the species-specific detection of *Penicillium expansum*. *Food Microbiology* 95: 103681. https://doi.org/10.1016/j.fm.2020.103681

Frisch L.M., Niessen L., 2019. Development and optimization of a group-specific loop-mediated isothermal amplification (LAMP) assay for the detection of patulin-producing Penicillium species. *International Journal of Food Microbiology* 346: 109177. https://doi.org/10.1016/j.ijfoodmicro.2019.03.010

Giovani B., Al-Jboory I., Chouibani M., Horn N., Mugnai L., D'Onghia A.M., 2022. Euphresco: a platform to link research and policy in the Mediterranean area and beyond. *Phytopathologia Mediterr*anea 61, 181 (abstract). https://doi.org/10.1038/s41477-020-0744-x

Horita M., Yano K., Tsuchiya K., 2004. PCR-based specific detection of *Ralstonia solanacearum* race 4 strains. *Journal of General Plant Pathology* 70: 278–283. https://doi.org/10.1007/s10327-004-0126-7

Hu L.X., Yang Z.H., Zhang D., Zhao D.M., Zhu J.H., 2016. Sensitive and rapid detection of *Pectobacterium atrosepticum* by targeting the *gyrB* gene using a real-time loop-mediated isothermal amplification assay. *Letters in Applied Microbiology* 63: 289–296. https://doi.org/10.1111/lam.12618.

Kader A.A., 2003. A perspective on postharvest horticulture (1978-2003). *HortScience* 38: 1004–1008.

Kasso M., Bekele M., 2018. Post-harvest loss and quality deterioration of horticultural crops in Dire Dawa Region, Ethiopia. *Journal of the Saudi Society of Agricultural Sciences* 17: 88–96. https://doi.org/10.1016/j.jssas.2016.01.005.

King K.M., Hawkins N.J., Atkins S., Dyer P.S., West J.S., Fraaije BA., 2019. First application of loop-mediated isothermal amplification (LAMP) assays for rapid identification of mating type in the heterothallic fungus *Aspergillus fumigatus*. *Mycoses* 62: 812–817. https://doi.org/10.1111/myc.12959

Kitinoja L., Tokala V., Mohammed M., 2019. Clean cold-chain development and the critical role of extension education. *Tropical Agriculture Association* 36: 19-25.

Klich M.A., Pitt J.I., 1988. Differentiation of *Aspergillus flavus* from *A. parasiticus* and other closely related species. *Transactions of the British Mycological Society* 91: 99–108. https://doi.org/10.1016/S0007-1536(88)80010-X

Kogovšek P., Mehle N., Pugelj A., Jakomin T., Schroers H.J., … Dermastia M., 2017. Rapid loop-mediated isothermal amplification assays for grapevine yellows phytoplasmas on crude leaf-vein homogenate has the same performance as qPCR. *European Journal of Plant Pathology* 148: 75–84. https://doi.org/10.1007/s10658-016-1070-z

Kubota R., Vine B.G., Alvarez A.M., Jenkins D.M., 2008. Detection of *Ralstonia solanacearum* by loop-mediated isothermal amplification. *Phytopathology* 98: 1045–51. https://doi.org/10.1094/PHYTO-98-9-1045

Lane C.R., Hobden E., Walker L., Barton V.C., Inman K.J.,…Barker I., 2007. Evaluation of a rapid diagnostic field test kit for identification of Phytophthora species, including *P. ramorum* and *P. kernoviae* at the point of inspection. *Plant Pathology* 56: 828–835. https://doi.org/10.1111/j.1365-3059.2007.01615.x

Larrea-Sarmiento A., Dhakal U., Boluk G., Fatdal L., Alvarez A., Arif M., 2018. Development of a genome-informed loop-mediated isothermal amplification assay for rapid and specific detection of *Xanthomonas euvesicatoria*. *Scientific Reports* 8: 14298. https://doi.org/10.1038/s41598-018-32295-4.

Le D.T., Vu N.T., 2017. Progress of loop-mediated isothermal amplification technique in molecular diagnosis of plant diseases. *Applied Biological Chemistry* 60: 169–180. https://doi.org/10.1007/s13765-017-0267-y

Lemma Z., Dawit W., Negari M., Chaka A., Sekvaraj T., Gebresenbet G., 2014. Identification of post-harvest rotting microorganisms from tomato fruits (*Solanum esculentum* Mill.) in Toke Kutaye District of West Shoa Zone, Ethiopia. *Journal of Stored Products and Postharvest Research* 5: 14–19. https://doi.org/10.5897/JSPPR2014.0171

Lenarčič R., Morisset D., Pirc M., Llop P., Ravnikar M., Dreo T., 2014. Loop-mediated isothermal ampli-

fication of specific endoglucanase gene sequence for detection of the bacterial wilt pathogen *Ralstonia solanacearum*. *PLoS One* 9: 96027. https://doi.org/10.1371/journal.pone.0096027.

Li H., Zhang H., Liu Z., Lin Z., Qiu Y., Qiu S., 2021. Rapid diagnosis of *Ralstonia solanacearum* infection sweet potato in China by loop-mediated isothermal amplification. *Archives of Microbiology* 203: 777–778. https://doi.org/10.1007/s00203-020-02059-8

Li W., Lee S.Y., Back C.G., Ten L.N., Jung H.Y., 2019. Loop-Mediated Isothermal Amplification for the Detection of *Xanthomonas arboricola* pv. *pruni* in Peaches. *Plant Pathology Journal* 35: 635–643. https://doi.org/10.5423/PPJ.OA.07.2019.0197.

Li X., Nie J., Ward L.J., Nickerson J., Solke H., De Boer S.H., 2011. Development and evaluation of a loop-mediated isothermal amplification assay for rapid detection and identification of *Pectobacterium atrosepticum*. *Canadian Journal of Plant Pathology* 33: 447–457. https://doi.org/10.1080/07060661.2011.603751

Logrieco A.F., 2022. From myco-key to myco-twin: mycotoxin management along food/feed chains. In: *Abstracts of invited, oral and poster papers presented at the 16th Congress of the Mediterranean Phytopathological Union*, April 4–8. Limassol, Cyprus. *Phytopathologia Mediterranea* 61(1): 181–239, 2022 DOI: 1036253/phyto-13613

Lu C., Zhang H., Wang Y., Zheng X., 2015. Rapid diagnosis of Fusarium root rot in soybean caused by *Fusarium equiseti* or *Fusarium graminearum* using loop-mediated isothermal amplification (LAMP) assays. *Australasian Plant Pathology* 44: 437–443. https://doi.org/10.1007/s13313-015-0361-8

Luo J., Vogel R.F, Niessen L., 2012. Development and application of a loop-mediated isothermal amplification assay for rapid identification of aflatoxigenic molds and their detection in food samples. *International Journal of Food Microbiology* 159: 214–224. https://doi.org/10.1016/j.ijfoodmicro.2012.08.018.

Luo J., Vogel R.F., Niessen L., 2014. Rapid detection of aflatoxin producing fungi in food by real-time quantitative loop-mediated isothermal amplification. *Food Microbiology* 44: 142–148. https://doi.org/10.1016/j.fm.2014.06.004

Moghimi H., Moradi A., Hamedi J., Basiri M., 2016. Development of a loop-mediated isothermal amplification assay for rapid and specific identification of ACT producing *Alternaria alternata*, the agent of brown spot disease in tangerine. *Applied Biochemistry and Biotechnology* 178: 1207–1219. https://doi.org/10.1007/s12010-015-1939-x

Moore K. J., Cahill J., Aidelberg G., Aronoff R., Bektaş A., Bezdan D., … gLAMP Consortium, 2021. Loop-Mediated Isothermal Amplification Detection of SARS-CoV-2 and Myriad Other Applications. *Journal of Biomolecular Techniques* 32(3): 228–275.

Mori Y., Nagamine K., Tomita N., Notomi T., 2001. Detection of loop-mediated isothermal amplification reaction by turbidity derived from magnesium pyrophosphate formation. *Biochemical and Biophysical Research Communications* 289: 150–154. https://doi.org/10.1006/bbrc.2001.5921

Mvumi B.M., Stathers T.E., 2015. Food security challenges in Sub-Saharan Africa: The potential contribution of postharvest skills, science and technology in closing the gap. *Proceedings of the 11th International Working Conference on Stored Product Protection. Department of Agriculture, Ministry of Agriculture and Cooperatives,* Bangkok, Thailand: 32–43. https://doi.org/10.14455/DOA.res.2014.7)

Nagamine K., Hase T., Notomi T., 2002. Accelerated reaction by loop-mediated isothermal amplification using loop primers. *Molecular and Cellular Probes* 16: 223–229. https://doi.org/10.1006/mcpr.2002.0415

Niessen L., 2013. Loop-mediated isothermal amplification-based detection of *Fusarium graminearum*. In: *Fungal Diagnostics: Methods and Protocols* (L. O´Connor, B. Glynn, ed.), Humana Press, Totowa, New Jersey, United States of America,177–193.

Niessen L., 2018. The application of loop-mediated isothermal amplification (LAMP) assays for the rapid diagnosis of food-borne mycotoxigenic fungi. *Current Opinion in Food Science* 23: 11–22. https://doi.org/10.1016/j.cofs.2018.02.007

Niessen L., Vogel R.F., 2010. Detection of *Fusarium graminearum* DNA using a loop-mediated isothermal amplification (LAMP) assay. *International Journal of Food Microbiology* 140: 183–191. https://doi.org/10.1016/j.ijfoodmicro.2010.03.036

Niessen L., Bechtner J., Fodil S., Taniwaki M.H., Vogel R.F., 2018. LAMP-based group specific detection of aflatoxin producers within Aspergillus section Flavi in food raw materials, spices, and dried fruit using neutral red for visible-light signal detection. *International Journal of Food Microbiology* 266: 241–250. https://doi.org/10.1016/j.ijfoodmicro.2017.12.013

Notomi T., Okayama H., Masubuchi H., Yonekawa T., Watanabe K., Hase T., 2000. Loop-mediated isothermal amplification of DNA. *Nucleic Acids Research* 28: E63. https://doi.org/10.1093/nar/28.12.e6

Notomi T., Mori Y., Tomita N., Kanda H., 2015. Loop-mediated isothermal amplification (LAMP): principle, features, and future prospects. *Journal of Micro-*

biology 53: 1–5. https://doi.org/10.1007/s12275-015-4656-9

Omotayo O.P., Omotayo A.O., Mwanza M., Babalola O.O., 2019. Prevalence of mycotoxins and their consequences on human health. *Toxicology Research* 35: 1–7. https://doi.org/10.5487/TR.2019.35.1.001

Ortega S. F., del Pilar Bustos López M., Nari L., Boonham N., Gullino M. L., Spadaro D., 2019. Rapid Detection of *Monilinia fructicola* and *Monilinia laxa* on Peach and Nectarine using Loop-Mediated Isothermal Amplification. *Plant Disease* 103: 2305–2314. https://doi.org/10.1094/PDIS-01-19-0035-RE

Ortega S.F., Siciliano I., Prencipe S., Gullino M.L., Spadaro D., 2020. Development of PCR, LAMP and qPCR assays for the detection of aflatoxigenic strains of *Aspergillus flavus* and *A. parasiticus* in hazelnut. *Toxins* 12: 757. https://doi.org/10.3390/toxins12120757

Ostry V., 2008. *Alternaria* mycotoxins: an overview of chemical characterization, producers, toxicity, analysis and occurrence in foodstuffs. *World Mycotoxin Journal* 1: 175–188. https://doi.org/10.3920/WMJ2008.x013

Palumbo J.D., O'Keeffe T.L., McGarvey J.A., 2011. Incidence of fumonisin B2 production within *Aspergillus* section Nigri populations isolated from California raisins. *Journal of Food Protection* 74: 672–675. https://doi.org/10.4315/0362-028X.JFP-10-412

Parfitt J., Barthel M., Macnaughton S., 2010. Food waste within food supply chains: quantification and potential for change to 2050. *Philosophical Transactions of the Royal Society B* 365**:** 3065–3081. https://doi.org/10.1098/rstb.2010.0126

Partida-Martinez L.P., Hertweck C., 2007. A gene cluster encoding rhizoxin biosynthesis in "*Burkholderia rhizoxina*", the bacterial endosymbiont of the fungus *Rhizopus microsporus*. *ChemBioChem* 8: 41–45. https://doi.org/10.1002/cbic.200600393

Pei S.C., Zhang Y.Y., Eremin S.A., Lee W.J. 2009. Detection of aflatoxin M1 in milk products from China by ELISA using monoclonal antibodies. *Food Control* 20, 1080–1085. https://doi.org/10.1016/j.foodcont.2009.02.004

Perrone G., Susca A., 2017. *Penicillium* species and their associated mycotoxins. In: *Mycotoxigenic Fungi, Methods in Molecular Biology* (A. Moretti, A. Susca, ed.), Humana Press, Totowa, New Jersey, United States of America, 107–119. https://doi.org/10.1007/978-1-4939-6707-0_5

Pitt J.I., Hocking A.D., Glenn D.R., 1983. An improved medium for the detection of *Aspergillus flavus* and *A. parasiticus*. *Journal of Applied Microbiology* 54, 109–114. https://doi.org/10.1111/j.1365-2672.1983.tb01307.x

Rodriguez A., Rodriguez M., Luque M.I., Martin A., Cordoba J.J., 2012. Real-time PCR assays for detection and quantification of aflatoxin producing molds in foods. *Food Microbiology* 31: 89–99. https://doi.org/10.1016/j.fm.2012.02.009.

Samson R.A., Noonim P., Meijer M., Houbraken J., Frisvad J.C., Varga, J., 2007. Diagnostic tools to identify black Aspergilli. *Studies in Mycology* 59: 129–145. https://doi.org/10.3114/sim.2007.59.13

Sanzani S.M., Reverberi M., Punelli M., Ippolito A., Fanelli C., 2012. Study on the role of patulin on pathogenicity and virulence of *Penicillium expansum*. *International Journal of Food Microbiology* 153: 323–331. https://doi.org/10.1016/j.ijfoodmicro.2011.11.021

Schaad N.W., Frederick R.D, 2002. Real-time PCR and its application for rapid plant disease diagnostics. *Canadian Journal of Plant Pathology* 24: 250–258. https://doi.org/10.1080/07060660209507006

Shapira R., Paster N., Eyal O., Mett A., Salomon R., 1996. Detection of aflatoxigenic molds in grains by PCR. *Applied and Environmental Microbiology* 62: 3270-3273. DOI: 10.1128/aem.62.9.3270-3273.1996

Shi X.C., Wang S.Y., Duan X.C., Wang Y.Z., Liu F.Q., Laborda P., 2020a. Biocontrol strategies for the management of *Colletotrichum* species in postharvest fruits. *Crop Protection* 141: 105454. https://doi.org/10.1016/j.cropro.2020.105454

Shi Y., Jin Z., Meng X., Wang L., Xie X., Li B., 2020b. Development and Evaluation of a Loop-mediated Isothermal Amplification Assay for the Rapid Detection and Identification of *Pectobacterium carotovorum* on Celery in the Field. *Horticultural Plant Journal* 6: 313–320. https://doi.org/10.1016/j.hpj.2020.07.004

Spadaro D., Gullino M.L., 2005. Improving the efficacy of biocontrol agents against soilborne pathogens. *Crop Protection* 24: 601–613. https://doi.org/10.1016/j.cropro.2004.11.003

Stakheev A.A., Ryazantsev D.Y., Gagkaeva T.Y., Zavriev S.K., 2011. PCR detection of Fusarium fungi with similar profiles of the produced mycotoxins. *Food Control* 22: 462–468. https://doi.org/10.1016/j.foodcont.2010.09.028

Storari M., Rohr R., Pertot I., Gessler C., Broggini G.A.L., 2013. Identification of ochratoxin A producing *Aspergillus carbonarius* and *A. niger* clade isolated from grapes using the loop-mediated isothermal amplification (LAMP) reaction. *Journal of Applied Microbiology* 114: 1193–1200. https://doi.org/10.1111/jam.12139

Storari M., Broggini G. A. L., 2017. Identification of Ochratoxin A-Producing Black Aspergilli from Grapes Using Loop-Mediated Isothermal Amplification

(LAMP) Assays. In: *Mycotoxigenic Fungi. Methods in Molecular Biology* (A. Moretti, A. Susca, ed.), Humana Press, Totowa, New Jersey, United States of America, 337–343. https://doi.org/10.1007/978-1-4939-6707-0

Suarez M.B., Walsh K., Boonham N., O'Neill T., Pearson S., Barker I., 2005. Development of real-time PCR (TaqMan ®) assays for the detection and quantification of *Botrytis cinerea* in planta. *Plant Physiology Biochemistry* 43: 890–899. https://doi.org/10.1016/j.plaphy.2005.07.003

Sun J., Li X., Zeng H., Xie Z., Lu C., Xi L., de Hoog G.S., 2010. Development and evaluation of loop-mediated isothermal amplification (LAMP) for the rapid diagnosis of *Penicillium marneffei* in archived tissue samples. *FEMS Immunology & Medical Microbiology* 58 : 381–388, https://doi.org/10.1111/j.1574-695X.2009.00647.x

Talibi I., Askarne L., Boubaker H., Boudyach E.H., Msanda F.,… Ben Aoumar A.A., 2012. Antifungal activity of Moroccan medicinal plants against citrus sour rot agent *Geotrichum candidum*. *Letters in Applied Microbiology* 55: 155–161. https://doi.org/10.1111/j.1472-765X.2012.03273.x

Tomlinson J.A., Dickinson M.J., Boonham N., 2010. Detection of *Botrytis cinerea* by loop-mediated isothermal amplification. *Letters in Applied Mycology* 51: 650–657. 10.1111/j.1472-765X.2010.02949.x

Tone K., Fujisaki R., Yamazaki T., Makimura K., 2017. Enhancing melting curve analysis for the discrimination of loop-mediated isothermal amplification products from four pathogenic molds: Use of inorganic pyrophosphatase and its effect in reducing the variance in melting temperature values. *Journal of Microbiological Methods* 132: 41–45. https://doi.org/10.1016/j.mimet.2016.10.020

Tripathi P., Dubey N. K., 2004. Exploitation of natural products as an alternative strategy to control postharvest fungal rotting of fruit and vegetables. *Postharvest Biology and Technology* 32: 235–245. https://doi.org/10.1016/j.postharvbio.2003.11.005

Tsai G.J., Cousin M.A., 1990. Enzyme-linked immunosorbent assay for detection of molds in cheese and yogurt. *Journal of Dairy Science* 73: 3366–3378. https://doi.org/10.3168/jds.S0022-0302(90)79032-7

Valentini F., Santoro F., Gallo M., Oualguirah L., D'Onghia A.M., 2022. An innovative protocol for the monitoring and onsite detection of *Erwinia amylovora* in Sicily. In: *Abstracts of invited, oral and poster papers presented at the 16th Congress of the Mediterranean Phytopathological Union*, April 4–8, 2022, Limassol, Cyprus. *Phytopathologia Mediterranea* 61(1): 181–239, 2022 DOI: 1036253/phyto-13613

van Egmond H.P., Schothorst R.C., Jonker M.A., 2007. Regulations relating to mycotoxins in food. *Analytical and Bioanalytical Chemistry* 389: 147–157. https://doi.org/10.1007/s00216-007-1317-9

Varga J., Frisvad J.C., Samson R.A., 2011. Two new aflatoxin producing species, and an overview of *Aspergillus* section Flavi. *Studies in Mycology* 69: 57–80. https://doi.org/10.3114/sim.2011.69.05

Vogt E.I., Kupfer V.M., Bechnter J.D., Frisch L.M., Vogel R.F., Niessen L., 2017. Detection of *Penicillium oxalicum* in grapes with a loop-mediated isothermal amplifcation (LAMP) assay. *Journal of Microbiology, Biotechnology and Food Sciences* 7: 265–270. 10.15414/jmbfs.2017/18.7.3.265-270

Xu M., Ye W., Zeng D., Wang Y., Zheng X., 2017. Rapid diagnosis of wheat head blight caused by *Fusarium asiaticum* using a loop-mediated isothermal amplification assay. *Australasian Plant Pathology* 46: 261–266.

Yahia E.M., Fonseca J.M., Kitinoja L., 2019. Postharvest losses and waste. In: *Postharvest Technology of Perishable Horticultural Commodities* (Yahia E.M., ed.). Oxford: Woodhead Publishing: 43–69. https://doi.org/10.1016/C2016-0-04890-8

Yang X., Qi Y.J., Al-Attala M.N., Gao Z.H., Yi X.K., Chen, Y., 2019. Rapid detection of *Alternaria* species involved in pear black spot using loop-mediated isothermal amplification. *Plant Disease* 103: 3002–3008. https://doi.org/10.1094/PDIS-01-19-0149-RE

Yaseen T., Drago S., Valentini F., Elbeaino T., Stampone G., …D'Onghia A.M., 2015. On-site detection of *Xylella fastidiosa* in host plants and in "spy insects" using the real-time loop mediated isothermal amplification method. *Phytopathologia Mediterranea* 54: 488–496. https//doi.org/10.14601/Phythopathol_Mediterr-15250

Yasuhara-Bell J., Marrero G., De Silva A., Alvarez A.M., 2016. Specific detection of *Pectobacterium carotovorum* by loop-mediated isothermal amplification. *Molecular Plant Pathology* 17: 1499–1505. https://doi.org/10.1111/mpp.12378.

Yasuhara-Bell J., Marrero G., Arif M., de Silva A., Alvarez A.M., 2017. Development of a Loop-Mediated Isothermal Amplification Assay for the Detection of *Dickeya* spp. *Phytopathology* 107: 1339–1345. https://doi.org/10.1094/PHYTO-04-17-0160-R.

Yokoyama E., Uchimura M., Ito K., 2010. Detection of enteroaggregative *Escherichia coli* by loop-mediated isothermal amplification. *Journal of Food Protection* 73: 1064–1072. https://doi.org/10.4315/0362-028x-73.6.

Wenderoth M., Garganese F., Schmidt-Heydt M., Soukup S.T., Ippolito A., … Fischer R., 2019. Alternariol as

virulence and colonization factor of *Alternaria alternata* during plant infection. *Molecular Microbiology* 112: 131–146 https://doi.org/10.1111/mmi.14258

Wenneker M., Thomma B.P.H.J., 2020. Latent postharvest pathogens of pome fruit and their management: from single measures to a systems intervention approach. *European Journal of Plant Pathology* 156: 663–681. https://doi.org/10.1007/s10658-020-01935-9

Wigmann É.F., Meyer K., Cendoya E., Maul R., Vogel R.F., Niessen L., 2020. A loop-mediated isothermal amplification (LAMP) based assay for the rapid and sensitive group-specific detection of fumonisin producing *Fusarium* spp. *International Journal of Food Microbiology* 325: 108627. https://doi.org/10.1016/j.ijfoodmicro.2020.108627

Williamson B., Tudzynski B., Tudzynski P., Van Kan J.A.L., 2007. *Botrytis cinerea*: the cause of grey mould disease. *Molecular Plant Pathology* 8: 561–580. https://doi.org/10.1111/j.1364-3703.2007.00417.x

Zeng D., Ye W., Xu M., Lu C., Tian Q., Zheng X., 2017. Rapid diagnosis of soya bean root rot caused by *Fusarium culmorum* using a loop-mediated isothermal amplification assay. *Journal of Phytopathology* 165: 249–256. https://doi.org/10.1111/jph.12556

Zhang G., Brown E.W., González-Escalona N., 2011. Comparison of real-time PCR, reverse transcriptase real-time PCR, loop-mediated isothermal amplification, and the FDA conventional microbiological method for the detection of *Salmonella* spp. in produce. *Applied and Environmental Microbiology* 77: 6495–6501. https://doi.org/10.1128/AEM.00520-11

Zhang X., Xu G., Tang H., Li Y., Liu C., 2017. Development of loop-mediated isothermal amplification (LAMP) assay for the rapid detection of *Alternaria alternata*. *Journal of AOAC International* 100: 99–103. https://doi.org/10.5740/jaoacint.16-0196

Zhang S. Y., Dai D. J., Wang H. D., Zhang C. Q., 2019. One-step loop-mediated isothermal amplification (LAMP) for the rapid and sensitive detection of *Fusarium fujikuroi* in bakanae disease through NRPS31, an important gene in the gibberellic acid biosynthesis. *Scientific Reports* 9: 1–9. https://doi.org/10.1038/s41598-019-39874-z

Zhao Y., Li P., Huang K., Hu H., Sun Y., 2013. Control of postharvest soft rot caused by *Erwinia carotovora* of vegetables by a strain of *Bacillus amyloliquefaciens* and its potential modes of action. *World Journal of Microbiology and Biotechnology* 29: 411–420. https://doi.org/10.1007/s11274-012-1193-0

Zhou Y., Zhang L., Fan F., Wang Z. Q., Huang Y., Luo C. X., 2021. Genome sequence of *Venturia carpophila*, the causal agent of peach scab. *Molecular Plant-Microbe Interactions* 34: 852–856. https://doi.org/10.1094/MPMI-11-20-0321-A

Phytopathologia Mediterranea
The international journal of the
Mediterranean Phytopathological Union

Firenze University Press
www.fupress.com/pm

60th MPU Anniversary Special Section - Review

Recent research accomplishments on early detection of *Xylella fastidiosa* outbreaks in the Mediterranean Basin

María P. VELASCO-AMO[1], Antonio VICENT[2], Pablo J. ZARCO-TEJADA[1,3], Juan A. NAVAS-CORTÉS[1], Blanca B. LANDA[1,*]

[1] *Institute for Sustainable Agriculture (IAS), Spanish National Research Council (CSIC), Córdoba, Spain*
[2] *Centro de Protección Vegetal y Biotecnología, Instituto Valenciano de Investigaciones Agrarias (IVIA), Moncada, Spain*
[3] *School of Agriculture and Food (SAF-FVAS) and Faculty of Engineering and Information Technology (IE-FEIT), University of Melbourne, Melbourne, Victoria, Australia*
*Corresponding author. E-mail: blanca.landa@csic.es

Summary. *Xylella fastidiosa* is a major transboundary plant pest, causing severe socio-economic impacts. Development of preventive strategies and methods for surveillance, early detection, monitoring, and accurate diagnosis of *X. fastidiosa* and its vectors, are keys to preventing the effects of this plant pathogen, and assist timely eradication or optimisation of containment measures. This review focuses on approaches for early detection of *X. fastidiosa* in the Mediterranean Basin, including development of climatic suitability risk maps to determine areas of potential establishment, and epidemiological models to assist in outbreak management through optimized surveillance and targeted responses. The usefulness of airborne hyperspectral and thermal images from remote sensing to discriminate *X. fastidiosa* infections from other biotic- and abiotic-induced spectral signatures is also discussed. The most commonly used methods for identifying *X. fastidiosa* in infected plants and vectors, and the molecular approaches available to genetically characterize *X. fastidiosa* strains, are described. Each of these approaches has trade-offs, but stepwise or simultaneous combinations of these methods may help to contain *X. fastidiosa* epidemics in the Mediterranean Basin.

Keywords. Climatic suitability risk maps, diagnostics, molecular approaches, quarantine plant pathogens, sequential adaptive survey.

OPEN ACCESS

Citation: M.P. Velasco-Amo, A. Vicent, P.J. Zarco-Tejada, J.A. Navas-Cortés, B.B. Landa (2022) Recent research accomplishments on early detection of *Xylella fastidiosa* outbreaks in the Mediterranean Basin. *Phytopathologia Mediterranea* 61(3): 549-561. doi: 10.36253/phyto-14171

Accepted: December 28, 2022

Published: January 13, 2023

Data Availability Statement: All relevant data are within the paper and its Supporting Information files.

Competing Interests: The Author(s) declare(s) no conflict of interest.

Editor: Anna Maria D'Onghia, CIHEAM/Mediterranean Agronomic Institute of Bari, Italy.

ORCID:
MPV-A: 0000-0001-7176-0435
AV: 0000-0002-3848-0631
PJZ-T: 0000-0003-1433-6165
JAN-C: 0000-0001-6480-1104
BBL: 0000-0002-9511-3731

INTRODUCTION

Xylella fastidiosa is a plant-associated bacterium that is a major transboundary plant health threat, and is a serious plant pathogen in terms of socioeconomic impacts. The bacterium causes diseases on a wide host range of plants including crops of economic importance in agriculture and forestry, and with cultural and heritage value. Diseases caused by *X. fastidiosa* include Pierce's Disease (PD) of grapevine, Citrus Variegated Chlorosis (CVC),

Almond Leaf Scorch (ALS), and Olive Quick Decline Syndrome (OQDS) (EFSA, 2022). A recent study by the Joint Research Center (JRC) and European Food Safety Authority (EFSA) (Sanchez *et al*., 2019) has identified *X. fastidiosa* as the quarantine pathogen with the greatest potential impact in the European Union (EU), in all economic, social, and environmental domains. That study estimated that *X. fastidiosa* could ultimately cost the EU over €5.5 billion per year due to production losses, and €0.7 billion per year in export losses, since the bacterium has the potential to affect 70% of EU production value of full-productive old (>30 years) olive trees, 13% of almond, 11% of citrus, and between 1 to 2% of grape production, in a full spread scenario across the EU.

Early detection of *X. fastidiosa* is important for taking timely measures for its eradication, containment or management (Almeida 2016; Zarco-Tejada *et al.* 2018). Consequently, development of efficient methods and strategies for surveillance, early detection and monitoring of *X. fastidiosa* have been the foci of several EU research projects such as XF-ACTORS (https://www.xfactorsproject.eu/) and POnTE (https://www.ponteproject.eu/), and grants by the EFSA. A major effort is currently being made in the EU to detect and assign *X. fastidiosa* strains from outbreaks to subspecies and, within them, to Sequence Types (STs). This is to infer relationships between ST and host range, and to trace back the possible origins of the introductions. Accurate diagnoses of *X. fastidiosa* at subspecies levels in the EU is essential for regulatory measures on outbreak response and management (e.g., removal of plants and replanting) (Regulation EU 2021/1688; EC, 2021). Currently, methods for *X. fastidiosa* identification are based on the European and Mediterranean Plant Protection Organization (EPPO) diagnostic protocol (EPPO, 2019).

The present review is based on an oral presentation entitled 'Current situation of *Xylella fastidiosa* impacts in Spain: ongoing research initiatives to understand and tackle this pathogen', which was presented at the 16th Congress of the Mediterranean Phytopathological Union in April 2022, Limassol, Cyprus (Landa, 2022). This review describes research outputs from the framework of the EU projects POnTE and XF-ACTORS for early detection of *X. fastidiosa*, together with current knowledge reported in *X. fastidiosa* literature and experienced gained during current EU outbreaks of the pathogen in the Mediterranean Basin. It is not intended, however, to provide a detailed state of the art summary on this topic. Topics covered include development of climatic suitability risk maps, how they can assist to determine areas of potential *X. fastidiosa* establishment, and how epidemiological models and surveillance strategies can help to track the outbreaks of *X. fastidiosa* and their potential spread. Other topics include the usefulness of remote sensing to support surveillance and monitoring of areas affected by *X. fastidiosa* outbreaks, and how to discriminate *X. fastidiosa* infections from other biotic and abiotic-induced stresses. Also provided are an extended description of the most commonly used methods to identify *X. fastidiosa* in infected plants and vectors, molecular approaches available to characterize *X. fastidiosa* strains at subspecies and ST level, and future directions for efficient molecular diagnostics and genetic characterization of *X. fastidiosa* strains.

Although the procedures for field sampling of plant material, in places of production and in consignments, as well as laboratory sample preparation, are all essential for obtaining reliable diagnostic results, description of these procedures is beyond the scope of this review. Detailed information on these aspects can be found in PM 7/24 Diagnostics for *Xylella fastidiosa* (EPPO, 2019), PM 3/81 Inspection of consignments for *Xylella fastidiosa* (EPPO, 2022a), PM 3/82 Inspection of places of production for *Xylella fastidiosa* (EPPO, 2022b), Methodologies for Sampling of Consignments ISPM 31 (IPPC, 2008), and in D'Onghia *et al.* (2022) and Loconsole *et al.* (2021).

CLIMATIC SUITABILITY RISK MAPS TO ESTIMATE REGIONS FOR POTENTIAL ESTABLISHMENT OF *XYLELLA FASTIDIOSA*

Xylella fastidiosa occurs in a variety of climatic zones, although it is particularly prevalent in the tropics and sub-tropics. The pathogen is also found in areas where climatic conditions are similar to those prevailing in Mediterranean climate zones, such as California, and in various European regions including Corsica in southern Italy, the Côte d'Azur in France, southern Portugal and the Balearic Islands and the Valencian Community in Spain. Records of diseases caused by *X. fastidiosa* also occur from much colder climates, such as New Jersey and Washington in the United States of America and the Niagara Peninsula, southern Ontario, British Columbia, Saskatchewan and Alberta in Canada (EFSA, 2015).

Different approaches have been used to infer areas with favourable climatic conditions for *X. fastidiosa*. Feil and Purcell (2001) used isotherms of winter minimum temperatures to propose the following severity levels and thermal ranges (minimum winter temperatures) for PD in grapevine: severe impact, >4.5°C; moderate, from 1.7 to 4.5°C; occasional, from 1.7 to -1.1°C; and rare, <-1.1°C. However, Anas *et al.* (2008) established areas at risk for PD at much lower temperatures, based on the number of days with minimum temperature below

-12.2ºC or -9.4ºC. Following this criterion of minimum temperatures in winter, most southern European countries have climatic conditions that would allow survival of *X. fastidiosa,* and these regions overlap with the production areas for several crops relevant to the EU economy, including olive and grapevine. All of these regions where *X. fastidiosa* has been described in Europe, including the outbreaks in Italy, France, Portugal and Spain, have climatic conditions that are considered favourable for *X. fastidiosa* survival, demonstrating the validity of this criterion. In contrast, Hoddle (2004) used the CLIMEX model to map the potential distribution of PD, and its Californian vector *Homalodisca vitripennis*, based on data from Feil and Purcell (2001), and concluded that regions with tropical, semi-tropical, temperate and moderate Mediterranean climates are suitable for both organisms. These additional criteria indicate that most wine-growing regions of southern France, central and southern Spain and Italy have climatic conditions suitable for PD. Conversely, low winter temperatures would exclude this disease from vineyard-growing areas in France, northern Spain, and Italy (Hoddle, 2004).

In 2019, the Plant Health Panel of EFSA evaluated the potential for establishment of *X. fastidiosa* in the EU. In that study, Köppen-Geiger climate matching revealed that most parts of the EU could be suitable for establishment of the bacterium, excluding only some higher altitude and northern EU regions. However, analyses using species distribution ensemble modelling identified areas in southern Europe to be at more risk, mainly in southern regions of Portugal, Spain, France, Italy, Greece, Malta, and Cyprus (EFSA, 2019), as well as coastal regions of Morocco, Algeria, Tunisia, Libya, Turkey, Syria, and Israel within the Mediterranean Basin (POnTE project, 2019). These results agree with those of Cardone *et al.* (2022), who evaluates risks of establishment and spread of *X. fastidiosa* in the EU, the Balkans and the Middle East and North Africa regions. They identified Malta, followed by Lebanon, Greece, Portugal, Algeria, Spain, Turkey, Egypt, Morocco, and Albania, as the most vulnerable countries with respect to climate suitability. The North European and Arabian Gulf countries were less vulnerable to the spread of the bacterium. When developing these models at pathogen subspecies level, it has been estimated that *X. fastidiosa* subsp. *multiplex* presents the greatest potential for establishment in the EU, compared with that predicted for subspp. *fastidiosa* and *pauca,* with subsp. *multiplex* able to establish the furthest north in the EU (EFSA, 2019).

Using species distribution ensemble modelling, Arias-Giraldo *et al.* (2022) determined relationships between sample location for *X. fastidiosa* with associated regional environmental variables for Andalusia, Southern Spain; the area with the largest olive production in the world. They analyzed ecological requirements for the three main *X. fastidiosa* subspecies, and estimated that the Eastern part of Andalusia was at the greatest relative risk.

Future directions for this research include development of modelling tools that integrate the main components of *X. fastidiosa* epidemics at different spatial and temporal scales, including the effects of environmental drivers (increased precision of weather and land use, and inclusion of insect vector distribution databases), and of climate change. These models will allow prioritization of surveillance programmes for *X. fastidiosa*, based on risk levels in areas free of the pathogen or with recent outbreaks (Arias-Giraldo *et al.*, 2022).

EPIDEMIOLOGICAL MODELS TO ASSIST OUTBREAK RESPONSE PROGRAMMES FOR *XYLELLA FASTIDIOSA*

After an outbreak of *X. fastidiosa* in a region, official surveys are implemented, initially to delimit the infested area, and then to maintain the pest-free status of a surrounding buffer zone (Commission Implementing Regulation (EU) 2020/1201; EC, 2020). Surveillance is a large proportion of the resources required in outbreak response programmes, so several methods have been developed for optimizing survey efficiency. A sequential adaptive delimiting survey for *X. fastidiosa* with increasing spatial resolution was evaluated, using occurrence data of *X. fastidiosa* in Alicante, Spain (Lázaro *et al.*, 2021). Inspection and sampling intensities were adjusted using an optimization algorithm, considering the results obtained in a previous coarse spatial resolution, with three-phase or two-phase designs. With this sequential adaptive survey strategy, it was possible to delimit the distribution of *X. fastidiosa* in the study area, with substantial reduction of the total number of samples to be collected and tested. With some adjustments, this approach could also be used to optimize delimiting surveys in other *X. fastidiosa* outbreaks in Europe and elsewhere.

Effects of climatic and spatial factors on the geographic distribution of *X. fastidiosa* in Lecce, Italy, and Alicante, Spain, were studied with Bayesian hierarchical models (Cendoya *et al.*, 2020). These two outbreaks represent different, but simple, epidemiological scenarios, one with OQDS, caused by *X. fastidiosa* subsp. *pauca* ST53, in Lecce (Morelli *et al.*, 2021; Saponari *et al.*, 2013), and other with ALS, caused by *X. fastidiosa* subsp. multiplex ST6, in Alicante (Landa *et al.*, 2020; Marco-Noales

et al., 2021). The climate covariates presented low variabilities and were not relevant in the resulting models, so they were not related with the distribution of *X. fastidiosa* in the study areas. These results indicate that climate is not likely to stop the spread of the pathogen from outbreaks to adjacent areas. Furthermore, the models were mainly driven by the spatial components, so probability of *X. fastidiosa* presence substantially increased with proximity to infested area. Overall, these results highlight the importance of implementing control measures based on reduction of inoculum and vector populations, to limit further disease spread from outbreak areas.

In epidemiological models, spatial dependence is often considered as direction-invariant and uniform (i.e., isotropic and stationary). However, these assumptions do not hold when there are elements limiting disease spread. This is the case when geographic barriers are present, or control measures are implemented to contain disease spread. Using the outbreak in Alicante, Spain, as a case study, *X. fastidiosa* occurrence data were analyzed through stationary and nonstationary models (Cendoya *et al*., 2022). The nonstationary models considered a cordon sanitaire surrounding the infested area, where host plants were removed and measures applied to impede disease spread. The mean value of the spatial range of the stationary model indicated that host plants closer than 4 km to the infested area would be at risk of *X. fastidiosa* infections. Consequently, the plant health authority increased by 10 km the minimum width of 2.5 km established by the Regulation (EU) 2020/1201 (EC, 2020) for buffer zones surrounding infested zones (Generalitat Valenciana, 2020). The nonstationary models with the cordon sanitaire resulted in a substantial reduction of the probability of *X. fastidiosa* presence outside the infested area. Nevertheless, these models assume that barriers are completely impermeable to pathogen spread, which is not realistic for those causing most plant diseases. Further methodological research is thus required to consider realistic barriers with different levels of permeability.

AIRBORNE HYPERSPECTRAL AND THERMAL IMAGES FROM REMOTE SENSING TO DETECT *XYLELLA FASTIDIOSA* INFECTED HOST PLANTS

Remote sensing studies on *X. fastidiosa* have manily focused on development of algorithms for early detection of symptoms induced by infections either using unmanned (e.g., Castrignanò *et al*., 2021) or manned (e.g., Zarco *et al*., 2018; 2021b) aerial vehicles. Zarco-Tejada *et al.* (2018) studied the Italian *X. fastidiosa* outbreak, evaluating more than 7000 olive trees using high-resolution hyperspectral and thermal imagery. This revealed that pre-visual detection of *X. fastidiosa*-infected trees was feasible using radiative transfer modelling and spectral plant-trait retrievals from imaging spectroscopy and thermal data. Their study showed that changes in specific plant functional traits detected using hyperspectral and thermal imagery could reveal *X. fastidiosa* infections occurring months before symptoms were visible. Important inputs identified for *X. fastidiosa* detection included spectral ratios in the blue region, plant traits such as leaf anthocyanin and carotenoid pigment content estimated using a radiative transfer model inversion, tree temperature, and estimates of solar-induced chlorophyll fluorescence emission. Later Poblete *et al.* (2020) used high-resolution hyperspectral and thermal imagery to assess performance of spectrally constrained machine-learning algorithms to measuring multispectral bandsets, selected from the original hyperspectral imagery, that were compatible with large-scale monitoring from unmanned platforms and a manned aircraft, as well as the contribution of solar–induced chlorophyll fluorescence (SIF) and the temperature-based Crop Water Stress Index (CWSI) retrieved, respectively, from hyperspectral and thermal imaging. This research demonstrated that large-scale *X. fastidiosa* monitoring could be supported using airborne platforms carrying multispectral and thermal cameras with limited numbers of spectral bands (e.g., six to 12 bands with 10 nm bandwidths), as long as the bands were selected for their sensitivity to distinguish *X. fastidiosa* symptoms.

Although these studies have shown that spectral screening methods can detect non-visual symptoms of early infection by *X. fastidiosa*, and can help prevent pathogen spread, the subtle pathogen-induced host physiological alterations detected by imaging spectroscopy can be entangled with dynamics of abiotic stresses. Zarco-Tejada *et al.* (2021b) used airborne spectroscopy and thermal scanning to monitor different EU areas covering more than one million trees, including different host species (olive and almond), affected by two vascular pathogens (*X. fastidiosa* and *Verticillium dahliae*), and comprising a gradient in water stress levels. This study demonstrated the existence of divergent pathogen- and host-specific spectral pathways, that could disentangle biotic-induced symptoms, and showed that uncoupling biotic and abiotic spectral dynamics diminished uncertainty in *X. fastidiosa* detection to less than 6% across different hosts (almond and olive). The study also assessed these deviating pathways against *V. dahliae,* another vascular pathogen that produces symptoms analogous to *X. fastidiosa*, and showed that the divergent

routes remained pathogen- and host-specific, with detection accuracies exceeding 92% across the pathosystems.

Recent studies have also correlated chemical compounds closely associated with *X. fastidiosa* infection in olive plants (i.e., higher contents of malic acid, formic acid, mannitol and sucrose and lower contents of oleuropein; Jlilat *et al*., 2021) with hyperspectral signals, by identifying specific wavelength packages also associated with bacterial infection. This combined spectro-metabolomic approach may represent a new paradigm for reliable detection of *X. fastidiosa* by remote sensing at the early stages of bacterial infection (Ahmed *et al*., 2021; A.M. D'Onghia, *personnal communication*).

The research described above has shown that early detection of *X. fastidiosa*-induced symptoms is feasible with high-resolution hyperspectral and thermal imagery and physically based plant trait retrievals. New research (Poblete *et al*., *in press*) has demonstrated that high resolution multispectral satellite imagery failed to detect early symptoms of infection, but was able to monitor medium and advanced severity levels at large scales. Results from these studies are essential for implementation of effective management of plant diseases, using airborne, drone and satellite based remote sensing technologies. These imaging methods could also contribute to future operational monitoring of infected crop areas at large scales, well beyond what is possible from field surveys and laboratory analyses (Zarco-Tejada *et al*., 2021a).

MOLECULAR DIAGNOSTIC TESTS FOR EARLY DETECTION AND SUBSPECIES DETERMINATION OF *XYLELLA FASTIDIOSA*

The EPPO Diagnostic protocol PM 7/24 (4) for *X. fastidiosa* is the most complete source for current screening tests available for detection of this bacterium and subspecies determination (EPPO, 2019), which includes a detailed description of each screening test with validation data. Among all the screening tests described, those based on molecular approaches are the most sensitive and rapid for *X. fastidiosa* detection and will be the focus of this review.

Most molecular tests used for *X. fastidiosa* diagnoses are based on conventional end-point PCR or real-time PCR (qPCR). However, for some of the PCR protocols, if the amplicon product is sequenced it can also provide information for subspecies assignation. The Commission Implementing Regulation (EU) 2021/1688 (EC, 2021) indicates which tests from those described in the EPPO Diagnostic protocol PM 7/24 should be used for official surveys and identification of *X. fastidiosa* and its subspecies.

There are several conventional PCR tests for *X. fastidiosa* diagnoses, and one of the most commonly used is that developed by Minsavage *et al.* (1994). This test is based on amplification of the RNA polymerase sigma-factor 70 (*rpo*D). A search on Google Scholar using 'Minsavage and *Xylella fastidiosa*' retrieved more than 800 publication records. This test can also be used to assign *X. fastidiosa* at the subspecies level, by sequencing the *rpo*D amplicon, and comparing its sequence using the Basic Local Alignment Search Tool (BLASTN; http://www.ncbi.nlm.nih.gov/) available at the National Center for Biotechnology Information, against the RefSeq Genome database of *Xylella fastidiosa* (taxid: 2371) as the search organism. This tool also allows a distance tree of results to be obtained, that clusters the target sequence with those *rpo*D sequences included in the reference genomes of different strains of *X. fastidiosa* belonging to different subspecies (Figure 1).

Other conventional PCR diagnostic tests are based on the gene encoding the β-subunit polypeptide of the DNA gyrase (*gyrB*). Although this methodology is not included in the EPPO Diagnostic protocol PM 7/24, it was used for developing a mini sequencing or single-nucleotide primer extension (SNuPE) approach for the multiplex amplification of six *X. fastidiosa gyrB* sequences targeting subspp. *fastidiosa, multiplex* and *sandyi*, and three genotypes within subspecies *pauca* present in the EU territory, and including strains from coffee and citrus from Brazil, and the type isolate infecting olive in Italy (Montes-Borrego *et al*., 2015; Saponari *et al*., 2016).

Several qPCR tests are available and have been validated at different laboratories (EPPO, 2019), including tests described by Harper *et al.* (2010), Francis *et al.* (2006), Ouyang *et al.* (2013), and Li *et al.* (2013). The target sequences for these tests are, respectively, the 16S rRNA processing RimM protein, the hypothetical protein HL gene, the cobalamin synthesis protein-coding gene, and the 16S rRNA. Because of their greater analytical sensitivity than other molecular tests, the use of qPCR is recommended for detection surveys to substantiate pest freedom in areas where *X. fastidiosa* is not known, and for asymptomatic plants (EPPO, 2019). These qPCR tests have been widely used in studies assessing distribution and host range of *X. fastidiosa* in Europe (e.g., Saponari *et al*., 2013; Jacques *et al*., 2016; Moralejo *et al*., 2020; Olmo *et al*., 2021), potential insect vectors of *X. fastidiosa* (e.g., Elbeaino *et al*., 2014; Cavalieri *et al*., 2019; Cunty *et al*., 2020; Moralejo *et al*., 2020; Marco-Noales *et al*., 2021), and in remote sensing studies (e.g., Zarco-Tejada *et al*., 2018; Poblete *et al*., 2020; Zarco-Tejada *et al*., 2021b; Camino *et al*., 2022) to outline examples of their usefulness.

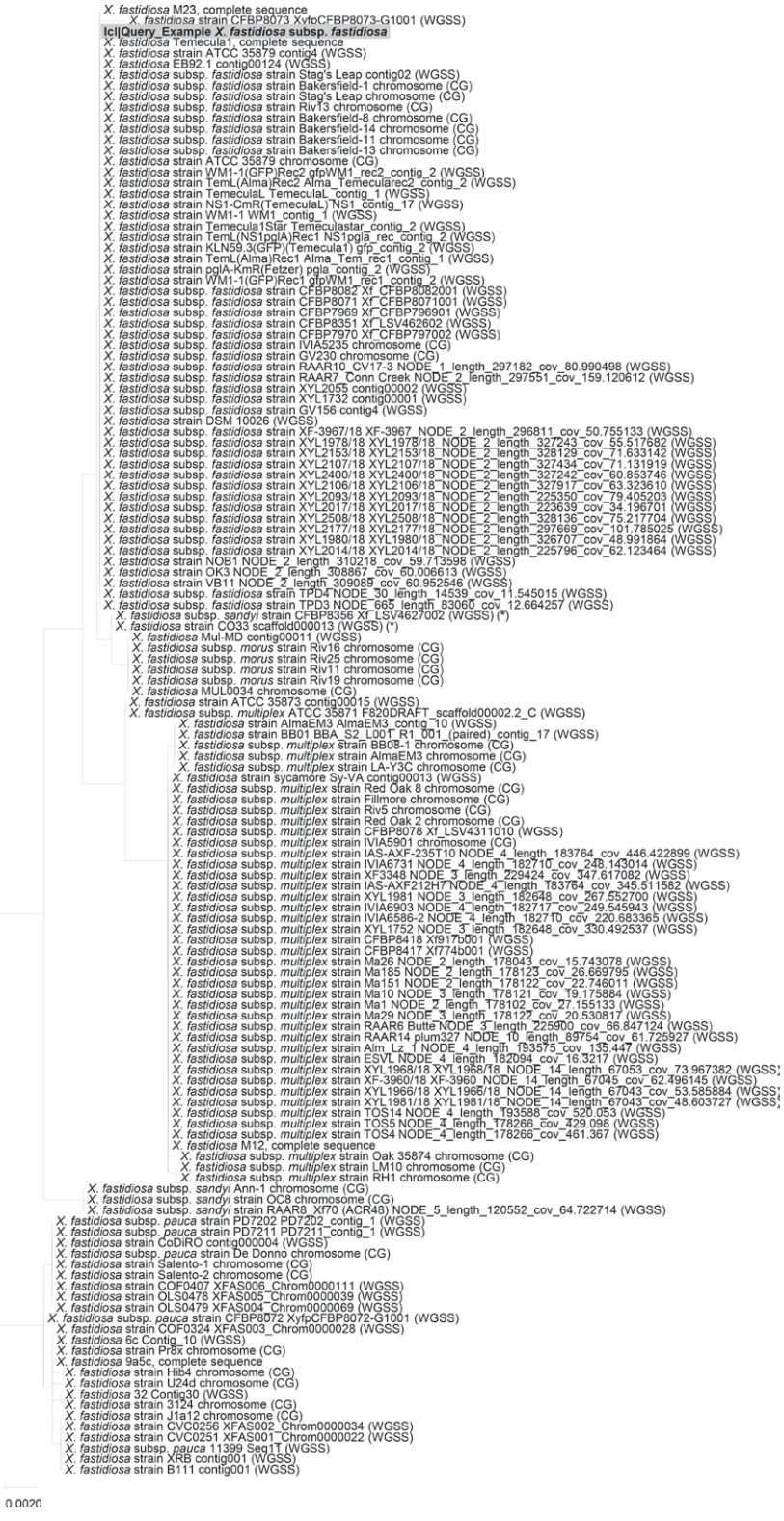

Figure 1. Phylogenetic distance tree of RNA polymerase sigma-factor 70 (*rpo*D) partial sequences obtained after BLAST analysis (http://www.ncbi.nlm.nih.gov/) of a query sequence against the RefSeq Genome database of *Xylella fastidiosa* (taxid: 2371). The different clusters correlate with main *X. fastidiosa* subspecies. lcl|Query= Represents an example of a query made for the *rpo*D sequence of a *X. fastidiosa* subsp. *fastidiosa* strain. (CG)= Complete Genome; (WGSS)= Whole Genome Shotgun Sequence. (*)= recombinant subspecies *morus/sandyi*.

Where a positive result is obtained in areas outside of demarcated areas (i.e., pest-free areas), the Commission Implementing Regulation (EU) 2020/1201 (EC, 2020) indicated that presence of *X. fastidiosa* must be confirmed by two tests targeting different parts of the bacterial genome, as recommended by EPPO (2019). To facilitate diagnosis of *X. fastidiosa* with two tests, Bonants *et al.* (2019) implemented a triplex qPCR test based on the primers and probes included in Harper qPCR and Ouyang qPCR tests, and an additional primer pair and probe for internal controls. This test facilitates two diagnostic tests simultaneously, saving time and resources, and can provide the same analytical sensitivity as each test independently (Bonants *et al.*, 2019).

Results from test performance studies (TPS) and proficiency tests (PT) performed in the frameworks of XF-ACTORS and POnTE, Euphresco PROMODE projects, have compared the performance characteristics of qPCR tests when used with plant or insect mock-inoculated matrices, and these results are available at the EPPO Database on Diagnostic Expertise (https://dc.eppo.int; EPPO, 2023). Results from these validation tests have indicated that all the qPCR diagnostic protocols were robust, and were suitable for the diagnoses of *X. fastidiosa* in plant and insect materials. However, although most qPCR protocols produced good performance values, their analytical sensitivity was slightly different when using mock-inoculated samples. A recent study has also shown greater analytic sensitivity of the Harper qPCR test compared to the Francis qPCR test, when using DNA samples extracted from naturally infected almond trees (Anguita-Maeso *et al.*, 2021).

For *X. fastidiosa* subspecies assignment, the Commission Implementing Regulation (EU) 2020/1201 (EC, 2020) determines Multilocus Sequence Type (MLST) analysis to be used (Yuan *et al.*, 2010), especially for new records (i.e., for a new outbreak or new hosts). This test is based on amplification and sequencing of seven housekeeping gene (HKG) loci (*cys*G, *glt*T, *hol*C, *leu*A, *mal*F, *nuo*L, *pet*C). Analysis of *rpo*D and *mal*F or *cys*G and *mal*F sequences have been shown to be sufficient for assignment of sample pathogens to subspecies (EPPO, 2019); whereas the sequences of the seven loci are needed to assign samples into STs. Originally, MSLT analysis was designed to be used with DNA extracted from *X. fastidiosa* pure cultures (Yuan *et al.*, 2010), and when used with plant DNA samples is partly efficient. To improve sensitivity, Cesbron *et al.* (2020) developed a direct nested-MLST assay for plant and insect extracted DNA, based on the same seven targeted HKG loci as those used in the Yuan *et al.* (2010) test. This nested-MLST assay improved detection threshold by 100 to 1000 times, compared to conventional MLST. Using this nested-MLST assay, plants that were previously not considered hosts (giving high or inconclusive Ct values in qPCR assays) tested positive, and novel alleles were revealed in France. In samples from Spanish outbreaks, the nested-MLST assay allowed to identify the *X. fastidiosa* subspecies or ST infecting new hosts in Europe at that time (Cesbron *et al.* 2020). This nested-MLST assay has been used to type *X. fastidiosa* positive samples to the subspecies and ST level in the outbreaks in Spain. These include three *X. fastidiosa* subspecies and four STs in the Balearic Islands: *X. fastidiosa* subsp. *fastidiosa* ST1 and *X. fastidiosa* subsp. *multiplex* ST7 in Mallorca, *X. fastidiosa* subsp. *pauca* ST80 in Ibiza, and *X. fastidiosa* subsp. *multiplex* ST81 in Mallorca and Menorca (Olmo *et al.*, 2021). Only a single subspecies and ST (i.e., *X. fastidiosa* subsp. *multiplex* ST6) was identified in the outbreak in Alicante (Marco-Noales *et al.*, 2021).

Some qPCR tests have been developed to specifically detect subspecies of *X. fastidiosa* (e.g., the tests of Burbank *et al.*, 2018; Dupas *et al.* 2019; Hodgetts *et al.*, 2021). These tests are based on Taqman probes, designed to specifically and simultaneously target one or several *X. fastidiosa* subspecies. The advantage of these protocols is, while the presence of the bacterium is detected, even at low concentration, the subspecies is also defined. The Burbank qPCR test was used by Moralejo *et al.* (2020) to track the *X. fastidiosa* DNA inside growth rings of infected almond trees, through dendrochronological analysis. The protocol allowed differentiation between subsp. *fastidiosa* and *multiplex* in rings of 25 trees, with nine infected by subsp. *fastidiosa*, and 19 infected by subsp. *multiplex,* and three trees had mixed infections. This qPCR test combined with the conventional and nested-MLST tests (described above) enabled dating infections back to 1998 for *X. fastidiosa* subsp. *fastidiosa* ST1, and before 2000 for *X. fastidiosa* subsp. *multiplex* ST81 (Moralejo *et al.*, 2020), indicating that the bacterium was introduced to the Balearic Islands earlier than previously thought.

Time and portability are also important factors in pathogen diagnoses, especially for quarantine plant pathogens (Aglietti *et al.*, 2019). Isothermal nucleic acid amplification tests have been developed for *X. fastidiosa* field diagnoses. These included loop-mediated isothermal amplification (LAMP) based on primers developed by Harper *et al.* (2010) that were modified by Yaseen *et al.* (2015), and the AmplifyRP® XRT+ test, using isothermal amplification based on recombinase polymerase amplification (RPA) (Kersting *et al.*, 2014), based on the protocol of Li *et al.* (2016). Both tests have kits and specific portable devices that are commercially available,

but other equipment can also be used. For instance, the AmplifyRP® XRT+ test uses the battery powered AmpliFire® Portable Fluorometer device, that is easy to transport, and does not require DNA extraction, since the test can be performed with the crude plant macerate and the amplification takes 20 min. This test is easy to use by untrained laboratory staff, and is well adapted to the field for preliminary on site screening, as it requires no particular expertise (Cesbron *et al*., 2022).

A constraint of these tests is that detection limits are greater than for qPCR tests. Nevertheless, negative or doubtful results can be verified with another, more sensitive test. During a field campaign in Mallorca, Spain, almond trees in 14 orchards under rainfed and irrigated conditions were visually scored for the presence of ALS. A total of 356 symptomatic and symptomless trees were sampled and analyzed using the AmplifyRP® XRT+ test and the AmpliFire® device by two operators in less of 5 days (Camino *et al*., 2022). When comparing results of this test with that of the Harper qPCR test using the same almond plant branch samples, 92.8% agreement for infected samples was obtained for the two methods. The samples that were negative by the AmplifyRP® XRT+ test showed cycle thresholds (Cts) >31 in the Harper qPCR test (Landa *et al*., unpublished).

Digital PCR (dPCR) is an innovative PCR tool based on partitioning of PCR reagents and DNA samples into thousands of droplets or microchambers (depending on thermocycler brand), that allows increased precision, sensitivity and absolute quantification without requirements for reference samples or standard curves. Detection of phytopathogenic bacteria by droplet PCR has provided successful results for pathogen diganoses, due to its detection efficiency at low pathogen concentrations and tolerance to PCR inhibitors (Dreo *et al*. 2014). Dupas *et al*. (2019) developed a droplet ddPCR protocol based on the Harper qPCR test. Both protocols showed the same detection limits for olive, *Polygala myrtifolia* and *Rosmarinus officinalis*, but the Harper qPCR test allowed better detection of 0.5 log for *Lavandula angustifolia*, and droplet dPCR allowed better detection of 0.5 log for *Quercus ilex*.

Investigation of pathogen strain origins in a new disease outbreaks requires whole genome sequencing (WGS) of pure bacterial cultures to resolve phylogenetic reconstruction. This is a challenge for *X. fastidiosa* due to its fastidious nature. For all the available nucleic acid based amplification methods described above for the detection of *X. fastidiosa,* the target sequence is a single locus, making the assays prone to false-positive or false-negative results (Bonants *et al*., 2019). High throughput Next Generation Sequencing (NGS) technologies allow sequencing of total DNA in samples, potentially providing detection of *X. fastidiosa* and characterization to subspecies and strain levels, without requirement for pathogen cultivation. NGS based on Illumina (Bonants *et al*., 2019; Román-Reyna *et al*., 2022) or Oxford Nanopore technologies (Johnson *et al*., 2022) have been explored for fast detection and identification of *X. fastidiosa*. The potential advantages and disadvantages of both of these technologies are beyond the scope of this review.

Using Illumina sequencing, Bonants *et al.* (2019) analyzed DNA extracts, by WGS, for presence of *X. fastidiosa* in artificially inoculated host plants and from naturally infected plants sampled or intercepted in different European countries. In all samples, even in samples with low infection levels, some DNA reads specific for *X. fastidiosa* were detected, and in several cases the pathogen could be identified to the subspecies level. Only for one sample was the whole genome assembled and the ST determined. Samples in which more *X. fastidiosa* genomic information was obtained corresponded to those with low Ct values (i.e., high *X. fastidiosa* titres). Thus, alinear relationship is found between the Log number of *X. fastidiosa* reads obtained by NGS and the Cts from Harper and Ouyang qPCR tests, and the time for positivity in a LAMP assay (Figure 2). Similarly, Anguita-Maeso *et al.* (2021) found a linear relationship between the Ct values obtained for the Harper and Francis qPCR tests and the Log of *X. fastidiosa* reads. Román-Reyna *et al.* (2021) developed a metagenomics pipeline using in-house short read Illumina sequencing to analyze samples from different plant species originating from Europe and the United States, and naturally infected by *X. fastidiosa*. They identified *X. fastidiosa* to the strain level in single and mixed infected plant samples at concentrations of 1 pg of bacterial DNA per gram of plant tissue, and in samples previously considered inconclusive when using qPCR (Ct >35), the protocol was able to confirm infection by *X. fastidiosa*. These results indicate that using the NGS approach, only in cases where DNA has been extracted from highly infected material, and where high genome coverage is used during sequencing, is possible to identify *X. fastidiosa* at the strain level.

To overcome this limitation, we have developed a Targeted Sequence Capture Enrichment (TSCE), in combination with High Throughput Sequencing (HTS). This uses an Illumina platform to provide adequate bacterial genome information for identification of *X. fastidiosa* at strain level (Velasco-Amo *et al*., 2021). Results indicated that although <0.25% of *X. fastidiosa* reads were detected by direct WGS of host DNA, this was increased by 41–73% when using the TSCE-HTS approach, for indi-

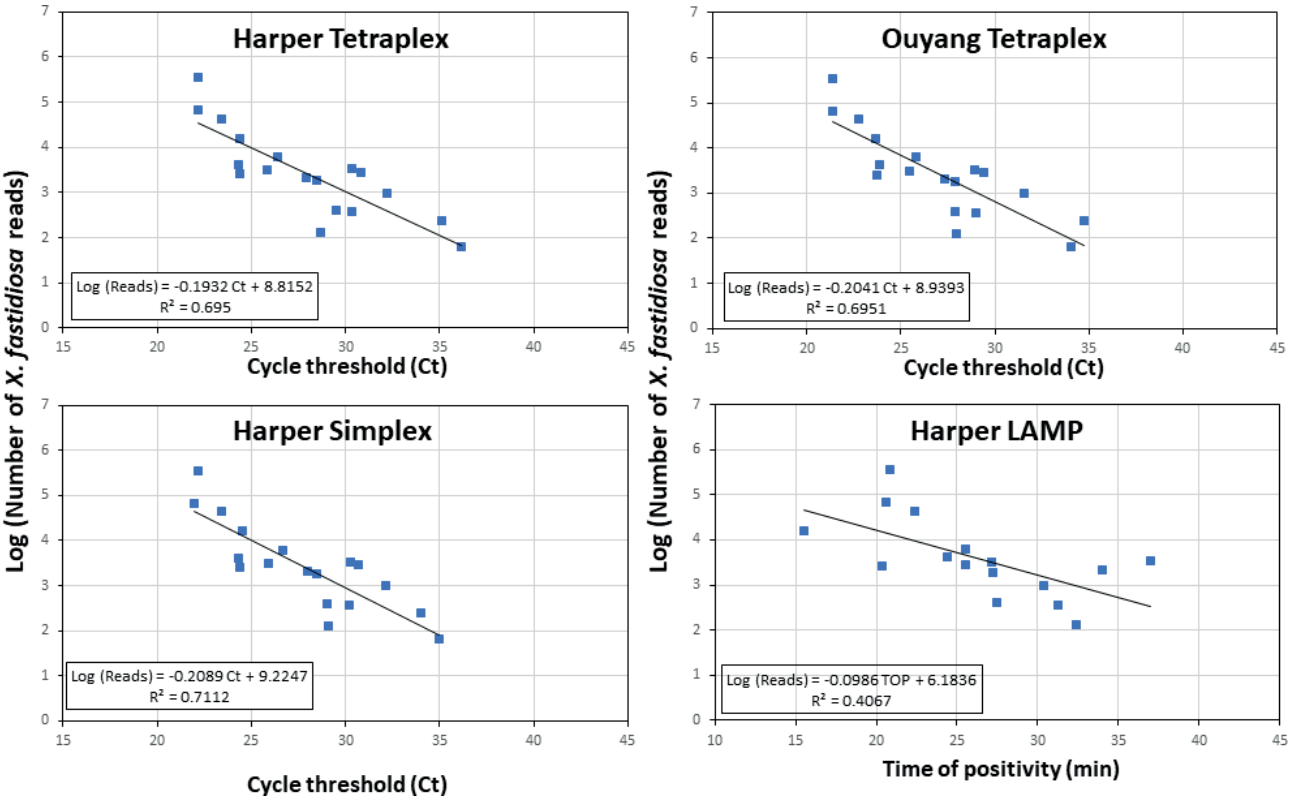

Figure 2. Linear regressions between Log [*Xylella fastidiosa* reads] obtained by next generation sequencing (NGS) and Ct values from quantitative polymerase chain reaction (qPCR) protocols of Ouyang tetraplex and Harper tetraplex (Bonants *et al.*, 2019), Harper Simplex (Harper *et al.* 2010), and LAMP test based in Harper *et al.* (2010). Data were obtained from Table 7 of Bonats *et al.* (2019), and represent the mean Ct value obtained for each sample.

vidual samples or in mixtures of up to four plant samples. The protocol was also validated using a range of insect and plant samples from different naturally infected host plants, and with levels of *X. fastidiosa* ranging from very high (CT >20) to close to the detection limit for Harper qPCR assay. More importantly, 80–100% of the 140 target sequences used to design the baits were captured, which allowed phylogenetic reconstruction of the *X. fastidiosa* strains infecting the samples, and identifying these at strain level (Landa *et al.*, 2021). This methodology may be useful for studies of *X. fastidiosa* introductions at outbreak stages, since a limited number of genetic markers do not provide sufficient phylogenetic resolution to determine dispersal paths or relationships among strains that are of biological and quarantine relevance.

ACKNOWLEDGEMENTS

Some of the research presented in this review was funded by the following projects: BeXyl (Beyond *Xylella*, Integrated Management Strategies for Mitigating *Xylella fastidiosa* impact in Europe; grant ID 101060593, from European Union's Horizon Europe 'Food, Bioeconomy Natural Resources, Agriculture and Environment' Programme); XF-ACTORS (*Xylella fastidiosa* Active Containment Through a Multidisciplinary-Oriented Research Strategy; grant 727987, from the European Union's Horizon 2020 Framework Research Programme); POnTE (Pest Organisms Threatening Europe; grant ID 635646, from the European Union's Horizon 2020 Framework Research Programme); E-RTA2017-00004-C06-02 (Desarrollo de estrategias de erradicación, contención y control de *X. fastidiosa* en España) from 'Programa Estatal de I+D+I Orientada a los Retos de la Sociedad of the Spanish Government AEI-INIA Spain' and the Spanish Olive Oil Interprofesional; Project P18-RT-4184 from Junta de Andalucia and the European Regional Development Fund; and the Intramural Project 201840E111 and the Thematic Interdisciplinary Platform on *X. fastidiosa* (PTI Sol-Xyl) from CSIC.

LITERATURE CITED

Aglietti C., Luchi N., Pepori A.L., Bartolini P., Pecori F., … Santini A., 2019. Real-time loop-mediated isothermal amplification: an early-warning tool for quarantine plant pathogen detection. *AMB Express* 9: 50. https://doi.org/10.1186/s13568-019-0774-9

Ahmed E. M. F. M. H., Musio B., Gualano S., Santoro F., Latronico M., … Gallo V., 2021. Early-detection of *Xylella fastidiosa* in olive trees by hyperspectral reflectance and non-targeted metabolomics. In: *Book of abstracts-Part IV, XXVII Congresso Nazionale della Società Chimica Italiana "La chimica guida lo sviluppo sostenibile"*, September 14-23, 2021 (online event): TEC OR026.

Almeida R.P.P., 2016. Can Apulia's olive trees be saved? *Science* 353: 346–348. https://doi.org/10.1126/science.aaf9710

Anas O., Brannen P., Sutton T., 2008. The effect of warming winter temperatures on the severity of Pierce's disease in the southeastern United States. *Plant Health Progress*: 6, https://doi.org/10.1094/PHP-2008-0718-01-RS.

Anguita-Maeso M., Ares-Yebra A., Haro C., Román-Écija M., Olivares-García C., … Landa B.B., 2021. *Xylella fastidiosa* infection reshapes microbial composition and network associations in the xylem of almond trees. *Frontiers in Microbiology* 13:866085. https://doi.org/10.3389/fmicb.2022.866085

Arias-Giraldo L.F., Landa B.B., Navas-Cortés J.A., 2022. Modelling potential climatic suitability for olive vascular diseases in southern Spain. In: L. Mugnai, "*Abstracts of invited, oral and poster papers presented at the 16th Congress of the Mediterranean Phytopathological Union*, April 4–8, May 2022, Limassol, Cyprus". *Phytopathologia Mediterranea* 61(1): 181–239. https://doi.org/1036253/phyto-13613

Bonants P., Griekspoor Y., Houwers I., Krijger M., van der Zouwen P., …. van der Wolf., 2019. Development and evaluation of a triplex taqMan assay and Next-Generation Sequence analysis for improved detection of *Xylella* in plant material. *Plant Disease* 103: 645–655. https://doi.org/10.1094/PDIS-08-18-1433-RE

Burbank L.P., Ortega B.C., 2018. Novel amplification targets for rapid detection and differentiation of *Xylella fastidiosa* subspecies *fastidiosa* and *multiplex* in plant and insect tissues. *Journal of Microbiological Methods* 155: 8–18. https://doi.org/10.1016/j.mimet.2018.11.002

Camino C., Araño K., Berni J.A., Dierkes H., Trapero-Casas J.L., … Beck P.S.A., 2022. Detecting *Xylella fastidiosa* in a machine learning framework using Vcmax and leaf biochemistry quantified with airborne hyperspectral imagery. *Remote Sensing of Environment* 282: 113281. https://doi.org/10.1016/j.rse.2022.113281

Cardone G., Digiaro M., Djelouah K., Frem M., Rota C., … Fucilli V., 2022. Socio-economic risks posed by a new plant disease in the Mediterranean basin. *Diversity* 14(11): 975. https://doi.org/10.3390/D14110975

Castrignanò A., Belmonte A., Antelmi I., Quarto R., Quarto F., ...Nigro F., 2021. Semi-automatic method for early detection of *Xylella fastidiosa* in olive trees using UAV multispectral imagery and geostatistical discriminant analysis. *Remote Sensing* 13: 14. https://doi.org/10.3390/rs13010014

Cavalieri V., Altamura G., Fumarola G., di Carolo M., Saponari M., …. Dongiovanni C., 2019. Transmission of *Xylella fastidiosa* subspecies *pauca* sequence type 53 by different insect species. *Insects* 10: 324. https://doi.org/10.3390/insects10100324

Cendoya M., Martínez-Minaya J., Dalmau V., Ferrer A., Saponari M., … Vicent A., 2020. Spatial Bayesian modeling applied to the surveys of *Xylella fastidiosa* in Alicante (Spain) and Apulia (Italy). *Frontiers in Plant Science* 11: 1204. https://doi.org/10.3389/fpls.2020.01204

Cendoya M., Hubel A., Conesa D., Vicent, A., 2022. Modeling the spatial distribution of *Xylella fastidiosa*: A nonstationary approach with dispersal barriers. *Phytopathology* 112: 1036–1045. https://doi.org/10.1094/PHYTO-05-21-0218-R

Cesbron S., Dupas E., Beaurepère Q., Briand M., Montes-Borrego M., … Jacques M.-A., 2020. Development of A Nested-MultiLocus Sequence Typing approach for a highly sensitive and specific identification of *Xylella fastidiosa* subspecies directly from plant samples. *Agronomy* 10: 1099. https://doi.org/10.3390/agronomy10081099

Cesbron S., Dupas E., Jacques M.-A., 2022. Evaluation of the AmplifyRP® XRT+ kit for the detection of Xylella fastidiosa by 2 Recombinase Polymerase Amplification (RPA). *PhytoFrontiers* in press, First look. https://doi.org/10.1094/PHYTOFR-03-22-0025-FI

Cunty A., Legendre B., de Jerphanion P., Juteau V., Forveille A., … Poliakoff F., 2020. *Xylella fastidiosa* subspecies and sequence types detected in *Philaenus spumarius* and in infected plants in France share the same locations. *Plant Pathology* 69:1798–1811. https://doi.org/10.1111/ppa.13248

D'Onghia A.M., Santoro F., Minutillo S.A., Frasheri D., Gallo M., … Valentini F., 2022. Optimisation of sampling and testing for asymptomatic olive trees infected by *Xylella fastidiosa* in Apulia region, Italy. *Phyto-*

pathologia Mediterranea 61(3): 439–449. https://doi.org/10.36253/phyto-13732

Dreo T., Manca P., Živa R., Jernej P., Mojca M., … Gruden K., 2014. Optimising droplet digital PCR analysis approaches for detection and quantification of bacteria: a case study of fire blight and potato brown rot. *Analytical and Bioanalytical Chemistry* 406 (26): 6513–6528. https://doi.org/10.1007/s00216-014-8084-1

Dupas E., Legendre B., Olivier V., Poliakoff F., Manceau C., Cunty A., 2019. Comparison of real-time PCR and droplet digital PCR for the detection of *Xylella fastidiosa* in plants. *Journal of Microbiological Methods* 162: 86–95. https://doi.org/10.1016/j.mimet.2019.05.010

EFSA, 2015. Scientific Opinion on the risk to plant health posed by *Xylella fastidiosa* in the EU territory, with the identification and evaluation of risk reduction options. *EFSA Journal* 13: 3989, 262 pp. https://10.2903/j.efsa.2015.3989

EFSA, 2019. Update of the Scientific Opinion on the risks to plant health posed by *Xylella fastidiosa* in the EU territory. *EFSA Journal*, 17(5), e05665. https://doi.org/10.2903/j.efsa.2019.5665

EFSA, 2022. Scientific Report on the update of the *Xylella* spp. host plant database – systematic 203 literature search up to 30 June 2021. *EFSA Journal*, 20, 67pp. https://doi.org/10.2903/j.efsa.2022.7039

Elbeaino T., Yaseen T., Valentini F., Ben Moussa I.E., Mazzoni V., D'Onghia A.M., 2014. Identification of three potential insect vectors of *Xylella fastidiosa* in southern Italy. *Phytopathologia Mediterranea* 53: 328–332. https://doi.org/10.14601/Phytopathol_Mediterr-14113

EPPO 2023. EPPO Database on Diagnostic Expertise. Available at: https://dc.eppo.int/ (accessed January 3, 2023).

EPPO, 2019. PM 7/24 (4) *Xylella fastidiosa*. *EPPO Bulletin* 49: 175-227. https://doi.org/10.3390/plants11121562

EPPO, 2022a. PM 3/81 (3) Inspection of consignments for *Xylella fastidiosa*. *EPPO Bulletin* 00: 1–13. https://doi.org/10.1111/epp.12880

EPPO, 2022b. PM 3/82 (3) Inspection of places of production for *Xylella fastidiosa*. *EPPO Bulletin* 00: 1–15. https://doi.org/10.1111/epp.12882

European Commission, 2020. Commission implementing regulation (EU) 2020/1201 of 14 August 2020 of the European Parliament and of the council as regards measures to prevent the introduction into and the spread within the union of *Xylella fastidiosa* (Wells *et al.*). Available online: https://eur-lex.europa.eu/legal-content/en/TXT/?uri=CELEX:32020R1201 (accessed December 31, 2022).

European Commission, 2021. Commission implementing regulation (EU) 2021/1688 of 20 September 2021 Commission Implementing Regulation (EU) 2021/1688 of 20 September 2021 amending Implementing Regulation (EU) 2020/1201 as regards the lists of host plants and specified plants, and the tests for the identification of *Xylella fastidiosa*. Available online: https://eur-lex.europa.eu/legal-content/EN/TXT/?uri=CELEX%3A32021R1688 (accessed December 31, 2022).

Feil H., Purcell A.H., 2001. Temperature-dependent growth and survival of *Xylella fastidiosa* in vitro and in potted grapevines. *Plant Disease* 85 (12): 1230–1234. https://doi.org/10.1094/PDIS.2001.85.12.1230

Francis M., Lin H., Cabrera-La Rosa J., Doddapaneni H., Civerolo E.L., 2006. Genome-based PCR primers for specific and sensitive detection and quantification of *Xylella fastidiosa*. *European Journal of Plant Pathology* 115: 203–213. https://doi.org/10.1007/s10658-006-9009-4

Generalitat Valenciana, 2020. Plan de acción frente a *Xylella fastidiosa* en la Comunitat Valenciana. Dirección general de Agricultura, Ganadería y Pesca. Servicio de Sanidad Vegetal. Available online: https://agroambient.gva.es/documents/163214705/163847802/Plan+acción+Diciembre+2020_firmado.pdf/856ce97f-f733-4ea8-8095-88149f6e78e7

Harper S.J., Ward L.I., Clover G.R.G., 2010 Development of LAMP and real-time PCR methods for the rapid detection of *Xylella fastidiosa* for quarantine and field applications. *Phytopathology* 100: 1282–1288. 10. https://doi.org/1094/PHYTO-06-10-0168

Hoddle M.S., 2004. The potential adventive geographic range of glassy-winged sharpshooter, *Homalodisca coagulata* and the grape pathogen *Xylella fastidiosa*: implications for California and other grape growing regions of the world. *Crop Protection* 23: 691–699. https://doi.org/10.1016/j.cropro.2003.11.017

Hodgetts J., Glover R., Cole J., Hall J., Boonham N., 2021. Genomics informed design of a suite of real-time PCR assays for the specific detection of each *Xylella fastidiosa* subspecies. *Journal of Applied Microbiology* 131: 855–872. https://doi.org/10.1111/jam.14903

IPPC, 2008. Methodologies for sampling of consignments (ISPM no. 31). Rome: International Plant Protection Convention, FAO.

Jacques M.A., Denancé N., Legendre B., Morel E., Briand M., … Crouzillat D., 2016. New coffee plant-Infecting *Xylella fastidiosa* variants derived via homologous recombination. *Applied and Environmental Microbiology* 82(5): 1556–1568. https://doi.org/10.1128/aem.03299-15

Jlilat A., Gallo V., Ragone R., Gualano G., Santoro F., … D'Onghia A.M., 2021. A non-targeted metabolomics study on *Xylella fastidiosa* infected olive plants grown under controlled conditions. *Scientific Reports* 11: 1070. https://doi.org/10.1038/s41598-020-80090-x

Johnson M.A., Liu H., Bush E., Sharma P., Yang S., … Vinatzer B.A., 2022. Investigating plant disease outbreaks with long-read metagenomics: sensitive detection and highly resolved phylogenetic reconstruction applied to *Xylella fastidiosa*. *Microbial Genomics* 8(5). https://doi.org/10.1099/mgen.0.000822

Kersting S., Rausch V., Bier F.F., von Nickisch-Rosenegk M., 2014. Rapid detection of *Plasmodium falciparum* with isothermal recombinase polymerase amplification and lateral flow analysis. *Malaria Journal* 13: 99. https://doi.org/10.1186/1475-2875-13-99

Landa B.B., Castillo A.I., Giampetruzzi A., Kahn A., Román-Écija M., … Almeida R.P., 2020. Emergence of a plant pathogen in Europe associated with multiple intercontinental introductions. *Applied and Environmental Microbiology* 86: e01521-19. https://doi.org/10.1128/AEM.01521-19

Landa B.B., 2022. Current situation of *Xylella fastidiosa* impacts in Spain: ongoing research initiatives to understand and tackle this pathogen. In: L. Mugnai, "*Abstracts of invited, oral and poster papers presented at the 16th Congress of the Mediterranean Phytopathological Union,* April 4–8, May 2022, Limassol, Cyprus". *Phytopathologia Mediterranea* 61(1): 181–239. https://doi.org/1036253/phyto-13613

Lázaro E., Sesé M., López-Quílez A., Conesa D., Dalmau V., …Vicent A., 2021. Tracking the outbreak: an optimized sequential adaptive strategy for *Xylella fastidiosa* delimiting surveys. *Biological Invasions* 23: 3243–3261. https://doi.org/10.1007/s10530-021-02572-x

Li R., Russell P., Mcowen N., Davenport B., Zhang S., 2016. Development of a rapid and reliable isothermal AmplifyRP diagnostic assay for specific detection of *Xylella fastidiosa*. *Phytopathology* 106: 109.

Li W., Teixeira D.C., Hartung J.S., Huang Q., Duan Y., … Levy L., 2013. Development and systematic validation of qPCR assays for rapid and reliable differentiation of *Xylella fastidiosa* strains causing citrus variegated chlorosis. *Journal of Microbiological Methods* 92: 79–89. https://doi.org/10.1016/j.mimet.2012.10.008

Loconsole G., Zicca S., Manco L., El Hatib O., Altamura G., … Saponari M., 2021. Diagnostic Procedures to Detect *Xylella fastidiosa* in Nursery Stocks and Consignments of Plants for Planting. *Agriculture* 11: 922. https://doi.org/10.3390/agriculture11100922

Marco-Noales E., Barbé S., Monterde A., Navarro I., Ferrer A., … Roselló M., 2021. Evidence that *Xylella fastidiosa* is the causal agent of almond leaf scorch disease in Alicante, mainland Spain (Iberian Peninsula). *Plant Disease* 105: 3349–3352. https://doi.org/10.1094/PDIS-03-21-0625-SC

Minsavage G.V., Thompson C.M., Hopkins D.L., Leite R.M.V.B.C., Stall R.E., 1994. Development of a polymerase chain reaction protocol for detection of *Xylella fastidiosa* in plant tissue. *Phytopathology* 84:456–461. https://doi.org/10.1094/Phyto-84-456

Montes-Borrego M., Lopes J.R., Jiménez-Díaz R.M., Landa B.B., 2015. Combined use of a new SNP-based assay and multilocus SSR markers to assess genetic diversity of *Xylella fastidiosa* subsp. *pauca* infecting citrus and coffee plants. *International Microbiology* 18: 13–24. https://doi.org/10.2436/20.1501.01.230

Moralejo E., Gomila M., Montesinos M., Borràs D., Pascual A., … Olmo D., 2020. Phylogenetic inference enables reconstruction of a long-overlooked outbreak of almond leaf scorch disease (*Xylella fastidiosa*) in Europe. *Communications Biology* 3: e560. https://doi.org/10.1038/s42003-020-01284-7

Morelli M., García-Madero J.M., Jos Á.; Saldarelli P., Dongiovanni C., … Compant S., 2021. *Xylella fastidiosa* in Olive: A Review of Control Attempts and Current Management. *Microorganisms* 9: 1771. https://doi.org/10.3390/microorganisms908177 1

Olmo D., Nieto A., Borràs D., Montesinos M., Adrover F., …Landa B.B., 2021. Landscape Epidemiology of *Xylella fastidiosa* in the Balearic Islands. *Agronomy* 11: 473–488. https://doi.org/10.3390/agronomy11030473

Ouyang P., Arif M., Fletcher J., Melcher U., Ochoa Corona F.M., 2013. Enhanced reliability and accuracy for field deployable bioforensic detection and discrimination of *Xylella fastidiosa* subsp. *pauca*, causal agent of citrus variegated chlorosis using Razor Ex technology and TaqMan Quantitative PCR. *PLoS ONE* 8: e81647. https://doi.org/10.1371/journal.pone.0081647

Poblete T., Camino C., Beck P.S.A., Hornero A., Kattenborn T., … Zarco-Tejada P.J., 2020. Detection of *Xylella fastidiosa* infection symptoms with airborne multispectral and thermal imagery: Assessing bandset reduction performance from hyperspectral analysis. ISPRS *Journal of Photogrammetry and Remote Sensing* 162: 27–40. https://doi.org/10.1016/j.isprsjprs.2020.02.010

POnTE, 2019. Pest Organisms Threatening Europe H2020 Grant Agreement Number: 635646. Deliverable D8.1. Selection of the most appropriate modelling method to estimate the potential distribution of pests and diseases. 85 pp. Available at https://cordis.europa.eu/project/id/635646/results.

Román-Reyna V., Dupas E., Cesbron S., Marchi G., Campigli S., …. Jacobs J.M., 2022. Metagenomic sequencing for identification of *Xylella fastidiosa* from leaf samples. *mSystems* 6:e0059121. https://doi.org./10.1128/mSystems.00591-21

Sanchez B., Barreiro J., Soto I., Rodriguez E., 2019. The impact indicator for priority pests (I2P2): a tool for ranking pests according to regulation (EU) 2016/2031. Maastricht: Europen Union. https://doi.org/10.2760/585182

Saponari M., Boscia D., Nigro F., Martelli G.P., 2013. Identification of DNA sequences related to *Xylella fastidiosa* in oleander, almond and olive trees exhibiting leaf scorch symptoms in Apulia (Southern Italy). *Journal of Plant Pathology* 95: 668.

Saponari M., D'attoma G., Montes- Borrego M., De La Fuente L., Loconsole G., Landa B.B., 2016. Rapid screening tests for differentiating *Xylella fastidiosa* isolates. *22th Congress of the Italian Society of Plant Pathology*, 19–22 September 2016, Roma (Italy). https://doi.org/10.5281/zenodo.583428

Velasco Amo M.P., Arias-Giraldo L. F., Marín Sanz J. A., Fernández Soria V. M., Juan Imperial J., Landa B.B., 2021. Assessing genome-wide diversity in Xylella fastidiosa through target enrichment via hybridization-based capture from natural host plant and insect samples. In: *Book of Abstracts of the 3rd European conference on* Xylella fastidiosa *and XF-ACTORS final meeting*, 61, April 26-30, On-line event, 2021.

Yaseen T., Drago S., Valentini F., Elbeaino T., Stampone G., … D'Onghia, 2015 On-site detection of *Xylella fastidiosa* in host plants and in "spy insects" using the real-time loop-mediated isothermal amplification method. *Phytopathologia Mediterranea* 54: 488–496.

Yuan X., Morano L., Bromley R., Spring-Pearson S., Stouthamer R., Nunney L., 2010 Multilocus Sequence Typing of *Xylella fastidiosa* Causing Pierce's Disease and Oleander Leaf Scorch in the United States. *Phytopathology* 100: 601–611. https://doi.org/10.1094/PHYTO-100-6-0601

Zarco-Tejada P.J., Camino C., Beck P.S.A., Calderon R., Hornero A., … Navas-Cortes, J.A., 2018. Previsual symptoms of *Xylella fastidiosa* infection revealed in spectral plant-trait alterations. *Nature Plants* 4(7): 432–439. https://doi.org/10.1038/s41477-018-0189-7

Zarco-Tejada P.J., Poblete T., Camino C., Calderon R., Hornero A., … Navas-Cortes, J.A., 2021a. Progress and achievements on the early detection of *Xylella fastidiosa* infection and symptom development with hyperspectral and thermal remote sensing imagery. In: *Book of Abstracts of the 3rd European conference on* Xylella fastidiosa *and XF-ACTORS final meeting*, page 54, April 26-30, On-line event, 2021.

Zarco-Tejada P.J., Poblete T., Camino C., Gonzalez-Dugo V., Calderon R., … Navas-Cortes J.A., 2021b. Divergent abiotic spectral pathways unravel pathogen stress signals across species. *Nature Communications* 12: 1–11. https://doi.org/10.1038/s41467-021-26335-3

Phytopathologia Mediterranea
The international journal of the
Mediterranean Phytopathological Union

Firenze University Press
www.fupress.com/pm

60th MPU Anniversary Special Section - Review

Fungal trunk diseases of fruit trees in Europe: pathogens, spread and future directions

Vladimiro GUARNACCIA[1,2,*], Christian KRAUS[3], Emmanouil MARKAKIS[4], Artur ALVES[5], Josep ARMENGOL[6], Ales EICHMEIER[7], Stephane COMPANT[8], David GRAMAJE[9]

[1] *Department of Agricultural, Forest and Food Sciences (DISAFA), University of Torino, Largo Braccini 2, 10095 Grugliasco, TO, Italy*
[2] *Centre for Innovation in the Agro-Environmental Sector, AGROINNOVA, University of Torino, Largo Braccini 2, 10095 Grugliasco, TO, Italy*
[3] *Julius Kühn-Institute, Federal Research Centre of Cultivated Plants, Plant Protection in Fruit Crops and Viticulture, 76833 Siebeldingen, Germany*
[4] *Institute of Olive Tree, Subtropical Crops and Viticulture, Hellenic Agricultural Organization - DIMITRA, 32A Kastorias street, Mesa Katsabas 71307, Heraklion, Crete, Greece*
[5] *Centre for Environmental and Marine Studies (CESAM), Department of Biology, University of Aveiro, 3810-193 Aveiro, Portugal*
[6] *Instituto Agroforestal Mediterráneo, Universitat Politècnica de València, Camino de Vera S/N, 46022-Valencia, Spain*
[7] *Mendeleum – Institute of Genetics, Mendel University in Brno, Valtická 334, 691 44 Lednice, Czech Republic*
[8] *AIT Austrian Institute of Technology, Center for Health and Bioresources, Bioresources Unit, Konrad Lorenz Strasse 24, 3430 Tulln, Austria*
[9] *Instituto de Ciencias de la Vid y del Vino (ICVV), Consejo Superior de Investigaciones Científicas, Universidad de la Rioja, Gobierno de La Rioja, Ctra. LO-20 Salida 13, 26007, Logroño, Spain*
*Corresponding author. E-mail: vladimiro.guarnaccia@unito.it

Summary. Production from crops of pome, stone fruit, nut, berry fruit, citrus, grapevine, and olive is increasingly threatened by fungal trunk diseases (FTD). These diseases and the consequent production losses are major problems. Many fungi (including *Botryosphaeriaceae*, *Calosphaeriaceae*, *Diaporthaceae*, *Diatrypaceae*, *Nectriaceae*, *Phaeomoniellaceae*, *Pleosporaceae*, *Togniniaceae*, *Valsaceae*) infect host wood, mainly through wounds and subsequent colonization of woody tissues, causing symptoms such as cankers, gummosis, wood rotting, blight and dieback. Propagative plant material, seedlings and fruit play a significant role in pathogen spread. Several abiotic factors (e.g. shifts in cultural practices and climate change) are involved in the disease development. This paper reviews recent literature on FTD of fruit crops, particularly focusing on the European status of pathogen occurrence. Case studies are described related to diseases of apple, citrus, grapevine, berry, nut and stone fruit, and olive trees. Aspects related to epidemiology and the increase in disease incidence along with the future perspectives on the FTD research are also discussed.

Keywords. Wood cankers, dieback, *Botryosphaeriaceae*, abiotic factors, epidemiology.

OPEN ACCESS

Citation: V. Guarnaccia, C. Kraus, E. Markakis, A. Alves, J. Armengol, A. Eichmeier, S. Compant, D. Gramaje (2022) Fungal trunk diseases of fruit trees in Europe: pathogens, spread and future directions. *Phytopathologia Mediterranea* 61(3): 563-599. doi: 10.36253/phyto-14167

Accepted: December 27, 2022

Published: January 13, 2023

Data Availability Statement: All relevant data are within the paper and its Supporting Information files.

Competing Interests: The Author(s) declare(s) no conflict of interest.

Editor: Alan J.L. Phillips, University of Lisbon, Portugal.

ORCID:
VG: 0000-0003-3188-7743
CK: 0000-0002-3830-8620
EM: 0000-0002-8791-0669
AA: 0000-0003-0117-2958
JA: 0000-0003-3815-8578
AE: 0000-0001-7358-3903
SC: 0000-0003-0709-6087
DG 0000-0003-1755-3413

INTRODUCTION

Trees cultivated in plantations are increasingly threatened by fungal trunk diseases (FTD) (van Niekerk *et al.,* 2004; Gramaje *et al*., 2016). There is increasing evidence that trees share pathogens with plants of forestry environments and with woody hosts that are not considered to be trees (Crous and Wingfield, 2018). Examples are pathogens in the family *Botryosphaeriaceae*, which are polyphagous, being often involved in diseases affecting diverse crops and plants of forest importance (Van Niekerk *et al.,* 2004; Guarnaccia *et al*., 2022). High incidence of FTD in fruit crops, such as pome and stone fruits, nut, berry fruit, citrus and olive, has been reported (Gramaje *et al.,* 2012; Úrbez-Torres *et al.,* 2013b; Carlucci *et al.,* 2015b; Guarnaccia and Crous, 2017), demonstrating a need for focus on this group of host plants. FTD have become major concerns for fruit industry stakeholders, and their occurrence in orchards and consequent production losses, is likely to have resulted from several causes, including shifts in cultural practices and climate change (Doll *et al.,* 2013).

Canker diseases of fruit crops are caused by a broad range of fungi that infect host wood, mainly through different kinds of wounds and subsequent colonization of vascular tissues (Crous and Wingfield, 2018). Wood pathogens cause symptoms such as cankers, gummosis, wood rotting, blight and dieback (Fig. 1; Gramaje *et al.,* 2012). Dieback of shoots, branches, and main trunks can lead to tree death in severe cases (Slippers and Wingfield 2007). Several FTD pathogens have been identified as species within *Botryosphaeriaceae*, *Calosphaeriaceae*, *Diaporthaceae*, *Diatrypaceae*, *Nectriaceae*, *Phaeomoniellaceae*, *Pleosporaceae*, *Togniniaceae*, and *Valsaceae,* as well as *Basidiomycota* (Rumbos 1988; Moral *et al.,* 2010; Kaliterna *et al.,* 2012; Carlucci *et al.,* 2013; 2015; Úrbez-Torres *et al.,* 2013a; Guarnaccia *et al.,* 2018b).

Some of these fungal pathogens live as endophytes in hosts after entering through wounds or natural openings, and pathogen spread occurs through asymptomatic plant material, seedlings and fruit, frequently circumventing country and region quarantine measures (Slippers and Wingfield, 2007).

Abiotic factors are strongly involved with FTD. High planting densities are required to maximize production and land resources, and these are combined with plant nutrient programmes, giving stressed cultivated plants. For example, almond production in Spain has increased in recent years, and new agronomic practices were adopted to increase yields from new plantations (León *et al*., 2020). However, incidence of almond associated FTD, such as twig cankers and shoot blight caused by *Diaporthe* spp., has also increased (León *et al.,* 2020). Abundant pruning wounds also promote chances of infections through possible airborne pathogen entry points (Henderson *et al.,* 2021). Similarly, wounds induced by mechanical shaking of trunks for fruit harvesting can increase host infection (Holland *et al.,* 2021a). Tree crop nurseries are important for meeting demands for plant material, and a lack of top-quality plants means greater incidence of FTD pathogens in the orchards. Global warming and climate change can increase plant stress and generate favourable conditions for the development of FTD, as for diseases caused by *Botryosphaeriaceae* (Pour *et al.,* 2020), which are serious threats to different crops (Slippers *et al.,* 2006).

The present paper aims to review recent literature on FTD, with a particular focus on the European situation of their causal agents, distribution and host associations, particularly relating to case studies on apple, citrus, grapevine, berry, nut and stone fruit, and olive trees. Moreover, epidemiology and hypotheses on the increase of FTD incidence are discussed, and future prospects and direction of trunk disease research are presented with the purpose of achieving sustainable disease management.

PATHOGEN DISTRIBUTION AND HOST RANGE IN EUROPE

In Europe, the group of fungi causing FTD is diverse and expands as new reports demonstrate (Table 1). While some of these fungi are probably host-specific, others have broad host ranges, including members of the *Botryosphaeriaceae*. This family is the most prevalent, and members can infect many different fruit crops. For example, *B. dothidea* is ubiquitous in Europe, and has been associated with FTD of walnut, hazelnut, almond, stone fruit, grapevine, olive, pistachio, apple and blueberry (Moral *et al.,* 2010; Gramaje *et al.,* 2012; Akgül *et al.,* 2014; Fischer *et al.,* 2016; Baránek *et al.,* 2018; Hilário *et al.,* 2020a; López-Moral *et al.,* 2020a,b). In contrast, *Neofusicoccum luteum* has only been isolated from grapevines in Portugal and France (van Niekerk *et al.,* 2004). *Diplodia seriata* can has also been found in different parts of Europe on many hosts, including walnut, grapevine, pear, quince, apple, apricot, plum, nectarine, almond and olive (Luque *et al.,* 2009; Gramaje *et al.,* 2012; Phillips *et al.,* 2012; Carlucci *et al.,* 2013; Kraus *et al.,* 2019; Bien and Damm 2020; Eichmeier *et al.,* 2020; López-Moral *et al.,* 2020a). *Diplodia mutila* is also common and infects grapevine, and trees of walnut, apricot, olive, plum, pear and apple (Phillips *et al.,* 2012; Carlucci *et al.,* 2013; Alves *et al.,* 2014; Gierl and Fischer,

Figure 1. FTD symptoms on different fruit trees. Natural dieback of *Vaccinium corymbosum* 'Blue Ribbon' in the field (**A**); branch canker on *Citrus sinensis* caused by *Diaporthe* spp. (**B**, from Guarnaccia *et al*., 2020); trunk canker on apple caused by *Neonectria ditissima* (**C**); internal discolouration of *Citrus reticulata* branch affected by *Botryosphaeriaceae* (**D**, from Bezerra *et al*., 2022); internal discolouration of avocado twig caused by *Neofusicoccum* spp. (**E**); cross-section showing a central white rot surrounded by black spots and sectorial necrosis of an esca infected vine (**F**), wedge-shaped canker in a Eutypa dieback affected vine (**G**), black spots and dark brown to black streaking of the xylem tissue in almond branches (**H**), sectorial necrosis of walnut affected trees (**I**), wood discolouration in pear branches (**J**).

Table 1. Distribution and host range of fungal pathogens associated with FTD on fruit crops in Europe based on literature research.

Division	Family	Genus	Species	Host	Country	References
Ascomycota	*Bionectriaceae*	*Acremonium*	*Acremonium sclerotigenum*	*Olea*, *Vitis*	Spain, Italy	Agustí-Brisach *et al.*, 2021; Lorenzini *et al.*, 2016
Ascomycota	*Xylariaceae*	*Biscogniauxia*	*Biscogniauxia nummularia*	*Prunus* (Plum), *Prunus* (Cherry)	Germany	Bien and Damm, 2020
Ascomycota	*Xylariaceae*	*Biscogniauxia*	*Biscogniauxia rosacearum*	*Cydonia*, *Prunus* (Plum), *Pyrus*	Italy	Raimondo *et al.*, 2016
Basidiomycota	*Phanerochaetaceae*	*Bjerkandera*	*Bjerkandera adusta*	*Prunus* (Plum), *Prunus* (Cherry), *Vitis*	Germany	Bien and Damm, 2020; Kraus *et al.*, 2018
Ascomycota	*Botryosphaeriaceae*	*Botryosphaeria*	*Botryosphaeria dothidea*	*Juglans*, *Prunus*, *Vitis*, *Prunus*, *Olea*, *Pistacia*, *Malus*, *Prunus* (Almond), *Vaccinium*, *Mangifera*	Spain, Switzerland, Portugal, Italy, Germany, Turkey, France, Czech Republic	López-Moral *et al.*, 2020a,b; van Niekerk *et al.*, 2004; Batista *et al.*, 2020; Carlucci *et al.*, 2013; Fischer *et al.*, 2016, Akgül *et al.*, 2014; Pintos *et al.*, 2018; Turkolmez *et al.*, 2016; Moral *et al.*, 2010; Baránek *et al.*, 2018; Gramaje *et al.*, 2012; Hilário *et al.*, 2019; Aiello *et al.*, 2022
Ascomycota	*Botryosphaeriaceae*	*Botryosphaeria*	*Botryosphaeria lutea* (= *Neofusicoccum luteum*)	*Vitis*	Portugal	van Niekerk *et al.*, 2004
Ascomycota	*Ploettnerulaceae*	*Cadophora*	*Cadophora fastigiata*	*Vitis*	Germany, Switzerland	Fischer *et al.*, 2016; Casieri *et al.*, 2009
Ascomycota	*Ploettnerulaceae*	*Cadophora*	*Cadophora luteo-olivacea*	*Vitis*, *Vaccinium*, *Olea*, *Prunus* (Plum)	Germany, Spain, France, Italy	Fischer *et al.*, 2016; Pintos *et al.*, 2018; Guarnaccia *et al.*, 2020; Agustí-Brisach *et al.*, 2021; Bien and Damm, 2020; Raimondo *et al.*, 2019, Casieri *et al.*, 2009
Ascomycota	*Ploettnerulaceae*	*Cadophora*	*Cadophora malorum*	*Malus*, *Actinidia*	Germany, Italy	Gierl and Fischer, 2017; Prodi *et al.*, 2008
Ascomycota	*Ploettnerulaceae*	*Cadophora*	*Cadophora melinii*	*Vitis*	Spain	Gramaje *et al.*, 2011
Ascomycota	*Ploettnerulaceae*	*Cadophora*	*Cadophora novi-eboraci*	*Juglans*, *Malus*, *Prunus* (Cherry)	Czech Republic, Germany	Eichmeier *et al.*, 2020; Gierl and Fischer, 2017; Bien and Damm, 2020
Ascomycota	*Ploettnerulaceae*	*Cadophora*	*Cadophora prunicola*	*Prunus* (Plum), *Prunus* (Cherry)	Germany	Bien and Damm, 2020
Ascomycota	*Ploettnerulaceae*	*Cadophora*	*Cadophora ramosa*	*Prunus* (Cherry), *Juglans*	Germany, Czech Republic	Bien and Damm, 2020; Eichmeier *et al.*, 2020
Ascomycota	*Calosphaeriaceae*	*Calosphaeriophora*	*Calosphaeria pulchella*	*Prunus* (Cherry)	Spain	Berbegal *et al.*, 2014
Ascomycota	*Glomerellaceae*	*Colletotrichum*	*Colletotrichum fruticola*	*Persea*	Italy	Guarnaccia *et al.*, 2016
Ascomycota	*Glomerellaceae*	*Colletotrichum*	*Colletotrichum gloeosporioides*	*Citrus*, *Persea*	Italy	Guarnaccia *et al.*, 2016,, 2017
Ascomycota	*Glomerellaceae*	*Colletotrichum*	*Colletotrichum karstii*	*Citrus*	Portugal	Ramos *et al.*, 2016
Ascomycota	*Tympanidaceae*	*Collophorina*	*Collophorina africana*	*Prunus* (Apricot), *Prunus* (Almond), *Prunus* (Plum)	Germany	Gierl and Fischer, 2017; Bien and Damm, 2020
Ascomycota	*Tympanidaceae*	*Collophorina*	*Collophorina badensis*	*Prunus* (Plum)	Germany	Bien and Damm, 2020
Ascomycota	*Tympanidaceae*	*Collophorina*	*Collophorina germanica*	*Prunus* (Cherry)	Germany	Bien and Damm, 2020

(Continued)

Table 1. (Continued).

Division	Family	Genus	Species	Host	Country	References
Ascomycota	*Tympanidaceae*	*Collophorina*	*Collophorina hispanica*	*Prunus* (Apricot), *Prunus* (Almond)	Germany, Spain	Gierl and Fischer, 2017; Gramaje *et al.*, 2012
Ascomycota	*Tympanidaceae*	*Collophorina*	*Collophorina neorubra*	*Prunus* (Cherry)	Germany	Bien and Damm, 2020
Ascomycota	*Tympanidaceae*	*Collophorina*	*Collophorina paarla*	*Prunus* (Cherry)	Germany	Gierl and Fischer, 2017
Ascomycota	*Diademaceae*	*Comoclathris*	*Comoclathris incompta*	*Olea*	Spain, Croatia, Italy	Moral *et al.*, 2017; Ivic *et al.*, 2010; Carlucci *et al.*, 2013
Ascomycota	*Coniochaetaceae*	*Coniochaeta*	*Coniochaeta hoffmannii*	*Vitis*	Germany	Fischer *et al.*, 2016
Ascomycota	*incertae sedis*	*Cryptovalsa*	*Cryptovalsa ampelina*	*Juglans*, *Vitis*	Czech Republic, Spain, Germany	Eichmeier *et al.*, 2020; Luque *et al.*, 2009,, 2012; Martin *et al.*, 2009; Kraus *et al.*, 2018
Ascomycota	*Nectriaceae*	*Cylindrocarpon*	*Cylindrocarpon destructans*	*Olea*, *Vitis*	Italy, Spain	Carlucci *et al.*, 2013; Gonzalez and Tello, 2011
Ascomycota	*Nectriaceae*	*Cylindrocarpon*	*Cylindrocarpon pauciseptatum*	*Vitis*, *Prunus* (Peach), *Prunus* (Plum)	Slovenia, Portugal, Italy, Spain, Bulgaria, France	Cabral *et al.*, 2012; Yaseen *et al.*, 2012; Martin *et al.*, 2011; Piperkova *et al.*, 2017; Pintos *et al.*, 2018
Ascomycota	*Nectriaceae*	*Cylindrocarpon*	*Cylindrocarpon peruviana*	*Persea*	Italy	Aiello *et al.*, 2020
Ascomycota	*Valsaceae*	*Cytospora*	*Cytospora chrysosperma*	*Prunus* (blackthorn), *Vitis*	Germany, Spain	Gierl and Fischer, 2017; Kraus *et al.*, 2018; González and Tello, 2011
Ascomycota	*Valsaceae*	*Cytospora*	*Cytospora oleina*	*Olea*	Greece, Italy	Rumbos, 1988; Carlucci *et al.*, 2013
Ascomycota	*Valsaceae*	*Cytospora*	*Cytospora pistaciae*	*Pistacia*	Italy	Aiello *et al.*, 2019
Ascomycota	*Valsaceae*	*Cytospora*	*Cytospora pruinosa*	*Olea*	Spain	López-Moral *et al.*, 2020b; Moral *et al.*, 2017
Ascomycota	*Nectriaceae*	*Dactylonectria*	*Dactylonectria hordeicola*	*Vitis*	France	Pintos *et al.*, 2018
Ascomycota	*Nectriaceae*	*Dactylonectria*	*Dactylonectria macrodidyma*	*Vitis*	France, Spain	Pintos *et al.*, 2018
Ascomycota	*Nectriaceae*	*Ilyonectria*	*Ilyonectria macrodidyma*	*Vitis*	Portugal, France, Turkey, Spain	Cabral *et al.*, 2012; Augustí-Brisach and Armengol, 2013
Ascomycota	*Nectriaceae*	*Dactylonectria*	*Dactylonectria pauciseptata*	*Vitis*	France, Spain	Pintos *et al.*, 2018
Ascomycota	*Nectriaceae*	*Dactylonectria*	*Dactylonectria torresensis*	*Vitis*	France, Spain	Pintos *et al.*, 2018
Ascomycota	*Diaporthaceae*	*Diaporthe*	*Diaporthe ampelina*	*Vitis*	France, Spain, Turkey, Czech Republic, Germany, UK, Croatia, Hungary	Pintos *et al.*, 2018; Akgül *et al.*, 2015; Baránek *et al.*, 2018; Kraus *et al.*, 2018; Guarnaccia *et al.*, 2018
Ascomycota	*Diaporthaceae*	*Diaporthe*	*Diaporthe amygdali*	*Prunus* (Almond), *Juglans*, *Vaccinium*, *Persea*	Portugal, Spain, Hungary, Italy	López-Moral *et al.*, 2020b; Varjas *et al.*, 2017; Guarnaccia *et al.*, 2016,, 2018
Ascomycota	*Diaporthaceae*	*Diaporthe*	*Diaporthe baccae*	*Vitis*, *Vaccinium*, *Citrus*, *Mangifera*	Spain, France, Italy, Croatia	Guarnaccia *et al.*, 2017,, 2018; Aiello *et al.*, 2022
Ascomycota	*Diaporthaceae*	*Diaporthe*	*Diaporthe bohemiae*	*Vitis*	Czech Republic	Guarnaccia *et al.*, 2018
Ascomycota	*Diaporthaceae*	*Diaporthe*	*Diaporthe celeris*	*Vitis*	UK	Guarnaccia *et al.*, 2018
Ascomycota	*Diaporthaceae*	*Diaporthe*	*Diaporthe cinerascens*	*Ficus*	Bulgaria	López-Moral *et al.*, 2020a,b

(Continued)

Table 1. (Continued).

Division	Family	Genus	Species	Host	Country	References
Ascomycota	*Diaporthaceae*	*Diaporthe*	*Diaporthe eres*	*Malus*, *Vitis*, *Prunus* (Cherry), *Vaccinium*, *Juglans*, *Prunus* (Peach), *Pyrus*	Germany, France, Spain, Czech Republic, UK, Italy, Hungary, Croatia, Poland, the Netherlands, Lithuanian, Greece, Switzerland	Gierl and Fischer, 2017; Pintos *et al.*, 2018; Bien and Damm, 2020; Guarnaccia *et al.*, 2018; Lombard *et al.*, 2014; Eichmeier *et al.*, 2020; Thomidis *et al.*, 2009; Prencipe *et al.*, 2017; Bertetti *et al.*, 2018; Casieri *et al.*, 2009
Ascomycota	*Diaporthaceae*	*Diaporthe*	*Diaporthe foeniculina*	*Ficus*, *Vitis*, *Citrus*, *Persea*, *Pyrus*, *Vaccinium*, *Juglans*, *Prunus* (Almond), *Mangifera*, *Litchi*	Germany, France, Spain, Greece, Malta, Portugal, Italy	Gierl and Fischer, 2017; Pintos *et al.*, 2018; Vakalounakis *et al.*, 2019; Guarnaccia *et al.*, 2016,, 2017; Mathioudakis *et al.*, 2020; Santos *et al.*, 2017; Hilario *et al.*, 2020; Lopez-Moral *et al.*, 2020; Gramaje *et al.*, 2012; Aiello *et al.*, 2022
Ascomycota	*Diaporthaceae*	*Diaporthe*	*Diaporthe hispaniae*	*Vitis*	Spain	Guarnaccia *et al.*, 2018
Ascomycota	*Diaporthaceae*	*Diaporthe*	*Diaporthe hungariae*	*Vitis*	Spain, Hungary	Guarnaccia *et al.*, 2018
Ascomycota	*Diaporthaceae*	*Diaporthe*	*Diaporthe limonicola*	*Citrus*	Malta	Guarnaccia *et al.*, 2017
Ascomycota	*Diaporthaceae*	*Diaporthe*	*Diaporthe mahothocarpus*	*Prunus* (Cherry)	Germany	Bien and Damm, 2020
Ascomycota	*Diaporthaceae*	*Diaporthe*	*Diaporthe melitensis*	*Citrus*	Malta	Guarnaccia *et al.*, 2017
Ascomycota	*Diaporthaceae*	*Diaporthe*	*Diaporthe novem*	*Vitis*, *Citrus*	France, Spain, Italy	Pintos *et al.*, 2018; Guarnaccia *et al.*, 2017
Ascomycota	*Diaporthaceae*	*Diaporthe*	*Diaporthe phaseolorum*	*Vitis*	Spain, Switzerland	Pintos *et al.*, 2018; Casieri *et al.*, 2009
Ascomycota	*Diaporthaceae*	*Diaporthe*	*Diaporthe rudis*	*Vitis*, *Vaccinium*, *Prunus* (Plum), *Prunus* (Cherry), *Litchi*	France, Spain, Italy, Germany, Portugal, UK, Switzerland, the Netherlands	Pintos *et al.*, 2018, Guarnaccia *et al.*, 2018,, 2020; Bien and Damm, 2020; Casieri *et al.*, 2009; Lombard *et al.*, 2014; Aiello *et al.*, 2022
Ascomycota	*Diaporthaceae*	*Diaporthe*	*Diaporthe vaccinii*	*Vaccinium*	the Netherlands, Lithuania, Latvia	Lombard *et al.*, 2014
Ascomycota	*Botryosphaeriaceae*	*Diplodia*	*Diplodia bulgarica*	*Malus*, *Pyrus*	Bulgaria, Germany, Turkey	Phillips *et al.*, 2012; Hinrichs-Berger *et al.*, 2021; Eken, 2021
Ascomycota	*Botryosphaeriaceae*	*Diplodia*	*Diplodia corticola*	*Vitis*	Italy	Carlucci *et al.*, 2015
Ascomycota	*Botryosphaeriaceae*	*Diplodia*	*Diplodia pseudoseriata*	*Pistacia*	Italy	Batista *et al.*, 2020
Ascomycota	*Botryosphaeriaceae*	*Diplodia*	*Diplodia juglandis*	*Juglans*	France	López-Moral *et al.*, 2020
Ascomycota	*Botryosphaeriaceae*	*Diplodia*	*Diplodia malorum*	*Malus*	Portugal	Phillips *et al.*, 2012; Alves *et al.*, 2014
Ascomycota	*Botryosphaeriaceae*	*Diplodia*	*Diplodia mutila*	*Vitis*, *Juglans*, *Prunus* (Apricot), *Olea*, *Prunus* (Plum), *Pyrus*, *Malus*	Portugal, Germany, Italy, Spain, France, Netherlands, England	López-Moral *et al.*, 2020, Gierl and Fischer, 2017; Carlucci *et al.*, 2013; Pintos *et al.*, 2018; Bien and Damm, 2020; Batista *et al.*, 2020; Phillips *et al.*, 2013; Alves *et al.*, 2014
Ascomycota	*Botryosphaeriaceae*	*Diplodia*	*Diplodia olivarum*	*Olea*, *Prunus* (Almond), *Pistacia*	Italy, Spain	Phillips *et al.*, 2012; Gramaje *et al.*, 2012; Alves *et al.*, 2014; Linaldeddu *et al.*, 2016
Ascomycota	*Botryosphaeriaceae*	*Diplodia*	*Diplodia sapinea*	*Malus*, *Vitis*, *Olea*	Portugal, France, Italy	Batista *et al.*, 2020; Comont *et al.*, 2016; Alves *et al.*, 2014; Phillips *et al.*, 2012

(Continued)

Table 1. (Continued).

Division	Family	Genus	Species	Host	Country	References
Ascomycota	*Botryosphaeriaceae*	*Diplodia*	*Diplodia scrobiculata*	*Olea*	Italy	Phillips *et al.*, 2012; Alves *et al.*, 2014
Ascomycota	*Botryosphaeriaceae*	*Diplodia*	*Diplodia seriata*	*Juglans*, *Vitis*, *Pyrus*, *Cydonia*, *Malus*, *Prunus (Apricot)*, *Olea*, *Prunus* (Plum), *Prunus* (Nectarine), *Prunus* (Almond), *Prunus* (Plum)	Czech Republic, Spain, Turkey, Spain, Germany, Germany, France, Italy, Bulgaria, Croatia, Portugal	Eichmeier *et al.*, 2020; López-Moral *et al.*, 2020; Kurbetli and Demirci, 2014; Moral *et al.*, 2010; Phillips *et al.*, 2012; Kaliterna *et al.*, 2012; Carlucci *et al.*, 2013; Ende *et al.*, 2016; Batista *et al.*, 2020; Kraus *et al.*, 2019; Akgül *et al.*, 2014; Luque *et al.*, 2009; Gramaje *et al.*, 2012; Bien and Damm, 2020
Ascomycota	*Botryosphaeriaceae*	*Dothiorella*	*Dothiorella iberica*	*Juglans*, *Prunus* (Apricot), *Corylus* (Hazelnut), *Malus*, *Vitis*	Spain, Germany, Italy	López-Moral *et al.*, 2020; Gierl and Fischer, 2017; Phillips *et al.*, 2005; Carlucci *et al.*, 2015
Ascomycota	*Botryosphaeriaceae*	*Dothiorella*	*Dothiorella omnivora*	*Juglans*, *Vitis*	Czech Republic, France, Hungary	Eichmeier *et al.*, 2020; Linaldeddu *et al.*, 2016; Vaczy *et al.*, 2018
Ascomycota	*Botryosphaeriaceae*	*Dothiorella*	*Dothiorella sarmentorum*	*Juglans*, *Malus*, *Prunus* (Almond), *Cydonia*, *Vitis*	Czech Republic, the Netherlands, Norway, Germany, Italy, Spain, Poland, Ukraine	López-Moral *et al.*, 2020; van Niekerk *et al.*, 2004; Gierl and Fischer, 2017; Carlucci *et al.*, 2015; Dissanayake *et al.*, 2016
Ascomycota	*Botryosphaeriaceae*	*Dothiorella*	*Dothiorella viticola*	*Vitis*	Spain, France	López-Moral *et al.*, 2020; Batista *et al.*, 2020; Comont *et al.*, 2016
Ascomycota	*Diatrypaceae*	*Eutypa*	*Eutypa lata*	*Juglans*, *Cydonia*, *Vitis*, *Pistacia*, *Prunus* (Almond), *Prunus* (Plum), *Prunus* (Cherry), *Olea*	Czech Republic, Germany, Spain, Italy, France	Eichmeier *et al.*, 2020; Gierl and Fischer, 2017; Luque *et al.*, 2009; López-Moral *et al.*, 2020b; Baránek *et al.*, 2018; Gramaje *et al.*, 2012; Bien and Damm, 2020; Tosi and Natalini, 2009; Aiello *et al.*, 2019; Baranek *et al.*, 2018; Laveau *et al.*, 2009; Kraus *et al.*, 2022
Ascomycota	*Diatrypaceae*	*Eutypella*	*Eutypella citricola*	*Vitis*	Spain	Luque *et al.*, 2012
Ascomycota	*Diatrypaceae*	*Eutypella*	*Eutypella leptoplaca*	*Vitis*	Spain	Luque *et al.*, 2009
Ascomycota	*Diatrypaceae*	*Eutypella*	*Eutypella microtheca*	*Vitis*	Spain	Luque *et al.*, 2012
Ascomycota	*Diatrypaceae*	*Eutypella*	*Eutypella vitis*	*Vitis*	Spain	Luque *et al.*, 2009
Basidiomycota	*Hymenochaetaceae*	*Fomitiporia*	*Fomitiporia mediterranea*	*Olea*, *Vitis*, *Actinidia*, *Citrus*, *Prunus* (Almond), *Pyrus*	Italy, Spain, Turkey, Czech Republic, Germany, France, Greece, Austria, Portugal, Slovenia, Switzerland	Carlucci *et al.*, 2013; Luque *et al.*, 2009; Akgül *et al.*, 2015; Baránek *et al.*, 2018; Kraus *et al.*, 2022; Laveau *et al.*, 2009; Elena and Paplomatis, 2009; Elena *et al.* , 2006; Rumbos and Rumbou, 2001; Moretti *et al.*, 2021; Olmo *et al.*, 2017; Markakis *et al.*, 2017
Basidiomycota	*Hymenochaetaceae*	*Fomitiporia*	*Fomitiporia punctata*	*Vitis*, *Actinidia*	Italy, Greece, France	Cortesi *et al.*, 2000; Elena and Paplomatas, 2007; Jamaux-Despréaux and Péros, 2003
Ascomycota	*Nectriaceae*	*Ilyonectria*	*Ilyonectria europea*	*Vitis*, *Actinidia*	Portugal, France	Cabral *et al.*, 2012
Ascomycota	*Nectriaceae*	*Ilyonectria*	*Ilyonectria liriodendri*	*Vitis*, *Malus*	France, Spain, Portugal, Switzerland, Turkey	Pintos *et al.*, 2018; Cabral *et al.*, 2012; Alaniz *et al.*, 2009; Casieri *et al.*, 2009; Savas *et al.*, 2015

(Continued)

Table 1. (Continued).

Division	Family	Genus	Species	Host	Country	References
Ascomycota	*Nectriaceae*	*Ilyonectria*	*Ilyonectria lusitanica*	*Vitis*	Portugal	Cabral *et al.*, 2012
Ascomycota	*Nectriaceae*	*Ilyonectria*	*Ilyonectria pseudodestructans*	*Vitis*	Portugal, Spain	Cabral *et al.*, 2012; Berlanas *et al.*, 2020
Ascomycota	*Nectriaceae*	*Ilyonectria*	*Ilyonectria robusta*	*Vitis*	France, Portugal, Spain	Pintos *et al.*, 2018; Cabral *et al.*, 2012; Berlanas *et al.*, 2020
Ascomycota	*Nectriaceae*	*Ilyonectria*	*Ilyonectria vitis*	*Vitis*	Portugal	Cabral *et al.*, 2012
Ascomycota	*Botryosphaeriaceae*	*Lasiodiplodia*	*Lasiodiplodia citricola*	*Vitis*	Italy	Carlucci *et al.*, 2015
Ascomycota	*Botryosphaeriaceae*	*Lasiodiplodia*	*Lasiodiplodia pseudotheobromae*	*Olea*, *Prunus* (Nectarine), *Pistacia*	Italy, Turkey, Spain	Carlucci *et al.*, 2013; Endes *et al.*, 2016; Akgül *et al.*, 2014; Aroca *et al.*, 2010; López-Moral *et al.*, 2020b
Ascomycota	*Botryosphaeriaceae*	*Lasiodiplodia*	*Lasiodiplodia theobromae*	*Olea*, *Prunus* (Nectarine), *Vitis*, *Vaccinium*, *Mangifera*	Italy, Turkey, Spain	Carlucci *et al.*, 2013, 2015; Endes *et al.*, 2016; Akgül *et al.*, 2014; Aroca *et al.*, 2010; Martin *et al.*, 2009; Borrero *et al.*, 2019; Aiello *et al.*, 2022
Ascomycota	*Botryosphaeriaceae*	*Lasiodiplodia*	*Lasiodiplodia viticola*	*Vitis*	France	Comont *et al.*, 2016
Ascomycota	*Phaeomoniellaceae*	*Minutiella*	*Minutiella pruni-avium*	*Prunus* (Cherry)	Germany	Bien and Damm, 2020
Ascomycota	*Sclerotiniaceae*	*Monilinia*	*Monilinia laxa*	*Prunus* (Plum)	Germany	Bien and Damm, 2020
Ascomycota	*Nectriaceae*	*Neocosmospora*	*Neocosmospora perseae*	*Persea*	Italy, Greece	Guarnaccia *et al.*, 2018, 2022
Ascomycota	*Botryosphaeriaceae*	*Neofusicoccum*	*Neofusicoccum australe*	*Mangifera*, *Prunus* (Almond), *Vitis*, *Olea*, *Vaccinium*	Italy, Spain, Portugal	Ismail *et al.*, 2013; Gramaje *et al.*, 2012; Aroca *et al.*, 2010; Lopes *et al.*, 2016; Hilário *et al.*, 2019
Ascomycota	*Botryosphaeriaceae*	*Neofusicoccum*	*Neofusicoccum hellenicum*	*Pistacia*	Greece, Italy	Lopes *et al.*, 2016; Gusella *et al.*, 2022
Ascomycota	*Botryosphaeriaceae*	*Neofusicoccum*	*Neofusicoccum luteum*	*Olea*, *Vitis*	Italy, Germany, Spain, France, Portugal	Carlucci *et al.*, 2013; Fischer *et al.*, 2016; Luque *et al.*, 2009; Pintos *et al.*, 2018; Lopes *et al.*, 2016
Ascomycota	*Botryosphaeriaceae*	*Neofusicoccum*	*Neofusicoccum mediterraneum*	*Juglans*, *Vitis*, *Olea*, *Pistacia*	Spain, Italy	López-Moral *et al.*, 2020a,b; Moral *et al.*, 2010, 2017; Brunetti *et al.*, 2022
Ascomycota	*Botryosphaeriaceae*	*Neofusicoccum*	*Neofusicoccum parvum*	*Juglans*, *Malus*, *Vitis*, *Castanea*, *Citrus*, *Ficus*, *Prunus* (Nectarine), *Prunus* (Peach), *Pistacia*, *Mangifera*, *Vaccinium*, *Prunus* (Almond), *Persea*, *Olea*	Spain, Portugal, Italy, Turkey, France, Greece, Croatia	López-Moral *et al.*, 2020a,b; Moral *et al.*, 2010; Batista *et al.*, 2020; Mondello *et al.*, 2013; Akgül *et al.*, 2014; Luque *et al.*, 2009; Pintos *et al.*, 2018; Ciordia *et al.*, 2022; Vakalounakis *et al.*, 2019; Aiello *et al.*, 2020; Thomidis *et al.*, 2011; Kaliterna *et al.*, 2013; Ismail *et al.*, 2013; Guarnaccia *et al.*, 2020; Gramaje *et al.*, 2012; Guarnaccia, 2016; Ismail *et al.*, 2013; Hilário *et al.*, 2019; Castillo *et al.*, 2013; Polizzi *et al.*, 2022
Ascomycota	*Botryosphaeriaceae*	*Neofusicoccum*	*Neofusicoccum vitifusiforme*	*Vitis*	Italy, Spain	Mondello *et al.*, 2013; Aroca *et al.*, 2010
Ascomycota	*Nectriaceae*	*Neonectria*	*Neonectria ditissima*	*Malus*	Portugal	Cabral *et al.*, 2012
Ascomycota	*Sporocadaceae*	*Neopestalotiopsis*	*Neopestalotiopsis rosae*	*Persea*	Italy	Fiorenza *et al.*, 2022
Ascomycota	*Sporocadaceae*	*Neopestalotiopsis*	*Neopestalotiopsis siciliana*	*Persea*	Italy	Fiorenza *et al.*, 2022

(Continued)

Table 1. (Continued).

Division	Family	Genus	Species	Host	Country	References
Ascomycota	*Botryosphaeriaceae*	*Neoscytalidium*	*Neoscytalidium dimidiatum*	*Citrus*, *Juglans*, *Vitis*, *Prunus* (Cherry), *Prunus* (Almond)	Italy, Turkey	Polizzi *et al.*, 2009; Dervis *et al.*, 2019; Oksal *et al.*, 2019; Oren *et al.*, 2020, 2022
Ascomycota	*Didymellaceae*	*Nothophoma*	*Nothophoma quercina*	*Olea*	Spain	Moral *et al.*, 2017
Ascomycota	*Diatrypaceae*	*Peroneutypa*	*Peroneutypa scoparia*	*Juglans*, *Vaccinium*	Czech Republic, Italy	Eichmeier *et al.*, 2020; Guarnaccia *et al.*, 2020
Ascomycota	*Togniniaceae*	*Phaeoacremonium*	*Phaeoacremonium alvesii*	*Olea*, *Vitis*	Italy, Turkey	Gramaje *et al.*, 2015
Ascomycota	*Togniniaceae*	*Phaeoacremonium*	*Phaeoacremonium amygdalinum*	*Prunus* (Almond)	Spain, Italy	Gramaje *et al.*, 2012; Raimondo *et al.*, 2021
Ascomycota	*Togniniaceae*	*Phaeoacremonium*	*Phaeoacremonium angustius*	*Cydonia*, *Vitis*	Germany, Portugal, Spain	Gierl and Fischer, 2017; Gramaje *et al.*, 2015
Ascomycota	*Togniniaceae*	*Phaeoacremonium*	*Phaeoacremonium cinereum*	*Vitis*	Spain	Gramaje *et al.*, 2015
Ascomycota	*Togniniaceae*	*Phaeoacremonium*	*Phaeoacremonium croatiense*	*Vitis*	Croatia	Essakhi *et al.*, 2008
Ascomycota	*Togniniaceae*	*Phaeoacremonium*	*Phaeoacremonium fraxinopennsylvanicum*	*Vitis*, *Actinidia*	Germany, Italy, Croatia, Hungary, Spain	Fischer *et al.*, 2016; Gramaje *et al.*, 2015
Ascomycota	*Togniniaceae*	*Phaeoacremonium*	*Phaeoacremonium griseorubrum*	*Vitis*	Italy	Gramaje *et al.*, 2015
Ascomycota	*Togniniaceae*	*Phaeoacremonium*	*Phaeoacremonium hispanicum*	*Vitis*	Spain	Gramaje *et al.*, 2015
Ascomycota	*Togniniaceae*	*Phaeoacremonium*	*Phaeoacremonium hungaricum*	*Prunus* (Plum), *Prunus* (Cherry)	Germany, Hungary	Bien and Damm, 2020; Gramaje *et al.*, 2015
Ascomycota	*Togniniaceae*	*Phaeoacremonium*	*Phaeoacremonium infatipes*	*Vitis*	Spain	González and Tello, 2011
Ascomycota	*Togniniaceae*	*Phaeoacremonium*	*Phaeoacremonium iranianum*	*Actinidia*, *Prunus* (Almond), *Prunus* (Plum), *Vitis*	Italy, Spain, Germany	Prodi *et al.*, 2008; Gramaje *et al.*, 2012; Bien and Damm, 2020
Ascomycota	*Togniniaceae*	*Phaeoacremonium*	*Phaeoacremonium italicum*	*Olea*, *Vitis*	Spain, Italy	Agustí-Brisach *et al.*, 2021; Gramaje *et al.*, 2015
Ascomycota	*Togniniaceae*	*Phaeoacremonium*	*Phaeoacremonium krajdenii*	*Vitis*	Spain	Gramaje *et al.*, 2011
Ascomycota	*Togniniaceae*	*Phaeoacremonium*	*Phaeoacremonium minimum*	*Vitis*, *Olea*, *Actinidia*, *Prunus* (Cherry), *Pistacia*	Spain, France, Turkey, Italy, Austria, Greece, Germany, Portugal	Pintos *et al.*, 2018; Akgül *et al.*, 2015, Agustí-Brisach *et al.*, 2021; Carlucci *et al.*, 2013; Luque *et al.*, 2019; Prodi *et al.*, 2008; Di Marco *et al.*, 2000; Mostert *et al.*, 2006; Lopez-Moral *et al.*, 2020; Garamaje *et al.*, 2015
Ascomycota	*Togniniaceae*	*Phaeoacremonium*	*Phaeoacremonium oleae*	*Olive*	Italy	Raimondo *et al.*, 2022

(Continued)

Table 1. (Continued).

Division	Family	Genus	Species	Host	Country	References
Ascomycota	*Togniniaceae*	*Phaeoacremonium*	*Phaeoacremonium parasiticum*	*Vitis*, *Olea*, *Actinidia*, *Prunus* (Cherry)	Spain, Italy, Greece	Aroca *et al.*, 2010; Agustí-Brisach *et al.*, 2021; Prodi *et al.*, 2008; Gramaje *et al.*, 2015
Ascomycota	*Togniniaceae*	*Phaeoacremonium*	*Phaeoacremonium rubrigenum*	*Olea*, *Vitis*, *Actinidia*	Italy, Croatia	Gramaje *et al.*, 2015; Di Marco *et al.*, 2010
Ascomycota	*Togniniaceae*	*Phaeoacremonium*	*Phaeoacremonium scolyti*	*Olea*, *Prunus* (Plum), *Vitis*	Spain, Germany, Italy, France, Turkey	Agustí-Brisach *et al.*, 2021; Bien and Damm, 2020; Carlucci *et al.*, 2015; Gramaje *et al.*, 2015; Ozben *et al.*, 2012
Ascomycota	*Togniniaceae*	*Phaeoacremonium*	*Phaeoacremonium sicilianum*	*Olea*, *Vitis*, *Juglans*	Italy, Spain, Czech Republic	Carlucci *et al.*, 2015; Gramaje *et al.*, 2015; Eichmeier *et al.*, 2020
Ascomycota	*Togniniaceae*	*Phaeoacremonium*	*Phaeoacremonium tuscanum*	*Vitis*	Italy	Gramaje *et al.*, 2015
Ascomycota	*Togniniaceae*	*Phaeoacremonium*	*Phaeoacremonium venezuelense*	*Prunus* (Apricot)	Spain	Gramaje *et al.*, 2015
Ascomycota	*Togniniaceae*	*Phaeoacremonium*	*Phaeoacremonium vibratile*	*Prunus* (Cherry)	Sweden	Gramaje *et al.*, 2015
Ascomycota	*Togniniaceae*	*Phaeoacremonium*	*Phaeoacremonium viticola*	*Vitis*, *Actinidia*, *Prunus* (Plum), *Prunus* (Cherry), *Olea*	Germany, Spain, Italy, France	Fischer *et al.*, 2016; Luque *et al.*, 2009; Prodi *et al.*, 2008; Bien and Damm, 2020; Mostert *et al.*, 2006; Gramaje *et al.*, 2015; Raimondo *et al.*, 2022
Ascomycota	*Phaeomoniellaceae*	*Phaeomoniella*	*Phaeomoniella chlamydospora*	*Vitis*, *Actinidia*	Spain, France, Turkey, Czech Republic, Portugal, Germany, Slovakia, Switzerland	Luque *et al.*, 2009; Pintos *et al.*, 2018; Akgül *et al.*, 2015; Baránek *et al.*, 2018; Agustí-Brisach *et al.*, 2021; Di Marco *et al.*, 2000; Chicau *et al.*, 2000; Fischer and Kassemeyer, 2003; Kakalikova *et al.*, 2006; Casieri *et al.*, 2009
Basidiomycota	*Hymenochaetaceae*	*Phellinus*	*Phellinus tuberculosus*	*Prunus* (Plum), *Prunus* (Cherry)	Germany	Bien and Damm, 2020
Ascomycota	*Nectriaceae*	*Pleiocarpon*	*Pleiocarpon algeriense*	*Persea*	Italy	Aiello *et al.*, 2020b
Ascomycota	*Pleurostomataceae*	*Pleurostoma*	*Pleurostoma richardsiae*	*Vitis*	Turkey, Spain	Ozben *et al.*, 2017; Pintos Varela *et al.*, 2016
Ascomycota	*Phaeomoniellaceae*	*Pseudophaeomoniella*	*Pseudophaeomoniella oleae*	*Olea*	Greece, Italy	Markakis *et al.*, 2022; Crous *et al.*, 2015
Ascomycota	*Phaeomoniellaceae*	*Pseudophaeomoniella*	*Pseudophaeomoniella oleicola*	*Olea*	Italy, Spain	Crous *et al.*, 2015; Agustí-Brisach *et al.*, 2021
Basidiomycota	*Stereaceae*	*Stereum*	*Stereum hirsutum*	*Prunus* (Almond), *Vitis*	Germany, Spain, France	Gierl and Fischer, 2017; Luque *et al.*, 2009; Larignon and Dubos, 1997; Fischer and Kassemeyer, 2003
Basidiomycota	*Polyporaceae*	*Trametes*	*Trametes versicolor*	*Prunus* (Plum), *Vitis*	Germany	Bien and Damm, 2020; Fischer and Kassemeyer, 2003

2017; Pintos *et al.,* 2018; Batista *et al.,* 2020; Bien and Damm, 2020; López-Moral *et al.,* 2020a). Other *Diplodia* spp. occur rarely and share different hosts: *Dip. corticola* (grapevines), *Dip. juglandis* (walnut), *Dip. malorum* (apple), *Dip. prunicola* (almond), *Dip. pseudoseriata* (pistachio), *Dip. scrobiculata* (olive) (Phillips *et al.,* 2012; Alves *et al.,* 2014; Carlucci *et al.,* 2015b; López-Moral *et al.,* 2020a; Batista *et al.,* 2020).

Neofusicoccum is another common member of the *Botryosphaeriaceae*, which is a predominant FTD pathogen. The host range of *N. parvum* is broad, including walnut, grapevine, apple, chestnut, citrus, fig, nectarine, peach, pistacia, mango, blueberry, almond, avocado, and olive (Moral *et al.,* 2010; Gramaje *et al.,* 2012; Ismail *et al.,* 2013; Akgül *et al.,* 2014; Guarnaccia *et al.,* 2016; Aiello *et al.,* 2020a; Guarnaccia *et al.,* 2020; Hilário *et al.,* 2020a; López-Moral *et al.,* 2020a). To date, this pathogen has only been isolated from plants in Croatia, France, Greece, Italy, Portugal, Spain, and Turkey, indicating a preference for warm climates. Further *Neofusicoccum* spp. probably restricted to the Mediterranean area and associated with FTD mainly of grapevine and olive trees, are *N. australe*, *N. hellenicum*, *N. luteum*, *N. mediterraneum* and *N. vitifusiforme* (Gramaje *et al.,* 2012; Ismail *et al*., 2013; Hilário *et al.,* 2020a; López-Moral *et al.,* 2020a; López-Moral *et al.,* 2020b; Gusella *et al.,* 2022).

Lasiodiplodia spp. were exclusively isolated from fruit crop plants in the south of Europe, including France, Italy, Spain, and Turkey. *Lasiodiplodia citricola* was isolated from grapevine, *L. pseudotheobromae* from olive, nectarine and pistachio, *L. theobromae* from olive, nectarine and grapevine, and *L. viticola* only from grapevine (Martin *et al.,* 2009; Aroca *et al.,* 2010; Carlucci *et al.,* 2013, 2015b; Akgül *et al.,* 2014; Comont *et al.,* 2016; Endes *et al.,* 2016; Borrero *et al.,* 2019; López-Moral *et al.,* 2020b). *Dothiorella sarmentorum*, however, was associated with FTD of walnut, apple, almond, pear and grapevine, mainly in areas with cool climates, such as the Czech Republic, Germany, the Netherlands, Norway, and Poland (van Niekerk *et al.,* 2004; Carlucci *et al.,* 2015b; Gierl and Fischer 2017; Dissanayake *et al.,* 2017; López-Moral *et al.,* 2020a). The closely related *Dip. omnivora* was also found in cool regions (the Czech Republic, France, Hungary) on walnut and grapevine (Linaldeddu *et al.,* 2016; Váczy *et al.,* 2018; Eichmeier *et al.,* 2020). *Dothoriella iberica* has been associated with FTD of walnut, apricot, hazelnut, apple and grapevine, in Spain, Germany and Italy (Phillips *et al.,* 2005; Carlucci *et al.,* 2015b; Gierl and Fischer 2017; López-Moral *et al.,* 2020a). *Neoscytalidium dimidiatum* has recently been related to canker and dieback of walnut, grapevine, cherry, almond and apricot in Turkey (Derviş *et al.,* 2019; Oksal *et al.,* 2019; Oksal *et al.,* 2020; Ören *et al.,* 2020; Ören *et al.,* 2022). This pathogen also caused shoot blight, canker and gummosis on citrus in Italy (Polizzi *et al.,* 2009).

Among *Diatrypaceae*, *Eutypa lata* has been commonly associated with FTD in Europe. This fungus was found on walnut, quince, grapevine, pistachio, almond, plum, cherry, blueberry, and olive, in the Czech Republic, France, Germany, Italy, and Spain (Prodorutti *et al.,* 2008; Laveau *et al.,* 2009; Luque *et al.,* 2009; Tosi and Natalini 2009; Wenneker *et al.,* 2011; Gramaje *et al.,* 2012; Gierl and Fischer, 2017; Baránek *et al.,* 2018; Aiello *et al.,* 2019; Bien and Damm 2020; Eichmeier *et al.,* 2020; Guarnaccia *et al.,* 2020; López-Moral *et al.,* 2020b; Kraus *et al.,* 2022). Other *Diatrypaceae* are less frequently associated with FTD in Europe; *Eutypella citricola*, *Eu. leptoplaca*, *Eu. microtheca* and *Eu. vitis* were found on grapevine in Spain (Luque *et al.,* 2009; Luque *et al.,* 2012). *Peroneutypa scoparia* was recently associated with dieback of walnut and blueberry in, respectively, the Czech Republic and Italy (Eichmeier *et al.,* 2020; Guarnaccia *et al.,* 2020). *Cryptovalsa ampelina* infected walnut and grapevine, in the Czech Republic, Germany, and Spain (Luque *et al.,* 2009; Martin *et al.,* 2009; Luque *et al.,* 2012; Kraus *et al.,* 2019; Eichmeier *et al.,* 2020).

Diaporthaceae is another diverse group of fungi causing FTD of fruit crops. Like some *Botryosphaeriaceae*, *Dia. eres* is ubiquitous in Europe, and affects a wide range of hosts including apple, blueberry, cherry, grapevine, peach, pear, and walnut (Casieri *et al.,* 2009; Thomidis and Michailides, 2009; Lombard *et al.,* 2014; Gierl and Fischer, 2017; Prencipe *et al.,* 2017; Bertetti *et al.,* 2018; Guarnaccia *et al.,* 2018; Pintos *et al.,* 2018; Bien and Damm, 2020; Eichmeier *et al.,* 2020). *Diaporthe foeniculina* caused FTD symptoms on almond, avocado, blueberry, chestnut, citrus, fig, grapevine, pear, and walnut, in France, Germany, Greece, Italy, Malta, Portugal, and Spain (Gramaje *et al.,* 2012; Annesi *et al.,* 2016; Guarnaccia *et al.,* 2016; Guarnaccia and Crous, 2017b; Gierl and Fischer, 2017; Santos *et al.,* 2017; Pintos *et al.,* 2018; Vakalounakis *et al.,* 2019; Mathioudakis *et al.,* 2020; Hilário *et al.,* 2020b; López-Moral *et al.,* 2020a). Other *Diaporthe* spp. have also been linked to FTD on many different crops, especially grapevine, but their occurrence is rare (Lombard *et al.,* 2014; Guarnaccia and Crous, 2017; Guarnaccia *et al.,* 2018; Pintos *et al.,* 2018), or some species such as *Dia. amygdali* are more host specific infecting mainly almond trees (León *et al*., 2020).

Species of *Phaeoacremonium* are well known for their involvement in FTD of grapevine. This group of fungi is diverse, with *P. minimum* being the most prevalent in Europe affecting grapevine, olive, blueberry,

cherry and pistachio (Di Marco *et al.,* 2004; Mostert *et al.,* 2006; Prodi *et al.,* 2008; Luque *et al.,* 2009; Carlucci *et al.,* 2013; Gramaje *et al.,* 2015; Akgül *et al.,* 2015; Pintos *et al.,* 2018; López-Moral *et al.,* 2020b; Agustí-Brisach *et al.,* 2021). *Phaeoacremonium viticola*, *Pm. iraniaum* and *Pm. parasiticum* are also common and have similar host ranges to *P. minimum,* including blueberry, grapevine, olive and *Prunus* trees (cherry, plum) (Mostert *et al.,* 2006; Prodi *et al.,* 2008; Luque *et al.,* 2009; Aroca *et al.,* 2010; Gramaje *et al.,* 2012; Gramaje *et al.,* 2015; Fischer *et al.,* 2016; Bien and Damm 2020; Agustí-Brisach *et al.,* 2021; Raimondo *et al.,* 2021). *Phaeoacremonium cinereum*, *Pm. croatiense*, *Pm. griseorubrum*, *Pm. hispanicum*, *Pm. infatipes*, *Pm. krajdenii* and *Pm. tuscanum* were only isolated from grapevine in Croatia, Italy, and Spain (Essakhi *et al.,* 2008; González and Tello, 2011; Gramaje *et al.,* 2011b, 2015). In contrast, *Pm. amygdalinum* (from almond), *Pm. hungaricum* (*Prunus* trees, plum and cherry), *Pm. olea* (olive), *Pm. venezuelense* (apricot), and *P. vibratile* (cherry) were only found on hosts other than grapevine (Gramaje *et al.,* 2012; Gramaje *et al.,* 2015; Bien and Damm, 2020; Raimondo *et al.,* 2021).

The *Nectriaceae* family includes diverse genera of FTD pathogens, currently named *Cylindrocarpon*-like asexual morphs, which are most known for their involvement in black foot of grapevine, mainly in France, Portugal and Spain (Alaniz *et al.,* 2011; González and Tello, 2011; Martin *et al.,* 2011; Cabral *et al.,* 2012; Agustí-Brisach and Armengol, 2013; Reis *et al.,* 2013; Pintos *et al.,* 2018; Berlanas *et al.,* 2020). However, these fungi have also been associated with decline of olive trees (in Italy), peach (Italy), plum (Bulgaria), apple (Portugal) and kiwifruit (Turkey) (Cabral *et al.,* 2012; Yaseen *et al.,* 2012; Carlucci *et al.,* 2013; Erper *et al.,* 2013; Piperkova *et al.,* 2017).

Investigation of wood necroses in crop trees often results in isolation of *Cadophora* spp., being *C. luteo-olivacea* the most common species in grapevine, but also occurs on olive, plum and blueberry, in Germany, Spain, France and Italy (Casieri *et al.,* 2009; Fischer *et al.,* 2016; Pintos *et al.,* 2018; Raimondo *et al.,* 2019; Bien and Damm, 2020; Guarnaccia *et al.,* 2020; Agustí-Brisach *et al.,* 2021). Furthermore, *C. fastigiata* (in Germany and Switzerland) and *C. viticola* (Spain) were exclusively found on grapevine (Casieri *et al.,* 2009; Gramaje *et al.,* 2015; Fischer *et al.,* 2016). More *Cadophora* spp., e.g. *Ca. malorum*, *Ca. viticola*, *Ca. novi-eboraci*, *Ca. prunicola* and *Ca. ramosa*, infected stone fruit trees (plum, cherry), walnut, apple and blueberry, in Germany, Italy and the Czech Republic (Prodi *et al.,* 2008; Gierl and Fischer, 2017; Eichmeier *et al.,* 2020; Bien and Damm, 2020).

Similar to *Cadophora* spp., *Collophorina* spp., including *Collop. australe*, *Collop. badensis*, *Collop. germanica*, *Collop. hispanica*, *Collop. neorubra*, and *Collop. paarla*, have been associated with wood necrosis, but mostly on stone fruit trees (apricot, almond, cherry, and plum) (Gramaje *et al.,* 2012; Gierl and Fischer 2017; Bien and Damm 2020). Only *Collop. hispanica* has also been linked to discolouration of chestnuts in Spain (Yurkewich *et al.,* 2017).

Besides the above-mentioned fungal families and genera, further species can cause FTD symptoms on different crops in Europe. For instance, *Phaeomoniella chlamydospora*, also associated with esca, appears in every European vineyard, and is probably host-specific for grapevine (Chicau *et al.,* 2000; Fischer and Kassemeyer, 2003; Kakalíková *et al.,* 2006; Casieri *et al.,* 2009; Luque *et al.,* 2009; Akgül *et al.,* 2015; Baránek *et al.,* 2018; Pintos *et al.,* 2018; Agustí-Brisach *et al.,* 2021). However, this fugus was also isolated from kiwifruit plants showing wood decay in Italy (Di Marco *et al.,* 2003). Relatives of *Pa. chlamydospora*, *Pseudophaeomoniella olea* and *Ps. oleicola*, are also host-specific, but for olive, and are linked to wood decay and shoot dieback in Greece, Italy and Spain (Crous *et al.,* 2015; Agustí-Brisach *et al.,* 2021; Markakis *et al.,* 2022). Species of *Colletotrichum*, such as *Col. fructicola*, *Col. gloeosporioides* and *Col. karstii*, have been related to canker and stem-end rot of avocado in Italy, and citrus disease in Italy and Portugal (Ramos *et al.,* 2016; Guarnaccia *et al.,* 2016, 2017). *Cytospora chrysosperma* affected grapevine and blackthorn (González and Tello, 2011; Gierl and Fischer, 2017; Kraus *et al.,* 2019). Its relatives *Cy. oleina*, *Cy. iistaciae* and *Cy. australe* were linked to dieback of olive and pistachio, in Greece, Italy and Spain (Rumbos 1988; Carlucci *et al.,* 2013; Moral *et al.,* 2017; Aiello *et al.,* 2019; López-Moral *et al.,* 2020b).

Several basidiomycetous fungi have been recorded as involved in FTD. *Fomitiporia mediterranea* is the predominant species in Europe, especially in vineyards, where it causes white rot in grapevine trunks (Rumbos and Rumbou 2001; Laveau *et al.,* 2009; Luque *et al.,* 2009; Akgül *et al.,* 2015; Baránek *et al.,* 2018; Moretti *et al.,* 2021; Kraus *et al.,* 2022). In addition, this fungus was also associated with decline symptoms on olive, kiwifruit, citrus, almond and pear (Elena *et al.,* 2006; Carlucci *et al.,* 2013; Markakis *et al.,* 2017; Olmo *et al.,* 2017). *Fomitiporia mediterranea* caused wood decay of kiwifruit, in Italy, Greece and France (Cortesi *et al.,* 2000; Elena and Paplomatas, 2002; Jamaux-Despréaux and Peros, 2003). *Stereum hirsutum*, was reported in Germany, Spain and France, where it was collected from decayed wood of grapevine, almond and chestnut

(Larignon and Dubos, 1997; Fischer and Kassemeyer, 2003; Luque *et al.,* 2009; Gierl and Fischer, 2017; Yurkewich *et al.,* 2017).

FUNGAL TRUNK DISEASES OF APPLE

Several pathogens infect trunks, branches and shoots of apple trees, causing cankers, twig blight, wood rot and, in severe cases, production losses and tree death (Sutton *et al.,* 2014). Symptoms on adult trees develop after long periods, while young plants can rapidly die (Marek *et al.,* 2013). Many Ascomycetes (approx. 36 species) have been associated with FTD of apple (Sutton *et al.,* 2014). Among these, *Neonectria ditissima* is the most serious threat as the cause of European canker, which has typical symptoms of elliptical, sunken areas of dark reddish-brown cankers. After the first year, the cankers become irregular and rough, with bark cracks and abundant production of perithecia (Sutton *et al.,* 2014; Weber and Børve, 2021). This disease has been reported in Germany, Ireland, Poland, and Portugal (Weber and Børve, 2021; Farr and Rossman, 2022).

The apple dieback syndrome is characterized by wood lesions, stunted plants, leaf chlorosis, bark discolouration and extensive cankers associated with wood decay, and progressive tree death (Sutton *et al.,* 2014; Mang *et al.,* 2022). Species in *Botryosphaeriaceae* and *Diaporthaceae* are considered the most relevant pathogens (Havenga *et al.,* 2019; Ali *et al.,* 2020; Diaz *et al.,* 2022). *Botryosphaeria dothidea* and *Dip. seriata* are the main pathogens found associated with dieback of apple trees in several countries (Havenga *et al.,* 2019; Diaz *et al.,* 2022; Ilyukhin *et al.,* 2022). Other *Diplodia* spp. recently reported as pathogenic on apple trees include *Dip. bulgarica* (Nourian *et al.,* 2021), *Dip. mutila* (Urbez-Torres *et al.,* 2016; Sessa *et al.,* 2017; Diaz *et al.,* 2019; Lodolo *et al.,* 2022), *Dip. intermedia* and *Dip. pseudoseriata* (Delgado-Cerrone *et al.,* 2016). Similarly, *Diaporthe* spp. were reported in association with dieback of apple, with *Dia. eres* dominating (Havenga *et al.,* 2019).

Considering the wide range of pathogens, apple dieback is considered as a disease complex (Mang *et al.,* 2022). However, only a few reports have been published on apple dieback in Europe. In Italy, *Dip. malorum*, *Phomopsis mali*, *Nectria* spp. and species in the *Botryosphaeriaceae* were reported as causing dieback, cracking and necrosis of trunks and from graft union sites of apple trees (Prodorutti *et al.,* 2012). Recently, Mang *et al.,* (2022) investigated apple orchards in Southern Italy, and characterized *N. parvum*, *Dia. eres*, *Dia. foeniculina*, *Pestalotiopsis australe*, *Trametes versicolor* and *Phomopsis* spp. The Basidiomycete *Inonotus hispidus* was also shown to be responsible for severe wood decay, canker and dieback symptoms on apple trees in southern Greece (Markakis *et al.,* 2017).

FUNGAL TRUNK DISEASES OF CITRUS

Twigs, branches and trunks of citrus plants affected by several FTD caused by diverse fungi have been reported in different continents (Timmer *et al.,* 2000; Mayorquin *et al.,* 2016; Bezerra *et al.,* 2021). *Colletotrichum* spp. are responsible of twig dieback in major producing areas in Asia and the USA (Huang *et al.,* 2013; Mayorquin *et al.,* 2019), and in Europe, where *Col. gloeosporioides* and *Col. karsti* were reported as dominant *Colletotrichum* spp. causing dieback of citrus twigs and shoots in Italy and Turkey (Aiello *et al.,* 2015; Uysal *et al.,* 2022).

Guarnaccia and Crous (2017) reported severe woody cankers of lemon trees caused by *Dia. limonicola* and *Dia. melitensis* in Malta, often showing gummous exudates and causing severe blight and dieback reported exclusively in Malta. Further *Diaporthe* species, including *Dia. baccae*, *Dia. foeniculina* and *Dia. novem*, are known as secondary pathogens causing wood diseases on citrus plants in Europe. *Diaporthe citri*, a key pathogen of citrus, was associated with shoot blight of *C. reticulata* in the Azores Islands, demonstrating for the first time the presence of a potential threat for citrus fruit production in Europe.

Several studies have recently revised species and genera of *Botryosphaeriaceae*, which include species largely distributed able to cause diseases of numerous plant species (Bezerra *et al.,* 2021; Zhang *et al.,* 2021). In particular, several studies have demonstrated the roles of *Diplodia*, *Dothiorella*, *Lasiodiplodia*, *Neofusicoccum,* and *Neoscytalidium* spp. as causal agents of FTD on *Citrus* spp. (Adesemoye *et al.,* 2011; Berraf-Tebbal *et al.,* 2020). Regarding European distribution, *Neoscytalidium dimidiatum* was reported to cause citrus branch canker in Italy (Polizzi *et al.,* 2009). A broad survey conducted by Bezerra *et al.,* (2021), through Greece, Italy, Portugal, Malta, and Spain, revealed the occurrence, genetic diversity, and pathogenicity of *Botryosphaeriaceae* species associated with symptomatic citrus cultivars. This study also demonstrated pathogenicity of *Botryosphaeriaceae* spp. in citrus-producing areas of these European countries. Phylogenetic multi-locus analyses identified four *Diplodia* species, with *Dip. pseudoseriata* being the most common, followed by three *Neofusicoccum* species, dominated by *N. parvum*, *Do. viticola* and *L. theobromae*.

Canker diseases of citrus are also caused by other fungal genera such as *Fusarium* and *Neocosmospora* (Sandoval-Denis *et al.,* 2018; Guarnaccia *et al.,* 2021), *Peroneutypa* (Timmer *et al.,* 2000), and *Phaeoacremonium* (Espargham *et al.,* 2020). Several *Fusarium* and *Neocosmospora* spp. were found in association with dry root rot, crown, trunk or twig cankers, or twig dieback, of citrus trees (Sandoval-Denis *et al.,* 2018).

FUNGAL TRUNK DISEASES OF GRAPEVINE

FTD of grapevine have become major problems in all grape producing countries, causing significant economic impacts from reduced production and vineyard longevity (AA.VV., 2022). Petri disease and black foot affect young grapevines while the diseases Eutypa, Botryosphaeria and Diaporthe diebacks, Cytospora canker and esca affect mature grapevines. These diseases are caused by a wide range of fungal pathogens producing diverse symptoms, including leaf and shoot distortion and discolouration, external wood cankers, internal wood necroses and staining, poor plant growth, mortality of roots, dieback and sudden grapevine collapse.

Petri disease is mainly caused by combinations of *Pa. chlamydospora* and 28 species of *Phaeoacremonium* (Gramaje *et al.,* 2018) with *Pm. minimum* being the most prevalent (Gramaje *et al.,* 2015). Other species associated with this disease include *Cadophora* spp. (Gramaje *et al.,* 2011a) and *Pleurostoma richardsiae* (Halleen *et al.,* 2007b). Up to 29 species of *Cylindrocarpon*-like asexual morphs belonging of *Campylocarpon*, *Cylindrocladiella*, *Cylindrodendrum*, *Dactylonectria*, *Ilyonectria*, *Neonectria*, *Pleiocarpon* and *Thelonectria* genera have been associated with black-foot of grapevine (Gramaje *et al.,* 2018; Aigoun-Mouhous *et al.,* 2019; Lawrence *et al.,* 2019; Akgül *et al.,* 2022). *Dactylonectria torresensis* is the most common species associated with this disease in Europe (Reis *et al.,* 2013, Carlucci *et al.,* 2017, Berlanas *et al.,* 2020) and Algeria (Aigoun-Mouhous *et al.,* 2019), while *Da. macrodidyma* has been considered the prevalent species in South Africa (Langenhoven *et al.,* 2018) and Canada (Úrbez-Torres *et al.,* 2014).

Eutypa dieback of grapevine is caused by 24 species of *Diatrypaceae* (Trouillas and Gubler 2010a; Luque *et al.,* 2012; Pitt *et al.,* 2013b; Rolshausen *et al.,* 2013), with *E. lata* being the most common and virulent fungus associated with this disease. Other genera of *Diatrypaceae* have been isolated from symptomatic wood, including *Anthostoma*, *Cryptosphaeria*, *Cryptovalsa*, *Diatrype*, *Diatrypella*, and *Eutypella* (Trouillas and Gubler 2010; Luque *et al.,* 2012).

At least 26 different species of *Botryosphaeria*, *Diplodia*, *Dothiorella*, *Lasiodiplodia*, *Neofusicoccum*, *Neoscytalidium*, *Phaeobotryosphaeria*, or *Spencermartinsia* have been reported as causal agents of Botryosphaeria dieback of grapevines (Úrbez-Torres and Gubler 2011; Pitt *et al.,* 2013a,c; Rolshausen *et al.,* 2013; Yang *et al.,* 2017). *Diplodia seriata*, *N. parvum* and *B. dothidea* are the most frequently isolated species (Úrbez-Torres, 2011). Several studies have indicated that most rapidly infecting wood-colonizing fungi, and therefore the most virulent, are species of *Lasiodiplodia* and *Neofusicoccum* (van Niekerk *et al.,* 2004; Úrbez-Torres *et al.,* 2008; Úrbez-Torres and Gubler, 2009).

Several species of *Diaporthe* have been associated with Diaporthe dieback of grapevines (Baumgartner *et al.,* 2013; Úrbez-Torres *et al.,* 2013a; Dissanayake *et al.,* 2015; Guarnaccia *et al.,* 2018). Among these, the disease is primarily caused by *Dia. ampelina* (formerly *Phomopsis viticola*) (Úrbez-Torres *et al.,* 2013a; Dissanayake *et al.,* 2015), which has long been known as the causal agent of the grapevine disease named Phomopsis cane and leaf spot in the United States of America, or excoriose in Europe (Phillips 2000; Úrbez-Torres *et al.,* 2013a).

Several *Cytospora* spp. have been associated with Cytospora canker in Iran (Fotouhifar *et al.,* 2010; Arzanlou and Narmani, 2015), Canada and United States of America (Lawrence *et al.,* 2017), although their pathogenicity on grapevine has only been evaluated for *Cy. viticola* and *C. vinacea*.

Regarding Basidiomycetes associated with esca disease in adult vineyards, these belong to the genera *Inocutis*, *Inonotus*, *Fomitiporella*, *Fomitiporia*, *Phellinus*, and *Stereum* (Cloete *et al*., 2015; Gramaje *et al*., 2018), being *F. mediterranea* the most frequent species in Europe.

FUNGAL TRUNK DISEASES OF BERRY FRUIT

Dieback, canker, and twig and stem blights are common diseases of berry fruit crops (e.g., blueberry, cranberry). These have been associated with diverse fungal pathogens, but most frequently with species of *Diaporthe* and several genera in the *Botryosphaeriaceae* (Lombard *et al.,* 2014; Guarnaccia *et al.,* 2020; Hilário *et al.,* 2020a; Hilário *et al.,* 2021a). Surveys of orchards have shown that dieback and blight are the most common symptoms, which affect plant longevity and fruit yields, and therefore represent threats to production (Lombard *et al.,* 2014; Cardinaals *et al.,* 2018; Guarnaccia *et al.,* 2020; Flor *et al.,* 2022). *Diaporthe vaccinii* (= *Phomopsis vaccinii*) has been regarded as the major species of *Diaporthe* occurring on *Vaccinium* spp. (until recently included in

the EPPO A2 list), causing Phomopsis canker and dieback, twig blight, leaf spots and viscid rot (fruit rot), mainly on highbush blueberry (*V. corymbosum*) and cranberry (*Vaccinium macrocarpon* and *V. oxycoccus*), and also known as upright dieback and viscid rot of cranberry (EPPO Bulletin 2009; Lombard *et al.,* 2014; Michalecka *et al.,* 2017). *Diaporthe vaccinii* is probably widespread in the United States of America and Canada, but there are only a few reports of this fungus in Europe (Germany, Latvia, Lithuania, the Netherlands, Poland, Romania, United Kingdom) (Lombard *et al.,* 2014; Michalecka *et al.,* 2017).

Several *Diaporthe* species have been reported from symptomatic blueberry plants rendering it questionable that *Dia. vaccinii* is a major pathogen of this crop. Its taxonomic status has also been the subject of debate, and Hilário *et al.,* (2021b) proposed that *Dia. vaccinii* is a synonym for *Dia. eres*. *Diaporthe eres* is emerging as the most common and widespread pathogen of highbush blueberry in Europe, being associated with dieback, twig and stem blight, and canker, in Croatia (Ivić *et al.,* 2018), Italy (Martino *et al.,* 2022), the Netherlands (Lombard *et al.,* 2014) and Portugal (as *Dia. vacuae*, a synonym of *Dia. eres*) (Hilário *et al.,* 2020b). This fungus has also been reported as causing cane blight of raspberry in Italy (Guarnaccia *et al.,* 2022b) and of blackberry in Croatia (Vrandecic *et al.,* 2011). In addition to *Dia. eres* and *Dia. vaccini* on *Vaccinium* spp. in different countries in Europe, Lombard *et al.* (2014) described three new species, *Dia. viticola* (= *Dia. rudis*) from the Netherlands, *Dia. baccae* and *Dia. sterilis* were from Italy, *Dia. rudis* has also been reported from symptomatic highbush blueberry plants in Italy (Guarnaccia *et al.,* 2020). A survey of highbush blueberry orchards in Portugal revealed the occurrence of ten *Diaporthe* species in symptomatic (dieback and twig blight) plants, namely *Dia. ambigua*, *Dia. amygdali*, *Dia. crousii*, *Dia. foeniculina*, *Dia. hybrida*, *Dia. leucospermi*, *Dia. phillipsii*, *Dia. malorum*, *Dia. rudis* and *Dia. vacuae* (= *Dia. eres*) (Hilário *et al.,* 2020b, 2021a). Inoculation trials showed that *Dia. amygdali* and *Dia. eres* were the most aggressive to blueberry plants (Hilário *et al.,* 2021a).

Species from at least four genera of *Botryosphaeriaceae*, namely *Botryosphaeria*, *Lasiodiplodia*, *Macrophomina* and *Neofusicoccum*, are known to cause disease on *Vaccinium* spp. Botryosphaeria stem canker is caused by *B. corticis*, a species considered an important pathogen of blueberry, but that has been reported only in the United States of America (Phillips *et al.,* 2006). *Botryosphaeria dothidea* is known to cause stem blight and dieback and has been reported from highbush blueberry in Portugal (Hilário *et al.,* 2020a). Of the 12 species of *Neofusicoccum* associated with stem blight and dieback of blueberry plants, *N. parvum* and *N. australe* have been reported in Portugal and Spain (Castillo *et al.,* 2013; Hilário *et al.,* 2020a), and *N. eucalyptorum* in Portugal. From these three species, *N. parvum* was the most aggressive in inoculation trials with highbush blueberry plants (Castillo *et al.,* 2013; Hilário *et al.,* 2020a).

Species of *Lasiodiplodia*, mostly *L. theobromae*, are important pathogens of blueberry in tropical and subtropical climates (e.g., Rodríguez-Gálvez *et al.,* 2020), but have been also reported in Europe associated with canker and dieback of highbush blueberry in Spain (Borrero *et al.,* 2019) and the Czech Republic (Pečenka *et al.,* 2021). *Macrophomina phaseolina*, a common soilborne fungus, has also been reported on highbush blueberry plants, causing charcoal rot in Spain (de los Santos *et al.,* 2019) and blight in Serbia (Popovič *et al.,* 2018).

Godronia cassandrae f. sp. *vaccinii* (= *Topospora myrtilli*, syn. *Fusicoccum putrefaciens*) causes Godronia canker, also known as Fusicoccum canker. This fungus may cause severe stem dieback of highbush blueberry, especially in young plants. This pathogen has been reported in North America and Europe, as a cause of severe losses in commercial highbush blueberry production (Strømeng and Stensvand, 2011). However, there are no recent reports of this fungus, so its status in Europe is uncertain.

Although not representing major pathogens, pestalotioid fungi of the *Sporocadaceae* have also been reported from blueberry plants with canker, dieback, and blight symptoms (Rodríguez-Gálvez *et al.,* 2020; Santos *et al.,* 2022). *Neopestalotiopsis clavispora* was reported from canker and twig dieback of highbush blueberry in Spain (Borrero *et al.,* 2018). Also on this host in Portugal, Santos *et al.,* (2022) reported three species of *Pestalotiopsis* (*P. australis*, *P. biseriata*, *P. chamaeropis*) and four species of *Neopestalotiopsis*, including *N. rosae* and the newly described *N. scalabiensis*, *N. vaccinii* and *N. vacciniicola*.

FUNGAL TRUNK DISEASES OF NUT TREES

Trunk pathogens of nut trees are underestimated phenomena associated with decline, even where the plants have shown obvious symptoms of trunk diseases. The first comprehensive study of fungal trunk pathogens detected in the wood of almond trees in Mallorca was published in 2012 (Gramaje *et al.,* 2012). Pathogens detected were: the *Botryosphaeriaceae*, *B. dothidea, Dip. olivarum, Dip. seriata, N. australe,* and *N. parvum*, confirmed by Olmo *et al.* (2016) and Arzanlou *et al.* (2016);

the *Diatrypaceae E. lata;* the *Togniniaceae Phaeoacremonium amygdalinum and P. iranianum*, confirmed by Raimondo *et al.* (2021); and the *Diaporthaceae Diaporthe amygdali*, later confirmed by Varjas *et al.* (2017), León *et al.* (2020), and Beluzán *et al.* (2022). Almond wood is also invaded by *Pleurostoma richardsiae* (Olmo *et al.,* 2015) and *Calosphaeria pulchella* (Arzanlou *et al.,* 2013). Holland *et al.* (2021b) described detailed symptoms on the almond wood associated with pathogens. They observed Botryosphaeriaceae canker, Ceratocystis canker, Cytospora canker, Diaporthe canker, Collophorina canker, Eutypa and Pallidophorina canker. Severe stem canker of almond trees caused by *Fusarium solani* was also reported by Markakis *et al.* (2021).

Walnut woody parts are commonly invaded by trunk pathogens, including *Diatrypaceae*, *Diaporthaceae*, *Botryosphaeriaceae* and *Togniniaceae*. In general, the spread of these fungi is similar in regions and countries such as: California (*Diaporthe*, *Neofusicoccum*) (Trouillas *et al.,* 2010; Agustí-Brisach *et al.,* 2019), Chile (*Diaporthe*, *Diplodia, Neofusicoccum*) (Díaz *et al.,* 2018; Luna *et al.,* 2022), China (*Botryoshpaeria*, *Lasiodiplodia, Neofusicoccum*) (Yu *et al.,* 2015; Li *et al.,* 2016), the Czech Republic (*Cadophora, Cryptovalsa, Diaporthe, Diplodia, Dothiorella, Eutypa, Eutypella, Peroneutypa, Phaeoacremonium*) (Eichmeier *et al.,* 2020), Italy (*Botryosphaeria, Neofusicoccum*) (Gusella *et al.,* 2021), Romania (*Diaporthe*) (Mihaescu *et al.,* 2020), Spain (*Botryosphaeria, Diaporthe, Diplodia, Dothiorella, Neofusicoccum*) (López-Moral *et al.,* 2020a; Moral *et al.,* 2010), and Turkey (*Botryosphaeria*, *Neofusicoccum*) (Kara *et al.,* 2021; Yildiz *et al.,* 2022). Walnut wood also hosts *Ca. spacidis* and *Ca. novi-eboraci* (*Incertae sedis*) and these pathogens were detected in most surveyed orchards in the Czech Republic (Eichmeier *et al.,* 2020).

Hazelnut plants can be hosts of *Diaporthe* as described for Turkey (Arciuolo *et al.,* 2020) and *Fomitiporia* in Italy (Pilotti *et al.,* 2010). Pistachio trunk pathogens are also known. Several pathogens were isolated in California, including *Col. karstii*, *Cy. californica*, *Cy. joaquinensis*, *Cy. parapistaciae*, *Cy. pistaciae*, *Dia. ambigua*, *Didymella glomerata*, *Dip. mutila*, *N. mediterraneum*, *Pm. canadense*, and *Schizophyllum commune* (Nouri *et al.,* 2019). Survey of FTD pathogens of pistachio in Iran revealed *Pm. parasiticum* as a dominant species, followed by *Pm. minimum*, *B. dothidea*, *N. parvum*, *Pm. cinereum*, *Pm. viticola* and *Do. viticola* (Mohammadi *et al.,* 2015). Chen *et al.* (2015) collected *L. americana* sp. nov. from blighted pistachio shoots in Arizona, United States of America, and *N. hellenicum* sp. nov. in Greece, while in Italy the new pathogen *Liberomyces pistaciae* sp. nov. was detected (Vitale *et al.,* 2018). Nut trees such as almonds, pistachios and walnuts were described in Iran as hosts of *Botryosphaeria, Collophorina, Cryptosphaeria, Diatrype, Diplodia, Dothiorella, Eutypella, Lasiodiplodia, Neofusicoccum, Pleurostoma* by Sohrabi *et al.* (2020).

FUNGAL TRUNK DISEASES OF STONE FRUIT TREES

Stone fruit trees are commonly affected by numerous wood-invading pathogens causing cankers and dieback. *Eutypa lata* was first reported as the causal agent of gummosis or dieback of apricot in Australia (Carter, 1957), and has since been known to affect several types of stone fruit trees (Matthee *et al.,* 1974; Carter 1982, 1995; Munkvold and Marois 1994; Rumbos, 1997). To date, at least 19 distinct species of *Togniniaceae* (i.e. *Pm. scolyti*, *Pm. minimum*, *Pm. australiense*, *Pm. alvesii*, *Pm. parasiticum*, *Pm. infatipes*, *Pm. iranianum*, *Pm. italicum*, *Pm. griseorubrum*, *Pm. junior*, *Pm. longicollarum*, *Pm. pallidum*, *Pm. prunicolum*, *Pm. subulatum*, *Pm. fuscum*, *Pm. griseorubrum*, *Togninia africana*, *T. griseo-olivacea* and *T. fraxinopennsylvanica*) have been associated with necrotic wood of stone fruit trees (Hawksworth *et al.,* 1976; Rumbos, 1986; Hausner *et al.,* 1992; Damm *et al*., 2008; Spies *et al.,* 2018). As well, four *Cytospora* species (*Cy. chrysosperma*, *Cy. longispora*, *Cy. plurivora, Cy. sorbicola*) have been identified as canker and dieback-causing pathogens in stone fruit trees including *Persica vulgaris*, *Prunus armeniaca*, *P. avium*, *P. cerasus*, *P. domestica* and *P. persica*, in several countries (Lawrence *et al.,* 2017).

Canker and branch dieback of sweet cherry trees caused by *Calosphaeriophora pulchella* has also been reported in California, Chile, South Australia and Spain (Trouillas *et al.,* 2012; Berbegal *et al.,* 2014; Auger *et al.,* 2021).

Studies conducted primarily in South Africa demonstrated the diversity of indigenous flora and the occurrence of newly identified fungi causing trunk diseases in adult stone fruit trees and propagation material (Damm *et al.,* 2007, 2010). The pathogenic potential of most of these species has been confirmed in pathogenicity trials. Damm *et al.* (2007) isolated several *Botryosphaeriaceae* species (*Dip. seriata*, *N. vitifusiforme, N. australe*, *Do. viticola, Dip. pinea*, *Dip. mutila, L. plurivora* and *Dip. africana*) from plum, peach, nectarine and apricot trees showing wood necrosis in South Africa. In another study on *Prunus* trees showing wood necrosis (Damm *et al*., 2010), identified species of *Coniochaeta* (*C. velutina* and the two new species, *C. africana* and *C. prunicola*) and *Phaeomoniellales* (*Pa. zymoides* on *Prunus salicina*, and the new species *Pa. dura*, *Pa. effusa*, *Pa. prunicola*

and *Pa. tardicola* mainly in plum wood). The new genus *Collophorina* was also proposed, comprising *Collop. africana*, *Collop. capensis*, *Collop. pallida* and *Collop. rubra* that occurred frequently in necrotic peach and nectarine wood. Also in South Africa, apricot and plum trees were inhabited by five *Diatrypaceae* species with *E. lata* the most dominant, followed by *Cryptovalsa ampelina*, *E. cremea*, *Eutypella citricola* and *Eu. microtheca*, whereas no *Diatrypaceae* were found on peach and nectarine (Moyo *et al.,* 2018).

In a similar study conducted in Germany, *Pallidophorina paarla*, *Collop. africana* and the two new species *Collop. badensis* and *Collop. germanica*, were associated with wood necroses on *Prunus* trees (Bien and Damm, 2020). Here, *Cadophora* was reported for the first time from *Prunus*, with *Ca. luteo-olivacea* and *Ca. novi-eboraci* dominating (Bien and Damm, 2020). *Cadophora prunicola*, *Ca. ramosa* and *Minutiella pruni-avium* were also described as new species.

A study in the western cape of South Africa (van der Merwe *et al.,* 2021) showed that stone fruit propagation material and nursery plants had latent infections of canker- and wood rot-associated fungi, with *Ca. luteo-olivacea* and *Dip. seriata* as the most frequently isolated. Sampled nursery trees were 22% infected, ungrafted rooted rootstock plants, 11%, dormant rootstock shoots, 6%, dormant buds, 1%, and green buds were 0.4% infected. Van der Merwe *et al.* (2021) also made 22 new records of fungal species on stone fruit, including (among others), three species of *Coniochaeta*, two of *Cadophora* and *Cytospora*, and one species of *Biscogniauxia*, *Eutypella* and *Peniophora*.

FUNGAL TRUNK DISEASES OF OLIVE TREES

FTD of olive have been considered as emerging problems for olive cultivation. Several studies have shown many wood-inhabiting fungi in diverse groups as causal agents of discrete diseases in adult and nursery olive plants. Numerous *Botryosphaeriaceae* species (i.e. *B. dothidea*, *B. obtusa*, *Dip. mutila*, *Dip. seriata, Do. iberica*, *L. theobromae*, *N. australe, N. stellenboschiana, N. luteum*, *N. mediterraneum, N. parvum* and *N. vitifusiforme*) have been shown as causing olive twig and branch dieback in California, Croatia, Italy, Tunisia, South Africa and Spain (Moral *et al.,* 2010, 2017; Carlucci *et al.,* 2013; Kaliterna *et al.,* 2013a; Úrbez-Torres *et al.,* 2013b; Spies *et al.,* 2020; van Dyk *et al.,* 2021b).

Several *Togniniaceae* (i.e. *Pm. africanum, Pm. alvesii, Pm. italicum, Pm. minimum, Pm. oleae*, *Pm. parasiticum, Pm. prunicola, Pm. rubrigenun, Pm. scolyti, Pm. sicilianum, Pm. spadicum* and *Pm. viticola*), *Phaeomoniellales* (i.e. *Neophaeomoniella niveniae*, *Pa. chlamydospora*, *Pseudophaeomoniella globose, Ps. oleae* and *Ps. oleicola)* and *Acremonium sclerotigenum, Ca. luteo-olivacea*, *Comoclathris incompta*, *Paracremonium* sp. and *Pleurostoma richardsiae* have also been indicated as causal agents of olive wood streaking, wilting, dieback and decline in California, Croatia, Greece, Italy, South Africa and Spain (Ivic *et al.,* 2010; Nigro *et al.,* 2013; Carlucci *et al.,* 2015; Markakis *et al.,* 2017, 2022; Spies *et al.,* 2020; Agustí-Brisach *et al.,* 2021; Lawrence *et al.,* 2021; van Dyk *et al.,* 2021b; Raimondo *et al.,* 2022).

The Basidiomycetes *F. mediterranea* (Fig. 2), *Fomitiporella viticola*, *Ganoderma lucidum*, *Phellinus linteus, P. robiniae, Schizophyllum commune* and *Trametes versicolor* have also been reported to be involved in olive wood rot and decay, in California, Greece and South Africa (Crous *et al.,* 2000; Úrbez-Torres *et al.,* 2013b; Markakis *et al.,* 2017, 2019; Lawrence *et al.,* 2021; van Dyk *et al.,* 2021b). Members of *Diatrypaceae* (i.e. *Diat. oregonensis*, *Diat. stigma*, *E. lata*), and species of *Cytospora* (i.e. *Cy. oleina*, *Cy. oleicola*, *Cy. olivarum*, *Cy. plurivora, Cy. pruinosa* and *Cy. sorbicola*) and *Diaporthe* (i.e. *Dia. viticola*, *Dia. rubis, Dia. foeniculina*) were associated with canker and twig and branch dieback diseases of olive trees in California, Greece, South Africa and Spain (Rumbos, 1988, 1993; Moral *et al.,* 2017; Lawrence *et. al.*, 2017; van Dyk *et al.,* 2021b).

A recent survey by van Dyk *et al.* (2021b), in the Western Cape Province, South Africa, and coupled with pathogenicity tests, showed *Ps. globosa* as a major olive trunk pathogen, and several lesser-known fungi were also associated with olive trunk disease symptoms. These included *Biscogniauxia rosacearum*, *Celerioriella umnquma*, *Coniochaeta velutina*, *Coniothyrium ferrarisianum*, *Didymocyrtis banksiae*, *Punctularia atropurpurascens*, *Vredendaliella oleae*, an undescribed *Cytospora* sp., *Geosmithia* sp., two undescribed *Neofusicoccum* spp., and four *Xenocylindrosporium* spp. Van Dyk *et al.* (2021a) also surveyed trunk pathogens in South African olive nurseries, and found several pathogens in *Nectriaceae, Diaporthaceae*, *Botryosphaeriaceae*, *Togniniaceae*, *Phaeomoniellaceae* and *Pleurostomataceae*, with *N. australe*, *Pleurostoma richardsiae* and *Pm. parasiticum* the most common fungi in propagating plant material.

EPIDEMIOLOGY OF TRUNK DISEASES

Most FTD pathogens can infect planting material during propagation processes in nurseries. Several studies have shown evidence to support non-pathogenic

Figure 2. Wood decay (Esca) symptoms in olive trees in Thrace, Northeastern Greece, infected by *Fomitiporia mediterranea*. Canker in the trunk (**A**); white rot appeared after removing a trunk sector due to incorrectly adjusted irrigation sprinklers which created conducive conditions for fungal infection (**B**); carpophore of *F. mediterranea* formed on the trunk surface (**C**); trunk cross section revealing light-coloured wood rot surrounded by a brown necrotic zone (**D**).

endophytic phases for these fungi, as they have been isolated from asymptomatic mother plants and propagation material (Halleen *et al.,* 2003; Aroca *et al.,* 2010; Berlanas *et al.,* 2020; van der Merwe *et al.,* 2021). Several studies have confirmed that plant propagation stages are potential infection points in grapevine nurseries (Edwards and Pascoe 2004; Aroca *et al.,* 2010; Halleen *et al.,* 2003; 2007a; Agustí-Brisach *et al.,* 2013), and recent studies indicate the role of infected planting material in the dissemination of fungal trunk pathogens in stone fruit trees (Marín-Terrazas *et al.,* 2016; van Dyk *et al.,* 2021a; van der Merwe *et al.,* 2021; Capote *et al.,* 2022) and apple (Havenga *et al.,* 2019).

Cylindrocarpon-like asexual morphs are soilborne. These fungi are commonly found in nursery fields and soils, so inoculum may already exist in soils before planting (Agustí-Brisach *et al.*, 2013; Berlanas *et al.,* 2017). However, most FTD pathogens are primarily spread through the dispersion of airborne spores. Depending on the fungal species, conidia or ascospores are released from pycnidia or perithecia embedded in the surfaces of dead wood and/or in bark tissues (Eskalen and Gubler, 2001; Rooney-Latham *et al.,* 2005; Úrbez-Torres *et al.,* 2014; van Niekerk *et al.,* 2010; Kraus *et al.,* 2020). This inoculum is released under favourable environmental conditions, which have been mostly associated with rain events and/or high relative humidity along with temperatures above freezing, which also favour spore germination (Úrbez-Torres *et al.,* 2010a; van Niekerk *et al.,* 2010). Spores then land on susceptible pruning wounds and/or natural openings to germinate and start colonization of xylem vessels and pith parenchyma cells (Mostert *et al.,* 2006).

Jiménez-Luna *et al.* (2022) showed the presence and diversity of air-borne spores of FTD pathogens in almond and walnut orchards in California, where incidence was influenced by host, age of the plants and precipitation. Arthropod-mediated dispersal of FTD pathogens has also been demonstrated in vineyards, indicating potential roles for arthropods in trunk diseases epidemiology (Moyo *et al.,* 2014; Kalvelage *et al.,* 2021, 2022). Agustí-Brisach *et al.* (2015) showed that pruning equipment can spread FTD pathogens under controlled conditions. They also found that high inoculum concentrations of FTD pathogens were required to produce successful infection. In grapevine, studies have shown that high risk infection periods may vary throughout each host growing season, and from year to year, but these periods can also overlap with host dormancy seasons in the Northern and Southern Hemispheres (Larignon and Dubos, 2001; Eskalen and Gubler, 2001; Amponsah *et al.,* 2009; Kuntzmann *et al.,* 2009; Quaglia *et al.,* 2009; Úrbez-Torres *et al.,* 2010; van Niekerk *et al.,* 2010; Cloete *et al.*, 2015; Valencia *et al.,* 2015; González-Domínguez *et al.,* 2020; Billones-Baaijens *et al.,* 2018). An epidemiological equation model for *Pa. chlamydospora* was developed by González-Domínguez *et al.* (2020) in Spanish vineyards. They showed that dispersal dynamics of this fungus was best explained by hydro-thermal time which takes account of effects of temperature and rainfall.

FTD fungi are cosmopolitan, and can colonize a range of hosts as saprotrophs or plant pathogens, infecting natural ecosystems and cultivated crops. Patterns of multiple host infections have been reported for *Botryosphaeriaceae* (Damm *et al.,* 2007; Slippers and Wingfield, 2007; Mojeremane *et al.*, 2020), *Diatrypaceae* (Moyo *et al.,* 2019), and *Togniniaceae* (Damm *et al.,* 2008). This is also the case for *F. mediterranea*, a lignicolous fungus that has been found as the causal agent of wood decay in several woody hosts (Markakis *et al.*, 2017). The overlap of trunk disease pathogens between agricultural systems and native plant ecosystems has also been indicated (Damm *et al.,* 2007, 2008; Moral *et al.,* 2010; Trouillas *et al.,* 2010; Markakis et al., 2017; Moyo *et al.,* 2019). The discovery of a single fungal species on multiple hosts has important epidemiological implications, giving circumstantial evidence that inocula travel between different woody hosts, so those hosts occurring in close proximity can provide inoculum to each other.

HYPOTHESES FOR INCREASED INCIDENCE OF TRUNK DISEASES

Crop intensification

Crop intensification can increase FTD incidence in the field. Intensive cropping systems provide favourable environments for infection, since microclimate resulting from high plant densities can increase wetness duration and decrease sunlight entry into tree canopies (Kraus *et al.,* 2018). Modern super-high-density systems also demand mechanization of cultural practices (e.g. pruning and harvesting), with consequential injuries that create conducive conditions to wound-penetrating fungi such as Basidiomycetes, *Botryosphaeriaceae*, *Diatrypaceae* and *Togniniaceae* (Moral *et al.,* 2010; Úrbez-Torres *et al.,* 2013b; Markakis *et al.,* 2017; Agustí-Brisach *et al.,* 2021). In viticulture, intensive pruning schemes (e.g. spur or cane pruning), can cause more frequent external FTD symptoms than minimal pruning schemes (Lecomte *et al.,* 2018, 2022; Kraus *et al.,* 2019). It was also assumed that intensive pruning causes more and larger pruning wounds on grapevine trunks, leading

to increased infections by wood degrading fungi, and consequent interruption of host vascular systems and increased symptoms (Travadon *et al.,* 2016; Kraus *et al.,* 2022).

Intensive crop production with high yields elevates plant water demand and in combination with the ongoing climate warming provokes drought stress, which enhances FTD development. For almond trees in southern Spain, water deficiency leads to increased dieback severity compared to well-watered trees (Agustí-Brisach *et al.,* 2020). In addition, under drought stress, grapevines were more susceptible to infection and colonization by FTD pathogens (Sosnowski *et al.,* 2016, 2021; Galarneau *et al.,* 2019; Hrycan *et al.,* 2020). The exact role of climate/environmental conditions (e.g. drought, rainfall, water availability) in FTD incidence is not completely clear and requires further investigation (Fischer and Peighami Ashnaei, 2019; Songy *et al.,* 2019).

Different woody crops (e.g. olive, grapevine and almonds) that are affected by the same fungal pathogens are commonly grown in neighbouring orchards in several Mediterranean countries (Fig. 3). This is likely to allow inoculum proliferation and flow among the orchards (Markakis *et al.,* 2017). Crop intensification is also likely to disturb microflora balances in agro-ecosystems, promoting transfer of trunk pathogens and their adaptation to new woody hosts. In recent years, emergence of new FTD has been shown for several woody crops (Damm *et al.,* 2010; Markakis *et al.,* 2017; van der Merwe *et al.,* 2021; van Dyk *et al.,* 2021a; b).

Figure 3. Typical landscape of adjacent vineyards and olive orchards in Crete, Southern Greece, which allows the inoculum flowing.

Planting material and nursery practices

Plant propagation in fruit crop and grapevine nurseries includes complex systems in which pathogen management is challenging. Infected nursery stock can be important long-distance vectors for FTD pathogens (Gramaje and Armengol, 2011). Studies in Europe on death of young or newly established fruit crop trees have shown that latent infections occurring during nursery propagation are important for development of cankers observed in the orchards (Brown *et al.,* 1994; Smit *et al.,* 1996; Marek *et al.,* 2013). Certified nursery trees are not commonly surveyed for latent fungal infections, which can lead to severe symptoms in newly established stone fruit orchards (Mostert *et al.,* 2016; van der Merwe *et al.,* 2021). McCracken *et al.* (2003) found that cankers caused by *N. ditissima* on scion shoots of 1-year-old commercial apple trees, developed after infections that occurred during the final stages of propagation. Marek *et al.* (2013) found that latent infections, occurring in nurseries, caused wood cankers during cold storage of propagation material or after planting. Havenga *et al.* (2019), in South Africa, showed presence of fungal pathogens causing FTD on the 65% of assessed certified apple tree nurseries. The pathogens isolated from 1-year-old diseased commercial trees were also recovered from latent infections in nursery trees, confirming the roles of rootstock wounds and bud unions as infection sites.

Van Diyk *et al.* (2021a) reported the presence of eight known FTD pathogens of olive and other woody host from plant portions which were in direct contact with perlite/soil and water. Infected grapevine propagation material is considered to have a major role for disease occurrence in the field (Halleen *et al.,* 2003; Gramaje and Armengol, 2011). Stone fruit nursery trees have also been investigated. Isolations conducted from scions and rootstocks have highlighted the importance of these materials as sources of latent infections for nursery trees, showing the presence of FTD pathogens on the 22% of 1080 trees tested (van der Merwe *et al.,* 2021).

This information emphasizes the importance of incorporating integrated disease management that combines different preventative control measures throughout the nursery propagation processes, storage, and during crop establishment, in order to reduce incidence and severity of FTD in orchards (Gramaje *et al.,* 2018). Cultural practices such as the removal of dead and affected material, which often bring fungal fruiting bodies and spores, is important in all phases of propagation and plant establishment (Van Zyl 2011). Authorized fungicides and biological control agents should be used to protect pruning wounds throughout plant propagation to reduce infections in nurseries (Fourie and Halleen 2004). For grapevine, hot water treatments of scions/

rootstocks before grafting, and of the dormant grafted nursery grapevines are recommended practices to reduce pathogen inocula (Fourie and Halleen 2004; Halleen *et al.,* 2007b; Bleach *et al.,* 2013; Eichmeier *et al.,* 2018).

Climate change

Increased incidence of FTD on woody hosts can be attributed to climate change (Chakraborty and Newton 2011; Kaliterna *et al.,* 2013a; Markakis *et al.,* 2017). Climate change prediction models foresee more frequent extreme weather conditions, along with increases in summer air temperature and drought stress for many crops in the Mediterranean region (Lung *et al.,* 2013). In California, Allen and Luptowitz (2017) predicted significant rainfall increases in response to warming climate. Alterations of wet and dry cycles, and extremely low and/or high temperature events will probably be more frequent, as consequences of the climate change. These phenomena may favour pathogen dispersal and adaptation to hosts other than their primary hosts, and this has been suggested for the extended host range of *F. mediterranea* (Elena *et al.,* 2006; Markakis *et al.,* 2017, 2019). This was also the case for the epidemic caused by *Dip. seriata* (a weak pathogen) that occurred in summer 2010 in Croatia, when severe dieback occurred in young olive trees previously exposed to low winter temperatures (Kaliterna *et al.,* 2013a). *Botryosphaeriaceae*-incited diseases are commonly more severe in years with high rainfall, when inoculum increases are followed by drought periods and host susceptibility increases (Ma *et al.,* 2001; Michailides and Morgan 2004; Marsberg *et al.,* 2017).

Microbiome balance

All plants contain microorganisms as parts of their holobionts (Berg *et al.,* 2020). These microbiota and their activities, the so-called microbiome, have been shown to change for all diseases, and as conditions alter (Bettenfeld *et al.,* 2020). There are functional core microbiota playing central roles in plant physiology and health. Increased numbers of (latent) pathogens in the core microbiota and detrimental effects on other microorganisms, which can take place when the plants are weakened by other biotic or abiotic factors, can lead to increase virulence and visible plant symptoms (Bettenfeld *et al.,* 2020). "Satellite microbiota" (i.e. not occurring in every plant) can be also be affected.

For FTD, Bruez *et al.* (2020) suggested that fungal microbiota from non-necrotic woody tissues were similar in healthy and esca diseased grapevines. In non-necrotic woody tissues, fungal and bacterial microbiota varied according to organs and seasons, but not according to disease status. *Phaeomoniella chlamydospora*, was the most abundant fungus in non-necrotic tissues from healthy plants. The only difference between healthy and diseased young grapevines was the presence of white rot necrotic tissues in cordons that were dominated by *F. mediterranea*, associated with *Pa. chlamydospora* and a few bacterial taxa. Increased numbers of pathogens, and changes in mycobiomes, were recorded in different plant tissues.

Meta barcoding studies of grapevines in Portugal (Del Frari *et al.,* 2019) and Greece (Bekris *et al.,* 2021) have assessed the mycobiomes of grapevine trunks with esca, and cultivar and biogeography-dependent patterns were identified that could be used as to distinguish between healthy and diseased grapevines. By analyzing the microbiomes of healthy and diseased grapevines, strong interactions between the bacterial and fungal wood microbiomes in asymptomatic grapevines could be used for discovery of novel biocontrol agents (Cobos *et al.,* 2022). However, specific bacteria isolated from healthy or diseased host tissues have been described as potentially increasing wood degradation by esca pathogens. This has been shown for *F. mediterranea* (Haidar *et al.,* 2021). Some bacterial strains that degrade grapevine wood components (cellulose and hemicellulose) did not inhibit *F. mediterranea* growth *in vitro*, but had synergistic interactions with *F. mediterranea* by enhancing the degradation of wood structures (Haidar *et al.,* 2021). One of these strains has been described as belonging to a new species, *Paenibacillus xylinteritus* sp. nov. (Haidar *et al*., 2022). Analyzing the microbiomes of healthy and diseased plants can pinpoint balance/imbalance that could lead to discovery of new types of interaction, such as other microorganisms that increase or decrease pathogen virulence.

Limited availability of fungicides

Chemical control using fungicides has been the main strategy for FTD management both in propagation material produced in nurseries and adult plants in orchards, for which pruning wound protection is essential to reduce FTD incidence. Nevertheless, limited products are currently registered to effectively control FTD in Europe and worldwide. Thus, future research should be focused on expanding the range of chemical and alternative options for this purpose (Gramaje *et al*., 2018). Available management strategies against FTD on grapevines have been widely investigated in the last decades and, for instance, many new biological control agents have been evaluated and registered to control FTD both in nurseries and vineyards, including fungi, bacteria and oomycet-

es, being *Trichoderma* spp. based products the most frequent (Gramaje *et al*., 2018; Mondello *et al*., 2018a,b). In the same way, it is necessary to progressively expand the range of treatments available for all types of fruit trees.

FUTURE DIRECTION OF FTD RESEARCH

Over the last years, fungal trunk pathogens incidence has globally increased in woody crops. The etiology is still complex, as many pathogens have been recently described associated with FTD symptoms. Disease management implies the adoption of precision farming technologies and alternative strategies to the use of synthetic fungicides (i.e., microbial biocontrol agents, plant defense elicitors and possible microbiome manipulations). This will provide a new scenario to understand the role of trunk pathogens in the whole cropping system. The integration of plant pathology concepts and methodologies with those of other disciplines will be needed to deliver new disease management strategies in a wider context. Here, we discuss the future direction of FTD research and identify some key issues that, we anticipate, must be faced to overcome the losses caused by these diseases.

A key challenge in this complex pathosystem is to develop tools and methodology that enable the rapid detection of FTD fungi in asymptomatic plants, especially in planting material, and the accurate diagnosis of the causal agents. High throughput sequencing (HTS) diagnostics is revolutionizing plant pathology. HTS methods are probably the most significant advances in molecular biology since the advent of the PCR process. Microbial/fungal genome sequencing or metagenomics/metabarcoding become a routine analysis and using the latest technology it is possible to generate near complete genomes (Robert-Siegwald *et al*., 2017; Eichmeier *et al*., 2022) or whole spectra of microbial/fungal communities (Eichmeier *et al*., 2018; Bruez *et al*., 2020; Gramaje et al. 2022). There are also other applications of HTS technology which can serve understanding of the plant pathogen interaction as transcriptomics (Romeo-Oliván *et al*., 2022) or small RNA sequencing (Eichmeier *et al*., 2019).

The advent of precision farming technologies coupled with remote sensing methods opens entire new fields of research, where the performance of cultural practices for FTD management can be addressed. Imaging analysis is one promising method for a non-invasive detection of FTD. For grapevine, with hyperspectral- or multispectral imaging analysis, esca symptomatic and asymptomatic plants can be diagnosed even before clear foliar-symptoms appear (Junges *et al*., 2018; Bendel *et al*., 2020; Pérez-Roncal *et al*., 2022). Even with unmanned aerial vehicles, whole vineyards could be monitored this way for FTD, which facilitates the assessment of the vineyard's health status (Di Gennaro *et al*., 2016). Furthermore, for Laurel wilt disease on avocado, it was possible to distinguish between healthy and asymptomatic trees based on hyperspectral analysis of the leaves (Hariharan *et al*., 2019, Abdulridha *et al*., 2016). In a trial with potted olive trees artificially infected with *F. mediterranea*, the uninfected population could be differentiated from the infected population with a good accuracy also by hyperspectral analysis of the leaves (Zapolska *et al*., 2020). These examples show that spectral imaging analysis of leaves are convenient diagnostic tools to detect FTD in different perennial crops. In the future, this tool could be implemented into the plant protection management process for an early detection of the disease. With that, proper curative countermeasures can be applied and, thus, preventing the plant from becoming symptomatic.

For many IPM programs, including the management of FTD, there is a crucial need of decision-support tools to determine disease risk and the best moments for any intervention (Rossi *et al*., 2012). Mathematical models that establish relationships between the amount of inoculum and disease development, integrating knowledge on the host-pathogen interactions and environmental data, are key components of any decision-support tool for plant disease management (Ojiambo *et al*., 2017), and have been consistently incorporated in decision support systems (DSSs) to assist users in operational and tactical decision-making in crop protection. Model-based forecasting has the potential to improve the timeliness, effectiveness, and foresight for managing crop diseases, while minimizing economic costs and environmental impacts (Newlands, 2018). For instance, improving our knowledge about the dispersal patterns of FTD spores and its relation to environmental conditions is essential for identifying periods with a high risk of spore dispersal and for adopting management strategies, such as pruning wound protection.

Regulatory changes are reducing the availability of fungicide options, as the health and ecological hazards of the chemicals are increasingly raising concerns. The consumer demand for residue free products have stimulated research into new tools for pest management. Alternatives to synthetic fungicides are mainly represented by a number of microbial active ingredients. Agronomic practices, i.e., reduction of the inoculum in the field, should be combined with biological control in order to reduce the input of synthetic fungicides on the crop.

Nanoparticles (NPs) in size 1–100 nm have demonstrated activity in suppressing plant diseases. These

NPs are mainly metalloids, metallic oxides, nonmetals, and carbon nanomaterials. NPs have been integrated into disease management strategies as fungicides or as nanofertilizers to enhance plant health. Although there are reports of different NPs of single element and carbon nanomaterials affecting plant pathogens. Mainly Ag, Cu, and Zn have received much attention thus far. Some NPs act directly as antimicrobial agents but others work more in altering the nutritional status of the host and they activate various defense mechanisms (Elmer *et al*., 2018). A recent study about the use of nanomaterials against selected FTD pathogens showed that AgSe nanoparticles (NPs), CuSe NPs, Ag NPs, Cu NPs and Se NPs can serve a significant inhibitory activity against *Dia. eres*, *Dip. seriata* and *E. lata* (Štůsková *et al*., 2022). Little information is still available on the use of NPs against FTD pathogens. In addition, more research is needed to evaluate the impact of these treatments on the microbiome and the environment.

Other alternatives to synthetic fungicides are the substances of botanical origin. Recently, several authors described the antimicrobial ability of wood extracts against various fungal species (Kawamura *et al*., 2011; Minova *et al*., 2015; Salem *et al*., 2015; Vek *et al*., 2021). Špetík *et al*. (2022) demonstrated that lignans extract from knotwood of Norway spruce function against *Cad. luteo-olivacea*, *Da. torresensis*, *Dia. ampelina*, *Dia. bohemiae*, *Dip. seriata*, *E. lata* and *Pm. minimum* affecting grapevine. Further research is needed to test the efficacy of these products under field conditions.

Over the last few years, the importance of the plant microbiome, the potential role of endophytes in disease control and/or development, and the interactions among microorganisms has been postulated (Blundell *et al*., 2022). The use of the most advanced technologies will contribute to the discovery of the next generation of microbial biofungicides. In recent years, designing microbial consortia (SynComs – synthetic microbial communities) has received a great deal of interest to overcome the variable results of bioncontrol agents under field conditions. SymComs are expected to be more robust to environmental changes than single-microbiome inoculants and are designed to mimic the natural microbiome function and structure. However, research is still needed to validate the consortia functionality at field scale.

LITERATURE CITED

AA.VV., 2022. Abstracts of oral and poster presentations given at the 12th International Workshop on Grapevine Trunk Diseases, Mikulov, Czech Republic, 10–14 July 2022", *Phytopathologia Mediterranea* 61: 319–369.

Abdulridha J., Ehsani R., De Castro A., 2016. Detection and differentiation between Laurel wilt disease, Phytophthora disease, and salinity damage using a hyperspectral sensing technique. *Agriculture* 6: 56.

Adesemoye A.O., Eskalen A., 2011. First report of *Spencermartinsia viticola*, *Neofusicoccum australe*, and *N. parvum* causing branch canker of citrus in California. *Plant Disease* 95: 770.

Agustí-Brisach C., Armengol J., 2013. Black-foot disease of grapevine: an update on taxonomy, epidemiology and management strategies. *Phytopathologia Mediterranea* 52S: 245–261.

Agustí-Brisach C., Cabral A., González-Domínguez E., Pérez-Sierra A., León M., … Armengol J., 2016. Characterization of *Cylindrodendrum*, *Dactylonectria* and *Ilyonectria* isolates associated with loquat decline in Spain, with description of *Cylindrodendrum alicantinum* sp. nov. *European Journal of Plant Pathology* 145: 103–118.

Agustí-Brisach C., Jiménez-Urbano J.P., Raya M.C. López-Moral A., Trapero A., 2021. Vascular fungi associated with branch dieback of olive in super-high-density systems in southern Spain. *Plant Disease* 105: 797–818.

Agustí-Brisach C., Moldero D., Raya M.D.C., Lorite I.J., Orgaz F., Trapero A., 2020. Water stress enhances the progression of branch dieback and almond decline under field conditions. *Plants* 9: 1213.

Agustí-Brisach C., Moral J., Felts D., Trapero A., Michailides T.J., 2019. Interaction between *Diaporthe rhusicola* and *Neofusicoccum mediterraneum* causing branch dieback and fruit blight of English walnut in California, and the effect of pruning wounds on the infection. *Plant Disease* 103: 1196–1205.

Aiello D., Carrieri R., Guarnaccia V., Vitale A., Lahoz E., Polizzi G., 2015. Characterization and pathogenicity of *Colletotrichum gloeosporioides* and *C. karstii* causing pre-harvest disease on *Citrus sinensis* in Italy. *Journal of Phytopathology* 163: 168–177.

Aiello D., Guarnaccia V., Costanzo M.B., Leonardi G.R., Epifani F., … Polizzi G., 2022. Woody canker and shoot blight caused by Botryosphaeriaceae and Diaporthaceae on mango and litchi in Italy. *Horticulturae* 8: 330.

Aiello D., Gusella G., Fiorenza A., Guarnaccia V., Polizzi G., 2020a. Identification of *Neofusicoccum parvum* causing canker and twig blight on *Ficus carica* in Italy. *Phytopathologia Mediterranea* 59: 213–218.

Aiello D., Gusella G., Vitale A., Guarnaccia V., Polizzi G., 2020b. *Cylindrocladiella peruviana* and *Pleiocarpon*

algeriense causing stem and crown rot on avocado (*Persea americana*). *European Journal of Plant Pathology* 158: 419–430.

Aiello D., Polizzi G., Gusella G., Fiorenza A., Guarnaccia V., 2019. Characterization of *Eutypa lata* and *Cytospora pistaciae* causing die-back and canker of pistachio in Italy. *Phytopathologia Mediterranea* 58: 699–706.

Aigoun-Mouhous W., Elena G., Cabral A., León M., Sabaou N., … Berraf-Tebbal A., 2019. Characterization and pathogenicity of Cylindrocarpon-like asexual morphs associated with black foot disease in Algerian grapevine nurseries, with the description of *Pleiocarpon algeriense* sp. nov. *European Journal of Plant Pathology* 154: 887–901.

Akgül D.S., Savas G.N., Teker T., Keykubat B., Mayorquin J.S., Eskalen A., 2015. Fungal trunk pathogens of Sultana Seedless vineyards in Aegean region of Turkey. *Phytopathologia Mediterranea* 54(2): 380–393.

Akgül D.S., Savas N.G., Eskalen A., 2014. First report of wood canker caused by *Botryosphaeria dothidea*, *Diplodia seriata*, *Neofusicoccum parvum*, and *Lasiodiplodia theobromae* on grapevine in Turkey. *Plant Disease* 98: S. 568.

Akgül D.S., Yildiz M., Güngör-Savas N., Bülbül I., Özarslandan M., … Armengol J. 2022. Occurrence and diversity of black-foot pathogens on asymptomatic nursery-produced grapevines in Turkiye. *European Journal of Plant Pathology* 164: 21–32.

Alaniz S., Abad-Campos P., García-Jiménez J., Armengol J., 2011. Evaluation of fungicides to control *Cylindrocarpon liriodendri* and *Cylindrocarpon macrodidymum* in vitro, and their effect during the rooting phase in the grapevine propagation process. *Crop Protection* 30: 489–494.

Ali S., Renderos W., Bevis E., Hebb J., Abbasi P.A., 2020. *Diaporthe eres* causes stem cankers and death of young apple rootstocks in Canada. *Canadian Journal of Plant Pathology* 42: 218–227.

Allen R.J., Luptowitz R. 2017. El Nino-like teleconnection increases California precipitation in response to warming. *Nature Communication* 8: 16055.

Alves A., Linaldeddu B.T., Deidda A., Scanu B., Phillips A.J.L., 2014. The complex of *Diplodia* species associated with Fraxinus and some other woody hosts in Italy and Portugal. *Fungal Diversity* 67S: 143–156.

Amponsah N.T., Jones E.E., Ridgway H.J., Jaspers M.V., 2009. First report of *Neofusicoccum australe* [*Botryosphaeria australis*], a cause of grapevine dieback in New Zealand. *Australasian Plant Disease Notes* 4: 6–8.

Annesi T., Luongo L., Vitale S., Galli M., Belisario A., 2016. Characterization and pathogenicity of *Phomopsis theicola* anamorph of *Diaporthe foeniculina* causing stem and shoot cankers on sweet chestnut in Italy. *Journal of Phytopathology* 164: 412–416.

Arciuolo R., Santos C., Soares C., Castello G., Spigolon N., … Battilani, P., 2020. Molecular characterization of *Diaporthe* species associated with hazelnut defects. *Frontiers in Plant Science* 11: 611–655.

Aroca Á., Gramaje D., Armengol J., García-Jiménez J., Raposo R. 2010. Evaluation of the grapevine nursery propagation process as a source of *Phaeoacremonium* spp. and *Phaeomoniella chlamydospora* and occurrence of trunk disease pathogens in rootstock mother vines in Spain. *European Journal of Plant Pathology* 126: 165–174.

Arzanlou M., Dokhanchi H., 2013. Calosphaeria canker of almond caused by *Calosphaeria pulchella* in Iran. *Archives of Phytopathology and Plant Protection* 46: 215–226.

Arzanlou M., Ghasemi S., Baradaran Bagheri M. 2016. *Collophora hispanica*, a new pathogen and potential threat to the almond industry in Iran. *Journal of Phytopathology* 164: 833–839.

Arzanlou M., Narmani A., 2015. ITS sequence data and morphology differentiate *Cytospora chrysosperma* associated with trunk disease of grapevine in northern Iran. *Journal of Plant Protection Research* 55: 117–25.

Auger J., Pozo L., Rubilar M., Briceño N., Osorio-Navarro C., Esterio M. 2021. First report of canker and branch dieback of sweet cherry trees caused by *Calosphaeria pulchella* in Chile. *Plant Disease* 105: 217.

Baranek M., Armengol J., Holleinová V., Pečenka J., Calzarano F., … Eichmeier A. 2018. Incidence of symptoms and fungal pathogens associated with grapevine trunk diseases in Czech vineyards. *Phytopathologia Mediterranea* 57 449–458.

Batista E., Lopes A., Alves A., 2020. Botryosphaeriaceae species on forest trees in Portugal: diversity, distribution and pathogenicity. *European Journal of Plant Pathology* 158: 693–720.

Baumgartner K., Fujiyoshi P.T., Travadon R., Castlebury L.A., Wilcox W.F., Rolshausen P.E. 2013. Characterization of species of *Diaporthe* from wood cankers of grape in eastern North American vineyards. *Plant Disease* 97: 912–920.

Bekris F., Vasileiadis S., Papadopoulou E., Samaras A., Testempasis S., … Karpouzas D.G. 2021. Grapevine wood microbiome analysis identifies key fungal pathogens and potential interactions with the bacterial community implicated in grapevine trunk disease appearance. *Environmental Microbiome*, 16 1–17.

Beluzán F., Miarnau X., Torguet L., Zazurca L., Abad-Campos P., … Armengol J. 2022. Susceptibility of

almond (*Prunus dulcis*) cultivars to twig canker and shoot blight caused by *Diaporthe amygdali*. *Plant Disease*, in press.

Bendel N., Kicherer A., Backhaus A., Klück H.C., Seiffert U., … Töpfer R., 2020. Evaluating the suitability of hyper-and multispectral imaging to detect foliar symptoms of the grapevine trunk disease Esca in vineyards. *Plant Methods* 16: 1–18.

Berbegal M., García-Jiménez J., Armengol J., 2014. First report of *Calosphaeria pulchella* causing canker and branch dieback of sweet cherry trees in Spain. *Plant Disease* 98: 1008.

Berg G., Rybakova D., Fischer D., Cernava T., Vergès M.C.C., … Schloter M., 2020. Microbiome definition re-visited: old concepts and new challenges. *Microbiome* 8: 1–22.

Berlanas C., López-Manzanares B., Gramaje D., 2017. Estimation of viable propagules of black-foot disease pathogens in grapevine cultivated soils and their relation to production systems and soil properties. *Plant and Soil* 417: 467–479.

Berlanas C., Ojeda S., López-Manzanares B., Andrés-Sodupe M., Bujanda R., … Gramaje D., 2020. Occurrence and diversity of black-foot disease fungi in symptomless grapevine nursery stock in Spain. *Plant Disease* 104: 94–104.

Berraf-Tebbal, A., Mahamedi A.E., Aigoun-Mouhous W., Špetík M., Céchová J., … Alves A. 2020. *Lasiodiplodia mitidjana* sp. nov. and other *Botryosphaeriaceae* species causing branch canker and dieback of *Citrus sinensis* in Algeria. *PLoS ONE* 15: e0232448.

Bertetti D., Guarnaccia V., Spadaro D., Gullino M.L. 2018. First report of fruit rot in European pear caused by *Diaporthe eres* in Italy. *Plant Disease* 102: 2651.

Bettenfeld P., Fontaine F., Trouvelot S., Fernandez O., Courty P.E., 2020. Woody plant declines. What's wrong with the microbiome? *Trends in Plant Sciences* 25: 381–394.

Bezerra J.D.P., Crous P.W., Aiello D., Gullino M.L., Polizzi G., Guarnaccia V., 2021. Genetic diversity and pathogenicity of Botryosphaeriaceae species associated with symptomatic citrus plants in Europe. *Plants* 10: 492.

Bien S., Damm U., 2020. Prunus trees in Germany–a hideout of unknown fungi? *Mycological Progress* 19: 667–690.

Billones-Baaijens R., Úrbez-Torres J.R., Liu M., Ayres M., … Savocchia S., 2018. Molecular methods to detect and quantify Botryosphaeriaceae inocula associated with grapevine dieback in Australia. *Plant Disease* 102: 1489–1499.

Bleach C., Jones E., Ridgway H., Jaspers M., 2013. Hot water treatment to reduce incidence of black foot pathogens in young grapevines grown in cool climates. *Phytopathologia Mediterranea* 52: 347–358.

Blundell R., Arreguin M., Eskalen A., 2021. In vitro evaluation of grapevine endophytes, epiphytes and sap micro-organisms for potential use to control grapevine trunk disease pathogens. *Phytopathologia Mediterranea* 60: 535–548.

Borrero C., Castaño R., Avilés M. 2018. First report of *Pestalotiopsis clavispora* (*Neopestalotiopsis clavispora*) causing canker and twig dieback on blueberry bushes in Spain. *Plant Disease* 102: 1178.

Borrero C., Pérez S., Avilés M., 2019. First report of canker disease caused by *Lasiodiplodia theobromae* on blueberry bushes in Spain. *Plant Disease* 103: 2684.

Brown A.E., Muthumeenakashi S., Swinburne T.R., Li R. 1994. Detection of the source of the infection of apple trees by *Cylindrocarpon heteronema* using DNA polymorphisms. *Plant Pathology* 43: 338–343.

Bruez E., Vallance J., Gautier,A., Laval V., Compant S.,… Rey P., 2020. Major changes in grapevine wood microbiota are associated with the onset of esca, a devastating trunk disease. *Environmental Microbiology* 22: 5189–5206.

Brunetti A., Matere A., Lumia V., Pasciuta V., Fusco V., … Pilotti M., 2022. *Neofusicoccum mediterraneum* is involved in a twig and branch dieback of olive trees observed in Salento (Apulia, Italy). *Pathogens* 11: 53.

Cabral A., Rego C., Nascimento T., Oliveira H., … Crous, P.W. 2012. Multi-gene analysis and morphology reveal novel *Ilyonectria* species associated with black foot disease of grapevines. *Fungal Biology* 116: 62–80.

Capote N., Del Río M.Á., Herencia J.F., Arroyo F.T., 2022. Molecular and pathogenic characterization of *Cylindrocarpon*-like anamorphs causing root and basal rot of almonds. *Plants* 11: 984.

Cardinaals J., Wenneker M., Voogd J.G.B., van Leeuwen G.C.M., 2018. Pathogenicity of *Diaporthe* spp. on two blueberry cultivars (*Vaccinium corymbosum*). *EPPO Bulletin* 48: 128–134.

Carlucci A., Cibelli F., Lops F., Raimondo M.L., 2015b. Characterization of Botryosphaeriaceae species as causal agents of trunk diseases on grapevines. *Plant Disease* 99: 1678–1688.

Carlucci A., Lops F., Cibelli F., Raimondo M.L. 2015a. *Phaeoacremonium* species associated with olive wilt and decline in southern Italy. *European Journal of Plant Pathology* 141: 717–729.

Carlucci A., Lops F., Mostert L., Halleen F., Raimondo M.L. 2017. Occurrence fungi causing black foot on

young grapevines and nursery rootstock plants in Italy. *Phytopathologia Mediterranea* 56: 10–39.

Carlucci A., Raimondo M.L., Cibelli F., Phillips A.J.L., Lops F., 2013. *Pleurostomophora richardsiae*, *Neofusicoccum parvum* and *Phaeoacremonium aleophilum* associated with a decline of olives in southern Italy. *Phytopathologia Mediterranea* 52: 517–527.

Carter M.V., 1957. *Eutypa armeniacae* Hansf. & Carter, sp. nov., and airborne vascular pathogen of *Prunus armeniaca* L. in southern Australia, *Australasian Journal of Botany* 5: 21–35.

Carter M.V., 1982. Additional hosts of *Eutypa armeniacae* in Australia. *Australasian Plant Pathology* 11: 46-48.

Carter M.V., 1995. Eutypa dieback. Pages 32-33 in: Compendium of Stone Fruit diseases. J. M. Ogawa, E.I. Zehr, G.W. Bird, D.F. Ritchie, K. Uriu, and J. K. Uyemoto, eds. APS Press, St. Paul, MN.

Casieri L., Hofstetter V., Viret O., Gindro K. 2009. Fungal communities living in the wood of different cultivars of young *Vitis vinifera* plants. *Phytopathologia Mediterranea* 48: 73–83.

Castillo S., Borrero C., Castaño R., Rodríguez A., Avilés M., 2013. First report of canker disease caused by *Neofusicoccum parvum* and *N. australe* on blueberry bushes in Spain. *Plant Disease* 97: 1112.

Chakraborty S., Newton A.C., 2011. Climate changes, plant diseases and food security: An overview. *Plant Pathology* 60: 2–14.

Chen S., Li G., Liu F., Michailides T.J., 2015. Novel species of Botryosphaeriaceae associated with shoot blight of pistachio. *Mycologia* 107: 780–792.

Chicau G., Cabral J., Cabral S. Aboim-Inglez M., 2000. *Phaeoacremonium chlamydosporum* and *Phaeoacremonium angustius* associated with esca and grapevine decline in 'Vinho Verde' grapevines in Northwest Portugal. *Phytopathologia Mediterranea* 39: 80–86.

Ciordia M., Loureiro M.D., González A.J., (2022): First Report of *Neofusicoccum parvum* Causing Canker on Castanea sativa in Spain. *Plant Disease* 106: 1299.

Cloete M., Fischer M., Mostert L., Halleen F., 2015. Hymenochaetales associated with esca-related wood rots on grapevine with a special emphasis on the status of esca in South African vineyards. *Phytopathologia Mediterranea* 54: 299–312.

Cobos R., Ibañez A., Diez-Galán A., Calvo-Peña C., Ghoreshizadeh S., Coque J.J.R. 2022. The grapevine microbiome to the rescue: implications for the biocontrol of trunk diseases. *Plants* 22: 840.

Comont G., Mayet V., Corio-Costet M.F., 2016. First report of *Lasiodiplodia viticola*, *Spencermartinsia viticola* and *Diplodia intermedia* associated with *Vitis vinifera* grapevine decline in French vineyards. *Plant Disease* 100: 2328.

Cortesi P., Fischer M., Milgroom M.G., 2000. Identification and spread of *Fomitiporia punctata* associated with wood decay of grapevine showing symptoms of Esca. *Phytopathology* 90: 967–972.

Crous P.W., Phillips A.J.L., Baxter A.P., 2000. Phytopathogenic fungi from South Africa. University of Stellenbosch, Department of Plant Pathology Press, South Africa.

Crous P.W., Wingfield M.J., 2018. Fungi infecting woody plants: emerging frontiers. *Persoonia-Molecular Phylogeny and Evolution of Fungi* 40: i–iii.

Crous P.W., Wingfield M.J., Guarro J., Hernández-Restrepo M., Sutton D.A., … Groenewald J.Z., 2015. Fungal planet description sheets: 320-370. *Persoonia-Molecular Phylogeny and Evolution of Fungi* 34: 167–266.

Damm U., Crous P.W., Fourie P.H., 2007. Botryosphaeriaceae as potential pathogens of *Prunus* species in South Africa, with descriptions of *Diplodia africana* and *Lasiodiplodia plurivora* sp. nov. *Mycologia* 99: 664–680.

Damm U., Fourie P.H., Crous P.W., 2010. *Coniochaeta* (*Lecythophora*), *Collophora* gen. nov. and *Phaeomoniella* species associated with wood necrosis of *Prunus* trees. *Persoonia* 24: 60–80.

Damm U., Mostert L., Crous P.W., Fourie P.H. 2008. Novel *Phaeoacremonium* species associated with necrotic wood of *Prunus* trees. *Persoonia* 20: 87–102.

de los Santos B., Aguado A., Borrero C., Viejobueno J., Avilés M., 2019. First report of charcoal rot caused by *Macrophomina phaseolina*, on blueberry in Southwestern Spain. *Plant Disease* 103: 2677.

Del Frari G., Gobbi A., Aggerbeck M.R., Oliveira H., Hansen L.H., Ferreira, R.B., 2019. Characterization of the wood mycobiome of *Vitis vinifera* in a vineyard affected by Esca. Spatial distribution of fungal communities and their putative relation with leaf symptoms. *Frontiers in Plant Science* 10: 910.

Delgado-Cerrone L., Mondino-Hintz P., Alaniz-Ferro S., 2016. Botryosphariaceae species associated with stem canker, dieback and fruit rot on apple in Uruguay. *European Journal of Plant Pathology* 146: 637–655.

Derviş S., Türkölmez Ş., Çiftçi O., Ulubaş Serçe Ç., Dikilitas M., 2019. First report of *Neoscytalidium dimidiatum* causing black canker and root rot of walnut in Turkey. *Plant Disease* 103: 2129.

Di Gennaro S.F., Battiston E., Di Marco S., Facini O., Matese A., … Mugnai L., 2016. Unmanned Aerial Vehicle (UAV)-based remote sensing to monitor grapevine leaf stripe disease within a vineyard affect-

ed by esca complex. *Phytopathologia Mediterranea* 55: 262–275.

Di Marco S., Calzarano F., Osti F., Mazzullo A., 2004. Pathogenicity of fungi associated with a decay of kiwifruit. *Australasian Plant Pathology* 33: 337.

Di Marco S., Osti F., Spada G., 2003. The wood decay of kiwifruit and first control measures. *Acta Horticolturae* 610: 291–294.

Díaz G.A., Latorre B.A., Ferrada E., Gutiérrez M., Bravo F., Lolas M., 2018. First report of *Diplodia mutila* causing branch dieback of English walnut cv. Chandler in the Maule Region, Chile. *Plant Disease* 102: 1451.

Díaz G.A., Mostert L., Halleen F., Lolas M., Gutierrez M., … Latorre B.A., 2019. *Diplodia seriata* associated with Botryosphaeria canker and dieback in apple trees in Chile. *Plant Disease* 103: 1025.

Díaz G.A., Valdez A., Halleen F., Ferrada E., Lolas M., Latorre B.A., 2022. Characterization and pathogenicity of *Diplodia*, *Lasiodiplodia*, and *Neofusicoccum* species causing Botryosphaeria canker and dieback of apple trees in central Chile. *Plant Disease* 106: 925–937.

Dissanayake A.J., Liu M., Zhang W., Chen Z., Udayanga D., … Hyde K.D. 2015. Morphological and molecular characterisation of *Diaporthe* species associated with grapevine trunk disease in China. *Fungal Biology* 119: 283–294.

Dissanayake A.J., Phillips A.J.L., Hyde K.D., Yan J.T., Li X.H., 2017. The current status of species in *Diaporthe*. *Mycosphere* 8: 1106–1156.

Doll D., Michailides T., Rolshausen P., 2013. Botryosphaeriaceae associated with almond trunk cankers: A threat to the almond industry? *Phytopathology* 103: S3.12.

Edwards J., Pascoe I.G., 2004. Occurrence of *Phaeomoniella chlamydospora* and *Phaeoacremonium aleophilum* associated with Petri disease and esca in Australian grapevines. *Australasian Plant Pathology* 33: 273–279.

Eichmeier A., Emilia D.L., Hakalova E., Pecenka J., Stuskova K., … Gramaje D., 2022. Draft genome sequence of Phyllosticta ampelicida, the cause of grapevine black rot. *Phytopathologia Mediterranea* 61: 279–282.

Eichmeier A., Kiss T., Penazova E., Pecenka J., Berraf-Tebbal A., … Grzebelus D., 2019. MicroRNAs in *Vitis vinifera* cv. Chardonnay are differentially expressed in response to *Diaporthe* species. *Genes* 10: 905.

Eichmeier A., Pečenka J., Peňázová E., Baránek M., Català-García S., … Gramaje D., 2018. High-throughput amplicon sequencing-based analysis of active fungal communities inhabiting grapevine after hot-water treatments reveals unexpectedly high fungal diversity. *Fungal Ecology* 36: 26–38.

Eichmeier A., Pečenka J., Spetik M., Necas T., Ondrasek I., … Gramaje D., 2020. Fungal trunk pathogens associated with *Juglans regia* in the Czech Republic. *Plant disease* 104: 761–771.

Elena K., Fischer M., Dimou K., Dimou D.M., 2006. *Fomitiporia mediterranea* infecting citrus trees in Greece. *Phytopathologia Mediterranea* 45: 35–39.

Elena K., Paplomatas E.J., 2002. First report of *Fomitiporia punctata* infecting kiwifruit. *Plant disease* 86: 1176.

Elmer W., Ma C., White J., 2018. Nanoparticles for plant disease management. *Current Opinion in Environmental Science & Health* 6: 66–70.

Endes A., Kayim M., Eskalen A., 2016. First report of *Lasiodiplodia theobromae*, *L. pseudotheobromae*, and *Diplodia seriata* causing bot canker and gummosis of nectarines in Turkey. *Plant disease* 100: 2321.

Erper I., Agustí-Brisach C., Tunali B., Armengol J., 2013. Characterization of root rot disease of kiwifruit in the Black Sea region of Turkey. *European Journal of Plant Pathology* 136: 291–300.

Eskalen A., Gubler W.D., 2001. Association of spores of *Phaeomoniella chlamydospora*, *Phaeoacremonium inflatipes*, and *Pm. aleophilum* with grapevine cordons in California. *Phytopathologia Mediterranea* 40: S429–S432.

Espargham N., Mohammadi H., Gramaje D., 2020. Survey of trunk disease pathogens within citrus trees in Iran. *Plants* 9: 754.

Essakhi S., Mugnai L., Crous P.W., Groenewald J.Z., Surico G., 2008. Molecular and phenotypic characterisation of novel *Phaeoacremonium* species isolated from esca diseased grapevines. *Persoonia Molecular Phylogeny and Evolution of Fungi* 21: 119–134.

Farr D.F., Rossman A.Y., 2022. Fungal Databases, U.S. National Fungus Collections, ARS, USDA. Retrieved May 11, 2022.

Fiorenza A., Gusella G., Aiello D., Polizzi G., Voglmayr H. 2022. *Neopestalotiopsis siciliana* sp. nov. and *N. rosae* causing tem lesion and dieback on avocado plants in Italy. *Journal of Fungi* 8: 562.

Fischer M., Ashnaei S.P., 2019. Grapevine, esca complex, and environment: The disease triangle. *Phytopathologia Mediterranea* 58: 17–37.

Fischer M., Kassemeyer H.H., 2003. Fungi associated with esca disease of grapevine in Germany. *Vitis* 42: 109–116.

Fischer M., Schneider P., Kraus C., Molnar M., Dubois C., … Haag N., 2016. Grapevine trunk disease in German viticulture: occurrence of lesser known fungi

and first report of *Phaeoacremonium viticola* and *P. fraxinopennsylvanicum*. *Vitis* 55: 145–156.

Flor N.C., Wright A.F., Huguet-Tapia J., Harmon, P.F., Liberti, D., 2022. Identification of fungi in the *Botryosphaeriaceae* family associated with stem blight of *Vaccinium* spp. in the Southeastern United States. *Fungal Biology* 126: 342–355.

Fotouhifar K.B., Hedjaroude G.A., Leuchtmann A., 2010. ITS rDNA phylogeny of Iranian strains of *Cytospora* and associated teleomorphs. *Mycologia* 102: 1369–1382.

Fourie P.H., Halleen F., 2004. Proactive control of Petri disease of grapevine through treatment of propagation material. *Plant Disease* 88: 1241–1245.

Galarneau E.R., Lawrence D.P., Travadon R., Baumgartner K., 2019. Drought exacerbates botryosphaeria dieback symptoms in grapevines and confounds host-based molecular markers of infection by *Neofusicoccum parvum*. Plant disease 103: 1738–1745.

Gierl L., Fischer M. 2017. Grapevine trunk disease in German viticulture II. Associated fungi occurring on non-Vitis hosts, and first report of *Phaeoacremonium angustius*. *Vitis* 56: 103–110.

González V., Tello M.L., 2011. The endophytic mycota associated with *Vitis vinifera* in central Spain. *Fungal diversity* 47: 29–42.

González-Domínguez E., Berlanas C., Gramaje D., Armengol J., Rossi V., Berbegal M., 2020. Temporal dispersal patterns of *Phaeomoniella chlamydospora*, causal agent of Petri disease and esca, in vineyards. *Phytopathology* 110: 1216–1225.

Gramaje D., Aguilar M.I., Armengol J., 2011b. First report of *Phaeoacremonium krajdenii* causing Petri disease of grapevine in Spain. *Plant disease* 95: 615.

Gramaje D., Agustí-Brisach C., Pérez-Sierra A., Moralejo E., Olmo D., … Armengol J., 2012. Fungal trunk pathogens associated with wood decay of almond trees on Mallorca (Spain). *Persoonia Molecular Phylogeny and Evolution of Fungi* 28: 1–13.

Gramaje D., Armengol J., 2011. Fungal trunk pathogens in the grapevine propagation process: potential inoculum sources, detection, identification, and management strategies. *Plant Disease* 95: 1040–1055.

Gramaje D., Baumgartner K., Halleen F., Mostert L., Sosnowski M.R., … Armengol J., 2016. Fungal trunk diseases: a problem beyond grapevines? *Plant Pathology* 65: 355–356.

Gramaje D., Eichmeier A., Spetik M., Carbone M.J., Bujanda R., … Rey P., 2022. Exploring the temporal dynamics of the fungal microbiome in rootstocks, the lesser-known half of the grapevine crop. *Journal of Fungi* 8: 421.

Gramaje D., Mostert L., Armengol J., 2011a. Characterization of *Cadophora luteo-olivacea* and *C. melinii* isolates obtained from grapevines and environmental samples from grapevine nurseries in Spain. *Phytopathologia Mediterranea* 50: S112–S126.

Gramaje D., Mostert L., Groenewald J.Z., Crous P.W., 2015. *Phaeoacremonium*: from esca disease to phaeohyphomycosis. Fungal Biology 119: 759–783.

Gramaje D., Úrbez-Torres J.R., Sosnowski M., 2018. Managing grapevine trunk diseases with respect to etiology and epidemiology: current strategies and future prospects. *Plant Disease* 102: 12–39.

Guarnaccia V., 2022. Fungal pathogens of wood: are they threats to Medi- terranean fruit crops? In: Abstracts of invited, oral and poster papers presented at the 16th Congress of the Mediterranean Phytopathological Union, April 4–8, 2022, Limassol, Cyprus. *Phytopathologia Mediterranea* 61: 181–239. DOI: 1036253/phyto-13613.

Guarnaccia V., Aiello D., Papadantonakis N., Polizzi G., Gullino M.L., 2022a. First report of branch cankers on avocado (*Persea americana*) caused by *Neocosmospora* (syn. *Fusarium*) *perseae* in Crete (Greece). *Journal of Plant Pathology* 104: 419–420.

Guarnaccia V., Crous P.W., 2017. Emerging citrus diseases in Europe caused by species of *Diaporthe*. *IMA fungus* 8: 317–334.

Guarnaccia V., Crous P.W., 2017. Emerging citrus diseases in Europe caused by species of *Diaporthe*. *IMA Fungus* 8: 317–334.

Guarnaccia V., Crous P.W., 2018. Species of *Diaporthe* on *Camellia* and *Citrus* in the Azores Islands. *Phytopathologia Mediterranea* 57: 307–319.

Guarnaccia V., Groenewald J.Z., Polizzi G., Crous P.W., 2017. High species diversity in *Colletotrichum* associated with citrus diseases in Europe: *Persoonia* 39: 32–50.

Guarnaccia V., Groenewald J.Z., Woodhall J., Armengol J., Cinelli T., … Crous P.W., 2018. *Diaporthe* diversity and pathogenicity revealed from a broad survey of grapevine diseases in Europe. *Persoonia* 40: 135–153.

Guarnaccia V., Martino I., Brondino L., Gullino M.L., 2022b. *Paraconiothyrium fuckelii*, *Diaporthe eres* and *Neocosmospora parceramosa* causing cane blight of red raspberry in Northern Italy. *Journal of Plant Pathology* 104: 683–698.

Guarnaccia V., Martino I., Tabone G., Brondino L. Gullino M.L., 2020. Fungal pathogens associated with stem blight and dieback of blueberry in northern Italy. *Phytopathologia Mediterranea* 59: 229–245.

Guarnaccia V., Sandoval-Denis M., Aiello D., Polizzi G., Crous P.W., 2018. *Neocosmospora perseae* sp. nov.,

causing trunk cankers on avocado in Italy. *Fungal Systematics and Evolution* 1: 131–140.

Guarnaccia V., Van Niekerk J., Crous P.W., Sandoval-Denis M., 2021. *Neocosmospora* spp. associated with dry root rot of citrus in South Africa. *Phytopathologia Mediterranea* 60: 79–100.

Guarnaccia V., Vitale A., Cirvilleri G., Aiello D., Susca A., … Polizzi G., 2016. Characterisation and pathogenicity of fungal species associated with branch cankers and stem-end rot of avocado in Italy. *European Journal of Plant Pathology* 146: 963–976.

Gusella G., Giambra S., Conigliaro G., Burruano S., Polizzi G., 2021. Botryosphaeriaceae species causing canker and dieback of English walnut (*Juglans regia*) in Italy. *Forest Pathology* 51: e12661.

Gusella G., Lawrence D.P., Aiello D., Luo Y., Polizzi G., Michailides T.J., 2022. Etiology of Botryosphaeria panicle and shoot blight of pistachio (*Pistacia vera*) caused by Botryosphaeriaceae in Italy. *Plant Disease* 106: 1192–1202.

Haidar R., Antonielli L., Compant S., Ursula U., 2022. *Paenibacillus xylinteritus* sp. nov., a novel bacterial species isolated from grapevine wood. bioRxiv.

Haidar R., Yacoub A., Vallance J., Compant S., Antonielli L., … Rey P., 2021. Bacteria associated with wood tissues of Esca-diseased grapevines: functional diversity and synergy with *Fomitiporia mediterranea* to degrade wood components. Environmental Microbiology 10: 6104–6121.

Halleen F., Crous P.W., Petrini O., 2003. Fungi associated with healthy grapevine cuttings in nurseries, with special reference to pathogens involved in the decline of young vines. *Australasian Plant Pathology* 32: 47–52.

Halleen F., Fourie P.H., Crous P.W., 2007a. Control of black foot disease in grapevine nurseries. *Plant Pathology* 56: 637–645.

Halleen F., Mostert L., Crous P.W., 2007b. Pathogenicity testing of lesser-known vascular fungi of grapevines. *Australasian Plant Pathology* 36: 277–285.

Hariharan J., Fuller J., Ampatzidis Y., Abdulridha J., Lerwill, A., 2019. Finite difference analysis and bivariate correlation of hyperspectral data for detecting Laurel wilt disease and nutritional deficiency in avocado. *Remote Sensing* 11: 1748.

Hausner G., Eyjólfsdóttir G.G., Reid J., Klassen G.R., 1992. Two additional species of the genus *Togninia*. *Canadian Journal of Botany* 70: 724–732.

Havenga M., Gatsi G.M., Halleen F., Spies C.F., van der Merwe R., Mostert L., 2019. Canker and wood rot pathogens present in young apple trees and propagation material in the Western Cape of South Africa. *Plant Disease* 103: 3129–3141.

Hawksworth D.L., Gibson I.A.S., Gams W., 1976. *Phialophora parasitica* associated with disease conditions in various trees. *Transactions of the British Mycological Society* 66: 427–431.

Henderson B., Sosnowski M.R., McCarthy M.G., Scott E.S., 2021. Incidence and severity of Eutypa dieback in grapevines are related to total surface area of pruning wounds. *Australian Journal of Grape and Wine Research* 27: 87–93.

Hilário S., Amaral I., Gonçalves M.F.M., Lopes A., Santos L., Alves A., 2020b. *Diaporthe* species associated with twig blight and dieback of *Vaccinium corymbosum* in Portugal with description of four new species. *Mycologia* 112: 293–308.

Hilário S., Gonçalves M.F.M., Alves A., 2021b. Using genealogical concordance and coalescent-based species delimitation to assess species boundaries in the *Diaporthe eres* complex. *Journal of Fungi* 7: 507.

Hilário S., Lopes A., Santos L., Alves A., 2020a. Botryosphaeriaceae species associated with blueberry stem blight and dieback in the Centre Region of Portugal. *European Journal of Plant Pathology* 156: 31–44.

Hilário S., Santos L., Alves A., 2021a. Diversity and pathogenicity of *Diaporthe* species revealed from a survey of blueberry orchards in Portugal. *Agriculture* 11: 1271.

Holland L.A., Travadon R., Lawrence D.P., Nouri M.T., Trouillas F., 2021a. Evaluation of pruning wound protection products for the management of almond canker diseases in California. *Plant Disease* 105: 3368–3375.

Holland L.A., Trouillas F., Nouri M.T., Lawrence D.P., Crespo M., … Fichtner E.J., 2021b. Fungal pathogens associated with canker diseases of almond in California. *Plant Disease* 105: 346-–360.

Hrycan J., Hart M., Bowen P., Forge T., Úrbez-Torres J.R. 2020. Grapevine trunk disease fungi: Their roles as latent pathogens and stress factors that favour disease development and symptom expression. Phytopathologia Mediterranea 59: 395–424.

Huang F., Chen G.Q., Hou X., Fu Y.S., Cai L., … Li H.Y., 2013. *Colletotrichum* species associated with cultivated citrus in China. *Fungal Diversity* 61: 61–74.

Ilyukhin E., Schneider K., Ellouze W., 2022. First report of *Botryosphaeria dothidea* causing stem canker and dieback of apple trees in Ontario, Canada. *Plant Disease*, 106: 2994.

Ismail A.M., Cirvilleri G., Lombard L., Crous P.W., Groenewald J.Z., Polizzi G., 2013. Characterisation of *Neofusicoccum* species causing mango dieback in Italy. *Journal of Plant Pathology* 95: 549–557.

Ivić D., Ivanovic A., Milicevic T., Cvjetkovic B., 2010. Shoot necrosis of olive caused by *Phoma incompta*, a

new disease of olive in Croatia. *Phytopathologia Mediterranea* 49: 414–416.

Ivić, D., Novak, A., Pilipović, P. 2018. *Diaporthe eres* Nitschke is the only *Diaporthe* species found on blueberry in Croatia. Fragm. Phytom. 32(2): 23-30.

Jamaux-Despréaux I., Peros J.P., 2003. Genetic structure in populations of the fungus *Fomitiporia punctata* associated with the esca syndrome in grapevine. *Vitis* 42: 43–51.

Jiménez Luna I., Doll D., Ashworth V.E., Trouillas F.P., Rolshausen P.E., 2022. Comparative profiling of wood canker pathogens from spore traps and symptomatic plant samples within California almond and walnut orchards. *Plant Disease* 106: 2182–2190.

Junges A.H., Ducati J.R., Lampugnani C.S., Almança M.A.K., 2018. Detection of grapevine leaf stripe disease symptoms by hyperspectral sensor. *Phytopathologia Mediterranea* 57: 399–406.

Kakalíková L., Jankura E., Šrobárová A., 2006. *Phaeomoniella chlamydospora*: causal agent of vine decline (*Vitis vinifera*) in the vineyards of Slovakia. *Plant Pathology* 55: 815–815.

Kaliterna J., Milicevic T., Bencic D., Duralija B., 2013b. First report of *Neofusicoccum parvum* associated with grapevine trunk diseases in Croatia. *Plant disease* 97: 1656–1656.

Kaliterna J., Miličević T., Cvjetković B., 2012. Grapevine trunk diseases associated with fungi from the Diaporthaceae family in Croatian vineyards. *Archives of industrial hygiene and toxicology* 63: 471–479.

Kaliterna J., Milicevic T., Ivic D., Bencic D., Mesic A., 2013a. First report of *Diplodia seriata* as causal agent of olive dieback in Croatia. *Plant Disease* 97: 231–244.

Kalvelage E.M., Behrens F.H., Rauch C., Voegele R.T., Fischer M., 2022. Arthropods as vectors of esca-related pathogens: Transmission efficiency of ants and earwigs and the potential of earwig feces as inoculum source in vineyards. *Vitis* 61: 77–85.

Kalvelage E.M., Voegele R.T., Fischer M., 2021. Dissemination of esca-related pathogens in German vineyards: do arthropods play roles in vectoring spores? *Phytopathologia Mediterranea* 60: 467–478.

Kara M., Soylu E.M., Soylu S., Uysal A., Kurt Ş., 2021. First report of *Neofusicoccum parvum* causing branch dieback on *Juglans regia* in Turkey. *Journal of Plant Pathology* 103: 335–335.

Kawamura F., Ramle S.F.M., Sulaiman O., Hashim R., Ohara S., 2011. Antioxidant and antifungal activities of extracts from 15 selected hardwood species of Malaysian timber. *European Journal of Wood and Wood Products* 69: 207–212.

Kim S.W., Jung J.H., Lamsal K., Kim Y.S., Min J.S., Lee Y.S., 2012. Antifungal effects of silver nanoparticles (AgNPs) against various plant pathogenic fungi. *Mycobiology* 40: 53–58.

Kraus C., Damm U., Bien S., Voegele R.T., Fischer M., 2020. New species of Phaeomoniellales from a German vineyard and their potential threat to grapevine (*Vitis vinifera*) health. *Fungal Systematics and Evolution* 6: 139–155.

Kraus C., Pennington T., Herzog K., Hecht A., Fischer M., … Kicherer A., 2018. Effects of canopy architecture and microclimate on grapevine health in two training systems. *Vitis* 57: 53–60.

Kraus C., Rauch C., Kalvelage E.M., Behrens F.H., d'Aguiar D., … Fischer M., 2022. Minimal versus intensive: how the pruning intensity affects occurrence of grapevine leaf stripe disease, wood integrity, and the mycobiome in grapevine trunks. *Journal of Fungi* 8: 247.

Kraus C., Voegele R.T., Fischer M. 2019. Temporal development of the culturable, endophytic fungal community in healthy grapevine branches and occurrence of GTD-associated fungi. *Microbial ecology* 77: 866–876.

Kubertli İ., Demirci F., 2014. Outbreak of stem canker and dieback of pear trees caused by *Botryosphaeria obtusa* (anamorph *Diplodia seriata*) in Turkey. *New Disease Reports* 30: 6–6.

Kuntzmann P., Vuillaume S., Larignon P., Bertsch C., 2009. Diagnosis of fungal diseases implicated in grapevine trunk disease in an Alsatian French vineyard. *Phytopathologia Mediterranea* 48: 166–166.

Langenhoven, S.D., Halleen, F., Spies, C.F.J., Stempien, E., Mostert, L. 2018. Detection and quantification of black foot and crown and root rot pathogens in grapevine nursery soils in the Western Cape of South Africa. Phytopathologia Mediterranea 57: 519–537.

Larignon P., Dubos B., 1997. Fungi associated with esca disease in grapevine. *European Journal of Plant Pathology* 103: 147–157.

Larignon P., Fulchic R., Cere L., Dubos B., 2001. Observations of black dead arm in French vineyards. *Phytopathologia Mediterranea* 40: 336–342.

Laveau C., Letouze A., Louvet G., Bastien S., Guerin-Dubrana L., 2009. Differential aggressiveness of fungi implicated in esca and associated diseases of grapevine in France. *Phytopathologia Mediterranea* 48: 32–46.

Lawrence D.P., Nouri M.T., Trouillas F.P., 2019. Taxonomy and multi-locus phylogeny of cylindrocarpon-like species associated with diseased roots of grapevine and other fruit and nut crops in California. *Fungal Systematic and Evolution* 4: 59–75.

Lawrence D.P., Nouri M.T., Trouillas F.P., 2021. Pleurostoma decline of olive trees caused by *Pleurostoma richardsiae* in California. *Plant disease* 105: 2149–2159.

Lawrence D.P., Travadon R., Pouzoulet J., Rolshausen P.E., Wilcox W.F., Baumgartner K., 2017. Characterization of *Cytospora* isolates from wood cankers of declining grapevine in North America, with the descriptions of two new *Cytospora* species. *Plant Pathology* 66: 713–725.

Lecomte P., Cholet C., Bruez E., Martigon T., Giudici M., … Rey P., 2022. Recovery after curettage of grapevines with esca leaf symptoms. *Phytopathologia Mediterranea* 61: 473–489.

Lecomte P., Diarra B., Carbonneau A., Rey P., Chevrier C., 2018. Esca of grapevine and training practices in France. *Phytopathologia mediterranea* 57 472–487.

León M., Berbegal M., Rodríguez-Reina J.M., Elena G., Abad-Campos P., … Armengol J., 2020. Identification and characterization of *Diaporthe* spp. associated with twig cankers and shoot blight of almonds in Spain. *Agronomy* 10: 1062.

Li G., Liu F., Li J., Liu Q., Chen S., 2016. Characterization of *Botryosphaeria dothidea* and *Lasiodiplodia pseudotheobromae* from English walnut in China. *Journal of Phytopathology* 164: 348–353.

Linaldeddu B.T., Deidda A., Scanu B., Franceschini A., Alves A., … Phillips A.J.L., 2016. Phylogeny, morphology and pathogenicity of Botryosphaeriaceae, Diatrypaceae and Gnomoniaceae associated with branch diseases of hazelnut in Sardinia (Italy). *European Journal of Plant Pathology* 146: 259–279.

Lódolo X.V., Lutz M.C., Mondino P., Ousset J., Sosa M.C., 2022. First report of *Diplodia seriata*, *Diplodia mutila*, and *Dothiorella omnivora* associated with apple cankers and dieback in Rio Negro, Argentina. *Plant Disease* 106: 325.

Lombard L., van Leeuwen G., Guarnaccia V., Polizzi G., van Rijswick P., … Crous P., 2014. *Diaporthe* species associated with *Vaccinium*, with specific reference to Europe. *Phytopathologia Mediterranea* 53: 287–299.

Lopes A., Barradas C., Phillips A.J.L., Alves A., 2016. Diversity and phylogeny of *Neofusicoccum* species occurring in forest and urban environments in Portugal. *Mycosphere* 7 906–920.

López-Moral A., Lovera M., Del Raya M.C., Cortés-Cosano N., Arquero O., … Agustí-Brisach C., 2020a. Etiology of branch dieback and shoot blight of english walnut caused by Botryosphaeriaceae and *Diaporthe* species in Southern Spain. *Plant disease* 104: 533–550.

López-Moral A., del Carmen Raya M., Ruiz-Blancas C., Medialdea I., Lovera M., … Agustí-Brisach C., 2020b. Aetiology of branch dieback, panicle and shoot blight of pistachio associated with fungal trunk pathogens in southern Spain. *Plant Pathology* 69: 1237–1269.

Luna I.J., Besoain X., Saa S., Peach-Fine E., Morales F.C., … Rolshausen P.E., 2022. Identity and pathogenicity of Botryosphaeriaceae and Diaporthaceae from *Juglans regia* in Chile. *Phytopathologia Mediterranea* 61: 79–94.

Lung T., Lavalle C., Hiederer R., Dosio A., Bouwer L.M., 2013. A multi-hazard regional level impact assessment for Europe combining indicators of climatic and non-climatic change. *Global Environmental Change* 23: 522–536.

Luque J., García-Figueres F., Legorburu F.J., Muruamendiaraz A., Armengol J., Trouillas F. 2012. Species of Diatrypaceae associated with grapevine trunk diseases in Eastern Spain. *Phytopathologia Mediterranea* 51: 528–540.

Luque J., Martos S., Aroca A., Raposo R., Garcia-Figueres F., 2009. Symptoms and fungi associated with declining mature grapevine plants in northeast Spain. *Journal of Plant Pathology* 91: 381–390.

Ma Z., Moran D.P., Michailides T.J., 2001. Effects of water stress on Botryosphaeriaceae blight of pistachio caused by *Botryosphaeria dothidea*. Plant disease 85: 745–749.

Mang S.M., Marcone C., Maxim A., Camele I., 2022. Investigations on fungi isolated from apple trees with die-back symptoms from Basilicata Region (Southern Italy). *Plants* 11: 1374.

Marek S.M., Yaghmour M.A., Bostock R.M., 2013. *Fusarium* spp., *Cylindrocarpon* spp., and environmental stress in the etiology of a canker disease of cold-stored fruit and nut tree seedlings in California. *Plant Disease* 97: 259–270.

Marín-Terrazas M., Ramos-Saez De Ojer J.L., López-Manzanares B., Gramaje D., 2016. First report of *Phaeoacremonium minimum* causing wood decay in nursery plants of almond in Spain. *Plant Disease* 100: 1244–1244.

Markakis E.A., Kavroulakis N., Ntougias S., Koubouris G.C., Sergentani C.K., Ligoxigakis E.K. 2017. Characterization of fungi associated with wood decay of tree species and grapevine in Greece. *Plant Disease* 101: 1929–1940.

Markakis E.A., Ligoxigakis E.K., Roussos P.A., Sergentani C.K., Kavroulakis N., … Koubouris G.C., 2019. Differential susceptibility responses of Greek olive cultivars to *Fomitiporia mediterranea*. *European Journal of Plant Pathology* 153: 1055–1066.

Markakis E.A., Soultatos S.K., Kanetis L., Goumas D.E., 2021. First report of stem canker of almond trees

caused by *Fusarium solani* in Greece. *Plant Disease* 105: 2724.

Markakis E.A., Soultatos S.K., Koubouris G.C., Psarras G., Kanetis L., … Goumas D.E., 2022. First report of *Pseudophaeomoniella oleae* causing wood streaking and decay on olive trees in Greece. *Plant disease* 106: 2263.

Marsberg A., Kemler M., Jami F., Nagel J.H., Postma-Smidt A., … Slippers B., 2017. *Botryosphaeria dothidea*: a latent pathogen of global importance to woody plant health. *Molecular Plant Pathology* 18: 477–488.

Martin M.T., Martin L., Cuesta M.J., García-Benavides P., 2011. First report of *Cylindrocarpon pauciseptatum* associated with grapevine decline from Castilla y León, Spain. *Plant disease* 95: 361.

Martin M.T., Martin L., de-Francisco M.T., Cobos R., 2009. First report of *Lasidiplodia theobromae* and *Cryptovalsa ampelina* associated with grapevine decline from Castilla y León, Spain. *Plant disease* 93: 545.

Martino I., Tabone G., Giordano R., Gullino M.L., Guarnaccia V., 2022. First report of *Diaporthe eres* causing stem blight and dieback on highbush blueberry (*Vaccinium corymbosum*) in Italy. Plant Disease (in press).

Mathioudakis M.M., Tziros G.T., Kavroulakis N., 2020. First report of *Diaporthe foeniculina* associated with branch canker of avocado in Greece. *Plant Disease* 104: 3057.

Matthee F.N., Thomas A.C., Erasmus H.D., 1974. Dieback of apricot trees in South Africa caused by *Eutypa armeniacae*. *Phytophylastica* 6: 131–132.

Mayorquin J.S. Nouri M.T., Peacock B.B., Trouillas F.P., Douhan G.W., … Eskalen A., 2019. Identification, pathogenicity, and spore trapping of *Colletotrichum karstii* associated with twig and shoot dieback in California. *Plant Disease* 103: 1464–1473.

Mayorquin J.S., Wang D.H., Twizeyimana M., Eskalen A., 2016. Identification, distribution, and pathogenicity of Diatrypaceae and Botryosphaeriaceae associated with *Citrus* branch canker in the southern California desert. *Plant Disease* 100: 2402–2413.

McCracken A.R., Berrie A., Barbara D.J., Locke T., Cooke L.R., … Langrell S.R.H., 2003. Relative significance of nursery infection and orchard inoculum in the development and spread of apple canker (*Nectria galligena*) in young orchards. *Plant Pathology* 52: 553–566.

Michailides T.J., Morgan D.P., 2004. Panicle and shoot blight of pistachio: A major threat to the California pistachio industry. APSnet Feature Story January.

Michalecka M., Bryk H., Seliga P., 2017. Identification and characterization of *Diaporthe vaccinii* Shear causing upright dieback and viscid rot of cranberry in Poland. *European Journal of Plant Pathology* 148: 595–605.

Mihaescu C., Dunea D., Bășa A.G., Frasin L.N., 2020. Characteristics of *Phomopsis juglandina* (Sacc.) Hohn. associated with dieback of walnut in the climatic conditions of Southern Romania. Agronomy 11: 46.

Minova S., Sešķēna R., Voitkāne S., Metla Z., Daugavietis M., Jankevica L., 2015. Impact of pine (L.) and spruce ((L.) Karst.) bark extracts on important strawberry pathogens. *In Proceedings of the Latvian Academy of Sciences. Section B. Natural, Exact, and Applied Sciences* 69: 62–67.

Mohammadi H., Sarcheshmehpour M., Mafi E., 2015. Fungal trunk pathogens associated with wood decay of pistachio trees in Iran. *Spanish Journal of Agricultural Research* 13: e1007.

Mojeremane K., Lebenya P., Du Plessis I.L., van der Rijst M., Mostert L., … Halleen F., 2020. Cross pathogenicity of *Neofusicoccum australe* and *Neofusicoccum stellenboschiana* on grapevine and selected fruit and ornamental trees. *Phytopathologia Mediterranea* 59: 581–593.

Mondello V., Larignon P., Armengol J., Kortekamp A., Vaczy K., … Fontaine F., 2018a. Management of grapevine trunk diseases: knowledge transfer, current strategies and innovative strategies adopted in Europe. *Phytopathologia Mediterranea* 57: 369–383.

Mondello V., Lo Piccolo S., Conigliaro G., Alfonzo A., Torta L., Burruano S., 2013. First report of *Neofusiccoccum vitifusiforme* and presence of other Botryosphaeriaceae species associated with Botryosphaeria dieback of grapevine in Sicily (Italy). *Phytopathologia Mediterranea* 52: 388–396.

Mondello V., Songy A., Battiston E., Pinto C., Coppin C., … Fontaine F., 2018b. Grapevine trunk diseases: a review of fifteen years of trials for their control with chemicals and biocontrol agents. *Plant Disease* 102: 1189–1217.

Moral J., Agusti-Brisach C., Perez-Rodriguez M., Xavier C., Raya M.C., … Trapero A., 2017. Identification of fungal species associated with branch dieback of olive and resistance of table cultivars to *Neofusicoccum mediterraneum* and *Botryosphaeria dothidea*. *Plant Disease* 101: 306–316.

Moral J., Muñoz-Díez C., González N., Trapero A., Michailides T.J., 2010. Characterization and pathogenicity of Botryosphaeriaceae species collected from olive and other hosts in Spain and California. *Phytopathology* 100: 1340–1351.

Moretti S., Pacetti A., Pierron R., Kassemeyer H.H., Fischer M., … Farine S., 2021. *Fomitiporia mediterranea*

M. Fisch., the historical Esca agent: A comprehensive review on the main grapevine wood rot agent in Europe. *Phytopathologia Mediterranea* 60 351–379.

Mostert L. Groenewald J.Z., Summerbell R.C., Gams W., Crous P.W., 2006. Taxonomy and pathology of *Togninia* (Diaporthales) and its *Phaeoacremonium* anamorphs. *Studies in Mycology* 54: 1–113.

Mostert L., Ferreira J., Van Zyl F., Havenga M., 2016. What is the phytosanitary status of nursery trees? *South Africa Fruit Journal* February/March: 53–57.

Moyo P., Allsopp E., Roets F., Mostert L., Halleen F., 2014. Arthropods vector grapevine trunk disease pathogens. *Phytopathology* 104: 1063–1069.

Moyo P., Mostert L., Halleen F., 2019. Diatrypaceae species overlap between vineyards and natural ecosystems in South Africa. *Fungal Ecology* 39: 142–151.

Moyo P., Mostert L., Spies C.F., Damm U., Halleen F., 2018. Diversity of Diatrypaceae species associated with dieback of grapevines in South Africa, with the description of *Eutypa cremea* sp. nov. *Plant Disease* 102: 220–230.

Munkvold G.P., Marois J.J., 1994. Eutypa dieback of sweet cherry and occurrence of *Eutypa lata* perithecia in the Central Valley of California. *Plant Disease* 78: 200–207.

Newlands N.K., 2018. Model-Based forecasting of agricultural crop disease risk at the regional scale, integrating airborne inoculum, environmental, and satellite-based monitoring data. *Frontiers in Environmental Science* 6: 63.

Nigro G., Boscia D., Antelmi I., Ippolito A. 2013. Fungal species associated with a severe decline of olive in southern Italy. *Journal of Plant Pathology* 95: 668.

Nouri M.T., Lawrence D.P., Holland L.A., Doll D.A., Kallsen C.E., … Trouillas F.P., 2019. Identification and pathogenicity of fungal species associated with canker diseases of pistachio in California. *Plant disease* 103: 2397–2411.

Nourian A., Salehi M., Safaie N., Khelghatibana F., Abdollahzadeh J. 2021. Fungal canker agents in apple production hubs of Iran. *Scientific reports* 11: 1–16.

Ojiambo P.S., Yuen J., van den Bosch F., Madden L.V., 2017. Epidemiology: past, present and future impacts on understanding disease dynamics and improving plant disease management – A summary of focus issue articles. *Phytopathology* 107: 1092–1094.

Oksal E., Çelik Y., Özer G., 2019. *Neoscytalidium dimidiatum* causes canker and dieback on grapevine in Turkey. *Australasian Plant Disease Notes* 14: 1–3.

Oksal E., Yiğit T., Özer G., 2020. First report of *Neoscytalidium dimidiatum* causing shoot blight, dieback and canker of apricot in Turkey. *Journal of Plant Pathology* 102: 579–580.

Olmo D., Armengol J., León M., Gramaje D., 2015. Pathogenicity testing of lesser-known fungal trunk pathogens associated with wood decay of almond trees. *European Journal of Plant Pathology* 143: 607–611.

Olmo D., Armengol J., León M., Gramaje D., 2016. Characterization and pathogenicity of Botryosphaeriaceae species isolated from almond trees on the island of Mallorca (Spain). *Plant Disease* 100: 2483–2491.

Olmo D., Gramaje D., Armengol J., 2017. Hongos asociados a las enfermedades de la madera del almendro en la Isla de Mallorca. *Revista de Fruticultura* 54: 18–29.

Ören E., Koca G., Gencer R., Bayraktar H., 2020. First report of *Neoscytalidium novaehollandiae* associated with stem canker and branch dieback of almond trees. *Australasian Plant Disease Notes* 15: 1–3

Ören E., Palacıoğlu G., Koca G., Ozan G.N., Bayraktar H., 2022. First report of *Neoscytalidium dimidiatum* causing branch dieback and canker on apple in Turkey. *Journal of Plant Pathology* 104: 429–429.

Panáček A., Kolář M., Večeřová R., Prucek R., Soukupová J., … Kvítek L., 2009. Antifungal activity of silver nanoparticles against *Candida* spp. *Biomaterials* 30: 6333–6340.

Pečenka J., Tekielska D., Kocanová M., Peňázová E., Berraf-Tebbal A., Eichmeier A., 2021. First report of *Lasiodiplodia theobromae* causing decline of blueberry (*Vaccinium corymbosum*) in the Czech Republic. *Plant Disease* 105: 215.

Pérez-Roncal C., Arazuri S., Lopez-Molina C., Jarén C., Santesteban L.G., López-Maestresalas A., 2022. Exploring the potential of hyperspectral imaging to detect Esca disease complex in asymptomatic grapevine leaves. *Computers and Electronics in Agriculture* 196: 1–12.

Phillips A., Alves A., Correia A., Luque J., 2005. Two new species of *Botryosphaeria* with brown, 1-septate ascospores and *Dothiorella* anamorphs. *Mycologia* 97: 513–529.

Phillips A.J.L. 2000. Excoriose, cane blight and related diseases of grapevines: A taxonomic review of the pathogen. *Phytopathologia Mediterranea* 39: 341–356.

Phillips A.J.L., Lopes J., Abdollahzadeh J., Bobev S., Alves A., 2012. Resolving the *Diplodia* complex on apple and other Rosaceae hosts. *Persoonia* 29: 29–38.

Phillips A.J.L., Oudemans P.V., Correia A., Alves A., 2006. Characterisation and epitypification of *Botryosphaeria corticis*, the cause of blueberry cane canker. *Fungal Diversity* 21: 141–155.

Pilotti M., Tizzani L., Brunetti A., Gervasi F., Di Lernia G., Lumia V., 2010. Molecular identification of *Fomitiporia mediterranea* on declining and decayed hazelnut. *Journal of Plant Pathology* 92: 115–129.

Pintos C., Redondo V., Costas D., Aguin O., Mansilla P., 2018. Fungi associated with grapevine trunk diseases in nursery-produced *Vitis vinifera* plants. *Phytopathologia Mediterranea* 57: 407–424.

Piperkova N., Cabral A., Mohamedova M., Milusheva S., Oliveira H., 2017. First report of *Dactylonectria pauciseptata* associated with Black Foot of frapevine and root rot of plum in Bulgaria. *Plant disease* 101: 2146.

Pitt W.M., Huang R., Steel C.C. Savocchia S., 2013a. Pathogenicity and epidemiology of Botryosphaeriaceae species isolated from grapevines in Australia. *Australasian Plant Pathology 42*: 573–582.

Pitt W.M., Trouillas F.P., Gubler W.D., Savocchia S., Sosnowski M.R., 2013b. Pathogenicity of diatrypaceous fungi on grapevines in Australia. *Plant Disease* 97: 749–756.

Pitt W.M., Úrbez-Torres J.R., Trouillas F.P. 2013c. *Dothiorella* and *Spencermartinsia*, new species and records from grapevines in Australia. *Australasian Plant Pathology* 44: 43–56

Polizzi G., Aiello, D., Vitale A., Giuffrida F., Groenewald J., Crous P.W., 2009. First report of shoot blight, canker, and gummosis caused by *Neoscytalidium dimidiatum* on citrus in Italy. *Plant Disease* 93: 1215.

Polizzi G., Di Pietro C., Gusella G., Ismail A.I., Aiello D., 2022. First report of seedling stem blight of mango caused by *Neofusicoccum parvum* in Italy. *Plant Disease* in press.

Popović T., Blagojević J., Aleksić G., Jelušić A., Krnjajić S., Milovanović P., 2018. A blight disease on highbush blueberry associated with *Macrophomina phaseolina* in Serbia. *Canadian Journal of Plant Pathology* 40: 121–127.

Pour F.N., Ferreira V., Félix C., Serôdio J., Alves A., … Esteves A.C., 2020. Effect of temperature on the phytotoxicity and cytotoxicity of Botryosphaeriaceae fungi. *Fungal biology* 124: 571–578.

Prencipe S., Nari L., Vittone G., Spadaro D., 2017. First report of *Diaporthe eres* causing stem canker on peach (*Prunus persica*) in Italy. *Plant disease* 101: 1052.

Prodi A., Sandalo S., Tonti S., Nipoti P., Pisi A., 2008. Phialophora-like fungi associated with kiwifruit elephantiasis. *Journal of Plant Pathology* 90: 487–494.

Prodorutti D., Cainelli C., Gualandri V., Profaizer D., Dallago G., … Angeli G., 2012. Moria e deperimento del melo in Trentino. *Atti delle Giornate Fitopatologiche* 2: 619–621.

Prodorutti D., Michelon L., Vanblaere T., Gobbin D., Pertot I., 2008. First report of *Eutypa lata* on red currant (*Ribes rubrum*) in Italy. *Plant Pathology* 57: 787.

Quaglia M., Covarelli L., Zazzerini A., 2009. Epidemiological survey on esca disease in Umbria, central Italy. *Phytopathologia Mediterranea* 48: 84–91.

Raimondo M.L., Carlucci A., Ciccarone C., Saddallah A., Lops F., 2019. Identification and pathogenicity of lignicolous fungi associated with grapevine trunk diseases in southern Italy. *Phytopathologia Mediterranea* 58: 639–662.

Raimondo M.L., Lops F., Carlucci A., 2021. First report of *Phaeoacremonium amygdalinum* associated with almond dieback and wood disease in Italy. *Plant Disease* 105: 4166.

Raimondo M.L., Lops F., Carlucci A., 2022. First report of *Phaeoacremonium oleae* and *P. viticola* associated with olive trunk diseases in Italy. *Plant disease* 106: 331.

Ramos, Ana Paula; Talhinhas, Pedro; Sreenivasaprasad, S.; Oliveira, Helena (2016): Characterization of *Colletotrichum gloeosporioides*, as the main causal agent of citrus anthracnose, and *C. karstii* as species preferentially associated with lemon twig dieback in Portugal. *Phytoparasitica* 44: 549–561.

Reis P., Cabral A., Nascimento T., Oliveira H., Rego C., 2013. Diversity of *Ilyonectria* species in a young vineyard affected by black foot disease. *Phytopatologia Mediterranea* 52: 335–346.

Robert-Siegwald G., Vallet J., Abou-Mansour E., Xu J., Rey P., … Lebrun M.H., 2017. Draft genome sequence of Diplodia seriata F98. 1, a fungal species involved in grapevine trunk diseases. *Genome announcements* 5: e00061-17.

Rodríguez-Gálvez E., Hilário S., Lopes L., Alves A., 2020. Diversity and pathogenicity of *Lasiodiplodia* and *Neopestalotiopsis* species associated with stem blight and dieback of blueberry plants in Peru. *European Journal of Plant Pathology* 157: 89–102.

Rolshausen P.E., Akgül D.S., Perez R., Eskalen A., Gispert C., 2013. First report of wood canker caused by *Neoscytalidium dimidiatum* on grapevine in California. *Plant Disease* 97: 1511.

Romeo-Oliván A., Chervin J., Breton C., Lagravère T., Daydé J., … Jacques A., 2022. Comparative transcriptomics suggests early modifications by Vintec® in grapevine trunk of hormonal signaling and secondary metabolism biosynthesis in response to *Phaeomoniella chlamydospora* and *Phaeoacremonium minimum*. *Frontiers in microbiology* 13: 898356.

Rooney-Latham S., Eskalen A., Gubler W.D., 2005. Occurrence of *Togninia minima* perithecia in esca-affected vineyards in California. *Plant Disease* 89: 867–871.

Rossi V., Caffi T., Salinari F., 2012. Helping farmers face the increasing complexity of decision-making for crop protection. *Phytopathologia Mediterranea* 51: 457–479.

Rumbos I., Rumbou A., 2001. Fungi associated with esca and young grapevine decline in Greece. *Phytopathology Mediterranea* 40: 330–335.

Rumbos I.C., 1986. *Phialophora parasitica*, causal agent of cherry dieback. *Journal of Phytopathology* 117: 283–287.

Rumbos I.C., 1988. *Cytospora oleina* causing canker and dieback of olive in Greece. *Plant Pathology* 37: 441–444.

Rumbos I.C., 1993. Dieback symptoms on olive trees caused by the fungus *Eutypa lata*. *EPPO Bulletin* 23: 441-445.

Rumbos I.C., 1997. Eutypa canker and dieback of almonds. *EPPO Bulletin* 27: 463–468.

Salem M.Z.M., Elansary H.O., Elkelish A.A., Zeidler A., Ali H.M., … Yessoufou K., 2016. In vitro bioactivity and antimicrobial activity of *Picea abies* and *Larix decidua* wood and bark extracts. *BioResources* 11: 9421–9437.

Sandoval-Denis M., Guarnaccia V., Polizzi G., Crous P.W., 2018. Symptomatic *Citrus* trees reveal a new pathogenic lineage in *Fusarium* and two new *Neocosmospora* species. *Persoonia* 40: 1–25.

Santos J., Hilário S., Pinto G., Alves A., 2022. Diversity and pathogenicity of pestalotioid fungi associated with blueberry plants in Portugal, with description of three novel species of *Neopestalotiopsis*. *European Journal of Plant Pathology* 162: 539–555.

Santos L., Phillips A.J.L., Crous P.W., Alves A., 2017. *Diaporthe* species on Rosaceae with descriptions of *D. pyracanthae* sp. nov. and *D. malorum* sp. nov. *Mycosphere* 8: 485–511.

Sessa L., Abreo E., Bettucci L., Lupo S., 2017. Diversity and virulence of *Diaporthe* species associated with wood disease symptoms in deciduous fruit trees in Uruguay. *Phytopathologia Mediterranea* 56: 431–444.

Slippers B., Boissin E., Phillips A.J.L., Groenewald J.Z., Lombard L., … Crous P.W., 2006. Phylogenetic lineages in the Botryosphaeriales: a systematic and evolutionary framework. *Studies in mycology* 55: 35–52.

Slippers B., Wingfield M.J., 2007. Botryosphaeriaceae as endophytes and latent pathogens of woody plants: diversity, ecology and impact. *Fungal biology reviews* 21: 90–106.

Smit W.A., Viljoen C.D., Wingfield B.D., Wingfield M.J., Calitz F.J., 1996. A new canker disease of apple, pear and plum rootstocks caused by *Diaporthe ambigua* in South Africa. *Plant Disease* 80: 1331–1335.

Sohrabi M., Mohammadi H., León M., Armengol J., Banihashemi Z., 2020. Fungal pathogens associated with branch and trunk cankers of nut crops in Iran. *European Journal of Plant Pathology* 157: 327–351.

Songy A., Fernandez O., Clément C., Larignon P., Fontaine F., 2019. Grapevine trunk diseases under thermal and water stresses. *Planta* 249: 1655–1679.

Sosnowski M., Ayres M., Scott E., 2016. Trunk diseases: the influence of water deficit on grapevine trunk disease. *Wine & Viticulture Journal* 31: 46–50.

Sosnowski M.R., Ayres M.R., Scott E.S., 2021. The influence of water deficit stress on the grapevine trunk disease pathogens *Eutypa lata* and *Diplodia seriata*. *Plant Disease* 105: 2217–2221.

Špetík M., Balík J., Híc P., Hakalová E., Štůsková K., … Eichmeier A., 2022. Lignans extract from knotwood of Norway spruce—A possible new weapon against GTDs. *Journal of Fungi* 8: 357.

Spies C.F.J., Mostert L., Carlucci A., Moyo P., Van Jaarsveld W.J., … Halleen F., 2020. Dieback and decline pathogens of olive trees in South Africa. *Persoonia* 45: 196–220.

Spies C.F.J., Moyo P., Halleen F., Mostert L., 2018. *Phaeoacremonium* species diversity on woody hosts in the Western Cape Province of South Africa. Persoonia 40, 2018: 26–62.

Strømeng G.M., Stensvand A., 2011. Godronia canker (*Godronia cassandrae* f. sp. *vaccinii*) in highbush blueberry. *The European Journal of Plant Science and Biotechnology* 5: 35–41.

Štůsková K., Pečenka J., Tekielska D.A., Špetík M., Bytešníková Z., … Eichmeier A. The in vitro effects of selected substances and nanomaterials against *Diaporthe eres*, *Diplodia seriata* and *Eutypa lata*. *Annals of Applied Biology*, in press.

Sutton T.B., Aldwinckle H.S., Agnello A.M., Walgenbach J.F. (Eds.) 2014. Compendium of apple and pear diseases and pests (pp. 20–21). St. Paul, MN: American Phytopathological Society.

Thomidis T., Michailides T.J., 2009. Studies on *Diaporthe eres* as a new pathogen of peach trees in Greece. *Plant Disease* 93: 1293–1297.

Thomidis T., Michailides T.J., Exadaktylou E., 2011. *Neofusicoccum parvum* associated with fruit rot and shoot blight of peaches in Greece. *European Journal of Plant Pathology* 131: 661–668.

Timmer L.W., Garnsey S.M., Graham J.H., 2000. Compendium of Citrus Diseases, 2nd ed.; American Phytopathological Society: Saint Paul, MN, USA.

Tosi L., Natalini G., 2009. First report of *Eutypa lata* causing dieback of olive trees in Italy. *Plant Pathology* 58: 398.

Travadon R., Lecomte P., Diarra B., Lawrence D.P., Renault D., … Baumgartner K., 2016. Grapevine pruning systems and cultivars influence the diversity of wood-colonizing fungi. *Fungal Ecology* 24: 82–93.

Trouillas F.P., Gubler W.D., 2010. Pathogenicity of Diatrypaceae species in grapevines in California. *Plant Disease* 94: 867–872.

Trouillas F.P., Peduto F., Lorber J.D., Sosnowski M.R., Grant J., … Gubler W.D., 2012. Calosphaeria canker of sweet cherry caused by *Calosphaeria pulchella* in California and South Australia. *Plant disease* 96: 648–658.

Trouillas F.P., Úrbez-Torres J.R., Peduto F., Gubler W.D., 2010. First report of twig and branch dieback of English walnut (*Juglans regia*) caused by *Neofusicoccum mediterraneum* in California. *Plant Disease* 94: 1267–1267.

Türkölmez Ş., Derviş S., Çiftçi O., Serçe Ç.U., 2016. First report of canker and dieback caused by *Botryosphaeria dothidea* on apple in Turkey. *Plant disease* 100: 1237.

Úrbez-Torres J.R., 2011. The status of Botryosphaeriaceae species infecting grapevines. Phytopathologia Mediterranea 50: S5–S45.

Úrbez-Torres J.R., Battany M., Bettiga l.J., Gispert C., McGourty G., … Gubler W.D. 2010. Botryosphaeriaceae species spore-trapping studies in California Vineyards. *Plant Disease* 94: 717–724.

Úrbez-Torres J.R., Boulé J., O'Gorman D.T., 2016. First report of *Diplodia seriata* and *D. mutila* causing apple dieback in British Columbia. *Plant Disease* 100: 1243.

Úrbez-Torres J.R., Gubler W.D. 2011. Susceptibility of grapevine pruning wounds to infection by *Lasiodiplodia theobromae* and *Neofusicoccum parvum*. *Plant Pathology* 60: 261–270.

Úrbez-Torres J.R., Gubler W.D., 2009. Pathogenicity of Botryosphaeriaceae spp. isolated from grapevine cankers in California. *Plant Disease* 93: 584–592.

Úrbez-Torres J.R., Haag P., Bowen P., O'Gorman D.T., 2014. Grapevine trunk diseases in British Columbia: Incidence and characterization of the fungal pathogens associated with black foot disease of grapevine. *Plant Disease* 98: 469–482.

Úrbez-Torres J.R., Leavitt G.M., Guerrero J.C., Guevara J., Gubler W.D., 2008. Identification and pathogenicity of *Lasiodiplodia theobromae* and *Diplodia seriata*, the causal agents of Bot canker disease of grapevines in Mexico. *Plant Disease* 92: 519–529.

Úrbez-Torres J.R., Peduto F., Smith R.J., Gubler W.D. 2013a. Phomopsis dieback: A grapevine trunk disease caused by *Phomopsis viticola* in California. *Plant Disease* 97: 1571–1579.

Úrbez-Torres J.R., Peduto F., Vossen P.M., Krueger W.H., Gubler W.D. 2013b. Olive twig and branch dieback: Etiology, incidence, and distribution in California. *Plant Disease* 97: 231–244.

Uysal A., Kurt Ş., Guarnaccia V., 2022. Distribution and characterization of *Colletotrichum* species associated with *Citrus* anthracnose in eastern Mediterranean region of Turkey. *European Journal of Plant Pathology* 163: 125–141.

Váczy K.Z., Németh M.Z., Csikós A., Kovács G.M., Kiss L., 2018. *Dothiorella omnivora* isolated from grapevine with trunk disease symptoms in Hungary. *European Journal of Plant Pathology* 150: 817–824.

Vakalounakis D.J., Ntougias S., Kavroulakis N., Protopapadakis E., 2019. *Neofusicoccum parvum* and *Diaporthe foeniculina* associated with twig and shoot blight and branch canker of citrus in Greece. *Journal of Phytopathology* 167: 527–537.

Valencia D., Torres C., Camps R., Lopez E., Celis-Diez J.L., Besoain X., 2015. Dissemination of Botryosphaeriaceae conidia in vineyards in the semiarid Mediterranean climate of the Valparaíso Region of Chile. *Phytopathologia Mediterranea* 54: 394–402.

van der Merwe R., Halleen F., van Dyk M., Jacobs V.G., Mostert L., 2021. Occurrence of canker and wood rot pathogens on stone fruit propagation material and nursery trees in the western Cape of South Africa. *Plant Disease* 105: 3586–3599.

van Dyk M., Spies C.F., Mostert L., Halleen F., 2021a. Survey of trunk pathogens in South African olive nurseries. *Plant Disease* 105: 1630–1639.

van Dyk M., Spies C.F., Mostert L., van der Rijst M., du Plessis I.L., … Halleen F., 2021b. Pathogenicity testing of fungal isolates associated with olive trunk diseases in South Africa. *Plant Disease* 105: 4060–4073.

van Niekerk J.M., Crous P.W., Groenewald J.Z., Fourie P.H., Halleen F. 2004. DNA phylogeny, morphology and pathogenicity of *Botryosphaeria* species on grapevines. *Mycologia* 96: 781–798.

van Niekerk J.M., Frikkie J.C., Halleen F., Fourie P.H., 2010. Temporal spore dispersal patterns of grapevine trunk pathogens in South Africa. *European Journal of Plant Pathology* 127: 375–90.

Van Zyl F., 2011. Stem cankers on stone fruit. South Africa Fruit Journal June/July: 22.

Varjas V., Vajna L., Izsépi F., Nagy G., Pájtli É., 2017. First report of *Phomopsis amygdali* causing twig canker on almond in Hungary. *Plant Disease* 101: 1674.

Vek, V.; Keržič, E.; Poljanšek, I.; Eklund, P.; Humar, M.; Oven, P. Wood extractives of silver fir and their antioxidant and antifungal properties. Molecules 2021, 26, 6412.

Vitale S., Aiello D., Guarnaccia V., Luongo L., Galli M., … Voglmayr H., 2018. *Liberomyces pistaciae* sp. nov., the causal agent of pistachio cankers and decline in Italy. *MycoKeys* 40: 29–51.

Vrandecic K., Jurkovic D., Cosic J., Postic J., Riccioni L., 2011. First report of cane blight on blackberry caused by *Diaporthe eres* in Croatia. *Plant Disease* 95: 612.

Weber R.W.S., Børve J., 2021. Infection biology as the basis of integrated control of apple canker (*Neonectria ditissima*) in Northern Europe. *CABI Agriculture and Bioscience* 2: 5.

Wenneker M., van Raak M.M., van Brouwershaven I.R., Martin W., Kox L.F., 2011. *Eutypa lata*, the causal agent of dieback in red currant (*Ribes rubrum*) and gooseberry (*R. uva-crispa*) in the Netherlands. *European journal of plant pathology* 131: 441–449.

Yang T., Groenewald J.Z., Cheewangkoon R., Jami F., Abdollahzadeh J., … Crous P.W., 2017. Families, genera, and species of Botryosphaeriales. *Fungal Biology* 121: 322–346.

Yaseen T., Ahmed Y., D'Onghia A.M., Digiaro M., 2012. First report of *Cylindrocarpon pauciseptatum* associated with root rot and decline of peach in Southern Italy (Apulia Region). *Plant disease* 96: 764.

Yildiz A., Benlioglu S., Benlioglu K., Korkom Y. 2022. Occurrence of twig blight and branch dieback of walnut caused by Botryosphaeriaceae species in Turkey. *Journal of Plant Diseases and Protection* 129: 687–693.

Yu Z., Tang G., Peng S., Chen H., Zhai M., 2015. *Neofusicoccum parvum* causing canker of seedlings of *Juglans regia* in China. *Journal of Forestry Research* 26: 1019–1024.

Yurkewich J.I., Castaño C., Colinas C., 2017. Chestnut red stain: Identification of the fungi associated with the costly discolouration of *Castanea sativa*. *Forest Pathology* 47: e12335.

Zapolska A., Kalaitzidis C., Markakis E., Ligoxigakis E., Koubouris G., 2020. Linear discriminant analysis of spectral measurements for discrimination between healthy and diseased trees of Olea europaea L. artificially infected by Fomitiporia mediterranea. *International Journal of Remote Sensing* 41: 5388–5398.

Zhang W., Groenewald J.Z., Lombard L., Schumacher R.K., Phillips A.J.L., Crous P.W., 2021. Evaluating species in Botryosphaeriales. *Persoonia* 46: 63–115.

We warmly thank for their kind cooperation the following referees who have reviewed papers during this year in order to publish this Volume (Phytopathologia Mediterranea 61, 2022):

de Abreu Lucas Magalhães, Vicosa, Brazil
Abad-Campos Paloma, Valencia, Spain
Abbes Zouhaier, Tunis, Tunisia
Abrantes Isabel, Coimbra, Portugal
Aglietti Chiara, Firenze, Italy
Aiello Dalia, Catania, Italy
Al Rwahnih Maher, Davis, CA, USA
Alves Artur, Aveiro, Portugal
Armengol Forti Josep, Valencia, Spain
Arzanlou Mahdi, Tabriz, Iran
Aydınlı Gökhan, Samsun, Turkey
Balestra Giorgio, Viterbo, Italy
Besoain Ximena, Valparaíso, Chile
Bezerra Jadson, Goiás, Brazil
Buonaurio Roberto, Perugia, Italy
Buzkan Nihal, Kahramanmaraş, Turkey
Castillo Pablo, Córdoba, Spain
Cheng Mingyuan, Fairbanks, AK, USA
Cimmino Alessio, Naples, Italy
Cobos Rebeca, León, Spain
Cohen Daniel, Auckland, New Zealand
Contaldo Nicoletta, Bologna, Italy
Damicone Jhon, Stillwater, OK, USA
Damm Ulrike, Görlitz, Germany
Danchin Etienne, Sophia Antipolis, France
De Jonghe Kris, Merelbeke, Belgium
Desbiez Cecile, Avignon, France
Di Marco Stefano, Bologna, Italy
Die José, Cordoba, Spain
Dill-Macky Ruth, Minneapolis, MN, USA
Dissanayake Asha, Chengdu, Sichuan, China
Elbeaino Toufic, Bari, Italy
Elfar Karina, Davis, CA, USA
Erper Ismail, Samsun, Turkey
Eskalen Akif, Davis, CA, USA
Esteves Ivania, Coimbra, Portugal
Ezra David, Rishon LeZion, Israel
Farine Sibylle, Colmar , France
Fernando Dilantha, Winnipeg, MB, Canada
Fetch Tom, Morden, MB, Canada
Fikre Asnake, Addis Ababa, Ethiopia
Fontaine Florence, Reims, France
Fuchs Marc, Ithaca, NY, USA
Gallitelli Donato, Bari, Italy
Gamba Fernanda M., Montevideo, Uruguay
Gannibal Philipp, St. Petersburg, Russia
Gerič Stare Barbara, Ljubljana, Slovenia
Gramaje David, Córdoba, Spain
Gutiérrez-Barranquero José Antonio, Málaga, Spain
Haapalainen Minna, Helsinki, Finland
Habili Nuredin, Adelaide, Australia
Hernandez-Martinez Rufina, Ensenada, Baja California, Mexico
Holeva Maria, Athens, Greece
Huang Tzu-Pi, Taichung, Taiwan
Infantino Alessandro, Rome, Italy
Ioos Renaud, Fougères Cedex, France
Ippolito Antonio, Bari, italy
Isakeit Thomas, College Station, Texas, USA
Jamil Arshi, Aligarh, India
Kassemeyer Hanns-Heinz, Freiburg, Germany
Kolmer James A., St. Paul, Minnesota, USA
Lahlali Rachid, Meknès, Morocco
Linaldeddu Benedetto, Padova, Italy
Ling Kai-Shu, Charleston, SC, USA
Liu Jia, Lincang, China
Locatelli Gabriel, Recife, PE, Brasile
Loconsole Giuliana, Bari, Italy
Lolas Mauricio, Talca, Chile
Lotos Leonidas, Thessaloniki, Greece
Luque Jordi, Cabrils, Spain
Maleita Carla, Coimbra, Portugal
Marhadour Sylvie, Paris, France
Martínez Mónica, Valencia, Spain
Mascia Tiziana, Bari, Italy
Masi Marco, Naples, Italy
Mazzaglia Angelo, Viterbo, Italy
Menzel Wulf, Braunschweig, Germany
Moral Juan, Cordoba, Spain
Moretti Chiaraluce, Perugia, Italy
Moretti Samuele, Colmar, France
Morris Hugh, Wien, Austria
Mostert Lizel, Stellenbosch, South Africa
Munir Shahzad, Kunming, China
Nicolas Rispail, Córdoba, Spain
Nicolia Alessandro, Salerno, Italia
Nodet Patrice, Brest, France
Osti Fabio, Bologna, italy
Pacetti Andrea, Florence, Italy
Palmero Daniel, Madrid, Spain
Proença Diogo, Coimbra, Portugal
Saldarelli Pasquale, Bari, Italy
Sándor Erzsébet, Debrecen, Hungary
Savoie Jean-Michel, Villenave d'Ornon, France
Schena Leonardo, Reggio Calabria, Italy
Schirmer Tommy, Freiburg, Germany
Shiskoff Nina, Frederick, Maryland, USA
Silva Goncalo D R, Chatham, Kent, UK

Finito di stampare da
Logo s.r.l. – Borgoricco (PD) – Italia

Mediterranean Phytopathological Union

Founded by Antonio Ciccarone

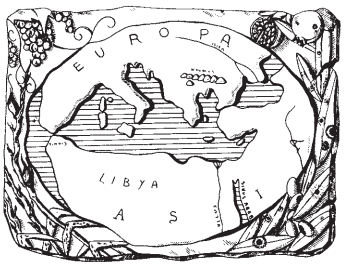

The Mediterranean Phytopathological Union (MPU) is a non-profit society open to organizations and individuals involved in plant pathology with a specific interest in the aspects related to the Mediterranean area considered as an ecological region. The MPU was created with the aim of stimulating contacts among plant pathologists and facilitating the spread of information, news and scientific material on plant diseases occurring in the area. MPU also intends to facilitate and promote studies and research on diseases of Mediterranean crops and their control.
The MPU is affiliated to the International Society for Plant Pathology.

MPU Governing Board

Affiliated Societies

Arab Society for Plant Protection (ASPP), http://www.asplantprotection.org/
French Society for Phytopathology (FSP), http://www.sfp-asso.org/
Hellenic Phytopathological Society (HPS), http://efe.aua.gr/
Israeli Phytopathological Society (IPS), http://www.phytopathology.org.il/
Italian Phytopathological Society (SIPAV), http://www.sipav.org/
Portuguese Phytopathological Society (PPS), http://www.spfitopatologia.org/
Spanish Society for Plant Pathology (SEF), http://www.sef.es/sef/

2022 MPU Membership Dues

Institutional MPU Membership: : € 200.00 (college and university departments, libraries and other facilities or organizations). Beside the open-access on-line version of *Phytopathologia Mediterranea*, the print version can be received with a € 50 contribution to mail charges (total € 250,00 to receive the print version). Researchers belonging to an Institution which is a member of the Union are entitled to publish with a reduced page contribution, as the Individual Regular members.
Individual Regular MPU Membership*: € 50.00 (free access to the open-access on-line version of Phytopathologia Mediterranea and can get the print version with a contribution to mail charges of € 50 (total € 100,00 to receive the print version).

*Students can join the MPU as a Student member on the recommendation of a Regular member. Student MPU members are entitled to a 50% reduction of the membership dues (proof of student status must be provided).

Payment information and online membership renewal and subscription at www.mpunion.com

For subscriptions and other information visit the MPU web site:
www.mpunion.com
or contact us at: Phone +39 39 055 2755861/862 – E-mail: phymed@unifi.it

Phytopathologia Mediterranea

Volume 61, December, 2022

Contents

Direttore responsabile: Giuseppe Surico • Autorizzazione del Tribunale di Firenze n. 4923 del 5-1-2000 • *Printed by* Logo S.r.l. - Padova, February 2023